NASA TECHNICAL TRANSLATION

NASA TT F-453

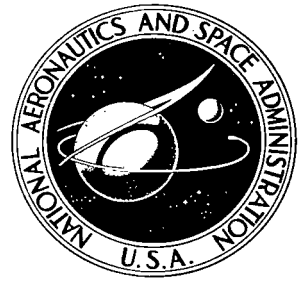

NASA TT F-453

LOAN COPY:
AFWL (W
KIRTLAND A
0069029
TECH LIBRARY KAFB, NM

SUPERSONIC GAS FLOW AROUND BLUNT BODIES

THEORETICAL AND EXPERIMENTAL INVESTIGATIONS

O. M. Belotserkovskiy, Editor

Computer Center of the Academy of Sciences USSR
Moscow, 1966

NATIONAL AERONAUTICS AND SPACE ADMINISTRATION • WASHINGTON, D. C. • JUNE 1967

TECH LIBRARY KAFB, NM
0069029

NASA TT F-453

SUPERSONIC GAS FLOW AROUND BLUNT BODIES

THEORETICAL AND EXPERIMENTAL INVESTIGATIONS

O. M. Belotserkovskiy, Editor

Translation of "Obtekaniye Zatuplennykh Tel Sverkhzvukovym Potokom Gaza. Teoreticheskoye i Eksperimental'noye Issledovaniya." Computer Center of the Academy of Sciences USSR, Moscow, 1966

NATIONAL AERONAUTICS AND SPACE ADMINISTRATION

For sale by the Clearinghouse for Federal Scientific and Technical Information
Springfield, Virginia 22151 – CFSTI price $3.00

SUPERSONIC GAS FLOW AROUND BLUNT BODIES

O. M. Belotserkovskiy, Editor

This review deals with certain characteristics of using the method of integral relations for the solution of the mixed problem of supersonic flow around blunt bodies, describes the construction of the numerical algorithms, and demonstrates their use for various cases of flow. Many calculations of two-dimensional and three-dimensional bodies of different shapes were performed. An investigation was made of an ideal gas with constant values of heat capacities, flows with equilibrium and non-equilibrium dissociation, ionization, vibrational-dissociation relaxation, and radiation. Viscous gas flows were also calculated. The results of the calculations are given in the form of tables and graphs. Supersonic flow around blunt bodies was also studied experimentally. A comparison of the calculated and the experimental data is presented.

PREFACE

During flights at high supersonic velocities problems of the heat protection of bodies compel the wide use of blunt aerodynamic shapes. Therefore, the construction of the pattern of flow past such bodies is of considerable practical interest.

Despite the fact that bluntness can be geometrically small in comparison with the overall dimension of the body, it has a very important effect of the overall flow pattern, forming a specific pattern of flow with a detached shock wave.

For a number of years the Computer Center of the Academy of Sciences USSR, the Leningrad Physicotechnical Institute im. A. F. Ioffe of the Academy of Sciences USSR, and other organizations under the supervision of O. M. Belotserkovskiy and Yu. P. Lun'kin have been developing numerical algorithms for calculating flow around blunt bodies with a detached shock wave. When constructing the indicated solution in the region of influence of bluntness, we used the method of integral relations [1,2], proposed by A. A. Dorodnitsyn for solving certain nonlinear problems of aerodynamics, which was developed by O. M. Belotserkovskiy for calculating mixed gas flows in a region with an unknown boundary. Calculations in the supersonic zone were performed by the method of characteristics or also by means of the method of integral relations.

Of the other published numerical schemes permitting solution of the problem of supersonic flow around blunt bodies, we need to point out the works of S. Utid and M. Yasukhar; M. Van Dyke; P. Garabedyan and Kh. Libershteyn; R. Vaglio-Laurin and A. Feri; S. K. Godunov, A. V. Zabrodin, and G. P. Prokopov; S. M. Gilinskiy and G. F. Telenin; G. P. Tinyakov; and L. I. Severinov.

The first solution of the direct problem of calculating supersonic flow around blunt bodies was given in an exact formulation in 1957 [3]. P. I. Chushkin [4] examined the limiting case of such a flow, viz., a sonic gas flow past bodies where the shock wave separated from the body at an infinitely great distance. M. Van Dyke [5] and others proposed a fundamentally different numerical scheme based on solving the inverse problem. Despite the fact that at present there are rather many numerical schemes for solving the mixed problem, their development and perfection continues even now since practice raises ever new, more complicated problems for study (investigation of flows with chemical reactions, radiation, viscous flows, calculation of flow around bodies having a discontinuity of the generatrix, etc.).

In this review we will dwell on certain characteristics of using the method of integral relations for this problem; we will describe the construction of the numerical algorithms; and we will demonstrate their use for various cases of flow.

Numerous calculations of two-dimensional (plane and axisymmetric) and three-dimensional bodies of different shapes (smooth, with a curvature discontinuity, with a discontinuity of the generatrix) were performed. We examined an ideal gas with constant values of heat capacities, flows with equilibrium and nonequilibrium dissociation, ionization, vibrational-dissociation relaxation, and radiation. Viscous gas flows which are described by Navier-Stokes equations were also calculated. The results of the calculations are given in the form of tables and graphs.

Along with the calculations, supersonic flow around blunt bodies was also studied experimentally. The eighth chapter was completely prepared by G. M. Ryabinkov and contains the results of his experimental investigations. The same chapter presents a comparison of calculated and experimental data.

The calculations were performed with the participation of A. I. Bykov, N. A. Vorob'yev, N. V. Leont'yev, N. V. Mel'tsis, R. M. Romanov, Ye. S. Sedov, and N. P. Shulishnin. A check of the differences of the tables presented in this book was performed at the Computer Center of the Academy of Sciences of the USSR under the supervision of L. S. Bark. The authors extend their gratitude to these comrades. The authors wish to thank Academician A. A. Dorodnitsyn for his constant attention to this work.

TABLE OF CONTENTS

	Pages
ANNOTATION	ii
PREFACE	iii
SYMBOLS	vi
CHAPTER 1. ALGORITHMS OF NUMERICAL SCHEMES OF THE METHOD OF INTEGRAL RELATIONS FOR CALCULATING MIXED GAS FLOWS	1
1. Statement of the Problem	1
2. Scheme I	8
3. Scheme II	22
4. Scheme III	31
5. Check of the Accuracy of the Calculations	41
CHAPTER 2. EQUILIBRIUM FLOWS	50
1. Equilibrium Blunt-Body Gas Flow	50
2. Description of Tables	62
3. Calculations of Flows at Low Supersonic Velocities	64
CHAPTER 3. NONEQUILIBRIUM FLOWS	105
1. Nonequilibrium Gas Flow Around Blunt Bodies	105
2. Combined Flows	117
3. Simultaneous Occurrence of Vibrational-Dissociation Relaxation	121
4. Description of Tables	128
CHAPTER 4. FLOW AROUND SOLIDS OF REVOLUTION WITH DISCONTINUITY OF GENERATRIX OR DISCONTINUITY OF CURVATURE OF THE CONTOUR	159
1. Calculation of Flow Around Solids of Revolution With Discontinuity of Generatrix	159
2. Calculation of Flow Around Bodies with Discontinuity of Contour Curvature (Scheme I)	172
CHAPTER 5. FLOWS WITH RADIATION	199
1. System of Equations	199
2. Statement of Problem and Scheme of Calculation	201
3. Results of Calculations	206
CHAPTER 6. VISCOUS FLOWS	225
1. Special Features of Calculating Viscous Flows	225
2. Statement of Problem	226
3. Construction of Solution	229
4. Some Results of Calculations	234
CHAPTER 7. THREE-DIMENSIONAL FLOWS	246
CHAPTER 8. EXPERIMENTAL INVESTIGATION OF FLOW AROUND SOLIDS OF REVOLUTION IN A SUPERSONIC GAS FLOW	255
1. Investigated Bodies and Measuring Equipment	255
2. Conduction and Analysis of Results of Experiments	263
3. Experimental Results	266
REFERENCES	312

SYMBOLS

s	-	length of arc measured along body contour;
n	-	normal to body ($n = 0$ corresponds to body contour);
t	-	time;
R	-	radius of curvature of body at arbitrary point;
r	-	distance along normal from axis of symmetry of body;
ε	-	distance along normal from surface of body to shock wave;
$\xi = n/\varepsilon(s)$;		
a, b	-	principal semiaxes of ellipsoid;
$\delta = b/a$;		
x, y	-	Cartesian coordinates;
θ, σ	-	angle formed by the tangent to the body contour and shock wave, respectively, and the direction of the oncoming flow;
u, v	-	velocity components in direction n, s, respectively, related to the maximal velocity value w_{max};
w	-	value of total velocity related to w_{max};
w_t, w_n	-	tangential and normal (to shock wave) components of velocity, respectively, related to w_{max};
w_x, w_y	-	velocity components along axes x, y, respectively, related to w_{max};
c	-	sound velocity related to w_{max};
c_*	-	critical sound velocity related to w_{max};
ψ	-	stream function;
C_p, C_v	-	specific heats at constant pressure and volume, respectively;
$\varkappa = C_p/C_v$;		
M, α	-	Mach number and angle, respectively;
Pr	-	Prandtl number;
Re	-	Reynolds number;
R	-	universal gas constant;
ρ	-	density referred to density in oncoming flow ρ_∞
p	-	pressure referred to $\rho_\infty w^2_{max}$;
μ	-	molecular weight referred to molecular weight of gas in oncoming flow μ_∞;
T	-	temperature related to $\mu_\infty w^2_{max}/R$;
S	-	entropy referred to $R/2\mu_\infty$;
h_i, h	-	specific enthalpy of i-th component and entire mixture, respectively, related to stagnation enthalpy $w^2_{max}/2$;
h_i°	-	enthalpy of formation of i-th component extrapolated to absolute zero;
C_i	-	mass concentration of i-th component;

ω_i - mass rate of formation of i-th component as a result of all chemical reactions;

x_i - molar concentration of i-th component;

T_{ij}, e_{ij}, τ_{ij} - temperature, specific internal energy, and relaxation time, respectively, of j-th vibrational degree of freedom of i-th component;

h_T, h_C, h_e - partial derivatives of enthalpy with respect to T, C_i, e_{ij} respectively;

K_p - equilibrium constant;

μ^* - viscosity coefficient;

$C_f = \frac{1}{\rho_\infty w_\infty^2} \left(\mu^* \frac{\partial v}{\partial n} \right)_{n=0}$ - friction coefficient;

A, E - magnitude of radiant energy absorbed and emitted, respectively, per unit volume in unit time;

B_ν - Planck function;

h_* - Planck constant;

k - Boltzmann constant;

b_* - Stefan-Boltzmann constant;

$\tilde{c}_*$ - light velocity;

$\tilde{\varepsilon}_*(\rho, T)$ - emission coefficient per unit length.

All the linear dimensions are related to the characteristic dimension of the body (to the radius for a sphere and to the vertical semiaxis b for ellipsoids). The subscript ∞ denotes quantities before the shock wave, ν = 0 or 1, respectively, for plane or axisymmetric cases.

CUT ALONG THIS LINE

FOLD LINE

NATIONAL AERONAUTICS AND SPACE ADMINISTRATION
WASHINGTON, D.C. 20546

OFFICIAL BUSINESS

POSTAGE AND FEES PAID
NATIONAL AERONAUTICS & SPACE ADMINISTRATION

NATIONAL AERONAUTICS AND SPACE ADMINISTRATION
CODE USS-T
WASHINGTON, D.C. 20546

NASA TTF No.
F-453

FOLD LINE

CUT ALONG THIS LINE

NATIONAL AERONAUTICS AND SPACE ADMINISTRATION

TECHNICAL TRANSLATION EVALUATION

Budget Bureau No. 104-R037
Approval Expires: Sept. 30, 1969

TO:
THE USERS OF THIS TRANSLATION

NASA TTF NO.
F-453

MAINTAINING THE QUALITY OF NASA TRANSLATIONS REQUIRES A CONTINUOUS EVALUATION PROGRAM. PLEASE COMPLETE AND MAIL THIS FORM TO AID IN THE EVALUATION OF THE USEFULNESS AND QUALITY OF THE TRANSLATING SERVICE.

THIS PUBLICATION *(Check one or more)*

- ☐ FURNISHED VALUABLE NEW DATA OR A NEW APPROACH TO RESEARCH.
- ☐ VERIFIED INFORMATION AVAILABLE FROM OTHER SOURCES.
- ☐ FURNISHED INTERESTING BACKGROUND INFORMATION.
- ☐ OTHER *(Explain)*: _____

FOLD LINE FOLD LINE

TRANSLATION TEXT *(Check one)*

- ☐ IS TECHNICALLY ACCURATE.
- ☐ IS SUFFICIENTLY ACCURATE FOR OUR PURPOSE.
- ☐ IS SATISFACTORY, BUT CONTAINS MINOR ERRORS.
- ☐ IS UNSATISFACTORY BECAUSE OF *(Check one or more)*:
  - ☐ POOR TERMINOLOGY.
  - ☐ NUMERICAL INACCURACIES.
  - ☐ INCOMPLETE TRANSLATION.
  - ☐ ILLEGIBLE SYMBOLS, TABULATIONS, OR CURVES.
  - ☐ OTHER *(Explain)*:

FOLD LINE FOLD LINE

REMARKS

FROM

DATE

NOTE: REMOVE THIS SHEET FROM THE PUBLICATION, FOLD AS INDICATED, STAPLE OR TAPE, AND MAIL. NO POSTAGE NECESSARY.

NASA Form 1332 AUG 66

GPO 915-777

CUT ALONG THIS LINE

CUT ALONG THIS LINE

CHAPTER 1

ALGORITHMS OF NUMERICAL SCHEMES OF THE METHOD OF INTEGRAL RELATIONS FOR CALCULATING MIXED GAS FLOWS

1. Statement of the Problem

The complete system of equations describing motion in a mixed-flow region /7* consists of equations of gas dynamics and relaxation equations. A stationary flow is examined. The problem consists of determining the solution in the region of influence of the initial system, i.e., in the region bounded by the shock wave, body contour, and boundary characteristics. The solution is set up in a class of functions with a continuous limited derivative.

The idea of the method of integral relations is, as is known, that by covering the integration range with a certain curvilinear calculated network and by introducing the representation of functions with respect to one of the directions into the partial differential equations, we obtain in the two-dimensional case an approximating system of ordinary differential equations, the solution of which is found by means of the well-developed numerical apparatus. Representation of the functions in both directions is also possible, which leads to a system of algebraic transcendental equations. An additional trigonometric approximation of the unknown functions in the transverse plane is introduced for three-dimensional flows.

The statement of the problem and general scheme of using the method of integral relations permit setting up the algorithm in a matrix form of classes of numerical schemes. Their realization on electronic computers substantially facilitates the process of programming and permits calculation for various approximations of the system with respect to single programs. The type of algorithm depends only on the variable with respect to which the approximation is performed. Consideration of specific properties of flows, the use of various complete systems of base functions, and the diverse structure of the calculated networks do not change the essence of the algorithms. It is possi- /8 ble to write out the general form of the approximating operator also for an arbitrary system of base functions.

1. The selection of a suitable system of coordinates plays an important role both for investigating equations and for automation of the calculating process.

It is convenient to write the system of differential equations of the problem either in orthogonal coordinates s, n, where s is the length of the arc measured along the body, n is a normal to the body (n = 0 corresponds to the body contour), or in coordinates s, $\xi = n/\varepsilon(s)$, where $n = \varepsilon(s)$ is the equation of a shock wave. In the system s, n it is easy to change from one body shape to another, which permits calculating flow around bodies of different shapes

*Numbers in the margin indicate pagination in original foreign text.

(smooth or with a discontinuity) by a single program. Furthermore, in these coordinates the approximating system has a comparatively simple form, and the data obtained can be used directly for calculating the boundary layer or heat transfer.

In the system s, ξ the shock wave becomes parallel to the body, which enables us to set up integral relations along s.

2. In a number of cases for constructing numerical schemes it is convenient to use different forms of writing the initial system of equations and boundary conditions. The fact is that mathematically equivalent forms of the equations and boundary conditions are not always equivalent from the point of view of the accuracy of their approximate representation.

Partial differential equations of the initial system are written in a divergent form as laws of conservations. Such a form of equations is convenient in that integration with respect to one of the variables is performed exactly, and the expressions (complexes of functions) which usually change more smoothly than the individual functions entering them, are approximated.

Actually, in the method of integral relations the integral which is a smoother function than the integrand is approximated. In this case, the accuracy of approximation increases and a good representation is achieved more quickly with an increase of the number of approximation. Finally, the integral permits a continuous representation in the case when the integrand has a discontinuity of the first kind (for example, a discontinuity of curvature of the generatrix of the body).

The initial system can be simplified if we incorporate into it known integrals and write certain partial differential equations along the lines of flow in the form of ordinary differential equations. Then the initial system will contain fewer partial differential equations which, in essence, are represented by means of the method of integral relations. The final relations and ordinary differential equations of the initial system are written along the boundaries of zones and, consequently, are used in the approximating system in an exact form. Thus, the boundary-value problem for such an approximating system will be simpler and it will represent more accurately the corresponding initial system of equations. /9

In this connection, when examining nonequilibrium flows, it is expedient to introduce equations of material balance and the Dalton equation in place of certain kinetic equations of the system, and to write the remaining kinetic equations and adiabatic condition along the lines of flow. The introduction of the Bernoulli integral to the system is also useful. For flows of an ideal and equilibrium-dissociating gases the adiabatic condition is taken in the form of constancy of entropy along the lines of flow.

If we also take into account equilibrium heat radiation of the gas, assuming that the shock layer is optically thin (we disregard energy dissipation), then the divergence of the vector of the radiation flux, which is represented as the difference of the radiation energy emitted and absorbed (is a unit volume in unit time) will enter the energy equation. Calculation of radiation

equilibrium with consideration of absorption is substantially complicated by the fact that in this case the energy equation becomes integro-differential.

If in the region of influence of a smooth body there is a discontinuity of the generatrix and the flow pattern changes so that the sonic point on the body will be at the point of discontinuity (sonic discontinuity), then a Prandtl-Meyer flow will occur in the supersonic neighborhood of this point. The characteristic of the second family in this case degenerates to a point, and the discontinuity itself will be essentially a singular point of the flow. Difficulties are encountered when constructing numerical schemes of calculating flow past such bodies, especially in the neighborhood of the discontinuity. In a number of cases it is expedient to use an asymptotic expansion such as the solution of R. Vaglio-Laurin [6], which holds true for a plane and axisymmetric vortex flow in a certain zone of the "boundary layer" joining the subsonic and supersonic neighborhoods of the sonic discontinuity. /10

3. We will point out certain features in the formulation of the problem. Let us examine, for simplicity, the case of the adiabatic flow of an ideal gas. The system of equations describing such a flow in coordinates x, y, where the x-axis is directed along a tangent to the body and the y-axis is directed along the normal (Fig. 1.1), can be written in the usual form:

$$\left.\begin{aligned}(w_x^2-c^2)\frac{\partial w_x}{\partial x}+w_x w_y\left(\frac{\partial w_x}{\partial y}+\frac{\partial w_y}{\partial x}\right)+(w_y^2-c^2)\frac{\partial w_y}{\partial y}=\nu c^2 w_y/y;\\ \frac{\partial w_y}{\partial x}-\frac{\partial w_x}{\partial y}=\Omega,\end{aligned}\right\} \qquad (1.1)$$

where $\Omega=\frac{1}{2}y^{\nu}\rho T\frac{dS}{d\psi}$ is the vortex value; c is the velocity of sound; $\nu = 0$ or 1, respectively, for the plane of the axisymmetric case; S is entropy.

The problem consists of determining the single-valued and continuous solution together with its derivatives (with the exception, perhaps, of the boundary points) in a minimal region of influence, the boundaries of which are the shock wave AB_3, axis of symmetry AE (in the two-dimensional case), body contour DE, and the boundary characteristic B_3D (Figs. 1.1 - 1.3).

By region of influence of the problem we will denote the part of the region containing the entire elliptic subregion AB_1D_1E and a minimal characteristic triangle including transitional line B_1D_1 (Fig. 1.4). The boundary conditions for the initial system are set up at the front of the shock wave, axis of symmetry, and surface of the body. Thus, we obtain a problem with an "open" upper bound, wherein only the condition of regularity distinguishing the class of solutions with a limited derivative makes the problem single-valued. /11

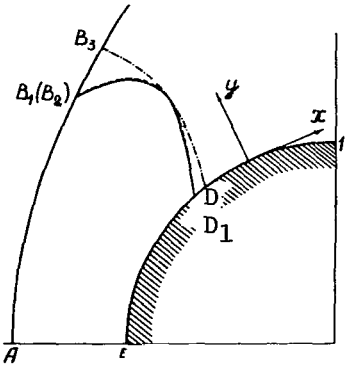

Figure 1.1. Flow of a perfect gas ($M_\infty = 4$; $\varkappa = 1.4$) around a circular cylinder ($\nu = 0$; $\delta = 1$): —— sonic line ($w = c$)-B_1D_1; --- singular line ($w_x = c$)-B_2D_1; -•-•- boundary characteristic -B_3D.

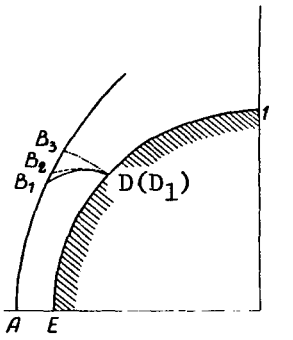

Figure 1.2. Flow of a perfect gas ($M_\infty = 4$; $\varkappa = 1.4$) around a sphere ($\nu = 1$; $\delta = 1$): —— sonic line ($w = c$)-B_1D_1; --- singular line ($w_x = c$)-B_2D_1; -•-•- boundary characteristic -B_3D.

Let L (y) be a certain line $x = x_1(y)$ lying in the integration range. Let us determine on this line the values of all derivatives of the unknown functions, for which purpose we must add to system (1.1) the relations being realized along L,

$$\frac{\partial w_y}{\partial y} + \frac{\partial w_y}{\partial x} x_1' = \frac{dw_y}{dy}; \quad \frac{\partial w_x}{\partial y} + \frac{\partial w_x}{\partial x} x_1' = \frac{dw_x}{dy}. \tag{1.2}$$

Then from (1.1) and (1.2) we obtain:

$$\left.\begin{aligned} &\frac{\partial w_y}{\partial x} = \frac{\Delta_y}{\Delta}; \quad \frac{\partial w_x}{\partial x} = \frac{\Delta_x}{\Delta}; \\ &\frac{\partial w_y}{\partial y} = \frac{dw_y}{dy} - \frac{\partial w_y}{\partial x} x_1'; \quad \frac{\partial w_x}{\partial y} = \frac{dw_x}{dy} - \frac{\partial w_x}{\partial x} x_1'. \end{aligned}\right\} \tag{1.3}$$

Here Δ is the determinant of system (1.1) - (1.2) and the determinants $\Delta_y(\Delta_x)$ are obtained from Δ by replacing the elements of the first (second) column by corresponding values of the right sides of the system.

We will write the condition that the line L (y) is a characteristic, i.e., the condition of the impossibility of a single-valued determination of the derivatives of all unknown functions on this line. It follows from (1.3) that

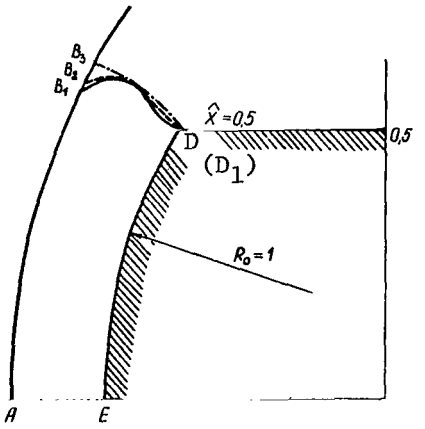

Figure 1.3. Flow of an ideal gas ($M_\infty = 4$; $\varkappa = 1.4$) past a sphere ($\nu = 1$; $R_0 = 1$) with a sonic discontinuity ($\hat{x} = 0.5$); —— sonic line ($w = c$)-B_1D_1; --- singular line ($w_x = c$)-B_2D_1; -·-·- boundary characteristic-B_3D.

when $\Delta = 0$ system (1.1) - (1.2) can allow only indeterminate solutions. In order that these solutions remain finite we must require the vanishing of all determinants composed by successive introduction of the right sides into the columns of the determinant of the system, i.e., there should be $\Delta_y = 0$ (the equality $\Delta_x = 0$ follows from $\Delta = 0$ and $\Delta_y = 0$). /12

Consequently, the condition

$$\Delta_y = 0 \text{ when } \Delta = 0 \qquad (1.4)$$

ensures the boundedness of all derivatives of the unknown functions w_x, w_y on the characteristic line.

Let us now examine the solution of the local Cauchy problem for initial system of equation (1.1) in the neighborhood of line x = const and y = const since later, when deriving the numerical solution, the approximating operator will be used in precisely this form.

In the neighborhood of x = const, we have

$$\frac{\partial w_y}{\partial x} = \Omega + \frac{dw_x}{dy}; \quad \frac{\partial w_x}{\partial x} = \frac{E_x}{w_x^2 - c^2}, \qquad (1.5)$$

where

$$E_x = \nu \frac{c^2 w_y}{y} - w_x w_y \left(2\frac{dw_x}{dy} - \Omega\right) - \left(w_y^2 - c^2\right)\frac{dw_y}{dy}.$$

Analogously for y = const,

$$\frac{\partial w_x}{\partial y} = -\Omega + \frac{dw_y}{dx}; \quad \frac{\partial w_y}{\partial y} = \frac{E_y}{w_y^2 - c^2}; \qquad (1.6)$$

$$E_y = \nu \frac{c^2 w_y}{y} - w_x w_y \left(2\frac{dw_y}{dx} - \Omega\right) - \left(w_x^2 - c^2\right)\frac{dw_x}{dx}.$$

In the integration range, let the velocity component w_x pass through the sonic value (which occurs in our problem), then when $w_x = c$, if a definite solution of the Cauchy problem (1.5) exists, then it need not be the only one. The /13

points at which $w_x = c$ will be singular points of the system. The totality of such points we will hereafter call the singular line of the initial system.

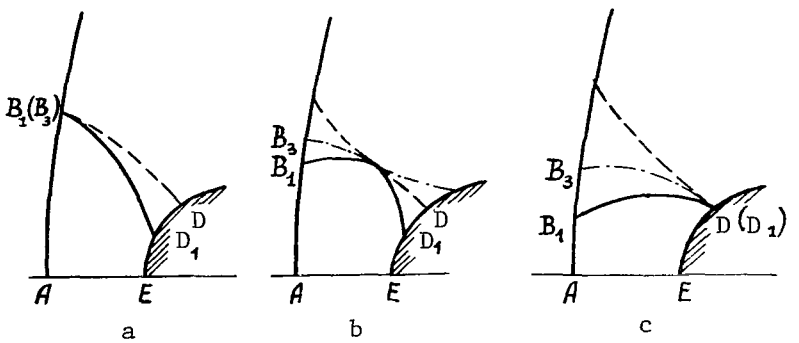

Figure 1.4. Types of regions of influence: --- characteristic of I family; - - - characteristic of II family; B_1D_1 - sonic line ($M = 1$); B_3D - boundary characteristic.

As follows from (1.5), for boundedness of the derivatives at points of the singular line we must realize a special condition

$$E_x = 0 \text{ when } w_x = c. \tag{1.7}$$

Otherwise, infinite values of the derivatives, i.e., infinite accelerations, will be on this line; motion cannot continue beyond the singular line (the singular line itself will be a limiting line) and the entire solution will not have any physical meaning.

The nature of such singular points is obvious - at them, the direction $x = \text{const}$ applies to one of the characteristics of the initial system of equations. Actually, at points where $w_x = c$ we have $\frac{w_x}{w} = \frac{c}{w} = \frac{1}{M} = \sin\alpha$, where α is the Mach angle. Depending upon the sign of the velocity component w_y, the direction $x = \text{const}$ applies to the characteristics of the first ($w_y > 0$) or the second ($w_y < 0$) family at points of the singular line.

In other words, the singular line is a locus of points at which the direction of integration becomes perpendicular to the characteristic. When selecting other unknown functions the position of the singular points remains as before, whereas on changing the system of coordinates (and, consequently, the direction along which the derivatives are determined) the position of the singular line can also change. The solution of the local Cauchy problem (1.6) in direction y is always single-valued and is bounded in our problem since in the entire integration range $|w_y| \ll c$.

Thus, at each point of the singular line, the condition of regularity of the solution which makes the problem unique can be written in the form $\Delta_y = 0$ along the corresponding characteristic, or as $E_x = 0$, $w_x = c$ along the ray $x = \text{const}$. If the singular line coincides with the characteristic, which occurs, for example, in Tricomi's second mixed problem, then these conditions will be identical. /14

In schemes I of the method of integral relations where integration of the approximating system is done with respect to x, the solution "encounters" the singular line and condition (1.7) isolates the only regular solution and thus closes the problem. Here, of course, all boundary conditions in the region of influence of blunting should be satisfied. The conditions of compatibility (1.4) along the boundary characteristic are now fulfilled automatically.

In schemes II where the representation of functions along the shock layer is introduced, the solution of the approximating system is found in the y-direction. The integration range here is limited above by the boundary characteristic which cuts out the exact region of influence of blunting. In this case, condition (1.4) ensures regularity of the solution along the upper bound and thus closes the approximating system. Derivatives only along the characteristic itself enter this condition, consequently it is used in the approximating system in each approximation in an exact form.

The regularity of solution within the integration range follows from corresponding representations of unknown functions along the shock layer, from the regularity of the solution at the limits of the integration range, and from the iterative method of constructing the sought numerical solution of the boundary-value problem for the approximating system. This solution is found by multiple iteration of the solutions of the Cauchy problem with initial data on the shock wave until the corresponding conditions on the body are fulfilled. In each iteration the regular solution is determined without limiting lines. Condition (1.7) is fulfilled here automatically on the singular line. It is not convenient to use it directly for closing the system in schemes II since derivatives with respect to both directions enter condition (1.7).

In schemes III where the representation of functions are introduced simultaneously in two directions and the initial system of partial differential equations is replaced in the two-dimensional case by a system of algebraic transcendental equations, both forms of writing the conditions closing the approximating system were used (depending on the order of constructing the algorithm of schemes III). In this case, a completely identical solution is obtained. /15

4. For simplicity, a system of polynomial functions is usually used as the complete base system of functions. The introduction of trigonometric representations is valid in the problem of sonic flow around bodies [4]. It seems to us inexpedient to use here base functions of another form (for example, Lagrange polynomials) because the computer algorithm is complicated without a noticeable increase in the accuracy of the calculations.

It is required that a numerical solution be constructed of a system of k second-order partial differential equations containing k unknown functions. When solving the problem by the method of integral relations, the coordinate system is selected so that the two opposite limits of the region are coordinate lines. The integral relations are also set up in this direction.

If, at the opposite limits of the region there is a sum of k boundary conditions, then the corresponding approximating system of ordinary differential equations proves to be completely closed. If one of the boundaries of the region is not known beforehand, an additional boundary condition is required. In the presence of a singular line, the corresponding boundary conditions can be absent, the conditions of regularity replace them. Here the simple method of integral relations is used. The laws of conservation expressed by the initial system are written across the zone in the form of integral relations.

Three types of numerical schemes have proved convenient for different flow regimes [7, 8, 9]. We will demonstrate their construction in the two-dimensional case.

2. Scheme I

1. The construction of the algorithm for calculating an arbitrary approximation by scheme I of the method of integral relations is presented for the example of flow around a blunt axisymmetric body with consideration of equilibrium dissociation of the gas.

The initial system of equations is written in coordinates s, n; the integration range is divided by lines passing between the surface of the body and the shock wave (Fig. 1.5), and the functions (and the integrals themselves) are represented by interpolation polynomials across the shock layer with points of interpolation at the zone boundaries [2, 3, 7, 8, 10-19]. /16

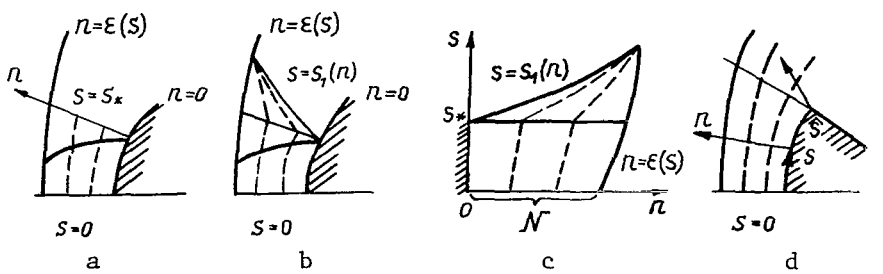

Figure 1.5. Scheme I

For equilibrium flows, the complete system of equations (projection of the motion equation onto n, continuity equation, stream functions, entropy, Bernoulli integral, and thermodynamic relations) in dimensionless form looks like:

$$\left.\begin{aligned}
&\frac{\partial \bar{z}}{\partial s}+\frac{\partial}{\partial n}(A\bar{H})=\bar{Y}; \quad \frac{\partial \bar{t}}{\partial s}+\frac{\partial}{\partial n}(A\bar{l})=0;\\
&\frac{d\psi}{ds}=\bar{t}\frac{dn}{ds}-A\bar{l}; \quad S=S_*(\psi);\\
&w^2+h=1; \quad TdS=dh-2\frac{dp}{\rho};\\
&h=h(p,T); \quad \rho=\rho(p,T)=\frac{p}{T}G(p,T),
\end{aligned}\right\} \tag{1.8}$$

here $\bar{z}=rz;\ \bar{l}=rl;\ \bar{t}=r\bar{t};\ \bar{H}=rH;\ \bar{g}=rg;$

$z=\rho uv;\quad l=\rho u;\quad t=\rho v;\quad H=p+\rho u^2;\quad g=p+\rho v^2;$

$\bar{Y}=\bar{g}/R+Ap\cos\theta;\quad A=1+n/R;\quad r=r_0+n\cos\theta.$

The boundary conditions are as follows: on the surface of the body (n = 0): u = 0, ψ = 0, $S_*(0)$ = 0; on the shock wave (n = ε(s)):

$$w_\tau=w_\infty\cos\sigma;\quad \rho w_n=w_\infty\sin\sigma;\quad p=p_\infty-\rho w_n^2+(w_\infty\sin\sigma)^2;$$

$$\psi=\frac{r^2}{2}w_\infty;\quad \frac{dw_n}{d\sigma}=\frac{w_\infty h_T\cos\sigma-w_n(De+\rho_T e_1)}{\rho h_T-w_n(Dw_\infty\sin\sigma+2\rho_T w_n)};$$

$$\frac{dp}{d\sigma}=e-w_\infty\sin\sigma\frac{dw_n}{d\sigma};$$

$$\frac{dS}{d\sigma}=-\frac{2}{T}\left[w_n\frac{dw_n}{d\sigma}+\frac{1}{\rho}\frac{dp}{d\sigma}-\frac{e_1}{2}\right];$$

$$\frac{dT}{d\sigma}=\frac{1}{h_T}\left[e_1-h_p\frac{dp}{d\sigma}-2w_n\frac{dw_n}{d\sigma}\right],$$

here $e_1=w_\infty^2\sin 2\sigma$; $e=e_1-w_n w_\infty\cos\sigma$. On the axis of symmetry (s = 0): v = 0, ψ = 0, S = 0. /17

Two partial differential equations, which are presented here approximately, enter the initial system (1.8).

We will approximate the functions $\bar{z}$, $\bar{t}$, $\bar{Y}$ in the following manner:

$$\bar{z}(n,s)=\sum_{i=1}^{N}{}^{i}z(s)\xi^i;\quad \bar{t}(n,s)=\sum_{i=0}^{N}{}^{i}t(s)\xi^i;\quad \bar{Y}(n,s)=\sum_{i=0}^{N}{}^{i}Y(s)\xi^i.$$

We will divide the integration range into N zones by lines ξ = k/N, k = 1, 2, ..., N-1, and integrate each of the partial differential equations, introducing

into them approximations, with respect to n from zero to each of the N remaining lines:

$$\int_0^{\frac{k}{N}\varepsilon(s)} \frac{\partial}{\partial s}\left[\sum_{i=1}^{N} {}^{i}z(s)\xi^{i}\right]dn + \int_0^{\frac{k}{N}\varepsilon(s)} \frac{\partial}{\partial n}(A\bar{H})dn = \int_0^{\frac{k}{N}\varepsilon(s)} \sum_{i=0}^{N} {}^{i}Y(s)\xi^{i}dn;$$

$$\frac{d}{ds}\left[\varepsilon(s)\int_0^{\frac{k}{N}} \sum_{i=1}^{N} {}^{i}z(s)\xi^{i}d\xi\right] - \frac{k}{N}\varepsilon'(s)z_k(s) +$$

$$+(A\bar{H})_k-(A\bar{H})_0 = \varepsilon(s)\int_0^{\frac{k}{N}} {}^{i}Y(s)\xi^{i}d\xi;$$

$$\varepsilon(s)\sum_{i=0}^{N}\frac{1}{i+1}\left(\frac{k}{N}\right)^{i+1} {}^{i}z'(s)+\varepsilon'(s)\sum_{i=1}^{N}\frac{1}{i+1}\left(\frac{k}{N}\right)^{i+1} {}^{i}z - \frac{k}{N}z_k\varepsilon'(s)+$$

$$+(A\bar{H})_k-(A\bar{H})_0-\varepsilon(s)\sum_{i=0}^{N}\frac{1}{i+1}\left(\frac{k}{N}\right)^{i+1} {}^{i}Y(s)=0; \quad k=1,2,\ldots,N.$$

Analogously, the second equation of (1.8) is transformed to the system

/18

$$\varepsilon(s)\sum_{i=0}^{N}\frac{1}{i+1}\left(\frac{k}{N}\right)^{i+1} {}^{i}t'(s)+\varepsilon'(s)\sum_{i=0}^{N}\frac{1}{i+1}\left(\frac{k}{N}\right)^{i+1} {}^{i}t(s) -$$

$$-\frac{k}{N}t_k\varepsilon'(s)+(A\bar{h})_k-(A\bar{h})_0=0; \quad k=1,2,\ldots,N.$$

Here f_k denotes $f(s, \xi = k/N)$.

In a vector form we can write:

$$\varepsilon(s)B^{*}\bar{z}'+\varepsilon'(s)B^{*}\bar{z}-\bar{f}-\varepsilon(s)B^{*}\bar{Y}=0;$$

$$\varepsilon(s)\bar{M}t_0'+\varepsilon(s)B^{*}\bar{t}'+\varepsilon'(s)\bar{M}t_0+\varepsilon'(s)B^{*}\bar{t}-\bar{G}=0,$$

here

$$B=\|b_{ki}\|; \quad k,i=1,\ldots,N; \quad b_{ki}=\frac{1}{i+1}\left(\frac{k}{N}\right)^{i+1};$$

$$\bar{M}=\|m_k\|; \quad m_k=k/N; \quad {}^{*}\bar{z}=\|{}^{k}z\|; \quad {}^{*}\bar{t}=\|{}^{k}t\|;$$

$$\bar{f} = \| f_k \|; \quad f_k = \varepsilon'(s)\frac{k}{N} z_k - (A\bar{H})_k + (A\bar{H})_0 + \varepsilon(s)\frac{k}{N} Y_0;$$

$$\bar{G} = \| g_k \|; \quad g_k = \varepsilon'(s)\frac{k}{N} t_k - (A\bar{h})_k + (A\bar{h})_0 .$$

Using the relation between the coefficients of approximate polynomials and functions on the lines of approximation

$$^*\bar{z} = W^{-1}\bar{z}_*; \quad ^*\bar{t} = W^{-1}(\bar{t}_* - \bar{t}_0); \quad ^*\bar{Y} = W^{-1}(\bar{Y}_* - \bar{Y}_0);$$

$$W = \| w_{ki} \|; \quad w_{ki} = \left(\frac{k}{N}\right)^i, \quad k, i = 1, \ldots, N,$$

we obtain a system of equations in the form

$$\bar{z}_*' + \bar{b} = 0; \quad \bar{a}\bar{t}_0' + \bar{t}_*' + \bar{c} = 0,$$

where

$$\bar{a} = WB^{-1}\bar{M} - 1;$$

$$\bar{b} = \frac{1}{\varepsilon}(\varepsilon'\bar{z}_* - \bar{Y}_* + \bar{Y}_0 - WB^{-1}\bar{f});$$

$$\bar{c} = \frac{1}{\varepsilon}[\varepsilon'(\bar{t}_* - \bar{t}_0) + WB^{-1}(\varepsilon'\bar{M}t_0 - G)].$$

The obtained system consists of 2N equations with 2N + 2 unknown functions t_0, $\bar{t}_*$, $\bar{Z}_*$, ε_0.

At the shock wave /19

$$v_N = w_n \sin(\sigma - \theta); \quad u_N = w_n \cos(\sigma - \theta).$$

From where

$$\alpha v_N' - \beta u_N' + w_n \frac{dw_n}{d\sigma}\theta' = 0; \quad \sigma' = \frac{v_N' + w_n\theta'\cos(\sigma-\theta)}{\alpha} = \frac{E_\sigma}{\alpha},$$

here

$$\alpha = \frac{dw_n}{d\sigma}\cos(\sigma-\theta) - w_n\sin(\sigma-\theta); \quad \beta = \frac{dw_n}{d\sigma}\sin(\sigma-\theta) + w_n\cos(\sigma-\theta).$$

Knowing $\sigma(s)$, the function $\varepsilon(s)$ is found from the geometric relation

$$\varepsilon'(s) = \left(1 + \frac{\varepsilon(s)}{R}\right)\tan(\sigma-\theta).$$

The equations for ε' and σ' close the approximating system. Having expressed the functions t, z, Y, etc., in terms of unknown functions u, v, p, ρ, we obtain a system of the form, $\Phi\bar{\varphi}' = \bar{\Theta}$, where

$$\bar{\varphi}' = \begin{Vmatrix} v_0' \\ v_1' \\ \vdots \\ v_N' \\ u_1' \\ \vdots \\ u_N' \end{Vmatrix}; \quad \Phi = \left\| \begin{array}{c|c|c} 0 & n_{11} \; \circ & n_{12} \; \circ \\ \vdots & \circ \; \ddots & \circ \; \ddots \\ 0 & \circ \; \ddots \; n_{N1} & \circ \; \ddots \; n_{N2} \\ \hline m_{00} & m_{11} \; \circ & m_{12} \; \circ \\ \vdots & \circ \; \ddots & \ddots \\ m_{00} & \circ \; \ddots \; m_{N1} & \circ \; \ddots \; m_{N2} \\ \hline 0 & 0 \quad 0\alpha & 0 \ldots 0 - \beta \end{array} \right\|; \quad \bar{\Theta} = \begin{Vmatrix} -b_1 \\ \vdots \\ -b_N \\ -c_1 \\ \vdots \\ -c_N \\ -w_n \dfrac{dw_n}{d\sigma}\theta' \end{Vmatrix};$$

$$m_{00} = \frac{r\rho}{c^2}(c^2 - v^2)\Big|_0; \quad n_{k1} = \frac{r\rho u}{c^2}(c^2 - v^2)\Big|_k;$$

$$m_{k1} = \frac{r\rho}{c^2}(c^2 - v^2)\Big|_0; \quad n_{k2} = \frac{r\rho v}{c^2}(c^2 - u^2)\Big|_k;$$

$$m_{k2} = -\frac{\rho u v r}{c^2}\Big|_k,$$

$c^2 = \dfrac{\rho h_T}{D\rho + 2\rho_T}$ is the square of the velocity of sound, $D = \rho_p h_T - \rho_T h_p$.

The complete approximating system of equations for numerical integration has the following form in scheme I:

/2

$$\left.\begin{array}{l} \bar{\varphi}' = \Phi^{-1}\bar{\Theta}; \quad \sigma' = \dfrac{v_N' + w_n\,\theta'\cos(\sigma-\theta)}{\alpha}; \\ \varepsilon' = \left(1 + \dfrac{\varepsilon}{R}\right)\tan(\sigma-\theta); \quad w_n' = \dfrac{dw_n}{d\sigma}\sigma'; \quad p_N' = \dfrac{dp_N}{d\sigma}\sigma'; \\ T_N' = \dfrac{dT_N}{d\sigma}\sigma'; \quad S_N' = \dfrac{dS_N}{d\sigma}\sigma'; \quad p_0' = -\rho_0 v_0 v_0'; \\ T_0' = \dfrac{1}{(h_T)_0}[(h_p)_0\rho_0 - 2]v_0 v_0'; \quad \psi_i' = \varepsilon'\dfrac{i}{N}(r\rho v)_i - \\ \qquad - \left(1 + \dfrac{i}{N}\dfrac{\varepsilon}{R}\right)(r\rho u)_i, \quad i = 1, 2, \ldots, N; \\ p_i' = -\dfrac{\rho_i}{2}[(w_i^2)' + T_i S_i']; \quad T_i' = -\dfrac{1}{(h_T)_i^2}[(w_i^2)' + \\ \qquad + (i_T)p_i'], \quad i = 1, 2, \ldots, N-1. \end{array}\right\} \qquad (1.9)$$

The prime everywhere denotes a derivative with respect to s;

$$h_p = \left(\frac{\partial h}{\partial p}\right)_T ; \quad h_T = \left(\frac{\partial h}{\partial T}\right)_p ; \quad \rho_p = \left(\frac{\partial \rho}{\partial p}\right)_T ; \quad \rho_T = \left(\frac{\partial \rho}{\partial T}\right)_p .$$

When s = 0 the values of $u_i(0)$, i = 1, 2, ..., N-1, and $\varepsilon(0)$ are unknown, i.e., of N quantities (u_N is found from relations on the shock wave). It is obvious from the form n_{kl}, m_{kl} and m_{00} that when $v_k = c_k$ the matrix Φ degenerates when k = 0, 1, ..., N-1 (when k = N there is no degeneration owing to α). The conditions of regularity of the solution at these N points permit a unique determination of N unknown parameters.

Thus, we have a system of ordinary differential equations (1.9) with initial data when s = 0

$$\varepsilon(0) = \varepsilon_0 ; \quad u_i(0) = u_i^0 ; \quad v_i(0) = 0; \quad u_0(0) = 0;$$
$$\psi_i(0) = 0; \quad \sigma(0) = \pi/2 ; \quad S_N(0) = 0; \quad w_n(0) = w_n^0 ;$$
$$p_i(0) = p_i^0 ; \quad T_i(0) = T_i^0, \quad i = 1, 2, \ldots, N.$$

Integration of system (1.9) is performed from the axis of symmetry to the upper limit (closing ray or boundary characteristic, see Fig. 5, a,b). In this case, we need satisfy the conditions of regularity at the singular points and the boundary conditions of the problem in a minimal region of influence.

We cannot use the conditions of constancy of entropy along the line of flow for nonequilibrium flows, and system (1.8) must be supplemented by a corresponding equation. In order not to introduce projections of the equations of motion onto the s-axis (the approximation of which proves to be less accurate than the approximation of other equations), we use the adiabatic flow condition along the lines of flow /21

$$\frac{dh}{dt} - \frac{2}{\rho}\frac{dp}{dt} = 0 \quad (t - \text{time}).$$

In this case, the equation of state is written as:

$$\rho = \rho(p, T, C_i),$$

and the expression for enthalpy h will have the form: $h = h(T, C_i)$ for the case of nonequilibrium dissociation and $h = h(T, C_i, T_{ij})$ for the case of vibrational-dissociation relaxation. Here T_{ij} is the vibrational temperature of the j-th vibrational degree of freedom of the i-th component.

Furthermore, to the initial system of gas dynamic equations, we must add relaxation equations describing the change of mass concentration of the components C_i and vibrational energies $e_{ij} = e_{ij}(T_{ij})$ and also the Dalton equation and

equations of material balance. If the gas mixture consists of q different components containing different types of atoms, the Dalton equation has the form

$$\sum_{i=1}^{q} C_i = 1, \tag{1.10}$$

and (a - 1) equations of material balance are written as:

$$\frac{\sum_{i=1}^{q} n_{im} \frac{C_i}{\mu_i}}{\sum_{i=1}^{q} n_{i1} \frac{C_i}{\mu_i}} = \beta_{m1} \quad \text{or} \quad \sum_{i=1}^{q} G_i^{(k)} C_i = \Delta^{(k)}, \quad k = 1, 2, \ldots, a-1, \tag{1.11}$$

where n_{im} is the number of atoms of type m (m = 1, 2, 3, ..., a) in component i (i = 1, 2, ..., q); β_{m1} = const; $\beta_{11} = 1$.

The form of the relaxation equations depends on the character of the kinetic processes in question.

For vibrational relaxation we have:

$$\frac{de_{ij}(T_{ij})}{dt} = \frac{e_{ij}(T) - e_{ij}(T_{ij})}{\tau_{ij}(p, T)}, \tag{1.12}$$

where e_{ij}, τ_{ij} are the specific internal energy and relaxation time, respectively, of the j-th vibrational degree of freedom of the i-th component. /22

For nonequilibrium dissociation in equilibrium vibrations we have

$$\frac{dC_i}{dt} = \frac{\omega_i(p, T, C_i)}{\rho}. \tag{1.13}$$

If we take into account simultaneous occurrence of vibrational dissociation relaxation, then equations (1.12) and (1.13) are written as:

$$\frac{de_{ij}(T_{ij})}{dt} = \frac{Q_{ij}(p, T, C_i, T_{ij})}{\rho}; \quad \frac{dC_i}{dt} = \frac{\omega_i(p, T, C_i, T_{ij})}{\rho}. \tag{1.14}$$

The form of the functions Q_{ij} and ω_i depends on the details of the kinetic processes and their interaction with each other. It is best not to approximate the relaxation equations and the adiabatic condition but to write them along the lines of flow and project them onto the line $\xi = k/N$, k = 1, 2, ..., N-1. Thus, for the case of vibrational-dissociation relaxation the approximating system with respect to scheme I will have the form:

$$
\left.
\begin{aligned}
&\vec{\varphi}' = \Phi^{-1}\vec{\omega};\quad \sigma' = \frac{v_N + w_n\theta'\cos(\sigma-\theta)}{\alpha_0};\quad \varepsilon' = A_1\tan(\sigma-\theta);\\
&w_n' = \frac{dw_n}{d\sigma}\sigma';\quad p_N' = \frac{dp_N}{d\sigma}\sigma';\quad T_N' = \frac{dT_N}{d\sigma}\sigma';\\
&p_k' = -\rho_k(u_k u_k' + v_k v_k') + \left[\frac{\partial p}{\partial n} + \frac{\rho}{2}\frac{\partial(w^2)}{\partial n}\right]_k \cdot \left(\xi\varepsilon' - A_k\frac{u_k}{v_k}\right);\\
&T_k' = -\frac{1}{(h_T)_k}\left\{\left[\sum_{i=1}^{q}(h_C)_i C_i'\right]_k + \left[\sum_{i=1}^{q}\sum_{j=1}^{r_i}(h_e)_{ij}e_{ij}\right]_k + \right.\\
&\qquad\qquad \left. + 2(v_k v_k' + u_k u_k')\right\};\\
&(C_i)_0' = \frac{1}{v_0}\left(\frac{dC_i}{dt}\right)_0;\quad (e_{ij})_0' = \frac{1}{v_0}\left(\frac{de_{ij}}{dt}\right)_0;\\
&(C_i)_k' = \frac{A_k}{v_k}\left(\frac{dC_i}{dt}\right)_k + \left(\frac{\partial C_i}{\partial n}\right)_k\left[\xi\varepsilon' - A_k\frac{u_k}{v_k}\right];\\
&(e_{ij})_k' = \frac{A_k}{v_k}\left(\frac{de_{ij}}{dt}\right)_k + \left(\frac{\partial e_{ij}}{\partial n}\right)_k\left[\xi\varepsilon' - A_k\frac{u_k}{v_k}\right],\\
&i = 1,2,\ldots,q;\quad j = 1,2,\ldots,r_{ij};\quad k = 1,2,\ldots,N-1,
\end{aligned}
\right\} \qquad (1.15)
$$

where r_i is the number of vibrational degrees of freedom of the i-th component and /23

$$
h_T = \left(\frac{\partial h}{\partial T}\right)_{C_i, e_{ij}};\quad h_{C_i} = \left(\frac{\partial h}{\partial C_i}\right)_{T,\, C_m \neq C_i, e_{ij}};
$$

$$
h_e = \left(\frac{\partial h}{\partial e_{ij}}\right)_{T,\, C_i,\, e_{mn} \neq e_{ij}}.
$$

The approximating system has singularities at the points where the tangential components of velocity v_k prove to be equal to the "frozen" velocities of sound

$$
c_k = \left(\frac{h_T T}{h_{T^{\mu}} - 2}\right)_k^{1/2},\quad k = 0,1,\ldots,N-1. \qquad (1.16)
$$

We note that in this case, both vibrations and dissociation are frozen.

2. Let us examine for the most general case, vibrational-dissociation relaxation, the approximating system in the second approximation (N = 2). Later, we will present the results of calculations with respect to scheme I for N = 2.

Let us designate all quantities on the body by the subscript "0", on the

intermediate line by the subscript "2", and on the shock wave by the subscript "1". Solving the first equation of system (1.15) relative to the unknown function, we obtain

$$v_0^* = \frac{E_0}{N_0}; \quad v_2' = \frac{E_2}{N_2}; \quad u_2' = \frac{1}{\bar{t}_2}(\bar{z}_2' - \bar{t}_2' u_2).$$

The form of the remaining equations of system (1.15) in this case does not change. The quantity E_σ entering the equation for $\sigma' = E_\sigma/\alpha_0$, when N = 2 is equal to

$$E_\sigma = \begin{cases} \dfrac{2(2A_2^2H_2 - A_1^2H_1 - A_2p_0)}{A_1\varepsilon} + \dfrac{p_1}{R} - \alpha_1 & \text{when } s = 0; \\ \dfrac{1}{u}(\bar{z}_1' - z_1 z_1' - \alpha_1 r_1) & \text{when } s > 0, \end{cases}$$

where

$$\bar{z}_1' = \frac{1}{3}(a_2 - 2a_1);$$

$$a_1 = \frac{\varepsilon'}{\varepsilon}(4\bar{z}_2 - 5\bar{z}_1) + \frac{6}{\varepsilon}(A_1\bar{H}_1 - H_0) - (\bar{Y}_0 + \bar{Y}_1 + 4\bar{Y}_2);$$

$$a_2 = -\frac{\varepsilon'}{\varepsilon}(\bar{z}_1 + 4\bar{z}_2) + \frac{24}{\varepsilon}(A_2\bar{H}_2 - \bar{H}_0) - (5\bar{Y}_0 - \bar{Y}_1 + 8\bar{Y}_2);$$

$$\alpha_1 = -\frac{\rho_1}{R}(u_1^2 - v_1^2); \quad \alpha_0 = \beta_0 u_1 + t_1 m_1;$$

/24

$$\beta_0 = M_1 m_1 - N_1 n_1 + L_1 \frac{dp_1}{d\sigma};$$

$$m_1 = \frac{dw_{t1}}{d\sigma}\sin(\sigma - \theta) - \frac{dw_{n1}}{d\sigma}\cos(\sigma - \theta) + v_1;$$

$$n_1 = u_1 - \frac{dw_{t1}}{d\sigma}\cos(\sigma - \theta) - \frac{dw_{n1}}{d\sigma}\sin(\sigma - \theta);$$

$$M_1 = \frac{2z}{(h_T)_1 T_1}; \quad N_1 = \rho_1\left(1 + \frac{2v_1^2}{(h_T)_1 T_1}\right); \quad L_1 = \frac{v_1}{T_1};$$

$$E_0 = \begin{cases} A_1 t_1' + \dfrac{2}{\varepsilon}(A_1^2 l_1 - 2A_2^2 l_2) & \text{when } s = 0; \\ \dfrac{1}{r_0}(\bar{t}_0' - t_0 r_0') - K_0(C_1)_0' - \Lambda_0 e_0' & \text{when } s > 0; \end{cases}$$

$$\bar{t}_0' = \frac{1}{3}(2b_1 - b_2); \quad b_1 = \frac{\varepsilon'}{\varepsilon}(\bar{t}_0 - 5\bar{t}_1 + 4\bar{t}_2) + \frac{6}{\varepsilon}A_1\bar{l}_1 + \bar{t}_1';$$

$$b_2 = \frac{\varepsilon'}{\varepsilon}(5\bar{t}_0 - \bar{t}_1 - 4\bar{t}_2) + \frac{24}{\varepsilon}A_2\bar{l}_2 - \bar{t}_1';$$

$$\bar{t}_1' = t_1' r_1 + t_1 r_1'; \quad t_1' = \beta_0\sigma' - \frac{e_1}{R};$$

$$K_k = t_k\left[\frac{(h_1^{(0)})_k - (h_2^{(0)})_k}{(h_T)_k T_k} - \frac{(\mu)_k}{\mu_2}\right];$$

$$\Lambda_k = \frac{t_k}{(h_T)_k T_k};\quad N_k = \rho_k\left(1-\frac{v_k^2}{c_k^2}\right);\quad c_k^2 = \frac{(h_T)_k T_k}{(h_T)_k(\mu)_k - 2},\quad k=0,2;$$

$$E_2 = \begin{cases} \frac{1}{2A_2}\left(\delta_0 + \frac{\delta_2}{R} - A_1 t_1\right) & \text{when } s = 0; \\ \frac{1}{r_2}(\bar{t}_2' - t_2 r_2') + \frac{z_2}{c_2^2}u_2' - L_2\left(\frac{\partial p}{\partial n} + \frac{\rho\partial w^2}{2\partial n}\right)_2\left(\frac{\varepsilon'}{2} - A_2\frac{u_2}{v_2}\right) - \\ - K_2(C_1)_2' - \Lambda_2 e_2', & \text{when } s > 0; \end{cases}$$

$$\delta_0 = \frac{1}{\varepsilon}\left(2A_2 l_2 - \frac{5}{2}A_1 l_1\right);\quad \delta_2 = A_2 l_2 - \frac{5}{2}A_1 l_1;$$

$$\bar{t}_2' = -\frac{1}{4}(b_1 + \bar{t}_0');\quad \bar{z}_2' = \frac{1}{8}(\bar{z}_1' - a_2);$$

$$r_1' = A_1 \sin\theta + \varepsilon' \cos\theta.$$

The derivatives dC/dt and de/dt are found from kinetic equations describing vibrational and dissociation relaxation. The quantities $dw_{n1}/d\sigma$, $dp_1/d\sigma$, $dT_1/d\sigma$ are determined by the corresponding differential equations for an oblique shock. Let us examine a diatomic gas on the assumption that immediately behind the shock the vibrations and dissociation are "frozen," then we must add $C = C(T_\infty)$, $e = e(T_\infty)$ to the boundary conditions of the problem on the shock wave. The specific enthalpy of the gas is determined here as: /25

$$h = C_1 h_1 + C_2 h_2;\quad h_T = \left(\frac{\partial h}{\partial T}\right)_{C,e};\quad h_i = h_i^{(0)} + e_i/C_i,\quad i = 1,2,$$

where C_1, C_2 and h_1, h_2 are the mass concentrations and specific enthalpies, respectively, of monatomic and diatomic components of the mixture; $h_i^{(0)}$ includes the internal energy of active degrees of freedom (translational, rotational), work of expansion, and energy of formation of the corresponding component D_i; e_i is the vibrational energy of the i-th component referred to as a unit mass of the mixture. If we take into account that the rotations of the molecules are fully excited, then for the monomatic component

$$h_1 = h_1^{(0)} = \frac{5}{\mu_1} T + D_1 \quad . \ (e_1 = 0),$$

and for the diatomic

$$h_2 = h_2^{(0)} + \frac{e_2}{C_2} = \frac{7}{\mu_2} T + \frac{e}{1 - C_1} \qquad (e_2 \equiv e).$$

To begin solving the approximating system we must assign, when s = 0, the values of the parameters ε_0 and $u_2(0)$ and approximate the velocity along the axis of symmetry in the form of the quadratic polynomial

$$u(0,n) = [4u_2(0) - u_1(0)] \frac{n}{\varepsilon_0} + 2[u_1(0) - 2u_2(0)] \left(\frac{n}{\varepsilon_0}\right)^2 .$$

Then, the wanting boundary conditions on the axis of symmetry are determined by integration, from the wave to the body, of the following system of equations:

$$\left.\begin{aligned} &\frac{dC_1}{dn} = \frac{1}{u} \frac{dC_1}{dt}; \quad \frac{de}{dn} = \frac{1}{u} \frac{de}{dt}; \quad \frac{dp}{dn} = -\rho u \frac{du}{dn}; \\ &\frac{dT}{dn} = -\frac{1}{(h_T)} \left[2u \frac{du}{dn} + (h_1^{(0)} - h_2^{(0)}) \frac{dC_1}{dn} + \frac{de}{dn} \right]. \end{aligned}\right\} \qquad (1.17)$$

/26

The unknown parameters ε_0 and $u_2(0)$ are found from the conditions of regularity of the solution at the singular points, $E_0 = 0$ when $v_0 = c_0$ and $E_2 = 0$ when $v_2 = c_2$.

We will now examine only nonequilibrium dissociation, taking into account that vibrations are excited in equilibrium. Equations for $(e)_k'$ (k = 0.2) will be absent in approximating system (1.15) and the expressions for T_0' and T_2' change:

$$T_0' = -\frac{1}{(h_T)_0} \{[(h_1)_0 - (h_2)_0](C_1)_0' + 2v_0 v_0'\};$$

$$T_2' = -\frac{1}{(h_T)_2} \{[(h_1)_2 - (h_2)_2](C_1)_2' + (w^2)_2'\},$$

wherein

$$h_T = \left(\frac{\partial h}{\partial T}\right)_{C_1} .$$

In the expressions for E_0 and E_2 when s > 0 we should also set $e_0' = 0$, $e_2' = 0$ and consider that

$$K_0 = t_0\left[\frac{(h_1)_0-(h_2)_0}{(h_T)_0T_0}-\frac{(\mu)_0}{\mu_2}\right];$$
$$K_2 = t_2\left[\frac{(h_1)_2-(h_2)_2}{(h_T)_2T_2}-\frac{(\mu)_2}{\mu_2}\right].$$

The parameters behind the shock wave and also their derivatives with respect to the angle of inclination of the shock wave $\sigma\left(\frac{dw_{n1}}{d\sigma}, \frac{dp_1}{d\sigma}, \frac{dT_1}{d\sigma}\right)$ will be determined on the assumption that immediately behind the shock only dissociation is "frozen" and the vibrations are in equilibrium.

The equation for de/dn will be absent in system (1.17) for determining the wanting boundary conditions on the axis of symmetry, and the expression for dT/dn will take the form

$$\frac{dT}{dn} = -\frac{1}{(h_T)}\left[2u\frac{du}{dn}+(h_1-h_0)\frac{dC_1}{dh}\right].$$

All other expressions remain unchanged. The "frozen" sonic velocities will be /27
determined as usual by formulas (1.16) where $h_T = \left(\frac{\partial h}{\partial T}\right)_{C_1}$, i.e., only dissociation is "frozen."

When calculating full equilibrium flows the enthalpy of the mixture h = h (p, T) and its molecular weight $\mu = \mu(p, T)$ are determined either from approximations or from solving a system of equations of chemical equilibrium. In this case the relaxation equations are absent in the approximating system (1.15) and

$$T_0' = -\frac{1}{(h_T)_0}\{(h_p)_0 p_0' + 2v_0 v_0'\};$$
$$T_2' = -\frac{1}{(h_T)_2}\{(h_p)_2' + (w^2)_2'\},$$

wherein $h_T = \left(\frac{\partial h}{\partial T}\right)_p$, $h_p = \left(\frac{\partial h}{\partial p}\right)_T$ are also found either from approximations or from equations of chemical equilibrium.

In the expressions for E_0 and E_2 when $s > 0$ we must set $e_k' = 0$ and $(C_1)_k' = 0$ (k = 0.2). The parameters behind the shock wave and their derivatives with respect to σ we will now find on the assumption of full equilibrium behind the shock. To determine the wanting boundary conditions on the axis of symmetry there is no need to set up the velocity profile in the form of a quadratic polynomial. As usual, only the two unknown parameters ε_0 and $u_2(0)$ are assigned,

and the quantities $p_2(0)$, $T_2(0)$, $p_0(0)$, $T_0(0)$ are determined by integration, along s = 0 from the wave to the body, of the equation

$$\frac{dT}{dp} = \frac{2 - \rho h_p}{2 h_T}.$$

The approximating system as usual has two singular points when $v_0 = c_0$ and $v_2 = c_2$, where c_0 and c_2 are "equilibrium" sonic velocities

$$c_0 = \left[\frac{\rho_0 (h_T)_0}{D_0 \rho_0 + 2(\rho_T)_0}\right]^{1/2}; \quad c_2 = \left[\frac{\rho_2 (h_T)_2}{D_2 \rho_2 + 2(\rho_T)_2}\right]^{1/2};$$

$$D = \rho_p h_T - \rho_T h_p; \quad \rho_p = \left(\frac{\partial \rho}{\partial p}\right)_T; \quad \rho_T = \left(\frac{\partial \rho}{\partial T}\right)_p.$$

The flow of an ideal gas with a constant heat capacity is a particular case of an equilibrium flow. When determining the thermodynamic quantities it is sufficient to set /28

$$h_T = C_p = \text{const}; \quad h_p = 0; \quad \rho_p = 1/T; \quad \rho_T = -\rho/T.$$

3. Thus, in scheme I in the second approximation for different cases of flow, we obtain a boundary-value problem for a system of ordinary differential equations wherein two unknown parameters on the axis of symmetry (ε_0 and $u_2(0)$) should be determined from the conditions of regularity of the solution at singular points

$$E_0 = 0 \text{ when } N_0 = 0 \quad \text{and} \quad E_2 = 0 \text{ when } N_2 = 0. \tag{1.18}$$

Usually such a problem is solved by multiple iteration of the solution of the Cauchy problem. Calculations show that to satisfy conditions (1.18) and a smooth extension of the solution beyond the singular points, a vastly higher accuracy of determining the parameters ε_0 and $u_2(0)$ than the accuracy of solving the problem itself (accuracy of the approximation of the initial system, accuracy of numerical integration) is needed. However, such a high accuracy is necessary not over the entire interval of change of the independent variable s but only in a rather narrow neighborhood of the singular points themselves. Therefore, when solving the boundary-value problem according to scheme I, it is best to set out in the following manner. As soon as the parameters become so refined that in a certain range $0 \leq s \leq s_k$ the "fork" values of these parameters ($\varepsilon_0^{(1)}$, $u_2^{(1)}$ and $\varepsilon_0^{(2)}$, $u_2^{(2)}$) give a solution with the required accuracy $\left(\frac{f_i^{(1)} - f_i^{(2)}}{f_i^{(1)}} \leq \delta\right)$, we can begin solving the Cauchy problem not from s = 0 but from $s = s_k$, linearly interpolating the boundary conditions for $s = s_k$ between $f_i^{(1)}$ and $f_i^{(2)}$. Here the value of s_k

can be successively increased and, consequently, we can continue to integrate the approximating system in an ever narrower interval. This method is rather easily automated and yields a great gain in time, and in calculations of severely blunt bodies ($\delta \gg 1$) is simply necessary since the required accuracy of the parameters chosen when $s = 0$ can prove to be limited in a number of cases of the computer matrix.

Calculations also show that to retain a continuous dependence of the solution upon the parameters, integration in the region of singular points must be performed with control of accuracy and automatic step selection. However, as /29
a criterion for "fork" values of the parameters it is not expedient to use the conditions $E_i < 0$ or $N_i < 0$ since in this case the step will be severely diminished. In place of them it is necessary to examine the conditions $E_i < \delta$ or $N_i < \delta$, where δ is a certain small number selected in conformity with a prescribed accuracy of integration. If both conditions $E_i < \delta$ and $N_i < \delta$ are simultaneously fulfilled as the parameters are refined, then as the criterion it is convenient to use the signs of the second derivatives of velocities v_0'' and v_2'' which can be found numerically.

To extend the solution beyond singular points the method of "complexes" has proved to be sufficiently effective [20]. In this case, the approximating system is written so that in place of equations for the tangential components of velocities, pressures, and temperatures along the body and intermediate lines (these equations have singularities), we introduce equations relative to the "complexes" of these quantities standing under the sign of partial derivatives with a divergent writing of the initial equations. The approximating system in "complexes" does not have singularities in the entire shock layer, For example, in place of six equations for v_0', P_0', T_0', v_2', p_2', T_2' of system (1.15) describing vibrational-dissociation relaxation according to scheme I in the second approximation, we can introduce the equivalent equations with derivatives of the "complexes"

$$t_0' = \bar{E}_0; \quad g_0' = \bar{E}_0 v_0; \quad q_0' = 0; \quad t_2' = \bar{E}_2; \quad g_2' = \bar{E}_2 v_2 + \bar{P}_2; \quad q_2' = 0,$$

where

$$q_0 = (h)_0 + v_0^2; \qquad q_2 = (h)_2 + v_2^2 + u_2^2;$$

$$\bar{E} = \frac{1}{r_0}(\bar{t}_0' - r_0' t_0); \qquad \bar{E}_2 = \frac{1}{r_2}(\bar{t}_2' - r_2' t_2);$$

$$\bar{P}_2 = -\rho_2 u_2 u_2' + \left(\frac{\partial p}{\partial n} + \frac{\rho}{2}\frac{\partial (w^2)}{\partial n}\right)_2 \left(\frac{\varepsilon'}{2} - A_2 \frac{u_2}{v_2}\right).$$

These equations together with the remaining equations of system (1.15) can be integrated with any predetermined accuracy in the entire shock layer, including points where $v_i = c_i$ $(i = 0.2)$. Here, however, since the right sides of the equations depend not only on the "complexes" but also on the gas dynamic quantities themselves, at each step of integration we must solve the following algebraic systems. /30

$$\left.\begin{array}{ll} \rho_0 v_0 = t_0; & \rho_2 v_2 = t_2; \\ p_0 + \rho_0 v_0^2 = g_0; & p_2 + \rho_2 v_2^2 = g_2; \\ (h)_0 + v^2 = 1; & (h)_2 + v_2^2 = 1 - u_2^2; \\ p_0/\rho_0 = T_0/(\mu)_0; & p_2/\rho_2 = T_2/(\mu)_2. \end{array}\right\} \qquad (1.19)$$

Here, the known quantities are t_0, g_0, t_2, g_2, u_2, $(C_1)_0$, e_0, $(C_1)_2 e_2$, since they are found from solving differential equations and the values ρ_i, v_i, p_i, T_i ($i = 0.2$) are unknown. Each of the systems (1.19) has two solutions. Investigations have shown that up to the point where $v_i = c_i$ ($i = 0.2$) we must take one solution, and beyond this point, we must take the other (at the singular point itself both solutions coincide). Thus, the singularity occurring in the problem and related with transition through sonic velocity does not disappear, and only the character of its manifestation changes. The solution of systems (1.19) for the case of a completely nonequilibrium flow and the flow of an ideal gas with a constant specific heat can be obtained in an analytical form. In the case of flow with nonequilibrium dissociation (equilibrium vibrations) each of the systems reduces to one transcendental equation and in the fully equilibrium case, to two (these equations are solved by iteration). To avoid excessive use of machine time to solve systems (1.19) we can change over to integration of the approximating system in "complexes" only upon approaching the singular points, and in the remaining region use the usual form of the approximating system.

4. We note that scheme I examined above gives more accurate information on the shock wave and on the body which is quite important for practice and for comparison with experiments. This scheme is suitable for calculating flows at high Mach values of the oncoming flow when the shock layer is comparatively thin and the law of distribution of the parameters across the layer has a sufficiently smooth character. The scheme is conveniently used when calculating flow around severely blunt bodies [10, 12, 13], as well as bodies with a discontinuity of the configuration [11, 15, 18] or discontinuity of the curvature of the generatrix [19].

3. Scheme II.

1. The initial system of equations is written in coordinates s, ξ ($\xi = n/\varepsilon(s)$); the range of integration is divided by lines $\eta = s/s_i(\xi) = \text{const}$ passing between the axis of symmetry $s = 0$ and the boundary characteristic $s = s_1(\xi)$ (Fig. 1.6); the functions are approximated along the shock layer by polynomials in terms of s with consideration of symmetry when $s = 0$ [2, 7, 8, 21-25]. /31

Let us construct the algorithm of the calculation in this scheme for cases of axisymmetric gas flows incorporating a fully equilibrium state, equilibrium state with radiation (volume luminenscence), or a nonequilibrium state.

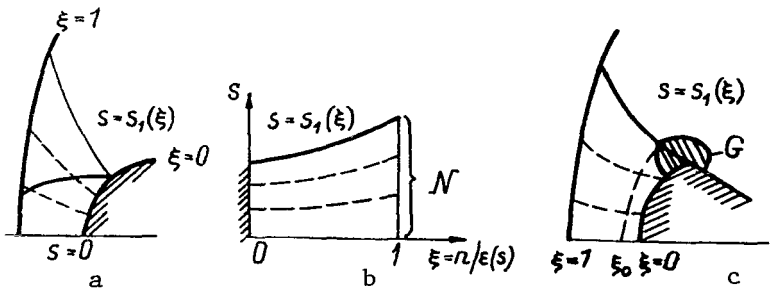

Figure 1.6. Scheme II.

The complete system of equations for all these cases contains the equations of motion and continuity

$$\left.\begin{aligned} &\frac{\partial}{\partial s}(\bar{z}\varepsilon)+\frac{\partial}{\partial \xi}\bar{M}=\bar{Y}\varepsilon;\quad \frac{\partial}{\partial s}(\bar{g}\varepsilon)+\frac{\partial}{\partial \xi}\bar{L}=\bar{X}\varepsilon;\\ &\frac{\partial}{\partial s}(\bar{t}\varepsilon)+\frac{\partial}{\partial \xi}\bar{N}=0, \end{aligned}\right\} \tag{1.20}$$

where

$$\begin{aligned} \bar{M} &= M\cos\theta; \quad M=(AH-\xi\varepsilon_s' z)P;\\ \bar{N} &= N\cos\theta; \quad N=(Al-\xi\varepsilon_s' t)P;\\ \bar{L} &= L\cos\theta; \quad L=(Az-\xi\varepsilon_s' g)P;\\ \bar{Y}\varepsilon &= Y\cos\theta; \quad Y=\left(g\frac{P}{R}-Ap\right)\varepsilon;\\ \bar{X} &= -\bar{z}/R+Ap\sin\theta;\\ r &= r_0+\xi\varepsilon\cos\theta=P\cos\theta; \quad P=r_0/\cos\theta+\xi\varepsilon, \end{aligned}$$

and also the Dalton equation (1.10), equation of material balance (1.11), and the equation of state /32

$$\rho=\frac{p}{T\sum\limits_{i=1}^{q}\frac{C_i}{\mu_i}}. \tag{1.21}$$

Furthermore, in the case of a complete equilibrium state, this system includes the equation of energy

$$h+w^2=1, \tag{1.22}$$

the equation of the law of mass action

$$\Phi(C_i) = K_p(T), \tag{1.23}$$

where K_p is the equilibrium constant, and the expression for enthalpy of the gas

$$h = \sum_{i=1}^{q} C_i h_i(T). \tag{1.24}$$

In the case of a thermodynamically equilibrium radiating gas (without absorption) we use the equation of energy in the form

$$\frac{dh}{dt} - \frac{2}{\rho}\frac{dp}{dt} + \frac{2\bar{E}}{\rho} = 0,$$

and also equations (1.23) and (1.24). Here $\bar{E}$ is the quantity of radiant energy emitted by a unit volume in unit time referred to $\rho_\infty w_{max}^2 / R_0$.

With consideration of dissociation relaxation and the absence of radiation of the gas, we use equations (1.22), (1.24), and relaxation equations (1.13).

In the case of vibrational-dissociation relaxation we use equations (1.22), the expression of enthalpy

$$h = \sum_{i=1}^{q} C_i h_i(T, T_{ij})$$

and relaxation equations (1.14).

The boundary conditions of the problem contain, additionally, the continuation $C_i = C_i(T_\infty)$ on the shock wave ($\xi = 1$) and the relation along the boundary characteristic ($s = s_1(\xi)$) for a sphere:

$$\frac{v}{w^2}\frac{du}{d\xi} - \frac{u}{w^2}\frac{dv}{d\xi} - \frac{1}{R}\frac{ds_1}{d\xi} \pm \frac{\operatorname{ctn}\alpha}{\rho w^2}\frac{dp}{d\xi} \pm \Gamma_1 = 0, \tag{1.25}$$

where /33

$$\Gamma_1 = \Gamma_0\left[(A \operatorname{tg}^{*}\theta + \xi\varepsilon_s')\frac{ds_1}{d\xi} + \varepsilon\right]\cos\theta;$$

$$\Gamma_0 = \frac{\sin\alpha}{\sin(\bar{\beta}\pm\alpha)}\left(\frac{1}{r}\sin\bar{\beta} + \Gamma_2\right); \quad \bar{\beta} = \beta + \theta;$$

$$\beta = \arctan\frac{u}{v}; \quad \alpha = \arcsin\frac{c}{w}; \quad c^2 = \frac{\rho h_T}{D\rho + 2\rho_T}; \quad D = \rho_p h_T - \rho_T h_p$$

*tg = tan

(the superscript pertains to the characteristics of the I family). In the case of a full equilibrium state

$$\Gamma_2 = 0;\ h_T = \left(\frac{\partial h}{\partial T}\right)_p;\ h_p = \left(\frac{\partial h}{\partial p}\right)_T;\ \rho_T = \left(\frac{\partial \rho}{\partial T}\right)_p;\ \rho_p = \left(\frac{\partial \rho}{\partial p}\right)_T,$$

whereby in the case of the equilibrium state of the radiating gas

$$\Gamma_2 = \frac{2E}{\rho w c^2 (\rho h_p - 2)},$$

and the remaining relations (1.26) do not change.

With dissociation relaxation

$$\Gamma_2 = \frac{1}{w} \sum_i \left(\frac{h_{C_i}}{T h_T} + \frac{\rho_{C_i}}{\rho}\right) \frac{dC_i}{dt} \frac{R_0}{w_{\max}};\quad h_T = \left(\frac{\partial h}{\partial T}\right)_{p, C_i};$$
$$h_p = 0,\ h_{C_i} = \left(\frac{\partial h}{\partial C_i}\right)_{p,\ T,\ C_j \neq C_i};\quad \rho_T = \left(\frac{\partial \rho}{\partial T}\right)_{p,\ C_i},$$
$$\rho_p = \left(\frac{\partial \rho}{\partial p}\right)_{T,\ C_i};\quad \rho_{C_i} = \left(\frac{\partial \rho}{\partial C_i}\right)_{p,\ T,\ C_j \neq C_i},$$

and in the case of vibrational-dissociation relaxation

$$\Gamma_2 = \frac{1}{w}\left[\sum_i \left(\frac{h_{C_i}}{T h_T} + \frac{\rho_{C_i}}{\rho}\right)\frac{dC_i}{dt} + \sum_{i,j}\left(\frac{h_{T_{ij}}}{T h_T} + \frac{\rho_{T_{ij}}}{\rho}\right)\frac{dC_{ij}}{dt}\right]\frac{R_0}{w_{\max}};$$
$$e_{ij} = e_{ij}(T_{ij});\quad h_T = \left(\frac{\partial h}{\partial T}\right)_{p,\ C_i,\ T_{ij}};\quad h_p = 0;\ h_{C_i} = \left(\frac{\partial h}{\partial C_i}\right)_{p,\ T,\ T_{ij},\ C_k \neq C_i};$$
$$\rho_T = \left(\frac{\partial p}{\partial T}\right)_{p,\ C_i,\ T_{ij}};\quad \rho_p = \left(\frac{\partial \rho}{\partial p}\right)_{T,\ C_i,\ T_{ij}};\quad \rho_{C_i} = \left(\frac{\partial \rho}{\partial C_i}\right)_{p,\ T,\ T_{ij},\ C_k \neq C_i}.$$

The equations of the lines of flow and the characteristic are written as:

$$\frac{ds_{f.l}}{d\xi} = \frac{\varepsilon v}{Au - \xi \varepsilon_s' v};\quad \frac{ds_1}{d\xi} = \frac{\varepsilon}{A \tan(\beta \pm \alpha) - \xi \varepsilon_s'}.$$

Partial differential equations (1.20) enter the complete system of equations. They are approximated across the shock layer. /34

Let us introduce $\eta = s/s_1(\xi)$, where $s = s_1(\xi)$ is the equation of the boundary characteristic.

The approximation directions here are the set of lines $\eta = k/N$, $k = 0, 1, \ldots, N$; and the functions are represented in the following manner:

$$\cos\theta(s) = \sum_{i=1}^{N} {}^{i}ns^{2i-1};$$

$$f(\xi, s) = \sum_{i=0}^{N} {}^{i}f(\xi)\eta^{2i} \quad \text{for even functions;}$$

$$L(\xi, s) = \sum_{i=1}^{N} {}^{i}L(\xi)\eta^{2i-1} \quad \text{for odd functions.}$$

The partial differential equations with the introduced approximations are integrated with respect to s from the zero line to each of the N remaining lines. For example,

$$\int_0^{\frac{k}{N}s_1(\xi)} \frac{\partial}{\partial\xi}\bar{M}ds + \int_0^{\frac{k}{N}s_1(\xi)} \frac{\partial}{\partial s}(\bar{z}\varepsilon)ds - \int_0^{\frac{k}{N}s_1(\xi)} (\bar{Y}\varepsilon)ds = 0;$$

$$\frac{d}{d\xi}\left\{s_1(\xi)\int_0^{\frac{k}{N}}\sum_{\substack{i=0\\j=1}}^{N} {}^{i}M^{j}ns_1^{2j-1}\eta^{2(i+j)-1}d\eta\right\} - \frac{k}{N}s_1'(M\cos\theta)_k +$$

$$+(\bar{z}\varepsilon)_k - \sum_{\substack{i=0\\j=1}}^{N} \frac{1}{2(i+j)}\left(\frac{k}{N}\right)^{2(i+j)} {}^{i}n^{i}Ys_1^{2j} = 0;$$

$$\sum_{\substack{i=0\\j=1}}^{N} {}^{i}M'^{j}n\left(\frac{k}{N}\right)^{2(i+j)} \frac{1}{2(i+j)}s_1^{2j} + s_1'\sum_{\substack{i=0\\j=0}}^{N} {}^{i}M^{j}n\left(\frac{k}{N}\right)^{2(i+j)} \frac{j}{i+j}s_1^{2j-1} -$$

$$-\frac{k}{N}s_1'(M\cos\theta)_k + (\bar{z}\varepsilon)_k - \sum_{\substack{i=0\\j=1}}^{N}\left(\frac{k}{N}\right)^{2(i+j)} \frac{1}{2(i+j)} {}^{j}n^{i}Ys_1^{2j} = 0, \quad k = 1,2,\ldots,N.$$

The remaining partial differential equations are analogously transformed. /3

It is convenient to write the system of ordinary differential equations obtained after integration of the three partial differential equations as:

$$G^*\bar{M}' + H^*\bar{M} - G^*\bar{Y} + \bar{q} = 0; \quad G^*\bar{N}' + H^*\bar{N} + \bar{k} = 0; \quad R^*\bar{L}' + S^*\bar{L} - T^*(\overline{\bar{X}\varepsilon}) + \bar{V} = 0.$$

Here and henceforth the prime denotes a derivative with respect to ξ.

$$G = \|g_{ki}\|, \quad g_{ki} = \sum_{j=1}^{N} \left(\frac{k}{N}\right)^{2(i+j)} \frac{1}{2(i+j)} {}^{j}ns_1^{2j}, \quad i = 0, 1, \ldots, N;$$

$$H = \|h_{ki}\|, \quad h_{ki} = \sum_{j=1}^{N} \left(\frac{k}{N}\right)^{2(i+j)} \frac{j}{2(i+j)} {}^{j}ns_1^{2j-1}s_1', \quad i = 0, 1, \ldots, N;$$

$$R = \|r_{ki}\|, \quad r_{ki} = \sum_{j=1}^{N} \left(\frac{k}{N}\right)^{2(i+j)-1} \frac{1}{2(i+j)-1} {}^{j}ns_1^{2j}, \quad i = 1, 2, \ldots, N;$$

$$S = \|s_{ki}\|, \quad s_{ki} = \sum_{j=1}^{N} \left(\frac{k}{N}\right)^{2(i+j)-1} \frac{2j}{2(i+j)-1} {}^{j}ns_1^{2j-1}s_1', \quad i = 1, \ldots, N;$$

$$T = \|t_{ki}\|, \quad t_{ki} = s_1 \frac{1}{i+1}\left(\frac{k}{N}\right)^{i+1}, \quad i = 0, 1, \ldots, N, \quad k = 1, \ldots, N.$$

For the even functions ${}^{*}\bar{f} = \|{}^{i}f\|$, $i = 0, 1, \ldots, N$; for the odd functions ${}^{*}\bar{L} = \|{}^{i}L\|$, $i = 1, \ldots, N$,

$$\bar{q} = \|q_k\|, \quad q_k = \left[(zP\varepsilon)_k - \frac{k}{N} s_1' M_k\right] \cos\theta_k;$$

$$\bar{k} = \|k_k\|, \quad k_k = \left[(tP\varepsilon)_k - \frac{k}{N} s_1' N_k\right] \cos\theta_k;$$

$$\bar{V} = \|V_k\|, \quad V_k = \left[(gP\varepsilon)_k - \frac{k}{N} s_1' L_k\right] \cos\theta_k.$$

Between the coefficients in approximations ${}^{i}f$ and the values of the functions at the boundaries of zones f_i there is a relation, respectively, for the even and odd functions

$$\bar{f}_* = \mathfrak{M}\,\bar{f}, \quad \bar{f}_* = \|f_i\|, \quad \mathfrak{M} = \|m_{ij}\|, \quad m_{ij} = \left(\frac{i}{N}\right)^{2j}, \quad i, j = 0, \ldots, N;$$

$$\bar{L}_* = W\,{}^{*}\bar{L}, \quad \bar{L}_* = \|L_i\|, \quad W = \|w_{ij}\|, \quad w_{ij} = \left(\frac{i}{N}\right)^{2j-1}, \quad i, j = 1, \ldots, N.$$

Into the obtained system of equations we substitute the quantities /36

$${}^{*}\bar{f} = \mathfrak{M}^{-1}\bar{f}_*; \quad {}^{*}\bar{L} = W^{-1}\bar{L}_*,$$

then we will have

$$AM_*' + Q = 0; \quad A\bar{N}_*' + V = 0; \quad C\bar{L}_*' + U = 0.$$

Here

$$Q = B\bar{M}_* - A\bar{Y}_* + \bar{q}; \quad A = G\mathfrak{M}^{-1}; \; D = sW^{-1};$$
$$V = B\bar{N}_* + \bar{k}; \qquad B = H\mathfrak{M}^{-1}; \; E = T\mathfrak{M}^{-1};$$
$$U = D\bar{L}_* - E(\overline{\bar{X}\varepsilon})_* - \bar{v}; \quad C = RW^{-1}.$$

We will now express the derivatives M_i', N_i', L_i' in terms of the derivatives of the unknown functions u_i, v_i, p_i, ρ_i, having eliminated some of them by means of the equation of state, the Bernoulli integral, and conditions on the zero line of flow and on the characteristic. Then we obtain

$$A_u\bar{u}' + A_v\bar{v}' + A_p\bar{p}' + A_0 = 0; \quad B_u\bar{u}' +$$
$$+ B_v\bar{v}' + B_p\bar{p}' + B_0 = 0, \; C_u\bar{u}' + C_v\bar{v}' + C_p\bar{p} + C_0 = 0.$$

Here $\bar{u}' = \|u_i'\|$, $i = 0, 1, \ldots, N$; $\bar{v}' = \|v_i'\|$, $i = 1, \ldots, N$; $\bar{p}' = \|p_i'\|$, $i = 0, 1, \ldots, N$; A_u, B_u, C_u are matrices of dimension N x (N + 1); A_v, B_v, C_v are matrices of dimension N x N; A_p, B_p, C_p are matrices of dimension N x (N - 1); A_0, B_0, C_0 are columns of dimension N.

In a more compact form the system appears as:

$$\Phi\bar{\varphi}' = \bar{\Theta},$$

where the matrix Φ in the integration range does not have degeneration. The obtained system of 3N ordinary differential equations can be solved for all $0 < \xi \leq 1$.

The complete approximating system of equations for numerical integration in scheme II has the form (for a q-component gas mixture containing different types of atoms):

$$\left.\begin{aligned} &\bar{\varphi}' = \Phi^{-1}\bar{\Theta}; \; p_0' = \delta_{01}u_0'; \; p_N' = \delta_{N1}u_N' + \delta_{N2}v_N' + \delta_{N3}; \\ &T_j' = -\frac{1}{h_{T_j}}[(h_{p_j})p_j' + H_j]; \quad \rho_j = \frac{p_j}{T_j \sum_{i=1}^{q} \frac{C_i}{\mu_i}}; \end{aligned}\right\} \qquad (1.26)$$

$$\sum_{i=1}^{q} G_{ij}^{(k)} C_{ij} = \Delta_j^{(k)}, \; k = 1,2,\ldots,a-1; \quad \sum_{i=1}^{q} C_{ij} = 1, \; j = 0,1,2,\ldots,N,$$

/37

whereby in the case of a full equilibrium state of the gas $H_j = (w_j^2)'$ and equations of the law of mass action (1.23) are added.

For an equilibrium state of the radiating gas

$$H_j = -\frac{2}{\rho_j} p_j' + \frac{2A_j}{\rho_j} \bar{E}_j \frac{s_j' - s_{f.1}'}{v_j} - \left[h_{T_j} \frac{\partial T_j}{\partial s} + \left(h_{p_j} - \frac{2}{\rho_j} \right) \frac{\partial p_j}{\partial s} \right] (s_j' - s_{f.1}'),$$

and, furthermore, equations (1.23) are added.

In the presence of only dissociation relaxation

$$H_j = (w_j^2)' + \sum_{i=1}^{q} h_{C_{ij}} C_{ij}'$$

and relaxation equations of the form

$$C_{ij}' = (C_{ij}')_{f.1} - (s_{f.1}' - s_j') \left(\frac{\partial C_i}{\partial s} \right)_j ;$$

$$(C_{ij}')_{f.1} = \frac{\omega_i}{\rho} \frac{R_0}{w_{max}} \frac{1}{u_j} (\varepsilon_j + \xi \varepsilon_j' s_{f.1}')$$

are used.

In the case of vibrational-dissociation relaxation

$$H_j^{(k)} = (w_j^2)' + \sum_{i=1}^{q} h(T_{ik}) C_{ij} C_{ij}'$$

and the following relaxation equations are added:

$$C_{ij}' = (C_{ij}')_{f.1} - (s_{f.1}' - s_j') \left(\frac{\partial C_i}{\partial s} \right)_j ;$$

$$(C_{ij}')_{f.1} = \frac{\omega_i(p, T, C_i, T_{ik})}{\rho} \frac{R_0}{w_{max}} \frac{1}{u_j} (\varepsilon_j + \xi \varepsilon_j' s_{f.1}') ;$$

$$e_{ik}'(T_{ik}) = (e_{ik}')_{f.1} - (s_{f.1}' - s_j') \left(\frac{\partial e_{ik}}{\partial s} \right)_j ;$$

$$(e_{ik}')_{f.1} = \frac{Q_{ik}(p, T, C_i, T_{ik})}{\rho} \frac{R_0}{w_{max}} \frac{1}{u_j} (\varepsilon + \xi \varepsilon_j' s_{f.1}')$$

$k = 1, 2, \ldots, r_i$, where r_i is the number of vibrational degrees of freedom of the i-th component.

2. Having assigned the position of the shock wave, determinable by parameters $\varepsilon_0, \varepsilon_1, \ldots, \varepsilon_N$, we find from the conditions on the wave, by means of the iterative method, the values of all unknown functions when $\xi = 1$. When solving system of equations (1.26) from the wave to the body, using the conditions u_i $(\xi = 0) = 0$, $i = 0, 1, \ldots, N$ ($N + 1$ is the condition of "nonflow" on the body), we find by means of the generalized Newton method [26] the quantities $\varepsilon_0, \varepsilon_1, \ldots, \varepsilon_N$, satisfying the problem. In this case, the corrections

/38

$\delta\varepsilon_j$ for the quantities ε_j are determined from the system of equations

$$\sum_{j=0}^{N} \frac{\partial u_i}{\partial \varepsilon_j} \delta\varepsilon_j = -u_i(\varepsilon_0, \ldots, \varepsilon_N), \quad i = 0, 1, \ldots, N,$$

wherein the derivatives $\partial u_i/\partial \varepsilon_j$ are replaced by means of the formulas

$$\frac{\partial u_i}{\partial \varepsilon_j} \approx \frac{u_i(\varepsilon_0, \ldots, \varepsilon_j + \Delta_1, \ldots, \varepsilon_N) - u_i(\varepsilon_0, \ldots, \varepsilon_j, \ldots, \varepsilon_N)}{\Delta}.$$

3. G. F. Telenin [27] proposed a numerical scheme of the straight-line method for calculating bodies of analytic form which was close to scheme II of the method of integral relations. In it he used rectilinear separation of the integration range wherein this range was limited above by an arbitrary ray (and not by a boundary characteristic) intersecting the sonic line. Calculations here are carried out by an "analytic" scheme, the calculations of each specific case being carried out until the boundary ray enters the transonic region and the data on it stop noticeably affecting the obtained numerical solution. The use here of a rectilinear separation network permits, generally speaking, a slight simplification of the form of the approximating operator.

Scheme II of the method of integral relations permits constructing a numerical solution of the problem in physical coordinates with an accurate examination of the region of influence of blunting and closure of the approximating system. Here, in conformity with the form of the boundary characteristic, is used a curvilinear calculated network for the given problem which is automatically set up during the calculations. We see from the construction of the algorithm of scheme II that the approximating system is written out with sufficient simplicity for an arbitrary number of the approximation and any complete base system of functions. The computer algorithm is completely automated and permits performing a stable calculation even at large values /39
of the number of the approximation (here all boundary conditions of the problem for any N are exactly satisfied). The data of the calculations obtained by this scheme are convenient for analysis and further use (for example, extension of the calculation by the method of characteristics).

Scheme II is suitable when the approximating functions change more weakly with respect to s than with respect to n. This takes place, for example, for bodies with a slowly changing curvature at small Mach numbers of the oncoming flow or in nonequilibrium flows when the distribution of the flow parameters across the shock layer is not smooth. In these cases, scheme II gives a good accuracy even at small values of the number of the approximation [21-23]. The developed algorithm also permits calculating flow around bodies with a discontinuity [24]. In this case, the asymptotic solution of R. Vaglio-Laurin [6] is used in the vicinity of the sonic discontinuity (region G, Figure 1.6,c).

For scheme II it is expedient to program the approximating system directly

in the n-th approximation. After assigning a specific accuracy of determination, the machine itself selects the necessary number of the approximation. Realization of the algorithm of scheme II on electronic computers requires, as a rule, less machine time than in scheme I.

4. Scheme III

Schemes I and II use an approximate representation of initial equations in one direction on a movable curvilinear calculated network with continuous approximations. For the problems under consideration, such a representation is convenient since it permits obtaining a satisfactory accuracy at a comparatively small number of the approximation. However, for approximating systems of ordinary differential equations we must solve the boundary-value problem of a rather high order, which is usually done by means of multiple solution of the Cauchy problem. In a number of cases this causes certain difficulties related, for example, with the passage of the singular points in omission scheme II. Therefore it is sometimes convenient to use finite-difference representations on the selected calculated network in both directions (scheme III) [2, 8, 9]. Here, when representing the functions with respect to the second direction, integration of the system need not be done. /40

The algebraic transcendental equations obtained as a result of approximation, which are solved numerically by the iterative method, give values of the unknown parameters at the nodes of the network. Such an approach was used in 1952 by P. I. Chushkin when examining the problem of supersonic flow past a wedge with a detached shock wave.

We note that if we use a linear and not a continuous approximation, we will have an ordinary finite-difference scheme.

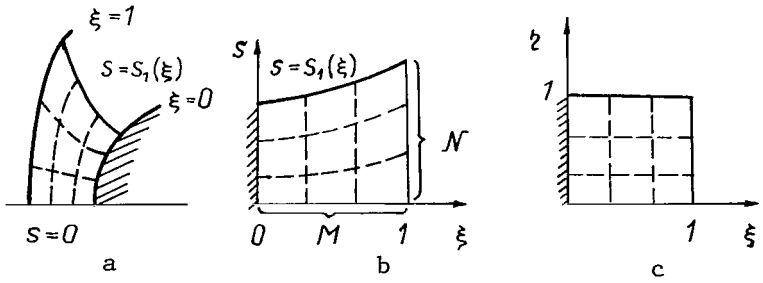

Figure 1.7. Scheme III.

1. Let us construct the approximating system for scheme III, using at first approximations along the shock layer (scheme II) and then across it (Figure 1.7). In scheme II we have a system of 3N ordinary differential equa-

tions of the type

$$\Phi \bar{\varphi}' = \bar{\Theta},$$

whereby in the integration range $|\Phi| > 0$. This system of equations is written along the lines $\eta = k/N = \text{const}$ in the region D ($0 \le \eta \le 1$, $0 \le \xi \le 1$), where $\eta = s/s_1(\xi)$, $\xi = n/\varepsilon(s)$; the value $\xi = 0$ corresponds to the surface of the body, $\xi = 1$ to the shock wave, $\eta = 0$ to the axis of symmetry, and $\eta = 1$ to the boundary characteristic (see Figure 1.7,c).

We will denote $1 - \xi = \zeta$ and introduce the following approximations:

$$\varphi_i - \varphi_{i0} = \sum_{j=1}^{M} {}^{j}\varphi_i \zeta^j; \quad \varphi_{i0} = \varphi_i(\zeta = 0), \quad i = 1, 2, \ldots, 3N,$$

having thus separated the integration range with respect to ξ between the wave and the body into M zones (see Figure 1.7,b). /41

If we designate $\varphi_{ij} = \varphi_i(\zeta = j/M)$, $j = 0, 1, \ldots, M$, then $\bar{\varphi}_{i*} - \bar{\varphi}_{i0} = \bar{M}^* \bar{\varphi}_i$,

where $\bar{\varphi}_{i*}, \bar{\varphi}_{i0}$ are columns of order M with the j-th element $\varphi_{ij}, \varphi_{i0}$, respectively; ${}^*\bar{\varphi}_i$ is a column of coefficients in the approximation; $\bar{M} = \|m_{ij}\|$ is a square matrix of rank M, $m_{ij} = \left(\frac{i}{M}\right)^j$.

Hence, we obtain

$${}^*\bar{\varphi}_i = \bar{M}^{-1}(\bar{\varphi}_{i*} - \bar{\varphi}_{i0}). \tag{1.27}$$

By virtue of the approximations introduced

$$\varphi_i' = \sum_{j=1}^{M} j^j \varphi_i \zeta^{j-1} \quad \text{or} \quad \bar{\varphi}_{i*}' = \chi^* \bar{\varphi}_i, \tag{1.28}$$

where $\chi = \|\chi_{ij}\|$ is a square matrix of rank M, $\chi_{ij} = j\left(\frac{i}{M}\right)^{j-1}$. Having substituted (1.27) for ${}^*\bar{\varphi}_i$ in (1.28). we will have

$$\bar{\varphi}_{i*}' = \chi \bar{M}^{-1}(\bar{\varphi}_{i*} - \bar{\varphi}_{i0}).$$

It remains to substitute the thus introduced approximations into the system

$$\bar{\varphi}' = \Phi^{-1}\bar{\Theta} \equiv \bar{b}$$

and write it for all $\zeta = j/M$, $j = 1, 2, \ldots, M$. Then we obtain a system of 3MN nonlinear algebraic equations

$$\chi \bar{M}^{-1} L - B = \chi \bar{M}^{-1} L_0. \qquad (1.29)$$

Here L, L_0, B are matrices of dimension M x 3N, whereby

$$L = \| l_{ji} \|, \quad l_{ji} = \varphi_i \left(\zeta = \frac{j}{M} \right) = \varphi_{ij};$$
$$L_0 = \| l_{0i} \|, \quad l_{0i} = \varphi_{i0};$$
$$B = \| b_{ji} \|, \quad b_{ji} = b_i \left(\zeta = \frac{j}{M} \right) = b_{ij},$$
$$i = 1, 2, \ldots, 3N; \quad j = 1, 2, \ldots, M.$$

To this system we add the remaining equations of the complete approximating system of equations (1.26) of scheme II with the introduced approximations with respect to ζ and which are written at the nodes of the calculated network. All boundary conditions are fulfilled at the nodes of the network lying at the boundary of the integration range. The obtained closed algebraic system is solved by the iterative method. The unknown quantities are the values of the gas dynamic functions at the nodes of the network and also the N + 1 parameter ε_i, i = 0, 1, ..., N, determining the position of the shock wave. With continuous approximation the calculations are performed directly in the entire integration range D with an exact examination of the region of influence of the problem. /42

2. Let us now construct the approximating system with respect to scheme III, using at first approximations of the functions across the shock layer (scheme I) and then along it. We will examine an equilibrium flow, but in place of the condition of isentropy S = S (ψ) we will use the projection of the equation of motion onto axis s. Proceeding in the same manner as when constructing the approximating system for scheme II, we obtain a system of 3N ordinary differential equations which in a matrix form can be written

$$\bar{z}_*' = -\bar{b}; \quad \bar{a} \bar{t}_0' + \bar{t}_*' = -\bar{c}; \quad \bar{a} \bar{g}_0' + \bar{g}_*' = -\bar{d}, \qquad (1.30)$$

where

$$\bar{a} = W B^{-1} \bar{M} - 1;$$
$$\bar{b} = \frac{\varepsilon'}{\varepsilon} \bar{z}_* - \bar{Y}_* + \bar{Y}_0 - \frac{1}{\varepsilon} W B^{-1} \bar{f};$$
$$\bar{c} = \frac{\varepsilon'}{\varepsilon} (\bar{t}_* - \bar{t}_0) + \frac{1}{\varepsilon} W B^{-1} (\varepsilon' \bar{M} t_0 - \bar{G});$$
$$\bar{d} = \frac{\varepsilon'}{\varepsilon} (\bar{g}_* - \bar{g}_0) + \frac{1}{\varepsilon} W B^{-1} (\varepsilon' \bar{M} g_0 - \bar{R}) - \bar{X}_* + \bar{X}_0,$$

$\bar{z}_*$, $\bar{t}_*$, $\bar{g}_*$, $\bar{Y}_*$, $\bar{X}_*$, $\bar{Y}_0$, $\bar{X}_0$ are columns with elements of the values of the functions on the intermediate lines, and the expressions for the matrices W, $\bar{M}$, $\bar{f}$, $\bar{G}$ are given in section 2 of this chapter:

$$\bar{R} = \| R_k \|, \qquad R_k = \varepsilon' \frac{k}{N} \bar{g}_k - (A\bar{z})_k + \varepsilon \frac{k}{N} \bar{X}_0.$$

We note that to construct the approximating system with respect to scheme III, there is no need to solve system (1.30) relative to the derivatives of the unknown hydrodynamic quantities u'_k, v'_k, T'_k, etc.

We will now draw M rays $s_\ell = \text{const}$ ($s_\ell = \frac{\ell}{M} s_M$) with N of them (M > N) drawn in such a manner that they pass through the singular points of system (1.30), /43 where on lines $n_k = \frac{k}{N}\varepsilon(s)$ (k = 0, ℓ, ..., N - 1) the corresponding tangential components of velocity prove to be equal to the sonic velocity ($v_k = c_k$). The position of these points is not known beforehand.

Let us now represent the form of the shock wave and the right sides of system (1.30) with consideration of evenness and oddness of the functions in the form

$$\varepsilon = \sum_{j=0}^{M} \left(\frac{s}{s_M}\right)^{2j} {}^j\varepsilon; \qquad b_k = \sum_{j=1}^{M} \left(\frac{s}{s_M}\right)^{2j-1} {}^j b_k;$$

$$c_k = \sum_{j=1}^{M} \left(\frac{s}{s_M}\right)^{2j-1} {}^j c_k; \qquad d_k = \sum_{j=0}^{M} \left(\frac{s}{s_M}\right)^{2j} {}^j d_k,$$

where $\bar{b} = \| b_k \|$, etc.

Having integrated each equation of system (1.30) from s = 0 to s = s_ℓ, ℓ = 1, 2, ..., M, we obtain a system of 3NM transcendental algebraic equations. We will now calculate the number of unknown quantities. Just as for scheme I, in the equilibrium case on the axis of symmetry, N - 1 values of velocity are unknown at the points of intersection of lines $n_k = \frac{k}{N}\varepsilon(s)$ with the axis. If we assign M + 1 values of the separation of the shock wave ε_ℓ, ℓ = 0, 1, ..., M and use the geometric relation for the angle of inclination of the wave, then at M + 1 points on the shock wave, all parameters can be determined from the conditions for an oblique shock. Further, having used the two finite relations (Bernoulli integral and the equation of state), at each node of the network, we can eliminate two of the five unknown quantities (p, ρ, T, u, v) and consider that at the MN remaining points of the region (except the wave and axis of symmetry) there will be 3MN-M unknown quantities (M values of the normal components of velocity on the body are equal to 0). As was already noted above, the position of the singular points s_i (i = 1, 2, ..., N) on lines $n_k = \frac{k}{N}\varepsilon(s)$

(k = 0, 1, ..., N - 1) are also unknown. Thus, we have 3MN + 2N unknown quantities determining the geometric pattern of flow and the gas dynamic parameters in the shock layer.

To obtain a closed system of equations for determining these quantities, we must add to the algebraic system of 3MN equations 2N conditions of regularity and the locations of the singular points ($E_k = 0$ when $v_k = c_k$, k = 0, 1, ..., N - 1). /44

3. The following difference scheme of types I - II is also possible. In the initial system of equations of equilibrium flow (where in place of $S = S(\psi)$ we will use the second equation of motion), we will introduce the substitution $\eta = \frac{s_*}{s_1(n)}$. In this case, the partial differential equations (1.8) to which we added the equation of motion in a projection onto s, are transformed to

$$\frac{\partial}{\partial\eta}(\bar{z}-\eta s_1' A\bar{H}) + \frac{\partial}{\partial n}(A\bar{H}s_1) = \bar{Y}s_1;$$

$$\frac{\partial}{\partial\eta}(\bar{g}-\eta s_1' A\bar{z}) + \frac{\partial}{\partial n}(A\bar{z}s_1) = \bar{X}s_1;$$

$$\frac{\partial}{\partial\eta}(\bar{t}-\eta s_1' A\bar{h}) + \frac{\partial}{\partial n}(A\bar{h}s_1) = 0.$$

The representation will be analogous to that in scheme I;

$$[\bar{z}-\eta s_1' A\bar{H}] = \sum_{i=1}^{N} {}^i z(\eta)\xi^i; \quad \bar{Y}s_1 = \sum_{i=1}^{N} {}^i Y(\eta)\xi^i;$$

$$[\bar{t}-\eta s_1' A\bar{h}] = \sum_{i=0}^{N} {}^i t(\eta)\xi^i; \quad \bar{X}s_1 = \sum_{i=0}^{N} {}^i X(\eta)\xi^i;$$

$$[\bar{g}-\eta s_1' A\bar{z}] = \sum_{i=0}^{N} {}^i g(\eta)\xi^i; \quad \xi = \frac{n}{\varepsilon(s)}.$$

Then, after transformations by scheme I, we obtain a system of 3N ordinary differential equations of the form:

$$\frac{d\bar{z}_*}{d\eta} + \bar{b}_1 = 0; \quad \bar{a}\frac{dt_0}{d\eta} + \frac{d\bar{t}_*}{d\eta} + \bar{c}_1 = 0; \quad \bar{a}\frac{dg_0}{d\eta} + \frac{d\bar{g}_*}{d\eta} + \bar{d}_1 = 0.$$

The unknowns in this system will be 3N + 3 functions t_0, g_0, ε, $\bar{t}_*$, $\bar{g}_*$, and also N values of $s_1(\xi = \frac{i}{N})$, i = 1, 2, ..., N. We will introduce approximations with respect to η

$$b_{1k} = \sum_{j=1}^{M} {}^{j}b_{1k}\eta^{2j-1}; \quad d_{1k} = \sum_{j=0}^{M} {}^{j}d_{1k}\eta^{2j};$$

$$c_{1k} = \sum_{j=1}^{M} {}^{j}c_{1k}\eta^{2j-1}; \quad \varepsilon = \sum_{j=0}^{M} (s_1\eta)^{2j}\, {}^{j}\varepsilon. \qquad /45$$

We will integrate our equations with the introduced approximations with respect to η from $\eta = 0$ to $\eta = \frac{j}{M}$, $j = 1, \ldots, M$. We obtain a system of 3MN algebraic equations

$$z + AB = 0; \quad \bar{t}_0\tilde{a}' + T + AC = 0; \quad \bar{g}_0\tilde{a}' + Y + \Omega = 0,$$

where $z = \|z_{\nu k}\|$; $T = \|t_{\nu k}\|$; $B = \|b_{1\nu k}\|$; $C = \|c_{1\nu k}\|$; $D = \|d_{1\nu k}\|$, $\nu = 1, \ldots, M$, $k=1, \ldots, N$, are matrices of dimension M x N, whereby $z_{\nu k} = z_k(\eta = \nu/M)$, etc;

$$A = Q\lambda^{-1}; \quad q_{ij} = \frac{1}{2j}\left(\frac{i}{M}\right)^{2j}; \quad \lambda_{ij} = \left(\frac{i}{M}\right)^{2j-1}$$

are matrices of dimension M x N; $\bar{d}_0 = \|d_{0i}\|$; $\bar{t}_0 = \|t_{0i}\|$; $\bar{g}_0 = \|g_{0i}\|$, $i = 1, \ldots, M$, are matrices-columns of dimension M; $d_{0i} = d_0(\eta = i/M)$, etc. Substituting in place of $z_{\nu k}$, $t_{\nu k}$, etc., their expressions in terms of $u_{\nu k}$, $v_{\nu k}$, $\rho_{\nu k}$ (the values $p_{\nu k}$ and $T_{\nu k}$ are eliminated by means of the Bernoulli integral and the equation of state), we obtain a system of transcendental algebraic equations relative to the unknown functions.

In this system, the unknowns are 3M(N - 1) values of the functions u, v, p at points (i, j), where i = 1, ..., M; j = 1, ..., N - 1. Furthermore, the values of v and p on the body are unknown, i.e., at points (i, 0), i = 1, ..., M (2M unknowns). On the axis of symmetry the unknowns are the values of u at points (0, i), i = i, ..., N - 1 (N - 1 unknowns). Further, the values of ε are unknown at points (i, N), i = 0, 1, ..., M (M + 1 unknowns), and also the values of $s_1(\xi)$ at points (M, j), j = 0, 1, ..., N (N + 1 unknowns). In all, we thus have 3MN + 2N + 1 unknown quantities. But, at point (M, 0) we have the relation u = c, i.e., 3MN + 2N unknowns remain in 3MN equations.

We obtain the lacking 2N relations from the characteristic conditions, having substituted into them the approximations of functions $s_1(\xi) = \sum_{i=0}^{N} {}^{i}s_1\xi^i$, and also u, v, p. Actually we have

$$\frac{ds_1}{d\xi} = \frac{\varepsilon(\eta s_1)}{A\tan(\beta \pm \alpha) - \xi\varepsilon_1'(\eta s_1)},$$

but ε and ε'_s, by virtue of the introduced approximations, represent polynomials /46
relative to s_1 since $\eta = 1$, then

$$\frac{ds_1}{d\xi} = \sum_{i=1}^{N} i\xi^{i-1}\, {}_i s_1 .$$

Writing the latter equality for $\xi = \frac{i}{N}$, $i = 1, 2, \ldots, N$, and expressing ${}_i s_1$ in terms of $s_{1i} = s_1(\xi = \frac{i}{N})$, we obtain N relationships of the type

$$\chi \bar{M}^{-1} \bar{s}_1 = \frac{\varepsilon(\bar{s}_1)}{\left(1 + \frac{\frac{i}{N}\varepsilon}{R}\right)\tan(\beta \pm \alpha) - \frac{i}{N}\varepsilon'(\bar{s}_1)},$$

where $\bar{s}_1 = \|s_{1i}\|$ is a column of dimension N, and χ, $\bar{M}^{-1}$ are matrices of dimension N x N.

Introducing analogously into the relation for the characteristic (1.25) the approximations for u, v, p we will have another N deficient relations. Thus, we obtain a closed system of transcendental algebraic equations on a rectilinear calculated network (see Figure 1.7,c).

4. Let us construct, as an example, an approximating system according to scheme III (type I - II) for the case of an equilibrium flow in approximation 2 x N. For this purpose we will divide the region between the shock wave and the body into a number of subregions, drawing one intermediate line $n = \varepsilon(s)/2$ along the shock layer and N rays $s = s_j$ ($j = 1, 2, \ldots, M$) in a transverse direction.

Having taken the first two equations of system (1.8) and having added to them the equation of motion in a projection onto axis s

$$\frac{\partial \bar{g}}{\partial s} + \frac{\partial (A\bar{z})}{\partial n} = \bar{X},$$

we integrate them from the body to the intermediate line $n = \varepsilon(s)/2$ and up to the shock wave $n = \varepsilon(S)$. Approximating the integrand quadratically with respect to n, we obtain the following relations:

$$\bar{g}'_0 = \omega_0^*;\ \bar{t}'_0 = \psi_0;\ \bar{z}'_1 = \varphi_1;\ \bar{g}'_2 = \omega_2;\ \bar{t}'_2 = \psi_2;\ \bar{z}'_2 = \varphi_2, \qquad (1.31)$$

where

$$\omega_0^* = \tfrac{1}{3}(2c_1 - c_2);\quad \omega_2 = \tfrac{1}{8}(c_2 + 5\bar{g}'_0);\quad \varphi_1 = \tfrac{1}{3}(a_2 - 2a_1);$$
$$\varphi_2 = \tfrac{1}{3}(\bar{z}'_1 - a_2);\quad \psi_0 = \tfrac{1}{3}(2b_1 - b_2);\quad \psi_2 = -\tfrac{1}{4}(b_1 + \bar{t}'_0);$$

/147

$$c_1 = \frac{\varepsilon'}{\varepsilon}[\bar{g}_0 + 4\bar{g}_2 - 5\bar{g}_1] + \frac{\varepsilon'}{\varepsilon}A_1\bar{z}_1 - (\bar{X}_0 + 4\bar{X}_2 + \bar{X}_1) + \bar{g}_1';$$

$$c_2 = \frac{\varepsilon'}{\varepsilon}[5\bar{g}_0 - \bar{g}_1 - 4\bar{g}_2] + \frac{24}{\varepsilon}A_2\bar{z}_2 - (5\bar{X}_0 - \bar{X}_1 + 8\bar{X}_2) - \bar{g}_1';$$

$$a_1 = \frac{\varepsilon'}{\varepsilon}[4\bar{z}_2 - 5\bar{z}_1] + \frac{6}{\varepsilon}(A_1\bar{H}_1 - \bar{H}_0) - (\bar{Y}_0 + \bar{Y}_1 + 4\bar{Y}_2);$$

$$a_2 = -\frac{\varepsilon'}{\varepsilon}(4\bar{z}_2 + \bar{z}_1) + \frac{24}{\varepsilon}(A_2\bar{H}_2 - H_0) - (5\bar{Y}_0 - \bar{Y}_1 + 8\bar{Y}_2);$$

$$b_1 = \frac{\varepsilon'}{\varepsilon}(\bar{t}_0 - 5\bar{t}_1 + 4\bar{t}_2) + \frac{6}{\varepsilon}A_1\bar{l}_1 + \bar{t}_1';$$

$$b_2 = \frac{\varepsilon'}{\varepsilon}(5\bar{t}_0 - \bar{t}_1 - 4\bar{t}_2) + \frac{24}{\varepsilon}A_2\bar{l}_2 - \bar{t}_1'.$$

We note that an exact relation $p_0' = t_0v_0'$ or $g_0' = v_0t_0'$ is realized along the body, therefore, the first equation of system (1.31) is written in the following manner: $\bar{g}_0' = \omega_0$, where $\omega_0 = \psi_0 v_0 + r_0' p_0$.

Let us now represent the right sides of system (1.31) by polynomials with respect to s with consideration of the evenness or oddness of the represented functions:

$$\omega_0 = \omega_{00} + \sum_{i=1}^{N} \bar{\omega}_{0i} s^{2i}; \quad \omega_2 = \omega_{20} + \sum_{i=1}^{N} \bar{\omega}_{2i} s^{2i};$$

$$\varphi_1 = \sum_{i=1}^{N} \bar{\varphi}_{1i} s_i^{2i-1}; \quad \varphi_2 = \sum_{i=1}^{N} \bar{\varphi}_{2i} s^{2i-1};$$

$$\psi_0 = \sum_{i=1}^{N} \bar{\psi}_{0i} s^{2i-1}; \quad \psi_2 = \sum_{i=1}^{N} \bar{\psi}_{2i} s^{2i-1},$$

where $\bar{\omega}_{0i}$, $\bar{\omega}_{2i}$, $\bar{\varphi}_{1i}$, $\bar{\varphi}_{2i}$, $\bar{\psi}_{0i}$, $\bar{\psi}_{2i}$ are coefficients of the interpolation polynomials.

Having integrated each of the equations of system (1.31) with respect to s from s = 0 to $s = s_j$ (j = 1, 2, ..., N), we obtain the approximating system of form

$$\left.\begin{aligned} \bar{g}_{0j} &= \sum_{i=0}^{N} \bar{\omega}_{0i} s_j^{2i+1} \frac{1}{2i+1}, \quad (\bar{\omega}_{00} = \omega_{00}); \\ \bar{g}_{2j} &= \sum_{i=0}^{N} \bar{\omega}_{2j} s_j^{2i+1} \frac{1}{2i+1}, \quad (\bar{\omega}_{20} = \omega_{20}); \end{aligned}\right\} \qquad (1.32)$$

/148

$$\left.\begin{aligned} \bar{z}_{1j} &= \sum_{i=1}^{N} \bar{\varphi}_{1i} s_j^{2i} \frac{1}{2i}; \quad \bar{t}_{0j} = \sum_{i=1}^{N} \bar{\psi}_{0i} s_j^{2i} \frac{1}{2i}; \\ \bar{z}_{2j} &= \sum_{i=1}^{N} \bar{\varphi}_{2i} s_j^{2i} \frac{1}{2i}; \quad \bar{t}_{2j} = \sum_{i=1}^{N} \bar{\psi}_{2i} s_j^{2i} \frac{1}{2i} \end{aligned}\right\}$$

$$(j = 1, 2, \ldots, N).$$

We will consider that the last two rays $s = s_{N-1}$ and $s = s_N$ pass, respectively, through points where the tangential components of velocity on the midline and on the body are equal to sonic velocities

$$v_{2(N-1)} = c_{2(N-1)}; \quad v_{0N} = c_{0N}. \tag{1.33}$$

We will add to system (1.32) the conditions of regularity of solution at these points

$$\left.\begin{aligned} E_{2(N-1)} &= \frac{1}{r_{2(N-1)}}\left[1 + L_{2(N-1)}\, v_{2(N-1)} + \right. \\ &+ \frac{M_{2(N-1)} u_{2(N-1)}}{t_{2(N-1)}}\psi_{2(N-1)} - L_{2(N-1)}\,\omega_{2(N-1)} - \\ &\left. - \frac{M_{2(N-1)}}{t_{2(N-1)}}\varphi_{2(N-1)} + r'_{2(N-1)}\left(L_{2(N-1)}\, p_{2(N-1)} - t_{2(N-1)}\right)\right] = 0; \\ E_{0N} &= \frac{1}{r_{0N}}\left[\psi_{0N} - t_{0N} r'_{0N}\right] = 0, \end{aligned}\right\} \tag{1.34}$$

where

$$L_{2(N-1)} = \frac{D_{2(N-1)}\, v_{2(N-1)}}{(h_T)_{2(N-1)}}; \quad M_{2(N-1)} = -\frac{2(\rho_T)_{2(N-1)} u_{2(N-1)} v_{2(N-1)}}{(h_T)_{2(N-1)}};$$

$$D_{2(N-1)} = (\rho_p)_{2(N-1)}(h_T)_{2(N-1)} - (\rho_T)_{2(N-1)}(h_p)_{2(N-1)},$$

and also relation (1.33). The obtained system of 6N + 4 algebraic transcendental equations is also an approximating system with respect to scheme III in approximation 2 x N.

We will describe the order of calculation. Let us assign on the axis of symmetry (s = 0), a certain value of the magnitude of separation of the shock wave ε_0, and also the velocity at the point of intersection of the axis with the midline u_{20}, and on all remaining rays the magnitude of the derivative ε'_j, three quantities at the point of intersection of the ray with the midline (for example, p_{2j}, T_{2j}, u_{2j}, j = 1, 2, ..., N) and two quantities at the point of intersection of the ray with the surface of the body (for example, p_{0j}, v_{0j}, j = 1, 2, ..., N; $u_{0j} \equiv 0$). We will also consider unknown the parameters s_{N-1} and s_N which determine the position of the singular points. Thus, in all /49

we have 6N + 4 unknown parameters.

Let us represent the function $\varepsilon'(s)$ with respect to s in the form $\varepsilon'(s) = \sum_{i=1}^{N} \bar{\varepsilon}_i s^{2i-1}$; then, having solved the system of linear equations $\varepsilon'_j = \sum_{i=1}^{N} \bar{\varepsilon}_i s_j^{2i-1}$, we find the coefficients of approximation $\bar{\varepsilon}_i$ and determine the magnitudes of the separations on each ray

$$\varepsilon_j = \varepsilon_0 + \sum_{i=1}^{N} \bar{\varepsilon}_i s_j^{2i} \frac{1}{2i}.$$

Using the geometric relation, we determine the angle of inclination of the shock wave σ_j for each $s = s_j$

$$\sigma_j = \text{arc tan} \frac{(1+\varepsilon_j/R_{0j})\ \theta_{0j} + \varepsilon'_j}{(1+\varepsilon_j/R_{0j}) - \varepsilon'_j},$$

where R_{0j} and θ_{0j} are known for a given body shape. From the relations for an oblique shock we determine all parameters behind the shock wave for each $s = s_j$. By means of the equation of state $p/\rho = RT/\mu\ (T,p)$, we determine all lacking gas dynamic quantities at the nodes of the network, after which on each ray the right sides of system (1.31) can be calculated.

Solving the systems of linear equations

$$\omega_{0j} - \omega_{00} = \sum_{i=1}^{N} \bar{\omega}_{0i} s_j^{2i}; \qquad \omega_{2j} - \omega_{20} = \sum_{i=1}^{N} \bar{\omega}_{2i} s_j^{2i};$$

$$\varphi_{1j} = \sum_{i=1}^{N} \bar{\varphi}_{1i} s_j^{2i-1}; \qquad \varphi_{2j} = \sum_{i=1}^{N} \bar{\varphi}_{2i} s_j^{2i-1};$$

$$\psi_{0j} = \sum_{i=1}^{N} \bar{\psi}_{0i} s_j^{2i-1}; \qquad \psi_{2j} = \sum_{i=1}^{N} \bar{\psi}_{2i} s_i^{2i-1},$$

we find the coefficients of approximations $\bar{\omega}_{0i}$, $\bar{\omega}_{2i}$, etc., and check the realization of 6N + 4 equations of the approximating system. If these equations are not satisfied, then having changed the values of the parameters, we repeat the entire process. The selection of parameters is accomplished by some iterative method, for example, by Newton's method or by the method of steepest descent.

Scheme III of the method of integral relations was successfully used, for example, to calculate supersonic flows at small Mach numbers of the oncoming flow. The results of the calculations of flow past a sphere for $1.05 \leq M_\infty \leq 2$ obtained by this scheme are given in the second chapter. /50

5. Check of the Accuracy of the Calculations

In the general case of nonlinear systems of partial differential equations, it is quite difficult to obtain an analytic estimate of the accuracy and convergence of the method of integral relations. Therefore, numerical estimates of a different kind should be considered as the basic criteria here. For this purpose, calculations of the same cases of flow were performed by different numerical schemes, and within each scheme with a different number of approximations.

Let us examine, at first, the effect of the number of the approximations on the accuracy of the calculations. Table 1.1 shows certain results of calculations for a circular cylinder around which flows an ideal gas ($\varkappa = 1.4$) at $M_\infty = 3$ obtained by scheme I for the first, second, and third approximations ($N = 1, 2, 3$). The table illustrates the practical convergence with respect to the approximations of the geometric pattern of flow (separation of shock wave) and profiles of gas dynamic quantities (velocity, pressure, and temperature) on the body. The data of this table indicates a sufficiently rapid convergence of the method of integral relations. It should be taken into account that the examined case is less favorable for scheme I owing to the comparatively large thickness of the shock layer.

Calculation experience has shown that in scheme I a sufficient accuracy of the calculations (2.5 - 3 decimal points) is achieved in most cases for axisymmetric bodies ($\nu = 1$) even in the second approximation ($N = 2$) and for plane bodies ($\nu = 0$) when $N = 2; 3$. In this case, the algorithm is realized directly (the singular points in the process of calculation pass in sequence). For large values of N, it is expedient to use the iteration process [28] in which only one j-th singular point passes in each iteration, and the value of $v_i(s)$ on other lines of the approximations ($i = 0, 1, 2, \ldots, N = 1; i \neq j$) are stored.

Tables 1.2 - 1.4 present the results of calculations for a sphere by scheme II for different approximations (from $N = 2$ to $N = 6$) for $M_\infty = 10$. Different types of flows are examined: an ideal gas with constant values of heat capacities $\varkappa = 1.4$ (see Table 1.2); equilibrium flow of oxygen $p_\infty = 0.001$ atm, $T_\infty = 290°K$ (see Table 1.3), and a nonequilibrium flow of $p_\infty = 0.001$ atm, $T_\infty = 290°K$, $R_0 = 0.1$ m (see Table 1.4). For all cases, the forms of the shock waves are given, as well as the profiles of the gas dynamic quantities (components of velocity, pressure, temperature, and concentration of oxygen for nonequilibrium flows) across the shock layer along the axis of symmetry ($s = 0$), intermediate line ($s = s_1/2$) and boundary characteristic ($s = s_1$). For the case of an ideal gas and equilibrium flow, the characteristic of the second family (- Mach Line) was used as the boundary characteristic when performing the calculations, and the characteristic of the first family (+ Mach Line), cutting off a minimal region of influence, was used for nonequilibrium flow.

/51

Upon calculation of flow around smooth bodies by scheme II for cases of an ideal gas, and also with consideration of equilibrium and nonequilibrium processes, it was established that the accuracy of the method increases within the integration range approximately by one decimal point in each new approximation (from 2.5 - 3 decimal points at N = 2-3 to 4-6 decimal points when N = 5-6).

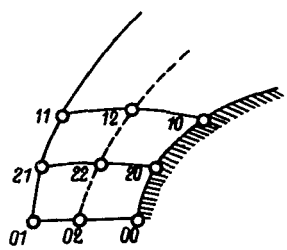

Figure 1.8. Points at which the results of calculations by schemes I and II are compared (Tables 1.5-1.6).

Another criterion of estimating the accuracy of integral relations can be a comparison of calculations of the same cases by different schemes and their comparison with data obtained by other methods. As an example, Table 1.5 gives the results of calculations for the case of flow of an ideal gas past a sphere $\varkappa = 1.4$ at $M_\infty = 10$, obtained by schemes I and II in the second approximation. It should be noted that here data are presented which were obtained by schemes in each of which an approximate representation of the functions in two diametrically opposite directions was used. At nine points of the flow field behind the shock wave (Figure 1.8), the values of density, temperature, and the tangential and normal components of velocity are compared and at three points, the magnitudes of separation of the shock wave. Table 1.6 presents analogous data for the case of an equilibrium flow of an oxygen stream around a sphere at $M_\infty = 10$, $p_\infty = 0.01$ atm, $T_\infty = 290°K$. /5?

We see that the results obtained by means of different schemes agree nicely with one another. This indicates reliability of the calculation results and also a sufficiently accurate approximation of the initial differential operator in the schemes in question.

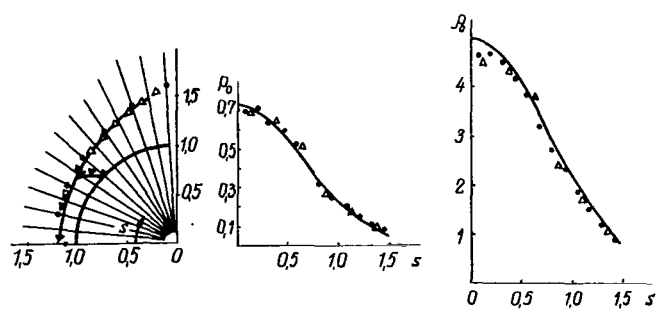

Figure 1.9. Comparison of the results of calculations by the method of integral relations and finite-difference method (sphere $M_\infty = 4$, ideal gas, $\varkappa = 1.4$):

—— Method of integral relations (scheme I, N = 2);
ΔΔΔ Calculation "A" } Method of finite difference [29].
●●● Calculation "B" }

In Figure 1.9 we have compared calculations (form and position of shock wave, sonic line; distribution of pressure p_0 and density ρ_0 along the body) obtained by means of the finite-difference scheme of S. K. Godunov [29] and scheme I for the sphere at $M_\infty = 4$, $\varkappa = 1.4$. Hence, it follows that with "dimunition" of the network (calculation "B") the results of the calculations by the finite-difference method approach the data obtained by the method of integral relations.

A check during numerical solutions of known exact relations which are not used in the approximating system (such as the integrals of the initial system, conditions of constancy of flow rates, constancy of entropy along the line of flow, etc.) can also serve as a check of the accuracy of the method. Calculations show that for scheme I, in the second approximation, the condition of constancy of the flow rate is fulfilled for all stream tubes with an error up to 0.1%, and in scheme II, where entropy is not introduced into the initial system of equations, the relation $S = S(\psi)$ is satisfied for the second approximation with an error up to 1%.

For scheme III, approximating systems (1.31)-(1.33) with a calculated /53
network of the form 2 x N (two steps across line shock layer and N steps along it) were examined to elicit the accuracy of the calculations and the convergence of the solution based on approximations. The results of the calculations for the case of an ideal gas ($M_\infty = 10$; $\varkappa = 1.4$, sphere) at different values of N ($N = 2, 3, 4, 5$) are given in Table 1.7; a comparison with the data of calculations by scheme I ($N = 2$) is also given there.

It is seen that in this scheme the establishment of the calculation results occurs rather quickly with an increase in the number of the approximation N (for example, the data when $N = 3$ and $N = 5$ differ from one another by 1%). A comparison with scheme I gives a difference of less than 3%. The solution of the transcendental system was performed here by the iterative method, and even if the initial approximation was rough (for example, with an accuracy up to 50%) the time of computing the third approximation of the BESM-2 computer did not exceed four minutes. The equations of the approximating system were satisfied with an error of the order of 10^{-7}.

TABLE 1.1

/54

IDEAL GAS. SCHEME I. (BASED ON APPROXIMATIONS). $M_\infty = 3$; $\varkappa = 1.4$; $\delta = 1$; $\nu = 0$, PLANE CIRCULAR CYLINDER.

Separation of Shock Wave and Distribution of Gas Dynamic Parameters Along Body

s	N	ε	v	p	T
0.0000	1	0.6969	0	0.6160	0.1429
0.0000	2	0.7086	0	0.6160	0.1429
0.0000	3	0.7036	0	0.6160	0.1429
0.1250	1	0.7018	0.0485	0.6100	0.1425
0.1250	2	0.7159	0.0558	0.6086	0.1424
0.1250	3	0.7091	0.0607	0.6071	0.1423
0.2500	1	0.7175	0.1011	0.5937	0.1414
0.2500	2	0.7370	0.1178	0.5864	0.1409
0.2500	3	0.7274	0.1239	0.5835	0.1407
0.3750	1	0.7469	0.1586	0.5635	0.1393
0.3750	2	0.7708	0.1827	0.5466	0.1381
0.3750	3	0.7591	0.1865	0.5439	0.1379
0.5000	1	0.7937	0.2192	0.5182	0.1360
0.5000	2	0.8181	0.2459	0.4945	0.1342
0.5000	3	0.8056	0.2477	0.4932	0.1341
0.6250	1	0.8626	0.2812	0.4618	0.1316
0.6250	2	0.8813	0.3063	0.4365	0.1295
0.6250	3	0.8687	0.3076	0.4342	0.1293
0.7500	1	0.9591	0.3446	0.3956	0.1259
0.7500	2	0.9635	0.3642	0.3739	0.1239
0.7500	3	0.9520	0.3653	0.3729	0.1238

TABLE 1.2

IDEAL GAS. SCHEME II (BASED ON APPROXIMATIONS). $M_\infty = 10$; $\varkappa = 1.4$; $\delta = 1$; $\nu = 1$, SPHERE.

Distribution of Gas Dynamic Parameters Along Axis of Symmetry ($s = 0$), Intermediate Line ($s = \frac{1}{2}s_1$), and Boundary Characteristic ($s = s_1$)

ξ	N	$s=0$				$s=\frac{1}{2}s_1$				$s=s_1$			
		u	v	p	T	u	v	p	T	u	v	p	T
1.00	2	-0.170781	0	0.792517	0.138690	-0.152194	0.275667	0.732532	0.128692	-0.090562	0.509820	0.587722	0.104555
1.00	3	-0.170782	0	0.792517	0.138690					-0.090195	0.508996	0.588498	0.104684
1.00	4	-0.170782	0	0.792517	0.138691	-0.151919	0.274525	0.733141	0.128794	-0.090195	0.508996	0.588496	0.104683
1.00	5	-0.170783	0	0.792517	0.138691					-0.090195	0.508996	0.588497	0.104684
1.00	6	-0.170783	0	0.792517	0.138691	-0.151919	0.274525	0.733141	0.128794	-0.090195	0.508996	0.588497	0.104684
0.50	2	-0.080861	0	0.859074	0.141923	-0.072675	0.243116	0.760957	0.133659	-0.041577	0.453190	0.534300	0.113270
0.50	3	-0.081050	0	0.858978	0.141919					-0.041199	0.451439	0.534454	0.113501
0.50	4	-0.081047	0	0.858983	0.141919	-0.072560	0.242172	0.761931	0.133727	-0.041248	0.451526	0.534305	0.113489
0.50	5	-0.081046	0	0.858984	0.141919					-0.041234	0.451500	0.534348	0.113492
0.50	6	-0.081046	0	0.858984	0.141919	-0.072560	0.242169	0.761933	0.133727	-0.041211	0.451468	0.534421	0.113497
0.00	2	-0.000017	0	0.879103	0.142861	-0.000014	0.208811	0.751668	0.136631	-0.00036	0.408292	0.464814	0.119044
0.00	3	-0.000002	0	0.879102	0.142861					-0.00013	0.407786	0.464940	0.119103
0.00	4	-0.000024	0	0.879103	0.142861	-0.000024	0.207945	0.753073	0.136684	-0.000055	0.408360	0.464025	0.119036
0.00	5	-0.000029	0	0.879103	0.142861					-0.000051	0.407976	0.464609	0.119081
0.00	6	-0.000029	0	0.879103	0.142861	-0.000022	0.207832	0.753203	0.136690	-0.000183	0.407324	0.465316	0.119157

Separation of Shock Wave

ε

N	$s=0$	$s=\frac{1}{2}s_1$	$s=s_1$
2	0.135623	0.143841	0.173651
3	0.135717		0.174606
4	0.135718	0.144255	0.174607
5	0.135718		0.174607
6	0.135718	0.144255	0.174607

TABLE 1.3

EQUILIBRIUM OXYGEN. SCHEME II (BASED ON APPROXIMATIONS). $M_\infty = 10$; $p_\infty = 0.001$ atm; $T_\infty = 290°K$; $\delta = 1$, $\nu = 1$, SPHERE.

Distribution of Gas Dynamic Parameters Along Axis of Symmetry ($s = 0$), Intermediate Line ($s = \frac{1}{2} s_1$), and Boundary Characteristic ($s = s_1$)

ξ	N	$s = 0$				$s = \frac{1}{2}s_1$				$s = s_1$			
		u	v	p	T	u	v	p	T	u	v	p	T
1.00	2	-0.088367	0	0.872946	0.069550	-0.077280	0.279930	0.799546	0.068123	-0.034557	0.515355	0.624932	0.064005
1.00	3	-0.088367	0	0.872946	0.069549					-0.033954	0.514237	0.626071	0.064361
1.00	4	-0.088366	0	0.872947	0.069549	-0.077188	0.279362	0.799874	0.068129	-0.033911	0.514159	0.626150	0.064038
1.00	5	-0.088367	0	0.872946	0.069549					-0.033910	0.514159	0.626150	0.064038
1.00	6	-0.088367	0	0.872946	0.069550	-0.077188	0.279362	0.799874	0.068130	-0.033912	0.514160	0.626149	0.064038
0.50	2	-0.037710	0	0.908856	0.069758	-0.033353	0.228105	0.792547	0.068596	-0.013177	0.429536	0.529787	0.065328
0.50	3	-0.037730	0	0.908847	0.069758					-0.012675	0.427124	0.530880	0.065372
0.50	4	-0.037725	0	0.908849	0.069758	-0.033348	0.228184	0.793106	0.068597	-0.012772	0.427249	0.530579	0.065368
0.50	5	-0.037725	0	0.908849	0.069758					-0.012786	0.427268	0.530537	0.065368
0.50	6	-0.037725	0	0.908849	0.069758	-0.033349	0.228186	0.793105	0.068597	-0.012813	0.427295	0.530466	0.065367
0.00	2	0.000000	0	0.917028	0.069805	0.000000	0.148454	0.768516	0.068986	0.000000	0.374393	0.446466	0.063636
0.00	3	0.000000	0	0.917028	0.069804					-0.000007	0.372459	0.446162	0.065756
0.00	4	-0.000063	0	0.917083	0.069805	-0.000026	0.166391	0.769212	0.068900	-0.00008	0.333320	0.443617	0.066155
0.00	5	-0.000060	0	0.917083	0.069805					-0.000100	0.333717	0.442948	0.066147
0.00	6	-0.000007	0	0.917028	0.069805	-0.000004	0.179930	0.769213	0.068833	-0.000130	0.334828	0.442136	0.066129

Separation of Shock Wave

ε

N	$s = 0$	$s = \frac{1}{2}s_1$	$s = s_1$
2	0.0727955	0.0797825	0.105961
3	0.0725941		0.106243
4	0.0725930	0.0797274	0.106256
5	0.0725930		0.106256
6	0.0725930	0.0797274	0.106256

TABLE 1.4

NONEQUILIBRIUM OXYGEN. SCHEME II (BASED ON APPROXIMATIONS). $M_\infty = 10$; $p_\infty = 0.001$ atm; $T_\infty = 290°K$; $R_0 = 0.1$ m; $\delta = 1$, $\nu = 1$, SPHERE.

Distribution of Gas Dynamic Parameters Along Axis of Symmetry ($s = 0$), Intermediate Line ($s = \frac{1}{2}s_1$), and Characteristic ($s = s_1$)

ξ	N	$s = 0$					$s = \frac{1}{2}s_1$					$s = s_1$				
		u	v	p	T	C_{0_2}	u	v	p	T	C_{0_2}	u	v	p	T	C_{0_2}
1.00	2	-0.126782	0	0.835457	0.108536	1.000000	-0.094064	0.423639	0.680415	0.091364	1.000000	0.070714	0.658724	0.455385	0.065866	1.000000
1.00	3	-0.126782	0	0.835457	0.108536	1.000000						0.069490	0.660325	0.453708	0.065676	1.000000
1.00	4	-0.126782	0	0.835457	0.108536	1.000000	-0.087242	0.406684	0.694191	0.092899	1.000000	0.069344	0.660759	0.453148	0.065607	1.000000
1.00	5	-0.126782	0	0.835457	0.108536	1.000000						0.069382	0.660761	0.453145	0.065606	1.000000
1.00	6	-0.126782	0	0.835457	0.108536	1.000000	-0.087394	0.407090	0.693370	0.092864	1.000000	0.069362	0.660762	0.453145	0.065606	1.000000
0.50	2	-0.053156	0	0.890847	0.091271	0.938582	-0.040790	0.275106	0.740382	0.089254	0.954756	0.000453	0.506811	0.459165	0.081634	0.990345
0.50	3	-0.051987	0	0.891481	0.091615	0.936653						-0.001063	0.489681	0.462436	0.081822	0.985876
0.50	4	-0.052371	0	0.891109	0.091557	0.936813	-0.044404	0.271056	0.749512	0.089634	0.955222	-0.001137	0.488700	0.463173	0.081841	0.985873
0.50	5	-0.052315	0	0.891110	0.091561	0.936822						-0.001004	0.489047	0.463447	0.081788	0.985012
0.50	6	-0.052377	0	0.891104	0.091565	0.936839	-0.044567	0.271634	0.748895	0.089638	0.955350	-0.000798	0.489845	0.463506	0.081781	0.985020
0.00	2	-0.000012	0	0.904452	0.078247	0.890285	-0.00002	0.177368	0.758145	0.075997	0.893426	-0.000013	0.335759	0.457104	0.069436	0.899149
0.00	3	0.000000	0	0.904438	0.077208	0.886164						-0.000001	0.333414	0.458055	0.068211	0.899500
0.00	4	-0.000061	0	0.904372	0.078623	0.891558	-0.000095	0.170952	0.766727	0.076635	0.894777	-0.000027	0.336881	0.459690	0.069939	0.901020
0.00	5	0.000000	0	0.904365	0.078621	0.891621						-0.000016	0.337086	0.459444	0.069920	0.901026
0.00	6	-0.000095	0	0.904367	0.078690	0.891787	-0.000019	0.171454	0.766222	0.076656	0.894907	-0.000021	0.337801	0.459123	0.069952	0.901279

Separation of Shock Wave

ε

N	$s = 0$	$s = \frac{1}{2}s_1$	$s = s_1$
2	0.095504	0.107485	0.192428
3	0.091321		0.195231
4	0.091164	0.111426	0.196384
5	0.091069		0.196723
6	0.091069	0.111172	0.196723

TABLE 1.5

/58

IDEAL GAS. SCHEMES I AND II (N = 2). $M_\infty = 10$; $\varkappa = 1.4$; $\delta = 1$; $\nu = 1$, SPHERE.

	SCHEME	NUMBER OF POINT								
		01	02	00	21	22	20	11	12	10
		COORDINATES OF POINT								
		s=0 ξ=1	s=0 ξ=0.5	s=0 ξ=0	s=0.3250 ξ=1	s=0.3450 ξ=0.5	s=0.3575 ξ=0	s=0.6500 ξ=1	s=0.6900 ξ=0.5	s=0.7151 ξ=0
ε	I	0.1360			0.1444			0.1744		
	II	0.1356			0.1438			0.1736		
u	I	-0.1710	-0.07920	0.0000	-0.1515	-0.07283	0.0000	-0.08992	-0.04166	0.0000
	II	-0.1708	-0.08086	0.0000	-0.1522	-0.07268	0.0000	-0.09056	-0.04158	0.0000
v	I	0.0000	0.00000	0.0000	0.2742	0.2431	0.2079	0.5084	0.4523	0.4091
	II	0.0000	0.00000	0.0000	0.2757	0.2431	0.2088	0.5098	0.4532	0.4083
p	I	0.7930	0.9000	0.8790	0.7336	0.7614	0.7526	0.5892	0.5332	0.4628
	II	0.7925	0.8591	0.8791	0.7325	0.7610	0.7517	0.5877	0.5343	0.4648
T	I	0.1387	0.1420	0.1429	0.1288	0.1337	0.1366	0.1046	0.1134	0.1189
	II	0.1387	0.1419	0.1429	0.1287	0.1336	0.1366	0.1046	0.1133	0.1190

TABLE 1.6

EQUILIBRIUM OXYGEN. SCHEMES I AND II (N = 2). $M_\infty = 10$; $p_\infty = 0.01$ atm; $T_\infty = 290°K$; $\delta = 1$; $\nu = 1$; SPHERE.

	SCHEME	NUMBER OF POINT								
		01	02	00	21	22	20	11	12	10
		COORDINATES OF POINT								
		s=0 ξ=1	s=0 ξ=0.5	s=0 ξ=0	s=0.3 ξ=1	s=0.3219 ξ=0.5	s=0.3367 ξ=0	s=0.6 ξ=1	s=0.6439 ξ=0.5	s=0.6733 ξ=0
ε	I	0.07886			0.08499			0.1072		
	II	0.07865			0.08473			0.1066		
u	I	-0.09605	-0.04202	0.0000	-0.08627	-0.03784	0.0000	-0.04885	-0.01966	0.0000
	II	-0.09597	-0.04154	0.0000	-0.08628	-0.03780	0.0000	-0.05039	-0.02155	0.0000
v	I	0.00000	0.00000	0.0000	0.2549	0.2083	0.1526	0.4733	0.3910	0.2965
	II	0.00000	0.00000	0.0000	0.2552	0.2085	0.1532	0.4762	0.3961	0.3040
p	I	0.8653	0.9039	0.9133	0.8050	0.8097	0.7964	0.6587	0.5952	0.5380
	II	0.8655	0.9043	0.9135	0.8051	0.8100	0.7962	0.6562	0.5855	0.5229
T	I	0.07654	0.07683	0.07690	0.07499	0.07560	0.07599	0.07055	0.07224	0.07344
	II	0.07650	0.07680	0.07686	0.07495	0.07556	0.07595	0.07042	0.07206	0.07323

TABLE 1.7

IDEAL GAS. SCHEME III (BASED ON APPROXIMATIONS) AND I (N = 2). $M_\infty = 10$; $\varkappa = 1.4$; $\delta = 1$; $\nu = 1$, SPHERE.

Distribution of Gas Dynamic Parameters Along Shock Wave ($\xi = 1.0$), Intermediate Line ($\xi = 0.5$), and Body ($\xi = 0$)

	N	s	$\xi = 1$							$\xi = 0.5$					$\xi = 0$				
			ε	σ	ρ	p	T	u	v	ρ	p	T	u	v	ρ	p	T	u	v
Scheme III	2	0.000	0.1507	1.571	5.714	0.7925	0.1387	-0.1708	0	6.047	0.8579	0.1419	-0.08329	0	6.153	0.8790	0.1428	0	0
	3	0.000	0.1351	1.571	5.714	0.7925	0.1387	-0.1708	0	6.052	0.8588	0.1419	-0.08149	0	6.153	0.8790	0.1428	0	0
	4	0.000	0.1351	1.571	5.714	0.7925	0.1387	-0.1708	0	6.051	0.8588	0.1419	-0.08151	0	6.153	0.8790	0.1428	0	0
	5	0.000	0.1354	1.571	5.714	0.7925	0.1387	-0.1708	0	6.051	0.8587	0.1419	-0.08170	0	6.153	0.8790	0.1428	0	0
I		0.000	0.1360	1.571	5.714	0.7930	0.1390	-0.1710	0	6.051	0.8590	0.1420	-0.08190	0	6.153	0.8790	0.1428	0	0
III	2	0.125	0.1513	1.455	5.710	0.7819	0.1369	-0.1687	0.1145	5.983	0.8431	0.1409	-0.08213	0.08288	6.113	0.8711	0.1425	0	0.05092
	3	0.125	0.1361	1.461	5.711	0.7830	0.1371	-0.1682	0.1095	6.002	0.8448	0.1408	-0.08034	0.09031	6.074	0.8633	0.1421	0	0.07165
	4	0.125	0.1362	1.461	5.711	0.7830	0.1371	-0.1682	0.1092	6.002	0.8449	0.1408	-0.08036	0.09026	6.074	0.8632	0.1421	0	0.07183
	5	0.125	0.1364	1.460	5.711	0.7829	0.1371	-0.1682	0.1099	6.000	0.8446	0.1408	-0.08044	0.09011	6.076	0.8636	0.1421	0	0.07113
I		0.125	0.1370	1.463	5.711	0.7830	0.1371	-0.1680	0.1080	6.004	0.8450	0.1408	-0.08020	0.08980	6.071	0.8630	0.1421	0	0.07320
III	2	0.250	0.1534	1.341	5.699	0.7515	0.1318	-0.1621	0.2252	5.798	0.8002	0.1380	-0.07859	0.1662	5.971	0.8428	0.1412	0	0.1093
	3	0.250	0.1395	1.354	5.701	0.7556	0.1325	-0.1602	0.2157	5.856	0.8048	0.1374	-0.07690	0.1791	5.830	0.8152	0.1398	0	0.1460
	4	0.250	0.1396	1.354	5.701	0.7558	0.1326	-0.1601	0.2153	5.857	0.8050	0.1374	-0.07691	0.1790	5.831	0.8153	0.1398	0	0.1458
	5	0.250	0.1397	1.353	5.701	0.7556	0.1325	-0.1602	0.2159	5.854	0.8047	0.1374	-0.07685	0.1787	5.829	0.8149	0.1398	0	0.1463
I		0.250	0.1410	1.357	5.702	0.7570	0.1327	-0.1600	0.2130	5.863	0.8060	0.1374	-0.07690	0.1780	5.830	0.8150	0.1398	0	0.1460
III	2	0.375	0.1575	1.234	5.681	0.7058	0.1242	-0.1497	0.3286	5.512	0.7342	0.1332	-0.07255	0.2497	5.666	0.7832	0.1382	0	0.1801
	3	0.375	0.1456	1.250	5.684	0.7134	0.1255	-0.1461	0.3164	5.626	0.7433	0.1321	-0.07103	0.2649	5.417	0.7354	0.1358	0	0.2229
	4	0.375	0.1458	1.250	5.684	0.7134	0.1255	-0.1461	0.3163	5.626	0.7433	0.1321	-0.07106	0.2647	5.427	0.7374	0.1359	0	0.2213
	5	0.375	0.1459	1.250	5.684	0.7134	0.1255	-0.1461	0.3164	5.626	0.7435	0.1322	-0.07106	0.2644	5.415	0.7351	0.1357	0	0.2232
I		0.375	0.1470	1.253	5.685	0.7150	0.1257	-0.1450	0.3140	5.630	0.7450	0.1322	-0.07120	0.2630	5.446	0.7410	0.1360	0	0.2180
III	2	0.500	0.1648	1.134	5.656	0.6508	0.1151	-0.1298	0.4216	5.162	0.6532	0.1265	-0.06378	0.3319	5.129	0.6813	0.1328	0	0.2650
	3	0.500	0.1551	1.149	5.660	0.6596	0.1165	-0.1256	0.4105	5.318	0.6657	0.1252	-0.06225	0.3463	4.882	0.6357	0.1302	0	0.2974
	4	0.500	0.1553	1.148	5.660	0.6591	0.1164	-0.1258	0.4110	5.312	0.6648	0.1252	-0.06223	0.3464	4.907	0.6404	0.1305	0	0.2942
	5	0.500	0.1553	1.148	5.660	0.6591	0.1165	-0.1258	0.4110	5.314	0.6652	0.1252	-0.06234	0.3462	4.900	0.6391	0.1304	0	0.2950
I		0.500	0.1570	1.153	5.661	0.6620	0.1168	-0.1250	0.4080	5.313	0.6670	0.1255	-0.06240	0.3430	4.942	0.6470	0.1308	0	0.2900
III	2	0.625	0.1766	1.045	5.624	0.5929	0.1054	-0.1007	0.5019	4.801	0.5697	0.1187	-0.05206	0.4082	4.294	0.5311	0.1237	0	0.3662
	3	0.625	0.1684	1.050	5.626	0.5960	0.1059	-0.09914	0.4986	4.921	0.5750	0.1168	-0.04908	0.4238	4.367	0.5439	0.1245	0	0.3580
	4	0.625	0.1685	1.050	5.626	0.5963	0.1060	-0.09900	0.4983	4.920	0.5751	0.1169	-0.04920	0.4235	4.336	0.5385	0.1242	0	0.3615
	5	0.625	0.1685	1.050	5.626	0.5962	0.1060	-0.09905	0.4984	4.919	0.5750	0.1169	-0.04919	0.4235	4.336	0.5385	0.1242	0	0.3615
I		0.625	0.1710	1.058	5.629	0.6020	0.1068	-0.09650	0.4930	4.925	0.5800	0.1177	-0.04990	0.4170	4.354	0.5420	0.1244	0	0.3590
III	2	0.750	0.1949	0.9684	5.588	0.5377	0.09622	-0.06101	0.5681	4.515	0.5032	0.1114	-0.03726	0.4674	3.406	0.3843	0.1128	0	0.4585
	3	0.750	0.1855	0.9470	5.577	0.5218	0.09356	-0.06914	0.5833	4.379	0.4662	0.1065	-0.02745	0.5040	3.666	0.4258	0.1161	0	0.4325
	4	0.750	0.1863	0.9597	5.584	0.5312	0.09514	-0.06423	0.5744	4.487	0.4843	0.1079	-0.03158	0.4934	3.662	0.4251	0.1161	0	0.4329
	5	0.750	0.1863	0.9759	5.583	0.5299	0.09492	-0.06491	0.5756	4.476	0.4826	0.1078	-0.03109	0.4943	3.672	0.4268	0.1162	0	0.4319
I		0.750	0.1910	0.9700	5.589	0.5380	0.09628	-0.06070	0.5670	4.483	0.4900	0.1092	-0.03280	0.4830	3.714	0.4330	0.1167	0	0.4280

CHAPTER 2

EQUILIBRIUM FLOWS

1. Equilibrium Blunt-Body Gas Flow

As is known, when a supersonic flow passes a body there is severe heating /60
of the gas in the layer behind the nose shock wave. As a consequence of this, effects associated with the variable heat capacity of the gas are observed behind the wave front: excitation of internal degrees of freedom of molecules and their dissociation and ionization. These effects substantially influence the position and form of the nose shock wave and also the distribution of hydrodynamic parameters in the shock layer.

We examined the effect of variable heat capacity on the supersonic flow of various gases around blunt bodies. The calculations were performed by schemes I and II of the method of integral relations.

One of them involves the direct solution of the system of equations of chemical equilibrium. It is worthwhile to resort to this method in the case of simple gas mixtures when the solution of the system of equations of chemical equilibrium at each step of integration does not require substantial expenditures of machine time. The values of enthalpies and constants of equilibrium of pure components that are needed for the calculation can be obtained from approximations with a high degree of accuracy since they are functions only of one variable, temperature.

For multicomponent gas mixtures, systems of equations of chemical equilibrium become cumbersome and their numerical solution causes an undesirable increase of machine time. Therefore, it is expedient to use the available tabular data on the composition and thermodynamic functions for multicomponent gas mixtures, approximating them as functions of pressure and temperature. Thus, many authors have proposed approximations of thermodynamic functions of air. I. N. Naumova [30] approximated the enthalpy h and molecular weight of air μ /61
with respect to two variables; and T for temperatures up to 16,800°K and pressures from 10^{-3} to 10^{3} atm. The relative error in calculating h and μ in absolute value is less than 1%. Less accurate, but simpler approximations were proposed by A. N. Kraiko [31]. He found analytic forms of the dependences of enthalpy h and density ρ as functions of pressure and temperature. The data of the calculation by these approximations coincide with the tabular data with an error of $\pm$ 3% for h and $\pm$ 1.5% for ρ in the temperature range of 400-20,000°K and pressures of 10^{-3} - 10^{3} atm.

We can also determine the thermodynamic functions of gas mixtures on the basis of differential relations obtained from equations of chemical equilibrium. In this case we must have only approximations of the molar components of the mixture. The advantages of this method of calculating thermodynamic functions of gas are that the obtained system of ordinary differential equations is joined to the initial approximating system of the numerical scheme of solving

the gas dynamic problem and is integrated simultaneously with it. This method requires less machine time in comparison with the iterative method of solving the system of equations of chemical equilibrium. Such a method of solution was worked by V. K. Molodtsov for air [32].

When calculating equilibrium flows of gas we used all the above-indicated methods of determining the thermodynamic functions; the selection of the specific method was determined by the requirement of convenience and minimal expenditure of machine time. A comparison of the various approaches shows a good agreement of the results obtained. As an example we will give the results of calculating equilibrium air flow around a sphere by scheme II in the second approximation when $M_\infty = 10$, $P_\infty = 0{,}01$ atm, $T_\infty = 300°K$. Calculation "A" corresponds to a calculation of thermodynamic functions by means of differential relations by V. K. Molodtsov's method of calculation "B" by the iterative method. Table 2.1 gives the distribution of the velocity components u_1, v_1, pressure p_1, and temperature T_1 along the boundary characteristic of the second family (-Mach line) and also its coordinates $s = s_1(\xi)$. It follows from the table that the results of the calculations coincide with a satisfactory degree of accuracy.

The approximating systems presented in the first chapter were used for calculations in a wide range of change of the initial parameters when it was necessary to take into account the processes of equilibrium dissociation and single and double ionization of the gas. The effect of equilibrium and also nonequilibrium processes on supersonic flow around blunt bodies was studied in oxygen, nitrogen, carbon dioxide, air, and other gas mixtures. Different body forms (sphere, ellipsoid of revolution, segmented bodies, blunt cones, etc.) were examined. /62

Let us dwell briefly on certain results of calculations which are presented in Figures 2.1-2.4, 2.6-2.19 for oxygen, in Figures 2.20, 2.21 for oxygen, nitrogen, and air, in Figures 2.5, 2.22, 2.23 for air, in Figure 2.24 for carbon dioxide, and also in Tables 2.2-2.9 (scheme I, N = 2); 2.10-2.28 (scheme II, N = 2, 3) and 2.29-2.30 (method of characteristics).

The influence of excitation of internal degrees of freedom, dissociation, and ionization is most clearly manifested for a pure gas; therefore, our examination will begin with oxygen.

Figure 2.1 shows the character of behavior of the magnitude of departure of the shock wave ε_0 along the axis of symmetry for a sphere past which flows equilibrium oxygen, as a function of the Mach number M_∞ and pressure p_∞ in the oncoming flow ($T_\infty = 290°K$). For comparison the curve for an ideal gas ($\varkappa = 1.4$) is also plotted. The nonmonotonic character of the dependence $\varepsilon_0 = \varepsilon_0(M_\infty)$ is distinctly seen, the nonmonotonic character increasing with a decrease of the values of p_∞. This law of behavior is explained by the effect of the variable heat capacity of the gas: excitation of vibrations, dissociation, and ionization of the gas occurs with an increase of M_∞.

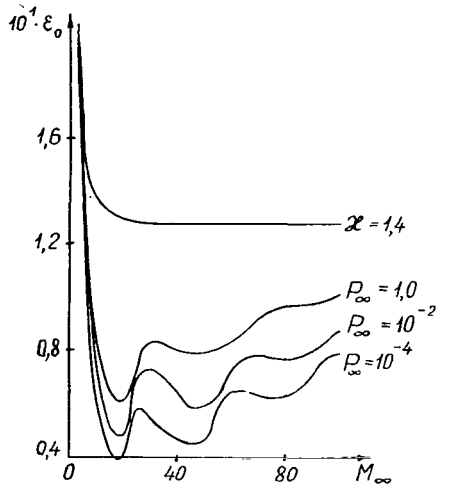

Figure 2.1. Separation of shock wave along axis of symmetry during flow of equilibrium oxygen around a sphere (T_∞ = 290°K, p_∞ = 1 atm, 10^{-2} atm, 10^{-4} atm) and an ideal gas ($\varkappa$ = 1.4).

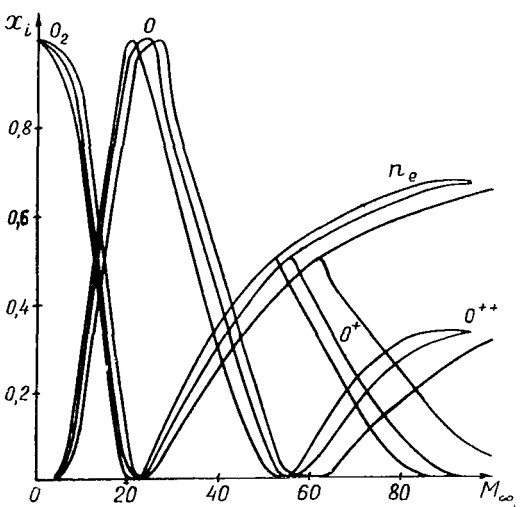

Figure 2.2. Behavior of molar concentration behind plane shock wave.

Figure 2.2 shows the values of the molar concentrations of molecular and atomic oxygen, ions, and electrons (O_2, O, O^+, O^{++}, and n_e) behind a plane shock wave as a function of M_∞. Such a change of concentrations leads to a nonmonotonic dependence on M_∞ of the gas density ρ_1 behind the shock wave of the axis of symmetry (Figure 2.3; flow around a sphere).

We will explain the character of the change of the dependence ε_0 (M_∞). When $M_\infty \sim 18$, when the gas is already noticeably dissociated, the density value ρ_1 reaches a maximum and the magnitude of separation of the shock wave ε_0 when p_∞ = const is minimal (see Figure 2.1). With an increase of M_∞ the gas becomes completely dissociated, compression diminishes (if we disregard the energy of dissociation and variable heat capacity of atomic oxygen, then $\rho_1 \to 4.0$), and the magnitude of departure of the wave correspondingly increases. Then primary ionization of the gas occurs with an increase of M_∞ (Figure 2.2), its heat capacity increases, and consequently, compression of the gas (Figure 2.3), which leads to a decrease in the magnitude of separation ε_0. A subsequent increase of M_∞ involves appreciable ionization of the gas (Figure 2.2), decrease of density ρ_1 (Figure 2.3), and an increase in the magnitude of separation. If we examine the flow at very large values of the Mach numbers of the oncoming flow (M_∞ > 60), then we must take into account secondary ionization of the gas (Figure 2.2). In this case compression of the gas again increases

/64

(Figure 2.3) and the magnitude of separation decreases. It is necessary to note that at high Mach numbers we must also take into account gas radiation.

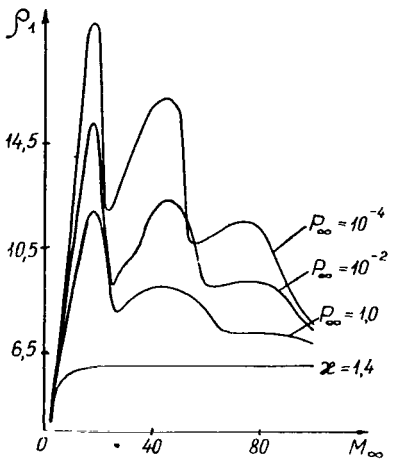

Figure 2.3. Density behind shock wave (on axis of symmetry) during flow around a sphere of equilibrium oxygen (T = 290°K, p_∞ = 1 atm, 10^{-2} atm, 10^{-4} atm) and an ideal gas ($\varkappa$ = 1.4).

Thus, the nonmonotonic dependence $\varepsilon_0 = \varepsilon_0 (M_\infty)$ on the whole is determined by the variable heat capacity of the gas and, primarily, by a nonmonotonic change of density behind the shock wave. It is seen that the magnitude of separation of the shock wave, owing to the variable heat capacity, can change severalfold. For an ideal gas when $\varkappa = C_p/C_v$ = const the dependence $\varepsilon_0 = \varepsilon_0 (M_\infty)$ is a monotonic function.

A change of density caused by dissociation and ionization is especially obvious for the case of oxygen. For air, which is a mixture of oxygen and nitrogen with markedly differing energies of vibration and dissociation, a nonmonotonic change of density, and, consequently, the nonmonotonic character of the dependence $\varepsilon_0 (M_\infty)$, is less pronounced. As an illustration, in Figure 2.4 (equilibrium oxygen, δ = 1, p_∞ = 0.01 atm, T_∞ = 290°K and in Figure 2.5 (equilibrium air, δ = 10, p_∞ = 0.01 atm, T_∞ = 290°K we present the results of calculations with consideration of ionization, where we have plotted (solid line) the dependences of the magnitude of shock-wave separation ε_0, density ρ_0, mass concentration C_{0_2}, C_0, C_0^+ (for oxygen) and the molar concentration of atomic oxygen x_0 (for air) at the critical point of the body as a function of M_∞. For comparison, the results of calculations without ionization (see Figure 2.4) and for ideal gas $\varkappa$ = 1.4 (Figure 2.5) are plotted by a dashed line.

A comparison of experimental data on the magnitude of shock-wave separation with the results of the calculations can serve, therefore, as a good criterion when investigating different physicochemical processes occurring in the shock layer.

Since the magnitude of the shock-wave separation ε_0 is related with gas density in the shock layer ρ_1, a number of authors have proposed an approximate dependence for $\varepsilon_0 = \varepsilon_0(\rho_1)$ which agree well with the calculations and /65

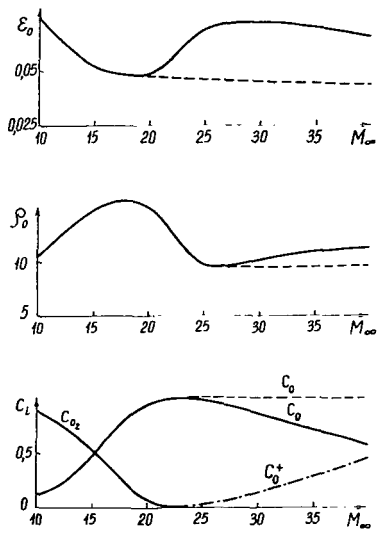

Figure 2.4. Magnitude of shock-wave separation, density, and mass concentrations at the critical point of the body (equilibrium oxygen, $\delta = 1$, $p_\infty = 0.01$ atm, $T_\infty = 290°K$): —— calculation with ionization; ---- calculation without ionization.

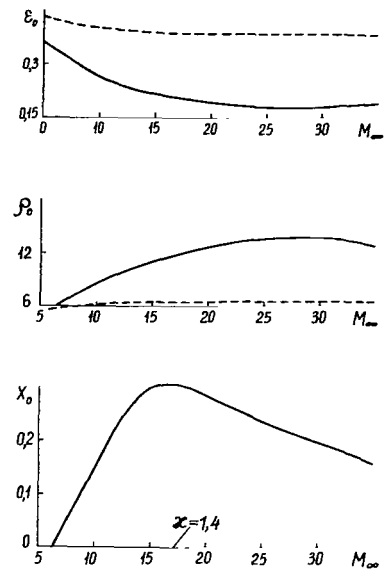

Figure 2.5. Magnitude of shock wave separation, density, and molar concentration of atomic oxygen at critical point of body (equilibrium air, $\delta = 10$, $p_\infty = 0.01$ atm, $T_\infty = 290°K$): —— calculation with ionization; ---- ideal gas $\varkappa = 1.4$.

experimental data. We note that the presence of such a dependence in an implicit form suggests a similarity of the flow field in the shock layer with respect to the Mach numbers of the oncoming flow. However, we can expect such a similarity only in the case of a monotonic change of density ρ_1 behind the shock wave from the number M_∞, i.e., at comparatively small Mach numbers, whereas in the region of a nonmonotonic change of density the similarity will be absent. This is confirmed by Figure 2.6 where the dependence $\varepsilon_0 = \varepsilon_0(\rho_1)$ calculated from the formula $\varepsilon_0 = 0.52(\rho_1-1)^{-0.86}$ (solid line) and the points obtained by the method of integral relations are shown for various cases. Only the points corresponding to small values of M_∞ when the monotonic dependence $\rho_1 = \rho_1(M_\infty)$ /66 are laid out on the solid curve.

To investigate more thoroughly the effect of variable heat capacity of the gas on the flow field in the region of nonmonotonic change of density, we will examine the results obtained on calculating the flow of equilibrium oxygen around a sphere when $M_\infty = 10; 25; 30$; $p_\infty = 0.01$ atm; $T_\infty = 290°K$.

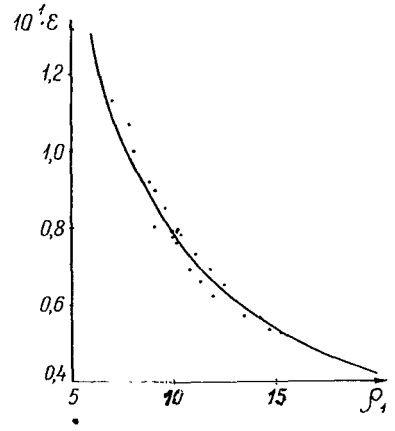

Figure 2.6. Curve of similarity and results of calculations (points).

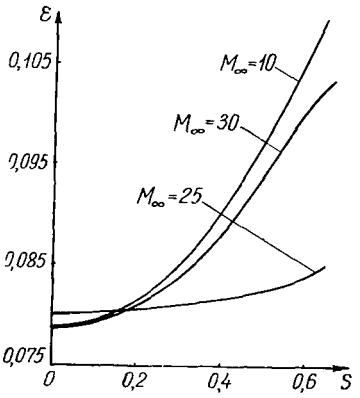

Figure 2.8. Separation of shock waves along surface of body (sphere, equilibrium oxygen, p_∞ = 0.01 atm, T_∞ = 290°K).

Figures 2.10-2.12 show the distribution of densities ρ_0, ρ_1 and ρ_2, respectively, along the surface of the sphere n = 0, shock wave n = ε(s), and intermediate line n = ε(s)/2 (scheme I, second approximation) for M_∞ = 10

Figures 2.7-2.9 show the position of shock waves for different Mach numbers of the oncoming flow. It is interesting to note that the shock wave for the case M_∞ = 30 is situated much closer to the shock wave when M_∞ = 10 than a wave when M_∞ = 25.

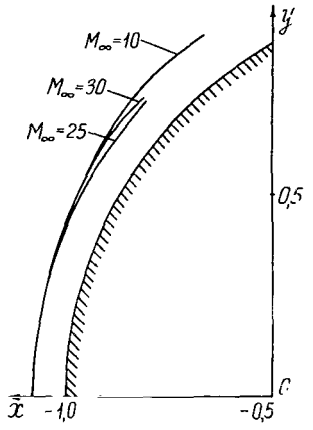

Figure 2.7. Flow of equilibrium oxygen around a sphere (p_∞ = 0.01 atm, T_∞ = 290°K). /67

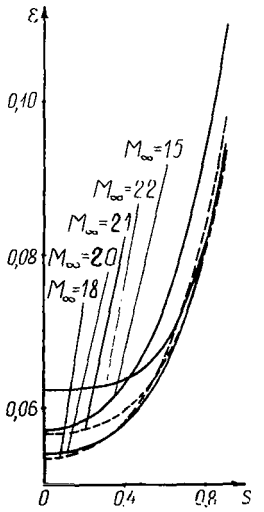

Figure 2.9. Separation of shock waves along surface of body (sphere, equilibrium oxygen, p_∞ = 0.01 atm, T_∞ = 290°K).

(Figure 2.10); $M_\infty = 25$ (Figure 2.11); $M_\infty = 30$ (Figure 2.12). It is seen that for the case $M_\infty = 10$ the density drops with distance from the axis of symmetry, this drop being more appreciable along the body and intermediate line than behind the shock wave. For the case $M_\infty = 25$ (Figure 2.11) there is also a drop of ρ_2 and ρ_0, wherein $\rho_2 > \rho_0$, and more appreciable difference of the profiles ρ_2 and ρ_0 is observed than when $M_\infty = 10$; it is interesting that ρ_1 here does not drop, but increases. For the case $M_\infty = 30$ (Figure 2.12) the change of densities is even more complex: ρ_2 can drop more appreciably than ρ_0, and the density behind the shock wave ρ_1 at first drops, as in the case of $M_\infty = 10$, and then increases as in the case of $M_\infty = 25$.

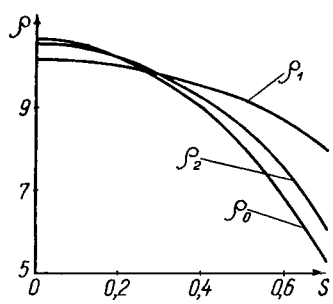

Figure 2.10. Distribution of densities along body ρ_0, shock wave ρ_1, and intermediate line ρ_2 (equilbrium oxygen, sphere, $M_\infty = 10$, $p_\infty = 0.01$ atm, $T_\infty = 290°K$).

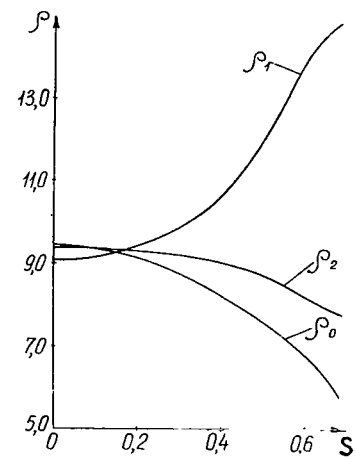

Figure 2.11. Distribution of densities along body ρ_0, shock wave ρ_1, and intermediate line ρ_2 (equilibrium oxygen, sphere, $M_\infty = 25$, $p_\infty = 0.01$ atm, $T_\infty = 290°K$).

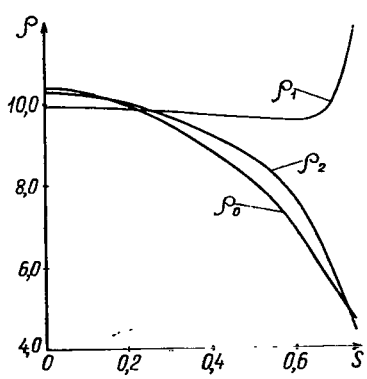

Figure 2.12. Distribution of densities along body ρ_0, shock wave ρ_1, and inmediate line ρ_2 (equilibrium oxygen, sphere, $M_\infty = 30$, $p_\infty = 0.01$ atm, $T_\infty = 290°K$).

Figures 2.13-2.15 show the distribution of temperature $\overline{T}_0 = T_0(s)/T_0(0)$, pressure $\overline{p}_0 = p_0(s)/p_0(0)$, and concentration of atomic oxygen $\overline{C}_0 = C_0(s)/C_0(0)$ ($C_0(0)$ is the concentration at the critical point) along the surface of a sphere for $M_\infty = 10; 25; 30$; $p_\infty = 0.01$ atm; $T_\infty = 290°K$.

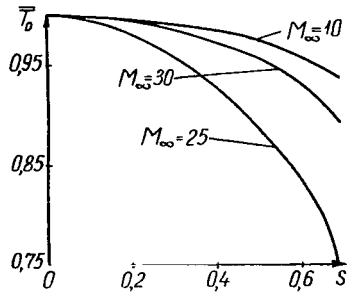

Figure 2.13. Distribution of temperature along sphere (equilibrium oxygen, $p_\infty = 0.01$ atm, $T_\infty = 290°K$).

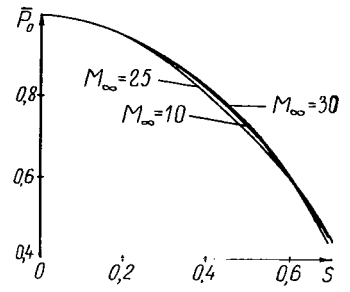

Figure 2.14. Distribution of pressure along sphere (equilibrium oxygen, $p_\infty = 0.01$ atm, $T_\infty = 290°K$).

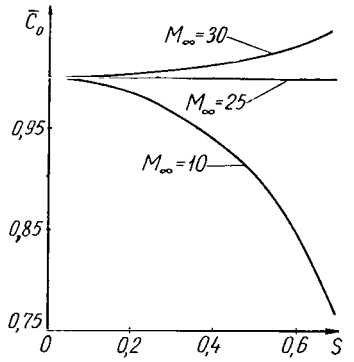

Figure 2.15. Distribution of mass concentrations of atomic oxygen along sphere (equilibrium oxygen, $p_\infty = 0.01$ atm, $T_\infty = 290°K$).

It is seen that the temperature profile for $M_\infty = 30$ is closer to the temperature profile when $M_\infty = 10$ than when $M_\infty = 25$; the pressure profiles for different M_∞ differ from one another very little, whereas the concentration profiles are completely different (for $M_\infty = 10$ the concentration drops, for $M_\infty = 25$ it is practically unchanged, and for $M_\infty = 30$ it even increases).

Figure 2.16 gives the position of the sonic points on the body (s_s) and the points of intersection of the boundary characteristic with the shock wave (s_{10}) for the case of equilibrium oxygen flow around a sphere when $p_\infty = 0.01$ atm, $T_\infty = 290°K$ for different M_∞. This dependence for s_{10} and s_s is also explicitly nonmonotonic.

Thus, Figures 2.7-2.16 clearly show that in the region of high Mach numbers similarity of the flow field is absent in the shock layer.

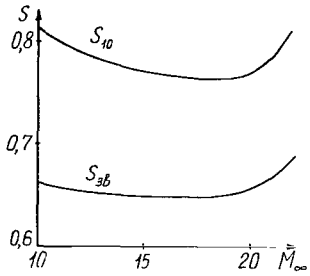

Figure 2.16. Position of sonic points on sphere s_s and points of intersection of boundary characteristic with shock wave s_{10} (equilibrium oxygen, p_∞ = 0.01 atm, T_∞ = 290°K).

The change of parameters along the shock layer was examined above. Now let us present certain results for a sphere (around which flows equilibrium oxygen at M_∞ = 10, p_∞ = 0.01 atm, T_∞ = 290°K) which characterize the change of gas dynamic parameters across the shock layer. The calculation was performed by scheme II when N = 2, 3.

Figures 2.17 and 2.18 give the distribution of the normal u_i and tangential v_i components of velocity along the axis of symmetry (i = 0), boundary characteristic (i = 1), and intermediate line (i = 2). As could be expected, for small Mach numbers the profiles of u_0, u_2, v_1, v_2 are close to linear, and the profile u_1 is completely nonlinear. The distribution of the concentration of atomic oxygen $(C_0)_i$ is presented in Figure 2.19.

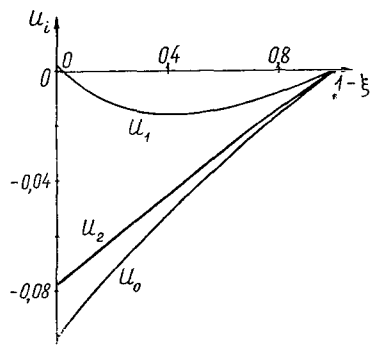

Figure 2.17. Distribution of normal velocity component along axis of symmetry u_0, boundary characteristic u_1, and intermediate line u_2 (sphere, equilibrium oxygen, M_∞ = 10, p_∞ = 0.01 atm, T_∞ = 290°K).

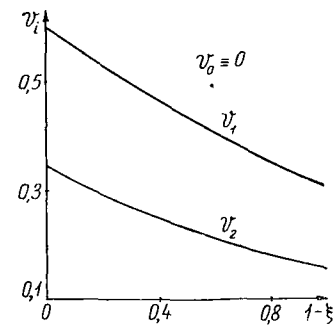

Figure 2.18. Distribution of tangential velocity component along axis of symmetry v_0, boundary characteristic v_1, and intermediate line v_2 (sphere, equilibrium oxygen, M_∞ = 10, p_∞ = 0.01 atm, T_∞ = 290°K).

From an examination of the results obtained for this case we can make the following conclusions: a) the density

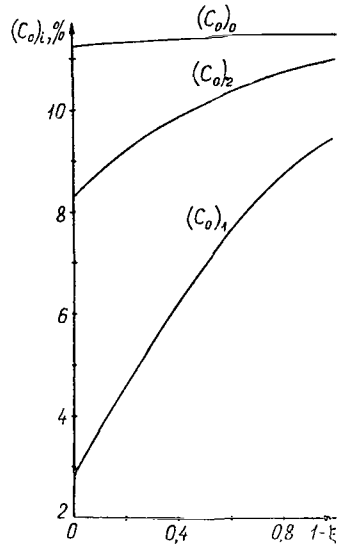

Figure 2.19. Distribution of concentration of atomic oxygen along axis of symmetry $(C_0)_0$, boundary characteristic $(C_0)_1$, and intermediate line $(C_0)_2$ (sphere, equilibrium oxygen, $M_\infty = 10$, $p_\infty = 0.01$ atm, $T_\infty = 290°K$).

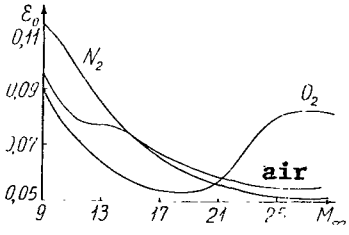

Figure 2.20. Separation of shock wave along axis of symmetry for oxygen, nitrogen, and air (sphere, $p_\infty = 0.01$ atm, $T_\infty = 290°K$).

along the zero line of flow increases and drops on the intermediate line and, especially, on the boundary characteristic; b) the change of pressure across the boundary layer is negligible; c) the change of temperature, concentration of atomic oxygen, and molecular weight of the mixture is especially substantial on the boundary characteristic (these parameters change little /71
along the zero line of flow and intermediate line).

A similar series of calculations was performed for nitrogen. The obtained regularities here have the same character as for oxygen, however, the effect of variable heat capacity is manifested only at large Mach numbers of the oncoming flow. Furthermore, the processes of dissociation and ionization in this case occur not sequentially as in oxygen but simultaneously owing to the smaller difference of the energies of dissociation and ionization of nitrogen. In this connection the nonmonotonic character of the magnitudes of wave separation and distribution of parameters in the shock layer are less evidenced for nitrogen than for oxygen. Numerous calculations were carried out for air. Figure 2.20 presents, for comparison, the dependence of the magnitude of wave separation along the axis of symmetry ε_0 on the Mach number of the oncoming flow M_∞ for oxygen, nitrogen, and air ($p_\infty = 0.01$ atm, $T_\infty = 290°K$). It is seen that at small values of M_∞, when the variable heat capacity of air is mainly due to dissociation of oxygen, the curve $\varepsilon_0 = \varepsilon_0 (M_\infty)$ for air is situated closer to the /72
corresponding curve for oxygen. However, with an increase of the Mach number, when dissociation of nitrogen begins to play a role, the character of the change of the curve $\varepsilon_0 = \varepsilon_0 (M_\infty)$ resembles the behavior of the analogous dependence for nitrogen, since this component predominates in air.

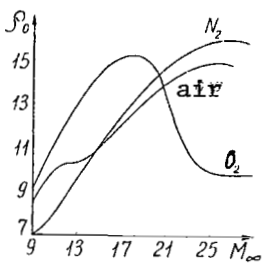

Figure 2.21. Density behind shock wave (on axis of symmetry) for oxygen, nitrogen, and air (sphere, p_∞ = 0.01 atm, T_∞ = 290°K).

Figure 2.21 gives the values of density behind a direct shock wave for oxygen, nitrogen, and air. In comparison with oxygen, in nitrogen and, accordingly, in air a shift of the density maximum toward larger values of M_∞ is observed. It also follows from an examination of Figures 2.20 and 2.21 that the character of behavior of the dependence $\varepsilon_0 = \varepsilon_0 (M_\infty)$ is determined mainly by the character of change of $\rho_1 (M_\infty)$. /71

The composite graph of Figure 2.22 shows the forms of the shock waves, sonic lines, distribution of pressure $\bar{p}_0$ and $\bar{T}_0$ (referred to the corresponding values at the critical point) along the surface of a sphere (δ = 1) and ellipsoids of revolution of different degrees of bluntness (δ = 10 and 100) for equilibrium dissociating air for M_∞ = 6, p_∞ = 1 atm, T_∞ = 300°K. The forms of shock waves and sonic lines in a case of an ideal gas (M_∞ = 6, $\varkappa$ = 1.4) are also given for comparison. Calculations were performed by scheme I, N = 2. It is seen that with an increase of bluntness (increase of δ) there is an ever weaker change of the flow parameters in the subsonic region; however, the law of behavior $\varepsilon(s)$ changes in this case.

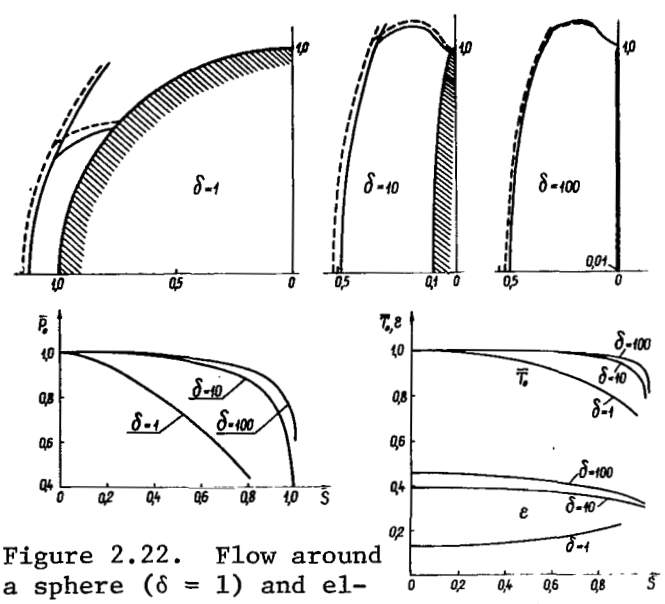

Figure 2.22. Flow around a sphere (δ = 1) and ellipsoids of revolution (δ = 10, 100) by equilibrium air when M_∞ = 6, p_∞ = 1 atm, T_∞ = 300°K (solid line) and an ideal gas M_∞ = 6, $\varkappa$ = 1.4 (dashed line).

Figure 2.23 presents the same dependences for M_∞ = 30, p_∞ = 0.01 atm, T_∞ = 300°K. Analogous calculations were carried out also for the intermediate values of M_∞. The approximations /73 of I. N. Naumova [30] were used here to calculate the thermodynamic functions of air.

Figure 2.24 shows the results of flow around bodies by equilibrium dissociating carbon dioxide CO_2 (M_∞ = 6, p_∞ = 1 atm, T_∞ = 300°K) and an ideal gas (M_∞ = 6, $\varkappa$ = 1.29). Here the system of equations of chemical equilibrium was integrated directly. Calculations were performed also for other mixtures of gases.

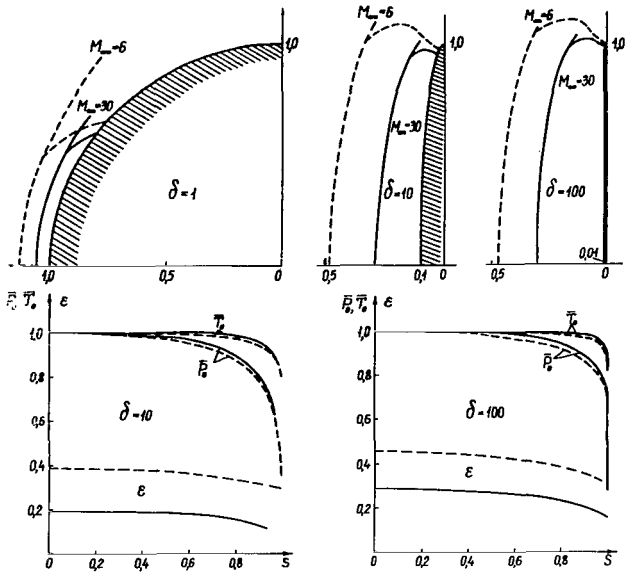

Figure 2.23. Flow around a sphere (δ = 1,) and ellipsoids of revolution (δ = 10, 100) by equilibrium air when M_∞ = 6, /73 p_∞ = 1 atm, T_∞ = 300°K (solid line).

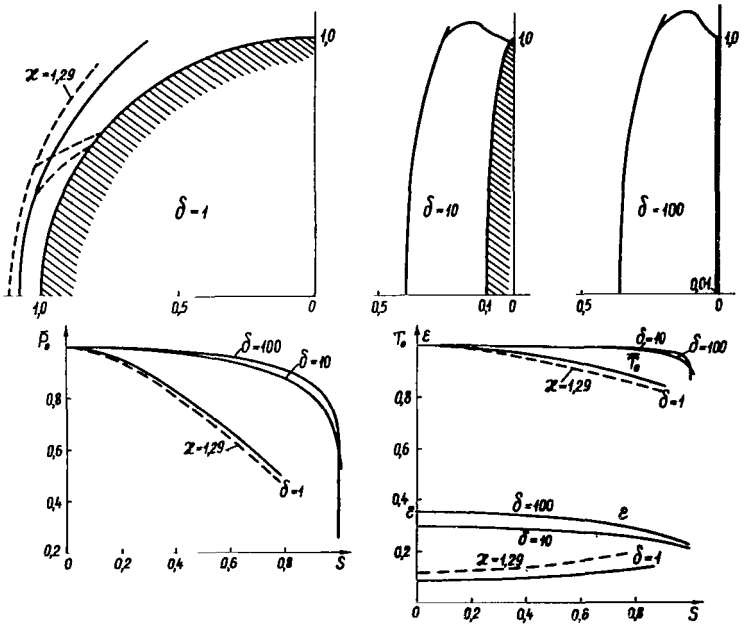

Figure 2.24. Flow past a sphere (δ = 1) and ellipsoids of revolution (δ=10,000) by an equilibrium stream of carbon dioxide when M_∞ = 6, p_∞ = 1 atm, T_∞ = 300°K (δ = 10, 100) (solid line) and by an ideal gas when M_∞ = 6, $\varkappa$ = 1.29 (dashed line).

2. Description of Tables

Tables 2.2-2.9 give the results of calculating the flow of equilibrium oxygen and equilibrium air around a sphere ($\delta = 1$) and ellipsoids of revolution ($\delta = 10, 100$). The calculations were performed by scheme I when N = 2. The following cases were examined:

1) Equilibrium oxygen /74

$M_\infty = 10$; $p_\infty = 0.01$ atm; $T_\infty = 290°K$; $\delta = 1$ (Table 2.2);

2) Equilibrium air

$M_\infty = 4$; $p_\infty = 1$ atm, $T_\infty = 300°K$; $\delta = 10, 100$ (Tables 2.3, 2.4);

$M_\infty = 6$; $p_\infty = 1$ atm, $T_\infty = 300°K$; $\delta = 10, 100$ (Tables 2.5, 2.6);

$M_\infty = 10$; $p_\infty = 0.01$ atm; $T_\infty = 300°K$; $\delta = 10, 100$ (Tables 2.7, 2.8);

$M_\infty = 15$; $p_\infty = 0.01$ atm; $T_\infty = 300°K$; $\delta = 10$ (Table 2.9).

The tables consist of two parts. In the first part the following data on the shock wave and on the surface of the body are given in relation to the length of the arc along the surface of the body s: ε is the distance along the normal from the surface of the body to the shock wave; σ is the angle of inclination of the shock wave to the direction of the oncoming flow; S_1, S_1' are the values of entropy on the shock wave and its derivative with respect to s, respectively; $\overline{p}_0 = p_0(s)/p_0(0)$, $\overline{T}_0 = T_0(s)/T_0(0)$ are the pressure and temperature on the surface of the body respectively, referred to the value of these quantities at the stagnation point.

The second part of the tables presents, depending upon s, the distribution of the following gas dynamic quantities: u_i, v_i are the velocity components along n, s, respectively; p_i is pressure; T_i is temperature; c_i^2 is the square of sound velocity; $w_i^2 = u_i^2 + v_i^2$; ψ_i is the stream function, and the Cartesian coordinates of the boundaries of the zones x_i, y_i are also given (the origin of the coordinates is placed at the center of the body). The values of the functions are given on the surface of the body $\xi = n/\varepsilon(s) = 0 (i = 0)$, on the intermediate line $\xi = 0.5 (i = 2)$, and on the boundary characteristic $\xi = 1 (i = 1)$.

Tables 2.10-2.28 give the results of calculating the flow of equilibrium oxygen, nitrogen, and air around a sphere. The calculations were performed by scheme II when N = 2,3. The following cases were examined:

1) Equilibrium oxygen: $M_\infty = 10$; 15; 18; 20; 21; 22; 23; 24; and 25; $p_\infty = 0.01$ atm; T_∞ 290°K (Tables 2.10-2.18); $M_\infty = 10$; $p_\infty = 0.001$ atm; $T_\infty = 288°K$ (Table 2.19);

2) Equilibrium nitrogen: $M_\infty = 10$; 15; 20; 25; and 27; $p_\infty = 0.01$ atm,

T_∞ = 290°K (Tables 2.20 - 2.24);

3) Equilibrium air: M_∞ = 4; 6; 10; and 30; p_∞ = 1 atm; 0.1 atm; T_∞ = 300°K (Tables 2.25-2.8).

The tables give the values of the following quantities on the axis of symmetry (s = 0), intermediate lines, and boundary characteristic ($s = s_1$): s, u, v, p, T, ρ, h (enthalpy).

Tables 2.29-2.30 present the results of calculations, by the method of characteristics, of gas dynamic quantities in the supersonic region for a smooth body "spherical blunt-cylinder" (Figure 2.25, Table 2.29) and a body with a discontinuity of the generatrix "spherical segment-cylinder" (Figure 2.26, Table 2.30). For flow of equilibrium oxygen (M_∞ = 10, p_∞ = 0.001 atm, T_∞ = 288°K) the initial data were obtained by scheme II of the method of integral relations. The Tables present the following quantities on the surface of the body: x_0, y_0, = r_0 - Cartesian coordinates of points on the body (the origin of the coordinates is placed at the critical point of the body), p_0, T_0, ρ_0, w_0, $\zeta_0 = \tan\theta$ - tangent of the angle of inclination of the velocity vector with the x-axis, $(C_0)_0$ - mass concentration of atomic oxygen. The coordinates of the nose shock wave x_B, $y_B = r_B$ are also given there. /75 /76

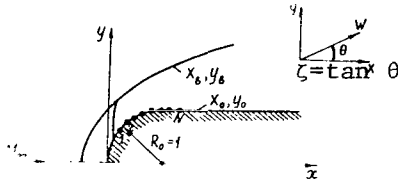

Figure 2.25. Form of smooth body "spherical blunt-cylinder" and position of points at which the data of Table 2.29 are given (calculation of supersonic region by the method of characteristics).

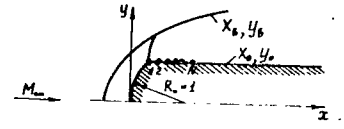

Figure 2.26. Body form with discontinuity "spherical segment-cylinder" and location of points at which data of Table 2.30 are given (calculation of supersonic region by the method of characteristics).

We must bear in mind that the values of velocity are referred to w_{max}, of pressure to $\rho_\infty w^2_{max}$, of density to ρ_∞, of temperature to $\mu_\infty w^2_{max}/R$, of enthalpy to $w^2_{max}/2$, of entropy to $R/2\mu_\infty$. All linear dimensions are referred to the characteristic dimension of the body (to the radius for a sphere and to the vertical semiaxis b for ellipsoids). The values before the shock wave are indicated by the subscript ∞.

3. Calculations of Flows at Low Supersonic Velocities

In concluding the chapter we will dwell on the results of calculating flows at low supersonic velocities. In a number of cases such flows are of considerable practical interest.

Some data on the flow of air around a sphere at Mach numbers of the oncoming flow of $1.05 \leq M_\infty \leq 2$ are given below. We note that at such velocities the effects associated with excitation of internal degrees of freedom of molecules can be disregarded and we can treat the air as an ideal gas with a constant heat capacity ($\varkappa = 1.4$). The calculations were performed by S. D. Popov by scheme III of the method of integral relations. Between the wave and the body in all variants was drawn one intermediate line (second approximation with respect to n), and four rays, not counting the axis of symmetry (the fourth approximation with respect to s), were examined in the upper half-plane for $M_\infty \geq 1.5$, and five rays were used for $M_\infty < 1.5$.

Figures 2.27-2.29 show the form and position of the shock waves and sonic lines for $M_\infty = 2$ (Figure 2.27), $M_\infty = 1.7$ (Figure 2.28), and $M_\infty = 1.5$ (Figure 2.29). The lines of flow are also plotted on the graphs. Calculation of the lines of flow gives more complete information about the parameters in the shock layer and, in particular, permits a sufficiently accurate determination of the sonic line.

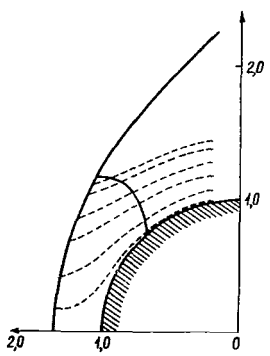

Figure 2.27. Position and form of shock wave, sonic line, and lines of flow (dashed lines) for $M_\infty = 2.0$ (sphere).

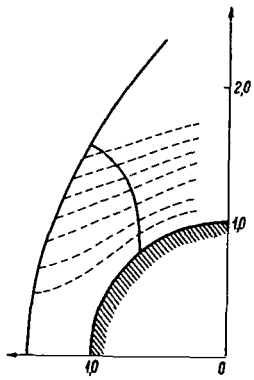

Figure 2.28. Position and form of shock wave, sonic line, and lines of flow (dashed lines) for $M_\infty = 1.7$ (sphere).

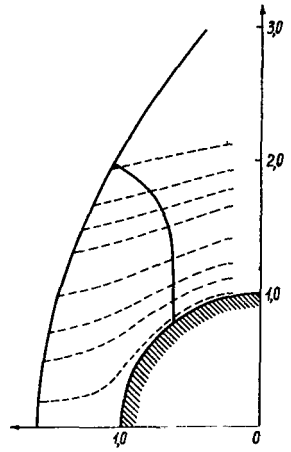

Figure 2.29. Position and form of shock wave, sonic line, and lines of flow (dashed lines) for $M_\infty = 1.5$ (sphere).

Figure 2.30 presents the separation of the shock wave ε_0 along the axis of the symmetry as a function of the change of the Mach number M_∞. The dots designate experimental data obtained by V. G. Maslennikov [33]. We see that

the coincidence of the results is good starting from $M_\infty = 1.25$. At lower Mach numbers of the oncoming flow the divergence of the experimental and theoretical data is noticeable. This is apparently explained by the insufficient accuracy of the calculations, since with a decrease of M_∞ the region of influence markedly increases this requires the use of a higher approximation with respect to n. /79

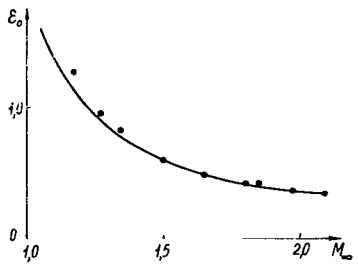

Figure 2.30. Dependence on M_∞ of the magnitude of shock-wave separation along axis of symmetry of sphere: —— scheme III of the method of integral relations; ... experimental data of V. G. Maslennikov [33].

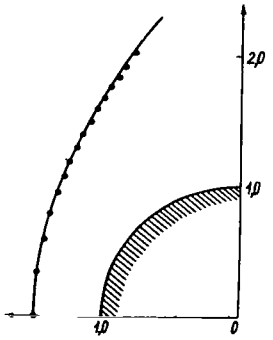

Figure 2.32. Comparison of experiemental data (dots) and theoretical results (curve) with respect to position and form of shock wave for M_∞ = 1.65.

Figures 2.31 and 2.32 show the position and form of shock waves for $M_\infty = 2.09$ and M_∞ = 1.65. Here the dots pertain to the experimental data of V. G. Maslennikov [34]. We see that the coincidence of the results is very good.

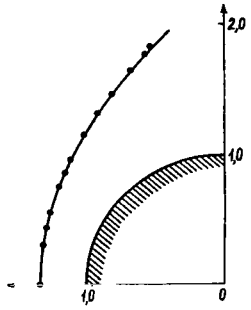

Figure 2.31. Comparison of experimental data (dots) and theoretical results (curve) with respect to position and form of shock wave for $M_\infty = 2.09$.

Figures 2.33 and 2.34 give the distribution of pressure on the surface of a sphere (referred to the pressure at the stagnation point) and the position of shock waves for different values of M_∞. The curves pertain, respectively, to M_∞ = 1.05; 1.1; 1.2; 1.3; 1.5; 1.7; and 2.0. With a decrease of M_∞ the distribution of pressure differs more appreciably from Newtonian, which is usually used in the theory of supersonic flows. In this case the nose shock wave separates ever farther from the body and straightens out.

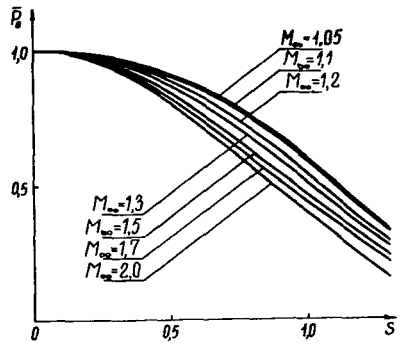

Figure 2.33. Distribution of pressure p_0 over surface of sphere for different values of M_∞.

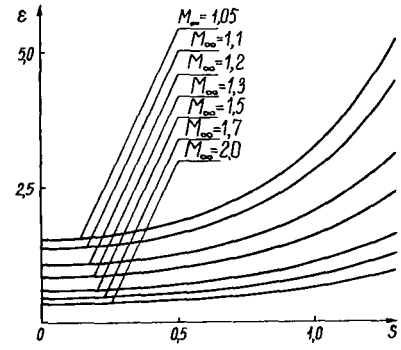

Figure 2.34. Form of shock waves for various values of M_∞.

Scheme III of the method of integral relations proved to be effective for calculating flow around bodies at low supersonic velocities. The use of schemes I and II for this purpose causes appreciable computational difficulties when solving the corresponding boundary-value problems for approximating systems, since with a decrease of the Mach number of the oncoming flow the dependence of the solution on the initial data increases, the round-off errors increase, and instability appears in the calculation. We note that in scheme II at M_∞ numbers close to unity a singularity appears in the approximating system analogous to that in scheme I, since the normal component of the flow velocity proves to be close to the velocity of sound. In scheme III, where the approximating system is a system of algebraic equations, there are no such singularities, therefore the procedure of calculation of different cases, for example when $M_\infty = 10$ and $M_\infty = 1.05$, is completely analogous and requires approximately the same expenditure of machine time (about 10 min on the BESM-2 electronic computer for approximation 2 x 5).

TABLE 2.1

COMPARISON OF COMPUTATIONAL RESULTS BY DIFFERENT METHODS OF CALCULATING THERMODYNAMIC FUNCTIONS OF AIR

/80

(Sphere: $M_\infty = 10$; $p_\infty = 0.01$ atm; $T_\infty = 300°K$)

	ξ	$s_1(\xi)$	u_1	v_1	p_1	T_1
Calculation "A"	1.000	1.000	0.0634	0.676	0.437	0.06119
	0.891	0.949	0.0402	0.644	0.434	0.06407
	0.766	0.901	0.0210	0.598	0.433	0.06718
	0.641	0.863	0.00837	0.550	0.434	0.06981
	0.516	0.833	+0.000414	0.503	0.436	0.07192
	0.391	0.808	−0.00313	0.460	0.437	0.07355
	0.266	0.789	−0.00415	0.422	0.438	0.07482
	0.141	0.773	−0.00306	0.388	0.437	0.07581
	0.000	0.760	+0.0000888	0.357	0.435	0.07663
Calculation "B"	1.000	1.000	0.0628	0.678	0.436	0.06112
	0.891	0.949	0.0397	0.644	0.433	0.06402
	0.766	0.901	0.0206	0.599	0.432	0.06711
	0.641	0.864	0.00800	0.551	0.432	0.06974
	0.516	0.833	+0.000441	0.504	0.433	0.07181
	0.391	0.809	−0.00331	0.461	0.434	0.07343
	0.266	0.789	−0.00426	0.424	0.435	0.07469
	0.141	0.773	−0.00310	0.390	0.434	0.07567
	0.000	0.762	+0.0000428	0.359	0.432	0.07648

EQUILIBRIUM OXYGEN. SCHEME I. N = 2

TABLE 2.2

$M_\infty = 10$; $p_\infty = 0.01$ atm; $T_\infty = 290°K$; $\rho_\infty = 0.01345$ kg/m^3;

$w_{max} = 3328.1$ m/sec; $h_{00} = 21\ 315°K$; $\delta = 1$

ξ	ε	σ	$\bar{p}_0$	$\bar{T}_0$
0.0000	0.0758	1.570	1.000	1.000
0.0625	0.0791	1.515	0.995	0.999
0.1250	0.0798	1.460	0.981	0.998
0.1875	0.0811	1.406	0.958	0.996
0.2500	0.0830	1.352	0.927	0.993
0.3125	0.0855	1.299	0.888	0.989
0.3750	0.0887	1.247	0.844	0.985
0.4375	0.0926	1.196	0.792	0.980
0.5000	0.0974	1.146	0.738	0.974
0.5625	0.103	1.099	0.682	0.967
0.6250	0.110	1.056	0.629	0.960
0.6875	0.118	1.016	0.577	0.953
0.7500	0.129	0.979	0.528	0.946
0.8125	0.141	0.942	0.482	0.938

s	u	v	p	T	c^2	w^2	-x	y	C_0
				$\xi = 0$					
0.0000	0	0.0000	0.913	0.0769	0.0974	0.000000	1.000	0.0000	0.114
0.0625	0	0.0285	0.909	0.0768	0.0973	0.000816	0.998	0.0624	0.114
0.1250	0	0.0569	0.896	0.0767	0.0971	0.00323	0.992	0.124	0.114
0.1875	0	0.0850	0.875	0.0766	0.0969	0.00723	0.982	0.186	0.113
0.2500	0	0.113	0.847	0.0764	0.0965	0.0128	0.968	0.247	0.112
0.3125	0	0.141	0.811	0.0761	0.0960	0.0200	0.951	0.307	0.110
0.3750	0	0.169	0.770	0.0757	0.0953	0.0287	0.930	0.366	0.108
0.4375	0	0.198	0.724	0.0753	0.0946	0.0392	0.905	0.423	0.106
0.5000	0	0.226	0.673	0.0749	0.0938	0.0511	0.877	0.479	0.103
0.5625	0	0.252	0.623	0.0743	0.0929	0.0639	0.845	0.533	0.101
0.6250	0	0.277	0.574	0.0738	0.0920	0.0771	0.810	0.585	0.0985
0.6875	0	0.301	0.527	0.0733	0.0910	0.0910	0.772	0.634	0.0956
0.7500	0	0.324	0.483	0.0727	0.0901	0.105	0.731	0.681	0.0926
0.8125	0	0.345	0.441	0.0721	0.0891	0.119	0.687	0.726	0.0896

TABLE 2.2 Continued

s	u	v	p	T	c^2	w^2	$-x$	y	C_0
				$\xi = 0.5$					
0.0000	-0.0420	0.0000	0.903	0.0768	0.0972	0.00176	1.039	0.0000	0.114
0.0625	-0.0415	0.0409	0.900	0.0767	0.0971	0.00340	1.037	0.0649	0.114
0.1250	-0.0411	0.0818	0.888	0.0766	0.0969	0.00829	1.031	0.129	0.112
0.1875	-0.0404	0.122	0.870	0.0764	0.0964	0.0166	1.022	0.193	0.110
0.2500	-0.0394	0.162	0.845	0.0760	0.0957	0.0280	1.009	0.257	0.108
0.3125	-0.0380	0.202	0.815	0.0756	0.0949	0.0423	0.992	0.320	0.104
0.3750	-0.0362	0.241	0.778	0.0751	0.0939	0.0594	0.971	0.382	0.100
0.4375	-0.0338	0.278	0.738	0.0745	0.0928	0.0788	0.947	0.443	0.0955
0.5000	-0.0308	0.315	0.694	0.0739	0.0915	0.100	0.920	0.502	0.0904
0.5625	-0.0269	0.349	0.650	0.0732	0.0902	0.122	0.889	0.560	0.0850
0.6250	-0.0216	0.381	0.608	0.0724	0.0889	0.146	0.855	0.617	0.0794
0.6875	-0.0146	0.411	0.567	0.0717	0.0875	0.169	0.818	0.672	0.0740
0.7500	-0.00571	0.438	0.527	0.0709	0.0862	0.192	0.778	0.725	0.0687
0.8125	0.00576	0.463	0.489	0.0701	0.0849	0.214	0.736	0.777	0.0635
				$\xi = 1$					
0.0000	-0.0960	0.0000	0.865	0.0765	0.0967	0.00922	1.078	0.0000	0.112
0.0625	-0.0956	0.0543	0.862	0.0764	0.0966	0.0121	1.077	0.0674	0.112
0.1250	-0.0944	0.108	0.854	0.0762	0.0961	0.0207	1.071	0.134	0.109
0.1875	-0.0923	0.161	0.841	0.0759	0.0954	0.0346	1.062	0.201	0.106
0.2500	-0.0893	0.213	0.822	0.0754	0.0944	0.0537	1.049	0.267	0.101
0.3125	-0.0853	0.264	0.800	0.0748	0.0931	0.0774	1.032	0.333	0.0951
0.3750	-0.0802	0.314	0.773	0.0741	0.0917	0.105	1.013	0.398	0.0879
0.4375	-0.0737	0.361	0.744	0.0732	0.0900	0.136	0.989	0.462	0.0801
0.5000	-0.0659	0.407	0.711	0.0723	0.0882	0.170	0.962	0.525	0.0716
0.5625	-0.0561	0.449	0.678	0.0712	0.0863	0.205	0.933	0.588	0.0631
0.6250	-0.0436	0.487	0.645	0.0701	0.0845	0.239	0.900	0.649	0.0550
0.6875	-0.0283	0.521	0.614	0.0689	0.0826	0.273	0.864	0.709	0.0474
0.7500	-0.0106	0.552	0.583	0.0677	0.0808	0.305	0.825	0.769	0.0402
0.8125	+0.00876	0.581	0.552	0.0663	0.0790	0.338	0.784	0.828	0.0333

EQUILIBRIUM AIR. SCHEME I. N = 2

/83

TABLE 2.3

$M_\infty = 4$; $p_\infty = 1$ atm; $T_\infty = 300°K$; $\rho_\infty = 1.1765$ kg/m^3;

$w_{max} = 1591$ m/sec; $h_{00} = 4408°K$; $\delta = 10$

s	ε	σ	S_1	S_1'	$\bar{p}_0$	$\bar{T}_0$
0.0000	0.483	1.570	0.00000	0.0000	1.000	1.000
0.0625	0.483	1.553	-0.00110	- 0.0354	0.999	1.000
0.1250	0.482	1.536	-0.00443	- 0.0711	0.998	0.999
0.1875	0.480	1.518	-0.00999	- 0.106	0.996	0.999
0.2500	0.477	1.501	-0.0177	- 0.142	0.993	0.998
0.3125	0.474	1.484	-0.0278	- 0.180	0.990	0.997
0.3750	0.470	1.466	-0.0404	- 0.221	0.985	0.996
0.4375	0.465	1.448	-0.0556	- 0.266	0.979	0.994
0.5000	0.460	1.429	-0.0738	- 0.318	0.971	0.993
0.5625	0.454	1.410	-0.0955	- 0.376	0.962	0.990
0.6250	0.448	1.389	-0.121	- 0.443	0.949	0.987
0.6875	0.440	1.368	-0.151	- 0.522	0.933	0.982
0.7500	0.433	1.345	-0.186	- 0.616	0.911	0.977
0.8125	0.424	1.321	-0.229	- 0.744	0.881	0.969
0.8750	0.416	1.294	-0.281	- 0.986	0.836	0.956
0.9375	0.408	1.255	-0.364	- 1.895	0.757	0.934
0.9531	0.406	1.241	-0.398	- 2.601	0.725	0.924
0.9688	0.406	1.220	-0.449	- 4.052	0.679	0.909
0.9844	0.407	1.187	-0.536	- 7.812	0.603	0.883
1.0000	0.420	1.118	-0.746	- 23.82	0.421	0.808

s	u	v	p	T	c^2	w^2	ψ	$-x$	y
				$\xi = 0$					
0.0000	0	0.0000	0.722	0.134	0.177	0.000000	0	0.1000	0.0000
0.0625	0	0.0101	0.722	0.134	0.177	0.000103	0	0.0998	0.0625
0.1250	0	0.0202	0.721	0.134	0.177	0.000411	0	0.0992	0.125
0.1875	0	0.0304	0.720	0.134	0.177	0.000927	0	0.0982	0.187
0.2500	0	0.0408	0.718	0.134	0.177	0.00166	0	0.0968	0.250
0.3125	0	0.0515	0.715	0.134	0.177	0.00265	0	0.0949	0.312
0.3750	0	0.0627	0.712	0.134	0.177	0.00393	0	0.0927	0.374
0.4375	0	0.0745	0.708	0.133	0.176	0.00556	0	0.0899	0.437
0.5000	0	0.0874	0.702	0.133	0.176	0.00764	0	0.0866	0.499
0.5625	0	0.101	0.695	0.133	0.176	0.0103	0	0.0827	0.562

TABLE 2.3 Continued

s	u	v	p	T	c^2	w^2	ψ	−x	y
0.6250	0	0.117	0.686	0.132	0.175	0.0137	0	0.0781	0.624
0.6875	0	0.135	0.674	0.132	0.174	0.0183	0	0.0726	0.686
0.7500	0	0.156	0.659	0.131	0.173	0.0246	0	0.0662	0.748
0.8125	0	0.183	0.637	0.130	0.172	0.0335	0	0.0585	0.810
0.8750	0	0.217	0.604	0.128	0.170	0.0471	0	0.0488	0.872
0.9375	0	0.268	0.547	0.125	0.166	0.0723	0	0.0357	0.933
0.9531	0	0.288	0.524	0.124	0.165	0.0832	0	0.0315	0.948
0.9688	0	0.315	0.490	0.122	0.162	0.0993	0	0.0267	0.963
0.9844	0	0.357	0.436	0.118	0.158	0.128	0	0.0208	0.978
1.0000	0	0.457	0.304	0.108	0.145	0.209	0	0.0129	0.991
				$\xi = 0.5$					
0.0000	−0.0828	0.0000	0.704	0.133	0.176	0.00686	0.000000	0.341	0.0000
0.0625	−0.0823	0.0116	0.704	0.133	0.176	0.00690	0.000888	0.341	0.0640
0.1250	−0.0825	0.0233	0.704	0.133	0.176	0.00735	0.00355	0.340	0.128
0.1875	−0.0830	0.0352	0.702	0.133	0.176	0.00813	0.00799	0.338	0.192
0.2500	−0.0838	0.0474	0.701	0.133	0.176	0.00927	0.0142	0.335	0.256
0.3125	−0.0849	0.0599	0.698	0.133	0.176	0.0108	0.0223	0.332	0.320
0.3750	−0.0863	0.0728	0.695	0.133	0.175	0.0127	0.0322	0.327	0.384
0.4375	−0.0880	0.0863	0.691	0.132	0.175	0.0152	0.0440	0.322	0.448
0.5000	−0.0900	0.100	0.686	0.132	0.174	0.0181	0.0577	0.316	0.513
0.5625	−0.0925	0.115	0.680	0.131	0.174	0.0218	0.0735	0.309	0.577
0.6250	−0.0954	0.131	0.673	0.131	0.173	0.0263	0.0915	0.301	0.642
0.6875	−0.0990	0.148	0.663	0.130	0.172	0.0317	0.111	0.292	0.707
0.7500	−0.103	0.167	0.651	0.129	0.171	0.0385	0.134	0.281	0.773
0.8125	−0.107	0.188	0.635	0.128	0.170	0.0471	0.160	0.268	0.840
0.8750	−0.111	0.213	0.615	0.127	0.168	0.0581	0.189	0.253	0.909
0.9375	−0.109	0.245	0.589	0.125	0.166	0.0719	0.225	0.233	0.985
0.9531	−0.104	0.254	0.583	0.125	0.166	0.0756	0.236	0.226	1.007
0.9688	−0.0942	0.264	0.578	0.124	0.165	0.0789	0.248	0.217	1.032
0.9844	−0.0709	0.276	0.576	0.124	0.165	0.0813	0.263	0.205	1.064
1.0000	−0.00208	0.298	0.563	0.123	0.164	0.0891	0.284	0.179	1.119
				$\xi = 1$					
0.0000	−0.178	0.0000	0.641	0.130	0.172	0.0316	0.00000	0.583	0.0000
0.0625	−0.178	0.0131	0.641	0.130	0.172	0.0319	0.00187	0.582	0.0655
0.1250	−0.178	0.0263	0.640	0.130	0.172	0.0325	0.00750	0.581	0.131
0.1875	−0.179	0.0395	0.639	0.130	0.172	0.0337	0.0168	0.578	0.196
0.2500	−0.180	0.0527	0.638	0.130	0.172	0.0353	0.0300	0.574	0.262
0.3125	−0.181	0.0660	0.636	0.130	0.172	0.0373	0.0470	0.569	0.328
0.3750	−0.183	0.0795	0.634	0.129	0.171	0.0398	0.0677	0.562	0.393
0.4375	−0.185	0.0934	0.631	0.129	0.171	0.0429	0.0924	0.555	0.460
0.5000	−0.187	0.107	0.628	0.128	0.170	0.0466	0.121	0.546	0.526
0.5625	−0.189	0.122	0.624	0.128	0.169	0.0509	0.153	0.536	0.593
0.6250	−0.192	0.138	0.620	0.127	0.169	0.0560	0.190	0.524	0.660
0.6875	−0.194	0.155	0.614	0.127	0.168	0.0620	0.231	0.511	0.728
0.7500	−0.197	0.173	0.608	0.126	0.167	0.0691	0.277	0.496	0.797
0.8125	−0.199	0.194	0.601	0.125	0.165	0.0774	0.330	0.479	0.869
0.8750	−0.198	0.220	0.592	0.123	0.164	0.0878	0.390	0.458	0.945
0.9375	−0.190	0.259	0.578	0.121	0.161	0.103	0.469	0.430	1.036
0.9531	−0.185	0.275	0.572	0.121	0.160	0.110	0.496	0.421	1.065
0.9688	−0.175	0.298	0.564	0.119	0.159	0.120	0.529	0.408	1.101
0.9844	−0.154	0.335	0.549	0.117	0.156	0.136	0.579	0.389	1.151
1.0000	−0.0923	0.408	0.515	0.113	0.150	0.175	0.679	0.346	1.247

TABLE 2.4

/85

$M_\infty = 4$; $p_\infty = 1$ atm; $T_\infty = 300°K$; $\rho_\infty = 1.1765$ kg/m^3;

$w_{max} = 1591$ m/sec: $h_{00} = 4408°K$; $\delta = 100$

s	ε	σ	S_1	S_1'	$\bar{p}_0$	$\bar{T}_0$
0.0000	0.501	1.570	0.00000	0.0000	1.000	1.000
0.0625	0.501	1.553	-0.00106	- 0.0342	0.999	1.000
0.1250	0.499	1.536	-0.00427	- 0.0686	0.998	1.000
0.1875	0.497	1.519	-0.00964	- 0.103	0.997	0.999
0.2500	0.493	1.502	-0.0171	- 0.138	0.995	0.999
0.3125	0.489	1.485	-0.0269	- 0.175	0.992	0.998
0.3750	0.483	1.467	-0.0391	- 0.215	0.988	0.997
0.4375	0.476	1.449	-0.0540	- 0.263	0.983	0.996
0.5000	0.468	1.430	-0.0722	- 0.319	0.977	0.994
0.5625	0.459	1.411	-0.0942	- 0.388	0.968	0.992
0.6250	0.449	1.389	-0.121	- 0.474	0.957	0.989
0.6875	0.437	1.366	-0.154	- 0.583	0.943	0.985
0.7500	0.424	1.340	-0.194	- 0.729	0.923	0.980
0.8125	0.409	1.312	-0.246	- 0.937	0.893	0.973
0.8750	0.392	1.278	-0.314	- 1.288	0.848	0.960
0.9375	0.372	1.233	-0.417	- 2.197	0.769	0.938
0.9882	0.350	1.155	-0.628	- 11.034	0.618	0.889
0.9941	0.344	1.123	-0.727	- 27.427	0.564	0.869
0.9990	0.327	0.948	-1.387	- 641.47	0.357	0.774

/86

s	u	v	p	T	c^2	w^2	ψ	-x	y
					$\xi = 0$				
0.0000	0	0.00000	0.722	0.134	0.177	0.0000000	0	0.01000	0.0000
0.0625	0	0.00911	0.722	0.134	0.177	0.0000829	0	0.00998	0.0625
0.1250	0	0.0181	0.721	0.134	0.177	0.000329	0	0.00992	0.125
0.1875	0	0.0272	0.720	0.134	0.177	0.000741	0	0.00982	0.187
0.2500	0	0.0365	0.719	0.134	0.177	0.00134	0	0.00968	0.250
0.3125	0	0.0460	0.717	0.134	0.177	0.00212	0	0.00949	0.312
0.3750	0	0.0561	0.714	0.134	0.177	0.00315	0	0.00927	0.375
0.4375	0	0.0669	0.710	0.134	0.177	0.00448	0	0.00899	0.437
0.5000	0	0.0788	0.706	0.133	0.176	0.00621	0	0.00866	0.500
0.5625	0	0.0920	0.700	0.133	0.176	0.00847	0	0.00826	0.562
0.6250	0	0.107	0.692	0.133	0.175	0.0114	0	0.00780	0.625
0.6875	0	0.124	0.681	0.132	0.175	0.0155	0	0.00726	0.687
0.7500	0	0.146	0.667	0.131	0.174	0.0213	0	0.00661	0.750
0.8125	0	0.172	0.645	0.130	0.173	0.0298	0	0.00582	0.812
0.8750	0	0.208	0.613	0.129	0.171	0.0434	0	0.00484	0.874
0.9375	0	0.261	0.556	0.126	0.167	0.0683	0	0.00348	0.937
0.9882	0	0.349	0.446	0.119	0.158	0.122	0	0.00153	0.988
0.9941	0	0.378	0.408	0.116	0.155	0.143	0	0.00108	0.994
0.9990	0	0.494	0.258	0.104	0.139	0.244	0	0.000471	0.999

TABLE 2.4 Continued

/86

s	u	v	p	T	c^2	w^2	ψ	−x	y
				$\xi = 0.5$					
0.0000	−0.0802	0.0000	0.705	0.133	0.176	0.00643	0.000000	0.260	0.0000
0.0625	−0.0794	0.0105	0.705	0.133	0.176	0.00642	0.000823	0.260	0.0626
0.1250	−0.0797	0.0211	0.705	0.133	0.176	0.00680	0.00328	0.259	0.125
0.1875	−0.0803	0.0319	0.704	0.133	0.176	0.00748	0.00740	0.258	0.187
0.2500	−0.0814	0.0431	0.703	0.133	0.176	0.00848	0.0131	0.256	0.250
0.3125	−0.0827	0.0546	0.701	0.133	0.176	0.00983	0.0206	0.253	0.313
0.3750	−0.0845	0.0666	0.698	0.133	0.175	0.0115	0.0298	0.250	0.375
0.4375	−0.0867	0.0792	0.695	0.132	0.175	0.0138	0.0407	0.247	0.438
0.5000	−0.0894	0.0925	0.690	0.132	0.175	0.0165	0.0534	0.242	0.501
0.5625	−0.0927	0.106	0.685	0.132	0.174	0.0200	0.0680	0.238	0.564
0.6250	−0.0969	0.122	0.677	0.131	0.173	0.0243	0.0844	0.232	0.626
0.6875	−0.102	0.139	0.668	0.130	0.173	0.0297	0.102	0.225	0.689
0.7500	−0.109	0.158	0.654	0.130	0.172	0.0369	0.123	0.218	0.752
0.8125	−0.117	0.180	0.636	0.128	0.170	0.0465	0.146	0.210	0.815
0.8750	−0.129	0.208	0.609	0.127	0.168	0.0604	0.172	0.200	0.878
0.9375	−0.145	0.248	0.564	0.124	0.165	0.0828	0.200	0.189	0.942
0.9882	−0.153	0.311	0.489	0.119	0.159	0.120	0.224	0.176	0.999
0.9941	−0.145	0.331	0.469	0.118	0.157	0.130	0.226	0.172	1.009
0.9990	−0.0753	0.543	0.205	0.0993	0.133	0.301	0.225	0.160	1.032

/87

				$\xi = 1$					
0.0000	−0.178	0.0000	0.641	0.130	0.172	0.0316	0.00000	0.511	0.0000
0.0625	−0.178	0.0118	0.641	0.130	0.172	0.0319	0.00172	0.511	0.0628
0.1250	−0.178	0.0238	0.640	0.130	0.172	0.0325	0.00689	0.509	0.125
0.1875	−0.179	0.0357	0.639	0.130	0.172	0.0336	0.0155	0.507	0.188
0.2500	−0.181	0.0476	0.638	0.130	0.172	0.0351	0.0275	0.503	0.251
0.3125	−0.183	0.0596	0.636	0.130	0.172	0.0371	0.0430	0.498	0.314
0.3750	−0.185	0.0717	0.634	0.129	0.171	0.0396	0.0620	0.492	0.376
0.4375	−0.188	0.0841	0.631	0.129	0.171	0.0426	0.0844	0.485	0.439
0.5000	−0.192	0.0969	0.628	0.128	0.170	0.0462	0.110	0.477	0.502
0.5625	−0.196	0.110	0.624	0.128	0.169	0.0507	0.139	0.467	0.565
0.6250	−0.201	0.124	0.620	0.127	0.169	0.0560	0.172	0.457	0.628
0.6875	−0.207	0.139	0.614	0.126	0.168	0.0626	0.208	0.444	0.691
0.7500	−0.215	0.156	0.607	0.125	0.166	0.0707	0.248	0.430	0.754
0.8125	−0.224	0.174	0.598	0.124	0.165	0.0809	0.292	0.415	0.818
0.8750	−0.237	0.194	0.586	0.123	0.163	0.0942	0.339	0.396	0.882
0.9375	−0.254	0.222	0.569	0.120	0.160	0.114	0.392	0.375	0.947
0.9882	−0.283	0.271	0.534	0.115	0.154	0.153	0.446	0.351	1.010
0.9941	−0.292	0.293	0.518	0.113	0.151	0.172	0.459	0.344	1.025
0.9990	−0.358	0.398	0.418	0.0988	0.132	0.287	0.496	0.320	1.066

TABLE 2.5

/88

$M_\infty = 6$; $p_\infty = 1$ atm; $T_\infty = 300°K$; $\rho_\infty = 1.1765$ kg/m^3;

$w_{max} = 2223$ m/sec; $h_{00} = 8612°K$; $\delta = 10$

s	ε	σ	S_1	S_1'	$\bar{p}_0$	$\bar{T}_0$
0.0000	0.399	1.570	0.00000	0.0000	1.000	1.000
0.0625	0.399	1.553	-0.00146	- 0.0470	0.999	0.999
0.1250	0.398	1.536	-0.00588	- 0.0944	0.998	0.999
0.1875	0.396	1.519	-0.0132	- 0.142	0.996	0.999
0.2500	0.393	1.502	-0.0237	- 0.193	0.994	0.998
0.3125	0.390	1.484	-0.0375	- 0.247	0.990	0.997
0.3750	0.386	1.466	-0.0548	- 0.309	0.985	0.996
0.4375	0.382	1.447	-0.0764	- 0.381	0.980	0.995
0.5000	0.377	1.428	-0.102	- 0.465	0.972	0.993
0.5625	0.371	1.407	-0.135	- 0.567	0.962	0.991
0.6250	0.364	1.384	-0.174	- 0.691	0.949	0.988
0.6875	0.356	1.360	-0.222	- 0.848	0.932	0.984
0.7500	0.348	1.334	-0.281	- 1.057	0.909	0.979
0.8125	0.339	1.304	-0.356	- 1.358	0.875	0.971
0.8750	0.329	1.270	-0.455	- 1.904	0.824	0.959
0.9375	0.319	1.221	-0.616	- 3.661	0.731	0.935
0.9531	0.317	1.202	-0.682	- 4.899	0.694	0.923
0.9687	0.315	1.178	-0.775	- 7.379	0.643	0.908
0.9843	0.314	1.140	-0.931	- 13.713	0.556	0.879
1.0000	0.321	1.059	-1.318	- 52.648	0.396	0.814

s	u	v	p	T	c^2	w^2	ψ	$-x$	y
				$\xi = 0$					
0.0000	0	0.00000	0.827	0.124	0.158	0.0000000	0	0.1000	0.0000
0.0625	0	0.00951	0.827	0.124	0.158	0.0000905	0	0.0998	0.0624
0.1250	0	0.0189	0.826	0.124	0.158	0.000360	0	0.0992	0.124
0.1875	0	0.0285	0.824	0.124	0.157	0.000815	0	0.0982	0.187
0.2500	0	0.0383	0.822	0.124	0.157	0.00147	0	0.0968	0.249
0.3125	0	0.0485	0.819	0.124	0.157	0.00235	0	0.0949	0.312
0.3750	0	0.0592	0.815	0.124	0.157	0.00350	0	0.0927	0.374
0.4375	0	0.0707	0.811	0.124	0.157	0.00500	0	0.0899	0.437
0.5000	0	0.0833	0.804	0.124	0.157	0.00694	0	0.0866	0.499
0.5625	0	0.0973	0.796	0.123	0.156	0.00946	0	0.0827	0.562

TABLE 2.5 Continued

/89

s	u	v	p	T	c^2	w^2	ψ	−x	y
0.6250	0	0.113	0.785	0.123	0.156	0.0127	0	0.0781	0.624
0.6875	0	0.131	0.771	0.122	0.155	0.0172	0	0.0726	0.686
0.7500	0	0.153	0.752	0.122	0.154	0.0235	0	0.0662	0.748
0.8125	0	0.180	0.724	0.121	0.153	0.0326	0	0.0585	0.810
0.8750	0	0.217	0.681	0.119	0.151	0.0472	0	0.0488	0.872
0.9375	0	0.274	0.605	0.116	0.148	0.0752	0	0.0357	0.933
0.9531	0	0.295	0.574	0.115	0.148	0.0874	0	0.0315	0.948
0.9687	0	0.323	0.532	0.113	0.146	0.104	0	0.0267	0.963
0.9843	0	0.370	0.460	0.109	0.142	0.137	0	0.0208	0.978
1.0000	0	0.456	0.328	0.101	0.132	0.208	0	0.0129	0.991
				$\xi = 0.5$					
0.0000	−0.0680	0.0000	0.812	0.124	0.157	0.00463	0.000000	0.299	0.0000
0.0625	−0.0676	0.0120	0.812	0.124	0.157	0.00472	0.000900	0.299	0.0637
0.1250	−0.0678	0.0241	0.811	0.124	0.157	0.00519	0.00359	0.298	0.127
0.1875	−0.0683	0.0364	0.810	0.124	0.157	0.00600	0.00810	0.296	0.191
0.2500	−0.0691	0.0491	0.808	0.124	0.157	0.00718	0.0144	0.293	0.255
0.3125	−0.0700	0.0620	0.805	0.123	0.156	0.00876	0.0225	0.290	0.318
0.3750	−0.0713	0.0755	0.802	0.123	0.156	0.0107	0.0326	0.285	0.382
0.4375	−0.0728	0.0895	0.797	0.123	0.156	0.0133	0.0445	0.280	0.446
0.5000	−0.0747	0.104	0.791	0.123	0.155	0.0164	0.0583	0.274	0.510
0.5625	−0.0769	0.119	0.784	0.122	0.155	0.0202	0.0742	0.267	0.574
0.6250	−0.0797	0.136	0.775	0.122	0.154	0.0250	0.0921	0.259	0.639
0.6875	−0.0830	0.155	0.763	0.121	0.153	0.0309	0.112	0.250	0.703
0.7500	−0.0869	0.175	0.747	0.120	0.152	0.0384	0.134	0.239	0.768
0.8125	−0.0912	0.199	0.726	0.119	0.151	0.0481	0.159	0.226	0.834
0.8750	−0.0951	0.228	0.697	0.118	0.149	0.0612	0.188	0.211	0.901
0.9375	−0.0922	0.266	0.655	0.116	0.147	0.0796	0.220	0.190	0.974
0.9531	−0.0869	0.278	0.643	0.115	0.148	0.0852	0.229	0.183	0.994
0.9687	−0.0759	0.292	0.630	0.114	0.148	0.0911	0.238	0.175	1.017
0.9843	−0.0506	0.309	0.615	0.114	0.147	0.0980	0.248	0.163	1.045
1.0000	+0.0216	0.351	0.552	0.111	0.144	0.123	0.259	0.140	1.089
				$\xi = 1$					
0.0000	−0.151	0.0000	0.753	0.122	0.154	0.0230	0.00000	0.499	0.0000
0.0625	−0.152	0.0143	0.753	0.122	0.154	0.0233	0.00198	0.498	0.0649
0.1250	−0.152	0.0287	0.752	0.122	0.154	0.0240	0.00792	0.497	0.130
0.1875	−0.153	0.0431	0.751	0.122	0.154	0.0253	0.0178	0.494	0.195
0.2500	−0.154	0.0577	0.750	0.121	0.154	0.0271	0.0317	0.490	0.260
0.3125	−0.155	0.0725	0.747	0.121	0.153	0.0295	0.0495	0.485	0.325
0.3750	−0.157	0.0877	0.745	0.121	0.153	0.0324	0.0714	0.479	0.390
0.4375	−0.159	0.103	0.741	0.120	0.152	0.0361	0.0974	0.471	0.455
0.5000	−0.161	0.120	0.737	0.120	0.152	0.0406	0.127	0.463	0.521
0.5625	−0.164	0.137	0.733	0.119	0.151	0.0461	0.161	0.452	0.587
0.6250	−0.168	0.156	0.727	0.119	0.150	0.0527	0.200	0.441	0.653
0.6875	−0.171	0.176	0.719	0.118	0.149	0.0607	0.243	0.427	0.720
0.7500	−0.176	0.199	0.711	0.117	0.147	0.0706	0.291	0.412	0.788
0.8125	−0.179	0.225	0.700	0.115	0.150	0.0830	0.344	0.394	0.857
0.8750	−0.181	0.257	0.685	0.114	0.147	0.0992	0.405	0.373	0.930
0.9375	−0.177	0.305	0.663	0.111	0.144	0.124	0.482	0.345	1.014
0.9531	−0.172	0.324	0.653	0.109	0.142	0.135	0.507	0.335	1.040
0.9687	−0.162	0.351	0.641	0.108	0.140	0.149	0.537	0.323	1.070
0.9843	−0.141	0.392	0.619	0.105	0.137	0.173	0.579	0.305	1.111
1.0000	−0.0753	0.473	0.569	0.0989	0.128	0.230	0.660	0.267	1.186

/90

TABLE 2.6

/90

$M_\infty = 6$; $p_\infty = 1$ atm; $T_\infty = 300°K$; $\rho_\infty = 1.1765$ kg/m^3;

$w_{max} = 2223$ m/sec; $h_{00} = 8612°K$; $\delta = 100$

s	ε	σ	S_1	S_1'	$\bar{p}_0$	$\bar{T}_0$
0.0000	0.459	1.570	0.00000	0.0000	1.000	1.000
0.0625	0.459	1.555	-0.00113	- 0.0365	0.999	0.999
0.1250	0.458	1.540	-0.00456	- 0.0733	0.999	0.999
0.1875	0.455	1.525	-0.0103	- 0.110	0.997	0.999
0.2500	0.452	1.510	-0.0183	- 0.148	0.996	0.998
0.3125	0.448	1.495	-0.0289	- 0.189	0.993	0.998
0.3750	0.443	1.479	-0.0422	- 0.235	0.990	0.997
0.4375	0.437	1.463	-0.0585	- 0.289	0.986	0.996
0.5000	0.430	1.445	-0.0786	- 0.353	0.981	0.995
0.5625	0.422	1.427	-0.103	- 0.430	0.975	0.994
0.6250	0.413	1.408	-0.132	- 0.526	0.966	0.992
0.6875	0.402	1.387	-0.169	- 0.646	0.955	0.989
0.7500	0.391	1.364	-0.214	- 0.802	0.939	0.986
0.8125	0.377	1.339	-0.270	- 1.011	0.917	0.981
0.8750	0.362	1.309	-0.342	- 1.319	0.883	0.973
0.9375	0.345	1.275	-0.440	- 1.893	0.824	0.959
0.9882	0.327	1.228	-0.591	- 6.842	0.720	0.931
0.9941	0.323	1.211	-0.652	- 16.25	0.686	0.921
1.0000	0.301	0.977	-1.762	-4034.9	0.318	0.773

/91

s	u	v	p	T	c^2	w^2	ψ	-x	y
				$\xi = 0$					
0.0000	0	0.00000	0.827	0.124	0.158	0.0000000	0	0.0100	0.0000
0.0625	0	0.00776	0.827	0.124	0.158	0.0000603	0	0.00998	0.0625
0.1250	0	0.0154	0.826	0.124	0.158	0.000239	0	0.00992	0.125
0.1875	0	0.0232	0.825	0.124	0.157	0.000540	0	0.00982	0.187
0.2500	0	0.0311	0.824	0.124	0.157	0.000971	0	0.00968	0.250
0.3125	0	0.0393	0.822	0.124	0.157	0.00154	0	0.00949	0.312
0.3750	0	0.0479	0.819	0.124	0.157	0.00230	0	0.00927	0.375
0.4375	0	0.0572	0.816	0.124	0.157	0.00327	0	0.00899	0.437
0.5000	0	0.0673	0.812	0.124	0.157	0.00453	0	0.00866	0.500
0.5625	0	0.0786	0.807	0.124	0.157	0.00618	0	0.00826	0.562
0.6250	0	0.0914	0.800	0.123	0.156	0.00835	0	0.00780	0.625
0.6875	0	0.106	0.790	0.123	0.156	0.0112	0	0.00726	0.687
0.7500	0	0.124	0.777	0.123	0.155	0.0153	0	0.00661	0.750
0.8125	0	0.146	0.759	0.122	0.155	0.0213	0	0.00582	0.812
0.8750	0	0.174	0.730	0.121	0.153	0.0305	0	0.00484	0.875
0.9375	0	0.217	0.682	0.119	0.151	0.0471	0	0.00348	0.937
0.9882	0	0.281	0.596	0.116	0.146	0.0789	0	0.00153	0.988
0.9941	0	0.300	0.567	0.115	0.149	0.0901	0	0.00108	0.994
1.0000	0	0.502	0.263	0.0964	0.125	0.252	0	0.000190	0.999

TABLE 2.6 Continued

s	u	v	p	T	c^2	w^2	ψ	$-x$	y
				$\xi = 0.5$					
0.0000	-0.0661	0.00000	0.813	0.124	0.157	0.00437	0.000000	0.239	0.0000
0.0625	-0.0656	0.00992	0.813	0.124	0.157	0.00441	0.000844	0.239	0.0626
0.1250	-0.0658	0.0199	0.812	0.124	0.157	0.00473	0.00337	0.238	0.125
0.1875	-0.0664	0.0301	0.811	0.124	0.157	0.00532	0.00759	0.237	0.187
0.2500	-0.0672	0.0406	0.810	0.124	0.157	0.00617	0.0135	0.235	0.250
0.3125	-0.0683	0.0514	0.808	0.124	0.157	0.00731	0.0211	0.233	0.313
0.3750	-0.0696	0.0626	0.806	0.123	0.156	0.00877	0.0305	0.231	0.375
0.4375	-0.0714	0.0742	0.803	0.123	0.156	0.0106	0.0417	0.227	0.438
0.5000	-0.0735	0.0865	0.799	0.123	0.156	0.0128	0.0547	0.223	0.501
0.5625	-0.0761	0.0995	0.794	0.123	0.155	0.0157	0.0696	0.219	0.563
0.6250	-0.0793	0.113	0.787	0.122	0.155	0.0191	0.0864	0.214	0.626
0.6875	-0.0834	0.128	0.778	0.122	0.154	0.0235	0.105	0.208	0.689
0.7500	-0.0887	0.145	0.766	0.121	0.153	0.0291	0.126	0.202	0.752
0.8125	-0.0957	0.165	0.750	0.120	0.152	0.0365	0.149	0.194	0.815
0.8750	-0.105	0.189	0.726	0.119	0.151	0.0468	0.175	0.186	0.878
0.9375	-0.118	0.220	0.689	0.118	0.149	0.0625	0.205	0.176	0.942
0.9882	-0.126	0.260	0.638	0.115	0.149	0.0835	0.232	0.165	0.998
0.9941	-0.120	0.268	0.631	0.115	0.149	0.0864	0.236	0.162	1.008
1.0000	+0.0447	0.469	0.336	0.101	0.131	0.222	0.239	0.133	1.069
				$\xi = 1$					
0.0000	-0.151	0.0000	0.753	0.122	0.154	0.0230	0.00000	0.469	0.0000
0.0625	-0.152	0.0118	0.753	0.122	0.154	0.0232	0.00184	0.469	0.0627
0.1250	-0.152	0.0238	0.752	0.122	0.154	0.0238	0.00739	0.468	0.125
0.1875	-0.153	0.0357	0.752	0.122	0.154	0.0248	0.0166	0.465	0.188
0.2500	-0.154	0.0477	0.750	0.121	0.154	0.0262	0.0295	0.462	0.251
0.3125	-0.156	0.0597	0.749	0.121	0.154	0.0280	0.0462	0.458	0.313
0.3750	-0.158	0.0720	0.747	0.121	0.153	0.0303	0.0665	0.452	0.376
0.4375	-0.161	0.0847	0.744	0.121	0.153	0.0331	0.0905	0.446	0.439
0.5000	-0.164	0.0979	0.741	0.120	0.152	0.0365	0.118	0.439	0.502
0.5625	-0.167	0.111	0.737	0.120	0.152	0.0406	0.149	0.430	0.565
0.6250	-0.172	0.126	0.733	0.119	0.151	0.0457	0.185	0.421	0.628
0.6875	-0.178	0.142	0.727	0.119	0.150	0.0519	0.223	0.410	0.691
0.7500	-0.184	0.159	0.721	0.118	0.149	0.0594	0.266	0.397	0.754
0.8125	-0.193	0.177	0.712	0.117	0.148	0.0688	0.313	0.383	0.817
0.8750	-0.203	0.198	0.702	0.116	0.146	0.0808	0.364	0.367	0.881
0.9375	-0.216	0.223	0.687	0.114	0.148	0.0967	0.420	0.348	0.946
0.9882	-0.228	0.262	0.666	0.111	0.144	0.120	0.477	0.328	1.009
0.9941	-0.229	0.279	0.658	0.110	0.143	0.130	0.490	0.323	1.023
1.0000	-0.195	0.505	0.514	0.0917	0.119	0.293	0.608	0.266	1.139

/92

TABLE 2.7

$M_\infty = 10$; $p_\infty = 0.01$ atm; $T_\infty = 300°K$; $\rho_\infty = 0.01176$ kg/m^3;

$w_{max} = 3559$ m/sec; $h_{00} = 22\ 064°K$; $\delta = 10$

s	ε	σ	S_1	S_1'	$\bar{p}_0$	$\bar{T}_0$
0.0000	0.294	1.570	0.00000	0.0000	1.000	1.000
0.0625	0.294	1.555	-0.00226	- 0.0726	0.999	0.999
0.1250	0.293	1.539	-0.00910	- 0.146	0.998	0.999
0.1875	0.292	1.523	-0.0206	- 0.224	0.997	0.999
0.2500	0.290	1.507	-0.0373	- 0.309	0.994	0.999
0.3125	0.287	1.490	-0.0595	- 0.405	0.991	0.999
0.3750	0.283	1.472	-0.0883	- 0.517	0.987	0.998
0.4375	0.279	1.454	-0.124	- 0.652	0.982	0.997
0.5000	0.275	1.434	-0.170	- 0.816	0.975	0.997
0.5625	0.269	1.413	-0.227	- 1.024	0.966	0.995
0.6250	0.263	1.389	-0.299	- 1.293	0.953	0.994
0.6875	0.256	1.363	-0.391	- 1.659	0.936	0.992
0.7500	0.248	1.334	-0.510	- 2.188	0.911	0.988
0.8125	0.239	1.299	-0.671	- 3.050	0.873	0.983
0.8750	0.229	1.253	-0.910	- 4.872	0.808	0.975
0.9375	0.218	1.177	-1.384	- 13.26	0.673	0.954
0.9531	0.214	1.133	-1.705	- 14.23	0.364	0.899
0.9687	0.210	1.081	-2.117	- 32.29	0.335	0.891
0.9843	0.206	1.006	-2.775	- 53.90	0.272	0.871
1.0000	0.201	0.884	-3.986	- 114.7	0.112	0.790

s	u	v	p	T	c^2	w^2	ψ	$-x$	y
				$\xi = 0$					
0.0000	0	0.00000	0.910	0.0834	0.107	0.0000000	0	0.1000	0.0000
0.0625	0	0.00737	0.910	0.0834	0.107	0.0000544	0	0.0998	0.0624
0.1250	0	0.0147	0.909	0.0833	0.107	0.000218	0	0.0992	0.124
0.1875	0	0.0223	0.907	0.0833	0.107	0.000499	0	0.0982	0.187
0.2500	0	0.0301	0.905	0.0833	0.107	0.000910	0	0.0968	0.249
0.3125	0	0.0383	0.903	0.0833	0.107	0.00147	0	0.0949	0.312
0.3750	0	0.0471	0.899	0.0832	0.107	0.00222	0	0.0927	0.374
0.4375	0	0.0567	0.894	0.0832	0.107	0.00322	0	0.0899	0.437
0.5000	0	0.0673	0.888	0.0831	0.107	0.00453	0	0.0866	0.499
0.5625	0	0.0792	0.879	0.0830	0.107	0.00628	0	0.0827	0.562
0.6250	0	0.0930	0.868	0.0829	0.106	0.00866	0	0.0781	0.624
0.6875	0	0.109	0.852	0.0827	0.106	0.0120	0	0.0726	0.686
0.7500	0	0.129	0.829	0.0824	0.106	0.0168	0	0.0662	0.748
0.8125	0	0.156	0.794	0.0820	0.105	0.0245	0	0.0585	0.810
0.8750	0	0.195	0.736	0.0813	0.103	0.0381	0	0.0488	0.872
0.9375	0	0.264	0.613	0.0796	0.100	0.0701	0	0.0357	0.933
0.9531	0	0.410	0.331	0.0750	0.0930	0.168	0	0.0315	0.948
0.9687	0	0.426	0.305	0.0743	0.0918	0.181	0	0.0267	0.963
0.9843	0	0.463	0.248	0.0726	0.0891	0.214	0	0.0208	0.978
1.0000	0	0.589	0.102	0.0659	0.0788	0.347	0	0.0129	0.991

/93

TABLE 2.7 Continued

/93

s	u	v	p	T	c^2	w^2	ψ	−x	y
				$\xi = 0.5$					
0.0000	−0.0432	0.0000	0.901	0.0833	0.107	0.00187	0.000000	0.247	0.0000
0.0625	−0.0432	0.0111	0.900	0.0833	0.107	0.00199	0.000857	0.247	0.0634
0.1250	−0.0434	0.0223	0.900	0.0832	0.107	0.00238	0.00343	0.246	0.126
0.1875	−0.0438	0.0337	0.898	0.0832	0.107	0.00305	0.00772	0.244	0.190
0.2500	−0.0443	0.0453	0.896	0.0832	0.107	0.00402	0.0137	0.241	0.253
0.3125	−0.0450	0.0573	0.894	0.0831	0.107	0.00531	0.0215	0.238	0.317
0.3750	−0.0459	0.0697	0.890	0.0830	0.107	0.00697	0.0310	0.234	0.380
0.4375	−0.0470	0.0827	0.885	0.0829	0.106	0.00906	0.0423	0.229	0.444
0.5000	−0.0485	0.0964	0.879	0.0828	0.106	0.0116	0.0554	0.223	0.507
0.5625	−0.0502	0.111	0.872	0.0827	0.106	0.0148	0.0704	0.217	0.571
0.6250	−0.0524	0.127	0.861	0.0825	0.105	0.0189	0.0872	0.209	0.634
0.6875	−0.0552	0.145	0.847	0.0823	0.105	0.0240	0.106	0.200	0.698
0.7500	−0.0587	0.165	0.828	0.0819	0.104	0.0308	0.127	0.189	0.762
0.8125	−0.0629	0.190	0.799	0.0815	0.104	0.0402	0.150	0.176	0.827
0.8750	−0.0671	0.223	0.782	0.0808	0.102	0.0544	0.175	0.161	0.892
0.9375	−0.0640	0.284	0.644	0.0792	0.0999	0.0851	0.201	0.141	0.961
0.9531	−0.0553	0.335	0.540	0.0776	0.0972	0.115	0.205	0.134	0.979
0.9687	−0.0502	0.384	0.439	0.0759	0.0941	0.149	0.208	0.125	0.999
0.9843	−0.0237	0.420	0.370	0.0745	0.0918	0.177	0.208	0.114	1.021
1.0000	+0.0536	0.494	0.234	0.0708	0.0860	0.247	0.203	0.0928	1.052
				$\xi = 1$					
0.0000	−0.103	0.0000	0.858	0.0828	0.106	0.0106	0.00000	0.394	0.0000
0.0625	−0.103	0.0143	0.858	0.0828	0.106	0.0108	0.00202	0.394	0.0643
0.1250	−0.103	0.0287	0.857	0.0827	0.106	0.0115	0.00808	0.392	0.128
0.1875	−0.104	0.0433	0.856	0.0827	0.106	0.0127	0.0181	0.390	0.193
0.2500	−0.105	0.0581	0.855	0.0826	0.106	0.0144	0.0323	0.386	0.257
0.3125	−0.106	0.0735	0.853	0.0825	0.106	0.0167	0.0505	0.382	0.321
0.3750	−0.108	0.0894	0.850	0.0824	0.105	0.0197	0.0728	0.376	0.386
0.4375	−0.110	0.106	0.846	0.0823	0.105	0.0234	0.0992	0.369	0.450
0.5000	−0.112	0.124	0.842	0.0821	0.105	0.0281	0.129	0.361	0.515
0.5625	−0.116	0.143	0.836	0.0818	0.104	0.0340	0.164	0.351	0.580
0.6250	−0.119	0.164	0.830	0.0816	0.104	0.0413	0.203	0.340	0.645
0.6875	−0.124	0.187	0.821	0.0812	0.103	0.0507	0.246	0.327	0.710
0.7500	−0.129	0.214	0.809	0.0807	0.102	0.0628	0.294	0.312	0.776
0.8125	−0.136	0.245	0.794	0.0801	0.101	0.0790	0.347	0.295	0.843
0.8750	−0.143	0.287	0.772	0.0791	0.0992	0.102	0.406	0.274	0.912
0.9375	−0.151	0.356	0.728	0.0772	0.0956	0.149	0.477	0.246	0.988
0.9531	−0.160	0.394	0.698	0.0759	0.0933	0.181	0.498	0.237	1.010
0.9687	−0.165	0.439	0.661	0.0742	0.0905	0.220	0.522	0.225	1.035
0.9843	−0.165	0.505	0.603	0.0714	0.0861	0.282	0.554	0.207	1.065
1.0000	−0.120	0.614	0.501	0.0657	0.0786	0.392	0.605	0.172	1.113

/94

TABLE 2.8

/95

$M_\infty = 10$; $p_\infty = 0.01$ atm; $T_\infty = 300°K$; $\rho_\infty = 0.01176$ kg/m^3;

$w_{max} = 3559$ m/sec; $h_{00} = 22\,064°K$; $\delta = 100$

s	ε	σ	S_1	S_1'	$\bar{p}_0$	$\bar{T}_0$
0.0000	0.373	1.570	0.00000	0.0000	1.000	1.000
0.0625	0.372	1.558	-0.00143	- 0.0459	0.999	1.000
0.1250	0.371	1.545	-0.00576	- 0.0925	0.999	0.999
0.1875	0.369	1.533	-0.0130	- 0.140	0.998	0.999
0.2500	0.367	1.520	-0.0234	- 0.192	0.997	0.999
0.3125	0.363	1.507	-0.0372	- 0.249	0.995	0.999
0.3750	0.359	1.493	-0.0548	- 0.315	0.993	0.999
0.4375	0.354	1.479	-0.0769	- 0.392	0.990	0.998
0.5000	0.348	1.464	-0.104	- 0.486	0.986	0.998
0.5625	0.341	1.448	-0.138	- 0.600	0.982	0.997
0.6250	0.333	1.430	-0.179	- 0.743	0.975	0.997
0.6875	0.325	1.411	-0.231	- 0.925	0.967	0.995
0.7500	0.314	1.390	-0.296	- 1.162	0.954	0.994
0.8125	0.303	1.367	-0.378	- 1.477	0.937	0.992
0.8750	0.290	1.340	-0.483	- 1.911	0.909	0.988
0.9375	0.275	1.309	-0.622	- 2.603	0.861	0.982
0.9882	0.260	1.272	-0.806	- 7.257	0.772	0.969
0.9941	0.257	1.261	-0.867	- 16.01	0.745	0.965
1.0000	0.249	1.176	-1.392	-1382.9	0.658	0.803

s	u	v	p	T	c^2	w^2	ψ	$-x$	y
				$\xi = 0$					
0.0000	0	0.00000	0.910	0.0834	0.107	0.0000000	0	0.01000	0.0000
0.0625	0	0.00542	0.910	0.0834	0.107	0.0000294	0	0.00998	0.0625
0.1250	0	0.0109	0.909	0.0834	0.107	0.000119	0	0.00992	0.125
0.1875	0	0.0164	0.909	0.0833	0.107	0.000271	0	0.00982	0.187
0.2500	0	0.0222	0.907	0.0833	0.107	0.000493	0	0.00968	0.250
0.3125	0	0.0281	0.906	0.0833	0.107	0.000795	0	0.00949	0.312
0.3750	0	0.0345	0.904	0.0833	0.107	0.00119	0	0.00927	0.375
0.4375	0	0.0414	0.901	0.0833	0.107	0.00171	0	0.00899	0.437
0.5000	0	0.0489	0.898	0.0832	0.107	0.00239	0	0.00866	0.500
0.5625	0	0.0573	0.894	0.0832	0.107	0.00328	0	0.00826	0.562

TABLE 2.8 Continued

/96

s	u	v	p	T	c^2	w^2	ψ	−x	y
0.6250	0	0.0669	0.888	0.0831	0.107	0.00448	0	0.00780	0.625
0.6875	0	0.0781	0.880	0.0830	0.107	0.00610	0	0.00726	0.687
0.7500	0	0.0915	0.869	0.0829	0.106	0.00838	0	0.00661	0.750
0.8125	0	0.108	0.853	0.0827	0.106	0.0117	0	0.00582	0.812
0.8750	0	0.131	0.828	0.0824	0.105	0.0171	0	0.00484	0.875
0.9375	0	0.164	0.784	0.0819	0.105	0.0270	0	0.00348	0.937
0.9882	0	0.215	0.703	0.0809	0.103	0.0462	0	0.00153	0.988
0.9941	0	0.229	0.678	0.0805	0.102	0.0525	0	0.00108	0.994
1.0000	0	0.603	0.599	0.0670	0.0811	0.363	0	0.000190	0.999
				$\xi = 0.5$					
0.0000	−0.0419	0.00000	0.901	0.0833	0.107	0.00176	0.000000	0.196	0.0000
0.0625	−0.0421	0.00850	0.901	0.0833	0.107	0.00184	0.000813	0.196	0.0626
0.1250	−0.0423	0.0170	0.901	0.0833	0.107	0.00208	0.00325	0.195	0.125
0.1875	−0.0427	0.0257	0.900	0.0832	0.107	0.00249	0.00734	0.194	0.187
0.2500	−0.0432	0.0346	0.899	0.0832	0.107	0.00307	0.0130	0.193	0.250
0.3125	−0.0439	0.0437	0.897	0.0832	0.107	0.00384	0.0204	0.191	0.313
0.3750	−0.0448	0.0531	0.895	0.0831	0.107	0.00483	0.0295	0.189	0.375
0.4375	−0.0459	0.0629	0.893	0.0831	0.107	0.00607	0.0403	0.186	0.438
0.5000	−0.0472	0.0732	0.889	0.0830	0.106	0.00760	0.0528	0.182	0.501
0.5625	−0.0490	0.0841	0.885	0.0829	0.106	0.00948	0.0670	0.179	0.563
0.6250	−0.0511	0.0958	0.879	0.0828	0.106	0.0118	0.0832	0.174	0.626
0.6875	−0.0539	0.108	0.872	0.0827	0.106	0.0147	0.101	0.169	0.689
0.7500	−0.0576	0.122	0.862	0.0825	0.106	0.0184	0.121	0.164	0.751
0.8125	−0.0625	0.139	0.847	0.0823	0.105	0.0232	0.143	0.157	0.814
0.8750	−0.0695	0.158	0.826	0.0820	0.104	0.0300	0.169	0.150	0.877
0.9375	−0.0797	0.184	0.792	0.0814	0.104	0.0403	0.197	0.141	0.941
0.9882	−0.0873	0.215	0.745	0.0808	0.102	0.0539	0.225	0.131	0.996
0.9941	−0.0832	0.220	0.740	0.0807	0.102	0.0556	0.229	0.129	1.005
1.0000	+0.00967	0.303	0.603	0.0788	0.0992	0.0922	0.239	0.110	1.057
				$\xi = 1$					
0.0000	−0.103	0.0000	0.858	0.0828	0.106	0.0106	0.00000	0.383	0.0000
0.0625	−0.103	0.0109	0.858	0.0828	0.106	0.0107	0.00192	0.382	0.0627
0.1250	−0.103	0.0219	0.858	0.0828	0.106	0.0112	0.00768	0.381	0.125
0.1875	−0.104	0.0330	0.857	0.0827	0.106	0.0119	0.0172	0.379	0.188
0.2500	−0.105	0.0442	0.856	0.0827	0.106	0.0130	0.0307	0.376	0.250
0.3125	−0.106	0.0557	0.855	0.0826	0.106	0.0144	0.0480	0.373	0.313
0.3750	−0.108	0.0675	0.853	0.0826	0.106	0.0162	0.0691	0.368	0.376
0.4375	−0.110	0.0799	0.851	0.0825	0.105	0.0185	0.0941	0.363	0.439
0.5000	−0.112	0.0929	0.848	0.0824	0.105	0.0213	0.122	0.357	0.502
0.5625	−0.115	0.106	0.845	0.0822	0.105	0.0248	0.155	0.350	0.564
0.6250	−0.119	0.121	0.841	0.0820	0.105	0.0291	0.192	0.341	0.627
0.6875	−0.124	0.137	0.836	0.0818	0.104	0.0344	0.232	0.332	0.690
0.7500	−0.130	0.155	0.830	0.0816	0.104	0.0410	0.277	0.321	0.753
0.8125	−0.137	0.174	0.822	0.0812	0.103	0.0494	0.325	0.309	0.816
0.8750	−0.147	0.196	0.812	0.0808	0.102	0.0601	0.378	0.295	0.880
0.9375	−0.158	0.221	0.799	0.0803	0.101	0.0741	0.435	0.279	0.944
0.9882	−0.165	0.255	0.781	0.0795	0.100	0.0926	0.492	0.261	1.004
0.9941	−0.164	0.268	0.776	0.0793	0.0995	0.0987	0.505	0.257	1.017
1.0000	−0.0679	0.382	0.727	0.0772	0.0956	0.150	0.607	0.221	1.115

/97

TABLE 2.9

$M_\infty = 15$; $p_\infty = 0.01$ atm; $T_\infty = 300°K$; $\rho_\infty = 0.01176$ kg/m^3;

$w_{max} = 5267$ m/sec; $h_{00} = 48\ 339°K$; $\delta = 10$

s	ε	σ	S_1	S_1'	$\bar{p}_0$	$\bar{T}_0$
0.0000	0.270	1.570	0.00000	0.0000	1.000	1.000
0.0625	0.270	1.556	-0.00277	- 0.0889	0.999	1.000
0.1250	0.269	1.541	-0.0111	- 0.180	0.998	1.000
0.1875	0.268	1.526	-0.0255	- 0.278	0.997	0.999
0.2500	0.266	1.510	-0.0462	- 0.386	0.995	0.999
0.3125	0.263	1.494	-0.0741	- 0.508	0.992	0.999
0.3750	0.260	1.478	-0.110	- 0.649	0.989	0.998
0.4375	0.257	1.460	-0.155	- 0.817	0.984	0.998
0.5000	0.252	1.442	-0.213	- 1.022	0.978	0.997
0.5625	0.247	1.421	-0.284	- 1.278	0.970	0.996
0.6250	0.242	1.400	-0.374	- 1.624	0.958	0.995
0.6875	0.235	1.375	-0.489	- 2.089	0.943	0.993
0.7500	0.228	1.347	-0.639	- 2.745	0.922	0.991
0.8125	0.220	1.314	-0.840	- 3.761	0.890	0.987
0.8750	0.212	1.273	-1.128	- 5.733	0.839	0.981
0.9375	0.203	1.211	-1.633	- 11.951	0.750	0.969
0.9531	0.200	1.188	-1.851	- 16.485	0.718	0.965
0.9687	0.198	1.155	-2.174	- 26.612	0.684	0.960
0.9843	0.197	1.093	-2.862	- 48.137	0.473	0.924
1.0000	0.198	0.989	-4.220	- 138.48	0.391	0.904

/98

s	u	v	p	T	c^2	w^2	ψ	$-x$	y
				$\xi = 0$					
0.0000	0	0.00000	0.938	0.0632	0.0934	0.0000000	0	0.1000	0.0000
0.0625	0	0.00638	0.938	0.0632	0.0934	0.0000407	0	0.0998	0.0625
0.1250	0	0.0129	0.937	0.0632	0.0934	0.000166	0	0.0992	0.125
0.1875	0	0.0195	0.936	0.0631	0.0934	0.000383	0	0.0982	0.187
0.2500	0	0.0265	0.934	0.0631	0.0933	0.000704	0	0.0968	0.250
0.3125	0	0.0338	0.931	0.0631	0.0933	0.00114	0	0.0949	0.312
0.3750	0	0.0416	0.928	0.0631	0.0933	0.00173	0	0.0927	0.374
0.4375	0	0.0501	0.924	0.0631	0.0932	0.00251	0	0.0899	0.437
0.5000	0	0.0594	0.918	0.0630	0.0931	0.00353	0	0.0866	0.499
0.5625	0	0.0699	0.910	0.0630	0.0930	0.00488	0	0.0827	0.562
0.6250	0	0.0819	0.900	0.0629	0.0929	0.00671	0	0.0781	0.624
0.6875	0	0.0961	0.886	0.0628	0.0927	0.00924	0	0.0726	0.686
0.7500	0	0.113	0.866	0.0626	0.0924	0.0129	0	0.0662	0.748
0.8125	0	0.135	0.836	0.0624	0.0920	0.0184	0	0.0585	0.810
0.8750	0	0.166	0.788	0.0620	0.0889	0.0277	0	0.0488	0.872
0.9375	0	0.212	0.704	0.0612	0.0882	0.0452	0	0.0357	0.933
0.9531	0	0.227	0.674	0.0610	0.0880	0.0519	0	0.0315	0.948
0.9687	0	0.243	0.642	0.0606	0.0876	0.0594	0	0.0267	0.963
0.9843	0	0.338	0.444	0.0584	0.0841	0.127	0	0.0208	0.978
1.0000	0	0.376	0.367	0.0571	0.0825	0.150	0	0.0129	0.991

TABLE 2.9 Continued

s	u	v	p	T	c^2	ω^2	ψ	$-x$	y
				$\xi = 0.5$					
0.0000	-0.0361	0.0000	0.931	0.0631	0.0933	0.00130	0.000000	0.289	0.0000
0.0625	-0.0363	0.0104	0.930	0.0631	0.0933	0.00143	0.000842	0.239	0.0603
0.1250	-0.0365	0.0210	0.929	0.0631	0.0933	0.00178	0.00337	0.233	0.126
0.1875	-0.0368	0.0316	0.928	0.0631	0.0932	0.00236	0.00759	0.232	0.190
0.2500	-0.0372	0.0425	0.926	0.0630	0.0932	0.00320	0.0135	0.229	0.253
0.3125	-0.0378	0.0536	0.924	0.0630	0.0931	0.00431	0.0211	0.226	0.316
0.3750	-0.0385	0.0652	0.921	0.0630	0.0930	0.00574	0.0304	0.222	0.380
0.4375	-0.0394	0.0772	0.916	0.0629	0.0929	0.00752	0.0415	0.218	0.443
0.5000	-0.0405	0.0899	0.911	0.0628	0.0928	0.00973	0.0544	0.212	0.507
0.5625	-0.0419	0.103	0.904	0.0627	0.0926	0.0124	0.0690	0.206	0.570
0.6250	-0.0437	0.118	0.894	0.0626	0.0924	0.0158	0.0855	0.198	0.634
0.6875	-0.0459	0.134	0.881	0.0625	0.0921	0.0202	0.105	0.190	0.697
0.7500	-0.0484	0.152	0.864	0.0623	0.0917	0.0257	0.124	0.179	0.761
0.8125	-0.0513	0.174	0.839	0.0620	0.0888	0.0331	0.146	0.167	0.826
0.8750	-0.0537	0.202	0.799	0.0616	0.0884	0.0438	0.171	0.153	0.891
0.9375	-0.0489	0.242	0.731	0.0609	0.0878	0.0611	0.196	0.134	0.959
0.9531	-0.0427	0.256	0.703	0.0606	0.0875	0.0678	0.202	0.127	0.977
0.9687	-0.0298	0.277	0.661	0.0602	0.0870	0.0778	0.206	0.120	0.997
0.9843	-0.00203	0.322	0.555	0.0590	0.0856	0.105	0.207	0.109	1.020
1.0000	+0.0786	0.364	0.435	0.0574	0.0834	0.138	0.201	0.0916	1.051
				$\xi = 1$					
0.0000	-0.0885	0.0515	0.893	0.0628	0.0928	0.00784	0.00000	0.370	0.0000
0.0625	-0.0887	0.0137	0.893	0.0628	0.0928	0.00805	0.00203	0.370	0.0641
0.1250	-0.0890	0.0276	0.893	0.0628	0.0928	0.00869	0.00815	0.368	0.128
0.1875	-0.0896	0.0417	0.892	0.0628	0.0927	0.00977	0.0183	0.366	0.192
0.2500	-0.0905	0.0561	0.890	0.0627	0.0926	0.0113	0.0326	0.363	0.256
0.3125	-0.0916	0.0710	0.888	0.0627	0.0925	0.0134	0.0509	0.358	0.321
0.3750	-0.0931	0.0862	0.885	0.0626	0.0923	0.0161	0.0734	0.353	0.385
0.4375	-0.0949	0.102	0.882	0.0625	0.0921	0.0196	0.100	0.346	0.449
0.5000	-0.0971	0.120	0.878	0.0623	0.0919	0.0239	0.130	0.339	0.514
0.5625	-0.0998	0.139	0.873	0.0622	0.0916	0.0292	0.165	0.330	0.578
0.6250	-0.103	0.159	0.867	0.0620	0.0888	0.0360	0.204	0.319	0.643
0.6875	-0.107	0.182	0.859	0.0617	0.0885	0.0446	0.248	0.307	0.708
0.7500	-0.111	0.208	0.848	0.0614	0.0882	0.0557	0.296	0.293	0.774
0.8125	-0.116	0.238	0.834	0.0609	0.0877	0.0706	0.349	0.277	0.841
0.8750	-0.121	0.277	0.814	0.0602	0.0869	0.0917	0.409	0.257	0.910
0.9375	-0.122	0.336	0.780	0.0589	0.0853	0.128	0.479	0.232	0.985
0.9531	-0.119	0.359	0.765	0.0583	0.0845	0.143	0.501	0.224	1.006
0.9687	-0.113	0.391	0.744	0.0574	0.0833	0.166	0.525	0.213	1.031
0.9843	-0.101	0.450	0.700	0.0553	0.0805	0.214	0.557	0.199	1.061
1.0000	-0.0416	0.547	0.620	0.0506	0.0739	0.300	0.611	0.170	1.112

/99

EQUILIBRIUM OXYGEN. SCHEME II. N = 2 /100

M_∞ = 10-25; p_∞ = 0.01 atm; T_∞ = 290°K; ρ_∞ = 0.01345 kg/m^3;

δ = 1

TABLE 2.10

M_∞ = 10; w_{max} = 3328.1 m/sec; h_{00} = 21 315°K; ε_0 = 0.07957;

ε_1 = 0.1385; ε_2 = 0.09065

ξ	s	u	v	p	T	ρ	h
			$s = 0$				
1.0000	0	-0.0959	0	0.865	0.0765	10.169	0.990
0.8906	0	-0.0827	0	0.877	0.0765	10.293	0.993
0.7656	0	-0.0686	0	0.888	0.0766	10.408	0.995
0.6406	0	-0.0554	0	0.897	0.0767	10.496	0.996
0.5156	0	-0.0431	0	0.903	0.0767	10.562	0.998
0.3906	0	-0.0315	0	0.908	0.0768	10.609	0.998
0.2656	0	-0.0207	0	0.911	0.0768	10.640	0.999
0.1406	0	-0.0106	0	0.912	0.0768	10.657	0.999
0.0000	0	0.0000	0	0.913	0.0768	10.664	0.999
			$s = s_1/2$				
1.0000	0.410	-0.0776	0.344	0.755	0.0735	9.488	0.875
0.8906	0.393	-0.0689	0.313	0.766	0.0741	9.501	0.896
0.7656	0.377	-0.0587	0.282	0.776	0.0746	9.517	0.916
0.6406	0.364	-0.0484	0.254	0.784	0.0749	9.530	0.932
0.5156	0.354	-0.0383	0.230	0.790	0.0752	9.536	0.945
0.3906	0.346	-0.0285	0.208	0.794	0.0755	9.535	0.955
0.2656	0.340	-0.0189	0.188	0.797	0.0757	9.525	0.964
0.1406	0.335	-0.00983	0.169	0.798	0.0758	9.505	0.970
0.0000	0.332	0.00000	0.151	0.798	0.0759	9.469	0.976
			$s = s_1$				
1.0000	0.820	+0.00169	0.601	0.531	0.0653	7.904	0.638
0.8906	0.786	-0.00736	0.563	0.531	0.0670	7.628	0.682
0.7656	0.754	-0.0132	0.519	0.531	0.0686	7.379	0.729
0.6406	0.729	-0.0156	0.476	0.532	0.0699	7.185	0.772
0.5156	0.708	-0.0155	0.436	0.533	0.0709	7.030	0.808
0.3906	0.692	-0.0134	0.399	0.533	0.0717	6.900	0.840
0.2656	0.680	-0.0101	0.364	0.532	0.0723	6.785	0.866
0.1406	0.671	-0.00575	0.333	0.529	0.0728	6.674	0.888
0.0000	0.665	0.00000	0.303	0.524	0.0732	6.555	0.906

TABLE 2.11

/100

$M_\infty = 15$; $w_{max} = 4925.6$ m/sec; $h_{00} = 46\ 690°K$;

$\varepsilon_0 = 0.05714$; $\varepsilon_1 = 0.06532$; $\varepsilon_2 = 0.1090$

ξ	s	u	v	p	T	ρ	h
			$s = 0$				
1.0000	0	-0.0690	0	0.913	0.0437	14.328	0.995
0.8906	0	-0.0589	0	0.922	0.0438	14.454	0.996
0.7656	0	-0.0482	0	0.930	0.0438	14.567	0.997
0.6406	0	-0.0384	0	0.936	0.0439	14.651	0.998
0.5156	0	-0.0293	0	0.941	0.0439	14.711	0.999

/101

ξ	s	u	v	p	T	ρ	h
0.3906	0	-0.0211	0	0.944	0.0439	14.753	0.999
0.2656	0	-0.0136	0	0.946	0.0439	14.779	0.999
0.1406	0	-0.00683	0	0.947	0.0439	14.793	0.999
0.0000	0	0.00000	0	0.947	0.0439	14.798	0.999
			$s = s_1/2$				
1.0000	0.450	-0.0508	0.395	0.765	0.0416	13.563	0.840
0.8906	0.431	-0.0453	0.356	0.773	0.0420	13.382	0.870
0.7656	0.414	-0.0386	0.316	0.780	0.0423	13.231	0.898
0.6406	0.400	-0.0317	0.281	0.786	0.0426	13.118	0.919
0.5156	0.389	-0.0248	0.249	0.791	0.0428	13.029	0.936
0.3906	0.380	-0.0182	0.220	0.794	0.0429	12.956	0.950
0.2656	0.374	-0.0120	0.194	0.797	0.0430	12.893	0.961
0.1406	0.368	-0.00613	0.170	0.799	0.0431	12.837	0.970
0.0000	0.364	0.00000	0.147	0.799	0.0432	12.780	0.978
			$s = s_1$				
1.0000	0.900	+0.0391	0.673	0.483	0.0369	11.224	0.545
0.8906	0.862	+0.0237	0.626	0.475	0.0378	10.402	0.607
0.7656	0.828	+0.0117	0.570	0.469	0.0386	9.701	0.674
0.6406	0.801	+0.00414	0.516	0.467	0.0393	9.192	0.733
0.5156	0.779	-0.000297	0.465	0.466	0.0399	8.816	0.782
0.3906	0.761	-0.00242	0.418	0.466	0.0403	8.532	0.824
0.2656	0.748	-0.00266	0.374	0.465	0.0407	8.311	0.859
0.1406	0.737	-0.00203	0.334	0.465	0.0410	8.132	0.887
0.0000	0.728	0.00000	0.295	0.464	0.0412	7.980	0.910

TABLE 2.12

/10

$M_\infty = 18$; $w_{max} = 5891.1$ m/sec; $h_{00} = 66\ 787°K$;

$\varepsilon_0 = 0.05334$; $\varepsilon_1 = 0.09804$; $\varepsilon_2 = 0.05988$

ξ	s	u	v	p	T	ρ	h
			$s = 0$				
1.0000	0	-0.0649	0	0.922	0.0348	15.277	0.995
0.8906	0	-0.0552	0	0.931	0.0349	15.401	0.996
0.7656	0	-0.0450	0	0.939	0.0349	15.510	0.997
0.6406	0	-0.0357	0	0.945	0.0349	15.591	0.998
0.5156	0	-0.0272	0	0.949	0.0349	15.649	0.999
0.3906	0	-0.0194	0	0.952	0.0350	15.688	0.999
0.2656	0	-0.0125	0	0.953	0.0350	15.712	0.999
0.1406	0	-0.00624	0	0.954	0.0350	15.725	0.999
0.0000	0	0.00000	0	0.955	0.0350	15.729	0.999
			$s = s_1/2$				
1.0000	0.450	-0.0470	0.402	0.771	0.0325	14.969	0.835
0.8906	0.431	-0.0419	0.361	0.777	0.0328	14.645	0.867
0.7656	0.415	-0.0356	0.320	0.784	0.0332	14.371	0.895
0.6406	0.402	-0.0291	0.284	0.789	0.0335	14.163	0.918
0.5156	0.391	-0.0228	0.251	0.793	0.0337	13.999	0.936

/10

ξ	s	u	v	p	T	ρ	h
0.3906	0.383	-0.0167	0.221	0.796	0.0339	13.866	0.950
0.2656	0.377	-0.0109	0.194	0.799	0.0340	13.757	0.962
0.1406	0.371	-0.00557	0.169	0.800	0.0342	13.665	0.971
0.0000	0.367	0.00000	0.145	0.801	0.0343	13.579	0.978
			$s = s_1$				
1.0000	0.900	+0.0404	0.685	0.479	0.0282	13.030	0.528
0.8906	0.863	+0.0252	0.633	0.467	0.0290	11.778	0.598
0.7656	0.830	+0.0132	0.573	0.460	0.0297	10.761	0.670
0.6406	0.804	+0.00558	0.517	0.457	0.0304	10.049	0.732
0.5156	0.783	+0.00100	0.465	0.456	0.0309	9.537	0.783
0.3906	0.767	-0.00135	0.417	0.455	0.0313	9.153	0.825
0.2656	0.754	-0.00209	0.372	0.455	0.0317	8.856	0.860
0.1406	0.743	-0.00161	0.331	0.455	0.0320	8.617	0.889
0.0000	0.735	0.00000	0.292	0.454	0.0323	8.422	0.912

TABLE 2.13

/102

$M_\infty = 20$; $w_{max} = 6536.2$ m/sec; $h_{00} = 82\ 215°K$;

$\varepsilon_0 = 0.05413$; $\varepsilon_1 = 0.09437$; $\varepsilon_2 = 0.05947$

ξ	s	u	v	p	T	ρ	h
			$s = 0$				
1.0000	0	-0.0675	0	0.922	0.0326	14.716	0.995
0.8906	0	-0.0573	0	0.931	0.0327	14.832	0.996
0.7656	0	-0.0466	0	0.939	0.0327	14.933	0.997
0.6406	0	-0.0369	0	0.946	0.0328	15.007	0.998
0.5156	0	-0.0280	0	0.950	0.0328	15.060	0.999
0.3906	0	-0.0201	0	0.953	0.0328	15.095	0.999
0.2656	0	-0.0129	0	0.955	0.0328	15.117	0.999
0.1406	0	-0.00645	0	0.956	0.0328	15.129	0.999
0.0000	0	0.00000	0	0.956	0.0328	15.133	0.999
			$s = s_1/2$				
1.0000	0.450	-0.0475	0.407	0.770	0.0287	15.283	0.831
0.8906	0.431	-0.0425	0.365	0.777	0.0292	14.819	0.864
0.7656	0.415	-0.0361	0.323	0.783	0.0297	14.416	0.894
0.6406	0.402	-0.0296	0.286	0.788	0.0302	14.102	0.916
0.5156	0.392	-0.0232	0.253	0.792	0.0306	13.848	0.934
0.3906	0.384	-0.0170	0.224	0.795	0.0310	13.638	0.949
0.2656	0.378	-0.0112	0.197	0.798	0.0313	13.463	0.960
0.1406	0.373	-0.00571	0.172	0.799	0.0316	13.315	0.970
0.0000	0.369	0.00000	0.148	0.800	0.0318	13.182	0.977
			$s = s_1$				
1.0000	0.900	+0.0401	0.691	0.476	0.0242	13.972	0.520
0.8906	0.863	+0.0250	0.637	0.462	0.0249	12.417	0.592
0.7656	0.831	+0.0131	0.575	0.454	0.0257	11.164	0.668
0.6406	0.805	+0.00551	0.517	0.451	0.0264	10.302	0.731
0.5156	0.785	+0.000966	0.465	0.449	0.0270	9.687	0.783
0.3906	0.769	-0.00137	0.418	0.449	0.0276	9.225	0.824
0.2656	0.756	-0.00209	0.375	0.449	0.0281	8.861	0.859
0.1406	0.746	-0.00161	0.335	0.448	0.0286	8.562	0.887
0.0000	0.738	0.00000	0.297	0.447	0.0291	8.313	0.908

TABLE 2.14

/10

$M_\infty = 21$; $w_{max} = 6959.1$ m/sec; $h_{00} = 90\ 538°K$;

$\varepsilon_0 = 0.05674$; $\varepsilon_1 = 0.09362$; $\varepsilon_2 = 0.06098$

ξ	s	u	v	p	T	ρ	h
			$s = 0$				
1.0000	0	-0.0735	0	0.917	0.0342	13.511	0.994
0.8906	0	-0.0622	0	0.927	0.0344	13.617	0.996
0.7656	0	-0.0504	0	0.936	0.0345	13.707	0.997
0.6406	0	-0.0399	0	0.943	0.0345	13.773	0.998
0.5156	0	-0.0303	0	0.947	0.0346	13.819	0.999
0.3906	0	-0.0217	0	0.951	0.0346	13.850	0.999
0.2656	0	-0.0140	0	0.952	0.0346	13.869	0.999
0.1406	0	-0.00705	0	0.953	0.0346	13.879	0.999
0.0000	0	0.00000	0	0.954	0.0346	13.883	1.000
			$s = s_1/2$				
1.0000	0.450	-0.0495	0.411	0.767	0.0275	15.162	0.828
0.8906	0.431	-0.0445	0.367	0.774	0.0283	14.563	0.862
0.7656	0.415	-0.0380	0.325	0.781	0.0291	14.025	0.892
0.6406	0.402	-0.0314	0.288	0.786	0.0299	13.592	0.915
0.5156	0.392	-0.0247	0.256	0.791	0.0307	13.233	0.933
0.3906	0.384	-0.0183	0.227	0.794	0.0313	12.932	0.947
0.2656	0.378	-0.0121	0.201	0.796	0.0319	12.678	0.959
0.1406	0.373	-0.00621	0.177	0.797	0.0324	12.466	0.968
0.0000	0.369	0.00000	0.155	0.798	0.0329	12.275	0.975
			$s = s_1$				
1.0000	0.900	+0.0394	0.694	0.473	0.0226	14.353	0.516
0.8906	0.863	+0.0246	0.642	0.458	0.0233	12.658	0.586
0.7656	0.830	+0.0127	0.578	0.449	0.0241	11.250	0.665
0.6406	0.805	+0.00504	0.518	0.446	0.0249	10.281	0.730
0.5156	0.785	+0.000511	0.465	0.445	0.0257	9.594	0.782
0.3906	0.769	-0.00176	0.419	0.445	0.0265	9.078	0.823
0.2656	0.757	-0.00238	0.378	0.445	0.0272	8.664	0.856
0.1406	0.747	-0.00175	0.342	0.444	0.0279	8.313	0.882
0.0000	0.739	0.00000	0.307	0.443	0.0286	8.011	0.903

TABLE 2.15

$M_\infty = 22$; $w_{max} = 7182.1$ m/sec; $h_{00} = 99\ 267°K$;

$\varepsilon_0 = 0.06237$; $\varepsilon_1 = 0.09316$; $\varepsilon_2 = 0.06447$

ξ	s	u	v	p	T	ρ	h
			$s = 0$				
1.0000	0	-0.0832	0	0.908	0.0380	11.954	0.993
0.8906	0	-0.0698	0	0.920	0.0382	12.060	0.995
0.7656	0	-0.0564	0	0.930	0.0383	12.147	0.996
0.6406	0	-0.0447	0	0.938	0.0384	12.209	0.998
0.5156	0	-0.0341	0	0.943	0.0385	12.253	0.998
0.3906	0	-0.0246	0	0.946	0.0385	12.282	0.999
0.2656	0	-0.0159	0	0.948	0.0386	12.300	0.999
0.1406	0	-0.00808	0	0.950	0.0386	12.310	0.999
0.0000	0	0.00000	0	0.950	0.0386	12.314	1.000

ξ	s	u	v	p	T	ρ	h
			$s = s_1/2$				
1.0000	0.450	-0.0543	0.418	0.761	0.0269	14.743	0.821
0.8906	0.431	-0.0492	0.372	0.768	0.0284	13.871	0.858
0.7656	0.414	-0.0427	0.329	0.775	0.0300	13.075	0.889
0.6406	0.402	-0.0355	0.293	0.781	0.0316	12.468	0.912
0.5156	0.392	-0.0282	0.262	0.785	0.0329	12.006	0.930
0.3906	0.384	-0.0209	0.234	0.788	0.0340	11.646	0.944
0.2656	0.378	-0.0138	0.209	0.790	0.0349	11.360	0.955
0.1406	0.374	-0.00715	0.187	0.792	0.0356	11.128	0.964
0.0000	0.371	0.00000	0.165	0.792	0.0363	10.927	0.972
			$s = s_1$				
1.0000	0.900	+0.0374	0.698	0.469	0.0211	14.662	0.510
0.8906	0.862	+0.0230	0.649	0.452	0.0218	12.858	0.576
0.7656	0.829	+0.0109	0.583	0.442	0.0228	11.247	0.659
0.6406	0.804	+0.00317	0.520	0.439	0.0238	10.132	0.728
0.5156	0.784	-0.00120	0.468	0.439	0.0249	9.349	0.780
0.3906	0.769	-0.00318	0.425	0.439	0.0260	8.751	0.818
0.2656	0.757	-0.00341	0.389	0.438	0.0272	8.250	0.848
0.1406	0.748	-0.00233	0.357	0.437	0.0284	7.802	0.872
0.0000	0.742	0.00000	0.326	0.435	0.0298	7.405	0.891

TABLE 2.16 /10

$M_\infty = 23$; $w_{max} = 7505.3$ m/sec; $h_{00} = 108\ 402°K$;

$\varepsilon_0 = 0.06961$; $\varepsilon_1 = 0.09283$; $\varepsilon_2 = 0.06899$

ξ	s	u	v	p	T	ρ	h
			$s = 0$				
1.0000	0	-0.0918	0	0.900	0.0414	10.842	0.991
0.8906	0	-0.0770	0	0.914	0.0416	10.953	0.994
0.7656	0	-0.0627	0	0.925	0.0417	11.044	0.996
0.6406	0	-0.0501	0	0.933	0.0418	11.109	0.997
0.5156	0	-0.0385	0	0.938	0.0419	11.155	0.998
0.3906	0	-0.0279	0	0.942	0.0420	11.187	0.999
0.2656	0	-0.0182	0	0.945	0.0420	11.208	0.999
0.1406	0	-0.00929	0	0.946	0.0420	11.219	0.999
0.0000	0	0.00000	0	0.947	0.0420	11.223	1.000
			$s = s_1/2$				
1.0000	0.450	-0.0621	0.427	0.751	0.0275	13.855	0.813
0.8906	0.430	-0.0573	0.381	0.758	0.0301	12.669	0.851
0.7656	0.414	-0.0498	0.338	0.765	0.0326	11.772	0.882
0.6406	0.401	-0.0414	0.303	0.772	0.0345	11.185	0.906
0.5156	0.391	-0.0327	0.272	0.776	0.0360	10.767	0.924
0.3906	0.384	-0.0241	0.244	0.779	0.0373	10.449	0.939
0.2656	0.378	-0.0159	0.219	0.781	0.0383	10.200	0.951
0.1406	0.374	-0.00820	0.195	0.782	0.0390	10.004	0.961
0.0000	0.371	0.00000	0.175	0.782	0.0396	9.847	0.969

/10

ξ	s	u	v	p	T	ρ	h
			$s = s_1$				
1.0000	0.900	+0.0346	0.703	0.464	0.0198	14.909	0.504
0.8906	0.861	+0.0198	0.654	0.446	0.0206	12.974	0.570
0.7656	0.828	+0.00758	0.586	0.438	0.0217	11.184	0.655
0.6406	0.803	+0.000165	0.526	0.435	0.0231	9.938	0.723
0.5156	0.783	-0.00362	0.479	0.434	0.0247	9.026	0.770
0.3906	0.769	-0.00498	0.442	0.433	0.0264	8.286	0.804
0.2656	0.757	-0.00440	0.409	0.431	0.0283	7.646	0.832
0.1406	0.748	-0.00275	0.377	0.429	0.0303	7.097	0.857
0.0000	0.742	0.00000	0.347	0.425	0.0321	6.669	0.877

/10

TABLE 2.17

/105

$M_\infty = 24$; $w_{max} = 7828.7$ m/sec; $h_{00} = 117\ 943°K$;

$\varepsilon_0 = 0.07601$; $\varepsilon_1 = 0.09361$; $\varepsilon_2 = 0.07340$

ξ	s	u	v	p	T	ρ	h
			$s = 0$				
1.0000	0	-0.0973	0	0.895	0.0433	10.232	0.990
0.8906	0	-0.0826	0	0.909	0.0435	10.345	0.993
0.7656	0	-0.0680	0	0.920	0.0436	10.440	0.995
0.6406	0	-0.0547	0	0.929	0.0437	10.511	0.996
0.5156	0	-0.0423	0	0.935	0.0438	10.564	0.998
0.3906	0	-0.0308	0	0.940	0.0439	10.600	0.999
0.2656	0	-0.0201	0	0.942	0.0439	10.624	0.999
0.1406	0	-0.0103	0	0.944	0.0439	10.637	0.999
0.0000	0	0.0000	0	0.945	0.0439	10.642	0.999
			$s = s_1/2$				
1.0000	0.450	-0.0719	0.434	0.740	0.0295	12.548	0.806
0.8906	0.430	-0.0658	0.390	0.748	0.0326	11.463	0.843
0.7656	0.414	-0.0566	0.349	0.756	0.0352	10.731	0.874
0.6406	0.401	-0.0465	0.313	0.763	0.0371	10.256	0.899
0.5156	0.392	-0.0364	0.282	0.768	0.0386	9.913	0.919
0.3906	0.384	-0.0268	0.252	0.771	0.0397	9.654	0.935
0.2656	0.379	-0.0176	0.225	0.773	0.0406	9.457	0.948
0.1406	0.374	-0.00907	0.202	0.774	0.0413	9.309	0.959
0.0000	0.371	0.00000	0.182	0.774	0.0418	9.197	0.966
			$s = s_1$				
1.0000	0.900	+0.0322	0.707	0.460	0.0187	15.102	0.488
0.8906	0.861	+0.0153	0.653	0.445	0.0196	12.932	0.573
0.7656	0.828	+0.00428	0.587	0.438	0.0211	11.039	0.654
0.6406	0.803	-0.00235	0.535	0.434	0.0230	9.677	0.712
0.5156	0.784	-0.00522	0.496	0.431	0.0252	8.614	0.752
0.3906	0.769	-0.00575	0.462	0.428	0.0277	7.741	0.786
0.2656	0.758	-0.00481	0.427	0.425	0.0303	7.028	0.816
0.1406	0.749	-0.00290	0.394	0.422	0.0326	6.478	0.844
0.0000	0.742	0.00000	0.364	0.419	0.0344	6.102	0.865

TABLE 2.18

$M_\infty = 25$; $w_{max} = 8152.1$ m/sec; $h_{00} = 127\ 890°K$;

$\varepsilon_0 = 0.08008$; $\varepsilon_1 = 0.09703$; $\varepsilon_2 = 0.07748$

ξ	s	u	v	p	T	ρ	h
			$s = 0$				
1.0000	0	−0.100	0	0.893	0.0439	9.960	0.989
0.8906	0	−0.0863	0	0.906	0.0441	10.069	0.992
0.7656	0	−0.0715	0	0.918	0.0442	10.168	0.994
0.6406	0	−0.0578	0	0.927	0.0443	10.246	0.996
0.5156	0	−0.0448	0	0.934	0.0443	10.304	0.997
0.3906	0	−0.0327	0	0.938	0.0444	10.345	0.998
0.2656	0	−0.0215	0	0.942	0.0444	10.371	0.999
0.1406	0	−0.0110	0	0.943	0.0444	10.386	0.999
0.0000	0	0.0000	0	0.944	0.0444	10.392	0.999
			$s = s_1/2$				
1.0000	0.450	−0.0796	0.434	0.733	0.0323	11.332	0.805
0.8906	0.430	−0.0715	0.393	0.743	0.0350	10.573	0.839
0.7656	0.414	−0.0606	0.354	0.752	0.0372	10.053	0.870
0.6406	0.402	−0.0494	0.319	0.759	0.0388	9.696	0.895
0.5156	0.393	−0.0386	0.286	0.764	0.0401	9.434	0.916
0.3906	0.385	−0.0283	0.255	0.767	0.0410	9.236	0.933
0.2656	0.379	−0.0186	0.228	0.770	0.0417	9.088	0.947
0.1406	0.374	−0.00962	0.204	0.771	0.0423	8.978	0.957
0.0000	0.370	0.00000	0.186	0.771	0.0426	8.896	0.965
			$s = s_1$				
1.0000	0.900	+0.0306	0.710	0.458	0.0178	15.234	0.494
0.8906	0.861	+0.0133	0.645	0.445	0.0191	12.621	0.583
0.7656	0.828	+0.00195	0.586	0.439	0.0212	10.612	0.656
0.6406	0.804	−0.00354	0.545	0.434	0.0238	9.173	0.702
0.5156	0.786	−0.00570	0.510	0.430	0.0267	8.065	0.738
0.3906	0.771	−0.00591	0.475	0.426	0.0296	7.192	0.773
0.2656	0.759	−0.00465	0.438	0.423	0.0324	6.525	0.807
0.1406	0.749	−0.00280	0.402	0.421	0.0347	6.049	0.837
0.0000	0.741	0.00000	0.372	0.417	0.0363	5.746	0.859

EQUILIBRIUM OXYGEN. SCHEME II. N = 3 /107

TABLE 2.19

$M_\infty = 10$; $p_\infty = 0.001$ atm; $T_\infty = 288°K$; $\rho_\infty = 0.001354$ kg/m^3;

$w_{max} = 3307$ m/sec; $h_{00} = 21\,055.3°K$; $\delta = 1$;

$\varepsilon_1 = 0.07871$; $\varepsilon_2 = 0.09861$; $\varepsilon_3 = 0.1429$

ξ	s	u	v	p	T	ρ	h	C_0
			$s = 0$					
1.000	0	-0.0890	0	0.872	0.0702	10.965	0.991	0.132
0.875	0	-0.0749	0	0.884	0.0702	11.108	0.993	0.133
0.750	0	-0.0617	0	0.894	0.0703	11.220	0.995	0.133
0.625	0	-0.0495	0	0.902	0.0703	11.306	0.997	0.134
0.500	0	-0.0381	0	0.908	0.0704	11.370	0.998	0.134
0.375	0	-0.0274	0	0.912	0.0704	11.414	0.998	0.134
0.250	0	-0.0175	0	0.914	0.0704	11.443	0.999	0.134
0.125	0	-0.00846	0	0.916	0.0704	11.458	0.999	0.134
0.000	0	0.00000	0	0.916	0.0704	11.462	0.999	0.134
			$s = s_1/3$					
1.000	0.291	-0.0802	0.248	0.814	0.0690	10.560	0.931	0.116
0.875	0.277	-0.0686	0.222	0.826	0.0693	10.642	0.945	0.119
0.750	0.266	-0.0573	0.199	0.836	0.0695	10.707	0.956	0.123
0.625	0.257	-0.0464	0.179	0.843	0.0697	10.757	0.965	0.125
0.500	0.249	-0.0360	0.161	0.849	0.0698	10.792	0.972	0.127
0.375	0.243	-0.0261	0.144	0.853	0.0699	10.814	0.977	0.129
0.250	0.239	-0.0168	0.129	0.856	0.0700	10.824	0.982	0.130
0.125	0.235	-0.00813	0.115	0.858	0.0700	10.823	0.986	0.131
0.000	0.233	0.00000	0.102	0.858	0.0701	10.811	0.989	0.132
			$s = 2s_1/3$					
1.000	0.583	-0.0480	0.466	0.669	0.0657	9.463	0.779	0.0752
0.875	0.554	-0.0453	0.421	0.677	0.0666	9.369	0.819	0.0860
0.750	0.532	-0.0406	0.381	0.685	0.0672	9.305	0.852	0.0950
0.625	0.514	-0.0348	0.345	0.691	0.0677	9.257	0.878	0.102
0.500	0.499	-0.0282	0.312	0.696	0.0681	9.217	0.900	0.108
0.375	0.487	-0.0213	0.282	0.700	0.0685	9.178	0.918	0.113
0.250	0.478	-0.0141	0.254	0.702	0.0687	9.139	0.933	0.118
0.125	0.471	-0.00704	0.228	0.703	0.0689	9.095	0.946	0.121
0.000	0.466	0.00000	0.204	0.702	0.0690	9.042	0.957	0.124
			$s = s_1$					
1.000	0.875	+0.0218	0.628	0.501	0.0604	8.039	0.603	0.0326
0.875	0.832	+0.00660	0.577	0.501	0.0623	7.677	0.665	0.0474
0.750	0.798	-0.00251	0.529	0.502	0.0637	7.427	0.718	0.0610
0.625	0.771	-0.00741	0.485	0.503	0.0647	7.244	0.763	0.0729
0.500	0.749	-0.00932	0.444	0.504	0.0655	7.100	0.801	0.0834
0.375	0.731	-0.00906	0.405	0.504	0.0661	6.980	0.833	0.0924
0.250	0.717	-0.00720	0.370	0.504	0.0666	6.874	0.861	0.100
0.125	0.706	-0.00412	0.337	0.502	0.0670	6.771	0.885	0.107
0.000	0.699	0.00000	0.306	0.499	0.0673	6.663	0.904	0.112

EQUILIBRIUM NITROGEN. SCHEME II. N = 2 /108

M_∞ = 10-27; p_∞ = 0.01 atm; T_∞ = 290°K; ρ = 0.01177 kg/m^3;

δ = 1

TABLE 2.20

M_∞ = 10; w_{max} = 3557.8 m/sec; h_{00} = 21 315°K;

ε_0 = 0.1078; ε_1 = 0.1864; ε_2 = 0.1225

ξ	s	u	v	p	T	ρ	h
			$s = 0$				
1.0000	0	-0.131	0	0.830	0.111	7.423	0.982
0.8906	0	-0.114	0	0.846	0.111	7.538	0.986
0.7656	0	-0.0963	0	0.861	0.111	7.646	0.990
0.6406	0	-0.0789	0	0.872	0.111	7.733	0.993
0.5156	0	-0.0622	0	0.881	0.112	7.800	0.996
0.3906	0	-0.0462	0	0.888	0.112	7.850	0.997
0.2656	0	-0.0309	0	0.893	0.112	7.884	0.999
0.1406	0	-0.0161	0	0.896	0.112	7.904	0.999
0.0000	0	0.0000	0	0.897	0.112	7.912	0.999
			$s = s_1/2$				
1.0000	0.450	-0.103	0.374	0.709	0.0998	7.093	0.849
0.8906	0.428	-0.0933	0.342	0.723	0.102	7.068	0.874
0.7656	0.409	-0.0806	0.310	0.737	0.104	7.056	0.897
0.6406	0.394	-0.0675	0.282	0.748	0.105	7.050	0.915
0.5156	0.382	-0.0543	0.258	0.756	0.106	7.043	0.930
0.3906	0.372	-0.0410	0.237	0.763	0.107	7.034	0.941
0.2656	0.364	-0.0278	0.218	0.767	0.108	7.019	0.951
0.1406	0.358	-0.0146	0.201	0.769	0.109	6.996	0.959
0.0000	0.354	0.0000	0.185	0.768	0.109	6.960	0.965
			$s = s_1$				
1.0000	0.900	+0.0120	0.642	0.475	0.0719	6.604	0.586
0.8906	0.857	-0.00275	0.602	0.477	0.0775	6.156	0.636
0.7656	0.819	-0.0127	0.559	0.480	0.0830	5.781	0.687
0.6406	0.789	-0.0174	0.519	0.482	0.0877	5.503	0.730
0.5156	0.764	-0.0184	0.482	0.484	0.0915	5.288	0.766
0.3906	0.745	-0.0167	0.449	0.484	0.0946	5.115	0.797
0.2656	0.729	-0.0129	0.420	0.483	0.0971	4.968	0.823
0.1406	0.717	-0.00756	0.394	0.480	0.0991	4.835	0.844
0.0000	0.708	0.00000	0.370	0.474	0.100	4.706	0.861

TABLE 2.21

/108

$M_\infty = 15$; $w_{max} = 5265.7$ m/sec; $h_{00} = 46\ 690°K$;

$\varepsilon_0 = 0.07338$; $\varepsilon_1 = 0.1426$; $\varepsilon_2 = 0.08546$

ξ	s	u	v	p	T	ρ	h
			$s = 0$				
1.0000	0	-0.0889	0	0.893	0.0698	11.118	0.992
0.8906	0	-0.0765	0	0.904	0.0699	11.243	0.994
0.7656	0	-0.0633	0	0.915	0.0699	11.358	0.995
0.6406	0	-0.0510	0	0.923	0.0700	11.446	0.997
0.5156	0	-0.0395	0	0.929	0.0700	11.511	0.998

/109

ξ	s	u	v	p	T	ρ	h
0.3906	0	-0.0288	0	0.933	0.0700	11.557	0.999
0.2656	0	-0.0188	0	0.936	0.0701	11.587	0.999
0.1406	0	-0.00964	0	0.937	0.0701	11.604	0.999
0.0000	0	0.00000	0	0.938	0.0701	11.610	0.999
			$s = s_1/2$				
1.0000	0.450	-0.0675	0.383	0.756	0.0666	10.251	0.848
0.8906	0.429	-0.0605	0.347	0.766	0.0672	10.223	0.875
0.7656	0.411	-0.0519	0.310	0.776	0.0677	10.207	0.900
0.6406	0.396	-0.0430	0.278	0.784	0.0681	10.197	0.920
0.5156	0.384	-0.0341	0.249	0.791	0.0685	10.188	0.936
0.3906	0.374	-0.0253	0.224	0.796	0.0687	10.177	0.948
0.2656	0.367	-0.0168	0.201	0.799	0.0689	10.160	0.959
0.1406	0.361	-0.00875	0.180	0.801	0.0690	10.139	0.967
0.0000	0.356	0.00000	0.159	0.801	0.0692	10.107	0.974
			$s = s_1$				
1.0000	0.900	+0.0316	0.652	0.495	0.0578	8.302	0.572
0.8906	0.859	+0.0163	0.613	0.491	0.0597	7.887	0.623
0.7656	0.822	+0.00461	0.564	0.490	0.0615	7.521	0.680
0.6406	0.793	-0.00242	0.516	0.490	0.0629	7.248	0.732
0.5156	0.769	-0.00597	0.470	0.490	0.0640	7.042	0.778
0.3906	0.749	-0.00695	0.427	0.491	0.0648	6.882	0.816
0.2656	0.734	-0.00605	0.388	0.491	0.0654	6.751	0.848
0.1406	0.722	-0.00375	0.353	0.490	0.0659	6.637	0.874
0.0000	0.713	0.00000	0.319	0.487	0.0663	6.528	0.895

TABLE 2.22

/109

$M_\infty = 20$; $w_{max} = 6985.5$ m/sec; $h_{00} = 82\ 215°K$;

$\varepsilon_0 = 0.05773$; $\varepsilon_1 = 0.1115$; $\varepsilon_2 = 0.06634$

ξ	s	u	v	p	T	ρ	h
			$s=0$				
1.0000	0	-0.0699	0	0.919	0.0463	14.208	0.995
0.8906	0	-0.0597	0	0.929	0.0463	14.336	0.996
0.7656	0	-0.0489	0	0.937	0.0463	14.450	0.997
0.6406	0	-0.0389	0	0.944	0.0464	14.535	0.998
0.5156	0	-0.0298	0	0.948	0.0464	14.597	0.999
0.3906	0	-0.0214	0	0.951	0.0464	14.639	0.999
0.2656	0	-0.0138	0	0.953	0.0464	14.665	0.999
0.1406	0	-0.00695	0	0.954	0.0464	14.680	0.999
0.0000	0	0.00000	0	0.955	0.0464	14.684	0.999
			$s=s_1/2$				
1.0000	0.450	-0.0515	0.396	0.771	0.0442	13.338	0.840
0.8906	0.431	-0.0460	0.357	0.779	0.0445	13.184	0.870
0.7656	0.413	-0.0392	0.317	0.787	0.0449	13.057	0.897
0.6406	0.400	-0.0322	0.281	0.793	0.0451	12.964	0.919
0.5156	0.389	-0.0253	0.250	0.798	0.0453	12.890	0.936

ξ	s	u	v	p	T	ρ	h
0.3906	0.380	-0.0186	0.221	0.802	0.0455	12.828	0.950
0.2656	0.373	-0.0122	0.195	0.804	0.0456	12.775	0.961
0.1406	0.367	-0.00625	0.171	0.806	0.0457	12.726	0.970
0.0000	0.363	0.00000	0.147	0.807	0.0458	12.675	0.978
			$s=s_1$				
1.0000	0.900	+0.0392	0.674	0.488	0.0392	10.919	0.544
0.8906	0.862	+0.0238	0.627	0.480	0.0402	10.159	0.605
0.7656	0.827	+0.0116	0.572	0.475	0.0411	9.509	0.672
0.6406	0.800	+0.00398	0.518	0.473	0.0418	9.035	0.731
0.5156	0.778	-0.000487	0.467	0.472	0.0424	8.686	0.781
0.3906	0.760	-0.00260	0.420	0.472	0.0429	8.423	0.823
0.2656	0.746	-0.00300	0.376	0.472	0.0433	8.218	0.858
0.1406	0.735	-0.00212	0.336	0.471	0.0436	8.052	0.886
0.0000	0.727	0.00000	0.296	0.470	0.0438	7.910	0.909

/110

TABLE 2.23

/110

$M_\infty = 25$; $w_{max} = 8712.5$ m/sec; $h_{00} = 127\ 890°K$;

$\varepsilon_0 = 0.05157$; $\varepsilon_1 = 0.09676$; $\varepsilon_2 = 0.05830$

ξ	s	u	v	p	T	ρ	h
			$s=0$				
1.0000	0	-0.0627	0	0.930	0.0342	15.883	0.996
0.8906	0	-0.0533	0	0.939	0.0342	16.010	0.997
0.7656	0	-0.0434	0	0.947	0.0343	16.122	0.998
0.6406	0	-0.0344	0	0.952	0.0343	16.205	0.998
0.5156	0	-0.0262	0	0.956	0.0343	16.264	0.999
0.3906	0	-0.0187	0	0.959	0.0343	16.304	0.999
0.2656	0	-0.0120	0	0.961	0.0343	16.328	0.999
0.1406	0	-0.00602	0	0.962	0.0343	16.341	0.999
0.0000	0	0.00000	0	0.962	0.0343	16.346	0.999
			$s = s_1/2$				
1.0000	0.450	-0.0455	0.403	0.777	0.0322	15.365	0.834
0.8906	0.431	-0.0404	0.362	0.784	0.0325	15.056	0.866
0.7656	0.415	-0.0343	0.321	0.799	0.0328	14.796	0.895
0.6406	0.402	-0.0281	0.284	0.795	0.0331	14.601	0.918
0.5156	0.392	-0.0219	0.251	0.799	0.0333	14.448	0.936
0.3906	0.383	-0.0160	0.221	0.802	0.0334	14.325	0.950
0.2656	0.377	-0.0105	0.193	0.805	0.0335	14.224	0.962
0.1406	0.372	-0.00536	0.168	0.806	0.0337	14.139	0.971
0.0000	0.368	0.00000	0.143	0.807	0.0337	14.060	0.979
			$s = s_1$				
1.0000	0.900	+0.0415	0.687	0.482	0.0282	13.195	0.525
0.8906	0.863	+0.0262	0.634	0.470	0.0289	11.938	0.596
0.7656	0.830	+0.0141	0.574	0.463	0.0296	10.925	0.669
0.6406	0.805	+0.00632	0.517	0.460	0.0302	10.221	0.731
0.5156	0.784	+0.00160	0.464	0.459	0.0307	9.716	0.783
0.3906	0.767	-0.000892	0.416	0.458	0.0311	9.341	0.826
0.2656	0.754	-0.00176	0.371	0.458	0.0315	9.052	0.862
0.1406	0.744	-0.00141	0.329	0.458	0.0317	8.822	0.891
0.0000	0.736	0.00000	0.288	0.457	0.0320	8.635	0.914

TABLE 2.24

$M_\infty = 27$; $w_{max} = 9404.2$ m/sec; $h_{00} = 149\ 002°K$;

$\varepsilon_0 = 0.05086$; $\varepsilon_1 = 0.09347$; $\varepsilon_2 = 0.05698$

ξ	s	u	v	p	T	ρ	h
			$s=0$				
1.0000	0	-0.0621	0	0.932	0.0315	16.034	0.996
0.8906	0	-0.0528	0	0.940	0.0316	16.160	0.997
0.7656	0	-0.0429	0	0.948	0.0316	16.270	0.998
0.6406	0	-0.0340	0	0.954	0.0316	16.352	0.998
0.5156	0	-0.0258	0	0.958	0.0316	16.409	0.999
0.3906	0	-0.0184	0	0.960	0.0316	16.448	0.999
0.2656	0	-0.0118	0	0.962	0.0316	16.472	0.999
0.1406	0	-0.00592	0	0.963	0.0316	16.485	0.999
0.0000	0	0.00000	0	0.963	0.0316	16.489	0.999
			$s=s_1/2$				
1.0000	0.450	-0.0445	0.406	0.778	0.0291	15.825	0.833
0.8906	0.431	-0.0397	0.364	0.784	0.0295	15.442	0.865
0.7656	0.415	-0.0337	0.322	0.790	0.0298	15.118	0.894
0.6406	0.403	-0.0276	0.285	0.795	0.0301	14.872	0.917
0.5156	0.392	-0.0215	0.252	0.799	0.0304	14.678	0.936
0.3906	0.384	-0.0157	0.221	0.802	0.0306	14.522	0.950
0.2656	0.378	-0.0103	0.193	0.804	0.0307	14.395	0.962
0.1406	0.373	-0.00525	0.168	0.806	0.0309	14.289	0.971
0.0000	0.369	0.00000	0.143	0.806	0.0310	14.193	0.979
			$s=s_1$				
1.0000	0.900	+0.0417	0.691	0.480	0.0251	13.944	0.520
0.8906	0.863	+0.0264	0.636	0.467	0.0258	12.472	0.593
0.7656	0.831	+0.0143	0.575	0.459	0.0265	11.307	0.669
0.6406	0.806	+0.00660	0.517	0.456	0.0271	10.508	0.732
0.5156	0.785	+0.00188	0.464	0.454	0.0277	9.940	0.784
0.3906	0.769	-0.000655	0.415	0.454	0.0281	9.517	0.827
0.2656	0.756	-0.00158	0.370	0.454	0.0285	9.190	0.862
0.1406	0.746	-0.00131	0.329	0.454	0.0288	8.929	0.891
0.0000	0.738	0.00000	0.288	0.453	0.0291	8.716	0.914

EQUILIBRIUM AIR. SCHEME II. N = 2

$\delta = 1$

TABLE 2.25

$M_\infty = 4$; $p_\infty = 1$ atm; $T_\infty = 300°K$; $\rho_\infty = 1.177$ kg/m^3;

$w_{max} = 1591$ m/sec; $h_{00} = 4410°K$; $\varepsilon_0 = 0.1679$;

$\varepsilon_1 = 0.3129$; $\varepsilon_2 = 0.1935$

ξ	s	u	v	p	T	ρ	h
			$s = 0$				
1.0000	0	-0.0621	0	0.932	0.0315	16.034	0.996
0.8906	0	-0.0528	0	0.940	0.0316	16.160	0.997
0.7656	0	-0.0429	0	0.948	0.0316	16.270	0.998
0.6406	0	-0.0340	0	0.954	0.0316	16.352	0.998
0.5156	0	-0.0258	0	0.958	0.0316	16.409	0.999
0.3906	0	-0.0184	0	0.960	0.0316	16.448	0.999
0.2656	0	-0.0118	0	0.962	0.0316	16.472	0.999
0.1406	0	-0.00592	0	0.963	0.0316	16.485	0.999
0.0000	0	0.00000	0	0.963	0.0316	16.489	0.999
			$s = s_1/2$				
1.0000	0.450	-0.0445	0.406	0.778	0.0291	15.825	0.833
0.8906	0.431	-0.0397	0.364	0.784	0.0295	15.442	0.865
0.7656	0.415	-0.0337	0.322	0.790	0.0298	15.118	0.894
0.6406	0.403	-0.0276	0.285	0.795	0.0301	14.872	0.917
0.5156	0.392	-0.0215	0.252	0.799	0.0304	14.678	0.936
0.3906	0.384	-0.0157	0.221	0.802	0.0306	14.522	0.950
0.2656	0.378	-0.0103	0.193	0.804	0.0307	14.395	0.962
0.1406	0.373	-0.00525	0.168	0.806	0.0309	14.289	0.971
0.0000	0.369	0.00000	0.143	0.806	0.0310	14.193	0.979
			$s = s_1$				
1.0000	0.900	+0.0417	0.691	0.480	0.0251	13.944	0.520
0.8906	0.863	+0.0264	0.636	0.467	0.0258	12.472	0.593
0.7656	0.831	+0.0143	0.575	0.459	0.0265	11.307	0.669
0.6406	0.806	+0.00660	0.517	0.456	0.0271	10.508	0.732
0.5156	0.785	+0.00188	0.464	0.454	0.0277	9.940	0.784
0.3906	0.769	-0.000655	0.415	0.454	0.0281	9.517	0.827
0.2656	0.756	-0.00158	0.370	0.454	0.0285	9.190	0.862
0.1406	0.746	-0.00131	0.329	0.454	0.0288	8.929	0.891
0.0000	0.738	0.00000	0.288	0.453	0.0291	8.716	0.914

TABLE 2.26

/112

$M_\infty = 6$; $p_\infty = 1$ atm; $T_\infty = 300°K$; $\rho_\infty = 1.177$ kg/m^3; $w_{max} = 2223$ m/sec;

$h_{00} = 8610°K$; $\varepsilon_0 = 0.1309$; $\varepsilon_1 = 0.2487$; $\varepsilon_2 = 0.1510$

ξ	s	u	v	p	T	ρ	h
			$s = 0$				
1.0000	0	-0.151	0	0.753	0.121	6.182	0.977
0.8906	0	-0.133	0	0.769	0.122	6.288	0.982
0.7656	0	-0.112	0	0.785	0.122	6.390	0.987
0.6406	0	-0.0930	0	0.798	0.123	6.472	0.991
0.5156	0	-0.0741	0	0.809	0.123	6.538	0.994
0.3906	0	-0.0556	0	0.816	0.123	6.588	0.996
0.2656	0	-0.0376	0	0.822	0.124	6.623	0.998
0.1406	0	-0.0198	0	0.825	0.124	6.645	0.999
0.0000	0	0.0000	0	0.827	0.124	6.653	1.000

/113

ξ	s	u	v	p	T	ρ	h
			$s = s_1/2$				
1.0000	0.500	-0.114	0.392	0.625	0.106	5.885	0.833
0.8906	0.473	-0.104	0.358	0.641	0.109	5.871	0.860
0.7656	0.449	-0.0920	0.325	0.657	0.112	5.867	0.885
0.6406	0.429	-0.0782	0.296	0.670	0.114	5.868	0.905
0.5156	0.414	-0.0637	0.272	0.680	0.115	5.869	0.921
0.3906	0.401	-0.0487	0.251	0.688	0.117	5.866	0.934
0.2656	0.391	-0.0334	0.233	0.693	0.118	5.857	0.944
0.1406	0.383	-0.0178	0.218	0.696	0.119	5.841	0.952
0.0000	0.376	0.0000	0.204	0.696	0.119	5.812	0.958
			$s = s_1$				
1.0000	1.000	+0.0352	0.643	0.406	0.0778	5.217	0.585
0.8906	0.947	+0.0142	0.614	0.408	0.0821	4.971	0.622
0.7656	0.898	+0.00170	0.578	0.411	0.0872	4.719	0.665
0.6406	0.859	-0.0109	0.541	0.414	0.0919	4.506	0.706
0.5156	0.828	-0.0151	0.506	0.416	0.0961	4.331	0.743
0.3906	0.802	-0.0154	0.474	0.417	0.0996	4.186	0.774
0.2656	0.782	-0.0127	0.447	0.416	0.102	4.060	0.799
0.1406	0.766	-0.00776	0.424	0.413	0.104	3.946	0.820
0.0000	0.752	0.00000	0.404	0.407	0.106	3.836	0.834

TABLE 2.27

/113

$M_\infty = 10$; $p_\infty = 0.01$ atm; $T_\infty = 300°K$; $\rho_\infty = 0.01177$ kg/m^3; $w_{max} = 3557$ m/sec; $h_{00} = 22\,050°K$; $\varepsilon_0 = 0.08662$; $\varepsilon_1 = 0.1854$; $\varepsilon_2 = 0.1028$

ξ	s	u	v	p	T	ρ	h
			$s = 0$				
1.0000	0	-0.103	0	0.858	0.0827	9.469	0.989
0.8906	0	-0.0891	0	0.871	0.0829	9.589	0.992
0.7656	0	-0.0742	0	0.883	0.0830	9.699	0.994
0.6406	0	-0.0602	0	0.892	0.0831	9.785	0.996
0.5156	0	-0.0470	0	0.899	0.0832	9.850	0.997
0.3906	0	-0.0346	0	0.904	0.0832	9.896	0.998
0.2656	0	-0.0228	0	0.907	0.0833	9.928	0.999
0.1406	0	-0.0118	0	0.909	0.0833	9.945	0.999
0.0000	0	0.0000	0	0.910	0.0833	9.952	0.999
			$s = s_1/2$				
1.0000	0.500	-0.0732	0.413	0.702	0.0760	8.727	0.823
0.8906	0.474	-0.0670	0.373	0.715	0.0773	8.683	0.855
0.7656	0.450	-0.0585	0.333	0.728	0.0784	8.656	0.884
0.6406	0.432	-0.0492	0.299	0.739	0.0793	8.640	0.907
0.5156	0.417	-0.0395	0.269	0.747	0.0800	8.628	0.925
0.3906	0.404	-0.0297	0.243	0.753	0.0805	8.616	0.939
0.2656	0.395	-0.0200	0.219	0.757	0.0809	8.600	0.951
0.1406	0.387	-0.0105	0.199	0.760	0.0813	8.580	0.960
0.0000	0.380	0.0000	0.179	0.761	0.0816	8.552	0.967

/114

ξ	s	u	v	p	T	ρ	h
			$s = s_1$				
1.0000	1.000	+0.0619	0.678	0.434	0.0610	7.062	0.536
0.8906	0.948	+0.0389	0.644	0.431	0.0639	6.648	0.582
0.7656	0.901	+0.0199	0.599	0.430	0.0671	6.264	0.640
0.6406	0.864	+0.00751	0.551	0.431	0.0697	5.976	0.696
0.5156	0.834	+0.0000946	0.504	0.432	0.0718	5.763	0.745
0.3906	0.809	-0.00354	0.461	0.434	0.0734	5.602	0.786
0.2656	0.790	-0.00438	0.423	0.434	0.0746	5.475	0.820
0.1406	0.775	-0.00314	0.390	0.434	0.0756	5.366	0.847
0.0000	0.761	0.00000	0.359	0.431	0.0764	5.266	0.868

TABLE 2.28

/114

$M_\infty = 30$; $p_\infty = 0.01$ atm; $T_\infty = 300°K$; $\rho_\infty = 0.01177$ kg/m^3; $w_{max} = 10\ 445$ m/sec; $h_{00} = 190\ 050°K$; $\varepsilon_0 = 0.06074$; $\varepsilon_1 = 0.1326$; $\varepsilon_2 = 0.06736$

ξ	s	u	v	p	T	ρ	h
			$s = 0$				
1.0000	0	-0.0720	0	0.923	0.0323	13.832	0.994
0.8906	0	-0.0610	0	0.933	0.0323	13.958	0.996
0.7656	0	-0.0497	0	0.942	0.0324	14.064	0.997
0.6406	0	-0.0395	0	0.948	0.0324	14.142	0.998
0.5156	0	-0.0303	0	0.953	0.0324	14.198	0.999
0.3906	0	-0.0218	0	0.956	0.0324	14.236	0.999
0.2656	0	-0.0142	0	0.958	0.0325	14.260	0.999
0.1406	0	-0.00721	0	0.959	0.0325	14.273	0.999
0.0000	0	0.00000	0	0.959	0.0325	14.278	1.000
			$s = s_1/2$				
1.0000	0.550	-0.0408	0.492	0.703	0.0248	14.910	0.755
0.8906	0.519	-0.0393	0.433	0.714	0.0262	13.942	0.810
0.7656	0.494	-0.0353	0.378	0.724	0.0276	13.191	0.855
0.6406	0.475	-0.0298	0.333	0.732	0.0287	12.699	0.888
0.5156	0.461	-0.0238	0.294	0.739	0.0295	12.364	0.912
0.3906	0.449	-0.0177	0.259	0.744	0.0302	12.124	0.932
0.2656	0.440	-0.0118	0.228	0.748	0.0306	11.949	0.947
0.1406	0.432	-0.00610	0.201	0.751	0.0310	11.821	0.959
0.0000	0.425	0.00000	0.178	0.754	0.0313	11.729	0.968
			$s = s_1$				
1.0000	1.100	0.114	0.768	0.363	0.0189	13.188	0.396
0.8906	1.0397	0.0811	0.723	0.341	0.0198	11.067	0.469
0.7656	0.988	0.0514	0.651	0.331	0.0210	9.288	0.573
0.6406	0.951	0.0312	0.582	0.328	0.0221	8.209	0.659
0.5156	0.922	0.0181	0.526	0.329	0.0232	7.526	0.722
0.3906	0.898	0.00966	0.479	0.330	0.0242	7.030	0.770
0.2656	0.880	0.00439	0.436	0.331	0.0253	6.632	0.809
0.1406	0.864	0.00143	0.397	0.332	0.0264	6.311	0.841
0.0000	0.851	0.00000	0.362	0.332	0.0273	6.079	0.866

CALCULATION OF FLOW IN THE SUPERSONIC REGION BY THE METHOD OF CHARACTERISTICS. EQUILIBRIUM OXYGEN

$M_\infty = 10$; $p_\infty = 0.001$ atm; $T_\infty = 288°K$; $\rho_\infty = 0.00135$ kg/m^3;

$w_{max} = 3236$ m/sec

TABLE 2.29

Spherical Blunt-Cylinder ($\delta = 1$; $\omega = 0°$)

Distribution of Gas Dynamic Parameters Along Surface of Body

x_0	r_0	p_0	T_0	ρ_0	w_0	ζ_0	$(C_0)_0$
0.284	0.698	0.424	0.0662	5.780	0.343	1.025	0.108
0.307	0.721	0.396	0.0659	5.437	0.357	0.959	0.106
0.360	0.768	0.340	0.0652	4.735	0.387	0.831	0.101
0.420	0.815	0.285	0.0643	4.042	0.418	0.710	0.0956
0.490	0.860	0.231	0.0634	3.351	0.452	0.591	0.0888
0.594	0.914	0.168	0.0619	2.526	0.497	0.443	0.0792
0.667	0.942	0.135	0.0608	2.077	0.525	0.352	0.0726
0.760	0.970	0.101	0.0595	1.604	0.559	0.246	0.0642
0.896	0.994	0.0658	0.0575	1.087	0.606	0.104	0.0520
0.970	0.999	0.0510	0.0563	0.865	0.631	0.0294	0.0453
1.071	1.000	0.0448	0.0557	0.770	0.643	0.000	0.0420
1.190	1.000	0.0429	0.0555	0.742	0.646	0.000	0.0410

Coordinates of Nose Shock Wave

x_B	-0.0756	-0.0455	0.0423	0.181	0.366	0.435	0.525	0.641	0.772	0.896	0.974	1.068	1.182
r_B	0.0000	0.266	0.523	0.762	0.986	1.054	1.137	1.232	1.330	1.413	1.463	1.520	1.585

TABLE 2.30

Spherical Segment-Cylinder ($\delta = 1$; $\chi = 43.8°$; $\omega = 0°$)

Distribution of Gas Dynamic Parameters Along Surface of Body

x_0	r_0	p_0	T_0	ρ_0	w_0	ζ_0	$(C_0)_0$
0.297	0.692	0.0580	0.0570	0.970	0.617	0	0.0489
0.374	0.692	0.0579	0.0569	0.968	0.618	0	0.0488
0.477	0.692	0.0570	0.0569	0.955	0.619	0	0.0484
0.559	0.692	0.0549	0.0567	0.924	0.623	0	0.0474
0.660	0.692	0.0522	0.0565	0.884	0.627	0	0.0462
0.786	0.692	0.0491	0.0562	0.836	0.633	0	0.0446
0.944	0.692	0.0457	0.0559	0.785	0.640	0	0.0428
1.071	0.692	0.0434	0.0556	0.749	0.644	0	0.0415
1.299	0.692	0.0399	0.0552	0.695	0.652	0	0.0395
1.635	0.692	0.0362	0.0548	0.637	0.660	0	0.0371
2.140	0.692	0.0340	0.0545	0.602	0.666	0	0.0357
2.730	0.692	0.0302	0.0539	0.542	0.676	0	0.0329

TABLE 2.30 Continued

Coordinates of Nose Shock Wave

x_B	-0.0756	-0.0455	0.0423	0.181	0.366
r_B	0	0.266	0.523	0.762	0.986

CHAPTER 3

NONEQUILIBRIUM FLOWS

1. Nonequilibrium Gas Flow Around Blunt Bodies

In the preceding chapter the results of calculating equilibrium gas flow around blunt bodies were presented. However, in a number of cases the flow field between the detached shock wave and the body surface can be essentially nonequilibrium. /116

In the examination of such processes certain difficulties arise because very abrupt changes of concentrations may occur in the shock layer, and approximations of the relaxation equations at a given number of the approximation prove to be substantially less accurate than approximations of the initial equations of motion and continuity. Furthermore, in nonequilibrium flows we must use the approximate representation of the second equation of motion (projection onto axis n) in place of the condition of conservation of entropy along the lines of flow. Calculation experience has shown that this approximation in scheme I is not accurate enough and may lead to instability of the calculations.

Scheme I of the method of integral relations for calculating nonequilibrium gas flows was developed [12], where these difficulties managed to be avoided. The relaxation equations and the second equation of motion were not approximated, but were written along the lines of flow and projected onto the lines of separation of the integration range. The method of calculating nonequilibrium gas flows by scheme II is presented in [21,22]. Here the relaxation equations were also written along the lines of flow, which made it possible to increase the accuracy of the calculations and to construct the entire flow field behind the shock-wave front. In the nonequilibrium case, as is known, the distribution of the gas dynamic parameters in the shock layer is affected not only by temperature, pressure, and Mach number in the oncoming flow (as in the equilibrium case), but also by the dimensions of the streamline body.

We will dwell at first on certain results of calculating the flow of nonequilibrium dissociating oxygen around bodies of different shape on the assumption that all internal degrees of freedom are in a state of equilibrium. /117

Certain results of the calculations are presented in Tables 3.1-3.7, 3.18 (scheme I, N = 2), 3.8-3.17 (scheme II, N = 2,3), and also in Figures 3.1-3.11.

Figure 3.1 shows the position and shape of shock waves and sonic lines for a sphere ($\delta = 1$) of radius $R_0 = 1$ cm (curve 2) and $R_0 = 10$ cm (curve 3) when $M_\infty = 10$, $p_\infty = 0.01$ atm, $T_\infty = 290°K$. For comparison the figure also shows data for the case of a fully equilibrium flow (curve 4) and a "frozen" flow corresponding to $\varkappa = 1.4$ (curve 1).

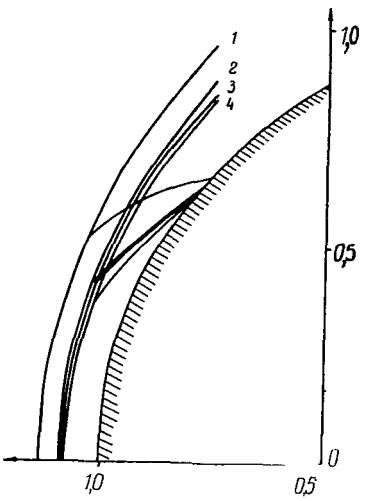

Figure 3.1. Position and shape of shock waves and sonic lines. Flow of nonequilibrium dissociated oxygen stream past sphere when $M_\infty = 10$, $p_\infty = 0.01$ atm, $T_\infty = 290°K$: 1) completely "frozen" flow, $\varkappa = 1.4$; 2) nonequilibrium flow, $R_0 = 1$ cm; 3) nonequilibrium flow, $R_0 = 10$ cm; 4) fully equilibrium flow.

To obtain more complete information on the flow field in the shock layer, /118
the streamlines were also constructed for all variants. In Figure 3.2 the dashed lines indicate streamlines for sphere $R_0 = 10$ cm when $M_\infty = 10$, $p_\infty = 0.01$ atm, $T_\infty = 290°K$ intersecting the shock wave, respectively at points $x = -1.082$, $y = 0.069$; $x = 1.077$, $y = 0.136$; $x = -1.005$, $y = 0.27$; $x = 0.97$, $y = 0.53$ (the origin of the coordinates is located at the center of the body). Here the dot-dash line denotes the line corresponding to the points of local equilibrium. Upstream from this line the process of dissociation (the rate of dissociation is greater than the rate of recombination) predominates, and downstream the process of recombination (the rate of dissociation is less than the rate of recombination) predominates. It is obvious that the region where recombination plays a substantial role, becomes rather noticeable far from the critical point. This is related with expansion of the flow in this zone and with a corresponding temperature drop which leads to a noticeable decline of the rate of dissociation.

The construction of streamlines is especially useful for bodies of a complex shape, for example when calculating flow around severely blunted bodies. Figures 3.3 and 3.4 show the shape and position of shock waves, sonic lines, and streamlines for ellipsoids of revolution with a ratio of semiaxes $\delta = b/a = 10$ (Figure 3.3) and 100 (Figure 3.4) when $b = 1$ cm ($M_\infty = 10$, $p_\infty = 0.01$ atm, $T_\infty = 290°K$). We see that for severely blunted bodies the sonic line has a more complex shape than, for example, the flow around a sphere. Only by constructing the streamlines was it possible to determine correctly the position and shape of the sonic lines for each body type.

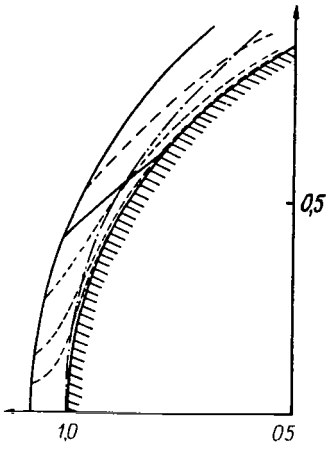

Figure 3.2. Position of streamline and line of local equilibrium dissociated oxygen stream around sphere when $M_\infty = 10$, $p_\infty = 0.01$ atm, $T_\infty = 290°K$, $R_0 = 10$ cm. Dashed lines, streamlines, dot-dash line, line of local equilibrium.

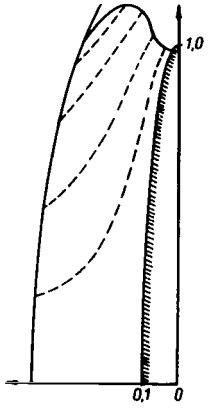

Figure 3.3. Position and shape of shock wave, sonic line, and streamlines. Flow of nonequilibrium dissociated oxygen stream around ellipsoid of revolution when $M_\infty = 10$, $p_\infty = 0.01$ atm, $T_\infty = 290°K$, $\delta = b/a = 10$, $b = 1$ cm.

/119

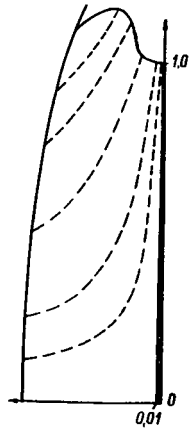

Figure 3.4. Position and shape of shock wave, sonic line, and streamlines. Flow of nonequilibrium dissociated oxygen stream around ellipsoid of revolution when $M_\infty = 10$, $p_\infty = 0.01$ atm, $T_\infty = 290°K$, $\delta = b/a = 100$, $b = 1$ cm.

The magnitude of separation of the shock wave ($\delta = 1.0$, curve 1; $\delta = 10$, curve 2; $\delta = 100$, curve 3) is shown as a function of the coordinate s in Figure 3.5 for $M_\infty = 10$, $p_\infty = 0.01$ atm, $T_\infty = 290°K$. As we see from the graph,

these dependences have a different character for different bluntness.

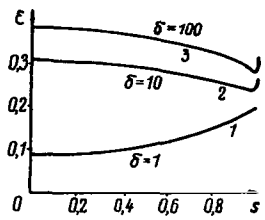

Figure 3.5. Magnitude of separation of shock wave. Flow of nonequilibrium dissociated oxygen stream around sphere and ellipsoids of revolution when $M_\infty = 10$, $p_\infty = 0.01$ atm, $T_\infty = 290°K$: 1) $\delta = 1$; 2) $\delta = 10$; 3) $\delta = 100$, $R_0 = b = 1$ cm.

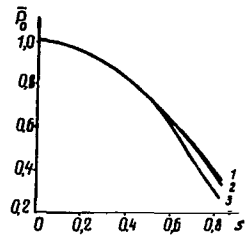

Figure 3.6. Distribution of pressure along surface of sphere. Flow of nonequilibrium dissociated oxygen stream around sphere when $M_\infty = 10$, $p_\infty = 0.01$ atm, $T_\infty = 290°K$: 1) nonequilibrium flow, $R_0 = 4$ cm; 2) nonequilibrium flow, $R_0 = 10$ cm; 3) fully equilibrium flow.

/120

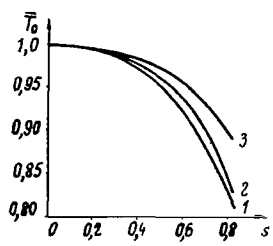

Figure 3.7. Distribution of temperature along surface of sphere. Flow of nonequilibrium dissociated oxygen stream around sphere when $M_\infty = 10$, $p_\infty = 0.01$ atm, $T_\infty = 290°K$: 1) nonequilibrium flow, $R_0 = 4$ cm; 2) nonequilibrium flow, $R_0 = 10$ cm; 3) fully equilibrium flow.

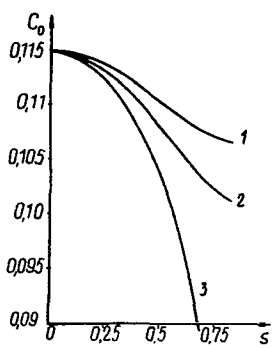

Figure 3.8. Distribution of concentration of atomic oxygen along surface of sphere. Flow of nonequilibrium dissociated oxygen stream around sphere and ellipsoids of revolution when $M_\infty = 10$, $p_\infty = 0.01$ atm, $T_\infty = 290°K$: 1) nonequilibrium flow, $R_0 = 4$ cm; 2) nonequilibrium flow, $R_0 = 10$ cm; 3) fully equilibrium flow.

Figures 3.6-3.8 show the distribution of pressure, temperature (referred to corresponding values at the critical point), and degree of dissociation along the surface of a sphere of radius R_0 = 4 cm (curve 1) and R_0 = 10 cm (curve 2) when M_∞ = 10, p_∞ = 0.01 atm, T_∞ = 290°K. For comparison the figures also show the corresponding data for an equilibrium flow (curve 3) at the same initial conditions. Hence it follows that the absence of dissociation equilibrium has a substantial effect on the temperature profiles and degree of dissociation and a comparatively negligible effect on the pressure profile. With an increase of the radius of the sphere the profiles approach the corresponding equilibrium values. Figures 3.9-3.11 show analogous curves for bodies of different bluntness, δ = 1.0 (curve 1), δ = 10 (curve 2), δ = 100 (curve 3), with the same characteristic dimension b = 1 cm when M_∞ = 10, p_∞ = 0.01 atm, T_∞ = 290°K.

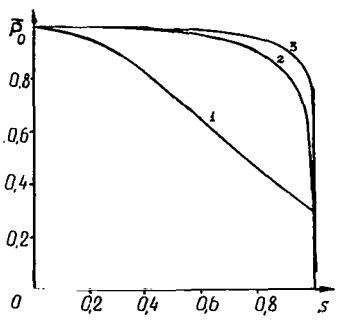

Figure 3.9. Distribution of pressure along surface of blunt bodies. Flow of nonequilibrium dissociated oxygen stream around sphere and ellipsoids of revolution when M_∞ = 10, p_∞ = 0.01 atm, T_∞ = 290°K: 1) δ = 1; 2) δ = 10; 3) δ = 100, R_0 = = b = 1 cm.

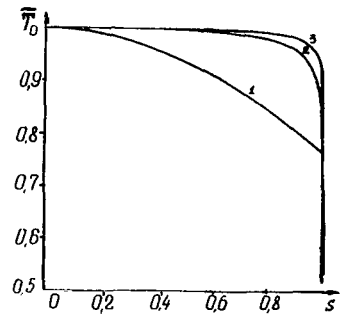

Figure 3.10. Distribution of temperature along surface of blunt bodies. Flow of nonequilibrium dissociated oxygen stream around sphere and ellipsoids of revolution when M_∞ = 10, p_∞ = 0.01 atm, T_∞ = 290°K: 1) δ = 1; 2) δ = 10; 3) δ = 100, R_0 = b = 1 cm.

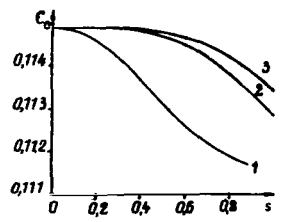

Figure 3.11. Distribution of concentration of atomic oxygen along surface of blunt bodies. Flow of nonequilibrium dissociated oxygen stream around sphere and ellipsoids of revolution when M_∞ = 10, p_∞ = 0.01 atm, T_∞ = 290°K: 1) δ = 1; 2) δ = 10; 3) δ = 100; R_0 = b = 1 cm.

Let us now examine the flow of a stream of nonequilibrium dissociating air around blunt bodies, which is, of course, of considerable practical interest. In this case several reactions occur simultaneously which are complexly related with one another. The first results of investigating the flow of a nonequilibrium dissociating air around blunt bodies were obtained by means of inverse methods [35,36], when the shape of the shock wave was given and when the body corresponding to it was found. Calculations by direct methods were performed quite recently. Certain results are contained also in [16,27].

The results are presented of a calculation of nonequilibrium air flow around blunt bodies with consideration of six dissociation reactions obtained by scheme II of the method of integral relation. The effect of the totality of the various reactions on the profiles of gas dynamic quantities and concentrations of all components both in the shock layer and on the surface of the body are examined in detail. It is assumed that the following reactions occur in air:

$$\begin{cases} O_2 + M \rightleftarrows 2O + M; & \text{(I)} \\ N_2 + M \rightleftarrows 2N + M; & \text{(II)} \\ NO + M \rightleftarrows N + O + M; & \text{(III)} \\ N + O_2 \rightleftarrows NO + O; & \text{(IV)} \\ N_2 + O \rightleftarrows NO + N; & \text{(V)} \\ N_2 + O_2 \rightleftarrows 2NO, & \text{(VI)} \end{cases}$$

where M is any of the examined components.

The complete system of relaxation equations for this case is written in the following form [22]: /122

$$\frac{dC_{O_2}}{dt} = \rho\mu_{O_2}\left\{\left[\frac{\rho}{K_{pI}}\left(\frac{C_O}{\mu_O}\right)^2 - \frac{C_{O_2}}{\mu_{O_2}}\right]\sum_{i=1}^{6} K_I^{(i)}\frac{C_i}{\mu_i} + K_{IV}\left[\frac{1}{K_{pIV}}\frac{C_O}{\mu_O}\frac{C_{NO}}{\mu_{NO}} - \frac{C_N}{\mu_N}\frac{C_{O_2}}{\mu_{O_2}}\right] + K_{VI}\left[\frac{1}{K_{pVI}}\left(\frac{C_{NO}}{\mu_{NO}}\right)^2 - \frac{C_{O_2}}{\mu_{O_2}}\frac{C_{N_2}}{\mu_{N_2}}\right]\right\}; \quad (3.1)$$

$$\frac{dC_{N_2}}{dt} = \rho\mu_{N_2}\left\{\left[\frac{\rho}{K_{pII}}\left(\frac{C_N}{\mu_N}\right)^2 - \frac{C_{N_2}}{\mu_{N_2}}\right]\sum_{i=1}^{6} K_{II}^{(i)}\frac{C_i}{\mu_i} + K_V\left[\frac{1}{K_{pV}}\frac{C_N}{\mu_N}\frac{C_{NO}}{\mu_{NO}} - \frac{C_{N_2}}{\mu_{N_2}}\frac{C_O}{\mu_O}\right] + K_{VI}\left[\frac{1}{K_{pVI}}\left(\frac{C_{NO}}{\mu_{NO}}\right)^2 - \frac{C_{O_2}}{\mu_{O_2}}\frac{C_{N_2}}{\mu_{N_2}}\right]\right\}; \quad (3.2)$$

$$\frac{dC_{NO}}{dt} = \rho\mu_{NO}\left\{\left[\frac{\rho}{K_{pIII}}\frac{C_N}{\mu_N}\frac{C_0}{\mu_0} - \frac{C_{NO}}{\mu_{NO}}\right]\sum_{i=1}^{6} K_{III}^{(i)}\frac{C_i}{\mu_i} + K_{IV}\left[\frac{C_N}{\mu_N}\frac{C_{0_2}}{\mu_{0_2}} - \right.\right.$$

$$- \frac{1}{K_{pIV}}\frac{C_{NO}}{\mu_{NO}} - \frac{C_0}{\mu_0}\Bigg] + K_V\left[\frac{C_{N_2}}{\mu_{N_2}}\frac{C_0}{\mu_0} - \frac{1}{K_{pV}}\frac{C_{NO}}{\mu_{NO}}\frac{C_N}{\mu_N}\right] +$$

$$\left. + 2K_{VI}\left[\frac{C_{N_2}}{\mu_{N_2}}\frac{C_{0_2}}{\mu_{0_2}} - \frac{1}{K_{pVI}}\left(\frac{C_{NO}}{\mu_{NO}}\right)^2\right]\right\}; \qquad (3.3)$$

$$\frac{dC_0}{dt} = \rho\mu_0\left\{2\left[\frac{C_{0_2}}{\mu_{0_2}} - \frac{\rho}{K_{pI}}\left(\frac{C_0}{\mu_0}\right)^2\right]\sum_{i=1}^{6} K_I^{(i)}\frac{C_i}{\mu_i} + \left[\frac{C_{NO}}{\mu_{NO}} - \right.\right.$$

$$- \frac{\rho}{K_{pIII}}\frac{C_N}{\mu_N}\frac{C_0}{\mu_0}\Bigg]\sum_{i=1}^{6} K_{III}^{(i)}\frac{C_i}{\mu_i} + K_{IV}\left[\frac{C_N}{\mu_N}\frac{C_{0_2}}{\mu_{0_2}} - \frac{1}{K_{pIV}}\frac{C_0}{\mu_0}\frac{C_{NO}}{\mu_{NO}}\right] +$$

$$\left. + K_V\left[\frac{1}{K_{pV}}\frac{C_N}{\mu_N}\frac{C_{NO}}{\mu_{NO}} - \frac{C_{N_2}}{\mu_{N_2}}\frac{C_0}{\mu_0}\right]\right\}; \qquad (3.4)$$

$$\frac{dC_N}{dt} = \rho\mu_N\left\{2\left[\frac{C_{N_2}}{\mu_{N_2}} - \frac{\rho}{K_{pII}}\left(\frac{C_N}{\mu_N}\right)^2\right]\sum_{i=1}^{6} K_{II}^{(i)}\frac{C_i}{\mu_i} + \right.$$

$$+ \left[\frac{C_{NO}}{\mu_{NO}} - \frac{\rho}{K_{pIII}}\frac{C_N}{\mu_N}\frac{C_0}{\mu_0}\right]\sum_{i=1}^{6} K_{III}^{(i)}\frac{C_i}{\mu_i} + K_{IV}\left[\frac{1}{K_{pIV}}\frac{C_0}{\mu_0}\frac{C_{NO}}{\mu_{NO}} - \right.$$

$$\left. - \frac{C_N}{\mu_N}\frac{C_{0_2}}{\mu_{0_2}}\right] + K_V\left[\frac{C_{N_2}}{\mu_{N_2}}\frac{C_0}{\mu_0} - \frac{1}{K_{pV}}\frac{C_N}{\mu_N}\frac{C_{NO}}{\mu_{NO}}\right]\Bigg\}; \qquad (3.5)$$

$$\frac{dC_{Ar}}{dt} = 0. \qquad (3.6)$$

Here K_{pI}, K_{pII}, ..., K_{pVI} are equilibrium constants, respectively, of reactions (I) - (VI); $K_I^{(i)}$, $K_{II}^{(i)}$, $K_{III}^{(i)}$, are constants of the rate of disintegration of molecules O_2, N_2, NO, when these molecules collide with component i; K_{IV}, K_V,

K_{VI} are constants of the rate of forward reactions (IV), (V), and (VI). The values of K_{pI}, K_{pII}, K_{pIII} were calculated from approximations given in tables [37]; the values of the remaining constants were selected from [36].

In place of certain relaxation equations we will introduce the Dalton equation

$$\sum_{i=1}^{6} C_i = 1 \tag{3.7}$$

and two equations of material balance, which are a consequence of the law of conservation of mass and of the Dalton equation

$$C_{O_2} + \frac{\mu_O}{\mu_{NO}} C_{NO} + C_O = (C_{O_2})_\infty; \tag{3.8}$$

$$C_{N_2} + \frac{\mu_N}{\mu_{NO}} C_{NO} + C_N = (C_{N_2})_\infty, \tag{3.9}$$

where $(C_{O_2})_\infty$ and $(C_{N_2})_\infty$ are values of the concentrations of C_{O_2} and C_{N_2} in the oncoming flow.

To determine the mass concentrations C_i we will use equations (3.1), (3.2), (3.4), (3.6) and equations (3.8), (3.9) in place of the six differential equations (3.1)-(3.6).

We note that the examined relaxation equations (3.1), (3.2), and (3.4) were not approximated, but written along the lines of flow in the form /124

$$\left(\frac{dC_j}{d\xi}\right)_{C.F.} = \frac{\omega_j}{\rho u}\left(\varepsilon + \xi\varepsilon_s' \frac{ds_{C.F}}{d\xi}\right)\frac{R_0}{w_{max}}$$

and used in the approximating system in an exact form. This substantially increased the accuracy of the calculations and made it possible to obtain the entire field of concentrations of individual components.

In the same manner we calculated flow of a nonequilibrium air stream around blunt bodies of different radius within a wide range of M_∞ and p_∞. We will dwell on certain results of the calculations.

In the shock layer nonequilibrium has a most pronounced effect on profiles of temperature and concentration of the gas components and a lesser effect on the velocity values. On the axis of symmetry the "nonequilibrium" temperature is higher than the "equilibrium" temperature owing to "lag" of the dissociation

process, whereas on the surface of the body it is lower owing to "lag" of the recombination process. An increase of the body radius R_0 at unchanged conditions in the oncoming flow brings the flow in the shock layer nearer to equilibrium. An analogous dependence is observed on raising pressure p_∞ in the oncoming flow.

To elicit the effect of individual reactions on establishing equilibrium in the region behind the shock wave, four variants of different aggregates of reactions were throughly investigated. In the first of them (this case it is depicted by a solid line in Figures 3.12, 3.18, and 3.19) all six reactions were taken into account, in the second (x's) reaction (VI) was excluded, in the third (dots) reaction (V) was excluded, and finally, in the fourth variant (triangles) reactions (IV), (V), and (VI) were excluded. When performing the calculations, the vanishing of the velocity of any of the six reactions was examined as a state of unstable equilibrium of this reaction which can be disturbed by a nonequilibrium flow of other reactions. The simultaneous vanishing of the velocities of all reactions taken into account was considered stable equilibrium. The results of the calculations showed that such equilibrium is established at the stagnation point.

As an example we examined flow around a sphere of radius R_0 = 1 cm when M_∞= 15, p_∞ = 0.01165 atm, T_∞ = 231.24°K, $(C_{O_2})_\infty$ = 0.2646, $(C_{N_2})_\infty$ = 0.7354, $(C_{Ar})_\infty$ = 0.

The results of the calculation are shown in Figures 3.12-3.19.

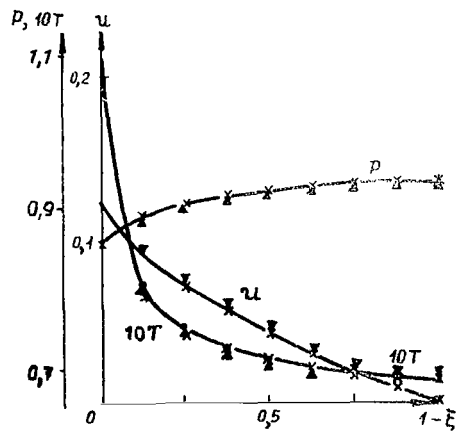

Figure 3.12. Distribution of pressure, temperature, and velocity along axis of symmetry. Flow of nonequilibrium dissociated air stream around sphere when M_∞ = 15, p_∞ = 0.01165 atm, T_∞ = 231.24°K, R_0 = 1 cm, $(C_{O_2})_\infty$ = 0.2646, $(C_{N_2})_\infty$ = 0.7354, $(C_{Ar})_\infty$ = 0: —— reactions I-VI; xxx - without reaction VI; ●●● - without reaction V; ▲▼▲ - without reactions IV - VI.

Figure 3.12 shows the profiles of the dimensionless magnitudes of pressure p, temperature T, and the normal component of velocity u along the axis of symmetry for all four variants. It is interesting that these parameters, and consequently the position of the shock wave, depend little on the number of reactions considered. For the case in question, as we see from the graph, the gas temperature as a result of dissociation drops almost by a factor of 2, whereas the pressure increases comparatively little. The velocity profile is close to linear. /125

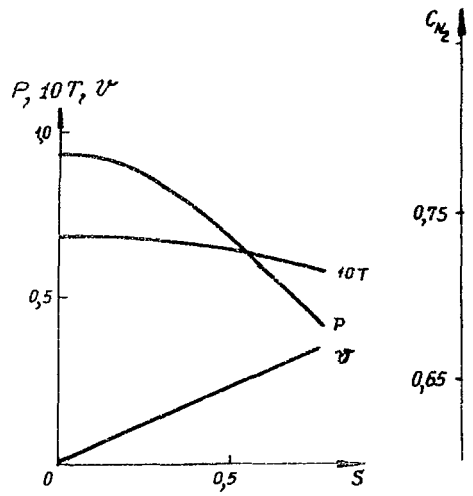

Figure 3.13. Distribution of pressure, temperature, and velocity along surface of body. Flow of nonequilibrium dissociated air stream around sphere when M_∞ = 15, p_∞ = 0.01165 atm, T_∞ = 231.24°K, R_0 = 1 cm, $(C_{O_2})_\infty$ = 0.2646, $(C_{N_2})_\infty$ = 0.7354, $(C_{Ar})_\infty$ = 0.

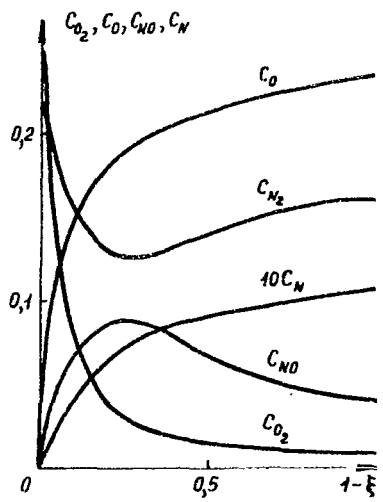

Figure 3.14. Distribution of concentrations of gas components along axis of symmetry s = 0. Flow of nonequilibrium dissociated air stream around sphere when M_∞ = 15, p_∞ = 0.01165 atm, T_∞ = 231.24°K, R_0 = 1 cm, $(C_{O_2})_\infty$ = 0.2646, $(C_{N_2})_\infty$ = 0.7354, $(C_{Ar})_\infty$ = 0.

/127

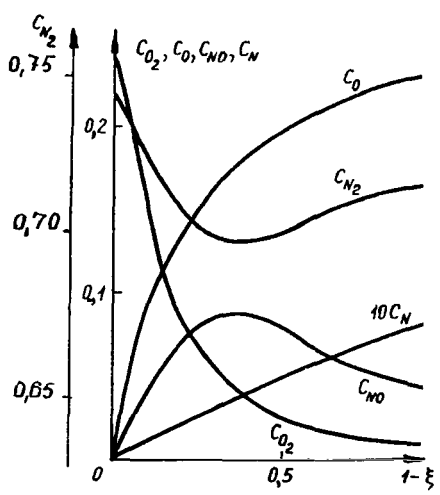

Figure 3.15. Distribution of concentrations of gas components along intermediate line s = s_1 (ξ)/2. Flow of nonequilibrium dissociated air stream around sphere when M_∞ = 15, p_∞ = 0.01165 atm, T_∞ = 231.24°K, R_0 = 1 cm, $(C_{O_2})_\infty$ = 0.2646, $(C_{N_2})_\infty$ = 0.7354, $(C_{Ar})_\infty$ = 0.

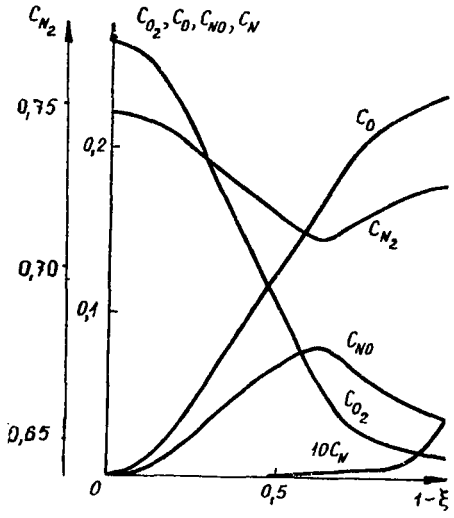

Figure 3.16. Distribution of concentrations of gas components along boundary characteristic $s = s_1(\xi)$. Flow of nonequilibrium dissociated air stream around sphere when M_∞ = 15, p_∞ = 0.01165 atm, T_∞ = 231.24°K R_0 = 1 cm, $(C_{O_2})_\infty$ = 0.2646, $(C_{N_2})_\infty$ = 0.7354, $(C_{Ar})_\infty$ = 0.

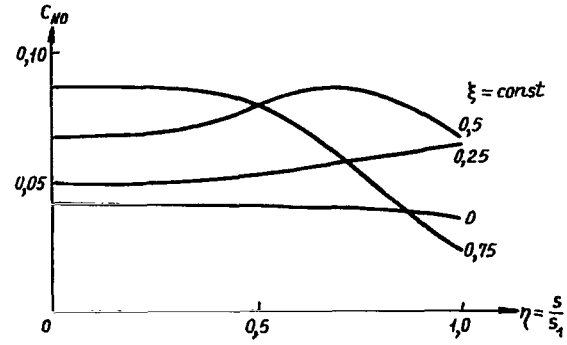

Figure 3.17. Distribution of nitric oxide concentration along lines $\xi = n/\varepsilon$ = const. Flow of nonequilibrium dissociated air stream around sphere when M_∞ = 15, p_∞ = 0.01165 atm, T_∞ = 231.24°K, R_0 = 1 cm, $(C_{O_2})_\infty$ = 0.2646, $(C_{N_2})_\infty$ = 0.7354, $(C_{Ar})_\infty$ = 0.

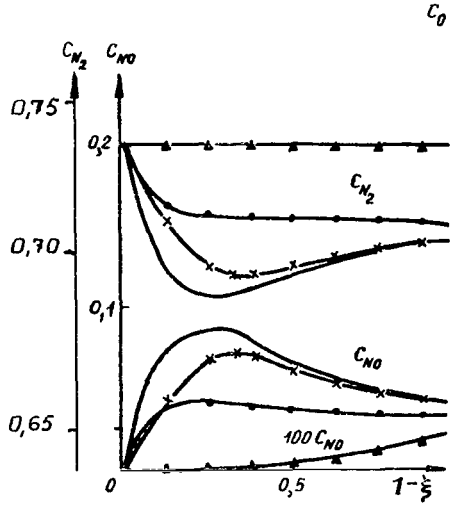

/128

Figure 3.18. Distribution of concentrations of molecular nitrogen and nitric oxide as a function of the considered reactions. Flow of nonequilibrium dissociated air flow around sphere when M_∞ = 15, p_∞ = 0.01165 atm, T_∞ = 231.24°K, R_0 = 1 cm, $(C_{O_2})_\infty$ = 0.2646, $(C_{N_2})_\infty$ = 0.7354, $(C_{Ar})_\infty$ = 0:
—— reactions I-VI; xxx - without reaction VI; ●●● - without reaction V; ▲▲▲ - without reactions IV-VI.

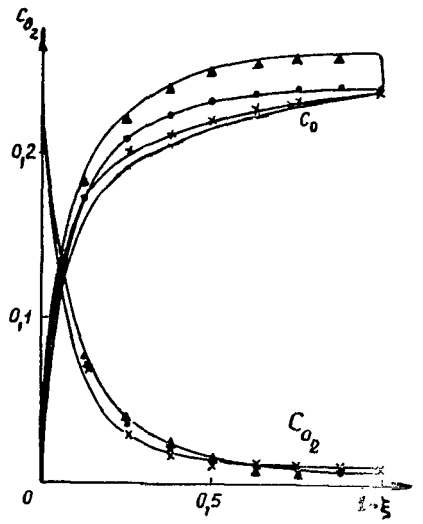

Figure 3.19. Distribution of concentrations of atomic and molecular oxygen as a function of the considered reactions. Flow of nonequilibrium dissociated air stream around sphere when $M_\infty = 15$, $p_\infty = 0.01165$ atm, $T_\infty = 231.24°K$, $R_0 = 1$ cm, $(C_{O_2})_\infty = 0.2646$, $(C_{N_2})_\infty = 0.7354$, $(C_{Ar})_\infty = 0$: —— reactions I-VI; xxx - without reaction VI; ●●● - without reaction V; ▲▲▲ - without reactions IV-VI.

Figure 3.13 shows the change of p, T, and v along the surface of a sphere. We see that the relative drop of temperature is less than that of pressure, and the velocity profile is close to linear just as along the axis of symmetry.

Figure 3.14 gives the distribution of concentrations of all components along the axis of symmetry with consideration of the six reactions. It is interesting to note the presence of a nitrogen concentration minimum C_{N_2} and a nitric oxide concentration maximum C_{NO}. Such a maximum was first noted in [38] for nonequilibrium dissociating air behind a direct shock wave. Since nitric oxide NO of all the components contained in the shock layer has the lowest ionization potential, the presence of a C_{NO} maximum leads to the appearance of an electron concentration in the shock layer appreciably exceeding the equilibrium concentration.

Figures 3.15 and 3.16 show the distribution of the concentrations of all components on the intermediate line $s = \frac{1}{2} s_1$ and on the boundary characteristic $s = s_1$ with consideration of all six reactions. Here we also observe a minimum C_{N_2} and a maximum C_{NO}. Figure 3.17 shows the distribution of C_{NO} with respect to $\eta = s/s_1$ at different values of $\xi = n/\varepsilon$ with consideration of the six reactions. For the examined case the concentration drops on the body ($\xi = 0$) and close to the shock wave ($\xi = 0.75$), whereas there is a maximum within the shock layer ($\xi = 0.5$).

Figures 3.18 and 3.19 show the change of profiles C_{N_2}, C_{NO}, C_O and C_{O_2} along the axis of symmetry in relation to the number of reactions taken into account. We see that all concentrations are very sensitive to this factor; the exclusion from the examination of bimolecular reaction VI (which is sometimes disregarded in the calculations) leads to a decrease of the nitric oxide concentration near the front of the shock wave and an increase of the concentration of molecular nitrogen. The maximum C_{NO} is retained, but somewhat /128

shifts away from the shock wave. The position of this maximum almost coincides with the position of the minimum C_{N_2}.

Calculation without consideration of reaction V gave a more substantial decrease of the nitric oxide concentration C_{NO} and increase of molecular nitrogen concentration C_{N_2} in comparison with consideration of all six reactions. The maximum C_{NO} in this case was retained, although it became less evidenced, and the minimum C_{N_2} disappeared. Hence we can conclude that reaction V at first proceeds forward and then back and plays a basic role in the formation of nitric oxide. The rate of this reaction is equal to zero in the region where C_{N_2} has a minimum. We note that the position of the maximum C_{NO} in this case (without reaction V) is the same as when all six reactions are examined. /129

Consideration of only the three reactions I, II, III showed the "frozen" character of dissociation of molecular nitrogen. This appearance of the maximum C_{NO} and of the minimum C_{N_2} and an appreciable decrease of C_N and C_{NO} in comparison with all previous cases are observed. This indicates that reaction IV, just as reaction V, at first proceeds forward and then back and plays a major role in the formation of NO. The velocity of reactions IV and V vanishes almost at the same place.

In all these three cases the content of atomic and molecular oxygen changes little. Consequently, reaction I of the dissociation of the molecular oxygen is the basic mechanism influencing the concentration of these components.

2. Combined Flows

We previously examined the flow field in a shock layer on the assumption that in the entire region the flow is completely "frozen" ($\varkappa$ = const), in equilibrium, or everywhere nonequilibrium. Calculation time correspondingly increases with a more detailed consideration of physicochemical transformations. Maximal expenditures, other things being equal, are observed on examining nonequilibrium flows of multicomponent gas mixtures, the state of which is close to equilibrium. Calculations carried out under different assumptions of the thermodynamic state of gas showed that, within a wide range of supersonic velocities of practical interest, the state of the gas in the region of influence of blunting deviates from full equilibrium. In most cases this deviation is negligible in the neighborhood of the axis of symmetry, where we can use the assumption of an equilibrium character of the change of thermodynamic parameters of the flow. Downstream the deviation increases and an essentially nonequilibrium, and in certain cases almost "frozen," flow occurs near the boundary characteristic.

Thus, when calculating flows in the region of influence of bluntness, it becomes necessary to simultaneously examine various states of the gas: from full equilibrium to "frozen." /130

Scheme II has proved convenient for investigating such mixed flows. We will examine the use of this scheme for calculating the flows of gas, the internal degrees of freedom of which are in equilibrium.

Calculation of such combined flows is performed by the usual method, only the initial parameters of the flow at the approximation points when $\xi = 1$ are determined twice: at first on the assumption of the "frozen character" of dissociation and then on the assumption of complete equilibrium of the physico-chemical transformations of gas passing through the shock wave.

The values of the derivative concentration of each of the newly formed components $dC_i/d\xi$ are determined successively at the approximation points with respect to the "frozen" parameters when $\xi = 1$, and then the value of the concentration itself at some small (in comparison with 1) distance ℓ from the shock wave: $(C_i)_{\xi=1-\ell} = \ell dC_i/d\xi$. This quantity is compared with the equilibrium value of the same concentration C_i^p. If $(C_i)_{\xi=1-\ell} > C_i^p$, then we assume an equilibrium state of the gas in that part of the region being calculated which lies upstream from the examined line of approximation, where this part of the region includes the line itself, and the initial parameters on it are assumed to correspond to a full equilibrium state. If $(C_i)_{\xi=1-\ell} < C_i^p$, then in this region the flow is assumed to be nonequilibrium, and the initial parameters on it are assumed to correspond to a state of "frozen" dissociation. After performing such an analysis and selecting the initial data at all approximation points, the approximating system is integrated along the boundaries of the zones. In the case of a full equilibrium state we additionally use the equation of the law of mass action, and in the case of nonequilibrium dissociation flows, relaxation equations and the corresponding values for the partial derivatives h_T, h_p, h_{C_i}, ρ_T, ρ_p, ρ_{C_i}.

Using this method we calculated flow around blunt bodies of different radius R_0 for a number of values of the parameters of the oncoming flow. It was assumed that the vibrations in the entire shock layer were in equilibrium /131
and we investigated only the effect of dissociation relaxation.

As an example we will present the results of calculating flow of oxygen around a sphere of radius $R_0 = 1$ m (full nonequilibrium flow), $R_0 = 10^3$ m (combined flow) when $M_\infty = 10$, $p_\infty = 0.001$ atm, $T_\infty = 288°K$. The calculation was performed by scheme II in the third approximation ($\ell = 0.001$).

The results of the calculations are shown in Table 3.17 and in Figures 3.20-3.22.

Figure 3.20 shows the shape and position of shock waves for the full equilibrium case ($R_0 = \infty$, curve 1), for a nonequilibrium dissociating flow ($R_0 = 1$ m, curve 2), and for a combined flow ($R_0 = 10^3$ m, curve 3). In the last case, on the basis of the stated criteria, equilibrium flow occurred along

the axis of symmetry s = 0 and intermediate lines $s = \frac{1}{3} s_1$ and $s = \frac{2}{3} s_1$ and a nonequilibrium flow along the boundary characteristic. The position of the shock wave near the axis of symmetry is analogous to the equilibrium case, whereas with motion downstream a deviation of the wave toward nonequilibirum is observed.

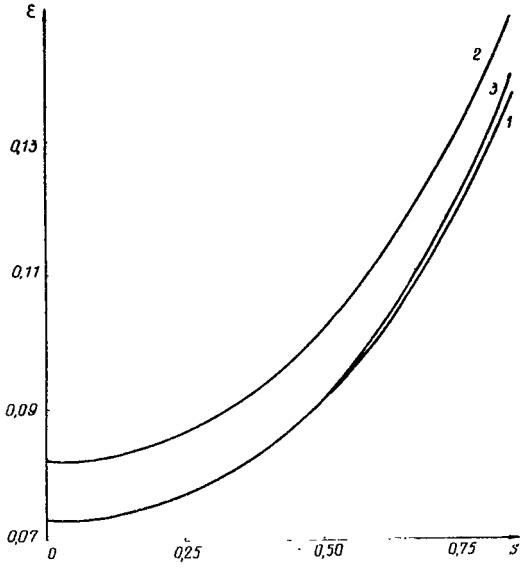

Figure 3.20. Magnitude of separation of shock wave. Flow of oxygen around sphere when $M_\infty = 10$, $p_\infty = 0.001$ atm, $T_\infty = 288°K$: 1) full equilibrium flow; 2) nonequilibrium dissociated flow, $R_0 = 1$ m; 3) combined flow, $R_0 = 10^3$ m. /132

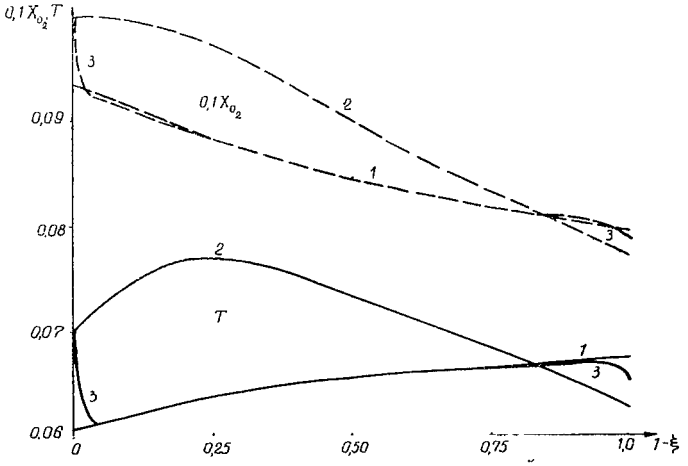

Figure 3.21. Distribution of temperature and molar concentration of molecular oxygen along boundary characteristic. Flow of oxygen around sphere when $M_\infty = 10$, $p_\infty = 0.001$ atm, $T_\infty = 288°K$: 1) full equilibrium flow; 2) nonequilibrium dissociated flow, $R_0 = 1$ m; 3) combined flow, $R_0 = 10^3$ m.

Figure 3.21 presents the profiles of temperature T (solid lines) and of the molar concentration of molecular oxygen x_{O_2} (dashed lines) along the boundary characteristic $s = s_1$. Curves 1 correspond to the case of equilibrium flow, curves 2 to nonequilibrium flow, and curves 3 to combined flow. It is interesting to note that although the calculations along lines $s = s_1$ were carried out on the assumption of nonequilibrium, profiles T and x_{O_2} in the greater part of the shock layer are close to the corresponding equilibrium values, the main difference being observed only in the neighborhood of the shock wave $\xi = 1$. Such behavior close to the wave is due to different boundary conditions for equilibrium and nonequilibrium flows, and near the body is due to the effect of recombination. The example of the calculation along the lines $s = s_1$ indicates that relaxation equations also describe those flows which are very close to equilibrium.

Figure 3.22 shows the profiles of T (solid lines) and x_{O_2} (dashed lines) along the surface of the body. Curves 1 correspond to the equilibrium case, curves 2 to nonequilibrium flow, and curves 3 to combined flow. We see that the combined flow deviates from equilibrium.

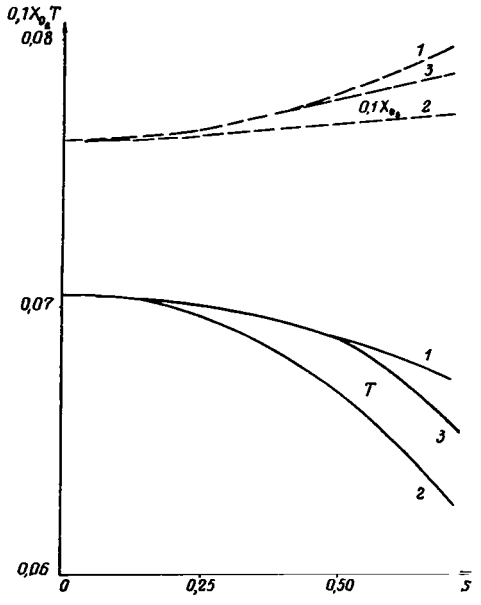

Figure 3.22. Distribution of temperature and molar concentration of molecular oxygen along surface of body. Flow of oxygen around sphere when $M_\infty = 10$, $p_\infty = 0.001$ atm, $T_\infty = 288°K$: 1) full equilibrium flow; 2) nonequilibrium dissociated flow, $R_0 = 1$ cm; 3) combined flow, $R_0 = 10^3$ m. /133

3. Simultaneous Occurrence of Vibrational-Dissociation Relaxation

In previous sections we examined the flow of nonequilibrium dissociating gas around blunt bodies. We always assumed that the vibrational degrees of freedom were excited in equilibrium and did not affect the rate of chemical reactions. However, as experimental and theoretical investigations have shown [39,40], with a rise of gas temperature the vibrational and dissociation relaxation times become commensurable with one another, therefore, here when considering processes on nonequilibrium dissociation we must take into account vibrational relaxation also.

The relation between vibrational and dissociation relaxation was first examined in [41] for a mixture of monatomic gas with a small admixture of a diatomic component. Only the effect of nonequilibrium excitation of vibrational degrees of freedom on the rate of dissociation described by the usual Landau-Teller equation. The effect of dissociation on vibrational relaxation was examined in [42] for the same mixture. The obtained relaxation equations were used to calculate the structure of a plane shock wave. /134

Equations were obtained in [13], which described the simultaneous occurrence of vibrational and dissociation relaxation in a pure diatomic gas. In these equations both the effect of vibrational relaxation on the rate of dissociation and the effect of dissociation relaxation on a change of the mean vibrational energy are taken into account. The equations describing the change of the number of molecules and atoms as a result of dissociation and recombination have the same general form regardless of the thermodynamic state of the vibrational degrees of freedom. The presence of vibrational relaxation will have an effect only on the implicit expression for specific reaction rates.

For a diatomic gas the relaxation equation is written as [43]:

$$\frac{dC_1}{dt} = \frac{2K'_d}{\mu_2}\rho C_1(1-C_1) + \frac{K''_d}{\mu_2}\rho(1-C_1)^2 - \frac{8K'_r}{\mu_2^2}C_1^3\rho^2 - \frac{4K''_r}{\mu_2^2}\rho^2 C_1^2(1-C_1), \tag{3.10}$$

here C_1 is the degree of dissociation, μ_2 is the molecular weight of the diatomic gas; K'_d, K'_r and K''_d, K''_r are the specific rates of dissociation and recombination when an atom or molecule, respectively, participates as the incident particle.

It is obvious that the absence of vibrational equilibrium will substantially affect the specific rate of dissociation and very little affect the specific rate of recombination. Therefore, to describe dissociation relaxation of the diatomic gas with consideration of nonequilibrium vibrations we used equations (3.10), in which K'_r and K''_r were expressed in terms of $(K'_d)_{eq}/K_c$ and $(K''_d)_{eq}/K_c$ (K_c is the equilibrium instant), and K'_d and K''_d were expressed, respectively, in terms of $(K'_d)_{eq}V^A$ and $(K''_d)_{eq}V^M$. The functions V^A and V^M characterize the deviation of the constants of the reaction rates from the case corresponding to /135

equilibrium of vibrational degrees of freedom.

Two models of the dissociation process were examined: 1) when dissociation occurs from an upper level; 2) when dissociation occurs from any vibrational level.

In the first case

$$V^A = \frac{Q(T)\exp\left[-\frac{(\gamma-1)h_*\nu}{kT_V}\right]}{Q(T_V)\exp\left[-\frac{(\gamma-1)h_*\nu}{kT}\right]};$$

$$V^M = \frac{Q^2(T)}{Q^2(T_V)}\,\frac{\exp\left[-\frac{(\gamma-1)h_*\nu}{kT_V}\right]\sum_j \exp\left(-\frac{jh_*\nu}{kT_V}\right)F(jh_*\nu)}{\exp\left[-\frac{(\gamma-1)h_*\nu}{kT}\right]\sum_j \exp\left(-\frac{jh_*\nu}{kT}\right)F(jh_*\nu)},$$

and the equation of vibrational relaxation is written as:

$$\frac{de}{dt} = \frac{e_{\text{eq}} - e}{\tau} - \frac{h_*\nu(\gamma-1)}{m_2}\frac{dC_1}{dt}.$$

In the second case

$$V^A = \frac{Q(T)Q(T_m)}{\gamma Q(T_V)};$$

$$V^M = \frac{Q^2(T)Q(T_m)}{Q^2(T_V)\gamma}\cdot\frac{\sum_j \exp\left(-\frac{jh_*\nu}{kT_V}\right)F(jh_*\nu)}{\sum_j \exp\left(-\frac{jh_*\nu}{kT}\right)F(jh_*\nu)},$$

and the relaxation equation takes the form

$$\frac{de}{dt} = \frac{e_{\text{eq}} - e}{\tau} - \frac{e_r}{m_2}\left(\frac{dC_1}{dt}\right)_r - \frac{e_d}{m_2}\left(\frac{dC_1}{dt}\right)_d.$$

Here T_V is the vibrational temperature, $1/T_m = 1/T_V - 1/T$; Q is the vibrational statistical sum; $\gamma = D/h_*\nu$; D is the dissociation energy; $F(jh_*\nu)$ is some function taking into account the change of vibrational energy of the incident molecule; e is the vibrational energy of a unit mass of gas; τ is relaxation time; m_2 is the mass of the molecule.

$$e_d = \frac{h_* \nu}{\exp\left(\frac{h_* \nu}{kT_m}\right)-1} - \frac{\gamma h_* \nu}{\exp\left(\frac{\gamma h_* \nu}{kT_m}\right)-1}; \quad e_r = \frac{\gamma-1}{2} h_* \nu; \qquad \text{/136}$$

$$\left(\frac{dC_1}{dt}\right)_r = \left(\frac{dC_1}{dt}\right)_{Ar} + \left(\frac{dC_1}{dt}\right)_{Mr} = -\frac{4C_1^2\rho^2}{\mu_2^2}[2C_1K_r' + (1-C_1)K_r''];$$

$$\left(\frac{dC_1}{dt}\right)_d = \left(\frac{dC_1}{dt}\right)_{Ad} + \left(\frac{dC_1}{dt}\right)_{Md} = \frac{(1-C_1)\rho}{\mu_2}[2C_1K_d' + (1-C_1)K_d''].$$

The values of the derivatives dC_1/dt and de/dt are found from the corresponding relaxation equations. For simplicity we will assume that

$$K_d' = K_d'' = K_d; \quad K_r' = K_r'' = K_r;$$

$$F(jh_*\nu) = 1, \text{i.e. } V^A = V^M = V.$$

Furthermore, we will examine the case where dissociation occurs from any vibrational level, since at high temperatures this case is, apparently, most probable [44,45]. Then we will have in a dimensionless form

$$\frac{dC_1}{dt} = \frac{\rho}{\mu_2}(1-C_1^2)V(K_d)_{eq}\left[1 - \frac{4C_1^2}{(1-C_1^2)\mu_2}\frac{p}{VK_p}\right];$$

$$\frac{de}{dt} = \frac{e_{eq}-e}{\tau} - \left[\frac{2T_x}{\exp\left(\frac{T_x}{T_m}\right)-1} - \frac{\mu_2 D}{\exp\left(\frac{\mu_2 D}{2T_m}\right)-1}\right]\left(\frac{dC_1}{dt}\right)_d -$$

$$-\frac{1}{2}[\mu_2 D - 2T_x]\left(\frac{dC_1}{dt}\right)_r,$$

where

$$\left(\frac{dC_1}{dt}\right)_d = \frac{\rho}{\mu_2}(1-C_1^2)V(K_d)_{eq}; \quad \left(\frac{dC_1}{dt}\right)_r = \frac{\rho}{\mu_2^2}4C_1^2\frac{p}{K_p}(K_d)_{eq};$$

$$\frac{dC_1}{dt} = \left(\frac{dC_1}{dt}\right)_d + \left(\frac{dC_1}{dt}\right)_r; \quad K_p = K_c RT.$$

To obtain the numerical solution, we used here scheme I of the method of integral relation.

Just as when calculating flows with nonequilibrium dissociation, for a more exact determination of derivatives of C_1 and e with respect to n, on the intermediate lines of approximation we introduce the additional lines /137

$$n_i(s) = \xi_i \varepsilon(s),$$

separating the integration range into a number of narrower zones. Along these additional lines we write the relaxation equations

$$(C_1)'_i = \frac{A_i}{v_i}\left(\frac{dC_1}{dt}\right)_i + \left(\frac{\partial C_1}{\partial n}\right)_i\left(\frac{dn_i}{ds} - A_i\frac{u_i}{v_i}\right);$$

$$e'_i = \frac{A_i}{v_i}\left(\frac{de}{dt}\right)_i + \left(\frac{\partial e}{\partial n}\right)_i\left(\frac{dn_i}{ds} - A_i\frac{u_i}{v_i}\right),$$

which are integrated simultaneously with the entire approximating system. The values of the hydrodynamic quantities u, v, p, T on these lines are determined by the corresponding known values of the wave, body, and on the intermediate lines of approximation. Four additional lines $\xi = 1/6$, $\xi = 1/3$, $\xi = 2/3$, $\xi = 5/6$ were used in the second approximation calculations.

The calculations were performed for different initial conditions in the oncoming flow. The case of pure oxygen was examined. Here, in conformity with [46,47], it was assumed that

$$(K_d)_{eq} = 1{,}06\cdot 10^{25}\cdot T^{-2{,}5}\exp\left(-\frac{59395}{T}\right) \text{ cm}^3/\text{mole.sec};$$

$$\tau = \frac{1}{p}\exp[(T^{-1/3} - 0{,}03)135{,}913 - 18{,}42] \text{ sec}$$

As an example we will dwell in detail on the results obtained (scheme I, N = 2) for a sphere of radius R_0 = 1 cm when M_∞ = 10, p_∞ = 0.01 atm, T_∞ = 290°K, and we will compare them with the corresponding data for equilibrium and "frozen" flows. The results of the calculation are presented in Table 3.18 and in Figures 3.23-3.28.

Figure 3.23 shows the shapes of shock waves and sonic lines for equilibrium flow (curve 1), flow with nonequilibrium dissociation but with vibrations (curve 2), with nonequilibrium dissociation and nonequilibrium vibrations (curve 3), and "frozen" flow corresponding to $\varkappa = 1.4$ (curve 4). We see that in comparison with nonequilibrium dissociation the shock wave with consideration of the simultaneous occurrence of vibrational and dissociation relaxation is situated somewhat farther from the body, but closer than in the case of a fully "frozen" /13

flow. Here the sonic line on the shock wave lies sufficiently high and the sonic line has a convexity toward the body unlike the "frozen" flow and the case with equilibrium vibrations.

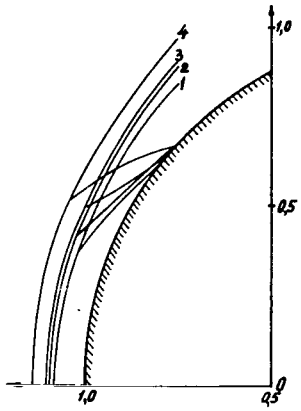

Figure 3.23. Position and shape of shock waves and sonic lines. Flow of oxygen past sphere when $M_\infty = 10$, $p_\infty = 0.01$ atm, $T_\infty = 290°K$, $R_0 = 1$ cm: 1) full equilibrium flow; 2) nonequilibrium dissociated flow with equilibrium excitation of internal degrees of freedom; 3) nonequilibrium dissociation and nonequilibrium excitation of vibration; 4) fully "frozen" flow, $\varkappa = 1.4$.

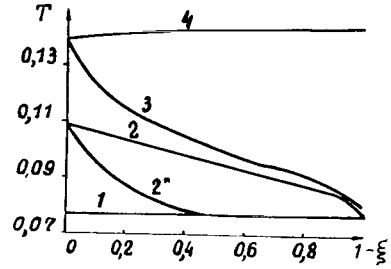

Figure 3.24. Distribution of temperature along axis of symmetry. Flow of oxygen around sphere when $M_\infty = 10$, $p_\infty = 0.01$ atm, $T_\infty = 290°K$, $R_0 = 1$ cm: 1) full equilibrium flow; 2) nonequilibrium dissociated flow with equilibrium excitation of internal degrees of freedom; 3) nonequilibrium dissociation and nonequilibrium excitation of vibrations; 4) fully "frozen" flow, $\varkappa = 1.4$.

Figure 3.24 shows the temperature profiles in the shock layer along the axis of symmetry. For equilibrium (curve 1) and "frozen" (curve 4) flows the temperature for all practical purposes does not change from the wave ($1 - \xi = 0$) toward the body ($1 - \xi = 1$), whereas for nonequilibrium flows this change is appreciable. For flow with nonequilibrium dissociation (curve 2) the greatest change of temperature in the case in question occurs close to the body, and for flow with nonequilibrium dissociation and nonequilibrium vibrations (curve 3) there are two regions of a marked drop of temperature: one near the shock wave and the other near the body. The first region is due to vibrational relaxation and the second to nonequilibrium dissociation. Curve 2* corresponds to the case of equilibrium vibrations, nonequilibrium dissociation when $R_0 = 10$ cm. Calculations showed that with an increase of body dimensions, Mach number, and pressure in the oncoming

/139

flow, the basic change of the temperature profile can occur close to the shock wave, whereas with a decrease of these quantities the change occurs near the body.

Figure 3.25 shows the profiles of the forward T and vibrational T_V temperatures along the axis of symmetry. We see that immediately behind the shock wave pronounced excitation of vibrational degrees of freedom and a corresponding increase of vibrational temperature occur, then the process of dissociation begins to develop which leads to a drop of the forward and vibrational temperatures. We note that complete equilibrium ensues only at the stagnation point and the vibrational temperature always remains lower than the forward temperature. For the case where the effect of nonequilibrium excitation of vibrational degrees of freedom on the rate of dissociation was examined, the profiles T and T_V have the same character as in Figures 3.25, but a region existed where the vibrational temperature exceeded the forward temperature.

Figure 3.26 shows the distribution of the mean vibrational energy e across the shock layer on rays s = 0, 0.25, 0.50. Just as the vibrational temperature, profile e has a maximum; we see that with distance from the axis of symmetry the maximum is displaced toward the body and becomes smaller. This is explained by the fact that downstream the gas temperature drops,which leads, on one hand, to an increase of the relaxation time of the excitation of vibrational degrees of freedom and, on the other hand, to a decrease of the vibrational energy itself.

Figure 3.27 shows the profiles of the concentration of atomic oxygen C_0 on rays s = 0, 0.25, 0.50. It is interesting to note that if along the zero line of flow the C_0 profile for the examined case is almost linear, excluding the region near the body, then with distance from the axis the C_0 profiles become ever increasingly nonlinear. On the last ray an appreciable increase of C_0 is observed only when $\xi < 0.5$. This slowdown in the dissociation process is explained by the drop of gas temperature downstream.

Calculations of the parameters of the gas on the body surface showed /140 that vibrational-dissociation relaxation had little effect on the velocity and pressure profile, but quite substantially affected the temperature profile.

Figure 3.28 shows that the distribution of temperature $\bar{T}_0 = T_0(s)/T_0(0)$ ($T_0(0)$ is the temperature at the stagnation point) along the surface of a sphere for equilibrium flow (curve 1), flow with nonequilibrium dissociation but with equilibrium vibrations (curve 2), flow with nonequilibrium dissociation and nonequilibrium vibrations (curve 3), and "frozen" flow corresponding to $\varkappa = 1.4$ (curve 4). Hence it follows that the temperature profiles depend strongly on the number of relaxation processes taken into account. For the examined case a decrease of $\bar{T}_0$ with consideration of vibrational-dissociation relaxation can exceed by 10% the decrease of $\bar{T}_0$ for equilibrium flow and by

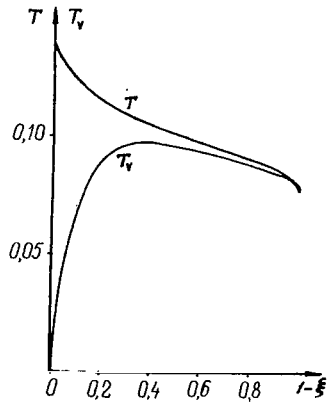

Figure 3.25. Distribution of forward T and vibrational T_V temperatures along axis of symmetry. Flow of nonequilibrium dissociating oxygen with nonequilibrium excitation of vibrations around sphere when $M_\infty = 10$, $p_\infty = 0.01$ atm, $T_\infty = 290°K$, $R_0 = 1$ cm.

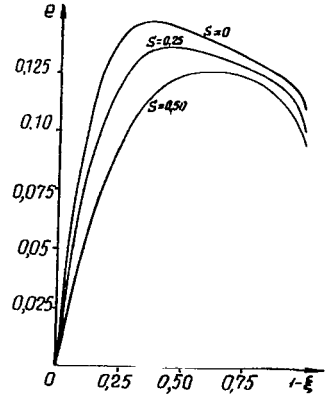

Figure 3.26. Distribution of mean vibrational energy e along lines s = const. Flow of nonequilibrium dissociating oxygen with nonequilibrium excitation of vibrations around sphere when $M_\infty = 10$, $p_\infty = 0.01$ atm, $T_\infty = 290°K$, $R_0 = 1$ cm.

5% the corresponding decrease of $\bar{T}_0$ with consideration of only dissociation relaxation. Intensive expansion of the gas in the supersonic region and the corresponding temperature drop along the surface of the body result in the profile $\bar{T}_0$, in the case of vibrational-dissociation relaxation, tending toward the corresponding value for "frozen" flow. This, of course, is not observed when only nonequilibrium dissociation is taken into account. /141

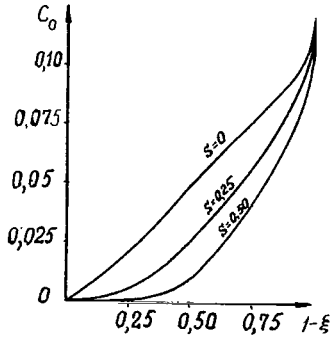

Figure 3.27. Distribution of concentration of atomic oxygen along lines s = const. Flow of nonequilibrium dissociating oxygen with nonequilibrium excitation of vibrations around a sphere when $M_\infty = 10$, $p_\infty = 0.01$ atm, $T_\infty = 290°K$, $R_0 = 1$ cm.

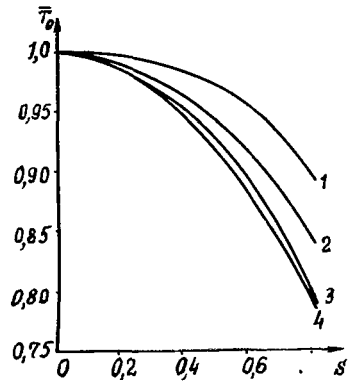

Figure 3.28. Distribution of temperature along surface of body. Flow of oxygen around sphere when M = 10, p = 0.01 atm, T = 290°K, R_0 = 1 cm: 1) full equilibrium flow; 2) nonequilibrium dissociated flow with equilibrium excitation of internal degrees of freedom; 3) nonequilibrium dissociation and nonequilibrium excitation of vibrations; 4) fully "frozen" flow, $\varkappa$ = 1.4.

4. Description of Tables

Tables 3.1-3.7 give the results of calculating the flow of nonequilibrium oxygen (equilibrium vibrations, nonequilibrium dissociation) around a sphere (δ = 1) and ellipsoids of revolution (δ = 10 and 100). The calculations were performed by scheme I when N = 2. The following cases were examined when M_∞ = 10, p_∞ = 0.01 atm, T_∞ = 290°K,

$\delta = 1$; $R_0 = 0{,}01$ m; 0,04 m; 0,1 m (Tables 3.1-3.3);
$\delta = 10$; $b = 0{,}01$ m (Tables 3.4, 3.5);
$\delta = 100$; $b = 0{,}01$ m (Tables 3.6, 3.7);

/142

Tables 3.1-3.4, 3.6 consist of two parts. In the first part the following data on the shock wave and on the surface of the body are given in relation to the length of arc along the surface of the body s: ε is the distance along the normal from the surface of the body to the shock wave; σ is the angle of inclination of the shock wave toward the oncoming flow; $\bar{P}_0 = P_0(s)/P_0(0)$, $\bar{T}_0 = T_0(s)/T_0(0)$ are the pressure and temperature on the surface of the body, respectively, referred to the value of these quantities at the stagnation point.

In the second part the distribution of the following gas dynamic quantities is given in relation to s: u_i, v_i are the velocity components along axes n, s, respectively; p_i is pressure; T_i is temperature; c_i^2 is the square of the sound velocity; $w_i^2 = u_i^2 + v_i^2$; Cartesian coordinates of

the boundaries of the zones x_i, y_i (the origin of the coordinates is placed at the center of the body); and also the mass concentration of atomic oxygen $(C_0)_i$. The values of the functions are given on the surface of the body $\xi = n/\varepsilon$ (s) = 0 (i = 0), on the intermediate line $\xi = 0.5$ (i = 2), and on the boundary characteristic $\xi = 1$ (i = 1).

Tables 3.5 and 3.7 give the values of x, y, u, v, p, T, ρ, c^2, C_0 along the streamlines for the corresponding cases.

Tables 3.8-3.16 give the results of calculating flow of nonequilibrium oxygen, nitrogen, and air around a sphere. The calculations were performed by scheme II when N = 2,3.

The following cases were examined:

1) nonequilibrium oxygen ("frozen" flow) $M_\infty = 10$, $p_\infty = 0.01$ atm, $T_\infty = 288°K$; $\delta = 1$ (Table 3.8);

2) nonequilibrium oxygen (equilibrium vibrations, nonequilibrium dissociation) $M_\infty = 10$, $p_\infty = 0.001$ atm, $T_\infty = 288°$, 290°K, $R_0 = 0.01$ m, 0.1 m, 1 m. (Tables 3.9, 3.10, 3.13);

$M_\infty = 15$; $p_\infty = 0.001$ atm, $T_\infty = 290°K$; $R_0 = 0.01$ m; 0.1 m (Tables 3.11, 3.12);

3) nonequilibrium nitrogen (equilibrium vibrations, nonequilibrium dissociation) $M_\infty = 15$, $p_\infty = 0.001$ atm, $T_\infty = 290°K$, $R_0 = 0.1$ m, 1 m (Tables 3.14, 3.15);

4) nonequilibrium air (equilibrium vibrations, nonequilibrium dissociation) $M_\infty = 10$, $p_\infty = 0.01$ atm, $T_\infty = 300°K$, $R_0 = 0.1$ m (Table 3.16).

The tables present the values of the following quantities on the axis of symmetry (s = 0), intermediate lines and boundary characteristic ($s = s_1$): s, u, v, p, T, ρ, h (enthalpy) and the values of concentrations (C_0 is the mass concentration of atomic oxygen, Tables 3.8-3.13; C_N is the mass concentration of atomic nitrogen, Tables 3.14-3.15; x_{O_2}, x_O, x_{N_2}, x_N, x_{NO} are the molar concentrations of molecular and atomic oxygen, nitrogen, and nitric oxide, respectively, Table 3.16). /143

Table 3.17 gives the results of calculating a combined (equilibrium-nonequilibrium) flow around a sphere ($M_\infty = 10$, $p_\infty = 0.001$ atm, $T_\infty = 288°K$, $R_0 = 1000$ m). The calculations were performed by scheme II when N = 3. The values of the quantities s, u, v, p, ρ, T, h, C_0 are given.

Table 3.18 gives the calculation of flow around a sphere with the simultaneous occurrence of vibrational and dissociation relaxation ($M_\infty = 10$, $p_\infty = 0.01$ atm, $T_\infty = 290°K$, $R_0 = 0.01$ m). The calculations were performed by scheme I when N = 2. The data of the following quantities are given:

ε, σ, $\bar{P}_0$, $\bar{T}_0$, u_i, v_i, p_i, T_i, c_i^2, w_i^2, x_i, y_i, $(C_0)_i$, e_i, (vibrational energy).

Tables 3.19-3.20 give the results of N. P. Shulishnina's calculations, by the method of characteristics, of gas dynamic quantities in the supersonic region for a smooth body "spherical blunting-cylinder" (Figure 2.25, Table 3.19) and a body with a discontinuity of the contour of the generatrix "spherical segment-cylinder" (Figure 2.26, Table 8.20) with a nonequilibrium oxygen flow (equilibrium vibrations, nonequilibrium dissociation). The following cases are examined: $M_\infty = 10$, $p_\infty = 0.001$ atm, $T_\infty = 288°K$, $R_0 = 1$ m. The initial data were obtained by scheme II of the method of integral relations. The tables show the following quantities on the surface of the body: x_0, $y_0 = r_0$ are Cartesian coordinates of the points on the body (the origin of the coordinates is placed at the critical point of the body); P_0, T_0, ρ_0, w_0, $\zeta = \tan\theta$ is the tangent of the angle of inclination of the velocity vector to the x-axis; $(C_0)_0$ is the mass concentration of atomic oxygen. The tables also give the coordinates of the nose shock wave x_B, $y_B = r_B$.

It is necessary to bear in mind that the values of velocity are referred to w_{max}^2, of pressure to $\rho_\infty w_{max}^2$, of density to ρ_∞, of temperature to $\mu_\infty w_{max}^2/R$, of enthalpy to $w_{max}^2/2$, and of entropy to $R/2\mu_\infty$. All linear dimensions are referred to the characteristic dimension of the body (to the radius for a sphere and to the vertical semiaxis b for ellipsoids). The subscript ∞ denotes quantities before the shock wave.

NONEQUILIBRIUM OXYGEN (EQUILIBRIUM VIBRATION, NONEQUILIBRIUM DISSOCIATION). Scheme I. N = 2

$M_\infty = 10$, $p_\infty = 0.01$ atm; $T_\infty = 290°K$; $\rho_\infty = 0.01345$ kg/m^3;

$w_{max} = 3328.1$ m/sec; $h_{oo} = 21315°K$; $\delta = 1\text{-}100$; $R_0(b) = 0.01\text{-}0.1$ m

TABLE 3.1

/144

$\delta = 1$; $R_0 = 0.01$ m

s	ε	σ	$\bar{p}_0$	$\bar{T}_0$
0.0000	0.0907	1.570	1.000	1.000
0.0625	0.0909	1.514	0.995	0.998
0.1250	0.0917	1.460	0.981	0.995
0.1875	0.0930	1.406	0.958	0.991
0.2500	0.0949	1.352	0.926	0.984
0.3125	0.0974	1.299	0.887	0.976
0.3750	0.100	1.246	0.841	0.965
0.4375	0.104	1.195	0.789	0.952
0.5000	0.109	1.145	0.732	0.938
0.5625	0.114	1.096	0.676	0.922
0.6250	0.121	1.050	0.618	0.904
0.6875	0.129	1.006	0.561	0.885
0.7500	0.139	0.965	0.505	0.865
0.8125	0.150	0.925	0.450	0.843

s	u	v	p	T	c^2	w^2	$-x$	y	C_0
				$\xi = 0$					
0.0000	0	0.0000	0.902	0.0769	0.111	0.000000	1.000	0.0000	0.114
0.0625	0	0.0288	0.898	0.0768	0.110	0.000832	0.998	0.0624	0.114
0.1250	0	0.0570	0.885	0.0765	0.110	0.00325	0.992	0.124	0.114
0.1875	0	0.0853	0.864	0.0762	0.110	0.00728	0.982	0.186	0.114
0.2500	0	0.113	0.836	0.0757	0.109	0.0129	0.968	0.247	0.114
0.3125	0	0.142	0.801	0.0750	0.108	0.0201	0.951	0.307	0.114
0.3750	0	0.170	0.759	0.0742	0.107	0.0290	0.930	0.366	0.113
0.4375	0	0.198	0.712	0.0732	0.105	0.0395	0.905	0.423	0.113
0.5000	0	0.227	0.661	0.0721	0.104	0.0516	0.877	0.479	0.113
0.5625	0	0.253	0.610	0.0709	0.102	0.0643	0.845	0.533	0.112
0.6250	0	0.279	0.558	0.0695	0.100	0.0781	0.810	0.585	0.112
0.6875	0	0.304	0.507	0.0681	0.0985	0.0929	0.772	0.634	0.112
0.7500	0	0.329	0.456	0.0665	0.0963	0.108	0.731	0.681	0.112
0.8125	0	0.354	0.406	0.0648	0.0939	0.125	0.687	0.726	0.111

TABLE 3.1 Continued

/145

s	u	v	p	T	c^2	w^2	$-x$	y	C_0
				$\xi = 0.5$					
0.0000	-0.0538	0.0000	0.889	0.0953	0.126	0.00289	1.045	0.0000	0.0510
0.0625	-0.0536	0.0438	0.885	0.0952	0.126	0.00480	1.043	0.0653	0.0506
0.1250	-0.0532	0.0881	0.875	0.0949	0.126	0.0106	1.037	0.130	0.0495
0.1875	-0.0523	0.131	0.857	0.0945	0.125	0.0201	1.028	0.195	0.0476
0.2500	-0.0510	0.175	0.833	0.0939	0.124	0.0332	1.014	0.259	0.0452
0.3125	-0.0492	0.217	0.802	0.0932	0.122	0.0497	0.997	0.322	0.0422
0.3750	-0.0469	0.259	0.767	0.0922	0.120	0.0693	0.977	0.384	0.0387
0.4375	-0.0441	0.299	0.727	0.0911	0.118	0.0916	0.953	0.445	0.0349
0.5000	-0.0406	0.338	0.683	0.0898	0.116	0.116	0.925	0.505	0.0310
0.5625	-0.0357	0.375	0.639	0.0883	0.114	0.142	0.894	0.563	0.0270
0.6250	-0.0298	0.410	0.595	0.0867	0.111	0.169	0.860	0.620	0.0230
0.6875	-0.0225	0.443	0.550	0.0850	0.109	0.196	0.822	0.675	0.0193
0.7500	-0.0136	0.473	0.506	0.0832	0.105	0.224	0.782	0.729	0.0158
0.8125	-0.00321	0.502	0.463	0.0813	0.103	0.252	0.739	0.780	0.0126
				$\xi = 1$					
0.0000	-0.126	0.0000	0.835	0.108	0.136	0.0161	1.090	0.0000	0
0.0625	-0.126	0.0553	0.832	0.108	0.134	0.0190	1.088	0.0681	0
0.1250	-0.124	0.109	0.824	0.107	0.133	0.0274	1.083	0.136	0
0.1875	-0.122	0.162	0.812	0.106	0.132	0.0412	1.073	0.203	0
0.2500	-0.118	0.214	0.795	0.104	0.129	0.0601	1.060	0.270	0
0.3125	-0.112	0.266	0.774	0.102	0.127	0.0837	1.044	0.337	0
0.3750	-0.106	0.316	0.749	0.0992	0.123	0.111	1.024	0.403	0
0.4375	-0.0986	0.364	0.721	0.0961	0.120	0.142	1.000	0.467	0
0.5000	-0.0891	0.410	0.690	0.0927	0.115	0.176	0.973	0.531	0
0.5625	-0.0778	0.454	0.658	0.0891	0.111	0.212	0.943	0.594	0
0.6250	-0.0642	0.494	0.625	0.0854	0.106	0.248	0.909	0.656	0
0.6875	-0.0485	0.531	0.593	0.0818	0.102	0.284	0.872	0.716	0
0.7500	-0.0305	0.565	0.561	0.0781	0.0982	0.320	0.833	0.776	0
0.8125	-0.0105	0.596	0.528	0.0744	0.0938	0.355	0.791	0.835	0

TABLE 3.2

/146

$\delta = 1$; $R_0 = 0.04$ m

s	ε	σ	$\bar{p}_0$	$\bar{T}_0$
0.0000	0.0867	1.570	1.000	1.000
0.0625	0.0870	1.516	0.995	0.998
0.1250	0.0877	1.460	0.981	0.996
0.1875	0.0890	1.405	0.958	0.993
0.2500	0.0908	1.351	0.926	0.987
0.3125	0.0932	1.298	0.887	0.981
0.3750	0.0963	1.245	0.841	0.972
0.4375	0.100	1.193	0.789	0.961
0.5000	0.104	1.141	0.731	0.948
0.5625	0.109	1.088	0.666	0.932
0.6250	0.115	1.033	0.593	0.911
0.6875	0.121	0.975	0.515	0.885
0.7500	0.128	0.914	0.436	0.854
0.8125	0.135	0.848	0.368	0.822

s	u	v	p	T	c^2	w^2	$-x$	y	C_0
$\xi = 0$									
0.0000	0	0.0000	0.905	0.0769	0.111	0.000000	1.000	0.0000	0.114
0.0625	0	0.0284	0.901	0.0768	0.110	0.000809	0.998	0.0624	0.114
0.1250	0	0.0571	0.888	0.0766	0.110	0.00326	0.992	0.124	0.114
0.1875	0	0.0855	0.867	0.0763	0.110	0.00731	0.982	0.186	0.114
0.2500	0	0.113	0.839	0.0759	0.109	0.0129	0.968	0.247	0.113
0.3125	0	0.142	0.803	0.0754	0.108	0.0202	0.951	0.307	0.112
0.3750	0	0.170	0.761	0.0747	0.107	0.0292	0.930	0.366	0.112
0.4375	0	0.199	0.714	0.0739	0.106	0.0397	0.905	0.423	0.111
0.5000	0	0.228	0.662	0.0729	0.104	0.0521	0.877	0.479	0.110
0.5625	0	0.258	0.603	0.0717	0.103	0.0670	0.845	0.533	0.109
0.6250	0	0.292	0.537	0.0700	0.100	0.0852	0.810	0.585	0.108
0.6875	0	0.326	0.467	0.0680	0.0979	0.106	0.772	0.634	0.107
0.7500	0	0.362	0.395	0.0657	0.0946	0.131	0.731	0.681	0.106
0.8125	0	0.399	0.334	0.0632	0.0907	0.159	0.687	0.726	0.106

TABLE 3.2 Continued

s	u	v	p	T	c^2	w^2	$-x$	y	C_0
				$\xi = 0.5$					
0.0000	-0.0498	0.0000	0.894	0.0852	0.118	0.00248	1.043	0.0000	0.0858
0.0625	-0.0494	0.0430	0.890	0.0851	0.118	0.00430	1.041	0.0625	0.0855
0.1250	-0.0489	0.0856	0.879	0.0848	0.117	0.00972	1.035	0.130	0.0844
0.1875	-0.0481	0.128	0.861	0.0845	0.117	0.0187	1.026	0.194	0.0826
0.2500	-0.0469	0.170	0.836	0.0839	0.116	0.0311	1.012	0.258	0.0801
0.3125	-0.0453	0.211	0.806	0.0833	0.114	0.0466	0.995	0.321	0.0771
0.3750	-0.0431	0.251	0.770	0.0824	0.113	0.0651	0.975	0.384	0.0736
0.4375	-0.0404	0.291	0.729	0.0814	0.111	0.0863	0.951	0.444	0.0699
0.5000	-0.0371	0.329	0.684	0.0802	0.109	0.109	0.923	0.504	0.0659
0.5625	-0.0332	0.367	0.633	0.0787	0.106	0.136	0.892	0.562	0.0619
0.6250	-0.0291	0.405	0.575	0.0768	0.103	0.165	0.857	0.618	0.0580
0.6875	-0.0248	0.444	0.513	0.0746	0.100	0.197	0.819	0.673	0.0542
0.7500	-0.0198	0.482	0.445	0.0720	0.0967	0.232	0.778	0.725	0.0508
0.8125	-0.0130	0.520	0.375	0.0690	0.0924	0.270	0.734	0.775	0.0479
				$\xi = 1$					
0.0000	-0.126	0.0000	0.835	0.108	0.135	0.0161	1.086	0.0000	0
0.0625	-0.126	0.0541	0.832	0.108	0.134	0.0189	1.084	0.0678	0
0.1250	-0.124	0.109	0.824	0.107	0.133	0.0274	1.079	0.135	0
0.1875	-0.122	0.162	0.812	0.106	0.132	0.0414	1.069	0.203	0
0.2500	-0.118	0.215	0.795	0.104	0.129	0.0605	1.056	0.269	0
0.3125	-0.113	0.267	0.773	0.101	0.127	0.0843	1.040	0.336	0
0.3750	-0.106	0.317	0.748	0.0991	0.123	0.112	1.020	0.401	0
0.4375	-0.0992	0.366	0.719	0.0960	0.119	0.144	0.996	0.466	0
0.5000	-0.0902	0.413	0.688	0.0925	0.115	0.179	0.969	0.529	0
0.5625	-0.0805	0.460	0.652	0.0885	0.110	0.218	0.938	0.591	0
0.6250	-0.0707	0.507	0.613	0.0841	0.105	0.262	0.904	0.652	0
0.6875	-0.0613	0.554	0.569	0.0791	0.0994	0.311	0.867	0.711	0
0.7500	-0.0531	0.603	0.519	0.0735	0.0926	0.366	0.825	0.769	0
0.8125	-0.0468	0.651	0.465	0.0672	0.0850	0.426	0.780	0.824	0

TABLE 3.3 /148

$\delta = 1$; $R_0 = 0.1$ m

s	ε	σ	$\bar{p}_0$	$\bar{T}_0$
0.0000	0.0842	1.570	1.000	1.000
0.0625	0.0846	1.518	0.995	0.999
0.1250	0.0855	1.461	0.980	0.997
0.1875	0.0867	1.405	0.957	0.994
0.2500	0.0885	1.350	0.925	0.990
0.3125	0.0908	1.296	0.886	0.984
0.3750	0.0937	1.243	0.840	0.977
0.4375	0.0973	1.191	0.788	0.968
0.5000	0.101	1.139	0.731	0.957
0.5625	0.106	1.086	0.666	0.943
0.6250	0.112	1.031	0.593	0.924
0.6875	0.118	0.974	0.515	0.900
0.7500	0.125	0.916	0.432	0.870
0.8125	0.132	0.857	0.348	0.831

s	u	v	p	T	c^2	w^2	−x	y	C_0
				$\xi = 0$					
0.0000	0	0.0000	0.907	0.0769	0.111	0.000000	1.000	0.0000	0.114
0.0625	0	0.0280	0.903	0.0768	0.110	0.000788	0.998	0.0624	0.114
0.1250	0	0.0576	0.890	0.0767	0.110	0.00332	0.992	0.124	0.114
0.1875	0	0.0862	0.869	0.0764	0.110	0.00743	0.982	0.186	0.113
0.2500	0	0.114	0.840	0.0761	0.109	0.0130	0.968	0.247	0.112
0.3125	0	0.142	0.805	0.0757	0.108	0.0204	0.951	0.307	0.111
0.3750	0	0.171	0.763	0.0751	0.108	0.0293	0.930	0.366	0.110
0.4375	0	0.199	0.716	0.0744	0.106	0.0399	0.905	0.423	0.109
0.5000	0	0.228	0.663	0.0736	0.105	0.0523	0.877	0.479	0.107
0.5625	0	0.259	0.604	0.0725	0.103	0.0673	0.845	0.533	0.106
0.6250	0	0.292	0.539	0.0711	0.101	0.0856	0.810	0.585	0.104
0.6875	0	0.328	0.467	0.0692	0.0990	0.107	0.772	0.634	0.103
0.7500	0	0.366	0.392	0.0669	0.0957	0.134	0.731	0.681	0.102
0.8125	0	0.406	0.316	0.0639	0.0915	0.165	0.687	0.726	0.101

TABLE 3.3 Continued

/149

s	u	v	p	T	c^2	w^2	$-x$	y	C_0
				$\xi = 0.5$					
0.0000	-0.0481	0.0000	0.897	0.0799	0.113	0.00231	1.042	0.0000	0.103
0.0625	-0.0473	0.0428	0.892	0.0798	0.113	0.00407	1.040	0.0650	0.103
0.1250	-0.0464	0.0840	0.881	0.0795	0.113	0.00922	1.034	0.129	0.102
0.1875	-0.0457	0.125	0.863	0.0792	0.112	0.0178	1.025	0.194	0.100
0.2500	-0.0446	0.166	0.838	0.0786	0.111	0.0297	1.011	0.258	0.0986
0.3125	-0.0430	0.207	0.807	0.0780	0.110	0.0448	0.994	0.321	0.0957
0.3750	-0.0410	0.247	0.771	0.0771	0.108	0.0627	0.974	0.383	0.0925
0.4375	-0.0384	0.285	0.730	0.0760	0.106	0.0830	0.949	0.444	0.0890
0.5000	-0.0351	0.323	0.685	0.0748	0.104	0.105	0.922	0.503	0.0854
0.5625	-0.0313	0.360	0.634	0.0733	0.101	0.131	0.891	0.561	0.0818
0.6250	-0.0273	0.398	0.577	0.0714	0.0991	0.159	0.856	0.617	0.0783
0.6875	-0.0233	0.435	0.514	0.0692	0.0958	0.189	0.818	0.672	0.0751
0.7500	-0.0198	0.472	0.447	0.0666	0.0920	0.223	0.777	0.724	0.0723
0.8125	-0.0172	0.509	0.380	0.0635	0.0877	0.259	0.733	0.773	0.0698
				$\xi = 1$					
0.0000	-0.126	0.0000	0.835	0.108	0.135	0.0161	1.084	0.0000	0
0.0625	-0.126	0.0519	0.832	0.108	0.134	0.0186	1.082	0.0677	0
0.1250	-0.124	0.108	0.824	0.107	0.133	0.0273	1.076	0.135	0
0.1875	-0.122	0.163	0.812	0.106	0.132	0.0416	1.067	0.202	0
0.2500	-0.118	0.216	0.794	0.104	0.129	0.0609	1.054	0.269	0
0.3125	-0.113	0.268	0.773	0.101	0.126	0.0850	1.038	0.335	0
0.3750	-0.107	0.319	0.747	0.0990	0.123	0.113	1.017	0.400	0
0.4375	-0.0997	0.367	0.718	0.0959	0.119	0.145	0.994	0.464	0
0.5000	-0.0908	0.415	0.686	0.0923	0.115	0.180	0.966	0.528	0
0.5625	-0.0811	0.461	0.651	0.0884	0.110	0.219	0.936	0.590	0
0.6250	-0.0713	0.508	0.612	0.0839	0.105	0.263	0.902	0.650	0
0.6875	-0.0618	0.555	0.568	0.0790	0.0992	0.312	0.864	0.709	0
0.7500	-0.0523	0.601	0.521	0.0736	0.0928	0.365	0.823	0.767	0
0.8125	-0.0423	0.645	0.472	0.0680	0.0860	0.418	0.778	0.821	0

TABLE 3.4 /150

$\delta = 10$; $b = 0.01$ m

s	ε	σ	$\bar{p}_0$	$\bar{T}_0$
0.0000	0.306	1.570	1.000	1.000
0.0625	0.306	1.554	0.999	0.999
0.1250	0.305	1.541	0.999	0.999
0.1875	0.303	1.528	0.998	0.999
0.2500	0.302	1.515	0.996	0.999
0.3125	0.300	1.500	0.994	0.998
0.3750	0.297	1.484	0.990	0.998
0.4375	0.294	1.466	0.985	0.997
0.5000	0.290	1.446	0.978	0.996
0.5625	0.285	1.425	0.969	0.994
0.6250	0.279	1.402	0.957	0.992
0.6875	0.273	1.377	0.941	0.989
0.7500	0.266	1.349	0.919	0.984
0.8125	0.258	1.318	0.887	0.977
0.8750	0.250	1.282	0.836	0.965
0.9156	0.245	1.254	0.784	0.952
0.9312	0.243	1.241	0.756	0.944
0.9468	0.241	1.227	0.722	0.935
0.9624	0.239	1.209	0.677	0.921
0.9781	0.239	1.186	0.612	0.901
0.9893	0.240	1.161	0.514	0.865
0.9971	0.245	1.140	0.312	0.770
1.0010	0.250	1.127	0.188	0.682
1.0049	0.262	1.113	0.0800	0.555
1.0055	0.264	1.109	0.0675	0.533

s	u	v	p	T	c^2	w^2	$-x$	y	C_0
$\xi = 0$									
0.0000	0	0.00000	0.905	0.0769	0.111	0.0000000	0.1000	0.0000	0.114
0.0625	0	0.00594	0.905	0.0768	0.110	0.0000353	0.0998	0.0624	0.115
0.1250	0	0.0117	0.904	0.0768	0.110	0.000138	0.0992	0.124	0.115
0.1875	0	0.0177	0.903	0.0768	0.110	0.000316	0.0982	0.187	0.115
0.2500	0	0.0244	0.902	0.0768	0.110	0.000599	0.0968	0.249	0.114

TABLE 3.4 Continued

/151

s	u	v	p	T	c^2	w^2	$-x$	y	C_0
0.3125	0	0.0321	0.899	0.0768	0.110	0.00103	0.0949	0.312	0.114
0.3750	0	0.0408	0.896	0.0767	0.110	0.00166	0.0927	0.374	0.114
0.4375	0	0.0504	0.891	0.0766	0.110	0.00254	0.0899	0.437	0.114
0.5000	0	0.0610	0.885	0.0766	0.110	0.00372	0.0866	0.499	0.114
0.5625	0	0.0726	0.877	0.0764	0.110	0.00528	0.0827	0.562	0.114
0.6250	0	0.0858	0.867	0.0763	0.110	0.00736	0.0781	0.624	0.114
0.6875	0	0.101	0.852	0.0760	0.109	0.0102	0.0726	0.686	0.114
0.7500	0	0.119	0.832	0.0757	0.109	0.0142	0.0662	0.748	0.114
0.8125	0	0.142	0.803	0.0751	0.108	0.0202	0.0585	0.810	0.113
0.8750	0	0.173	0.757	0.0742	0.107	0.0299	0.0488	0.872	0.113
0.9156	0	0.201	0.709	0.0732	0.105	0.0406	0.0408	0.912	0.113
0.9312	0	0.215	0.684	0.0726	0.104	0.0465	0.0372	0.928	0.113
0.9468	0	0.232	0.653	0.0719	0.103	0.0539	0.0332	0.943	0.113
0.9624	0	0.253	0.613	0.0708	0.102	0.0642	0.0286	0.958	0.112
0.9781	0	0.282	0.554	0.0692	0.100	0.0799	0.0231	0.972	0.112
0.9893	0	0.325	0.465	0.0665	0.0964	0.106	0.0184	0.982	0.112
0.9971	0	0.419	0.283	0.0592	0.0862	0.175	0.0143	0.989	0.112
1.0010	0	0.489	0.170	0.0525	0.0768	0.239	0.0120	0.992	0.112
1.0049	0	0.574	0.0724	0.0427	0.0629	0.329	0.00937	0.995	0.112
1.0055	0	0.587	0.0611	0.0409	0.0604	0.345	0.00896	0.995	0.112
				$\xi = 0.5$					
0.0000	-0.0449	0.0000	0.895	0.0856	0.118	0.00202	0.253	0.0000	0.0845
0.0625	-0.0465	0.0117	0.896	0.0858	0.118	0.00230	0.252	0.0634	0.0839
0.1250	-0.0478	0.0240	0.896	0.0859	0.119	0.00286	0.251	0.126	0.0833
0.1875	-0.0488	0.0366	0.895	0.0859	0.119	0.00372	0.250	0.190	0.0828
0.2500	-0.0495	0.0492	0.893	0.0860	0.119	0.00488	0.247	0.253	0.0822
0.3125	-0.0502	0.0618	0.890	0.0860	0.118	0.00634	0.244	0.317	0.0817
0.3750	-0.0509	0.0744	0.886	0.0860	0.118	0.00813	0.241	0.380	0.0811
0.4375	-0.0518	0.0872	0.882	0.0860	0.118	0.0103	0.236	0.444	0.0804
0.5000	-0.0530	0.100	0.876	0.0859	0.118	0.0129	0.231	0.508	0.0796
0.5625	-0.0546	0.114	0.869	0.0859	0.118	0.0161	0.225	0.571	0.0786
0.6250	-0.0567	0.130	0.859	0.0858	0.118	0.0201	0.217	0.635	0.0774
0.6875	-0.0593	0.147	0.847	0.0857	0.117	0.0252	0.208	0.699	0.0760
0.7500	-0.0625	0.166	0.831	0.0856	0.117	0.0316	0.198	0.763	0.0743
0.8125	-0.0663	0.189	0.808	0.0853	0.116	0.0401	0.186	0.828	0.0723
0.8750	-0.0701	0.216	0.776	0.0849	0.115	0.0518	0.172	0.894	0.0697

TABLE 3.4 Continued

/152

s	u	v	p	T	c^2	w^2	$-x$	y	C_0
0.9156	-0.0708	0.238	0.747	0.0845	0.115	0.0619	0.160	0.939	0.0677
0.9312	-0.0696	0.248	0.735	0.0842	0.114	0.0665	0.154	0.958	0.0669
0.9468	-0.0667	0.258	0.721	0.0840	0.114	0.0713	0.149	0.976	0.0661
0.9624	-0.0601	0.269	0.709	0.0838	0.113	0.0761	0.142	0.996	0.0652
0.9781	-0.0453	0.279	0.700	0.0836	0.113	0.0803	0.133	1.019	0.0643
0.9893	-0.0222	0.286	0.697	0.0834	0.113	0.0824	0.124	1.039	0.0637
0.9971	-0.00746	0.296	0.680	0.0831	0.112	0.0881	0.115	1.059	0.0632
1.0010	+0.0300	0.308	0.653	0.0824	0.111	0.0962	0.108	1.072	0.0629
1.0049	+0.0615	0.327	0.602	0.0811	0.109	0.111	0.0991	1.090	0.0624
1.0055	+0.0671	0.331	0.593	0.0808	0.109	0.114	0.0974	1.094	0.0622
				$\xi = 1$					
0.0000	-0.126	0.0000	0.835	0.108	0.135	0.0161	0.406	0.0000	0
0.0625	-0.127	0.0142	0.834	0.108	0.135	0.0163	0.405	0.0644	0
0.1250	-0.127	0.0265	0.834	0.108	0.135	0.0169	0.404	0.128	0
0.1875	-0.127	0.0381	0.833	0.108	0.135	0.0177	0.402	0.193	0
0.2500	-0.128	0.0501	0.832	0.108	0.134	0.0189	0.398	0.257	0
0.3125	-0.129	0.0633	0.831	0.108	0.134	0.0206	0.394	0.322	0
0.3750	-0.130	0.0781	0.828	0.107	0.134	0.0230	0.389	0.386	0
0.4375	-0.131	0.0944	0.825	0.107	0.133	0.0263	0.383	0.451	0
0.5000	-0.134	0.112	0.822	0.107	0.133	0.0305	0.376	0.516	0
0.5625	-0.136	0.131	0.817	0.106	0.132	0.0359	0.367	0.581	0
0.6250	-0.139	0.151	0.811	0.106	0.132	0.0426	0.357	0.646	0
0.6875	-0.143	0.174	0.803	0.105	0.131	0.0509	0.345	0.712	0
0.7500	-0.147	0.199	0.794	0.104	0.129	0.0614	0.331	0.778	0
0.8125	-0.151	0.227	0.782	0.102	0.128	0.0746	0.314	0.846	0
0.8750	-0.153	0.261	0.766	0.101	0.126	0.0919	0.295	0.916	0
0.9156	-0.151	0.290	0.753	0.0997	0.124	0.107	0.279	0.966	0
0.9312	-0.148	0.303	0.746	0.0989	0.123	0.114	0.273	0.986	0
0.9468	-0.143	0.319	0.738	0.0981	0.122	0.122	0.265	1.009	0
0.9624	-0.134	0.339	0.729	0.0970	0.121	0.133	0.256	1.034	0
0.9781	-0.116	0.367	0.715	0.0955	0.119	0.148	0.243	1.065	0
0.9893	-0.0879	0.396	0.700	0.0939	0.117	0.165	0.230	1.096	0
0.9971	-0.0476	0.421	0.687	0.0924	0.115	0.180	0.216	1.128	0
1.0010	-0.0129	0.434	0.679	0.0915	0.114	0.188	0.205	1.152	0
1.0049	+0.0402	0.445	0.669	0.0904	0.113	0.199	0.189	1.186	0
1.0055	+0.0500	0.446	0.667	0.0902	0.112	0.202	0.185	1.192	0

TABLE 3.5

/153

$\delta = 10$; $b = 0.01$ m

$-x$	y	u	v	p	T	ρ	c^2	C_0
Streamline intersecting shock wave at point $x_1 = -0.3989$, $y_1 = 0.2577$								
0.398	0.257	-0.128	0.0501	0.832	0.108	7.681	0.134	0.0000
0.289	0.318	-0.0699	0.0660	0.874	0.0886	9.208	0.121	0.0722
0.234	0.380	-0.0470	0.0747	0.881	0.0845	9.594	0.117	0.0865
0.199	0.442	-0.0346	0.0819	0.881	0.0824	9.776	0.115	0.0939
0.173	0.504	-0.0271	0.0894	0.877	0.0809	9.862	0.114	0.0985
0.152	0.566	-0.0222	0.0980	0.870	0.0799	9.887	0.113	0.101
0.135	0.629	-0.0189	0.108	0.860	0.0790	9.860	0.112	0.103
0.120	0.691	-0.0167	0.120	0.846	0.0783	9.781	0.111	0.105
0.106	0.753	-0.0152	0.136	0.827	0.0775	9.641	0.110	0.106
0.0918	0.815	-0.0143	0.156	0.799	0.0767	9.414	0.109	0.107
0.0768	0.877	-0.0135	0.184	0.757	0.0755	9.049	0.108	0.108
0.0587	0.941	-0.0116	0.228	0.682	0.0733	8.385	0.105	0.109
0.0291	1.007	+0.0138	0.401	0.356	0.0618	5.189	0.0896	0.110
0.0202	1.016	+0.0384	0.521	0.149	0.0500	2.693	0.0731	0.110
Streamline intersecting shock wave at point $x_1 = -0.3762$, $y_1 = 0.5164$								
0.376	0.516	-0.134	0.112	0.822	0.107	7.665	0.133	0.0000
0.309	0.577	-0.0996	0.128	0.839	0.0938	8.535	0.124	0.0482
0.261	0.639	-0.0796	0.140	0.840	0.0892	8.852	0.120	0.0640
0.223	0.700	-0.0668	0.151	0.833	0.0865	8.982	0.118	0.0728
0.191	0.763	-0.0582	0.165	0.819	0.0845	8.992	0.116	0.0787
0.162	0.825	-0.0522	0.181	0.796	0.0827	8.891	0.114	0.0828
0.135	0.888	-0.0475	0.204	0.761	0.0809	8.656	0.112	0.0860
0.106	0.954	-0.0401	0.238	0.702	0.0785	8.215	0.109	0.0895
0.0639	1.035	+0.0273	0.335	0.519	0.0715	6.634	0.101	0.0945
0.0538	1.048	+0.0529	0.378	0.423	0.0681	5.678	0.0966	0.0945
Streamline intersecting shock wave at point $x_1 = -0.3310$, $y_1 = 0.7788$								
0.331	0.778	-0.147	0.199	0.794	0.104	7.621	0.129	0.0000
0.278	0.841	-0.125	0.217	0.788	0.0954	8.016	0.123	0.0299
0.231	0.905	-0.108	0.238	0.765	0.0906	8.083	0.119	0.0445
0.185	0.974	-0.0889	0.267	0.724	0.0862	7.959	0.115	0.0561
0.116	1.077	+0.0312	0.302	0.677	0.0805	7.855	0.110	0.0714
0.0768	1.131	+0.200	0.486	0.209	0.0623	3.133	0.0863	0.0723

TABLE 3.6

/154

$\delta = 100$; $b = 0.01$ m

s	ε	σ	$\bar{p}_0$	$\bar{T}_0$
0.0000	0.382	1.570	1.000	1.000
0.0625	0.382	1.557	0.999	0.999
0.1250	0.381	1.546	0.999	0.999
0.1875	0.379	1.536	0.999	0.999
0.2500	0.377	1.527	0.998	0.999
0.3125	0.374	1.517	0.997	0.999
0.3750	0.370	1.506	0.995	0.999
0.4375	0.366	1.493	0.993	0.998
0.5000	0.361	1.479	0.989	0.998
0.5625	0.355	1.463	0.985	0.997
0.6250	0.349	1.446	0.979	0.996
0.6875	0.341	1.427	0.970	0.994
0.7500	0.332	1.406	0.959	0.992
0.8125	0.321	1.384	0.942	0.989
0.8750	0.309	1.361	0.916	0.984
0.9375	0.296	1.337	0.871	0.973
0.9687	0.289	1.326	0.833	0.964
0.9877	0.284	1.315	0.793	0.953
0.9980	0.278	1.285	0.714	0.931
0.9985	0.277	1.278	0.696	0.926
0.9990	0.276	1.268	0.666	0.916
0.9995	0.275	1.250	0.596	0.893
1.0000	0.276	1.197	0.400	0.829

s	u	v	p	T	c^2	w^2	$-x$	y	C_0
$\xi = 0$									
0.0000	0	0.00000	0.905	0.0769	0.111	0.0000000	0.01000	0.0000	0.113
0.0625	0	0.00403	0.905	0.0768	0.110	0.0000162	0.00998	0.0625	0.113
0.1250	0	0.00803	0.905	0.0768	0.110	0.0000645	0.00992	0.125	0.113
0.1875	0	0.0121	0.905	0.0768	0.110	0.000147	0.00982	0.187	0.113
0.2500	0	0.0165	0.904	0.0768	0.110	0.000273	0.00968	0.250	0.113
0.3125	0	0.0215	0.903	0.0768	0.110	0.000465	0.00949	0.312	0.113
0.3750	0	0.0273	0.901	0.0768	0.110	0.000749	0.00927	0.375	0.113
0.4375	0	0.0340	0.899	0.0768	0.110	0.00116	0.00899	0.437	0.113
0.5000	0	0.0417	0.896	0.0767	0.110	0.00174	0.00866	0.500	0.113
0.5625	0	0.0503	0.892	0.0767	0.110	0.00253	0.00826	0.562	0.113

TABLE 3.6 Continued

/15

s	u	v	p	T	c^2	w^2	$-x$	y	C_0
0.6250	0	0.0600	0.886	0.0766	0.110	0.00361	0.00780	0.624	0.113
0.6875	0	0.0712	0.879	0.0765	0.110	0.00507	0.00726	0.687	0.113
0.7500	0	0.0843	0.868	0.0763	0.110	0.00711	0.00661	0.749	0.113
0.8125	0	0.100	0.853	0.0760	0.109	0.0100	0.00582	0.812	0.113
0.8750	0	0.121	0.830	0.0756	0.109	0.0147	0.00484	0.874	0.113
0.9375	0	0.152	0.789	0.0748	0.108	0.0232	0.00348	0.937	0.113
0.9687	0	0.175	0.754	0.0741	0.107	0.0307	0.00248	0.968	0.113
0.9877	0	0.197	0.718	0.0733	0.105	0.0388	0.00156	0.987	0.113
0.9980	0	0.236	0.646	0.0716	0.103	0.0558	0.000645	0.997	0.113
0.9985	0	0.244	0.630	0.0712	0.102	0.0598	0.000565	0.998	0.113
0.9990	0	0.258	0.603	0.0705	0.101	0.0666	0.000473	0.998	0.113
0.9995	0	0.289	0.540	0.0687	0.0995	0.0837	0.000359	0.999	0.113
1.0000	0	0.361	0.392	0.0638	0.0926	0.131	0.000192	0.999	0.113
				$\xi = 0.5$					
0.0000	-0.0423	0.00000	0.897	0.0839	0.117	0.00179	0.201	0.0000	0.0904
0.0625	-0.0438	0.00901	0.897	0.0840	0.117	0.00200	0.201	0.0625	0.0899
0.1250	-0.0453	0.0184	0.898	0.0841	0.117	0.00239	0.200	0.125	0.0893
0.1875	-0.0466	0.0281	0.897	0.0842	0.117	0.00296	0.199	0.187	0.0888
0.2500	-0.0477	0.0381	0.896	0.0843	0.117	0.00372	0.198	0.250	0.0883
0.3125	-0.0486	0.0481	0.895	0.0844	0.117	0.00468	0.196	0.313	0.0878
0.3750	-0.0495	0.0581	0.893	0.0844	0.117	0.00584	0.194	0.375	0.0872
0.4375	-0.0505	0.0682	0.890	0.0844	0.117	0.00721	0.192	0.438	0.0867
0.5000	-0.0516	0.0785	0.886	0.0845	0.117	0.00883	0.189	0.501	0.0860
0.5625	-0.0531	0.0890	0.882	0.0845	0.117	0.0107	0.186	0.563	0.0853
0.6250	-0.0551	0.100	0.877	0.0845	0.117	0.0130	0.182	0.626	0.0845
0.6875	-0.0577	0.112	0.870	0.0845	0.117	0.0159	0.177	0.689	0.0835
0.7500	-0.0613	0.125	0.861	0.0845	0.117	0.0196	0.172	0.751	0.0823
0.8125	-0.0664	0.141	0.848	0.0844	0.116	0.0243	0.166	0.814	0.0808
0.8750	-0.0737	0.159	0.830	0.0843	0.116	0.0307	0.159	0.877	0.0789

TABLE 3.6 Continued

/156

s	u	v	p	T	c^2	w^2	$-x$	y	C_0
0.9375	-0.0848	0.181	0.802	0.0842	0.115	0.0402	0.151	0.941	0.0762
0.9687	-0.0919	0.196	0.781	0.0840	0.115	0.0469	0.147	0.974	0.0745
0.9877	-0.0942	0.206	0.768	0.0839	0.115	0.0517	0.143	0.996	0.0733
0.9980	-0.0776	0.213	0.775	0.0842	0.115	0.0514	0.138	1.019	0.0723
0.9985	-0.0725	0.213	0.779	0.0843	0.115	0.0508	0.137	1.022	0.0722
0.9990	-0.0641	0.213	0.785	0.0844	0.115	0.0497	0.135	1.027	0.0721
0.9995	-0.0472	0.214	0.793	0.0846	0.115	0.0482	0.132	1.036	0.0720
1.0000	+0.0124	0.223	0.788	0.0843	0.115	0.0501	0.122	1.063	0.0724
				$\xi = 1$					
0.0000	-0.126	0.0000	0.835	0.108	0.135	0.0161	0.392	0.0000	0
0.0625	-0.127	0.0110	0.835	0.108	0.135	0.0162	0.392	0.0627	0
0.1250	-0.127	0.0205	0.834	0.108	0.135	0.0166	0.391	0.125	0
0.1875	-0.127	0.0290	0.834	0.108	0.135	0.0172	0.389	0.188	0
0.2500	-0.128	0.0372	0.833	0.108	0.134	0.0178	0.386	0.250	0
0.3125	-0.129	0.0457	0.832	0.108	0.134	0.0188	0.383	0.313	0
0.3750	-0.130	0.0552	0.831	0.108	0.134	0.0200	0.380	0.376	0
0.4375	-0.131	0.0659	0.830	0.108	0.134	0.0217	0.375	0.439	0
0.5000	-0.133	0.0779	0.828	0.107	0.134	0.0239	0.370	0.502	0
0.5625	-0.136	0.0912	0.825	0.107	0.133	0.0269	0.364	0.564	0
0.6250	-0.139	0.105	0.822	0.107	0.133	0.0306	0.356	0.627	0
0.6875	-0.143	0.121	0.817	0.106	0.132	0.0354	0.348	0.690	0
0.7500	-0.148	0.138	0.812	0.106	0.132	0.0413	0.338	0.753	0
0.8125	-0.154	0.156	0.806	0.105	0.131	0.0484	0.327	0.816	0
0.8750	-0.161	0.175	0.798	0.104	0.130	0.0568	0.314	0.880	0
0.9375	-0.168	0.194	0.790	0.103	0.129	0.0662	0.300	0.945	0
0.9687	-0.170	0.205	0.785	0.103	0.128	0.0713	0.291	0.979	0
0.9877	-0.169	0.218	0.780	0.102	0.128	0.0762	0.285	1.005	0
0.9980	-0.158	0.256	0.767	0.101	0.126	0.0907	0.275	1.040	'
0.9985	-0.155	0.264	0.764	0.100	0.125	0.0940	0.273	1.046	0
0.9990	-0.149	0.277	0.760	0.100	0.125	0.0993	0.270	1.055	0
0.9995	-0.137	0.300	0.751	0.0994	0.124	0.109	0.265	1.072	0
1.0000	-0.0830	0.366	0.722	0.0963	0.120	0.141	0.245	1.127	0

TABLE 3.7

/157

$\delta = 100$; $b = 0.01$ m

$-x$	y	u	v	p	T	ρ	c^2	C_0
Streamline intersecting shock wave at point $x_1 = -0.3869$; $y_1 = 0.2509$								
0.386	0.250	-0.128	0.0372	0.833	0.108	7.682	0.134	0.0000
0.251	0.313	-0.0679	0.0511	0.880	0.0870	9.384	0.119	0.0784
0.187	0.375	-0.0457	0.0586	0.889	0.0833	9.772	0.116	0.0916
0.147	0.438	-0.0338	0.0643	0.890	0.0814	9.956	0.115	0.0982
0.118	0.500	-0.0265	0.0698	0.888	0.0801	10.054	0.113	0.102
0.0981	0.563	-0.0217	0.0757	0.885	0.0793	10.099	0.113	0.104
0.0821	0.625	-0.0184	0.0827	0.880	0.0787	10.106	0.112	0.106
0.0692	0.688	-0.0163	0.0911	0.873	0.0781	10.078	0.111	0.108
0.0585	0.750	-0.0150	0.101	0.862	0.0777	10.011	0.113	0.108
0.0494	0.813	-0.0145	0.115	0.848	0.0772	9.894	0.110	0.109
0.0412	0.875	-0.0147	0.133	0.825	0.0766	9.698	0.110	0.109
0.0334	0.938	-0.0159	0.160	0.786	0.0757	9.351	0.108	0.110
0.0231	1.007	-0.000933	0.580	0.0599	0.0389	1.367	0.0583	0.124
Streamline intersecting shock wave at point $x_1 = -0.3704$; $y_1 = 0.5020$								
0.370	0.502	-0.133	0.0779	0.828	0.107	7.674	0.134	0.0000
0.287	0.564	-0.0965	0.0953	0.851	0.0922	8.736	0.123	0.0564
0.233	0.626	-0.0765	0.106	0.856	0.0879	9.093	0.120	0.0717
0.193	0.689	-0.0642	0.115	0.855	0.0854	9.267	0.117	0.0800
0.162	0.751	-0.0563	0.125	0.848	0.0837	9.339	0.116	0.0853
0.135	0.814	-0.0516	0.136	0.837	0.0824	9.329	0.115	0.0890
0.112	0.876	-0.0496	0.151	0.818	0.0812	9.226	0.113	0.0916
0.0922	0.939	-0.0507	0.173	0.785	0.0799	8.981	0.112	0.0935
0.0653	1.021	-0.00975	0.391	0.368	0.0656	5.107	0.0937	0.100
Streamline intersecting shock wave at point $x_1 = -0.3386$; $y_1 = 0.7537$								
0.338	0.753	-0.148	0.138	0.812	0.106	7.650	0.132	0.0000
0.279	0.816	-0.125	0.154	0.818	0.0954	8.258	0.124	0.0378
0.232	0.879	-0.112	0.169	0.810	0.0910	8.460	0.121	0.0524
0.191	0.942	-0.107	0.187	0.789	0.0880	8.445	0.118	0.0608
0.122	1.063	+0.0132	0.224	0.774	0.0822	8.720	0.113	0.0797
0.0875	1.134	+0.117	0.505	0.194	0.0595	3.006	0.0841	0.0883
Streamline intersecting shock wave at point $x_1 = -0.3076$; $y_1 = 0.9127$								
0.307	0.912	-0.164	0.185	0.794	0.104	7.621	0.129	0.0000
0.251	0.978	-0.149	0.204	0.783	0.0954	7.974	0.123	0.0296
0.171	1.088	-0.120	0.247	0.797	0.0865	8.679	0.116	0.0616
0.125	1.174	+0.159	0.337	0.533	0.0751	6.601	0.103	0.0747

NONEQUILIBRIUM OXYGEN (FROZEN FLOW). /158

SCHEME II. N = 2

TABLE 3.8

$M_\infty = 10$, $p_\infty = 0.01$ atm, $T_\infty = 288°K$, $\rho_\infty = 0.0135$ kg/m^3, $w_{max} = 3317$ m/sec, $h_{00} = 21\ 168°K$, $\delta = 1$, $\varepsilon_0 = 0.1049$, $\varepsilon_1 = 0.1969$, $\varepsilon_2 = 0.1188$, $C_{O_2} = 1$

ξ	s	u	v	p	T	ρ	h
			$s = 0$				
1.000	0	-0.127	0	0.836	0.108	7.702	0.983
0.875	0	-0.108	0	0.853	0.108	7.829	0.988
0.750	0	-0.0903	0	0.866	0.109	7.931	0.991
0.625	0	-0.0735	0	0.877	0.109	8.011	0.994
0.500	0	-0.0576	0	0.886	0.109	8.073	0.996
0.375	0	-0.0423	0	0.892	0.109	8.118	0.998
0.250	0	-0.0277	0	0.896	0.110	8.149	0.999
0.125	0	-0.0136	0	0.898	0.110	8.166	0.999
0.000	0	0.0000	0	0.899	0.110	8.173	1.000
			$s = s_1/2$				
1.000	0.500	-0.0933	0.422	0.682	0.0916	7.442	0.814
0.875	0.471	-0.0838	0.377	0.699	0.0953	7.336	0.850
0.750	0.448	-0.0727	0.339	0.713	0.0982	7.266	0.880
0.625	0.430	-0.0610	0.307	0.725	0.100	7.217	0.902
0.500	0.415	-0.0489	0.278	0.734	0.102	7.179	0.920
0.375	0.403	-0.0366	0.253	0.740	0.103	7.147	0.934
0.250	0.394	-0.0244	0.232	0.745	0.104	7.115	0.946
0.125	0.386	-0.0122	0.213	0.748	0.105	7.083	0.954
0.000	0.380	0.0000	0.198	0.749	0.106	7.049	0.961
			$s = s_1$				
1.000	1.000	+0.0552	0.685	0.425	0.0624	6.825	0.528
0.875	0.942	+0.0292	0.647	0.423	0.0680	6.233	0.581
0.750	0.896	+0.0118	0.604	0.423	0.0736	5.751	0.636
0.625	0.860	+0.00101	0.560	0.424	0.0789	5.380	0.687
0.500	0.830	-0.00489	0.518	0.425	0.0834	5.098	0.732
0.375	0.806	-0.00713	0.480	0.425	0.0872	4.881	0.770
0.250	0.788	-0.00663	0.446	0.425	0.0904	4.710	0.801
0.125	0.772	-0.00406	0.418	0.424	0.0928	4.567	0.826
0.000	0.760	0.00000	0.394	0.420	0.0947	4.443	0.845

NONEQUILIBRIUM OXYGEN /159

(EQUILIBRIUM VIBRATIONS, NONEQUILIBRIUM DISSOCIATION).

SCHEME II. N = 2

TABLE 3.9

M_∞ = 10-15, p_∞ = 0.001 atm, T_∞ = 290°K, ρ_∞ = 0.001345 kg/m^3,

δ = 1, R_0 = 0.01-0.1 m

M_∞ = 10, w_{max} = 3328 m/sec, h_{00} = 21 315°K, R_0 = 0.01 m,

ε_0 = 0.1021, ε_1 = 0.1950, ε_2 = 0.1164

ξ	s	u	v	p	T	ρ	h	C_0
				$s=0$				
1.0000	0	-0.126	0	0.835	0.108	7.697	0.983	0.00000
0.8906	0	-0.110	0	0.850	0.108	7.847	0.987	0.00278
0.7656	0	-0.0921	0	0.865	0.107	8.002	0.991	0.00640
0.6406	0	-0.0751	0	0.876	0.106	8.145	0.994	0.0105
0.5156	0	-0.0589	0	0.885	0.105	8.279	0.996	0.0153
0.3906	0	-0.0435	0	0.892	0.103	8.411	0.998	0.0208
0.2656	0	-0.0288	0	0.896	0.102	8.551	0.999	0.0276
0.1406	0	-0.0149	0	0.899	0.0994	8.721	0.999	0.0367
0.0000	0	0.0000	0	0.900	0.0885	9.461	1.000	0.0743
				$s=s_1/2$				
1.0000	0.500	-0.0926	0.420	0.683	0.0916	7.452	0.814	0.00000
0.8906	0.474	-0.0845	0.382	0.698	0.0946	7.369	0.846	0.00063
0.7656	0.451	-0.0737	0.343	0.712	0.0971	7.318	0.876	0.00213
0.6406	0.432	-0.0620	0.310	0.724	0.0987	7.301	0.899	0.00466
0.5156	0.417	-0.0499	0.281	0.733	0.0995	7.311	0.918	0.00843
0.3906	0.405	-0.0376	0.256	0.740	0.0994	7.345	0.932	0.0136
0.2656	0.395	-0.0253	0.233	0.745	0.0986	7.406	0.944	0.0207
0.1406	0.387	-0.0132	0.212	0.748	0.0966	7.512	0.954	0.0309
0.0000	0.380	0.0000	0.185	0.749	0.0855	8.167	0.965	0.0728
				$s=s_1$				
1.0000	1.000	+0.0553	0.684	0.426	0.0624	6.822	0.528	0.00000
0.8906	0.948	+0.0321	0.650	0.424	0.0673	6.299	0.575	0.00001
0.7656	0.902	+0.0139	0.608	0.423	0.0729	5.813	0.629	0.00005
0.6406	0.864	+0.0236	0.564	0.424	0.0780	5.442	0.680	0.00037
0.5156	0.835	-0.00411	0.523	0.425	0.0822	5.168	0.726	0.00147
0.3906	0.810	-0.00680	0.484	0.426	0.0854	4.973	0.764	0.00418
0.2656	0.791	-0.00666	0.449	0.426	0.0871	4.845	0.797	0.00969
0.1406	0.775	-0.00436	0.416	0.424	0.0869	4.789	0.826	0.0202
0.0000	0.761	0.00000	0.367	0.420	0.0754	5.203	0.862	0.0726

TABLE 3.10

/160

$M_\infty = 10$, $w_{max} = 3328$ m/sec, $h_{00} = 21\ 315°K$, $R_0 = 0.1$ m,

$\varepsilon_0 = 0.09457$, $\varepsilon_1 = 0.1899$, $\varepsilon_2 = 0.11012$

ξ	s	u	v	p	T	ρ	h	C_0
				$s=0$				
1.0000	0	-0.126	0	0.835	0.108	7.697	0.983	0.0000
0.8906	0	-0.107	0	0.853	0.103	8.115	0.988	0.0204
0.7656	0	-0.0879	0	0.869	0.0984	8.509	0.992	0.0377
0.6406	0	-0.0705	0	0.881	0.0947	8.843	0.995	0.0512
0.5156	0	-0.0545	0	0.890	0.0916	9.136	0.997	0.0626
0.3906	0	-0.0397	0	0.896	0.0888	9.404	0.998	0.0727
0.2656	0	-0.0259	0	0.900	0.0861	9.663	0.999	0.0825
0.1406	0	-0.0131	0	0.903	0.0831	9.945	0.999	0.0930
0.0000	0	0.0000	0	0.904	0.0739	10.878	1.000	0.124
				$s=s_1/2$				
1.0000	0.500	-0.0914	0.417	0.685	0.0919	7.457	0.817	0.00000
0.8906	0.475	-0.0828	0.380	0.701	0.0933	7.465	0.848	0.00551
0.7656	0.452	-0.0712	0.343	0.715	0.0932	7.556	0.876	0.0157
0.6406	0.434	-0.0590	0.311	0.727	0.0918	7.701	0.899	0.0284
0.5156	0.419	-0.0466	0.281	0.737	0.0897	7.877	0.918	0.0422
0.3906	0.407	-0.0346	0.253	0.743	0.0872	8.068	0.934	0.0561
0.2656	0.397	-0.0229	0.228	0.748	0.0845	8.275	0.947	0.0699
0.1406	0.389	-0.0118	0.204	0.751	0.0813	8.517	0.957	0.0845
0.0000	0.382	0.0000	0.173	0.752	0.0712	9.403	0.969	0.122
				$s=s_1$				
1.0000	1.000	+0.0552	0.684	0.425	0.0624	6.822	0.528	0.00000
0.8906	0.950	+0.0324	0.649	0.424	0.0674	6.287	0.577	0.00008
0.7656	0.904	+0.0143	0.607	0.424	0.0728	5.826	0.630	0.00033
0.6406	0.868	+0.00297	0.566	0.425	0.0770	5.509	0.679	0.00335
0.5156	0.838	-0.00343	0.525	0.426	0.0792	5.322	0.724	0.0110
0.3906	0.814	-0.00619	0.484	0.426	0.0794	5.242	0.765	0.0246
0.2656	0.794	-0.00617	0.443	0.426	0.0777	5.251	0.803	0.0434
0.1406	0.778	-0.00410	0.402	0.424	0.0744	5.344	0.837	0.0665
0.0000	0.765	0.00000	0.344	0.420	0.0628	5.971	0.880	0.120

TABLE 3.11

/161

$M_\infty = 15$, $w_{max} = 4926$ m/sec, $h_{00} = 46\ 690°K$, $R_0 = 0.01$ m,

$\varepsilon_0 = 0.06831$, $\varepsilon_1 = 0.1463$, $\varepsilon_2 = 0.08026$

ξ	s	u	v	p	T	ρ	h	C_0
				$s=0$				
1.0000	0	-0.116	0	0.866	0.102	8.486	0.986	0.000
0.8906	0	-0.0876	0	0.893	0.0706	10.17	0.992	0.245
0.7656	0	-0.0671	0	0.910	0.0601	11.38	0.995	0.330
0.6406	0	-0.0517	0	0.921	0.0552	12.17	0.997	0.369
0.5156	0	-0.0387	0	0.928	0.0520	12.79	0.998	0.393
0.3906	0	-0.0274	0	0.933	0.0496	13.31	0.999	0.413
0.2656	0	-0.0173	0	0.936	0.0474	13.80	0.999	0.430
0.1406	0	-0.00852	0	0.938	0.0452	14.32	1.000	0.447
0.0000	0	0.00000	0	0.938	0.0397	15.86	1.000	0.489
				$s=s_1/2$				
1.0000	0.500	-0.0842	0.432	0.703	0.0845	8.320	0.806	0.000
0.8906	0.477	-0.0681	0.395	0.724	0.0688	9.194	0.838	0.144
0.7656	0.456	-0.0539	0.356	0.740	0.0597	10.00	0.869	0.239
0.6406	0.439	-0.0420	0.319	0.750	0.0547	10.58	0.896	0.297
0.5156	0.425	-0.0327	0.284	0.758	0.0513	11.03	0.918	0.339
0.3906	0.413	-0.0236	0.251	0.763	0.0486	11.42	0.938	0.374
0.2656	0.404	-0.0153	0.220	0.767	0.0463	11.81	0.951	0.402
0.1406	0.397	-0.00764	0.190	0.770	0.0439	12.25	0.963	0.430
0.0000	0.391	0.00000	0.151	0.771	0.0377	13.73	0.976	0.486
				$s=s_1$				
1.0000	1.000	+0.0563	0.710	0.419	0.0537	7.809	0.491	0.0000
0.8906	0.954	+0.0362	0.676	0.416	0.0564	7.248	0.541	0.0192
0.7656	0.912	+0.0203	0.633	0.413	0.0555	6.976	0.598	0.0660
0.6406	0.878	+0.00971	0.584	0.411	0.0522	6.929	0.658	0.136
0.5156	0.850	+0.00287	0.531	0.410	0.0485	6.984	0.717	0.208
0.3906	0.827	-0.000956	0.478	0.408	0.0451	7.101	0.771	0.276
0.2656	0.808	-0.00241	0.424	0.407	0.0419	7.269	0.819	0.336
0.1406	0.794	-0.00203	0.372	0.406	0.0388	7.510	0.861	0.391
0.0000	0.782	0.00000	0.300	0.403	0.0317	8.581	0.909	0.481

TABLE 3.12

/162

$M_\infty = 15$, $w_{max} = 4926$ m/sec, $h_{00} = 46\ 690°K$, $R_0 = 0.1$ m,

$\varepsilon_0 = 0.05706$, $\varepsilon_1 = 0.1293$, $\varepsilon_2 = 0.06792$

ξ	s	u	v	p	T	ρ	h	C_0
				$s = 0$				
1.0000	0	-0.116	0	0.866	0.102	8.486	0.986	0.000
0.8789	0	-0.0659	0	0.914	0.0490	13.17	0.995	0.415
0.7539	0	-0.0510	0	0.926	0.0448	14.26	0.997	0.448
0.6289	0	-0.0393	0	0.934	0.0427	14.92	0.998	0.466
0.5039	0	-0.0293	0	0.939	0.0412	15.40	0.999	0.478
0.3789	0	-0.0206	0	0.942	0.0402	15.77	0.999	0.485
0.2539	0	-0.0129	0	0.944	0.0394	16.06	0.999	0.491
0.1289	0	-0.00613	0	0.945	0.0388	16.26	1.000	0.496
0.0000	0	0.00000	0	0.946	0.0386	16.35	1.000	0.497
				$s = s_1/2$				
1.0000	0.500	-0.0855	0.435	0.700	0.0842	8.317	0.803	0.000
0.8789	0.476	-0.0507	0.392	0.736	0.0487	11.60	0.843	0.302
0.7539	0.456	-0.0404	0.350	0.748	0.0442	12.43	0.875	0.361
0.6289	0.440	-0.0321	0.310	0.756	0.0418	12.91	0.902	0.399
0.5039	0.427	-0.0246	0.274	0.762	0.0402	13.25	0.923	0.428
0.3789	0.416	-0.0177	0.241	0.766	0.0390	13.52	0.941	0.450
0.2539	0.408	-0.0113	0.210	0.769	0.0381	13.73	0.955	0.468
0.1289	0.401	-0.00552	0.181	0.771	0.0375	13.88	0.967	0.481
0.0000	0.394	0.00000	0.153	0.772	0.0372	13.90	0.976	0.490
				$s = s_1$				
1.0000	1.000	+0.0512	0.717	0.411	0.0528	7.785	0.482	0.000
0.8789	0.953	+0.0370	0.683	0.408	0.0477	7.946	0.532	0.076
0.7539	0.913	+0.0233	0.633	0.402	0.0432	8.026	0.597	0.159
0.6289	0.881	+0.0127	0.575	0.398	0.0398	8.071	0.668	0.238
0.5039	0.854	+0.00560	0.515	0.395	0.0371	8.143	0.734	0.308
0.3789	0.833	+0.00139	0.457	0.394	0.0350	8.236	0.790	0.367
0.2539	0.816	-0.000562	0.402	0.393	0.0333	8.323	0.837	0.415
0.1289	0.803	-0.000838	0.352	0.392	0.0322	8.371	0.875	0.452
0.0000	0.789	0.000000	0.302	0.404	0.0321	8.563	0.906	0.467

NONEQUILIBRIUM OXYGEN

(EQUILIBRIUM VIBRATIONS, NONEQUILIBRIUM DISSOCIATION).

SCHEME II. N = 3

TABLE 3.13

$M_\infty = 10$, $p_\infty = 0.001$ atm, $T_\infty = 288°K$, $\rho_\infty = 0.001354$ kg/m^3,

$w_{max} = 3307$ m/sec, $h_{00} = 21\,055°K$, $\delta = 1$, $R_0 = 1$ m,

$\varepsilon_0 = 0.08170$, $\varepsilon_1 = 0.08800$, $\varepsilon_2 = 0.1098$, $\varepsilon_3 = 0.1557$

ξ	s	u	v	p	T	ρ	h	C_0
				$s = 0$				
1.0000	0	-0.127	0	0.834	0.108	7.683	0.983	0.0000
0.8750	0	-0.0941	0	0.865	0.0887	9.110	0.990	0.0701
0.7500	0	-0.0750	0	0.880	0.0831	9.712	0.994	0.0901
0.6250	0	-0.0591	0	0.891	0.0798	10.125	0.996	0.102
0.5000	0	-0.0449	0	0.898	0.0774	10.448	0.997	0.106
0.3750	0	-0.0320	0	0.904	0.0754	10.716	0.998	0.117
0.2500	0	-0.0202	0	0.907	0.0737	10.949	0.999	0.123
0.1250	0	-0.00957	0	0.909	0.0721	11.161	0.999	0.129
0.0000	0	0.00000	0	0.909	0.0704	11.376	0.999	0.134
				$s = s_1/3$				
1.0000	0.291	-0.114	0.246	0.782	0.102	7.607	0.925	0.0000
0.8750	0.278	-0.0876	0.223	0.809	0.0882	8.691	0.942	0.0553
0.7500	0.267	-0.0705	0.203	0.823	0.0829	9.222	0.953	0.0772
0.6250	0.258	-0.0560	0.184	0.833	0.0795	9.597	0.962	0.0915
0.5000	0.251	-0.0428	0.166	0.841	0.0771	9.893	0.970	0.102
0.3750	0.245	-0.0307	0.150	0.846	0.0750	10.143	0.976	0.111
0.2500	0.240	-0.0196	0.134	0.849	0.0732	10.362	0.981	0.119
0.1250	0.237	-0.00933	0.118	0.851	0.0715	10.562	0.985	0.126
0.0000	0.235	0.00000	0.103	0.851	0.0697	10.768	0.989	0.133
				$s = 2s_1/3$				
1.0000	0.583	-0.0718	0.464	0.651	0.0882	7.377	0.779	0.0000
0.8750	0.556	-0.0624	0.424	0.666	0.0850	7.658	0.815	0.0230
0.7500	0.534	-0.0531	0.389	0.676	0.0814	7.945	0.845	0.0453
0.6250	0.517	-0.0439	0.355	0.684	0.0784	8.192	0.871	0.0641
0.5000	0.502	-0.0348	0.324	0.689	0.0759	8.407	0.893	0.0803
0.3750	0.490	-0.0258	0.293	0.693	0.0736	8.599	0.912	0.0945
0.2500	0.481	-0.0169	0.264	0.695	0.0715	8.774	0.929	0.107
0.1250	0.474	-0.00826	0.235	0.695	0.0695	8.942	0.944	0.119
0.0000	0.470	0.00000	0.205	0.693	0.0672	9.122	0.957	0.131
				$s = s_1$				
1.0000	0.875	+0.00751	0.632	0.490	0.0700	7.000	0.600	0.00000
0.8750	0.834	-0.00554	0.583	0.493	0.0753	6.530	0.659	0.00259
0.7500	0.802	-0.0120	0.541	0.496	0.0769	6.365	0.706	0.0133
0.6250	0.776	-0.0146	0.500	0.498	0.0756	6.381	0.748	0.0319
0.5000	0.754	-0.0146	0.461	0.498	0.0733	6.459	0.786	0.0523
0.3750	0.736	-0.0127	0.423	0.498	0.0708	6.555	0.820	0.0723
0.2500	0.722	-0.00944	0.385	0.496	0.0683	6.658	0.851	0.0912
0.1250	0.711	-0.00509	0.347	0.493	0.0657	6.766	0.879	0.109
0.0000	0.705	0.00000	0.306	0.487	0.0626	6.897	0.905	0.128

NONEQUILIBRIUM NITROGEN /164

(EQUILIBRIUM VIBRATIONS, NONEQUILIBRIUM DISSOCIATION).

SCHEME II. N = 2

TABLE 3.14

$M_\infty = 15$, $p_\infty = 0.001$ atm, $T_\infty = 290°K$, $\rho_\infty = 0.001177$ kg/m^3,

$w_{max} = 5266$ m/sec, $h_{00} = 46690°K$, $\delta = 1$

$R_0 = 0.1$ m, $\varepsilon_0 = 0.09187$, $\varepsilon_1 = 0.1822$, $\varepsilon_2 = 0.1065$

ξ	s	u	v	p	T	ρ	h	C_0
				$s = 0$				
1.0000	0	-0.127	0	0.834	0.108	7.683	0.983	0.0000
0.8750	0	-0.0941	0	0.865	0.0887	9.110	0.990	0.0701
0.7500	0	-0.0750	0	0.880	0.0831	9.712	0.994	0.0901
0.6250	0	-0.0591	0	0.891	0.0798	10.125	0.996	0.102
0.5000	0	-0.0449	0	0.898	0.0774	10.448	0.997	0.106
0.3750	0	-0.0320	0	0.904	0.0754	10.716	0.998	0.117
0.2500	0	-0.0202	0	0.907	0.0737	10.949	0.999	0.123
0.1250	0	-0.00957	0	0.909	0.0721	11.161	0.999	0.129
0.0000	0	0.00000	0	0.909	0.0704	11.376	0.999	0.134
				$s = s_1/3$				
1.0000	0.291	-0.114	0.246	0.782	0.102	7.607	0.925	0.0000
0.8750	0.278	-0.0876	0.223	0.809	0.0882	8.691	0.942	0.0553
0.7500	0.267	-0.0705	0.203	0.823	0.0829	9.222	0.953	0.0772
0.6250	0.258	-0.0560	0.184	0.833	0.0795	9.597	0.962	0.0915
0.5000	0.251	-0.0428	0.166	0.841	0.0771	9.893	0.970	0.102
0.3750	0.245	-0.0307	0.150	0.846	0.0750	10.143	0.976	0.111
0.2500	0.240	-0.0196	0.134	0.849	0.0732	10.362	0.981	0.119
0.1250	0.237	-0.00933	0.118	0.851	0.0715	10.562	0.985	0.126
0.0000	0.235	0.00000	0.103	0.851	0.0697	10.768	0.989	0.133
				$s = 2s_1/3$				
1.0000	0.583	-0.0718	0.464	0.651	0.0882	7.377	0.779	0.0000
0.8750	0.556	-0.0624	0.424	0.666	0.0850	7.658	0.815	0.0230
0.7500	0.534	-0.0531	0.389	0.676	0.0814	7.945	0.845	0.0453
0.6250	0.517	-0.0439	0.355	0.684	0.0784	8.192	0.871	0.0641
0.5000	0.502	-0.0348	0.324	0.689	0.0759	8.407	0.893	0.0803
0.3750	0.490	-0.0258	0.293	0.693	0.0736	8.599	0.912	0.0945
0.2500	0.481	-0.0169	0.264	0.695	0.0715	8.774	0.929	0.107
0.1250	0.474	-0.00826	0.235	0.695	0.0695	8.942	0.944	0.119
0.0000	0.470	0.00000	0.205	0.693	0.0672	9.122	0.957	0.131
				$s = s_1$				
1.0000	0.875	+0.00751	0.632	0.490	0.0700	7.000	0.600	0.00000
0.8750	0.834	-0.00554	0.583	0.493	0.0753	6.530	0.659	0.00259
0.7500	0.802	-0.0120	0.541	0.496	0.0769	6.365	0.706	0.0133
0.6250	0.776	-0.0146	0.500	0.498	0.0756	6.381	0.748	0.0319
0.5000	0.754	-0.0146	0.461	0.498	0.0733	6.459	0.786	0.0523
0.3750	0.736	-0.0127	0.423	0.498	0.0708	6.555	0.820	0.0723
0.2500	0.722	-0.00944	0.385	0.496	0.0683	6.658	0.851	0.0912
0.1250	0.711	-0.00509	0.347	0.493	0.0657	6.766	0.879	0.109
0.0000	0.705	0.00000	0.306	0.487	0.0626	6.897	0.905	0.128

TABLE 3.15 /1

$R_0 = 1$ m; $\varepsilon_0 = 0.07898$; $\varepsilon_1 = 0.1716$; $\varepsilon_2 = 0.09492$

ξ	s	u	v	p	T	ρ	h	C_N
			$s = 0$					
1.0000	0	−0.125	0	0.857	0.108	7.882	0.984	0.0000
0.8906	0	−0.0951	0	0.886	0.0870	9.368	0.991	0.0859
0.7656	0	−0.0751	0	0.902	0.0793	10.189	0.994	0.116
0.6406	0	−0.0590	0	0.913	0.0751	10.731	0.997	0.132
0.5156	0	−0.0448	0	0.922	0.0722	11.149	0.998	0.144
0.3906	0	−0.0321	0	0.927	0.0699	11.499	0.999	0.153
0.2656	0	−0.0207	0	0.931	0.0678	11.809	1.000	0.161
0.1406	0	−0.0103	0	0.933	0.0659	12.104	1.000	0.169
0.0000	0	0.0000	0	0.933	0.0633	12.496	1.000	0.178
			$s = s_1/2$					
1.0000	0.500	−0.0896	0.422	0.703	0.0921	7.630	0.813	0.0000
0.8906	0.476	−0.0749	0.386	0.723	0.0852	8.188	0.845	0.0372
0.7656	0.454	−0.0610	0.348	0.739	0.0792	8.723	0.874	0.0705
0.6406	0.437	−0.0490	0.313	0.751	0.0749	9.148	0.899	0.0959
0.5156	0.422	−0.0381	0.281	0.759	0.0716	9.500	0.919	0.116
0.3906	0.410	−0.0279	0.251	0.765	0.0689	9.804	0.936	0.132
0.2656	0.401	−0.0183	0.223	0.769	0.0665	10.080	0.950	0.146
0.1406	0.393	−0.00932	0.196	0.772	0.0643	10.354	0.961	0.159
0.0000	0.387	0.00000	0.167	0.773	0.0612	10.750	0.972	0.175
			$s = s_1$					
1.0000	1.000	+0.0574	0.699	0.429	0.0591	7.255	0.506	0.0000
0.8906	0.952	+0.0349	0.662	0.427	0.0648	6.583	0.560	0.0005
0.7656	0.909	+0.0175	0.620	0.427	0.0690	6.146	0.614	0.0067
0.6406	0.874	+0.00656	0.577	0.426	0.0695	5.982	0.666	0.0252
0.5156	0.845	+0.00000194	0.529	0.426	0.0677	5.984	0.719	0.0524
0.3906	0.821	−0.00326	0.480	0.425	0.0647	6.075	0.768	0.0827
0.2656	0.802	−0.00403	0.431	0.425	0.0614	6.217	0.813	0.112
0.1406	0.786	−0.00290	0.384	0.423	0.0581	6.390	0.851	0.139
0.0000	0.774	0.00000	0.331	0.420	0.0537	6.628	0.885	0.171

NONEQUILIBRIUM AIR

(EQUILIBRIUM VIBRATIONS, NONEQUILIBRIUM DISSOCIATION)

SCHEME II. N = 3

TABLE 3.16

$M_\infty = 10$, $p_\infty = 0.01$ atm, $T_\infty = 300°K$, $\rho_\infty = 0.01178$ kg/m^3,

$w_{max} = 3553$ m/sec, $h_{00} = 22\,050°K$, $\delta = 1$, $R_0 = 0.1$ m,

$\varepsilon_0 = 0.09294$, $\varepsilon_1 = 0.09252$, $\varepsilon_2 = 0.1217$, $\varepsilon_3 = 0.1682$

ξ	s	u	v	p	T	ρ	h	x_{O_2}	x_O	x_N	x_{NO}	x_{N_2}
						$s = 0$						
1.0000	0	-0.134	0	0.827	0.114	7.253	0.981	0.209	0.0000	0.000000	0.0000	0.780
0.8730	0	-0.106	0	0.853	0.102	8.020	0.988	0.156	0.0686	0.000168	0.0232	0.742
0.7480	0	-0.0857	0	0.870	0.0968	8.530	0.992	0.128	0.101	0.000257	0.0396	0.721
0.6230	0	-0.0676	0	0.882	0.0929	8.910	0.995	0.110	0.121	0.000319	0.0516	0.707
0.4980	0	-0.0514	0	0.890	0.0902	9.205	0.997	0.0976	0.135	0.000361	0.0596	0.697
0.3750	0	-0.0364	0	0.896	0.0880	9.434	0.998	0.0886	0.146	0.000384	0.0638	0.691
0.2500	0	-0.0234	0	0.900	0.0863	9.610	0.999	0.0825	0.156	0.000390	0.0643	0.687
0.1250	0	-0.0110	0	0.902	0.0849	9.749	0.999	0.0784	0.165	0.000353	0.0613	0.685
0.0000	0	0.0000	0	0.903	0.0836	9.851	0.999	0.0742	0.174	-0.00134	0.0559	0.684
						$s = s_1/3$						
1.0000	0.291	-0.121	0.246	0.776	0.107	7.194	0.924	0.209	0.0000	0.0000000	0.0000	0.780
0.8730	0.277	-0.0990	0.223	0.799	0.100	7.733	0.940	0.169	0.0514	0.0000937	0.0168	0.752
0.7480	0.266	-0.0795	0.203	0.814	0.0957	8.153	0.952	0.142	0.0843	0.000167	0.0322	0.731
0.6230	0.257	-0.0640	0.185	0.826	0.0920	8.489	0.961	0.121	0.107	0.000230	0.0453	0.716
0.4980	0.250	-0.0491	0.168	0.834	0.0893	8.759	0.969	0.106	0.124	0.000282	0.0554	0.704
0.3750	0.244	-0.0353	0.152	0.840	0.0871	8.971	0.975	0.0946	0.138	0.000319	0.0616	0.695
0.2500	0.239	-0.0226	0.137	0.843	0.0854	9.131	0.980	0.0864	0.150	0.000336	0.0635	0.689
0.1250	0.236	-0.0107	0.123	0.845	0.0839	9.253	0.984	0.0806	0.162	0.000340	0.0611	0.686
0.0000	0.234	0.0000	0.109	0.845	0.0824	9.358	0.987	0.0769	0.174	0.000418	0.0542	0.685
						$s = 2s_1/3$						
1.0000	0.583	-0.0779	0.464	0.645	0.0920	7.013	0.777	0.209	0.0000	0.0000000	0.00000	0.780
0.8730	0.554	-0.0705	0.424	0.660	0.0930	7.035	0.814	0.195	0.0180	0.0000129	0.00530	0.771
0.7480	0.533	-0.0610	0.389	0.671	0.0916	7.169	0.844	0.175	0.0441	0.0000409	0.0152	0.755
0.6230	0.515	-0.0507	0.357	0.680	0.0892	7.347	0.869	0.152	0.0709	0.0000819	0.0282	0.738
0.4980	0.500	-0.0402	0.326	0.686	0.0867	7.527	0.891	0.130	0.0952	0.000131	0.0419	0.722
0.3750	0.489	-0.0297	0.298	0.690	0.0845	7.697	0.910	0.112	0.116	0.000183	0.0535	0.708
0.2500	0.479	-0.0196	0.271	0.692	0.0826	7.810	0.925	0.0978	0.134	0.000242	0.0602	0.697
0.1250	0.473	-0.00956	0.244	0.692	0.0810	7.891	0.939	0.0873	0.152	0.000245	0.0603	0.691
0.0000	0.469	0.00000	0.219	0.689	0.0794	7.942	0.951	0.0801	0.170	0.000184	0.0526	0.684
						$s = s_1$						
1.0000	0.875	+0.00406	0.631	0.488	0.0727	6.721	0.600	0.209	0.00000	0.00000000	0.00000	0.780
0.8730	0.832	-0.00955	0.581	0.492	0.0786	6.252	0.660	0.206	0.00373	0.00000173	0.00127	0.778
0.7480	0.799	-0.0162	0.540	0.496	0.0825	5.978	0.706	0.201	0.0105	0.00000353	0.00300	0.775
0.6230	0.773	-0.0185	0.502	0.498	0.0835	5.880	0.746	0.186	0.0299	0.0000123	0.00956	0.764
0.4980	0.751	-0.0177	0.465	0.499	0.0823	5.895	0.782	0.163	0.0573	0.0000895	0.0222	0.747
0.3750	0.733	-0.0148	0.428	0.499	0.0801	5.950	0.815	0.138	0.0861	0.000243	0.0384	0.727
0.2500	0.719	-0.0100	0.393	0.497	0.0778	6.027	0.843	0.114	0.113	0.000429	0.0525	0.710
0.1250	0.709	-0.00552	0.359	0.493	0.0758	6.056	0.869	0.0960	0.139	0.000449	0.0586	0.697
0.0000	0.703	0.00000	0.325	0.487	0.0738	6.046	0.892	0.0841	0.165	0.000565	0.0503	0.690

COMBINED (EQUILIBRIUM-NONEQUILIBRIUM FLOW OXYGEN

SCHEME II. N = 3

TABLE 3.17

$M_\infty = 10$, $p_\infty = 0.001$ atm, $T_\infty = 288°K$, $\rho_\infty = 0.001354$ kg/m^3,

$w_{max} = 3307$ m/sec, $h_{00} = 21\,055.3°K$, $\delta = 1$, $R_0 = 1000$ m,

$\varepsilon_0 = 0.07312$, $\varepsilon_1 = 0.07855$, $\varepsilon_2 = 0.09932$, $\varepsilon_3 = 0.1455$

ξ	s	u	v	p	T	ρ	h	C_0
				$s = 0$				
1.0000	0	-0.0890	0	0.872	0.0702	10.965	0.991	0.132
0.8713	0	-0.0745	0	0.885	0.0702	11.111	0.994	0.133
0.7463	0	-0.0614	0	0.895	0.0703	11.223	0.995	0.133
0.6213	0	-0.0492	0	0.902	0.0703	11.308	0.997	0.134
0.4943	0	-0.0376	0	0.908	0.0704	11.372	0.998	0.134
0.3674	0	-0.0268	0	0.912	0.0704	11.416	0.998	0.134
0.2492	0	-0.0175	0	0.914	0.0704	11.443	0.999	0.134
0.1247	0	-0.00840	0	0.916	0.0704	11.458	0.999	0.134
0.0000	0	0.00000	0	0.916	0.0704	11.462	0.999	0.134
				$s = s_1/3$				
1.0000	0.291	-0.0802	0.248	0.814	0.0690	10.561	0.931	0.116
0.8713	0.278	-0.0682	0.223	0.826	0.0693	10.640	0.945	0.119
0.7463	0.268	-0.0569	0.200	0.835	0.0695	10.701	0.955	0.122
0.6213	0.259	-0.0460	0.181	0.842	0.0696	10.746	0.964	0.125
0.4943	0.252	-0.0355	0.163	0.848	0.0698	10.777	0.971	0.127
0.3674	0.247	-0.0256	0.146	0.852	0.0699	10.795	0.977	0.128
0.2492	0.243	-0.0169	0.132	0.854	0.0699	10.801	0.981	0.130
0.1247	0.240	-0.00825	0.118	0.855	0.0700	10.796	0.985	0.131
0.0000	0.238	0.00000	0.105	0.855	0.0701	10.780	0.988	0.132
				$s = 2s_1/3$				
1.0000	0.583	-0.0457	0.461	0.673	0.0658	9.500	0.784	0.0764
0.8713	0.556	-0.0429	0.418	0.681	0.0666	9.399	0.822	0.0867
0.7463	0.536	-0.0383	0.380	0.687	0.0672	9.326	0.852	0.0951
0.6213	0.519	-0.0327	0.346	0.691	0.0677	9.265	0.877	0.102
0.4943	0.505	-0.0262	0.313	0.695	0.0681	9.210	0.899	0.108
0.3674	0.495	-0.0194	0.283	0.698	0.0684	9.158	0.918	0.113
0.2492	0.487	-0.0128	0.257	0.699	0.0686	9.109	0.932	0.117
0.1247	0.481	-0.00599	0.231	0.699	0.0688	9.053	0.945	0.121
0.0000	0.477	0.00000	0.207	0.697	0.0690	8.985	0.956	0.124
				$s = s_1$				
1.0000	0.875	+0.00809	0.631	0.491	0.0611	7.003	0.601	0.0000
0.8713	0.834	+0.00615	0.572	0.497	0.0624	7.586	0.672	0.0494
0.7463	0.804	-0.00210	0.527	0.496	0.0637	7.325	0.722	0.0623
0.6213	0.779	-0.00667	0.485	0.495	0.0646	7.133	0.764	0.0735
0.4943	0.758	-0.00858	0.446	0.494	0.0654	6.974	0.801	0.0836
0.3674	0.742	-0.00837	0.408	0.493	0.0660	6.838	0.833	0.0926
0.2492	0.730	-0.00673	0.375	0.491	0.0664	6.717	0.859	0.0999
0.1247	0.721	-0.00378	0.342	0.487	0.0668	6.590	0.882	0.106
0.0000	0.716	0.00000	0.312	0.481	0.0653	6.591	0.902	0.118

NONEQUILIBRIUM OXYGEN /168

(NONEQUILIBRIUM VIBRATIONS, NONEQUILIBRIUM DISSOCIATIONS).

SCHEME I. N = 2

TABLE 3.18

$M_\infty = 10$, $p_\infty = 0.01$ atm, $T_\infty = 290°K$, $\rho_\infty = 0.01345$ kg/m^3,

$w_{max} = 3328.1$ m/sec, $h_{00} = 21\,315°K$, $\delta = 1$, $R_0 = 0.01$ m

s	ε	σ	$\bar{p}_0$	$\bar{T}_0$
0.0000	0.0997	1.570	1.000	1.000
0.0625	0.100	1.520	0.995	0.998
0.1250	0.101	1.464	0.980	0.994
0.1875	0.102	1.408	0.957	0.989
0.2500	0.104	1.354	0.925	0.981
0.3125	0.107	1.301	0.885	0.971
0.3750	0.110	1.249	0.839	0.959
0.4375	0.114	1.198	0.787	0.944
0.5000	0.119	1.147	0.730	0.927
0.5625	0.125	1.098	0.670	0.907
0.6250	0.132	1.050	0.607	0.884
0.6875	0.140	1.002	0.543	0.858
0.7500	0.149	0.955	0.477	0.829
0.8125	0.160	0.907	0.412	0.795

s	u	v	p	T	c^2	w^2	$-x$	y	C_0	e_0
					$\xi = 0$					
0.0000	0	0.0000	0.895	0.0774	0.124	0.000000	1.000	0.0000	0.119	0.108
0.0625	0	0.0290	0.891	0.0773	0.124	0.000795	0.998	0.0624	0.119	0.108
0.1250	0	0.0579	0.878	0.0770	0.124	0.00336	0.992	0.124	0.119	0.107
0.1875	0	0.0868	0.857	0.0765	0.123	0.00755	0.982	0.186	0.119	0.107
0.2500	0	0.115	0.828	0.0759	0.122	0.0133	0.968	0.247	0.119	0.106
0.3125	0	0.143	0.793	0.0752	0.120	0.0206	0.951	0.307	0.119	0.105
0.3750	0	0.172	0.751	0.0742	0.119	0.0296	0.930	0.366	0.118	0.104
0.4375	0	0.200	0.705	0.0731	0.117	0.0402	0.905	0.423	0.118	0.103
0.5000	0	0.228	0.654	0.0717	0.115	0.0524	0.877	0.479	0.118	0.102
0.5625	0	0.256	0.600	0.0702	0.112	0.0660	0.845	0.533	0.117	0.100
0.6250	0	0.284	0.544	0.0684	0.109	0.0812	0.810	0.585	0.117	0.0993
0.6875	0	0.313	0.486	0.0664	0.106	0.0981	0.772	0.634	0.117	0.0979
0.7500	0	0.341	0.427	0.0641	0.102	0.116	0.731	0.681	0.116	0.0965
0.8125	0	0.370	0.369	0.0616	0.0988	0.137	0.687	0.726	0.116	0.0953

TABLE 3.18 Continued

s	u	v	p	T	c^2	w^2	$-x$	y	C_0	e_0
					$\xi = 0.5$					
0.0000	-0.0634	0.0000	0.880	0.101	0.150	0.00402	1.049	0.0000	0.0490	0.143
0.0625	-0.0627	0.0459	0.876	0.100	0.149	0.00604	1.048	0.0655	0.0490	0.143
0.1250	-0.0618	0.0901	0.864	0.100	0.149	0.0119	1.042	0.130	0.0474	0.143
0.1875	-0.0608	0.134	0.847	0.100	0.148	0.0217	1.032	0.195	0.0453	0.142
0.2500	-0.0596	0.178	0.823	0.0996	0.146	0.0354	1.019	0.260	0.0424	0.142
0.3125	-0.0577	0.222	0.793	0.0988	0.145	0.0526	1.002	0.323	0.0388	0.141
0.3750	-0.0554	0.264	0.758	0.0978	0.142	0.0731	0.982	0.386	0.0347	0.139
0.4375	-0.0523	0.306	0.719	0.0965	0.140	0.0966	0.957	0.448	0.0303	0.138
0.5000	-0.0485	0.346	0.676	0.0950	0.137	0.122	0.930	0.508	0.0257	0.136
0.5625	-0.0438	0.385	0.631	0.0933	0.134	0.150	0.899	0.566	0.0211	0.133
0.6250	-0.0381	0.423	0.584	0.0912	0.130	0.180	0.864	0.623	0.0168	0.131
0.6875	-0.0312	0.459	0.535	0.0888	0.126	0.211	0.827	0.679	0.0128	0.128
0.7500	-0.0231	0.493	0.485	0.0861	0.121	0.244	0.786	0.732	0.00938	0.125
0.8125	-0.0137	0.526	0.434	0.0831	0.117	0.277	0.742	0.784	0.00642	0.121
					$\xi = 1$					
0.0000	-0.170	0.0000	0.792	0.138	0.194	0.0291	1.099	0.0000	0	0.0000466
0.0625	-0.169	0.0509	0.790	0.138	0.193	0.0314	1.098	0.0687	0	0.0000466
0.1250	-0.167	0.106	0.783	0.137	0.192	0.0396	1.092	0.137	0	0.0000466
0.1875	-0.164	0.161	0.771	0.135	0.189	0.0533	1.083	0.205	0	0.0000466
0.2500	-0.160	0.214	0.755	0.132	0.185	0.0717	1.070	0.273	0	0.0000466
0.3125	-0.153	0.266	0.736	0.129	0.181	0.0946	1.053	0.340	0	0.0000466
0.3750	-0.146	0.316	0.713	0.125	0.175	0.121	1.033	0.406	0	0.0000466
0.4375	-0.136	0.364	0.687	0.121	0.169	0.151	1.009	0.472	0	0.0000466
0.5000	-0.125	0.411	0.658	0.116	0.162	0.185	0.982	0.536	0	0.0000466
0.5625	-0.113	0.456	0.628	0.111	0.155	0.220	0.952	0.600	0	0.0000466
0.6250	-0.0990	0.498	0.596	0.105	0.148	0.258	0.918	0.662	0	0.0000466
0.6875	-0.0831	0.538	0.562	0.100	0.140	0.297	0.881	0.723	0	0.0000466
0.7500	-0.0658	0.577	0.527	0.0945	0.132	0.337	0.841	0.783	0	0.0000466
0.8125	-0.0474	0.614	0.491	0.0886	0.124	0.379	0.797	0.842	0	0.0000466

CALCULATION OF FLOW IN SUPERSONIC REGION /170

BY METHOD OF CHARACTERISTICS. NONEQUILIBRIUM OXYGEN.

$M_\infty = 10$, $p_\infty = 0.001$ atm, $T_\infty = 288°K$, $\rho_\infty = 0.00135$ kg/m^3,

$w_{max} = 3236$ m/sec.

TABLE 3.19

Spherical Blunting-Cylinder ($\delta = 1$; $R_0 = 1$ m; $\omega = 0°$)

Distribution of Gas Dynamic Parameters Along Surface of Body

x_0	r_0	p_0	T_0	ρ_0	w_0	ζ_0	$(C_0)_0$
0.286	0.700	0.434	0.0631	6.092	0.351	1.019	0.129
0.309	0.723	0.405	0.0621	5.774	0.365	0.954	0.129
0.353	0.762	0.355	0.0603	5.213	0.389	0.847	0.129
0.395	0.796	0.312	0.0586	4.719	0.410	0.758	0.128
0.470	0.848	0.247	0.0555	3.942	0.446	0.624	0.128
0.558	0.897	0.185	0.0519	3.169	0.483	0.492	0.128
0.652	0.937	0.134	0.0480	2.483	0.519	0.370	0.128
0.751	0.968	0.0949	0.0441	1.908	0.553	0.256	0.128
0.845	0.988	0.0669	0.0404	1.468	0.583	0.156	0.128
0.949	0.998	0.0443	0.0364	1.079	0.612	0.0508	0.128
1.050	1.000	0.0354	0.0344	0.913	0.627	0.0000	0.128
1.176	1.000	0.0343	0.0341	0.891	0.629	0.0000	0.128

Coordinates of Nose Shock Wave

x_B	-0.0840	-0.0539	0.0339	0.174	0.361	0.426	0.518	0.635	0.767	0.890
r_B	0.0000	0.269	0.527	0.769	0.994	1.058	1.141	1.236	1.332	1.413
x_B	0.967	1.059	1.169	1.304	1.474	1.693	1.984	2.389	4.276	6.593
r_B	1.461	1.515	1.577	1.649	1.735	1.837	1.963	2.124	2.744	3.357

TABLE 3.20

Spherical Segment-Cylinder (δ = 1, R_0 = 1 m, χ = 45°50', ω = 0°)

Distribution of Gas Dynamic Parameters Along Surface of Body

x_0	r_0	p_0	T_0	ρ_0	w_0	ζ_0	$(C_0)_0$
0.298	0.696	0.0386	0.0348	0.981	0.621	0	0.129
0.385	0.696	0.0402	0.0352	1.011	0.618	0	0.129
0.476	0.696	0.0403	0.0352	1.013	0.618	0	0.129
0.661	0.696	0.0390	0.0349	0.989	0.620	0	0.129
0.780	0.696	0.0380	0.0347	0.969	0.621	0	0.129
0.924	0.696	0.0367	0.0344	0.944	0.624	0	0.129
1.098	0.696	0.0353	0.0341	0.916	0.626	0	0.129
1.312	0.696	0.0335	0.0337	0.881	0.630	0	0.129
1.621	0.696	0.0313	0.0331	0.836	0.634	0	0.129
2.040	0.696	0.0293	0.0326	0.796	0.637	0	0.129
2.58	0.696	0.0263	0.0318	0.734	0.643	0	0.129
3.47	0.696	0.0219	0.0303	0.639	0.654	0	0.128
5.00	0.696	0.0168	0.0284	0.522	0.667	0	0.128
6.21	0.696	0.0142	0.0273	0.460	0.675	0	0.128
7.88	0.696	0.0119	0.0261	0.404	0.683	0	0.128
10.20	0.696	0.0102	0.0251	0.359	0.689	0	0.128
13.60	0.696	0.00884	0.0243	0.322	0.695	0	0.128
18.93	0.696	0.00766	0.0235	0.289	0.700	0	0.127
28.07	0.696	0.00672	0.0229	0.260	0.705	0	0.127

Coordinates of Nose Shock Wave

x_B	-0.0840	-0.0539	0.0339	0.174	0.361	0.485	0.630	0.884	1.087	1.376	1.801	2.450	3.490
r_B	0.0000	0.269	0.527	0.769	0.994	1.105	1.210	1.360	1.462	1.593	1.762	1.989	2.301

CHAPTER 4

FLOW AROUND SOLIDS OF REVOLUTION WITH DISCONTINUITY OF GENERATRIX OR DISCONTINUITY OF CURVATURE OF THE CONTOUR

Calculation of supersonic flow around bodies with a discontinuity of the /171
generatrix of the contour is of considerable practical importance, since the presence of a sonic discontinuity at a given radius of curvature of blunting lessens heat exchange near the stagnation point. Also of definite interest is an examination of flow around bodies with a discontinuity of curvature of the contour. However, when calculating flow around bodies with a sonic discontinuity, appreciable difficulties arise owing to the appearance of a singularity at the point of discontinuity [6]. A pronounced change of velocity both in magnitude and in direction occurs in the region of mixed flow in the neighborhood of the corner point. In the supersonic zone a "hanging" shock can occur near the side surface of the body in the flow.

The inverse problem of supersonic flow around bodies with a break was examined in the work of R. Vaglio-Laurin [48]. Calculations of flow up to the point of discontinuity were performed by G. F. Telenin's scheme in [49].

In this chapter we will solve the direct problem of supersonic flow around blunt bodies with a sonic break by the method of integral relations. The solution is constructed in the entire region of effect of blunting and is extended by means of the method of characteristics into the supersonic zone.

1. Calculation of Flow Around Solids of Revolution With Discontinuity of Generatrix.

1. Statement of problem. Let a supersonic flow of a ideal gas encounter a symmetric body with a break of the generatrix of the contour situated at a zero angle of attack (Figure 4.1). We will examine the case where a local sonic velocity is reached at the corner point and the body shape behind the discontinuity does not affect the pattern in the region of influence of blunting. In the neighborhood of the discontinuity the flow is described by /172
the asymptotic solution of R. Vaglio-Laurin [6], which at the corner coincides with the Pradtl-Meyer solution.

One of the ways of calculating flow around bodies with a sonic break is to perform the calculations by scheme I of the method of integral relations both before the discontinuity and with supersonic turn around it, where the initial equations are written in a polar coordinate system with the center at the corner point [11]. The second approach involves using scheme II with isolation of the neighborhood of the break where the asymptotic solution is used [24]. Finally, a third way is to replace the corner point by a "curvature" of finite

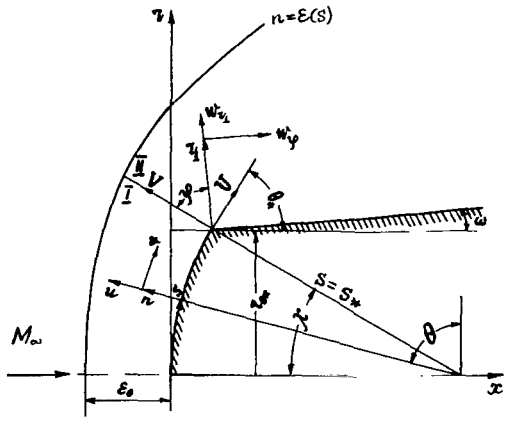

Figure 4.1. Diagram of designations used in flow around body with break of contour generatrix.

radius [19]. Such calculations are a certain approximation of the flow pattern around bodies with a break of the generatrix when the radius of "curvature" becomes sufficiently small.

Let us examine each of these methods separately.

2. Calculation by Scheme I. We will separate the flow field behind the detached shock wave into two regions (I and II) by means of ray $s = s_*$ (Figure 4.1). In region I, as usual, we will use the orthogonal coordinate system s, n and in region II the polar system r_1, ϕ with the center at the corner point. Here the magnitude of the derivative of velocity $w_0' = dw_0/d\phi$ is determined from the relation along the characteristic of the second family (- Mach line), which at the corner point takes the form

$$\frac{\sqrt{M_0^2-1}}{w_0}\,dw_0 + d\beta = 0,$$

where β is the angle of rotation of the velocity vector.

We note that the vector of sonic velocity on the body is situated normal to the ray separating regions I and II. Turn of the flow in the neighborhood of the break follows the angle of rotation of the velocity vector, therefore $v_0 = w_0$ and $d\phi = -d\beta$. As a result of simple transformations we obtain a differential equation for determining the velocity magnitude at the corner point

$$v_0' = v_0\sqrt{(1-v_0^2)\Big/\left(\frac{v_0^2}{c_*^2} - 1\right)}$$

(derivatives with respect to s in region I and with respect to ϕ in region II are denoted by primes).

The problem will be examined in the second approximation. To determine the unknown parameters $\varepsilon(0)$, $u_2(0)$, which enter the approximating system in region I, we use the following conditions at the corner point

$$N_0(s_*) = 0, \quad E_0(s_*) = 0,$$

where $v_0' = E_0/N_0$. The condition $N_0(s_*) = 0$ denotes that a sonic velocity has been reached at the corner point.

We note that the initial system of differential equations is approximated, generally speaking, in regions I and II with a different degree of accuracy. The values of the functions on the boundary ray $s = s_*$, obtained from calculations in region I are not completely exact data for solving in region II. Although the difference of these solutions is small and for practical purposes is insignificant, it cannot help but be taken into account in calculations by various approximating systems. Therefore, the data on ray $s = s_*$ are in need of some correction. To determine the new values of the functions $u_2(s_*)$, $v_2(s_*)$, in region II we use the conditions of regularity of the solution at singular points on the intermediate line and on the shock wave ($E_2 = 0$ when $N_2 = 0$, $E_\sigma = 0$ when $\alpha = 0$, where $v_2' = E_2/N_2$, a $\sigma' = E_\sigma/\alpha$). Thus the flow in the region of turn is approximately set up. As calculations showed, the proposed scheme gives good results.

The asymptotic form of R. Vaglio-Laurin is not used in this solution in the neighborhood of the sonic break and the value of the derivative of velocity at the corner point remains finite, although large in absolute value. Nevertheless, for segmental bodies with angles of half-opening $\chi = 30$-$35°$ there is a sufficiently good agreement of the obtained numerical solution and the asymptotic solution. The indicated range of angles χ can be expanded, if we smooth out the derivatives on approaching the boundary ray $s = s_*$. /174

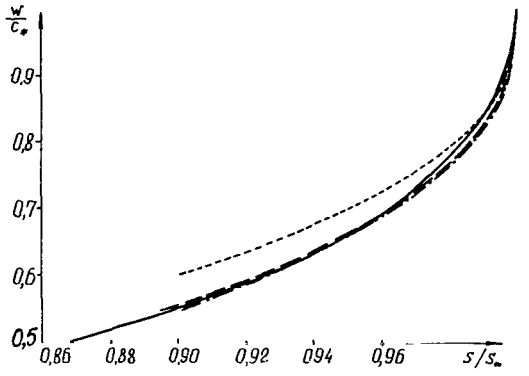

Figure 4.2. Distribution of velocity along surface of axisymmetric body with flat end ($\delta = \infty$; $M_\infty = 5.8$; $\varkappa = 1.4$), obtained from exact solution of R. Vaglio-Laurin and calculated by method of integral relations at different values of w_{fus} ($\Delta w = c_* - w_{fus}$):
- - - - - - - $\Delta w \cong 0.15\ c_*$
— — — $\Delta w \cong 0.30\ c_*$
—· — ·— · $\Delta w \cong 0.40\ c_*$
} solution of R. Vaglio-Laurin
———— method of integral relations

In Figure 4.2 the distribution of velocity (referred to the critical values c_*) along the surface of an axisymmetric body with a flat end (δ = obtained by the method of integral relations (solid line) and by the exact solution of R. Vaglio-Laurin (dashed line) is compared when $M_\infty = 5.8$, $\varkappa = 1.4$. The "fusion" of both solutions occurred in the subsonic region at different velocity values w_{fus} ($\Delta w = c_* - w_{fus}$).

For the solution in the region of influence of blunting to be extended to the supersonic zone, the initial data on the supersonic ray must be known with a high accuracy. After determining the flow in the mixed region the initial data on the supersonic ray are refined by the method of characteristics. For this purpose a triangular region bounded by the supersonic portion of the shock wave and the + Mach and - Mach lines is calculated by the method of characteristics from the shock wave plotted by the method of integral relations. In this case the functions on the ray passing from the corner point through the calculated region are determined. On the segment of the ray between the break and the characteristic triangle, the values of the functions are found by interpolation. In the calculations of the supersonic region the "hanging" shocks are constructed, the origin of which is determined by the point of intersection of the + Mach lines (Figures 4.3-4.7).

Certain results of the calculations are given in Figures 4.3-4.12 and in Tables 4.1-4.10.

In Figures 4.3-4.7 shock waves and "hanging" shocks are constructed for cones with segmental blunting ($\varkappa = 1.4$; $M_\infty = 5.8$; $\chi = 33°$, and also $M_\infty = 4$; 6; $\chi = 30°$) at different angles of half-opening of the cone ($\omega = -5°$; $0°$; $10°$).

In Figures 4.4, 4.6, and 4.7 the solid line corresponds to the case M_∞ = 4 and the dashed line to the case $M_\infty = 6$.

The intensity of the "hanging" shock at first rapidly increases, and then gradually decreases with distance from the blunting. In the calculations the maximal angle of rotation of the flow on passing through the "hanging" shock reaches several degrees. For example, at distance x = 40 (Figure 4.5) the angle of rotation of the flow reaches only 10'. The appearance of the "hanging' shock is explained by overexpansion of the flow as the flow turns around the corner point and by subsequent compression and stagnation near the side surface of the body. In Figure 4.3 the calculated data are compared with the experiment of D. Fraasa [50] (dots), and we see that the results agree. We note that the initial data on the supersonic ray obtained with a high degree of accuracy permitted calculating flow around long bodies at a distance of tens of diameters of blunting (Figure 4.5).

Figures 4.8 and 4.9 show the change of the boundaries of the zone of turn of the flow for different adiabatic exponents ($M_\infty = \infty$; $\delta = 1$; $\chi = 50°$; $\omega = 0°$ - Figure 4.8) and different angles of half-opening of the spherical segment ($M_\infty = 4$; $\varkappa = 1.4$; $\delta = 1$; $\omega = 0°$ - Figure 4.9). These figures show the plotted characteristics limiting the region of influence of blunting and the

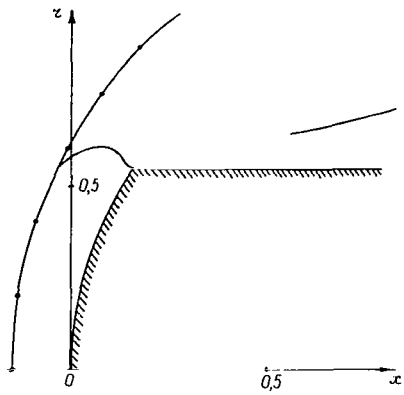

Figure 4.3. Flow pattern around body "spherical segment-cylinder" (M_∞ = 5.8; $\varkappa$ = 1.4; δ = 1; χ = 33°): _____, calculation by method of integral relations; · · ·, experiment of D. Fraasa [50].

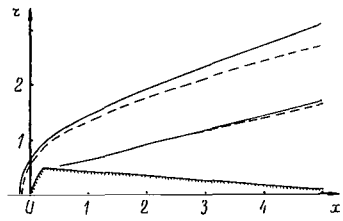

Figure 4.4. Position of nose shock wave and "hanging" shock in flow around cone with segmental blunting ($\varkappa$ = 1.4; δ = 1; χ = 30°; ω = -5°): _____ M_∞ = 4; ---- M_∞ = 6.

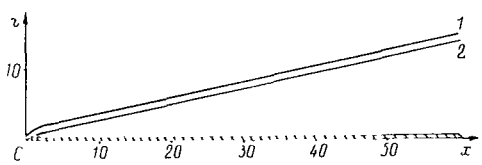

Figure 4.5. Position of nose shock wave and "hanging" shock in flow around cylinder with segmental blunting (M_∞ = 5.8; $\varkappa$ = 1.4; δ = 1; χ = 33°; ω = 0°): 1) Nose shock wave; 2) "hanging" shock.

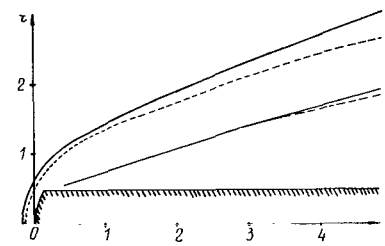

Figure 4.6. Position of nose shock wave and "hanging" shock in flow around cylinder with segmental blunting ($\varkappa$ = 1.4; δ = 1; χ = 30°; ω = 0°): _____ M_∞ = 4; ---- M_∞ = 6.

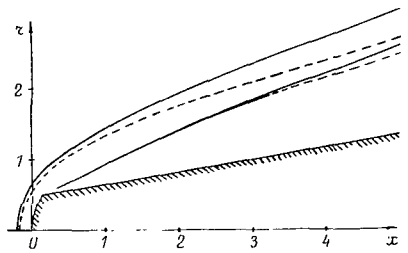

Figure 4.7. Position of nose shock wave and "hanging" shock in flow around cone with segmental blunting ($\varkappa$ = 1.4; δ = 1; χ = 30°; ω = 10°): ——— M_∞ = 4; ---- M_∞ = 6.

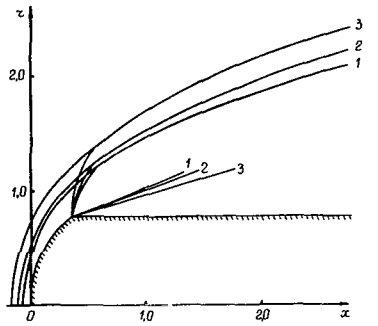

Figure 4.8. Change of boundaries of zone of turn in flow around a cylinder with segmental blunting (supersonic discontinuity) at different values of $\varkappa$ (M_∞ = ∞, χ = 50°): 1 - $\varkappa$ = 1.29; 2 - $\varkappa$ = 1.4; 3 - $\varkappa$ = 1.66 ...

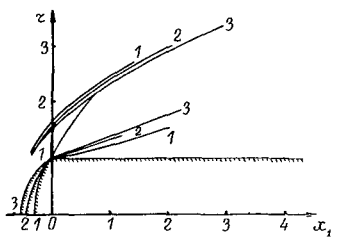

Figure 4.9. Change of boundaries of zone of turn in flow around cylinder with segmental blunting at various angles of half-opening of segment (M_∞ = 4; $\varkappa$ = 1.4; δ = 1): 1 - χ = 30° ; 2 - χ = 45°; 3 - χ = 55°.

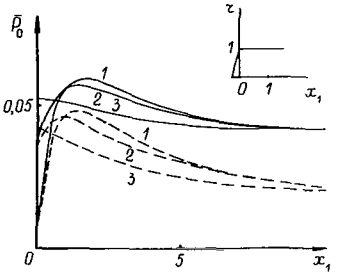

Figure 4.10. Distribution of pressure on side surface of cylinder with segmental blunting at different angles of half-opening of segment ($\varkappa$ = 1.4): 1 - χ = 30°; 2 - χ = 45°; 3 - χ = 90°; ——— M_∞ = 4, --- M_∞ = 6.

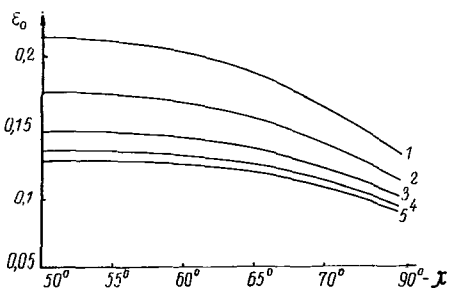

Figure 4.11. Magnitude of separation of shock wave on axis of symmetry $\varepsilon(0)$ from spherical segment in relation to angle of half-opening ($\varkappa$ = 1.4; δ = 1): 1 - M_∞ = 3; 2 - M_∞ = 4; 3 - M_∞ = 6; 4 - M_∞ = 10; 5 - M_∞ = ∞

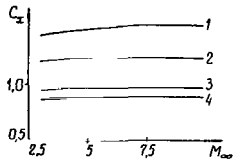

Figure 4.12. Dependence of wave drag coefficient C_x of spherical segments on M_∞ number ($\varkappa = 1.4$; $\delta = 1$): 1 - $\chi = 30°$; 2 - $\chi = 50°$; 3 - $\chi = 70°$; 4 - $\chi = 90°$.

discontinuity. In Figure 4.8, curve 1 corresponds to data for $\varkappa = 1.29$, curve 2 for $\varkappa = 1.4$, curve 3 for $\varkappa = 1.66$ ..... In Figure 4.9, curve 1 corresponds to the value $\chi = 30°$, curve 2 to $\chi = 45°$, and curve 3 to $\chi = 55°$. The linear dimensions here are referred to the ordinate of the point of discontinuity. /178

In Figure 4.10 when $M_\infty = 4$ (solid line) and $M_\infty = 6$ (dashed line) we show the distribution of pressure on the side surface of the cylinder with segmental blunting at different angles of half-opening of the spherical segment ($\varkappa = 1.4$; $\delta = 1$; $\omega = 0°$). Curve 1 pertains to the case when $\chi = 30°$, curve 2 when $\chi = 45°$, and curve 3 when $\chi = 90°$.

Figure 4.11 illustrates the law of change of the magnitude of separation $\varepsilon(0)$ of the shock wave from the body along the axis of symmetry at different positions of the sonic discontinuity. The case $\varkappa = 1.4$, $\delta = 1$ when $M_\infty = 3$ (curve 1), = 4 (curve 2), = 6 (curve 3), = 10 (curve 4), = ∞ (curve 5) is examined.

Figure 4.12 shows the dependence of the wave drag coefficient C_x of spherical segments ($\varkappa = 1.4$, $\delta = 1$) on the M_∞ number at the following values of the angle of half-opening: $\chi = 30°$ (curve 1), = 50° (curve 2), = 70° (curve 3), and = 90° (curve 4).

Table 4.1 gives the values of the gas dynamic quantities in the region of influence of blunting having the shape of a spherical segment. The calculations were performed by scheme I of the method of integral relations in the second approximation (N = 2) when $\varkappa = 1.4$. Flow around a spherical segment with an angle of half-opening of $\chi = 30°$ was examined at Mach numbers of the oncoming flow $M_\infty = 3$, 4, 6, and 10. The values of total velocity w, local Mach number M, pressure $\bar{p} = p(\xi,s)/p_0(0)$, temperature $\bar{T} = T(\xi,s)/T_0(0)$, density $\bar{\rho} = \rho(\xi,s)/\rho_0(0)$, where $p_0(0)$, $T_0(0)$, and $\rho_0(0)$ are values of the corresponding quantities at the stagnation point, are given in relation to s at values of $\xi = n/\varepsilon(s) = 0$ (body), 0.25, 0.50, 0.75, and 1 (shock wave). Cylindrical coordinates of points ξ, s are denoted by x, r (Figure 4.1).

Tables 4.2-4.10 give the distribution of the quantities $\bar{p}_0$, $\bar{T}_0$, $\bar{\rho}_0$, w_0, and M_0 along the side surface of the body in the supersonic region. The calculations were performed by the method of characteristics for the following values of the angle of half-opening of the spherical segments χ, of the angle of half-opening of the cone ω, and Mach number M_∞ (Figure 4.1):

$\chi = 30°$; $M_\infty = 4$; 6; $\omega = -5°$; 0°; 5°; 10° (Tables 4.2 - 4.9);
$\chi = 33°$; $M_\infty = 5.8$; $\omega = 0°$ (Table 4.10).

Furthermore, these tables give the coordinates x, r and the tangent of the angle of inclination, tan σ, of the "hanging" shock and also the values of certain quantities before the shock (designated by the index -) and after the shock (index +): ζ is the tangent of the angle of inclination of the velocity vector; S is entropy; $\beta_+ = \sqrt{M^2 - 1}$. /1

Tables 4.3, 4.7, and 4.10 also give the coordinates of the nose shock wave x_B, r_B.

For other cases examined here ($\omega \neq 0°$), in the region before the point of intersection of the nose shock wave and the "hanging" shock the position and shape of the shock wave coincide with the data, when $\omega = 0°$ for the corresponding values of the Mach numbers of the oncoming flow.

It is necessary to bear in mind that the values of velocity are referred to w_{max}, of pressure to $\rho_\infty w_{max}^2$, of density to ρ_∞, of temperature to $\mu_\infty w_{max}^2/R$, of enthalpy to w_{max}^2 and of entropy to $R/2\mu_\infty$. All linear dimensions are referred to the radius of curvature of the body R_0 at the critical point. The index ∞ denotes parameters of an undisturbed flow.

3. Calculation by Scheme II. As was already noted in the first chapter, scheme II of the method of integral relations was used also for calculating flow around bodies with a sonic discontinuity. In this case the asymptotic calculations, were examined in the neighborhood of the point of discontinuity (region G, Figure 4.13). Outside this region we used the algorithm of scheme II in the usual form, the additional conditions of "fusion" of both solutions made the problem single-valued.

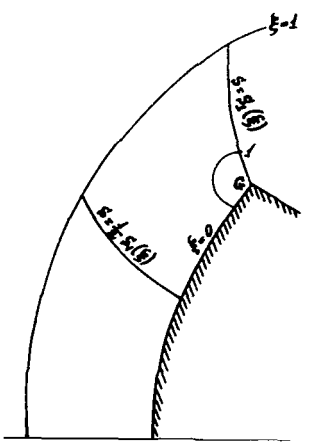

Figure 4.13. Diagram of separation of integration range when calculating flow around body with discontinuity of contour generatrix by the method of integral relations.

Let us first examine near-sonic flow in the neighborhood of G of the corner point. The solution has the form of a power series of distance $\bar{n}$ on the surface of the body ($\bar{n} = 0$) with coefficients depending upon the corresponding self-similar variable ζ

$$U/c_* = 1+(\varkappa+1)^{-1/3}\sum_{i=0}^{\infty}\bar{n}^{\frac{2+i}{4}}\tilde{u}_i(\zeta);\quad V/c_* = \sum_{i=0}^{\infty}\bar{n}^{\frac{3+i}{4}}\tilde{v}_i(\zeta), \tag{4.1}$$

where

$$\zeta = (\varkappa+1)^{-1/3}\bar{s}\bar{n}^{-5/4},\quad \bar{s} = (s-s_*)/r_{0*},\quad \bar{n} = n/r_{0*}. \qquad /180$$

The principal term of expansion (4.1) corresponding to two-dimensional potential flow in the neighborhood of the discontinuity has coefficients of the form (derivatives with respect to ζ are denoted by primes)

$$\tilde{u}_0 = g',\quad \tilde{v}_0 = (7g-5\zeta g')/4, \tag{4.2}$$

where

$$g'' = B_1(21g-25\zeta g')/16,\quad 1/B_1 = g'-\frac{25}{16}\zeta^2.$$

As follows from [51], the function g can be expressed in a parametric form in the following manner (C is the scale constant)

$$g = (25/42)\cdot 5^{-1/8}(5x^2+5x-4)(1-x)^{-7/8}(1+\tfrac{3}{5}x)^{-9/8}C^{-3};$$

$$\zeta = -2\cdot 5^{-3/8}x(1-x)^{-5/8}(1+\tfrac{3}{5}x)^{-3/8}C,\quad -\tfrac{5}{3} < x < 1.$$

If C = 1, then g'(1) = 0, and $g \sim (125/56)\cdot 2^{-1/5}(-\zeta)^{7/5}$ when $\zeta \to -\infty$, $\sim\zeta^3/3 - (675/96)\cdot 10^{-1/3}\zeta^{1/3}$ when $\zeta \to \infty$. The higher order terms of expansion (4.1) take into account the axisymmetric and eddy character of the flow. The system of differential equations for determining the coefficients of the terms up to third order inclusively is as follows

$$\left.\begin{aligned}
&\frac{d\tilde{u}_1}{d\zeta} = B_1[\tilde{v}_1 + \nu\sin\theta_* - \tilde{u}_1(\tilde{u}_0+\tfrac{15}{16}\zeta)];\\
&\frac{d\tilde{v}_1}{d\zeta} = \tfrac{1}{4}B_1[\tilde{u}_1(3\tilde{u}_0+5\zeta\tilde{u}_0')-5\zeta(\tilde{v}_1+\nu\sin\theta_*)];\\
&\frac{d\tilde{u}_2}{d\zeta} = B_1\{\tfrac{5}{4}\zeta[\nu K(\varkappa+1)^{1/3}-\tilde{u}_2]-B_2\};\\
&\frac{d\tilde{v}_2}{d\zeta} = B_1\{\tfrac{5}{4}\zeta B_2-\tilde{u}_0[\nu K(\varkappa+1)^{1/3}-\tilde{u}_2]\};\\
&\frac{d\tilde{u}_3}{d\zeta} = -B_1(B_3+\tfrac{25}{16}\zeta\tilde{u}_3);\quad \frac{d\tilde{v}_3}{d\zeta} = \tfrac{5}{4}B_1(\tilde{u}_0\tilde{u}_3+\zeta B_3),
\end{aligned}\right\} \tag{4.3}$$

where

$$B_2 = -\frac{5}{4}\tilde{v}_2 + \tilde{u}_0'\tilde{u}_2 + \tilde{u}_1'\tilde{u}_1 + (\varkappa+1)^{-1/3}\left\{\frac{3\varkappa-1}{4}\tilde{u}_0\tilde{v}_0 + \frac{1}{2}\tilde{u}_0^2\tilde{u}_0' + \right.$$

$$\left. + \tilde{v}_0\tilde{v}_0' - \frac{5}{4}\zeta[(\varkappa-1)\tilde{u}_0\tilde{v}_0' + \tilde{u}_0'\tilde{v}_0]\right\};$$

$$B_3 = -\frac{3}{2}\tilde{v}_3 + \tilde{u}_0'\tilde{u}_3 + \tilde{u}_1'\tilde{u}_2 + \tilde{u}_1\tilde{u}_2' + (\varkappa+1)^{-1/3}\left\{\frac{2\varkappa-1}{2}\tilde{u}_0\tilde{v}_1 + \frac{3}{4}\varkappa\tilde{u}_1\tilde{v}_0 + \right.$$

$$+ \frac{1}{2}\tilde{u}_0^2\tilde{u}_1' + \tilde{u}_0\tilde{u}_1\tilde{u}_0' + \tilde{v}_0'\tilde{v}_1 + \tilde{v}_0\tilde{v}_1' + \nu(\varkappa-2)\tilde{u}_0\sin\theta_* -$$

$$\left. - \frac{5}{4}\zeta[\tilde{v}_0\tilde{u}_1' + \tilde{u}_0'\tilde{v}_1 + (\varkappa-1)(\tilde{u}_0\tilde{v}_1' + \tilde{u}_1\tilde{v}_0')]\right\};$$

$$K = \frac{\rho_* w_* a r_{0*}(\varkappa+1)}{\varkappa-1}\left(\frac{\partial^2 v}{\partial r^2}\right)_{\xi=1}^{r=0}\left[\frac{2}{(\varkappa+1)^2 - (\varkappa-1)^2 a} - \frac{a-1}{2a}\right];$$

$$a = 1 + \frac{2}{\varkappa-1}M_\infty^{-2}.$$

The functions $\tilde{u}_i$, $\tilde{v}_i$ should satisfy the boundary conditions both in the subsonic region (zero equality of the normal component of velocity on the surface of the body) and in the supersonic zone, where the solution describes a flow of the Pradtl-Meyer type. In the first-order terms of the expansion (4.1) the coefficients are equal to $\tilde{u}_1 = 0$, $\tilde{v}_1 = -\nu \sin\theta_*$. Furthermore, in the plane case ($\nu = 0$) $\tilde{u}_3 = 0$, $\tilde{v}_3 = 0$.

The solution of (4.1) holds true in the supersonic region only at small angles ϕ of rotation of the flow (Figure 4.1). For example, when $\phi \to \pi/2$ the functions $\bar{n}^{\frac{2+i}{4}}\tilde{u}_i$, $\bar{n}^{\frac{3+i}{4}}\tilde{v}_i$ increase infinitely in absolute value, and the entire solution of (4.1) loses meaning. Let us examine the extension of this solution into the purely supersonic region, which is valid at finite values of angle ϕ.

We will seek this solution in the form

$$\left.\begin{aligned}\frac{w_{r_1}}{c_*} &= \frac{1}{c_*}\sin c_*\varphi + f_1^{(0)}r_1^{\alpha_1} + f_1^{(1)}r_1^{\alpha_2} + f_1^{(2)}r_1^{\alpha_3} + \ldots;\\ \frac{w_\varphi}{c_*} &= \cos c_*\varphi + f_2^{(0)}r_1^{\beta_1} + f_2^{(1)}r_1^{\beta_2} + f_2^{(2)}r_1^{\beta_3} + \ldots.\end{aligned}\right\} \qquad (4.4)$$

The principal term represents the Prandtl-Meyer solution, and the terms containing r_1 are corrections to it. In the case of a supersonic discontinuity the corrections for the potential axisymmetric flow are written out in work [52].

We will find the corrections for the case of a sonic discontinuity. The indexes on r_1 are determined here from the condition of "fusion" of the given

lution with the solution of R. Vaglio-Laurin:

$$\alpha_1 = \beta_1 = \frac{2}{3}; \quad \alpha_2 = \beta_2 = 1; \quad \alpha_3 = \beta_3 = 10/9.$$

e functions $f_i^{(j)}$ are expressed in the following manner:

$$f_1^{(0)} = C_1(\sin c_*\varphi)^{1/3}(\cos c_*\varphi)^{2/3};$$

$$f_2^{(0)} = \frac{C_1 c_*}{10(\varkappa-1)}[(5\varkappa-3)\cos 2c_*\varphi - 3\varkappa+1](\sin 2c_*\varphi)^{-2/3}(\cos c_*\varphi)^{\frac{\varkappa+1}{3(\varkappa-1)}};$$

$$f_1^{(1)} = \Lambda(\sin c_*\varphi)^{1/3}(\cos c_*\varphi)^{\frac{3\varkappa-1}{2(\varkappa-1)}};$$

$$f_2^{(1)} = \frac{1}{4}\bar{K} - \frac{c_*}{2\sin c_*\varphi}\frac{\varkappa-(2\varkappa-1)\cos 2c_*\varphi}{\varkappa-1}f_1^{(1)} +$$

$$+ \frac{\nu}{16\sin 2c_*\varphi}\{(1+3c_*)\sin[\theta_* - (1-c_*)\varphi] - (1-3c_*)\sin[\theta_* - (1+c_*)\varphi] +$$

$$+ (1+c_*)\sin[\theta_* + (3c_*-1)\varphi] - (1-c_*)\sin[\theta_* - (1+3c_*)\varphi]\};$$

$$f_1^{(2)} = C_3(\sin c_*\varphi)^{5/3}(\cos c_*\varphi)^{\frac{2}{9}\frac{7\varkappa-2}{\varkappa-1}};$$

$$f_2^{(2)} = \frac{C_3 c_*}{38(\varkappa-1)}[(19\varkappa-9)\cos 2c_*\varphi - 9\varkappa-1](\sin c_*\varphi)^{-4/3}(\cos c_*\varphi)^{\frac{5}{9}\frac{\varkappa+1}{\varkappa-1}};$$

$$\Lambda = C_2 - \frac{\nu K}{2}\left(\frac{2}{\varkappa+1}\right)^{1/(\varkappa-1)}\int_0^{\varphi}(\sin c_*\varphi)^{-1/2}(\cos c_*\varphi)^{\frac{\varkappa+1}{2(\varkappa-1)}}d\varphi +$$

$$+ \frac{\nu}{16}\int_{\varphi_0(C_2)}^{\varphi}\{(1+3c_*)\sin[\theta_* - (1-c_*)\varphi] + (3c_*-1)\sin[\theta_* - (1+c_*)\varphi] +$$

$$+ (1+c_*)\sin[\theta_* - (1-3c_*)\varphi] - (1-c_*)\sin[\theta_* - (1+3c_*)\varphi]\}(\sin c_*\varphi)^{-3/2}\times$$

$$\times(\cos c_*\varphi)^{-\frac{5\varkappa-3}{2(\varkappa-1)}}d\varphi;$$

$$\bar{K} = \nu K\left(\frac{2}{\varkappa+1}\right)^{1/(\varkappa-1)}(\cos c_*\varphi)^{2\varkappa/(\varkappa-1)},$$

re the constants C_1, C_2, and C_3 are also found from the condition of "fusion" /183
h the solution of R. Vaglio-Laurin. The obtained solution has a singularity
n $\phi = 0$.

Expansions (4.1) and (4.4) permit finding all parameters of the flow in the neighborhood of G of the sonic discontinuity with an accuracy up to the scale constant.

The approximating system of scheme II of the method of integral relations contains N + 1 unknown parameters ε_i, i = 0, 1, 2, ... N, where ε_i are in the values of the magnitude of detachment of the shock wave on the i-th line of separation. Furthermore, solution (4.1) includes an additional unknown parameter C, the scale constant. Thus, we have in all N + 2 unknown parameters which are determined from N boundary conditions on the body ($\tilde{u}_i = 0$, i = 0, 2, 3, ..., N) and two conditions of "fusion" for the velocity components u and v (Figure 4.13) at point 1 of the intersection of the boundary of region G with the boundary characteristic.

The order of calculation is as follows. When $\xi = 1$, the initial values of all unknown functions are determined from the conditions on the shock wave, after which the approximating system is integrated by the usual method up to point 1, where $\xi = \xi_0$. When $0 < \xi < \xi_0$, the approximating system is integrated simultaneously with equations (4.1)-(4.4) which describe near-sonic flow in the neighborhood of the discontinuity.

To determine the unknown parameters we used the method of steepest descent, and the accuracy of the solution of the boundary-value problem is determined by the value of the maximal permissible error

$$\{(u_0^2+u_2^2+\ldots+u_N^2)_{\xi=0}+[(u_1-u_{1v})^2+(v_1-v_{1v})^2]_{\xi=\xi_0}\}^{1/2}<\delta,$$

where u_{1v}, v_{1v} are the values of the velocity components at point 1 found by formulas (4.1).

We will present certain results of calculations carried out by the above-described scheme ($M_\infty = 10$, $\varkappa = 1.4$).

Figure 4.14, a,b, shows the shape of the shock wave generated upon flow around spherical segments with angles of half-opening $\chi = 43°30'$ (case 1) and 33° (case 2). The distribution of the velocity components u and v across the shock layer on the axis of symmetry s = 0, on the intermediate line s = 1/2 $s_1(\xi)$ and on the boundary characteristic $s = s_1(\xi)$ is given for the same bodies in Figures 4.15-4.17 and in Table 4.11. We see that the behavior of the quantity u on the boundary characteristic depends strongly on the angle of half-opening of the segment (Figures 4.15 and 4.16).

As the calculations show, an increase of the angle of half-opening of the segment leads to an increase of the scale constant C entering the solution of (4.1). When the angle of half-opening of the segment corresponds to the position of the sonic point on the sphere, the scale constant becomes infinite

and the principal term of expansion (4.1) degenerates to the Prandtl-Meyer solution.

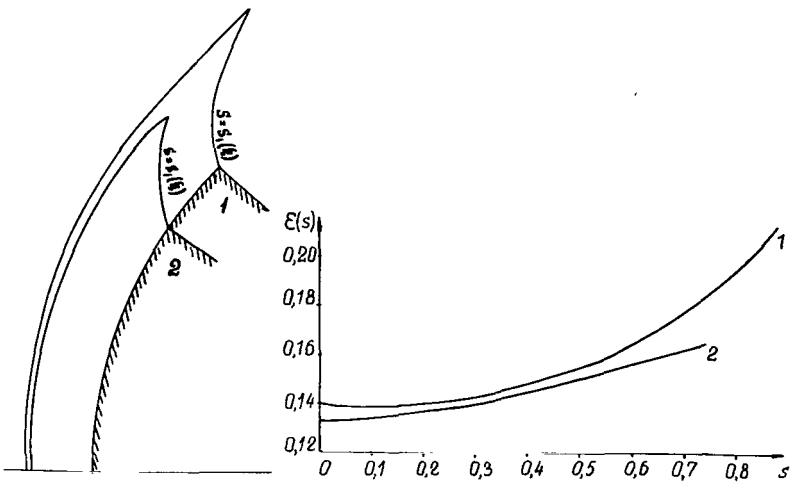

a b

Figure 4.14. Shock waves and boundary characteristics for flow around spherical segments with angles of half-opening $\chi = 43°30'$ and 33° ($M_\infty = 10$; $\varkappa = 1.4$; $\delta = 1$): a) position of shock wave and boundary characteristic; b) magnitude of separation of shock wave from surface of body; 1) $\chi = 43°30'$; 2) $\chi = 33°$.

Calculations were carried out in the second approximation (N = 2). An investigation of the algorithm of scheme II shows that the maximal error occurs on the boundary characteristic and does not exceed 2 percent here. The error of the calculations on the axis and midline is about 0.5 percent. We note that at the point of "fusion" of the two solutions the velocity components undergo a small discontinuity.

Two terms (zero and first order) in solution (4.1) were used to construct flow in the neighborhood of the discontinuity. Calculations showed that the effect of the higher order terms is negligible.

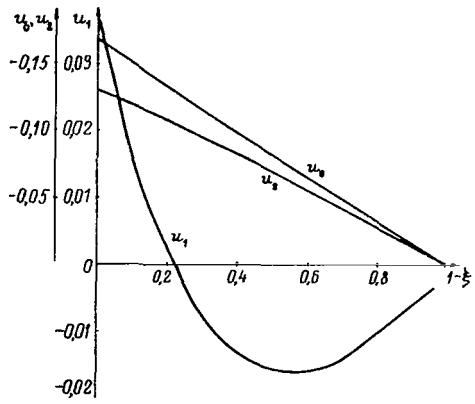

Figure 4.15. Distribution of normal velocity component along axis of symmetry (u_0), boundary characteristic (u_1), and intermediate line (u_2) (flow around spherical segment: $M_\infty = 10$; $\varkappa = 1.4$; $\delta = 1$; $\varkappa = 43°30'$).

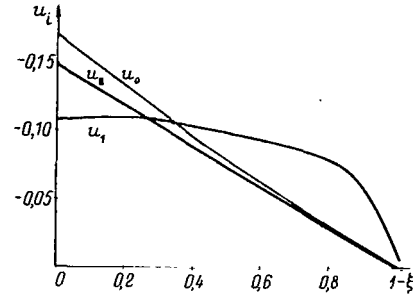

Figure 4.16. Distribution of normal velocity component along axis of symmetry (u_0), boundary characteristic (u_1), and intermediate line (u_2) (flow around spherical segment: $M_\infty = 10$; $\varkappa = 1.4$; $\delta = 1$; $\chi = 33°$).

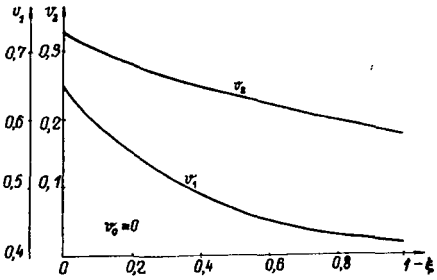

Figure 4.17. Distribution of tangential velocity component along boundary characteristic (v_1) and intermediate line (v_2).

2. Calculation of Flow Around Bodies With Discontinuity of Contour Curvature (Scheme I).

The approximating system of equations describing flow around bodies with a discontinuity of curvature of contour is completely analogous to the case for smooth bodies. However, at small values of the radius of "curvature" certain derivatives can have a discontinuity on the ray passing through the point of discontinuity of curvature. To extend the solution we must perform continuous smoothing of the derivatives.

We will present the technique of calculating bodies with a discontinuity of curvature. The values of $s_{\bar{r}}$ and $\bar{r}$, where $s_{\bar{r}}$ is the coordinate (length of arc) of the point of discontinuity and $\bar{r}$ is the dimensionless radius of "curvature" referred to the radius of the midsection, are given. Calculation

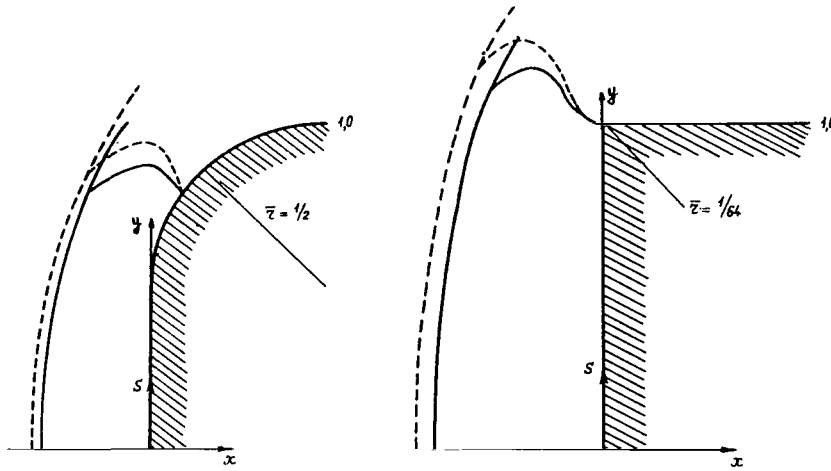

Figure 4.18. Shape of shock wave and sonic line in flow around a body with discontinuity of contour curvature (M_∞ = 5.8): ——— equilibrium air (p_∞ = 1 atm; T_∞ = 300°K); ---- ideal gas ($\varkappa$ = 1.4).

from s = 0 (axis of symmetry) to s = $s_{\bar{r}}$ is performed in the usual manner, and when s = $s_{\bar{r}}$ the equation of the body changes. The conditions of adjusting the parameters remain as before. Figures 4.18-4.21 and Tables 4.12-4.15 give the flow pattern and distribution of gas dynamic parameters in the region between the shock wave and the body when $1/\bar{r}$ = 2 and 64.

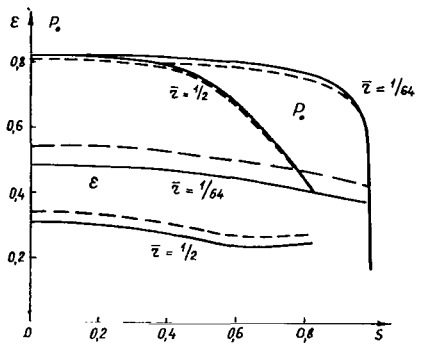

Figure 4.19. Distribution of pressure and magnitude of separation of shock wave upon flow around body with discontinuity of curvature M_∞ = 5.8 ; $1/\bar{r}$ = 2; 64): ——— equilibrium air (p_∞ = 1 atm; T_∞ = 300°K); ---- ideal gas ($\varkappa$ = 1.4).

/187

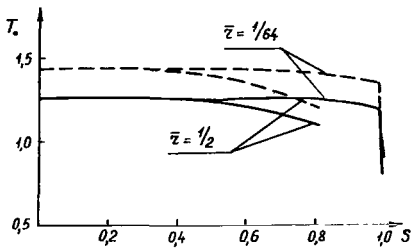

Figure 4.20. Distribution of temperature along surface for flow around body with discontinuity of curvature (M_∞ = 5.8 ; $1/\bar{r}$ = 2; 64): ——— equilibrium air (p_∞ = 1 atm; T_∞ = 300°K); ---- ideal gas ($\varkappa$ = 1.4).

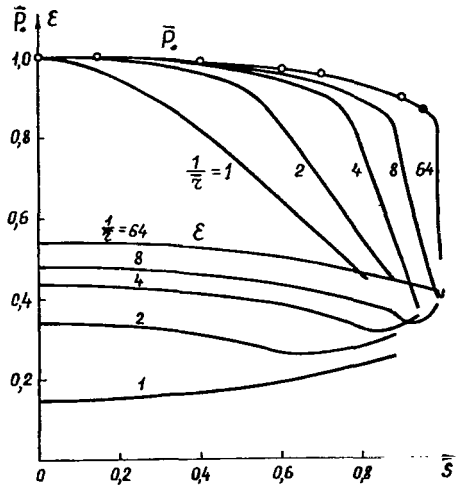

Figure 4.21. Distribution of pressure and magnitude of separation of shock wave for flow of ideal gas around body with discontinuity of curvature (M_∞ = 5.8; $\varkappa$ = 1.4; $1/\bar{r}$ = 2,4,8, and 64): ••• experiment of Fraasa [53].

Figure 4.18 shows the position of the shock wave and sonic line for flow of an ideal gas ($\varkappa$ = 1.4, dashed line) and equilibrium dissociating air (p_∞ = 1 atm; T_∞ = 300°K, solid line) around a body (M_∞ = 5.8). We note the unique form of the sonic line when $1/\bar{r}$ = 64, which is due to intense turning of the flow in the neighborhood of the sonic point. Figures 4.19 and 4.20 show the distribution of pressure and temperature along the surface of the body, and Figure 4.21 shows the dependence $p_0(s)$ and $\varepsilon_0(s)$ when $1/\bar{r}$ = 1-64. The corresponding experimental values taken from the work of D. Fraasa [sic! - Trans., 53] are also plotted here.

Tables 4.12 and 4.13 give the gas dynamic quantities of a body (ξ = 0), on the wave (ξ = 1), and on the intermediate line (ξ = 0.5) for flow of an ideal gas around a body (M_∞ = 5.8; $\varkappa$ = 1.4; $1/\bar{r}$ = 2 and 64).

Tables 4.14 and 4.15 give the vaules of the gas dynamic quantities in the case of flow of equilibrium dissociating air around bodies (M_∞ = 5.8; p_∞ = 1 atm; T_∞ = 300°K, $1/\bar{r}$ = 2 and 64).

CALCULATION OF FLOW IN THE REGION OF INFLUENCE OF BLUNTING /189

SCHEME I. N = 2

TABLE 4.1

Ideal Gas; $\varkappa = 1.4$.

Spherical Segment with a Sonic Discontinuity; $\delta = 1$; $\chi = 30°$

ξ	s	x	r	$\bar{p}$	$\bar{T}$	$\bar{\rho}$	w	M
				$M_\infty = 3$				
0.00	0.000	0.0000	0.000	1.000	1.000	1.000	0.0000	0.000
0.00	0.125	0.00780	0.124	0.981	0.994	0.987	0.0723	0.162
0.00	0.250	0.0311	0.247	0.927	0.978	0.947	0.146	0.330
0.00	0.375	0.0695	0.366	0.832	0.949	0.877	0.225	0.518
0.00	0.500	0.122	0.479	0.647	0.883	0.733	0.341	0.812
0.25	0.000	-0.0500	0.000	0.989	0.997	0.992	0.0542	0.121
0.25	0.125	-0.0422	0.131	0.973	0.991	0.981	0.0925	0.207
0.25	0.250	-0.0189	0.260	0.924	0.974	0.948	0.160	0.362
0.25	0.375	+0.0195	0.385	0.839	0.944	0.889	0.236	0.543
0.25	0.500	+0.0730	0.506	0.689	0.888	0.776	0.334	0.793
0.50	0.000	-0.100	0.000	0.960	0.988	0.971	0.106	0.240
0.50	0.125	-0.0922	0.137	0.946	0.982	0.963	0.131	0.297
0.50	0.250	-0.0690	0.272	0.903	0.964	0.937	0.188	0.428
0.50	0.375	-0.0303	0.405	0.831	0.933	0.890	0.258	0.597
0.50	0.500	+0.0235	0.533	0.714	0.883	0.808	0.342	0.813
0.75	0.000	-0.150	0.000	0.915	0.975	0.939	0.158	0.358
0.75	0.125	-0.142	0.143	0.903	0.968	0.933	0.177	0.402
0.75	0.250	-0.119	0.285	0.868	0.949	0.914	0.224	0.515
0.75	0.375	-0.0803	0.425	0.808	0.917	0.881	0.287	0.670
0.75	0.500	-0.0259	0.560	0.721	0.870	0.828	0.360	0.864
1.00	0.000	-0.200	0.000	0.856	0.956	0.895	0.207	0.475
1.00	0.125	-0.192	0.149	0.847	0.950	0.892	0.223	0.512
1.00	0.250	-0.169	0.298	0.820	0.930	0.881	0.264	0.612
1.00	0.375	-0.130	0.444	0.774	0.897	0.863	0.320	0.757
1.00	0.500	-0.0754	0.587	0.710	0.850	0.835	0.386	0.936
				$M_\infty = 4$				
0.00	0.000	0.00000	0.000	1.000	1.000	1.000	0.0000	0.000
0.00	0.125	0.00780	0.124	0.981	0.994	0.986	0.0730	0.163
0.00	0.250	0.0310	0.247	0.926	0.978	0.946	0.147	0.332
0.00	0.375	0.0694	0.366	0.833	0.949	0.877	0.225	0.516
0.00	0.500	0.122	0.479	0.655	0.886	0.739	0.337	0.800

TABLE 4.1 Continued

/19C

ξ	s	x	r	$\bar{p}$	$\bar{T}$	$\bar{\rho}$	w	M
0.25	0.000	-0.0420	0.000	0.992	0.997	0.994	0.0475	0.106
0.25	0.125	-0.0342	0.129	0.975	0.991	0.984	0.0910	0.204
0.25	0.250	-0.0109	0.258	0.925	0.973	0.950	0.162	0.369
0.25	0.375	+0.0274	0.382	0.840	0.942	0.892	0.240	0.554
0.25	0.500	+0.0807	0.502	0.691	0.885	0.781	0.339	0.805
0.50	0.000	-0.0840	0.000	0.968	0.990	0.977	0.0952	0.213
0.50	0.125	-0.0762	0.135	0.953	0.984	0.969	0.125	0.283
0.50	0.250	-0.0530	0.268	0.909	0.963	0.943	0.189	0.432
0.50	0.375	-0.0145	0.399	0.835	0.929	0.898	0.265	0.614
0.50	0.500	+0.0390	0.524	0.716	0.875	0.818	0.352	0.843
0.75	0.000	-0.126	0.000	0.929	0.979	0.949	0.143	0.323
0.75	0.125	-0.118	0.140	0.917	0.972	0.943	0.167	0.378
0.75	0.250	-0.0950	0.279	0.884	0.949	0.927	0.224	0.514
0.75	0.375	-0.0565	0.415	0.818	0.912	0.897	0.295	0.692
0.75	0.500	-0.00262	0.547	0.727	0.858	0.847	0.376	0.908
1.00	0.000	-0.168	0.000	0.878	0.963	0.911	0.190	0.434
1.00	0.125	-0.160	0.145	0.868	0.955	0.908	0.211	0.483
1.00	0.250	-0.137	0.290	0.838	0.930	0.901	0.263	0.610
1.00	0.375	-0.0985	0.432	0.790	0.890	0.888	0.330	0.784
1.00	0.500	-0.0443	0.570	0.724	0.834	0.867	0.407	0.996
				$M_\infty = 6$				
0.00	0.000	0.00000	0.000	1.000	1.000	1.000	0.0000	0.000
0.00	0.125	0.00780	0.124	0.981	0.994	0.986	0.0737	0.165
0.00	0.250	0.0310	0.247	0.925	0.978	0.946	0.148	0.334
0.00	0.375	0.0694	0.366	0.833	0.949	0.877	0.225	0.517
0.00	0.500	0.122	0.479	0.664	0.889	0.746	0.332	0.787
0.25	0.000	-0.0362	0.000	0.994	0.998	0.996	0.0426	0.0953
0.25	0.125	-0.0285	0.129	0.977	0.991	0.985	0.0909	0.204
0.25	0.250	-0.00525	0.256	0.926	0.972	0.952	0.166	0.377
0.25	0.375	+0.0331	0.380	0.840	0.939	0.894	0.245	0.566
0.25	0.500	+0.0862	0.499	0.698	0.884	0.790	0.340	0.809
0.50	0.000	-0.0725	0.000	0.974	0.992	0.981	0.0864	0.194
0.50	0.125	-0.0648	0.133	0.958	0.985	0.973	0.122	0.275
0.50	0.250	-0.0415	0.265	0.913	0.962	0.948	0.193	0.441
0.50	0.375	-0.00316	0.394	0.837	0.925	0.905	0.273	0.635
0.50	0.500	+0.0501	0.518	0.724	0.870	0.833	0.360	0.863

TABLE 4.1 Continued

/191

ξ	s	x	r	$\bar{p}$	$\bar{T}$	$\bar{\rho}$	w	M
0.75	0.000	-0.108	0.000	0.939	0.982	0.956	0.131	0.296
0.75	0.125	-0.101	0.138	0.927	0.974	0.951	0.161	0.365
0.75	0.250	-0.0779	0.275	0.888	0.948	0.936	0.227	0.522
0.75	0.375	-0.0394	0.409	0.825	0.906	0.910	0.306	0.719
0.75	0.500	+0.0140	0.538	0.738	0.848	0.870	0.389	0.946
1.00	0.000	-0.145	0.000	0.893	0.968	0.922	0.177	0.404
1.00	0.125	-0.137	0.142	0.883	0.958	0.921	0.203	0.465
1.00	0.250	-0.114	0.284	0.852	0.929	0.917	0.266	0.617
1.00	0.375	-0.0758	0.423	0.802	0.881	0.910	0.343	0.819
1.00	0.500	-0.0220	0.558	0.734	0.817	0.899	0.427	1.057
				$M_\infty = 10$				
0.00	0.000	0.00000	0.000	1.000	1.000	1.000	0.0000	0.000
0.00	0.125	0.00780	0.124	0.980	0.994	0.986	0.0742	0.166
0.00	0.250	0.0311	0.247	0.924	0.977	0.945	0.148	0.336
0.00	0.375	0.0695	0.366	0.832	0.948	0.877	0.226	0.518
0.00	0.500	0.122	0.479	0.667	0.890	0.749	0.330	0.782
0.25	0.000	-0.0333	0.000	0.995	0.998	0.997	0.0400	0.0895
0.25	0.125	-0.0255	0.128	0.978	0.991	0.986	0.0913	0.205
0.25	0.250	-0.00230	0.255	0.925	0.971	0.953	0.168	0.383
0.25	0.375	+0.0361	0.379	0.839	0.937	0.895	0.249	0.576
0.25	0.500	+0.0892	0.497	0.698	0.881	0.792	0.343	0.818
0.50	0.000	-0.0667	0.000	0.976	0.993	0.983	0.0817	0.183
0.50	0.125	-0.0589	0.133	0.961	0.985	0.975	0.121	0.273
0.50	0.250	-0.0356	0.264	0.914	0.961	0.951	0.196	0.449
0.50	0.375	+0.00280	0.392	0.838	0.921	0.909	0.279	0.650
0.50	0.500	+0.0561	0.515	0.724	0.864	0.838	0.367	0.884
0.75	0.000	-0.1000	0.000	0.945	0.984	0.960	0.125	0.282
0.75	0.125	-0.0922	0.137	0.931	0.974	0.955	0.158	0.359
0.75	0.250	-0.0690	0.273	0.892	0.946	0.942	0.231	0.530
0.75	0.375	-0.0305	0.405	0.827	0.901	0.918	0.314	0.740
0.75	0.500	+0.0229	0.533	0.739	0.838	0.881	0.401	0.979
1.00	0.000	-0.133	0.000	0.901	0.970	0.928	0.170	0.387
1.00	0.125	-0.125	0.141	0.890	0.959	0.928	0.200	0.457
1.00	0.250	-0.102	0.281	0.859	0.927	0.926	0.269	0.626
1.00	0.375	-0.0639	0.418	0.807	0.874	0.923	0.353	0.846
1.00	0.500	-0.0102	0.551	0.738	0.803	0.919	0.443	1.105

CALCULATION OF FLOW IN SUPERSONIC REGION
BY THE METHOD OF CHARACTERISTICS.
IDEAL GAS; $\varkappa = 1.4$; $M_\infty = 4\text{-}6$.

/1

TABLE 4.2

$M_\infty = 4$. Spherical Segment-Cone; $\delta = 1$; $\chi = 30°$; $\omega = -5°$.

Distribution of Gas Dynamic Parameters Along Surface of Body

x_0	$\bar{p}_0$	$\bar{T}_0$	$\bar{\rho}_0$	w_0	M_0
0.134	0.00710	0.243	0.0293	0.870	3.941
0.272	0.0201	0.327	0.0614	0.820	3.203
0.408	0.0309	0.370	0.0834	0.793	2.915
0.515	0.0371	0.390	0.0951	0.780	2.794
0.638	0.0417	0.403	0.103	0.772	2.718
0.771	0.0448	0.411	0.108	0.766	2.672
0.865	0.0461	0.415	0.111	0.764	2.653
1.025	0.0476	0.418	0.113	0.762	2.633
1.142	0.0481	0.420	0.114	0.761	2.625
1.296	0.0484	0.421	0.115	0.760	2.621
1.492	0.0483	0.420	0.114	0.760	2.622
1.748	0.0478	0.419	0.113	0.761	2.630
2.087	0.0468	0.416	0.112	0.763	2.643
2.545	0.0455	0.413	0.110	0.765	2.662
3.178	0.0445	0.411	0.108	0.767	2.675
4.079	0.0465	0.416	0.111	0.764	2.647

"Hanging" Shock

x	r	ζ_+	β_+	S_+	ζ_-	S_-	$tg\sigma$
0.424	0.528	-0.214	3.025	-0.811	-0.243	-0.811	0.0903
0.505	0.537	-0.167	2.815	-0.813	-0.241	-0.814	0.131
0.602	0.551	-0.147	2.724	-0.817	-0.230	-0.819	0.155
0.801	0.585	-0.127	2.665	-0.827	-0.205	-0.829	0.185
1.310	0.698	-0.0716	2.640	-0.865	-0.146	-0.866	0.247
2.813	1.110	-0.0143	3.068	-1.098	-0.0633	-1.098	0.276

TABLE 4.3

/193

$M_\infty = 4$. Spherical Segment-Cylinder; $\delta = 1$; $\chi = 30°$; $\omega = 0°$

Distribution of Gas Dynamic Parameters

Along Surface of Body

x_0	$\bar{p}_0$	$\bar{T}_0$	$\bar{\rho}_0$	w_0	M_0
0.134	0.0115	0.279	0.0411	0.849	3.594
0.269	0.0317	0.373	0.0851	0.791	2.897
0.395	0.0449	0.412	0.109	0.766	2.669
0.524	0.0532	0.432	0.123	0.753	2.561
0.662	0.0575	0.442	0.130	0.746	2.510
0.736	0.0587	0.444	0.132	0.745	2.497
0.838	0.0595	0.446	0.133	0.743	2.488
0.917	0.0598	0.447	0.133	0.743	2.485
1.021	0.0598	0.447	0.133	0.743	2.486
1.152	0.0592	0.446	0.132	0.744	2.492
1.321	0.0581	0.443	0.131	0.745	2.504
1.540	0.0562	0.439	0.128	0.748	2.525
1.826	0.0536	0.433	0.123	0.752	2.555
2.207	0.0504	0.426	0.118	0.757	2.595
2.726	0.0470	0.417	0.112	0.763	2.640
3.448	0.0440	0.409	0.107	0.768	2.683
4.541	0.0422	0.404	0.104	0.771	2.711
5.090	0.0420	0.404	0.103	0.771	2.713
5.727	0.0420	0.404	0.104	0.771	2.713
6.478	0.0422	0.404	0.104	0.771	2.711
7.376	0.0423	0.405	0.104	0.771	2.709
9.093	0.0427	0.406	0.105	0.770	2.702
10.57	0.0433	0.407	0.106	0.769	2.694
11.45	0.0436	0.408	0.106	0.768	2.689

"Hanging" Shock

x	r	ζ_+	β_+	S_+	ζ_-	S_-	$\operatorname{tg}\sigma$
0.398	0.555	-0.126	2.754	-0.813	-0.159	-0.813	0.204
0.471	0.572	-0.0835	2.584	-0.817	-0.156	-0.818	0.243
0.563	0.595	-0.0659	2.515	-0.823	-0.147	-0.824	0.266
0.787	0.658	-0.0431	2.476	-0.840	-0.121	-0.841	0.298
1.346	0.841	+0.00324	2.553	-0.903	-0.0673	-0.904	0.343
2.616	1.268	+0.0275	3.156	-1.222	-0.0184	-1.222	0.315
3.251	1.461	+0.0268	3.434	-1.372	-0.0110	-1.372	0.294
4.147	1.719	+0.0244	3.596	-1.458	-0.00771	-1.458	0.282
5.479	2.069	+0.0208	3.726	-1.526	-0.00492	-1.526	0.273

Coordinates of Nose Shock Wave

x_B	-0.168	-0.160	-0.137	-0.0986	-0.0443	0.0126	0.0371	0.0720	0.112	0.183	
r_B	0	0.145	0.290	0.432	0.570	0.680	0.719	0.767	0.816	0.890	
x_B	0.310	0.410	0.554	0.765	1.114	1.530	2.145	2.566	3.098	3.778	5.000
r_B	1.002	1.081	1.181	1.316	1.513	1.723	2.004	2.183	2.399	2.662	3.111

TABLE 4.4

$M_\infty = 4$. Spherical Segment-Cone; $\delta = 1$; $\chi = 30°$; $\omega = 5°$

Distribution of Gas Dynamic Parameters Along Surface of Body

x_0	$\bar{p}_0$	$\bar{T}_0$	$\bar{\rho}_0$	w_0	M_0
0.134	0.0178	0.316	0.0563	0.828	3.287
0.205	0.0337	0.379	0.0889	0.787	2.857
0.265	0.0476	0.419	0.113	0.762	2.633
0.397	0.0652	0.458	0.142	0.735	2.430
0.457	0.0699	0.467	0.149	0.729	2.385
0.525	0.0734	0.474	0.154	0.725	2.354
0.574	0.0751	0.477	0.157	0.722	2.339
0.665	0.0768	0.480	0.159	0.720	2.325
0.701	0.0771	0.480	0.160	0.720	2.322
0.824	0.0773	0.481	0.160	0.720	2.321
0.914	0.0768	0.480	0.160	0.720	2.325
1.028	0.0757	0.478	0.158	0.722	2.334
1.174	0.0739	0.475	0.155	0.724	2.350
1.361	0.0712	0.470	0.151	0.727	2.373
1.605	0.0678	0.463	0.146	0.732	2.405
1.927	0.0638	0.455	0.140	0.737	2.444
2.359	0.0597	0.447	0.133	0.743	2.486
2.954	0.0564	0.439	0.128	0.748	2.522
3.845	0.0547	0.436	0.125	0.750	2.543
4.210	0.0545	0.435	0.125	0.751	2.544
4.622	0.0545	0.435	0.125	0.751	2.545
5.094	0.0544	0.435	0.125	0.751	2.546
5.635	0.0544	0.435	0.125	0.751	2.546
6.614	0.0547	0.436	0.125	0.750	2.543
7.407	0.0551	0.436	0.126	0.750	2.538

"Hanging" Shock

x	r	ζ_+	β_+	S_+	ζ_-	S_-	tanσ
0.360	0.574	-0.0464	2.534	-0.816	-0.0766	-0.816	0.319
0.423	0.596	-0.00655	2.382	-0.820	-0.0766	-0.821	0.358
0.503	0.625	+0.0113	2.319	-0.828	-0.0695	-0.828	0.381
0.697	0.702	+0.0276	2.309	-0.849	-0.0489	-0.850	0.405
1.182	0.909	+0.0662	2.425	-0.929	-0.0571	-0.930	0.434
2.278	1.354	+0.0752	3.129	-1.303	+0.0282	-1.304	0.370
2.725	1.516	+0.0719	3.310	-1.399	+0.0307	-1.400	0.353
3.316	1.721	+0.0676	3.428	-1.460	+0.0319	-1.460	0.341
4.123	1.992	+0.0622	3.538	-1.509	+0.0321	-1.514	0.330

TABLE 4.5

/195

$M_\infty = 4$. Spherical Segment-Cone; $\delta = 1$; $\chi = 30°$; $\omega = 10°$

Distribution of Gas Dynamic Parameters Along Surface of Body

x_0	$\bar{p}_0$	$\bar{T}_0$	$\bar{\rho}_0$	w_0	M_0
0.134	0.0267	0.355	0.0752	0.802	3.013
0.195	0.0481	0.420	0.114	0.761	2.625
0.260	0.0684	0.464	0.147	0.731	2.399
0.319	0.0803	0.486	0.165	0.716	2.297
0.393	0.0908	0.504	0.180	0.704	2.218
0.458	0.0960	0.512	0.187	0.696	2.190
0.522	0.0990	0.516	0.191	0.695	2.163
0.570	0.100	0.518	0.193	0.693	2.155
0.634	0.101	0.519	0.194	0.693	2.150
0.742	0.100	0.519	0.194	0.693	2.151
0.820	0.100	0.518	0.193	0.694	2.156
0.920	0.0985	0.515	0.191	0.695	2.166
1.046	0.0961	0.512	0.187	0.698	2.182
1.208	0.0929	0.507	0.183	0.702	2.204
1.416	0.0888	0.500	0.177	0.706	2.233
1.689	0.0843	0.493	0.170	0.711	2.266
2.052	0.0802	0.486	0.164	0.716	2.297
2.545	0.0777	0.482	0.161	0.719	2.317
3.282	0.0771	0.480	0.160	0.720	2.323
3.932	0.0774	0.481	0.160	0.720	2.320
4.588	0.0781	0.482	0.161	0.719	2.314
5.187	0.0789	0.484	0.163	0.718	2.308
5.907	0.0800	0.486	0.164	0.716	2.299
6.471	0.0808	0.487	0.165	0.715	2.292

"Hanging" Shock

x	r	ζ_+	β_+	S_+	ζ_-	S_-	$\tan\sigma$
0.327	0.589	0.0332	2.318	-0.818	0.00441	-0.818	0.447
0.382	0.615	0.0699	2.188	-0.824	0.00254	-0.825	0.485
0.450	0.649	0.0886	2.127	-0.832	0.00744	-0.834	0.510
0.617	0.736	0.100	2.137	-0.860	0.0233	-0.861	0.527
1.036	0.961	0.131	2.299	-0.950	0.0571	-0.963	0.535
1.979	1.418	0.127	3.051	-1.368	0.0780	-1.368	0.437
2.285	1.549	0.123	3.156	-1.422	0.0782	-1.422	0.424
2.668	1.710	0.118	3.243	-1.465	0.0776	-1.466	0.412
3.155	1.908	0.112	3.332	-1.509	0.0764	-1.509	0.400
3.791	2.159	0.105	3.400	-1.540	0.0743	-1.540	0.389
4.644	2.487	0.0985	3.448	-1.557	0.0716	-1.557	0.380

TABLE 4.6

$M_\infty = 6$. Spherical Segment-Cone; $\delta = 1$; $\chi = 30°$; $\omega = -5°$

Distribution of Gas Dynamic Parameters Along Surface of Body

x_0	$\bar{p}_0$	$\bar{T}_0$	$\bar{\rho}_0$	w_0	M_0
0.134	0.00710	0.243	0.0293	0.870	3.941
0.258	0.0166	0.310	0.0535	0.830	3.334
0.386	0.0258	0.351	0.0734	0.805	3.035
0.445	0.0287	0.362	0.0792	0.798	2.963
0.520	0.0314	0.372	0.0844	0.792	2.905
0.593	0.0332	0.378	0.0879	0.788	2.867
0.715	0.0352	0.384	0.0917	0.784	2.828
0.836	0.0365	0.388	0.0940	0.782	2.805
0.919	0.0370	0.389	0.0949	0.781	2.796
1.021	0.0373	0.390	0.0955	0.780	2.791
1.147	0.0373	0.390	0.0955	0.780	2.790
1.305	0.0369	0.389	0.0948	0.781	2.797
1.505	0.0361	0.387	0.0932	0.782	2.813
2.093	0.0327	0.376	0.0868	0.789	2.878
2.733	0.0295	0.365	0.0808	0.796	2.945
3.163	0.0279	0.359	0.0777	0.800	2.982
3.408	0.0272	0.357	0.0762	0.801	2.999
3.677	0.0265	0.354	0.0749	0.803	3.015
3.971	0.0260	0.352	0.0738	0.804	3.029
4.295	0.0257	0.351	0.0731	0.805	3.038
4.652	0.0257	0.351	0.0732	0.805	3.037
5.046	0.0267	0.355	0.0753	0.802	3.010

"Hanging" Shock

x	r	ζ_+	β_+	S_+	ζ_-	S_-	tanσ
0.499	0.537	-0.190	3.052	-0.867	-0.224	-0.867	0.107
0.653	0.559	-0.131	2.845	-0.874	-0.207	-0.875	0.162
0.980	0.620	-0.0881	2.805	-0.897	-0.162	-0.899	0.211
1.545	0.755	-0.0360	2.921	-0.945	-0.0982	-0.949	0.260
1.919	0.856	-0.0138	3.034	-0.990	-0.0693	-0.991	0.276
2.409	0.994	+0.00556	3.222	-1.069	-0.0427	-1.070	0.283
3.070	1.177	+0.0192	3.641	-1.245	-0.0211	-1.271	0.268

TABLE 4.7

/197

$M_\infty = 6$. Spherical Segment-Cylinder; $\delta = 1$; $\chi = 30°$; $\omega = 0°$

Distribution of Gas Dynamic Parameters Along Surface of Body

x_0	$\bar{p}_0$	$\bar{T}_0$	$\bar{\rho}_0$	w_0	M_0
0.134	0.0115	0.279	0.0411	0.849	3.594
0.265	0.0280	0.360	0.0777	0.799	2.981
0.387	0.0389	0.395	0.0983	0.777	2.764
0.535	0.0450	0.412	0.109	0.766	2.669
0.642	0.0469	0.417	0.112	0.763	2.642
0.747	0.0477	0.419	0.113	0.761	2.630
0.818	0.0479	0.419	0.114	0.761	2.628
0.907	0.0478	0.419	0.113	0.761	2.630
1.015	0.0472	0.418	0.113	0.762	2.638
1.150	0.0461	0.415	0.111	0.764	2.653
1.318	0.0442	0.410	0.107	0.767	2.680
1.805	0.0384	0.394	0.0976	0.778	2.771
2.298	0.0336	0.379	0.0886	0.787	2.860
2.906	0.0292	0.364	0.0802	0.797	2.952
3.704	0.0253	0.350	0.0724	0.806	3.046
4.455	0.0231	0.341	0.0679	0.811	3.107
5.715	0.0213	0.332	0.0639	0.816	3.164
6.943	0.0201	0.327	0.0615	0.819	3.201
7.941	0.0196	0.325	0.0603	0.821	3.220

"Hanging" Shock

x	r	ζ_+	β_+	S_+	ζ_-	S_-	$\tan\sigma$
0.446	0.566	-0.116	2.839	-0.870	-0.141	-0.870	0.209
0.578	0.599	-0.0546	2.644	-0.879	-0.128	-0.881	0.266
0.859	0.679	-0.0180	2.634	-0.907	-0.0923	-0.908	0.306
1.333	0.834	+0.0228	2.787	-0.970	-0.0403	-0.971	0.339
1.603	0.926	+0.0371	2.902	-1.015	-0.0201	-1.016	0.345
1.943	1.044	+0.0493	3.094	-1.100	-0.00145	-1.101	0.342
2.384	1.190	+0.0572	3.474	-1.287	+0.0138	-1.287	0.320
2.967	1.368	+0.0603	3.983	-1.536	+0.0242	-1.536	0.292
3.766	1.592	+0.0599	4.478	-1.766	+0.0304	-1.766	0.267
4.909	1.884	+0.0563	4.958	-1.979	+0.0328	-1.979	0.246

Coordinates of Nose Shock Wave

x_B	-0.145	-0.137	-0.114	-0.0758	-0.0221	0.0189	0.0457	0.0785	0.118	0.182	0.288
r_B	0	0.142	0.284	0.423	0.558	0.639	0.683	0.728	0.775	0.840	0.932
x_B	0.398	0.501	0.683	0.938	1.305	1.698	2.016	3.000	4.000	5.000	
r_B	1.014	1.083	1.192	1.326	1.494	1.652	1.776	2.114	2.421	2.706	

TABLE 4.8

$M_\infty = 6$. Spherical Segment-Cone; $\delta = 1$; $\chi = 30°$; $\omega = 5°$

Distribution of Gas Dynamic Parameters Along Surface of Body

x_0	$\bar{p}_0$	$\bar{T}_0$	$\bar{\rho}_0$	w_0	M_0
0.134	0.0178	0.316	0.0563	0.828	3.287
0.199	0.0295	0.365	0.0807	0.796	2.945
0.266	0.0429	0.406	0.105	0.770	2.699
0.325	0.0509	0.427	0.119	0.756	2.589
0.403	0.0573	0.441	0.129	0.747	2.513
0.456	0.0599	0.447	0.133	0.743	2.484
0.522	0.0618	0.451	0.137	0.740	2.464
0.578	0.0628	0.453	0.138	0.739	2.454
0.670	0.0634	0.454	0.139	0.738	2.448
0.732	0.0634	0.454	0.139	0.738	2.448
0.809	0.0629	0.453	0.138	0.739	2.453
0.902	0.0619	0.451	0.137	0.740	2.463
1.017	0.0601	0.447	0.134	0.742	2.482
1.161	0.0576	0.442	0.130	0.746	2.510
1.340	0.0541	0.434	0.124	0.751	2.549
1.567	0.0500	0.425	0.117	0.758	2.600
1.867	0.0453	0.413	0.109	0.765	2.664
1.956	0.0441	0.410	0.107	0.768	2.681
2.050	0.0430	0.407	0.105	0.770	2.698
2.149	0.0418	0.403	0.103	0.772	2.716
2.253	0.0407	0.400	0.101	0.774	2.733
2.480	0.0386	0.394	0.0978	0.778	2.769
2.731	0.0366	0.388	0.0942	0.781	2.803
3.318	0.0335	0.379	0.0884	0.787	2.861
4.041	0.0314	0.372	0.0845	0.792	2.904
4.963	0.0296	0.366	0.0810	0.796	2.942
5.827	0.0287	0.362	0.0792	0.798	2.964
6.892	0.0280	0.360	0.0778	0.799	2.980
7.749	0.0277	0.359	0.0772	0.800	2.987

"Hanging" Shock

x	r	ζ_+	β_+	S_+	ζ_-	S_-	$\tan\sigma$
0.399	0.588	-0.0387	2.620	-0.874	-0.0602	-0.874	0.321
0.514	0.629	+0.0219	2.443	-0.885	-0.0514	-0.887	0.378
0.754	0.724	+0.0533	2.460	-0.920	-0.0218	-0.922	0.411
1.151	0.892	+0.0858	2.638	-0.995	+0.0207	-0.990	0.429
1.344	0.975	+0.0950	2.758	-1.047	+0.0348	-1.048	0.427
1.579	1.074	+0.102	2.958	-1.142	+0.0476	-1.143	0.414
1.871	1.191	+0.105	3.308	-1.319	+0.0579	-1.320	0.387
2.240	1.328	+0.106	3.713	-1.523	+0.0649	-1.523	0.357
2.717	1.493	+0.104	4.096	-1.707	+0.0691	-1.707	0.333
3.350	1.696	+0.100	4.500	-1.894	+0.0705	-1.895	0.310
4.215	1.956	+0.0942	4.833	-2.012	+0.0698	-2.040	0.291

TABLE 4.9

/199

$M_\infty = 6$. Spherical Segment-Cone; $\delta = 1$; $\chi = 30°$; $\omega = 10°$

Distribution of Gas Dynamic Parameters Along Surface of Body

x_0	$\bar{p}_0$	$\bar{T}_0$	$\bar{\rho}_0$	w_0	M_0
0.134	0.0267	0.355	0.0752	0.802	3.013
0.202	0.0469	0.417	0.112	0.763	2.642
0.263	0.0627	0.453	0.138	0.739	2.455
0.327	0.0735	0.474	0.155	0.724	2.353
0.393	0.0794	0.484	0.163	0.717	2.304
0.442	0.0819	0.489	0.167	0.714	2.284
0.524	0.0839	0.492	0.170	0.712	2.269
0.603	0.0844	0.493	0.171	0.711	2.265
0.658	0.0842	0.493	0.170	0.711	2.266
0.724	0.0834	0.491	0.169	0.712	2.272
0.805	0.0820	0.489	0.167	0.714	2.283
0.904	0.0798	0.485	0.164	0.717	2.301
1.026	0.0765	0.479	0.159	0.721	2.327
1.178	0.0723	0.472	0.153	0.726	2.363
1.369	0.0674	0.462	0.145	0.732	2.409
1.618	0.0618	0.451	0.137	0.740	2.464
1.881	0.0574	0.442	0.129	0.746	2.512
2.191	0.0536	0.433	0.123	0.752	2.555
2.366	0.0522	0.430	0.121	0.754	2.573
2.555	0.0510	0.427	0.119	0.756	2.587
2.760	0.0501	0.425	0.117	0.758	2.599
3.105	0.0488	0.422	0.115	0.760	2.616
3.505	0.0477	0.419	0.113	0.762	2.631
3.806	0.0472	0.417	0.112	0.762	2.638

"Hanging" Shock

x	r	ζ_+	β_+	S_+	ζ_-	S_-	$\tan\sigma$
0.377	0.613	0.0526	2.367	-0.881	0.0193	-0.881	0.457
0.496	0.671	0.103	2.248	-0.900	0.0290	-0.901	0.510
0.743	0.800	0.133	2.326	-0.955	0.0585	-0.956	0.532
1.027	0.952	0.152	2.525	-1.034	0.0860	-1.044	0.527
1.169	1.025	0.157	2.673	-1.114	0.0953	-1.115	0.513
1.337	1.110	0.160	2.912	-1.238	0.103	-1.239	0.483
1.787	1.314	0.158	3.535	-1.560	0.112	-1.561	0.428
2.093	1.442	0.155	3.847	-1.715	0.114	-1.716	0.404

TABLE 4.10

$M_\infty = 5.8$. Spherical Segment-Cylinder; $\delta = 1$; $\chi = 33°$; $\omega = 0°$

Distribution of Gas Dynamic Parameters Along Surface of Body

x_0	$\bar{p}_0$	$\bar{T}_0$	$\bar{\rho}_0$	w_0	M_0
0.161	0.0151	0.301	0.0500	0.835	3.400
0.191	0.0178	0.316	0.0564	0.826	3.284
0.426	0.0408	0.401	0.101	0.773	2.732
0.687	0.0472	0.418	0.112	0.762	2.678
0.972	0.0480	0.419	0.114	0.761	2.627
1.261	0.0462	0.415	0.111	0.764	2.652
1.555	0.0432	0.407	0.106	0.769	2.696
1.748	0.0411	0.401	0.102	0.773	2.728
2.282	0.0358	0.386	0.0928	0.783	2.817
2.985	0.0309	0.370	0.0834	0.793	2.915
3.962	0.0263	0.353	0.0745	0.803	3.020
5.002	0.0238	0.343	0.0692	0.810	3.089
5.980	0.0225	0.333	0.0665	0.813	3.127
7.679	0.0211	0.332	0.0636	0.817	3.170
8.752	0.0206	0.330	0.0626	0.818	3.185
10.03	0.0203	0.328	0.0618	0.819	3.197
11.57	0.0200	0.327	0.0612	0.820	3.205
13.45	0.0199	0.326	0.0610	0.820	3.209
17.18	0.0200	0.327	0.0613	0.820	3.205
22.58	0.0205	0.329	0.0622	0.818	3.190
27.67	0.0209	0.331	0.0632	0.817	3.176
34.56	0.0213	0.333	0.0641	0.816	3.162
44.59	0.0218	0.335	0.0651	0.815	3.147
59.43	0.0218	0.335	0.0651	0.815	3.147
69.74	0.0215	0.333	0.0644	0.816	3.157
83.09	0.0213	0.333	0.0640	0.816	3.164
100.7	0.0209	0.331	0.0632	0.817	3.176
154.9	0.0229	0.340	0.0674	0.812	3.114

TABLE 4.10 Continued

/201

"Hanging" Shock

x	r	ζ_+	β_+	S_+	ζ_-	S_-	$\operatorname{tg}\sigma$
0.560	0.640	-0.0977	2.777	-0.878	-0.117	-0.878	0.239
0.716	0.682	-0.0357	2.617	-0.891	-0.104	-0.892	0.293
0.984	0.764	-0.0114	2.659	-0.921	-0.0741	-0.921	0.317
1.392	0.899	+0.0182	2.791	-0.974	-0.0265	-0.974	0.339
1.651	0.988	+0.0313	2.891	-1.014	-0.0191	-1.015	0.344
1.978	1.100	+0.0430	3.048	-1.082	-0.00261	-1.083	0.343
2.396	1.241	+0.0516	3.358	-1.234	+0.0116	-1.234	0.326
2.943	1.412	+0.0558	3.811	-1.459	+0.0218	-1.459	0.300
3.681	1.625	+0.0568	4.244	-1.664	+0.0283	-1.664	0.277
4.714	1.899	+0.0546	4.709	-1.877	+0.0313	-1.877	0.255
6.231	2.272	+0.0500	5.064	-2.031	+0.0316	-2.031	0.238
8.600	2.820	+0.0438	5.296	-2.124	+0.0298	-2.125	0.225
12.63	3.708	+0.0365	5.433	-2.173	+0.0268	-2.173	0.215
20.41	5.351	+0.0288	5.506	-2.191	+0.0227	-2.191	0.207
38.52	9.030	+0.0209	5.544	-2.190	+0.0178	-2.190	0.206

Coordinates of Nose Shock Wave

x_B	-0.148	-0.118	0.003	0.0634	0.117	0.177	0.283	0.402	0.567	0.754	
r_B	0	0.285	0.628	0.734	0.806	0.872	0.970	1.064	1.177	1.289	
x_B	0.941	1.182	1.499	1.766	2.281	2.989	3.986	5.437	6.794	7.639	8.625
r_B	1.390	1.508	1.650	1.761	1.958	2.206	2.525	2.950	3.321	3.542	3.793
x_B	9.786	11.165	14.807	20.26	28.89	35.15	43.55	55.03	70.81		
r_B	4.081	4.413	5.257	6.459	8.272	9.547	11.22	13.46	16.49		

CALCULATION OF FLOW IN REGION OF INFLUENCE OF BLUNTING

SCHEME II. N = 2

TABLE 4.11

Ideal Gas; $\varkappa$ = 1.4; M_∞ = 10.

Spherical Segment with Sonic Discontinuity; δ = 1; χ = 33°

$\varepsilon_0 = 0.1333;\ \varepsilon_1 = 0.1643;\ \varepsilon_2 = 0.1436;\ C = 2.1$

ξ	s	u	v
		$s = 0$	
1.0	0	-0.171	0
0.8	0	-0.132	0
0.6	0	-0.0965	0
0.4	0	-0.0626	0
0.2	0	-0.0301	0
0.0	0	0.0000	0
		$s = s_1/2$	
1.0	0.380	-0.148	0.329
0.8	0.347	-0.119	0.281
0.6	0.325	-0.0895	0.246
0.4	0.313	-0.0590	0.218
0.2	0.297	-0.0279	0.195
0.0	0.288	0.0000	0.177
		$s = s_1$	
1.0	0.759	-0.108	0.648
0.8	0.695	-0.111	0.548
0.6	0.650	-0.106	0.490
0.4	0.617	-0.0943	0.452
0.2	0.593	-0.0791	0.428
0.0	0.576	-0.00705	0.415

TABLE 4.12

/203

IDEAL GAS, BODY WITH DISCONTINUITY OF CURVATURE

SCHEME I. N = 2

$M_\infty = 5.8$; $\varkappa = 1.4$; $1/\bar{r} = 2$

s	ε	σ	Φ_1	$\bar{p}_0$	$\bar{T}_0$
0.0000	0.341	1.570	0.00000	1.000	1.000
0.0625	0.340	1.547	-0.00229	0.999	1.000
0.1250	0.338	1.523	-0.00921	0.997	0.999
0.1875	0.334	1.499	-0.0207	0.994	0.998
0.2500	0.329	1.476	-0.0370	0.989	0.997
0.3125	0.322	1.451	-0.0585	0.982	0.995
0.3750	0.314	1.426	-0.0858	0.972	0.992
0.4375	0.304	1.400	-0.119	0.955	0.987
0.5000	0.292	1.366	-0.156	0.928	0.978
0.5625	0.276	1.319	-0.261	0.869	0.960
0.6250	0.267	1.260	-0.400	0.797	0.937
0.6875	0.265	1.198	-0.577	0.712	0.907
0.7500	0.268	1.140	-0.772	0.623	0.873
0.8125	0.278	1.094	-0.956	0.527	0.832
0.8750	0.299	1.079	-1.067	0.369	0.752
0.9375	0.322	0.902	-1.958	0.132	0.560
1.0000	0.345	0.820	-2.472	0.109	0.531

s	u	v	p	T	c^2	w^2	ψ	$-x$	y
$\xi = 0$									
0.0000	0	0.0000	0.809	0.142	0.200	0.000000	0	0	0.0000
0.0625	0	0.0130	0.808	0.142	0.199	0.000171	0	0	0.0625
0.1250	0	0.0261	0.807	0.142	0.199	0.000686	0	0	0.125
0.1875	0	0.0397	0.804	0.142	0.199	0.00157	0	0	0.187
0.2500	0	0.0542	0.800	0.142	0.199	0.00293	0	0	0.250
0.3125	0	0.0704	0.795	0.142	0.199	0.00495	0	0	0.312
0.3750	0	0.0894	0.786	0.141	0.198	0.00800	0	0	0.375
0.4375	0	0.113	0.773	0.141	0.197	0.0128	0	0	0.437
0.5000	0	0.145	0.751	0.139	0.195	0.0211	0	0	0.500
0.5625	0	0.197	0.703	0.137	0.192	0.0390	0	-0.00390	0.562

TABLE 4.12 Continued

s	u	v	p	T	c^2	w^2	ψ	$-x$	y
0.6250	0	0.250	0.645	0.133	0.187	0.0625	0	-0.0155	0.623
0.6875	0	0.304	0.576	0.129	0.181	0.0924	0	-0.0347	0.683
0.7500	0	0.355	0.504	0.124	0.174	0.126	0	-0.0612	0.739
0.8125	0	0.408	0.426	0.118	0.166	0.167	0	-0.0945	0.792
0.8750	0	0.497	0.298	0.107	0.150	0.247	0	-0.134	0.840
0.9375	0	0.662	0.106	0.0800	0.112	0.439	0	-0.179	0.883
1.0000	0	0.684	0.0885	0.0758	0.106	0.468	0	-0.229	0.920
				$\xi = 0.5$					
0.0000	-0.0796	0.0000	0.791	0.141	0.198	0.00634	0.000000	0.170	0.0000
0.0625	-0.0791	0.0155	0.791	0.141	0.198	0.00650	0.000860	0.170	0.0625
0.1250	-0.0800	0.0314	0.790	0.141	0.198	0.00739	0.00344	0.169	0.125
0.1875	-0.0817	0.0479	0.787	0.141	0.198	0.00897	0.00777	0.167	0.187
0.2500	-0.0842	0.0652	0.784	0.141	0.197	0.0113	0.0139	0.164	0.250
0.3125	-0.0879	0.0837	0.778	0.140	0.197	0.0147	0.0218	0.161	0.312
0.3750	-0.0932	0.103	0.770	0.140	0.196	0.0194	0.0318	0.157	0.375
0.4375	-0.101	0.125	0.758	0.139	0.194	0.0260	0.0440	0.152	0.437
0.5000	-0.107	0.156	0.740	0.137	0.192	0.0358	0.0590	0.146	0.500
0.5625	-0.107	0.195	0.713	0.135	0.190	0.0497	0.0805	0.133	0.579
0.6250	-0.0982	0.243	0.675	0.133	0.186	0.0687	0.103	0.114	0.656
0.6875	-0.0862	0.291	0.631	0.129	0.181	0.0921	0.127	0.0885	0.731
0.7500	-0.0707	0.337	0.583	0.125	0.176	0.119	0.152	0.0566	0.804
0.8125	-0.0527	0.377	0.539	0.122	0.170	0.145	0.178	0.0185	0.874
0.8750	-0.0385	0.463	0.414	0.112	0.156	0.216	0.208	-0.0246	0.942
0.9375	-0.0244	0.563	0.262	0.0974	0.136	0.318	0.233	-0.0762	1.007
1.0000	-0.00105	0.582	0.243	0.0945	0.132	0.338	0.255	-0.136	1.066
				$\xi = 1$					
0.0000	-0.178	0.0000	0.722	0.138	0.193	0.0319	0.00000	0.341	0.0000
0.0625	-0.179	0.0178	0.722	0.138	0.193	0.0323	0.00182	0.340	0.0625
0.1250	-0.180	0.0356	0.720	0.138	0.193	0.0338	0.00728	0.338	0.125
0.1875	-0.182	0.0533	0.718	0.137	0.192	0.0361	0.0164	0.334	0.187
0.2500	-0.185	0.0710	0.715	0.137	0.192	0.0394	0.0291	0.329	0.250
0.3125	-0.189	0.0890	0.712	0.136	0.191	0.0438	0.0455	0.322	0.312
0.3750	-0.194	0.107	0.707	0.135	0.190	0.0494	0.0656	0.314	0.375
0.4375	-0.200	0.125	0.701	0.134	0.188	0.0561	0.0892	0.304	0.437
0.5000	-0.204	0.157	0.692	0.133	0.187	0.0667	0.121	0.292	0.500
0.5625	-0.202	0.208	0.677	0.130	0.183	0.0844	0.166	0.270	0.596
0.6250	-0.189	0.274	0.654	0.126	0.177	0.111	0.222	0.244	0.689
0.6875	-0.168	0.340	0.626	0.122	0.171	0.144	0.284	0.211	0.780
0.7500	-0.139	0.399	0.596	0.117	0.164	0.179	0.351	0.174	0.868
0.8125	-0.0990	0.447	0.568	0.112	0.157	0.210	0.426	0.131	0.955
0.8750	-0.0445	0.467	0.552	0.110	0.154	0.220	0.509	0.0848	1.044
0.9375	-0.0289	0.596	0.435	0.0904	0.126	0.356	0.596	0.0270	1.131
1.0000	+0.0169	0.652	0.376	0.0806	0.112	0.425	0.685	-0.0429	1.211

TABLE 4.13

/205

$M_\infty = 5.8$; $\varkappa = 1.4$; $1/\bar{r} = 64$

s	ε	σ	s_1	$\bar{p}_0$	$\bar{T}_0$
0.0000	0.544	1.570	0.000000	1.000	1.000
0.0625	0.543	1.555	-0.000906	0.999	1.000
0.1250	0.542	1.541	-0.00364	0.999	1.000
0.1875	0.540	1.526	-0.00822	0.997	0.999
0.2500	0.536	1.511	-0.0146	0.996	0.999
0.3125	0.532	1.496	-0.0228	0.994	0.998
0.3750	0.527	1.481	-0.0331	0.991	0.997
0.4375	0.521	1.465	-0.0454	0.987	0.996
0.5000	0.514	1.449	-0.0601	0.983	0.995
0.5625	0.506	1.433	-0.0774	0.977	0.993
0.6250	0.497	1.416	-0.0977	0.969	0.991
0.6875	0.486	1.399	-0.121	0.960	0.988
0.7500	0.475	1.381	-0.148	0.946	0.984
0.8125	0.462	1.363	-0.178	0.928	0.978
0.8750	0.449	1.345	-0.209	0.901	0.970
0.9375	0.434	1.331	-0.237	0.858	0.957
0.9843	0.422	1.325	-0.249	0.807	0.940
0.9863	0.411	1.268	-0.379	0.710	0.906
0.9882	0.403	1.220	-0.510	0.598	0.863
0.9902	0.400	1.178	-0.639	0.478	0.810
0.9921	0.401	1.142	-0.766	0.364	0.749
0.9941	0.408	1.108	-0.893	0.263	0.683
0.9960	0.419	1.070	-1.047	0.190	0.622
0.9980	0.435	1.018	-1.282	0.149	0.581
1.0000	0.456	0.929	-1.740	0.132	0.562

TABLE 4.13 Continued

s	u	v	p	T	c^2	w^2	ψ	−x	y
					ξ = 0				
0.0000	0	0.00000	0.809	0.142	0.200	0.0000000	0	0	0.0000
0.0625	0	0.00816	0.809	0.142	0.199	0.0000667	0	0	0.0625
0.1250	0	0.0162	0.808	0.142	0.199	0.000264	0	0	0.125
0.1875	0	0.0244	0.807	0.142	0.199	0.000595	0	0	0.187
0.2500	0	0.0326	0.806	0.142	0.199	0.00106	0	0	0.250
0.3125	0	0.0411	0.804	0.142	0.199	0.00169	0	0	0.312
0.3750	0	0.0500	0.802	0.142	0.199	0.00250	0	0	0.375
0.4375	0	0.0594	0.799	0.142	0.199	0.00353	0	0	0.437
0.5000	0	0.0695	0.795	0.142	0.199	0.00484	0	0	0.500
0.5625	0	0.0807	0.790	0.141	0.198	0.00652	0	0	0.562
0.6250	0	0.0932	0.784	0.141	0.198	0.00869	0	0	0.625
0.6875	0	0.107	0.776	0.141	0.197	0.0115	0	0	0.687
0.7500	0	0.124	0.766	0.140	0.196	0.0154	0	0	0.750
0.8125	0	0.144	0.751	0.139	0.195	0.0209	0	0	0.812
0.8750	0	0.170	0.729	0.138	0.194	0.0292	0	0	0.875
0.9375	0	0.206	0.695	0.136	0.191	0.0425	0	0	0.937
0.9843	0	0.243	0.653	0.134	0.188	0.0593	0	0	0.984
0.9863	0	0.305	0.574	0.129	0.181	0.0930	0	−0.000121	0.986
0.9882	0	0.369	0.484	0.123	0.172	0.136	0	−0.000485	0.988
0.9902	0	0.435	0.387	0.115	0.162	0.189	0	−0.00108	0.990
0.9921	0	0.500	0.294	0.107	0.149	0.250	0	−0.00191	0.991
0.9941	0	0.562	0.213	0.0976	0.136	0.316	0	−0.00293	0.993
0.9960	0	0.614	0.154	0.0889	0.124	0.377	0	−0.00419	0.995
0.9980	0	0.647	0.121	0.0830	0.116	0.418	0	−0.00560	0.996
1.0000	0	0.661	0.107	0.0802	0.112	0.438	0	−0.00718	0.997
					ξ = 0.5				
0.0000	−0.0795	0.00000	0.791	0.141	0.198	0.00632	0.000000	0.272	0.0000
0.0625	−0.0788	0.00972	0.791	0.141	0.198	0.00630	0.000859	0.271	0.0625
0.1250	−0.0790	0.0195	0.791	0.141	0.198	0.00662	0.00343	0.271	0.125
0.1875	−0.0795	0.0294	0.790	0.141	0.198	0.00720	0.00772	0.270	0.187
0.2500	−0.0804	0.0396	0.789	0.141	0.198	0.00804	0.0137	0.268	0.250
0.3125	−0.0815	0.0501	0.787	0.141	0.198	0.00917	0.0215	0.266	0.312
0.3750	−0.0830	0.0610	0.785	0.141	0.197	0.0106	0.0310	0.263	0.375
0.4375	−0.0849	0.0722	0.782	0.141	0.197	0.0124	0.0424	0.260	0.437
0.5000	−0.0871	0.0840	0.779	0.140	0.197	0.0146	0.0557	0.257	0.500
0.5625	−0.0899	0.0963	0.774	0.140	0.196	0.0173	0.0708	0.253	0.562
0.6250	−0.0934	0.109	0.769	0.139	0.195	0.0207	0.0880	0.248	0.625
0.6875	−0.0978	0.123	0.761	0.139	0.195	0.0248	0.107	0.243	0.687
0.7500	−0.103	0.138	0.752	0.138	0.194	0.0299	0.129	0.237	0.750
0.8125	−0.111	0.155	0.739	0.137	0.192	0.0365	0.153	0.231	0.812
0.8750	−0.121	0.174	0.722	0.136	0.190	0.0453	0.180	0.224	0.875

TABLE 4.13 Continued

s	u	v	p	T	c^2	w^2	ψ	$-x$	y
0.9375	-0.136	0.197	0.696	0.134	0.188	0.0577	0.212	0.217	0.937
0.9843	-0.152	0.219	0.667	0.132	0.185	0.0714	0.239	0.211	0.984
0.9863	-0.122	0.226	0.683	0.133	0.186	0.0661	0.252	0.203	1.011
0.9882	-0.0852	0.236	0.693	0.133	0.187	0.0632	0.263	0.195	1.038
0.9902	-0.0441	0.251	0.689	0.133	0.186	0.0653	0.270	0.185	1.063
0.9921	-0.00198	0.273	0.666	0.132	0.185	0.0746	0.275	0.174	1.088
0.9941	+0.0391	0.302	0.622	0.129	0.181	0.0928	0.277	0.162	1.112
0.9960	+0.0793	0.337	0.559	0.125	0.175	0.120	0.278	0.149	1.137
0.9980	+0.121	0.377	0.481	0.120	0.168	0.157	0.278	0.134	1.163
1.0000	+0.175	0.443	0.355	0.110	0.154	0.227	0.278	0.133	1.189
					$\xi = 1$				
0.0000	-0.178	0.0000	0.722	0.138	0.193	0.0319	0.00000	0.544	0.0000
0.0625	-0.178	0.0111	0.722	0.138	0.193	0.0320	0.00182	0.543	0.0625
0.1250	-0.179	0.0224	0.721	0.138	0.193	0.0326	0.00728	0.542	0.125
0.1875	-0.180	0.0336	0.720	0.138	0.193	0.0335	0.0164	0.540	0.187
0.2500	-0.181	0.0448	0.719	0.137	0.193	0.0349	0.0291	0.536	0.250
0.3125	-0.182	0.0560	0.718	0.137	0.192	0.0366	0.0455	0.532	0.312
0.3750	-0.184	0.0672	0.716	0.137	0.192	0.0386	0.0656	0.527	0.375
0.4375	-0.187	0.0786	0.714	0.136	0.191	0.0412	0.0892	0.521	0.437
0.5000	-0.189	0.0902	0.711	0.136	0.191	0.0442	0.116	0.514	0.500
0.5625	-0.193	0.102	0.708	0.136	0.190	0.0477	0.147	0.506	0.562
0.6250	-0.196	0.114	0.705	0.135	0.189	0.0518	0.182	0.497	0.625
0.6875	-0.201	0.126	0.701	0.134	0.188	0.0565	0.220	0.486	0.687
0.7500	-0.206	0.139	0.696	0.134	0.187	0.0619	0.262	0.475	0.750
0.8125	-0.211	0.152	0.691	0.133	0.186	0.0679	0.307	0.462	0.812
0.8750	-0.217	0.163	0.686	0.132	0.185	0.0741	0.357	0.449	0.875
0.9375	-0.222	0.173	0.681	0.131	0.184	0.0796	0.410	0.434	0.937
0.9843	-0.224	0.177	0.679	0.131	0.183	0.0819	0.452	0.422	0.984
0.9863	-0.219	0.243	0.657	0.127	0.178	0.107	0.502	0.407	1.037
0.9882	-0.202	0.301	0.636	0.124	0.173	0.131	0.552	0.390	1.088
0.9902	-0.174	0.353	0.616	0.120	0.168	0.155	0.602	0.371	1.136
0.9921	-0.138	0.398	0.597	0.117	0.164	0.178	0.654	0.350	1.184
0.9941	-0.0954	0.437	0.577	0.114	0.159	0.200	0.708	0.328	1.232
0.9960	-0.0470	0.473	0.555	0.110	0.154	0.226	0.765	0.302	1.280
0.9980	+0.00393	0.514	0.522	0.104	0.146	0.265	0.826	0.273	1.330
1.0000	+0.0521	0.576	0.462	0.0949	0.132	0.335	0.890	0.239	1.381

TABLE 4.14

EQUILIBRIUM AIR. BODY WITH DISCONTINUITY OF CURVATURE
SCHEME I. N = 2

$M_\infty = 5.8$; $p_\infty = 1$ atm; $T_\infty = 300°K$; $\rho_\infty = 1.1765$ kg/m^3;

$w_{max} = 3657$ m/sec; $1/\bar{r} = 2$

s	ε	σ	Φ_1	$\bar{p}_0$	$\bar{T}_0$
0.0000	0.310	1.570	0.00000	1.000	1.000
0.0625	0.309	1.546	-0.00251	0.999	1.000
0.1250	0.307	1.526	-0.0100	0.997	1.000
0.1875	0.304	1.502	-0.0227	0.994	0.999
0.2500	0.299	1.479	-0.0409	0.990	0.998
0.3125	0.292	1.455	-0.0653	0.983	0.996
0.3750	0.284	1.430	-0.0973	0.974	0.994
0.4375	0.275	1.403	-0.137	0.958	0.991
0.5000	0.263	1.367	-0.184	0.930	0.984
0.5625	0.248	1.321	-0.306	0.873	0.971
0.6250	0.239	1.262	-0.467	0.803	0.953
0.6875	0.237	1.199	-0.680	0.717	0.926
0.7500	0.240	1.137	-0.924	0.629	0.900
0.8125	0.250	1.080	-1.187	0.528	0.865

s	u	v	p	T	c^2	w^2	ψ	-x	y
$\xi = 0$									
0.0000	0	0.0000	0.820	0.125	0.158	0.000000	0	0	0.0000
0.0625	0	0.0117	0.820	0.125	0.158	0.000138	0	0	0.0625
0.1250	0	0.0235	0.818	0.125	0.158	0.000553	0	0	0.125
0.1875	0	0.0357	0.816	0.125	0.158	0.00127	0	0	0.187
0.2500	0	0.0488	0.812	0.125	0.158	0.00238	0	0	0.250
0.3125	0	0.0636	0.807	0.125	0.158	0.00404	0	0	0.312
0.3750	0	0.0812	0.799	0.125	0.158	0.00659	0	0	0.375
0.4375	0	0.103	0.786	0.124	0.157	0.0107	0	0	0.437
0.5000	0	0.134	0.763	0.123	0.156	0.0179	0	0	0.500
0.5625	0	0.183	0.716	0.122	0.158	0.0335	0	-0.00390	0.562

TABLE 4.14 Continued

s	u	v	p	T	c^2	w^2	ψ	$-x$	y
0.6250	0	0.232	0.659	0.119	0.155	0.0538	0	-0.0155	0.623
0.6875	0	0.283	0.588	0.116	0.151	0.0805	0	-0.0347	0.683
0.7500	0	0.332	0.516	0.113	0.147	0.110	0	-0.0612	0.739
0.8125	0	0.386	0.433	0.108	0.141	0.149	0	-0.0945	0.792
				$\xi = 0.5$					
0.0000	-0.0674	0.0000	0.805	0.125	0.158	0.00455	0.000000	0.155	0.0000
0.0625	-0.0669	0.0148	0.805	0.125	0.158	0.00469	0.000839	0.159	0.0625
0.1250	-0.0676	0.0299	0.804	0.125	0.158	0.00547	0.00335	0.158	0.125
0.1875	-0.0691	0.0457	0.802	0.125	0.157	0.00687	0.00758	0.157	0.187
0.2500	-0.0714	0.0623	0.799	0.124	0.157	0.00898	0.0135	0.149	0.250
0.3125	-0.0746	0.0800	0.793	0.124	0.157	0.0119	0.0213	0.146	0.312
0.3750	-0.0793	0.0992	0.786	0.124	0.156	0.0161	0.0310	0.142	0.375
0.4375	-0.0864	0.120	0.774	0.123	0.155	0.0220	0.0429	0.137	0.437
0.5000	-0.0979	0.145	0.755	0.122	0.158	0.0308	0.0574	0.131	0.500
0.5625	-0.0919	0.188	0.728	0.121	0.156	0.0438	0.0778	0.119	0.577
0.6250	-0.0836	0.233	0.689	0.119	0.154	0.0616	0.0995	0.100	0.553
0.6875	-0.0726	0.280	0.640	0.116	0.151	0.0838	0.121	0.0757	0.726
0.7500	-0.0582	0.326	0.589	0.113	0.147	0.109	0.144	0.0444	0.797
0.8125	-0.0403	0.369	0.535	0.110	0.143	0.137	0.167	0.00684	0.865
				$\xi = 1$					
0.0000	-0.154	0.0000	0.745	0.123	0.155	0.0237	0.00000	0.310	0.0000
0.0625	-0.154	0.0175	0.745	0.123	0.155	0.0242	0.00182	0.309	0.0625
0.1250	-0.155	0.0352	0.744	0.123	0.159	0.0255	0.00729	0.307	0.125
0.1875	-0.158	0.0527	0.742	0.122	0.159	0.0277	0.0164	0.304	0.187
0.2500	-0.161	0.0706	0.739	0.122	0.158	0.0309	0.0291	0.299	0.250
0.3125	-0.165	0.0889	0.735	0.122	0.158	0.0351	0.0455	0.292	0.312
0.3750	-0.170	0.108	0.730	0.121	0.157	0.0406	0.0656	0.284	0.375
0.4375	-0.176	0.127	0.724	0.120	0.156	0.0475	0.0893	0.275	0.437
0.5000	-0.181	0.156	0.714	0.119	0.155	0.0574	0.121	0.263	0.500
0.5625	-0.179	0.209	0.699	0.117	0.152	0.0761	0.164	0.242	0.593
0.6250	-0.166	0.273	0.675	0.114	0.148	0.102	0.217	0.216	0.683
0.6875	-0.147	0.339	0.645	0.110	0.143	0.136	0.276	0.186	0.770
0.7500	-0.120	0.400	0.612	0.106	0.137	0.174	0.341	0.150	0.855
0.8125	-0.0843	0.455	0.577	0.101	0.132	0.214	0.411	0.108	0.938

TABLE 4.15

$M_\infty = 5.8$; $p_\infty = 1$ atm; $T_\infty = 300°K$; $\rho_\infty = 1.1765$ kg/m^3;

$w_{max} = 3657$ m/sec; $1/\bar{r} = 64$

s	ε	σ	Φ_1	$\bar{p}_0$	$\bar{T}_0$
0.0000	0.490	1.570	0.00000	1.000	1.000
0.0625	0.489	1.550	-0.00101	0.999	1.000
0.1250	0.488	1.542	-0.00407	0.999	1.000
0.1875	0.486	1.527	-0.00918	0.998	1.000
0.2500	0.483	1.513	-0.0163	0.996	0.999
0.3125	0.478	1.498	-0.0256	0.994	0.999
0.3750	0.473	1.483	-0.0373	0.991	0.998
0.4375	0.468	1.468	-0.0516	0.988	0.997
0.5000	0.461	1.452	-0.0688	0.983	0.996
0.5625	0.453	1.435	-0.0895	0.978	0.995
0.6250	0.444	1.418	-0.114	0.970	0.993
0.6875	0.433	1.399	-0.144	0.961	0.992
0.7500	0.422	1.379	-0.179	0.947	0.988
0.8125	0.409	1.358	-0.221	0.929	0.984
0.8750	0.395	1.337	-0.268	0.900	0.977
0.9375	0.380	1.316	-0.318	0.853	0.965
0.9843	0.367	1.304	-0.349	0.791	0.949
0.9863	0.356	1.249	-0.507	0.690	0.920
0.9882	0.349	1.204	-0.663	0.577	0.883
0.9904	0.345	1.158	-0.837	0.445	0.832
0.9921	0.346	1.125	-0.977	0.349	0.786
0.9941	0.350	1.084	-1.166	0.262	0.735
0.9960	0.358	0.966	-1.804	0.161	0.655

TABLE 4.15 Continued

/211

s	u	v	p	T	c^2	w^2	ψ	$-x$	y
				$\xi = 0$					
0.0000	0	0.00000	0.820	0.125	0.158	0.0000000	0	0	0.0000
0.0625	0	0.00741	0.820	0.125	0.158	0.0000550	0	0	0.0625
0.1250	0	0.0147	0.819	0.125	0.158	0.000218	0	0	0.125
0.1875	0	0.0221	0.818	0.125	0.158	0.000491	0	0	0.187
0.2500	0	0.0296	0.817	0.125	0.158	0.000880	0	0	0.250
0.3125	0	0.0374	0.815	0.125	0.158	0.00140	0	0	0.312
0.3750	0	0.0455	0.813	0.125	0.153	0.00207	0	0	0.375
0.4375	0	0.0542	0.810	0.125	0.158	0.00294	0	0	0.437
0.5000	0	0.0636	0.807	0.125	0.158	0.00405	0	0	0.500
0.5625	0	0.0740	0.802	0.125	0.158	0.00548	0	0	0.562
0.6250	0	0.0858	0.796	0.125	0.157	0.00737	0	0	0.625
0.6875	0	0.0994	0.788	0.124	0.157	0.00989	0	0	0.687
0.7500	0	0.115	0.777	0.124	0.156	0.0133	0	0	0.750
0.8125	0	0.135	0.762	0.123	0.156	0.0183	0	0	0.812
0.8750	0	0.161	0.739	0.123	0.159	0.0260	0	0	0.875
0.9375	0	0.197	0.700	0.121	0.157	0.0391	0	0	0.937
0.9843	0	0.239	0.649	0.119	0.154	0.0572	0	0	0.984
0.9863	0	0.298	0.566	0.115	0.150	0.0693	0	-0.000121	0.986
0.9882	0	0.360	0.473	0.111	0.144	0.130	0	-0.000485	0.988
0.9904	0	0.431	0.365	0.104	0.136	0.186	0	-0.00117	0.990
0.9921	0	0.485	0.287	0.0990	0.129	0.235	0	-0.00191	0.991
0.9941	0	0.538	0.215	0.0925	0.120	0.290	0	-0.00295	0.993
0.9960	0	0.612	0.132	0.0825	0.108	0.374	0	-0.00419	0.995
				$\xi = 0.5$					
0.0000	-0.0672	0.00000	0.805	0.125	0.158	0.00452	0.000000	0.245	0.0000
0.0625	-0.0666	0.00937	0.805	0.125	0.158	0.00452	0.000838	0.244	0.0625
0.1250	-0.0668	0.0188	0.805	0.125	0.158	0.00482	0.00334	0.244	0.125
0.1875	-0.0673	0.0284	0.804	0.125	0.158	0.00534	0.00753	0.243	0.187
0.2500	-0.0680	0.0383	0.803	0.125	0.158	0.00610	0.0134	0.241	0.250
0.3125	-0.0691	0.0484	0.802	0.125	0.157	0.00712	0.0209	0.239	0.312
0.3750	-0.0704	0.0589	0.800	0.124	0.157	0.00843	0.0303	0.236	0.375
0.4375	-0.0720	0.0698	0.797	0.124	0.157	0.0100	0.0413	0.234	0.437
0.5000	-0.0741	0.0813	0.793	0.124	0.157	0.0121	0.0542	0.230	0.500
0.5625	-0.0766	0.0933	0.789	0.124	0.156	0.0145	0.0690	0.226	0.562

TABLE 4.15 Continued

s	u	v	p	T	c^2	w^2	ψ	−x	y
0.6250	-0.0797	0.106	0.783	0.123	0.156	0.0176	0.0857	0.222	0.625
0.6875	-0.0837	0.120	0.776	0.123	0.155	0.0214	0.104	0.216	0.687
0.7500	-0.0889	0.135	0.766	0.123	0.159	0.0262	0.125	0.211	0.750
0.8125	-0.0958	0.152	0.753	0.122	0.158	0.0324	0.148	0.204	0.812
0.8750	-0.105	0.172	0.734	0.121	0.157	0.0409	0.175	0.197	0.875
0.9375	-0.120	0.197	0.705	0.119	0.155	0.0533	0.205	0.190	0.937
0.9843	-0.137	0.221	0.671	0.118	0.153	0.0677	0.231	0.183	0.984
0.9863	-0.105	0.227	0.687	0.118	0.154	0.0630	0.241	0.176	1.008
0.9882	-0.0681	0.239	0.692	0.118	0.154	0.0620	0.249	0.168	1.031
0.9904	-0.0228	0.260	0.675	0.118	0.153	0.0683	0.253	0.158	1.056
0.9921	+0.0127	0.284	0.639	0.116	0.151	0.0812	0.254	0.149	1.074
0.9941	+0.0536	0.325	0.567	0.113	0.147	0.108	0.254	0.139	1.095
0.9960	+0.128	0.648	0.0574	0.0825	0.108	0.436	0.253	0.126	1.117
				$\xi = 1$					
0.0000	-0.154	0.0000	0.745	0.123	0.155	0.0237	0.00000	0.490	0.0000
0.0625	-0.154	0.0111	0.745	0.123	0.155	0.0239	0.00182	0.489	0.0625
0.1250	-0.154	0.0224	0.745	0.123	0.155	0.0245	0.00729	0.488	0.125
0.1875	-0.155	0.0336	0.744	0.123	0.159	0.0253	0.0164	0.486	0.187
0.2500	-0.156	0.0448	0.743	0.123	0.159	0.0266	0.0291	0.483	0.250
0.3125	-0.158	0.0560	0.741	0.122	0.159	0.0282	0.0455	0.478	0.312
0.3750	-0.160	0.0675	0.739	0.122	0.158	0.0302	0.0656	0.473	0.375
0.4375	-0.162	0.0791	0.737	0.122	0.158	0.0327	0.0893	0.468	0.437
0.5000	-0.165	0.0912	0.735	0.121	0.157	0.0357	0.116	0.461	0.500
0.5625	-0.168	0.103	0.731	0.121	0.157	0.0393	0.147	0.453	0.562
0.6250	-0.173	0.116	0.728	0.121	0.156	0.0435	0.182	0.444	0.625
0.6875	-0.177	0.130	0.723	0.120	0.156	0.0486	0.220	0.433	0.687
0.7500	-0.183	0.144	0.718	0.119	0.155	0.0547	0.262	0.422	0.750
0.8125	-0.190	0.159	0.712	0.119	0.154	0.0617	0.308	0.409	0.812
0.8750	-0.197	0.174	0.705	0.118	0.153	0.0697	0.357	0.395	0.875
0.9375	-0.205	0.188	0.697	0.117	0.151	0.0780	0.410	0.380	0.937
0.9843	-0.210	0.197	0.693	0.116	0.151	0.0832	0.452	0.367	0.984
0.9863	-0.105	0.227	0.670	0.113	0.147	0.109	0.495	0.353	1.030
0.9882	-0.186	0.315	0.648	0.110	0.143	0.134	0.538	0.337	1.074
0.9904	-0.155	0.370	0.624	0.107	0.139	0.161	0.587	0.318	1.121
0.9921	-0.123	0.409	0.605	0.105	0.136	0.182	0.625	0.301	1.157
0.9941	-0.0830	0.452	0.580	0.101	0.132	0.211	0.670	0.281	1.198
0.9960	-0.0615	0.545	0.500	0.0913	0.119	0.301	0.716	0.257	1.239

CHAPTER 5

FLOWS WITH RADIATION

In this chapter we will solve the supersonic blunt-body problem with consideration of radiation [23]. Scheme II of the method of integral relations was used for the calculation. As a result of the calculations the distribution of gas dynamic parameters in the shock layer with consideration of radiation was obtained. /213

1. System of Equations

The equations of motion of a gas with consideration of radiation were examined earlier in astrophysics and meteorology. Other investigations [54, 55] give a complete system of equations of gasdynamics with consideration of radiation obtained under the most general assumptions.

In the case of an inviscid, non-heat-conducting, thermodynamically equilibrium, nonrelativistic gas flow, this system appears as

$$\frac{d\bar{w}}{dt} = -\frac{1}{\rho}\operatorname{grad} p; \tag{5.1}$$

$$\operatorname{div}(\rho\bar{w}) = 0; \tag{5.2}$$

$$\rho\frac{dh(p, T)}{dt} - \frac{dp}{dt} + q_R = 0; \tag{5.3}$$

$$q_R = 4\pi\int_0^\infty k'_\nu B_\nu d\nu - \int_0^\infty k'_\nu d\nu \int_\Omega I_\nu d\Omega; \tag{5.4}$$

$$\frac{dI_\nu}{dr_*} = k'_\nu(B_\nu - I_\nu); \quad \left(B_\nu = \frac{2h_*\nu^3}{\tilde{c}_*^2}\,\frac{1}{\exp\left(\frac{h_*\nu}{kT}\right) - 1}\right); \tag{5.5}$$

$$p = \rho RT/\mu(p, T), \tag{5.6}$$

where I_ν is the intensity of radiation; $k'_\nu = k_\nu\left[1 - \exp\left(-\frac{h_*\nu}{kT}\right)\right]$ - is the coefficient of absorption with consideration of stimulated emissions; $\tilde{c}_*$ is the velocity of light; k is the Boltzmann const; h_* is the Planck constant; r_* is the direction of radiation transfer; Ω is the volume of gas. /214

The equations of motion, continuity, and state (5.1), (5.2), and (5.6), reta the same form as in the case of flow without radiation. The equation of energy (5.3) contains an additional term q_R which takes into account the heat gain of the gas owing to radiation and is equal to the difference of the radiant energy (5.5) is a new equation. As we see from equation (5.3), when accounting for radiation we must deal with nonadiabatic and nonisentropic gas flows.

The known boundary conditions of gasdynamics for the given problem must be supplemented by special boundary conditions for radiation: in the case of radiating surfaces in the flow the magnitude of the intensity of radiation I_ν must be given.

The equations of gasdynamics with consideration of radiation (5.1)-(5.6) are an integro-differential system of equations, which appreciably complicates the solution of any problem in this region. However, in a number of cases of practical interest we must deal with a certain "limiting" state of the gas when disregarding absorption, we can take into account only radiation (case of volume luminescence). Then the integro-differential system of equations in question changes to a system of ordinary differential equations, and there is no need to solve the equation of transfer of radiant energy. The expression for q_R in this case takes the form

$$q_R = \bar{E} = 4\pi \int_0^\infty k'_\nu B_\nu d\nu, \tag{5.7}$$

where $\bar{E}$ is the quantity of radiant energy emitted by a unit volume in unit time. The quantity $\bar{E}$ is often represented as

$$\bar{E} = 2\tilde{\varepsilon}_* \sigma T^4. \tag{5.8}$$

Comparing (5.8) and (5.7), we find that

$$\tilde{\varepsilon}_* = \frac{2\pi}{\sigma_* T^4} \int_0^\infty k'_\nu B_\nu d\nu = 2\dot{k}_\nu. \tag{5.9}$$

The coefficient $\tilde{\varepsilon}$ characterizes the amount of radiation per unit length and is equal to the frequency-averaged doubled coefficient of absorption (coefficient 2 in the expression for $\bar{E}$ characterizes the radiation yield to both sides). The case where we can disregard absorption corresponds to an optically thin medium, i.e., $\dot{k}_\nu l = \frac{\tilde{\varepsilon}_*}{2} l \ll 1$, where l is a characteristic dimension (for example, thickness of the shock layer).

Another "limiting" case of flows with radiation corresponds to the condition $\dot{k}_\nu l \gg 1$ and leads to "blocking" of radiation [56]. Therefore, the

system in question also becomes differential. It is obvious that when solving different problems both of these cases and the intermediate case $k_\nu l \approx 1$ can be encountered.

The coefficients k'_ν, k_ν, E, characterizing the radiative properties of the gas medium are determined either experimentally or are calculated theoretically; the determination of these coefficients is quite difficult for complex gas mixtures.

2. Statement of Problem and Scheme of Calculation

As is known, behind the front of a detached shock wave formed near the surface of a blunt body during passage of a hypersonic gas flow, different physicochemical transformations, including radiation and absorption of radiant energy, occur. Depending upon the parameters of the medium (p_∞, ρ_∞, T_∞) in which motion occurs and upon the parameters of the medium of the body and flow velocity w_∞, flows differing from those named above can develop during flow of a radiating gas around a body. The case of flow around a blunt body will be examined below on the assumption of volume luminescence.

Let us examine a hypersonic flow of gas encountering, at a constant velocity w_∞, a flat or axisymmetric blunt body. The gas behind the front of the detached shock wave will be considered equilibrium dissociated and ionized. We will calculate flow in the region bounded by the shock wave, axis of symmetry, surface of the body, and boundary characteristic cutting off the region of influence of blunting. The coordinates s and $\xi = n/\varepsilon(s)$ will be considered independent variables here.

The equation of continuity and motion (in projections on the coordinate axes s and ξ) are written out in (1.20). After appropriate approximations they are given in section 3 of the first chapter and for N = 2 in [21]. /216

The equation of energy in the coordinate system s, ξ in a dimensionless form can be written as

$$\frac{\partial}{\partial s}(\bar{t}\,\varepsilon\bar{H}) + \frac{\partial}{\partial \xi}(\bar{N}\bar{H}) + 2EAr\varepsilon = 0, \tag{5.10}$$

where $\bar{H} = h + w^2$.

The equation of energy along the streamline can be written in the form

$$dh - \frac{2}{\rho}dp + \frac{2E}{\rho}dt = 0. \tag{5.11}$$

In equations (5.10) and (5.11) we will also use the designations: h, the specific enthalpy referred to $\frac{1}{2}w^2_{max}$; E, quantity of radiant energy emitted by

a unit volume in unit time referred to $\rho_\infty w_{max}^2/R_0$.

The equation of state in a dimensionless form is

$$\rho = p\mu(p,T)/T, \tag{5.1}$$

where T is temperature referred to $w_{max}^2 \mu_\infty/R$; $\mu(p,T)$ is the molecular weight of the gas at the examined point of the flow referred to the molecular weight of gas in the oncoming flow μ_∞; R is the universal gas constant.

Along the streamlines the well-known differential relation, which does not have its own form in a radiating gas, holds true

$$\rho w dw + dp = 0. \tag{5.1}$$

Along the characteristics in the radiating gas the ratio

$$\left.\begin{aligned} &\frac{v}{w^2}u' - \frac{u}{w^2}v' - \frac{1}{R}s_1' \pm \frac{\operatorname{ctn}\alpha}{\rho w^2}p' \pm \Gamma_1 = 0; \\ &\Gamma_1 = \Gamma_0[(A\tan\theta + \xi\varepsilon_s')s_1' + \varepsilon]\cos\theta; \\ &\Gamma_0 = \frac{\sin\alpha}{\sin(\bar{\beta}\pm\alpha)}\left[\frac{v}{r}\sin\bar{\beta} - \frac{2E}{\rho w c^2(2-\rho h_p)}\right]. \end{aligned}\right\}^* \tag{5.1}$$

holds true.

In the case of volume luminescence the boundary conditions relating the gas parameters on the shock wave have the same form as without consideration of radiation. This means that luminescence does not affect the flow parameters immediately upon passing through the front of the shock wave, but does have an effect on its state only as the gas particles advance from the shock wave toward the body.

The boundary condition on the body is the condition of nonflow

$$u \equiv 0. \tag{5.1}$$

In the case of volume luminescence there is no need to assign the boundary conditions on the body for radiation.

On the axis of symmetry s = 0 the condition

$$v_0 \equiv 0. \tag{5.1}$$

must be fulfilled.

Relation (5.14) must be fulfilled on the boundary characteristic $s_1 = s($

Since it is assumed that the gas behind the shock-wave front is in a state of equilibrium, we must have at our disposal tables of the thermodynamic functions of the corresponding gas at high temperatures. For example, for calculations of air flows we can use the tables in [37]. When conducting our calculations, we used the approximate analytic representations of the thermodymanic functions proposed by V. V. Mikhailov [57 and 58]. The function $\bar{E}$ characterizing the radiative properties of the gas depends, of course, on the type of gas, its temperature, and density. For air the values of $\bar{E}$ are calculated, for example, by B. Kibel [59] and are presented there in the form of graphs. The dependencies of $\bar{E}$ on ρ and T, borrowed from [59], were approximated in the form

$$\bar{E} = 10^5 \left(\frac{\rho}{\rho_0}\right)^{1,3} [10^{0,55(T/1000)} - 10^{1,1}] \tag{5.17}$$

and in this form were used in the calculations. Here ρ_0 is the density of air under normal conditions (p = 1 atm, T = 388°K). The range of applicability of approximations (5.17) is

$$2000^\circ\text{K} \leq T \leq 12\,000^\circ\text{K}, \quad 10^{-4} \leq \rho/\rho_0 \leq 1.$$

As was already noted, the method of integral relations underlies the solution of this problem. It is known that when examining problems of flow around blunt bodies without consideration of radiation by this method, the equation of energy is used as a finite relationship $h + w^2 = 1$, and the equations of motion and continuity are approximated by ordinary differential equations. Since when considering radiation the equation of energy cannot be represented as a finite relation, but has the form (5.10) or (5.11), we can, in this case, /218 either replace equation (5.10) by its approximating ordinary differential equation, or write equation (5.11) approximately along the boundaries of the zones. The second way, which is described below, was used in the calculations.

The equation of energy along the axis of symmetry is written as

$$h_{T_0} T_0' + (h_{p_0} - 2/\rho_0) p_0' + 2E_0 \varepsilon_0/\rho_0 u_0 = 0, \tag{5.18}$$

which follows from (5.11). Furthermore, along s = 0 the relation

$$p_0' = -\rho_0 u_0 u_0', \tag{5.19}$$

holds true, which follows from (5.13).

To write the equation of energy along the boundaries of the zones we will proceed in the following manner. Equation (5.11) is represented as

$$h_T T'_{\text{L.F.}} + \left(h_p - \frac{2}{\rho}\right) p'_{\text{L.F.}} + \frac{2AE}{\rho\nu} s'_{\text{L.F.}} = 0, \tag{5.20}$$

or, having designated $V' = h_T T' + (h_p - 2/\rho)p'$, we obtain (5.11) in the form

$$V'_{L.F.} = -\frac{2AE}{\rho v} s'_{L.F.}$$

Then the value of V' at the boundary of zone $s = s_i(\xi)$ can be determined in terms of the value of V' on the line of flow. Actually, from the obvious equalities

$$V'_{L.F.} = \frac{\partial V}{\partial s} s'_{L.F.} + \frac{\partial V}{\partial \xi}; \quad V'_i = \frac{\partial V}{\partial s} s'_i + \frac{\partial V}{\partial \xi}$$

it follows that

$$V'_i = V'_{L.F.} + \frac{\partial V}{\partial s}(s'_i - s'_{L.F.}). \tag{5.2}$$

This means that the equation of energy (5.11) along the boundary of the zone $s = s_i$ can be written in the form

$$\left[h_T T' + \left(h_p - \frac{2}{\rho}\right)p'\right]_i = -\left[\frac{2AE}{\rho v} s'_{L.F.} + \Lambda\right]_i, \tag{5.2}$$

where

$$\Lambda_i = \left[h_T \frac{\partial T}{\partial s} + \left(h_p - \frac{2}{\rho}\right)\frac{\partial p}{\partial s}\right]_i (s'_i - s'_{L.F.}).$$

The values of the derivatives $\partial T/\partial s$ and $\partial p/\partial s$ entering (5.22) can be found from approximations of p and T by the known values of these functions on the boundaries of the zones. To increase the accuracy of determining $\partial T/\partial s$ and $\partial p/\partial s$ we may introduce additional lines dividing the zones into a number of narrower zones.

Equations (5.12), (5.14), (5.18), (5.19), and (5.22), the equations of the line of flow, characteristics, and the equations obtained on approximating the equations of motion, represent a closed approximating system of ordinary differential equations for the problem in question. Having solved the system relative to derivatives of the unknown functions u_i, v_i, p_i, T_i, ρ_i, and s_1 ($i = 0, 1, 2, \ldots, N$), we obtain a system of equations used for numerical integration. In the second approximation ($N = 2$) this system will have the form

$$s'_1 = \frac{\varepsilon}{A_1 \tan(\beta \pm \alpha) - \xi \varepsilon'_s};$$

$$u'_0 = [-Q_{11}(F_{21}K_{31} - F_{31}K_{21}) + Q_{21}(F_{11}K_{31} - F_{31}K_{11}) - Q_{31}(F_{11}K_{21} - F_{21}K_{11})] / [E_{11}(F_{21}K_{31} - F_{31}K_{21}) - F_{21}(F_{11}K_{31} - F_{31}K_{11})];$$

$$v'_1 = \frac{F_{31}(F_{21}u'_0 + Q_{21}) - F_{21}Q_{31}}{F_{21}K_{31} - F_{31}K_{21}}; \quad u'_1 = -\frac{1}{F_{31}}(Q_{31} - K_{31}v'_1);$$

$$p_0' = \delta_{01} u_0'; \quad p_1' = \delta_{11} u_1' + \delta_{12} v_1' + \delta_{13};$$

$$p_2' = \frac{-Q_4(F_5K_6 - F_6K_5) + Q_5(F_4K_6 - F_6K_4) - Q_6(F_4K_5 - F_5K_4)}{E_4(F_5K_6 - F_6K_5) - E_5(F_4K_6 - F_6K_4) + E_6(F_4K_5 - F_5K_4)};$$

$$u_2' = \frac{Q_5K_4 - Q_4K_5 + (E_5K_4 - E_4K_5)p_2'}{F_4K_5 - F_5K_4};$$

$$v_2' = -\frac{1}{K_6}(F_6p_2' + F_6u_2' + Q_6); \qquad (5.23)$$

$$T_0' = -\frac{1}{h_{T0}}\left[\left(h_{p_0} - \frac{2}{\rho_0}\right)p_0' + \frac{2E_0'\varepsilon_0}{\rho_0 u_0}\right];$$

$$T_1' = -\frac{1}{h_{T1}}\left[\left(h_{p_1} - \frac{2}{\rho_1}\right)p_1' + \frac{2A_1E_1}{\rho_1 v_1}s_{L.F.}' - \Lambda_1\right];$$

$$T_2' = -\frac{1}{h_{T2}}\left[\left(h_{p_2} - \frac{2}{\rho_2}\right)p_2' + \frac{2A_2E_2}{\rho_2 v_2}s_{L.F.}' - \Lambda_2\right].$$

To determine ρ_0, ρ_1, ρ_2, the equation of state (5.12) is used. /220

Most coefficients entering system (5.23) are the same as in [21], except for some coefficients which appear here as

$$\gamma_{01} = \delta_{01}/c_1^2; \quad \gamma_{02} = \frac{2E_0\varepsilon_0}{\rho_0 u_0}\cdot\frac{\rho_{T_0}}{h_{T_0}}; \quad \gamma_{11} = \delta_{11}/c_1^2; \quad \gamma_{12} = \delta_{12}/c_1^2;$$

$$\gamma_{13} = \frac{\delta_{13}}{c_1^2} - \left(\frac{2A_1E_1}{\rho_1 v_1}s_{L.F.}' - \Lambda_1\right)\frac{\rho_{T_1}}{h_{T_1}}; \quad \gamma_{21} = \gamma_{22} = 0; \quad \gamma_{24} = 1/c_2^2;$$

$$\gamma_{23} = -\left(\frac{2A_2E_2}{\rho_2 v_2}s_{L.F.}' - \Lambda_2\right)\frac{\rho_{T_2}}{h_{T_2}}; \quad \delta_{13} = \pm\rho_1 w_1^2 \tan\alpha\left(\frac{s_1'}{R} - \Gamma_1\right),$$

where Γ_1 is taken from the relation along the characteristic (5.14).

Integration of equations (5.23) is performed from the shock wave ($\xi = 1$) up to the body ($\xi = 0$), the conditions on the shock wave serving as the initial conditions for the system. The unknown quantities in integration are the three parameters on the shock wave ε_0, ε_1, ε_2, which are determined from the

boundary conditions on the body (5.15). When performing calculations on an electronic computer the values of the quantities ε_0, ε_1 and ε_2 are found by means of the generalized Newton method.

3. Results of Calculations

Flow of equilibrium air around blunt bodies was calculated in the second approximation according to the scheme proposed in section 2 of this chapter with ($E \neq 0$) and without consideration of radiation ($E = 0$) under different conditions in the oncoming flow. Some of the calculations were made to evaluate the accuracy of the computations. As an investigation of the algorithm of scheme II shows in the case where radiation is disregarded and the equation of energy is used in the exact form $h + w^2 = 1$, the error of the second approximation does not exceed 1 percent. Since in this book we used an approximate writing of the equation of energy (5.21), the error of the computations can be estimated by comparing the results of calculations performed by the given scheme when $E = 0$ with the results of the computations in which the equations of energy is used in an exact form (without E). Such a comparison is given in Table 5.1. From this it follows that within the range of integration the error of the computations is not more than 0.5 percent and increases somewhat only in the region of intersection of the boundary characteristic with the shock wave. We note that the highest accuracy of the calculation is achieved when a minimal region of influence of blunting is examined. Since quantity E characterizing the radiative properties of air is presently determined with an error much larger than the error of computations when $N = 2$, it proved to be expedient to perform the calculations with consideration of radiation only with respect to the second approximation, without increasing the number of the approximation.

To explain the basic regularities characterizing flow around blunt bodies with consideration of radiation, the calculations were performed at different parameters of the oncoming flow ($M_\infty = 10\text{-}35$, $p_\infty = 0.01\text{-}0.00001$ atm, $T_\infty = 220\text{-}300°K$). It was found that in a quantitative respect the effect of radiation substantially depends upon M_∞, p_∞, R_0, and, in a number of cases, is quite appreciable.

As an example of the noticeable effect of radiation, Figures 5.1-5.20 and Tables 5.2-5.5 give certain results of the calculations of an air flow around a sphere of radius $R_0 = 1$ in the cases $E = 0$ and $E \neq 0$ at different M_∞ and p_∞.

As we see from an examination of the tables and graphs, consideration of radiation leads to an appreciable decrease of temperature T and increase of density ρ in the shock layer and on the surface of the streamline body. The change of T and ρ is especially noticeable near the stagnation point ($\xi \to 0$).

The effect of radiation on the profiles T and ρ decreases with distance from the stagnation point toward the characteristic ($s \to s_1$) (Figures 5.1, 5.2, 5.6, 5.7, 5.11, 5.12, 5.15, and 5.16).

Pressure p in the shock layer and on the surface of the body remains virtually unchanged owing to radiation. The slight change of pressure on the boundary characteristic s_1 (Figures 5.3, 5.8, 5.13, and 5.18) is explained both by the change in the angle of inclination of the shock wave and by the change in the position of the characteristic itself. Changes of the tangential component of velocity v in the shock layer owing to radiation also do not occur, except for a small region near the surface of the body ($\xi = 0$) where v noticeably drops (Figures 5.5, 5.10, 5.15, and 5.20). The normal component of velocity u remains virtually unchanged along the axis of symmetry and the

/222

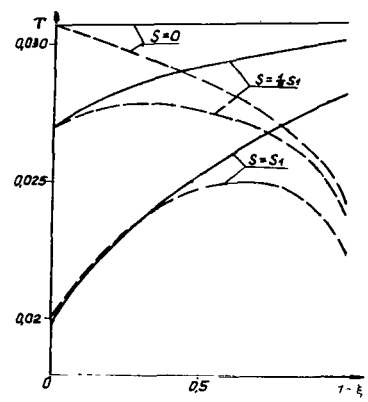

Figure 5.1. Change of temperature along axis of symmetry s = 0, boundary characteristic $s = s_1$, and intermediate line $s = \frac{1}{2}s_1$ for flow past sphere (R_0 = 1 m) of equilibrium dissociated air (M_∞ = 33, p_∞ = 0.0029 atm, and T_∞ = 257°K) with radiation $E \neq 0$ (dashed line) and without consideration of radiation E = 0 (solid line).

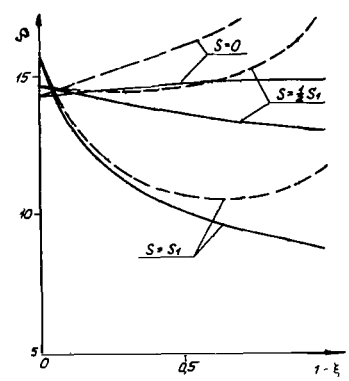

Figure 5.2. Change of density along axis of symmetry s = 0, boundary characteristic $s = s_1$, and intermediate line $s = \frac{1}{2}s_1$ for flow around (R_0 = 1 m) of equilibrium dissociated air (M_∞ = 33, p_∞ = 0.0029 atm, and T_∞ = 257°K) with radiation $E \neq 0$ (dashed line) and without consideration of radiation E = 0 (solid line).

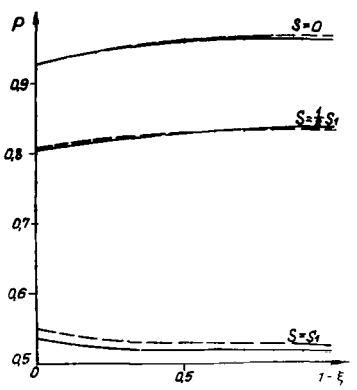

Figure 5.3. Change of pressure along axis of symmetry s = 0, boundary characteristic $s = s_1$, and intermediate line $s = \frac{1}{2}s_1$ for flow past sphere (R_0 = 1 m) of equilibrium dissociated air (M_∞ = 33, p_∞ = 0.0029 atm, and T_∞ = 257°K) with radiation $E \neq 0$ (dashed line) and without consideration of radiation E = 0 (solid line).

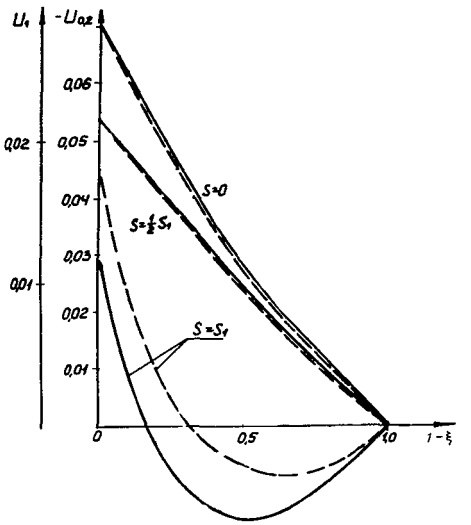

Figure 5.4. Change of normal component of velocity u along axis of symmetry s = 0, boundary characteristic $s = s_1$, and intermediate line $s = \frac{1}{2}s_1$ with flow past sphere (R_0 = 1 m) of equilibrium dissociated air (M_∞ = 33, p_∞ = 0.0029 atm, and T_∞ = 257°K) with radiation $E \neq 0$ (dashed line) and without consideration of radiation E = 0 (solid line).

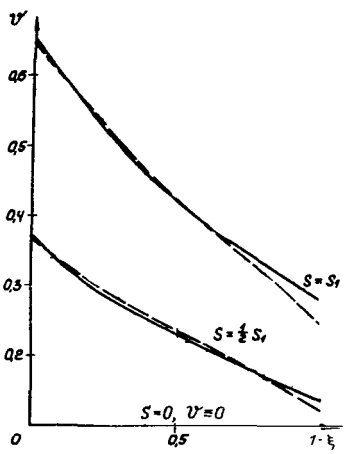

Figure 5.5. Change of tangential characteristic $s = s_1$ and intermediate $s = \frac{1}{2}s_1$ for flow past sphere (R_0 = 1 m) of equilibrium dissociated air (M_∞ = 33, p_∞ = 0.0029 atm, and T_∞ = 257°K) with radiation $E \neq 0$ (dashed line) and without consideration of radiation E = 0 (solid line).

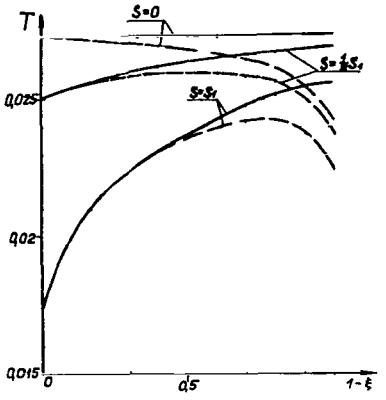

Figure 5.6. Change of temperature along axis of symmetry s = 0, boundary characteristic s = s_1, and intermediate s = $\frac{1}{2}s_1$ for flow past sphere (R_0 = 1 m) of equilibrium dissociated air (M_∞ = 33.5, p_∞ = 0.00047 atm, T_∞ = 270°K) with radiation E ≠ 0 (dashed line) and without consideration of radiation E = 0 (solid line).

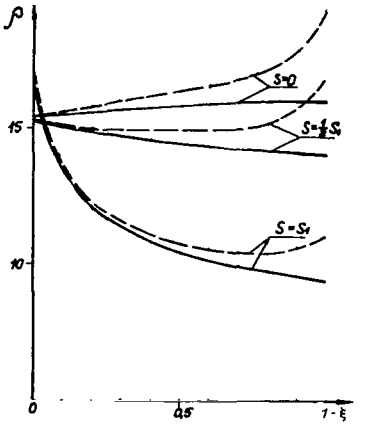

Figure 5.7. Change of density along axis of symmetry s = 0, boundary characteristic s = s_1, and intermediate line s = $\frac{1}{2}s_1$ for flow past sphere (R_0 = 1 m) of equilibrium dissociated air (M_∞ = 33.5, p_∞ = 0.00047 atm, T_∞ = 270°K) with radiation E ≠ 0 (dashed line) and without consideration of radiation E = 0 (solid line).

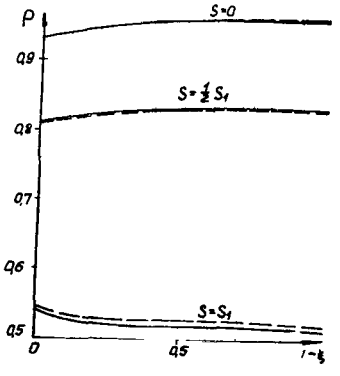

Figure 5.8. Change of pressure along axis of symmetry s = 0, boundary characteristic s = s_1, and intermediate line s = $\frac{1}{2}s_1$ for flow past sphere (R_0 = 1 m) of equilibrium dissociated air (M_∞ = 33.5, p_∞ = 0.00047 atm, T_∞ = 270° K) with radiation E ≠ 0 (dashed line) and without consideration of radiation E = 0 (solid line).

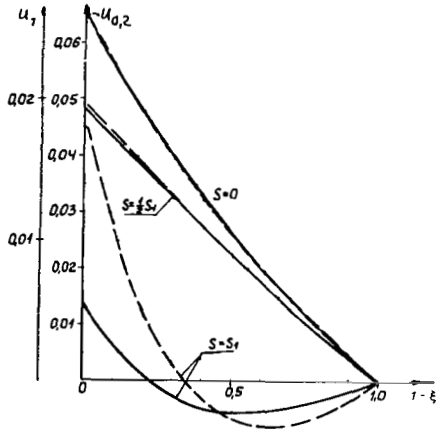

Figure 5.9. Change of normal component of velocity u along axis of symmetry s = 0, boundary characteristic $s = s_1$, and intermediate line $s = \frac{1}{2}s_1$ for flow past a sphere (R_0 = 1 m) of equilibrium dissociated air (M_∞ = 33.5, p_∞ = 0.00047 atm, T_∞ = 270°K) with radiation E ≠ 0 (dashed line) and without consideration of radiation E = 0 (solid line).

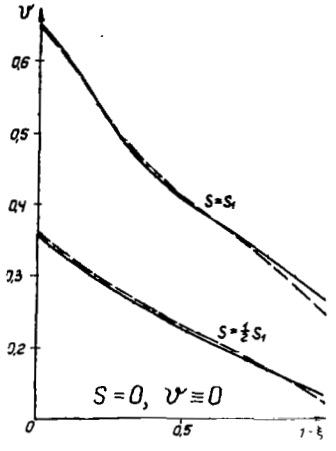

Figure 5.10. Change of the tangential component of velocity u along boundary characteristic $s = s_1$ and intermediate line $s = \frac{1}{2}s_1$ for flow past sphere (R_0 = 1 m) of equilibrium dissociated air (M_∞ = 33.5, p_∞ = 0.00047 atm, T_∞ = 270°K) with radiation E ≠ 0 (dashed line) and without consideration of radiation E = 0 (solid line).

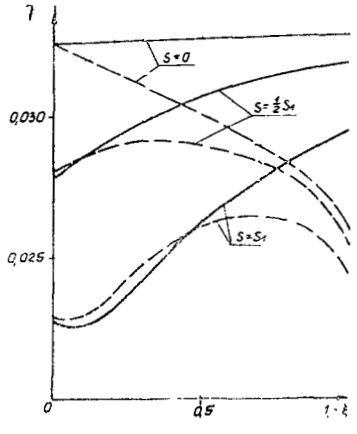

Figure 5.11. Change of temperature along axis of symmetry s = 0, boundary characteristic $s = s_1$, and intermediate line $s = \frac{1}{2}s_1$ for flow past sphere (R_0 = 1 m) of equilibrium dissociated air (M_∞ = 32, p_∞ = 0.01 atm, T_∞ = 250°K) with radiation E ≠ 0 (dashed line) and without consideration of radiation E = 0 (solid line).

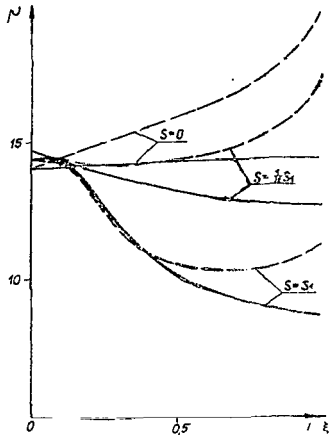

Figure 5.12. Change of density along axis of symmetry s = 0, boundary characteristic s = s_1, and intermediate s = $\frac{1}{2}s_1$ for flow past a sphere (R_0 = 1 m) of equilibrium dissociated air (M_∞ = 32, p_∞ = 0.01 atm, T_∞ = 250°K) with radiation E ≠ 0 (dashed line) and without consideration of radiation E = 0 (solid line).

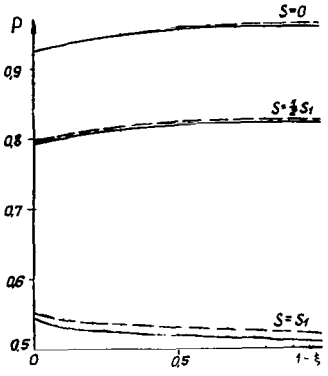

Figure 5.13. Change of pressure along axis of symmetry s = 0, boundary characteristic s = s_1, and intermediate line s = $\frac{1}{2}s_1$ for flow past sphere (R_0 = 1 m) of equilibrium air (M_∞ = 32, p_∞ = 0.01 atm, T_∞ = 250°K) with radiation E ≠ 0 (dashed line) and without consideration of radiation E = 0 (solid line).

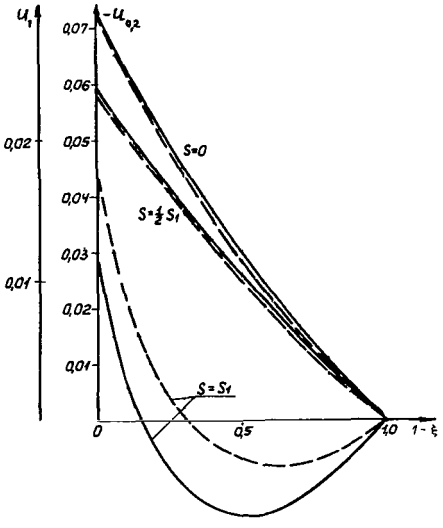

Figure 5.14. Change of normal component of velocity u along axis of symmetry s = 0, boundary characteristic s = s_1, and intermediate line s = $\frac{1}{2}s_1$ for flow past sphere (R_0 = 1 m) of equilibrium air (M_∞ = 32, p_∞ = 0.01 atm, T_∞ = 250°K) with radiation E ≠ 0 (dashed line) and without consideration of radiation E = 0 (solid line).

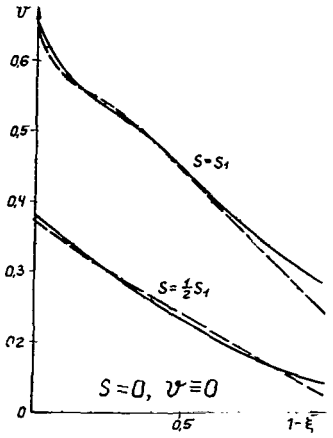

Figure 5.15. Change of tangential component of velocity v along boundary characteristic $s = s_1$ and intermediate line $s = \frac{1}{2}s_1$ for flow past sphere (R_0 = 1 m) of equilibrium dissociated air (M_∞ = 32, p_∞ = 0.01 atm, T_∞ = 250°K) with radiation $E \neq 0$ (dashed line) and without consideration of radiation E = 0 (solid line).

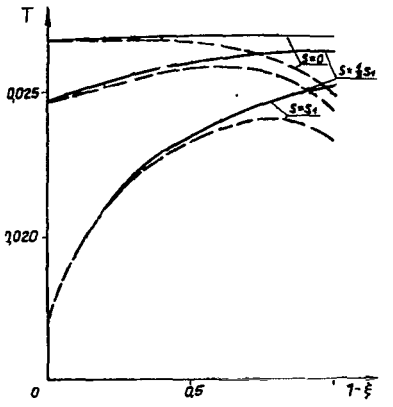

Figure 5.16. Change of temperature along axis of symmetry s = 0, boundary characteristic $s = s_1$, and intermediate line $s = \frac{1}{2}s_1$ for flow past sphere (R_0 = 1 m) of equilibrium dissociated air (M_∞ = 34.5, p_∞ = 0.000249 atm, T_∞ = 250°K) with radiation $E \neq 0$ (dashed line) and without consideration E = 0 (solid line).

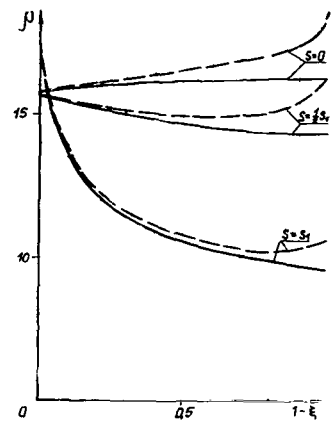

Figure 5.17. Change of density along axis of symmetry s = 0, boundary characteristic $s = s_1$, and intermediate line $s = \frac{1}{2}s_1$ for flow past sphere (R_0 = 1 m) of equilibrium dissociated air (M_∞ = 34.5, p_∞ = 0.000249 atm, T_∞ = 250°K) with radiation $E \neq 0$ (dashed line) and without consideration of radiation E = 0 (solid line).

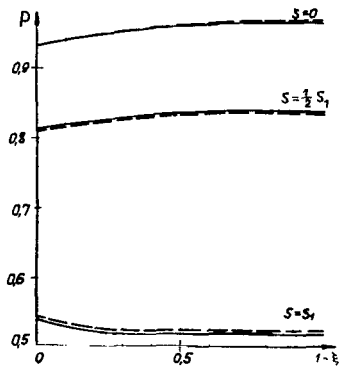

Figure 5.18. Change of pressure along axis of symmetry s = 0, boundary characteristic s = s_1, and intermediate line s = $\frac{1}{2}s_1$ for flow past sphere (R_0 = 1 m) of equilibrium dissociated air (M_∞ = 34.5, p_∞ = 0.000249 atm, T_∞ = 250°K) with radiation E ≠ 0 (dashed line) and without consideration of radiation E = 0 (solid line).

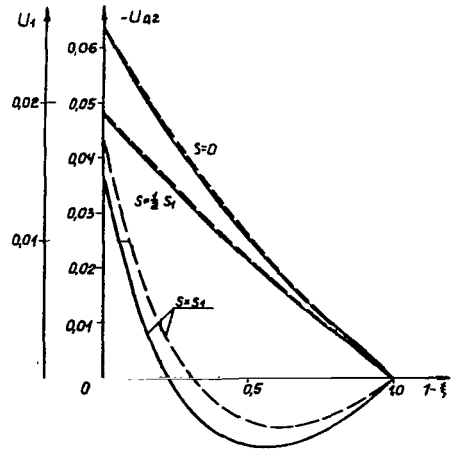

Figure 5.19. Change of normal component of velocity u along axis of symmetry s = 0, boundary characteristic s = s_1, intermediate line s = $\frac{1}{2}s_1$ for flow past sphere (R_0 = 1 m) of equilibrium dissociated air (M_∞ = 34.5, p_∞ = 0.000249 atm, T_∞ = 250°K) with radiation E ≠ 0 (dashed line) and without consideration of radiation E = 0 (solid line).

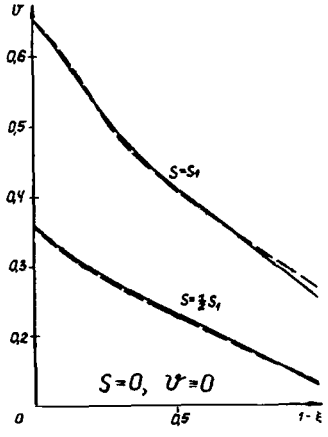

Figure 5.20. Change of tangential component of velocity v along boundary characteristic s = s_1 and intermediate line s = $\frac{1}{2}s_1$ for flow past sphere (R_0 = 1 m) of equilibrium dissociated air (M_∞ = 34.5, p_∞ = 0.000249 atm, T_∞ = 250°K) with radiation E ≠ 0 (dashed line) and without consideration of radiation E = 0 (solid line).

intermediate line, whereas it substantially changes along the boundary characteristic (Figures 5.4, 5.9, 5.14, and 5.19). However, close to the characteristic,u is much smaller than v in absolute value, consequently the value of total velocity w noticeably decreases owing to radiation only on the surface of the body, without changing in the shock layer.

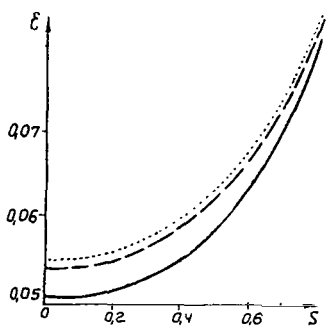

Figure 5.21. Change of the magnitude of separation of the shock wave in relation to s for flow of a dissociated air stream past sphere without consideration of radiation E = 0 (dotted line) and with radiation E ≠ 0 for different R_0 (R_0 = 0.1 m, dashed line; R_0 = 1 m, solid line).

As we see from Figure 5.21, the magnitude of separation of the shock wave from the surface of the streamline body decreases when radiation is taken into account, which is especially noticeable in the region of the stagnation point. This leads, in turn, to an increase of curvature of the detached shock wave in the zone of influence of radiation.

Tables 5.2-5.5 give the results of calculating flow of an equilibrium dissociated air stream past a sphere with radiation (E ≠ 0) and without consideration of radiation (E = 0) along the axis of symmetry (s = 0), boundary characteristic ($s = s_1$), and intermediate line ($s = \frac{1}{2}s_1$). The following data are given: u, v, the normal and tangential components of velocity w; p, pressure; T, temperature; ρ, density; E, quantity of radient energy emitted by a unit volume of gas in unit time. All quantities are given in a dimensionless form.

The program developed in this chapter permits us to perform calculations not only for air but also for other gas mixtures. The solution of the problem of flow past a blunt body with consideration of radiation can be extended to the supersonic region by the method of characteristics.

TABLE 5.1

/228

FLOWS WITH RADIATION

$M_\infty = 10$; $p_\infty = 0.01$ atm; $T_\infty = 300°K$;

$R_0 = 1$ m; $\rho_\infty = 0.01178$ kg/m^3; $w_{max} = 3555$ m/sec.

ξ	s		u		v	
	$E = 0$	without E	$E = 0$	without E	$E = 0$	without E
			$s = 0$			
1.0000	0	0	-0.103	-0.103	0	0
0.8906	0	0	-0.0890	-0.0892	0	0
0.7656	0	0	-0.0741	-0.0742	0	0
0.6406	0	0	-0.0601	-0.0602	0	0
0.5156	0	0	-0.0469	-0.0470	0	0
0.3906	0	0	-0.0345	-0.0346	0	0
0.2656	0	0	-0.0229	-0.0228	0	0
0.1406	0	0	-0.0118	-0.0118	0	0
0.0000	0	0	0.0000	0.0000	0	0
			$s = s_1/2$			
1.0000	0.500	0.500	-0.0727	-0.0733	0.412	0.413
0.8906	0.474	0.474	-0.0666	-0.0670	0.372	0.373
0.7656	0.450	0.450	-0.0581	-0.0585	0.332	0.334
0.6406	0.432	0.432	-0.0489	-0.0492	0.297	0.299
0.5156	0.417	0.417	-0.0393	-0.0395	0.268	0.269
0.3906	0.405	0.404	-0.0296	-0.0298	0.242	0.243
0.2656	0.395	0.395	-0.0200	-0.0201	0.219	0.219
0.1406	0.387	0.387	-0.0105	-0.0105	0.198	0.199
0.0000	0.380	0.380	0.0000	0.0000	0.178	0.179
			$s = s_1$			
1.0000	1.000	1.000	+0.0622	+0.0619	0.677	0.678
0.8906	0.948	0.948	+0.0393	+0.0388	0.646	0.644
0.7656	0.901	0.901	+0.0202	+0.0199	0.599	0.599
0.6406	0.864	0.864	+0.00771	+0.00747	0.550	0.551
0.5156	0.834	0.834	+0.000316	+0.0000570	0.502	0.504
0.3906	0.810	0.809	-0.00329	-0.00358	0.460	0.461
0.2656	0.790	0.790	-0.00410	-0.00442	0.422	0.423
0.1406	0.775	0.775	-0.00284	-0.00318	0.389	0.390
0.0000	0.761	0.761	0.00000	0.00000	0.356	0.359

SCHEME II.

$N = 2.\ \delta = 1;\ R_0 = 1$ m; 0.1 m

TABLE 5.1

$\varepsilon_0 = 0.08626;\ \varepsilon_2 = 0.1030;\ \varepsilon_1 = 0.1865$ (E = 0)

$\varepsilon_0 = 0.08665;\ \varepsilon_2 = 0.1028;\ \varepsilon_1 = 0.1854$ (without E)

p		T		ρ		h	
E = 0	without E	E = 0	without E	E = 0	without E	E = 0	without E
				$s = 0$			
0.858	0.858	0.0827	0.0827	9.465	9.465	0.989	0.989
0.871	0.871	0.0828	0.0828	9.586	9.585	0.992	0.992
0.883	0.883	0.0830	0.0830	9.696	9.695	0.994	0.994
0.892	0.892	0.0831	0.0831	9.782	9.781	0.996	0.996
0.899	0.899	0.0831	0.0831	9.846	9.846	0.997	0.997
0.904	0.904	0.0832	0.0832	9.893	9.893	0.998	0.998
0.907	0.907	0.0832	0.0832	9.924	9.924	0.999	0.999
0.909	0.909	0.0833	0.0833	9.942	9.942	0.999	0.999
0.910	0.910	0.0833	0.0833	9.951	9.948	1.000	0.999
				$s = s_1/2$			
0.703	0.702	0.0760	0.0760	8.729	8.723	0.824	0.823
0.717	0.715	0.0773	0.0772	8.687	8.679	0.856	0.855
0.729	0.728	0.0784	0.0784	8.662	8.652	0.885	0.884
0.740	0.738	0.0793	0.0793	8.649	8.636	0.907	0.907
0.748	0.747	0.0799	0.0799	8.639	8.625	0.925	0.925
0.754	0.753	0.0805	0.0805	8.627	8.612	0.939	0.939
0.758	0.757	0.0809	0.0809	8.611	8.597	0.950	0.951
0.761	0.760	0.0812	0.0812	8.590	8.577	0.959	0.960
0.763	0.761	0.0815	0.0815	8.561	8.548	0.967	0.967
				$s = s_1$			
0.435	0.434	0.0610	0.0609	7.062	7.059	0.536	0.536
0.432	0.431	0.0645	0.0639	6.582	6.646	0.592	0.582
0.431	0.430	0.0677	0.0670	6.196	6.262	0.653	0.640
0.432	0.431	0.0702	0.0696	5.928	5.973	0.707	0.696
0.433	0.432	0.0721	0.0717	5.735	5.760	0.754	0.745
0.435	0.434	0.0736	0.0733	5.588	5.600	0.793	0.786
0.435	0.434	0.0748	0.0746	5.470	5.472	0.824	0.820
0.435	0.434	0.0757	0.0756	5.367	5.364	0.850	0.847
0.433	0.431	0.0766	0.0764	5.330	5.264	0.859	0.868

TABLE 5.2

/230

$M_\infty = 33$; $p_\infty = 0.0029$ atm; $T_\infty = 257°K$;

$R_0 = 1$ m; $\rho_\infty = 0.003988$ kg/m^3; $w_{max} = 10\,623$ m/sec.

ξ	s		u		v	
	$E \neq 0$	$E = 0$	$E \neq 0$	$E = 0$	$E \neq 0$	$E = 0$
			$s = 0$			
1.0000	0	0	-0.0697	-0.0697	0	0
0.8906	0	0	-0.0588	-0.0593	0	0
0.7656	0	0	-0.0475	-0.0484	0	0
0.6406	0	0	-0.0374	-0.0383	0	0
0.5156	0	0	-0.0281	-0.0292	0	0
0.3906	0	0	-0.0198	-0.0209	0	0
0.2656	0	0	-0.0125	-0.0134	0	0
0.1406	0	0	-0.00603	-0.00670	0	0
0.0000	0	0	0.00000	0.00000	0	0
			$s = s_1/2$			
1.0000	0.400	0.400	-0.0532	-0.0533	0.364	0.364
0.8906	0.386	0.385	-0.0468	-0.0469	0.329	0.328
0.7656	0.374	0.372	-0.0393	-0.0394	0.296	0.292
0.6406	0.364	0.363	-0.0318	-0.0320	0.266	0.261
0.5156	0.357	0.355	-0.0245	-0.0250	0.238	0.233
0.3906	0.351	0.349	-0.0176	-0.0182	0.212	0.207
0.2656	0.346	0.344	-0.0112	-0.0119	0.185	0.183
0.1406	0.342	0.340	-0.00552	-0.00606	0.158	0.160
0.0000	0.339	0.337	0.00000	0.00000	0.121	0.137
			$s = s_1$			
1.0000	0.800	0.800	+0.0173	+0.0117	0.641	0.649
0.8906	0.772	0.770	+0.00882	+0.00303	0.592	0.593
0.7656	0.748	0.745	+0.00251	-0.00277	0.533	0.529
0.6406	0.729	0.726	-0.00110	-0.00558	0.478	0.475
0.5156	0.714	0.710	-0.00295	-0.00650	0.430	0.428
0.3906	0.702	0.698	-0.00358	-0.00615	0.386	0.387
0.2656	0.692	0.688	-0.00323	-0.00488	0.344	0.349
0.1406	0.685	0.680	-0.00208	-0.00288	0.301	0.313
0.0000	0.679	0.675	0.00000	0.00000	0.239	0.278

TABLE 5.2

$\varepsilon_0 = 0.05028$; $\varepsilon_2 = 0.05522$; $\varepsilon_i = 0.08091$ ($E \neq 0$)

$\varepsilon_0 = 0.05496$; $\varepsilon_2 = 0.05999$; $\varepsilon_1 = 0.08390$ ($E = 0$)

p		T		ρ		E
$E \neq 0$	$E = 0$	$E \neq 0$	$E = 0$	$E \neq 0$	$E = 0$	
			$s = 0$			
0.926	0.926	0.0306	0.0306	14.306	14.306	1.704
0.936	0.936	0.0303	0.0307	14.726	14.430	1.471
0.945	0.944	0.0298	0.0307	15.197	14.539	1.218
0.952	0.951	0.0293	0.0307	15.668	14.620	0.988
0.957	0.955	0.0288	0.0308	16.154	14.678	0.781
0.960	0.958	0.0281	0.0308	16.676	14.717	0.598
0.962	0.960	0.0274	0.0308	17.276	14.741	0.437
0.963	0.961	0.0265	0.0308	18.061	14.754	0.291
0.963	0.961	0.0242	0.0308	20.327	14.758	0.135
			$s = s_1/2$			
0.805	0.805	0.0270	0.0270	14.682	14.684	0.291
0.812	0.812	0.0275	0.0277	14.502	14.362	0.358
0.818	0.817	0.0277	0.0283	14.433	14.074	0.406
0.822	0.822	0.0278	0.0287	14.481	13.839	0.417
0.825	0.825	0.0276	0.0291	14.634	13.640	0.394
0.828	0.828	0.0273	0.0295	14.896	13.469	0.343
0.829	0.829	0.0268	0.0297	15.290	13.321	0.273
0.830	0.830	0.0260	0.0300	15.906	13.191	0.191
0.829	0.830	0.0237	0.0302	17.916	13.059	0.0904
			$s = s_1$			
0.549	0.539	0.0201	0.0199	15.531	15.488	0.00973
0.538	0.528	0.0215	0.0215	13.220	13.037	0.0165
0.533	0.522	0.0230	0.0229	11.865	11.666	0.0293
0.530	0.520	0.0240	0.0241	11.142	10.869	0.0452
0.529	0.519	0.0247	0.0251	10.737	10.300	0.0599
0.528	0.519	0.0250	0.0260	10.552	9.842	0.0681
0.526	0.518	0.0249	0.0269	10.564	9.453	0.0656
0.525	0.517	0.0244	0.0276	10.816	9.114	0.0518
0.522	0.514	0.0223	0.0283	11.725	8.812	0.0267

TABLE 5.3

/232

$M_\infty = 33$; $p_\infty = 0.0029$ atm; $T_\infty = 257°K$;

$R_0 = 0.1$ m; $\rho_\infty = 0.003988$ kg/m^3; $w_{max} = 10\,623$ m/sec.

ξ	s		u		v	
	$E \neq 0$	$E = 0$	$E \neq 0$	$E = 0$	$E \neq 0$	$E = 0$
			$s = 0$			
1.0000	0	0	-0.0697	-0.0697	0	0
0.8906	0	0	-0.0593	-0.0593	0	0
0.7656	0	0	-0.0484	-0.0484	0	0
0.6406	0	0	-0.0384	-0.0383	0	0
0.5156	0	0	-0.0292	-0.0292	0	0
0.3906	0	0	-0.0209	-0.0209	0	0
0.2656	0	0	-0.0134	-0.0134	0	0
0.1406	0	0	-0.00669	-0.00670	0	0
0.0000	0	0	0.00000	0.00000	0	0
			$s = s_1/2$			
1.0000	0.400	0.400	-0.0533	-0.0533	0.364	0.364
0.8906	0.385	0.385	-0.0469	-0.0469	0.328	0.328
0.7656	0.373	0.372	-0.0394	-0.0394	0.293	0.292
0.6406	0.363	0.363	-0.0321	-0.0320	0.262	0.261
0.5156	0.355	0.355	-0.0250	-0.0250	0.234	0.233
0.3906	0.349	0.349	-0.0183	-0.0182	0.208	0.207
0.2656	0.344	0.344	-0.0119	-0.0119	0.184	0.183
0.1406	0.340	0.340	-0.00606	-0.00606	0.160	0.160
0.0000	0.338	0.337	0.00000	0.00000	0.133	0.137
			$s = s_1$			
1.0000	0.800	0.800	+0.0129	+0.0117	0.647	0.649
0.8906	0.771	0.770	+0.00426	+0.00303	0.592	0.593
0.7656	0.746	0.745	-0.00162	-0.00277	0.529	0.529
0.6406	0.726	0.726	-0.00456	-0.00558	0.475	0.475
0.5156	0.711	0.710	-0.00563	-0.00650	0.429	0.428
0.3906	0.699	0.698	-0.00546	-0.00615	0.387	0.387
0.2656	0.689	0.688	-0.00437	-0.00488	0.348	0.349
0.1406	0.681	0.680	-0.00259	-0.00288	0.311	0.313
0.0000	0.676	0.675	0.00000	0.00000	0.266	0.278

TABLE 5.3

$\varepsilon_0 = 0.05397$; $\varepsilon_2 = 0.05902$; $\varepsilon_1 = 0.08335$ $(E \neq 0)$

$\varepsilon_0 = 0.05496$; $\varepsilon_2 = 0.05999$; $\varepsilon_1 = 0.08390$ $(E = 0)$

p		T		ρ		E
$E \neq 0$	$E = 0$	$E \neq 0$	$E = 0$	$E \neq 0$	$E = 0$	
			$s = 0$			
0.926	0.926	0.0306	0.0306	14.306	14.306	1.704
0.936	0.936	0.0306	0.0307	14.462	14.430	1.471
0.944	0.944	0.0306	0.0307	14.618	14.539	1.218
0.951	0.951	0.0305	0.0307	14.756	14.620	0.988
0.955	0.955	0.0305	0.0308	14.887	14.678	0.781
0.958	0.958	0.0303	0.0308	15.021	14.717	0.598
0.960	0.960	0.0302	0.0308	15.179	14.741	0.437
0.961	0.961	0.0299	0.0308	15.408	14.754	0.291
0.962	0.961	0.0287	0.0308	16.266	14.758	0.135
			$s = s_1/2$			
0.805	0.805	0.0270	0.0270	14.683	14.684	0.291
0.812	0.812	0.0276	0.0277	14.380	14.362	0.358
0.818	0.817	0.0282	0.0283	14.120	14.074	0.406
0.822	0.822	0.0286	0.0287	13.924	13.839	0.417
0.825	0.825	0.0289	0.0291	13.780	13.640	0.394
0.828	0.828	0.0291	0.0295	13.686	13.469	0.343
0.829	0.829	0.0292	0.0297	13.651	13.321	0.273
0.830	0.830	0.0292	0.0300	13.712	13.191	0.191
0.830	0.830	0.0281	0.0302	14.369	13.059	0.0904
			$s = s_1$			
0.541	0.539	0.0199	0.0199	15.497	15.488	0.00973
0.530	0.528	0.0215	0.0215	13.077	13.037	0.0165
0.525	0.522	0.0229	0.0229	11.710	11.666	0.0293
0.522	0.520	0.0241	0.0241	10.919	10.869	0.0452
0.521	0.519	0.0251	0.0251	10.368	10.300	0.0599
0.521	0.519	0.0259	0.0260	9.947	9.842	0.0681
0.520	0.518	0.0266	0.0269	9.626	9.453	0.0656
0.519	0.517	0.0270	0.0276	9.419	9.114	0.0518
0.516	0.514	0.0263	0.0283	9.684	8.812	0.0267

TABLE 5.4

/234

$M_\infty = 33.5$; $p_\infty = 0.0047$ atm; $T_\infty = 270°K$;

$R_0 = 1$ m; $\rho_\infty = 0.0006153$ kg/m^3; $w_{max} = 11\,053$ m/sec.

ξ	s		u		v	
	$E \neq 0$	$E = 0$	$E \neq 0$	$E = 0$	$E \neq 0$	$E = 0$
			$s = 0$			
1.0000	0	0	-0.0647	-0.0647	0	0
0.8906	0	0	-0.0548	-0.0548	0	0
0.7656	0	0	-0.0448	-0.0448	0	0
0.6406	0	0	-0.0355	-0.0356	0	0
0.5156	0	0	-0.0270	-0.0271	0	0
0.3906	0	0	-0.0192	-0.0193	0	0
0.2656	0	0	-0.0122	-0.0123	0	0
0.1406	0	0	-0.00596	-0.00612	0	0
0.0000	0	0	0.00000	0.00000	0	0
			$s = s_1/2$			
1.0000	0.400	0.400	-0.0490	-0.0484	0.360	0.358
0.8906	0.385	0.385	-0.0435	-0.0429	0.322	0.320
0.7656	0.374	0.373	-0.0366	-0.0361	0.289	0.286
0.6406	0.364	0.363	-0.0298	-0.0294	0.260	0.257
0.5156	0.357	0.356	-0.0232	-0.0229	0.234	0.230
0.3906	0.351	0.349	-0.0169	-0.0168	0.208	0.204
0.2656	0.346	0.344	-0.0109	-0.0109	0.184	0.180
0.1406	0.342	0.341	-0.00546	-0.00556	0.159	0.157
0.0000	0.339	0.338	0.00000	0.00000	0.124	0.132
			$s = s_1$			
1.0000	0.800	0.800	+0.0182	+0.0138	0.645	0.651
0.8906	0.771	0.770	+0.00980	+0.00533	0.597	0.595
0.7656	0.748	0.746	+0.00324	-0.000686	0.522	0.518
0.6406	0.729	0.727	-0.000520	-0.00384	0.463	0.461
0.5156	0.714	0.712	-0.00248	-0.00519	0.416	0.416
0.3906	0.702	0.699	-0.00319	-0.00526	0.376	0.377
0.2656	0.692	0.689	-0.00295	-0.00434	0.338	0.341
0.1406	0.685	0.682	-0.00194	-0.00264	0.299	0.306
0.0000	0.679	0.676	0.00000	0.00000	0.244	0.267

TABLE 5.4

$\varepsilon_0 = 0.04908$; $\varepsilon_2 = 0.05535$; $\varepsilon_1 = 0.08162$ ($E \neq 0$)

$\varepsilon_0 = 0.05104$; $\varepsilon_2 = 0.05793$; $\varepsilon_1 = 0.08349$ ($E = 0$)

p		T		ρ		E
$E \neq 0$	$E = 0$	$E \neq 0$	$E = 0$	$E \neq 0$	$E = 0$	
			$s = 0$			
0.931	0.931	0.0273	0.0273	15.400	15.400	0.555
0.940	0.940	0.0272	0.0273	15.620	15.530	0.548
0.948	0.948	0.0271	0.0274	15.852	15.639	0.532
0.954	0.954	0.0270	0.0274	16.084	15.721	0.507
0.958	0.958	0.0269	0.0274	16.328	15.780	0.474
0.961	0.961	0.0267	0.0274	16.604	15.820	0.432
0.963	0.963	0.0264	0.0274	16.951	15.845	0.378
0.964	0.964	0.0259	0.0274	17.468	15.858	0.305
0.965	0.964	0.0241	0.0274	19.372	15.862	0.170
			$s = s_1/2$			
0.811	0.812	0.0251	0.0251	15.332	15.331	0.167
0.817	0.818	0.0255	0.0255	15.115	15.056	0.199
0.822	0.823	0.0257	0.0259	14.967	14.824	0.228
0.826	0.827	0.0259	0.0262	14.891	14.635	0.247
0.829	0.830	0.0260	0.0264	14.879	14.483	0.257
0.831	0.832	0.0259	0.0266	14.939	14.350	0.255
0.832	0.834	0.0258	0.0267	15.096	14.236	0.239
0.833	0.835	0.0254	0.0269	15.436	14.134	0.203
0.833	0.835	0.0237	0.0270	17.060	14.029	0.116
			$s = s_1$			
0.546	0.539	0.0174	0.0172	16.954	16.942	0.00294
0.533	0.526	0.0201	0.0201	13.316	13.114	0.00950
0.529	0.521	0.0218	0.0218	11.998	11.796	0.0203
0.528	0.521	0.0228	0.0229	11.294	11.064	0.0327
0.528	0.521	0.0235	0.0237	10.854	10.559	0.0449
0.527	0.521	0.0239	0.0243	10.575	10.174	0.0549
0.527	0.521	0.0241	0.0248	10.432	9.863	0.0603
0.526	0.520	0.0240	0.0253	10.463	9.600	0.0578
0.523	0.518	0.0224	0.0256	11.103	9.362	0.0347

TABLE 5.5

/236

$M_\infty = 34.5$; $p_\infty = 0.000249$ atm; $T_\infty = 250°K$;

$R_0 = 1$ m; $\rho_\infty = 0.000353$ kg/m^3; $w_{max} = 10\,952$ m/sec.

ξ	s		u		v	
	$E \neq 0$	$E = 0$	$E \neq 0$	$E = 0$	$E \neq 0$	$E = 0$
			$s = 0$			
1.0000	0	0	-0.0634	-0.0634	0	0
0.8906	0	0	-0.0536	-0.0536	0	0
0.7656	0	0	-0.0438	-0.0438	0	0
0.6406	0	0	-0.0348	-0.0347	0	0
0.5156	0	0	-0.0264	-0.0264	0	0
0.3906	0	0	-0.0188	-0.0188	0	0
0.2656	0	0	-0.0120	-0.0120	0	0
0.1406	0	0	-0.00589	-0.00595	0	0
0.0000	0	0	0.00000	0.00000	0	0
			$s = s_1/2$			
1.0000	0.400	0.400	-0.0476	-0.0472	0.359	0.358
0.8906	0.385	0.385	-0.042[illegible]	-0.0419	0.321	0.319
0.7656	0.374	0.373	-0.035[illegible]	-0.0352	0.288	0.286
0.6406	0.364	0.364	-0.0289	-0.0287	0.259	0.256
0.5156	0.357	0.356	-0.0225	-0.0224	0.232	0.229
0.3906	0.351	0.350	-0.0164	-0.0163	0.206	0.204
0.2656	0.346	0.345	-0.0107	-0.0106	0.182	0.180
0.1406	0.342	0.341	-0.00538	-0.00541	0.157	0.156
0.0000	0.339	0.338	0.00000	0.00000	0.126	0.131
			$s = s_1$			
1.0000	0.800	0.800	+0.0171	+0.0143	0.648	0.652
0.8906	0.771	0.771	+0.00870	+0.00583	0.597	0.596
0.7656	0.748	0.747	+0.00229	-0.000218	0.519	0.517
0.6406	0.729	0.728	-0.00128	-0.00342	0.461	0.459
0.5156	0.714	0.812	-0.00307	-0.00484	0.415	0.414
0.3906	0.702	0.700	-0.00361	-0.00498	0.375	0.375
0.2656	0.692	0.690	-0.00320	-0.00415	0.337	0.339
0.1406	0.684	0.682	-0.00204	-0.00254	0.300	0.304
0.0000	0.679	0.677	0.00000	0.00000	0.250	0.265

TABLE 5.5

$\varepsilon_0 = 0.04883$; $\varepsilon_2 = 0.05533$; $\varepsilon_1 = 0.08116$ ($E \neq 0$)

$\varepsilon_0 = 0.04997$; $\varepsilon_2 = 0.05687$; $\varepsilon_1 = 0.08226$ ($E = 0$)

p		T		ρ		E
$E \neq 0$	$E = 0$	$E \neq 0$	$E = 0$	$E \neq 0$	$E = 0$	
			$s = 0$			
0.933	0.933	0.0268	0.0268	15.732	15.732	0.294
0.942	0.942	0.0268	0.0268	15.910	15.862	0.295
0.949	0.949	0.0268	0.0269	16.087	15.972	0.294
0.955	0.955	0.0267	0.0269	16.252	16.054	0.289
0.959	0.959	0.0266	0.0269	16.416	16.113	0.280
0.962	0.962	0.0265	0.0269	16.595	16.153	0.267
0.964	0.964	0.0263	0.0269	16.815	16.178	0.248
0.965	0.964	0.0260	0.0269	17.151	16.191	0.218
0.965	0.965	0.0248	0.0269	18.516	16.195	0.148
			$s = s_1/2$			
0.812	0.813	0.0247	0.0247	15.644	15.644	0.0937
0.818	0.819	0.0251	0.0251	15.396	15.362	0.112
0.824	0.824	0.0254	0.0255	15.206	15.125	0.130
0.827	0.828	0.0256	0.0257	15.077	14.934	0.143
0.830	0.831	0.0257	0.0260	14.999	14.775	0.153
0.832	0.833	0.0258	0.0261	14.976	14.640	0.158
0.834	0.835	0.0257	0.0263	15.022	14.523	0.157
0.834	0.835	0.0256	0.0264	15.197	14.420	0.146
0.834	0.835	0.0244	0.0265	16.308	14.313	0.103
			$s = s_1$			
0.543	0.539	0.0170	0.0169	17.336	17.324	0.00182
0.530	0.525	0.0198	0.0198	13.456	13.318	0.00579
0.526	0.521	0.0214	0.0215	12.114	11.984	0.0121
0.525	0.520	0.0225	0.0225	11.390	11.244	0.0194
0.524	0.520	0.0232	0.0233	10.915	10.733	0.0270
0.524	0.520	0.0237	0.0240	10.586	10.344	0.0339
0.524	0.520	0.0240	0.0245	10.369	10.029	0.0393
0.523	0.520	0.0241	0.0248	10.282	9.763	0.0412
0.521	0.518	0.0232	0.0252	10.627	9.524	0.0313

CHAPTER 6

VISCOUS FLOWS

1. Special Feature of Calculating Viscous Flows

At small Reynolds numbers the effect of viscosity in a number of cases can /238
be so substantial that it is impossible to isolate the regions of flow corresponding to the "external" inviscid flow and the boundary layer. Here is becomes necessary to consider the flow as being completely viscous and to investigate it by means of the Navier-Stokes equations. Such a situation can be created, e.g. in the case of flows of a supersonic gas stream of low density around blunt bodies.

The change to Navier-Stokes equations (henceforth the validity of the equations of continuum mechanics will be everywhere assumed) is associated with a number of difficulties. In particular, as a consequence of the ellipticity of this system a local investigation of flow (for example, in the neighborhood of the stagnation point) is impossible without knowledge of its subsequent history. Furthermore, owing to the high order of the equations the four relations obtained on the basis of the laws of conservation on passing through the shock (which can no longer be considered infinitely thin) and the three natural conditions on the surface of the body (the conditions of attachment or slippage and the conditions for temperature)prove to be inadequate for calculating flow in the region between the shock and the body. In a number of works [60-61, and others] an additional condition of equating to zero on the body surface the normal derivative of the normal velocity component ($\partial u/\partial n = 0$ when $n = 0$) obtained from the equation of continuity on the basis of requiring the finiteness of the density gradient on the wall ($\partial \rho/\partial n < \infty$ when $n = 0$),is used. This condition does not contain, however, new information and is a simple consequence of the equations themselves and of the ordinary boundary conditions on the body. By combining the equation of continuity with the equations of motion and energy we can show, for example, in the case of an insulated surface, that in the /239
presence of attachment the quantity $(\partial \rho/\partial n)_{n = 0}$ can never become infinite, and the equality $(\partial u/\partial n)_{n = 0} = 0$ is identically fulfilled.

To the difficulties of investigating this problem we must also add the additional computational difficulties associated with this cumbersome system and the complex character of behavior of its solutions.

There are a number of simplified approaches to calculate the characteristics of a viscous flow in the neighborhood of the stagnation point of a blunt body at hypersonic velocities [60-65]. They are based on the assumption of thinness of the viscous layer, i.e., smallness of the ration ε/R. For the plane case such an assumption is quite rough: for example, when $\varkappa = 1.4$ and at small Reynolds numbers, $\varepsilon/R = 0(1)$. On the basis of the thin-layer concept, further simplifying assumptions (about certain types of functional relations, concentricity of the shock and body, etc.) are made in [60-63] when investigating flow at the stagnation point, as a result of which the problem is reduced to integration of a system of ordinary differential equations. Unlike these works

H. Cheng [64] determined the flow characteristics in the entire region of blunting. The principal equations obtained from the Navier-Stokes equations with an accuracy up to terms of the order of ε/R are equations of the boundary-layer type. In view of their low order the number of boundary conditions on the body and shock becomes excessive, as a result of which the normal velocity component and temperature experience a discontinuity on the outer boundary of the viscous layer. Another direction developed by M. Van Dyke [65] consists of refining the "boundary layer-inviscid flow" system by means of terms of double asymptotic expansions. Such an approach apparently is worthwhile at sufficient ly large Reynolds numbers when two different regions actually exist.

The results of the calculations of supersonic flow of a viscous gas stream around blunt bodies obtained by the method of integral relations [14] are given later. The assumptions of the hypersonic nature of the flow, thinness of the viscous layer, etc. prove to be superfluous here. The proposed algorithm for calculations of viscous flows can be treated as a generalization of the method developed in [1, 2, and 7] and in other works for the case of an ideal gas. Owing to the complexity of the problem at the first steps of its investigation we did not set out to obtain a final solution. The results presented here were obtained by scheme I of the method of integral relations in the second approximation. It is possible that the numerical data are in need of refinement by improving individual details of the scheme.

2. Statement of Problem

Let us examine flow at a zero angle of attack around a plane symmetric blunt body with a contour having a continuous curvature (flows around axisymmet bodies are investigated in like manner). We will introduce an orthogonal coordinate system s, n (n = 0 - body contour, Fig. 6.1).

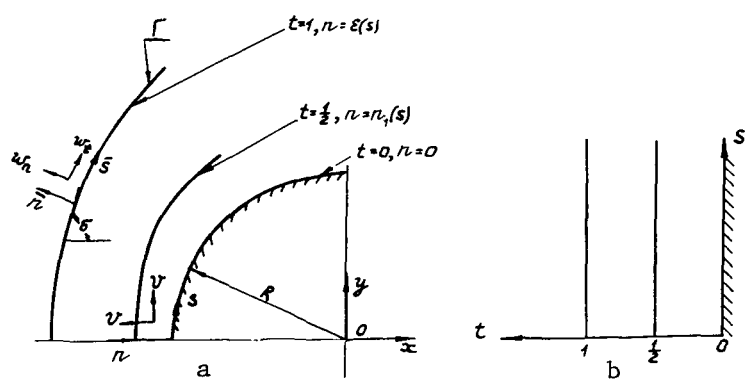

Figure 6.1. Corrdinate system and separation: a) Integration ranges in physical plane (flow around circular cylinder with insulated surface; M_∞ = 5.2; Re = 25; Pr = 0.72; $\varkappa$ = 1.4); b) integration ranges in fictitious plane s, t.

Let us consider the formulation of the problem [14]. We assume that the viscous flow in the region $n > 0$ is described by Navier-Stokes equations, and a unique solution of these equations exists so that when $n = \infty$ the unknown functions u, v, p, and h take given values of the parameters of an undisturbed flow u_∞, v_∞, p_∞, and h_∞ (moreover, $M_\infty^2 = \frac{w_\infty^2}{(\varkappa-1)h_\infty} > 1$ where $w_\infty^2 = u_\infty^2 + v_\infty^2$) and when $n = 0$ the three conditions on the surface of the body ($u = 0$, $v = 0$, and $h = h_0(s)$ or $\partial h/\partial n = 0$) are fulfilled.

At a finite distance from the body we will draw a certain sufficiently smooth line Γ, the equation of which is set as $n = n^*(s) \equiv \varepsilon(s)$ (Fig. 6.1). If we were able to construct the solution of the Navier-Stokes equations in an infinite region $n \geq n^*(s)$ (satisfying the conditions at infinity), then such a solution, depending on three arbitrary functions (for example, on three arbitrary given conditions when $n = n^*$), would determine on line Γ the necessary boundary conditions for a zone of finite width $0 \leq n \leq n^*$. Actually, in this case when $n = n^*(s)$ we will have seven conditions, $u(s)$, $v(s)$, $p(s)$, $h(s)$, $\frac{\partial u}{\partial \bar{n}}(s)$, $\frac{\partial h}{\partial \bar{n}}(s)$ and $\frac{\partial v}{\partial \bar{n}}(s)$ (here the coordinate $\bar{n}$ is reckoned along the normal to Γ), which are obtained with an accuracy up to three arbitrary functions of s. Now solving the problem in the zone $0 \leq n \leq n^*$ (the boundary $n = n^*(s)$ is known), we eliminate the three arbitrary functions by means of the three conditions on the body. In the general case the position of the line Γ can be determined not in an implicit form but by means of the relation

$$F\left[s, u(s,n^*), v(s,n^*), p(s,n^*), h(s,n^*), \left(\frac{\partial u}{\partial \bar{n}}\right)_{n=n^*} \left(\frac{\partial v}{\partial \bar{n}}\right)_{n=n^*} \left(\frac{\partial h}{\partial \bar{n}}\right)_{n=n^*}\right] = 0,$$

which also serves as an additional condition for constructing the boundary of the regions (here $\bar{n}$ is normal to the line $n = n^*(s)$).

In view of the considerable difficulties of determining the solution when $n \geq n^*$ it is expedient to simplify the Navier-Stokes operator in this region. Here, however, the method of constructing the boundary conditions for the zone $0 \leq n \leq n^*$ must be fully retained. It is necessary only to require that on the basis of the laws of conservation both the unknown functions themselves and the derivatives of enthalpy and the velocity components along the normal remain continuous on line Γ. The conditions obtained will now have, of course, an approximate character.

The method of simplifying the Navier-Stokes system is largely determined by the choice of line Γ. In particular, by relating this line to the region of the "diffused" shock wave we can seek the solution when $n \geq n^*$ in the form of an expansion in a small parameter proportional to the curvature of the line Γ or inversely proportional to the Reynolds number (the characteristic scale of viscosity in this case remains fixed). In the calculations carried out we used only the zero terms of this expansion. The order of the following

terms is equal to 0 (1/Re) and higher; moreover the radius of curvature of the body at the stagnation point can be treated in place of the radius of curvature of the line as a characteristic scale of the length upon a change of the functions along the shock wave. After single integration of the equations of zero approximation, the boundary conditions when n = n*(s) are written as

$$\left.\begin{aligned} &\rho w_n = w_{n\infty}; \quad \rho w_n w_t = \frac{\mu^*}{\mathrm{Re}} \frac{dw_t}{d\bar{n}} + w_{n\infty} w_{t\infty}; \\ &\rho w_n^2 + p = \frac{4}{3} \frac{\mu^*}{\mathrm{Re}} \frac{dw_n}{d\bar{n}} + w_{n\infty}^2 + p_\infty; \quad \rho w_n \left(h + \frac{u^2 + v^2}{2}\right) = \\ &= \frac{\mu^*}{\mathrm{Re\,Pr}} \frac{dh}{d\bar{n}} + \frac{\mu^*}{\mathrm{Re}} w_t \frac{dw_t}{d\bar{n}} + \frac{4}{3} \frac{\mu^*}{\mathrm{Re}} w_n \frac{dw_n}{d\bar{n}} + w_{n\infty} \left(h_\infty + \frac{1}{2}\right). \end{aligned}\right\} \qquad (6.1)$$

Here and henceforth in this chapter it is assumed that the gasdynamic quantities are reduced in the following manner to a dimensionless form: velocities are referred to w_∞, pressure to $\rho_\infty w_\infty^2$, density to ρ_∞ enthalpy to w_∞^2, coefficient of viscosity to the coefficient of viscosity μ_r^* when h = 1; $\mathrm{Re} = \rho_\infty w_\infty R_0 / \mu_r^*$.

The line Γ was selected so that regions with comparatively abrupt changes of functions, characteristic for the structure of a shock wave, were outside the zone $0 \leq n \leq n^*(s)$ and were defined as a line on which

$$dw_n / d\bar{n} = 0. \qquad (6.2)$$

This equality, which is fulfilled at certain points of the integral curves of systems (6.1) having a physical meaning, serve as a sign of the "trailing" front of the shock wave (Fig. 6.1). Here we must remember that system (6.1) is a more accurate approach to the Navier-Stokes system "inside" the shock wave and not on its "boundary." However, an expansion of the range of numerical integration "into" the shock wave would appreciably complicate the use of the method of integral relations. Now relations (6.1) - (6.2), together with the conditions on the body, give a sufficient number of boundary conditions, when n = 0 and n = n*, for solving the complete Navier-Stokes equations in region $0 \leq n \leq n^*$ with the unknown boundary

$$n^*(s) = \varepsilon(s).$$

From the point of view of the given formulation of the problem it is /2
expedient that the accuracy of the obtained solutions in zone $0 \leq n \leq n^*$ be determined with the accuracy with which the boundary conditions were found when n = n*. Therefore, to simplify the problem we will examine, when $n \leq n^*$, the equations obtained from the complete Navier-Stokes equations with an order of accuracy no less than the boundary conditions (6.1):

$$
\left.
\begin{aligned}
&\frac{\partial \rho v}{\partial s}+\frac{\partial}{\partial n}[(1+kn)\rho u]=0;\\
&\rho v\frac{\partial v}{\partial s}+(1+kn)\rho u\frac{\partial v}{\partial n}+k\rho uv=-\frac{\partial p}{\partial s}+\frac{1}{\mathrm{Re}}\frac{\partial}{\partial n}\left[(1+kn)\mu^*\frac{\partial v}{\partial n}\right]-\frac{k}{\mathrm{Re}}v\frac{\partial \mu^*}{\partial n};\\
&\rho v\frac{\partial u}{\partial s}+(1+kn)\rho u\frac{\partial u}{\partial n}-k\rho v^2=-(1+kn)\frac{\partial p}{\partial n}+\frac{4}{3\mathrm{Re}}\frac{\partial}{\partial n}\left[(1+kn)\mu^*\frac{\partial u}{\partial n}\right]-\\
&\qquad-\frac{2}{3\mathrm{Re}}\frac{\partial}{\partial n}\left(\mu^*\frac{\partial v}{\partial s}\right)+\frac{1}{\mathrm{Re}}\frac{\partial}{\partial s}\left(\mu^*\frac{\partial v}{\partial n}\right)-\frac{7k}{3\mathrm{Re}}\frac{\partial(\mu^* v)}{\partial s};\\
&\rho v\frac{\partial}{\partial s}\left(h+\frac{u^2+v^2}{2}\right)+(1+kn)\rho u\frac{\partial}{\partial n}\left(h+\frac{u^2+v^2}{2}\right)=\frac{1}{\mathrm{Pr}\,\mathrm{Re}}\frac{\partial}{\partial n}\left[\mu^*(1+kn)\frac{\partial h}{\partial n}\right]+\\
&+\frac{1}{\mathrm{Re}}\frac{\partial}{\partial n}\left[\mu^*(1+kn)v\frac{\partial v}{\partial n}\right]+\frac{4}{3\mathrm{Re}}\frac{\partial}{\partial n}\left[\mu^*(1+kn)u\frac{\partial u}{\partial n}\right]-\frac{k}{\mathrm{Re}}\frac{\partial}{\partial n}(\mu^* v^2).
\end{aligned}
\right\} \qquad (6.3)
$$

Here k is the curvature of the body referred to $1/R_0$.

System (6.3) contains all terms of the gasdynamic equations and boundary-layer equations. It differs from the Navier-Stokes system by the absence of terms with derivatives $\partial^2 v/\partial s^2$, $\partial^2 u/\partial s^2$, $\partial^2 u/\partial s \partial n$, $\partial^2 h/\partial s^2$, etc., the order of which in comparison with terms in the left side of the equations is equal to 0 (1/Re). As an exception, the "extra-order" term $\frac{7}{3}\frac{k}{\mathrm{Re}}\frac{\partial}{\partial s}(\mu^* v)$ is retained in the third equation of system (6.3) which, obviously, does not lessen the accuracy of this system. As calculations showed, unlike the other "extra-order" terms it can make no less a contribution to the solution than the terms written in the right sides of (6.3) when the Reynolds numbers are sufficiently small (Re < 10). This is explained by the presence of the coefficient 7/3 exceeding by a factor of 7 the coefficient obtained by mutual compensation of the two preceding terms.

Although system (6.3) is not elliptic, the disturbances it describes can propagate upstream; however, unlike the complete equations this propagation is determined not by secondary derivatives with respect to s, but by derivatives of pressure. Thus, the number of boundary conditions at the stagnation point /244 and on the axis of symmetry is insufficient for solving the problem with initial data on the line s = 0. By virtue of the fact that the higher derivatives with respect to n in (6.3) are the same as in the complete Navier-Stokes equations, the necessary boundary conditions of the problem, when n = 0 and n = n*, are determined by the conditions on the body and by relations (6.1) - (6.2).

3. Construction of Solution

To construct the solution of the system (6.3) we used scheme I of the method of integral relations. After introducing new functions the equivalent

$$\varphi = \partial v/\partial n; \quad \psi = \partial u/\partial n; \quad \eta = \partial h/\partial n \qquad (6.4)$$

system of first-order equations, which includes equalities (6.4), is reduced to a divergent form and is integrated over the coordinate from the surface of the body to the boundary of each of the zones $n = n_j(s)$ into which the integration range $0 \leq n \leq n^*$ is separated (Fig. 6.1):

$$n_0 \leq n_j \leq n \leq n_{j+1} \leq n_N, \quad n_0 = 0, \quad n_N = n^*, \quad j = 0, 1, \ldots, N-1.$$

For example, the second equation of system (6.3) is written as

$$\frac{d}{ds}\int_0^{n_j} \rho v^2 dn - (\rho v)_j \frac{dn_j}{ds} + (1+kn)(\rho uv)_j + k\int_0^{n_j} \rho uv dn = -\frac{d}{ds}\int_0^{n_j} p dn + \\ + p_j \frac{dn_j}{ds} + \frac{1}{\mathrm{Re}}(1+kn_j)\mu_j^* \varphi_j - \frac{1}{\mathrm{Re}}\mu_0^* \varphi_0 - \frac{k}{\mathrm{Re}}(\mu^* v)_j + \frac{k}{\mathrm{Re}}\int_0^{n_j} \mu^* \varphi dn. \tag{6.5}$$

Here and henceforth the values of the functions or their products on the corresponding zones are designated by an index. The integrands ρv^2, ρuv, $\rho v\left(h+\frac{u^2+v^2}{2}\right)$, ρv, p, φ, ψ, η, and also the viscosity μ^* are replaced by interpolation polynomials with the interpolation points on the boundaries of the zones. All other complexes of the functions (such as $\mu^*\phi$, etc.) are represented as the product of corresponding interpolation polynomials for cofactors.

Since within the integration range there is a sufficiently abrupt change of the profiles of the gasdynamic functions across the "shock" layer (corresponding to the "external" flow and "boundary layer"), interpolation of the functions is performed not with respect to the coordinate n, but for a certain new variable, $t(n,s)$, which approximately describes the profiles of the tangential velocity component at a fixed value of the coordinate s. With a successful selection of the function t (regardless of the relative dimensions of the "boundary-layer"), in the entire integration range $0 \leq n \leq n^*$ the dependence $v(t)$ (or $\rho v(t)$) will be close to linear, $\rho v^2(t)$ close to quadratic, etc. In this case transformation of $t(s, n)$ will produce such extension of the "boundary-layer" and compression of the "external" flow that the character of change of the interpolated functions will be sufficiently smooth and identical in the entire examined region. /2

Function t was defined as the solution of the equation

$$a\frac{d^2t}{d\xi^2} + \frac{dt}{d\xi} - c = 0 \tag{6.6}$$

with boundary conditions

$$t(0) = 0; \quad t(1) = 1; \quad \xi = \frac{n}{n^*}. \tag{6.7}$$

This equation is a rough one-dimensional analog of the investigated flow: when $a \to 0$ we obtain, by double asymptotic expansion, the "external flow" with a constant "vorticity" $dt/d\xi$ and the "boundary layer" with an exponential "velocity" profile t.

The solution of equation (6.6), satisfying the boundary conditions (6.7), has the form

$$t(\xi, a) = c\xi + (1-c)\frac{1-\exp(-\xi/a)}{1-\exp(-1/a)}, \qquad (6.8)$$

where parameter a plays the role of the effective thickness of the "boundary layer"; c is a constant.

After changing to variables s, t, the region $0 \leq n \leq n^*$ is transformed to a zone of constant width $0 \leq t \leq 1$, and separation of the integration range into N zones is accomplished by the lines

$$t_j(\xi_j, a) = j/N, \quad j = 0, 1, \ldots, N.$$

The rectilinear calculated network in the fictitious plane (s, t) (Fig. 6.1, b) corresponds to a certain uneven separation in the physical plane s, n (Fig. 6.1, a).

Setting in (6.8) $c = 1/N$ ($1 = 0, 1, \ldots, N-1$), we derive that in plane (s, t) the regions of flow corresponding to the "external" flow and to the "external" flow and to the "boundary layer" are "mapped" respectively onto ℓ and $N - \ell$ zones. This means that if $a \to 0$ together with the thickness of the boundary layer, then $\xi_{N-\ell-1} \to 0$, and the quantity $\xi_{N-\ell}$ is not zero. Thus, the flow pattern in the plane (s, t) should not greatly change with a change of the Reynolds number, provided that parameter a always has the order of relative thickness of the boundary layer. Therefore, the introduction of the variable t permits, generally speaking, performing calculations in a sufficiently wide range of Re numbers at a comparatively low number of the approximation. In the calculations, the results of which are given below, constant c in the solution of (6.8) was assumed to be equal to zero. This corresponds to small Reynolds numbers when the entire flow can be considered viscous. /246

The degrees of the approximating polynomials are determined by the character of behavior of the functions near the surface of the body and also by the number of the approximation. For example,

$$\rho v^2 = \sum_{k=2}^{N+1} A_k t^k; \quad \rho uv = \sum_{k=3}^{N+2} B_k t^k; \quad p = \sum_{k=0}^{N} P_k t^k.$$

When setting up these polynomials we also took into account, in addition to the boundary conditions of the body, that when $n \to 0$, $v = 0(n)$, $u = 0(n^2)$, $p = p_0 +$

O(n), etc. The sum of the highest powers of all polynomials is by one unit less than the corresponding sum with the usual approximation in the physical plane. This is related to the introduction of the parameter a which is treate here as an unknown function.

Coefficients A_k, B_k, P_k etc., are determined from the corresponding conditions at the interpolation nodes in the form

$$A_k = \sum_{i=1}^{N} a_i^{(k)} \rho_i v_i^2; \quad B_k = \sum_{i=1}^{N} b_i^{(k)} (\rho u v)_i; \quad P_k = \sum_{i=1}^{N} d_i^{(k)} p_i \quad \text{etc.},$$

where $a_i^{(k)}$, $b_i^{(k)}$, $d_i^{(k)}$ are numerical coefficients. After this the corresponding integrals are written as linear combinations of the values of the functions at the interpolation points with coefficients depending on a:

$$\int_0^{n_j} \rho v^2 dn = n^* \int_0^{\xi_j} \rho v^2 d\xi = n^* \sum_{i=1}^{N} \sigma_{ij}^a (a) \rho_i v_i^2 \qquad (6.9)$$

etc., where

$$\sigma_{ij}^a (a) = \sum_{k=2}^{N+1} a_i^{(k)} \int_0^{\xi_j} t^k d\xi.$$

When c = 0, $\xi = -a \ln \{1 - [1 - \exp(-1/a)]t\}$, the quadratures in (6.9) are calculated in a finite form and the integral relations change to a system of ordinary quasilinear first-order differential equations. To this system are added the boundary conditions on the surface of the body and line Γ (6.0) - (6 written in a differential form in a coordinate system s, n. The approximating system is closed by means of the obvious geometric relation

$$d\varepsilon/ds = (1 + k\varepsilon) tg\, \tau,$$

where $\varepsilon = n^*(s)$, and τ is the angle of inclination of line Γ to the contour of the body.

After eliminating the functions characterizing friction on the body surfa 4N + 4 equations, in the case of an insulated wall, form a closed approximatin system with unknown functions u_i, v_i, p_i, h_0, h_i (i = 1, 2, ..., N), a, ε, τ. The magnitude of pressure on the surface of the body is determined from the relation

$$p_0 = \frac{\varkappa - 1}{\varkappa} h_0 \frac{(\rho v)_{t=0}^2}{(\rho v^2)_{t=0}}.$$

For conciseness we write the obtained system of the N-th approximation in the form

$$S(\vec{z}, s)\frac{d\vec{z}}{ds} = \vec{b}(\vec{z}, s), \qquad (6.10)$$

where S is the matrix; $\vec{z}$ is a vector, the components of which are the unknown functions; $\vec{b}$ is a vector of the right-hand side. In view of its awkwardness we will introduce only simple equations obtained, for example, from the equation of continuity

$$\varepsilon \sum_{i=1}^{N} \sigma_{ij}^{r} \frac{d(\rho v)_i}{ds} + \varepsilon \frac{da}{ds}\left[\sum_{i=1}^{N} \bar{\sigma}_{ij}^{r} (\rho v)_i - (f\rho v)_j\right] =$$

$$= -(1+\varepsilon k\xi_j)(\rho u)_j - (1+\varepsilon k)\operatorname{tg}\tau\left[\sum_{i=1}^{N} \sigma_{ij}^{r}(\rho v)_i - (\xi\rho v)_j\right];$$

$$\rho_j = \frac{\varkappa}{\varkappa-1}\frac{p_j}{h_j},$$

here $\sigma_{ij}^{r}(a)$ are functions determined in accord with (6.9), /248

$$\bar{\sigma}_{ij}^{r}(a) = d\sigma_{ij}^{r}/da; \quad f_j = d\xi_j/da.$$

Since parameter a enters the equations as an unknown function, transformation of (6.8) itself depends upon the solution of system (6.10) and changes along the surface of the body. In this case the width of the zones $n_j(s)$ will change in the physical plane s, n together with the effective thickness of the "boundary layer."

Let us examine the singularities of the approximating system. On the axis of symmetry system (6.10) has a singularity as a consequence of degeneration of matrix S, when s = 0, therefore to start integration of the approximating system from the axis of symmetry all functions entering the system were represented as expansions which, by virtue of the conditions of symmetry ($\tau = 0$, $v_i = 0$, $du_i/ds = 0$ when $s = 0$) have the form

or

$$\left.\begin{aligned} z_i &= z_i^{(1)} s + z_i^{(3)} s^{(3)} + \dots \\ z_i &= z_i^{(0)} + z_i^{(2)} s^2 + \dots . \end{aligned}\right\} \qquad (6.11)$$

The system of algebraic equations obtained after substitution of series (6.11) into (6.10) are closed, but to determine the coefficients of these expansions N relations are insufficient. Thus, on integration of symmetry, N boundary conditions remain unknown. This is a consequence of the "elliptic" properties of the initial system (6.3), which are determined by the presence of partial derivatives of pressure in it. However, it turned out that N unknown parameters, when s = 0, are uniquely determined from the conditions of regularity at N singular points; moreover, N - 1 singularities have the sa form as in the case of an inviscid flow and are singular points of the saddle type. We can show that their origin is related to the absence of a term with a higher derivative $\partial^2 v/\partial s^2$ in equations (6.3), so that the coefficients of dv_i/ds in approximating system (6.10), which are determinable only by the gasdynamic terms of system (6.3), reduce, with appropriate transformations, t a form characteristic for the case of an ideal gas.

For the passage of the singular points the equations containing the derivatives dv_i/ds were represented in the form

$$M_j(\vec{z}, s)\, dv_i/ds = N_j(\vec{z}, s), \quad j = 1, 2, \ldots, N-1,$$

In so doing the integral curves of the solution were selected so that at the singular point the equalities $M_j = 0$ and $N_j = 0$ were fulfilled simultaneously In addition to the singularities of the saddle-point type, the approximating system has one node. We can show that determination of the derivative da/ds reduces the solution of the equation

$$P(\vec{z}, s)\, da/ds = Q(\vec{z}, s),$$

where P and Q vanish simultaneously at a certain value of the coordinate s. The change of functions P and Q in the neighborhood of P = 0, Q = 0, derived in the process of integration of system (6.10), has the character shown in Fig. 6.2, and is typical for a node. Among the integral curves (6.10) we selected those which had a holomorphic direction when P = 0, Q = 0.

4. Some Results of Calculations

When performing the calculations on a computer we used a general-purpose program suitable for computing the arbitrary approximation ($N \geq 2$) with prelimi adjustment for the parameter N. Prior to programming, the approximating syst (6.10) was not solved relative to the derivatives of the unknown functions -- reduction to a normal form was accomplished directly during integration. For this purpose we calculated the functions M_j, N_j, P, and Q, which are necessar for satisfying the conditions of regularity at the singular points.

Before starting the calculation we assigned the parameters a (0) and ε (0) when N = 2,(and the parameters a(0), $\varepsilon(0)$, $u_j(0)$ (j = 2, ..., N - 1) when n > 2. To calculate the coefficients of expansions (6.11) $z_i^{(0)}$, $z_i^{(2)}$, z(

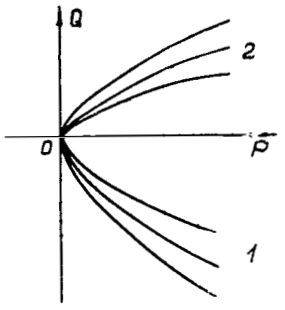

Figure 6.2. Pattern of behavior of functions P and Q in neighborhood of node P = 0, Q = 0.

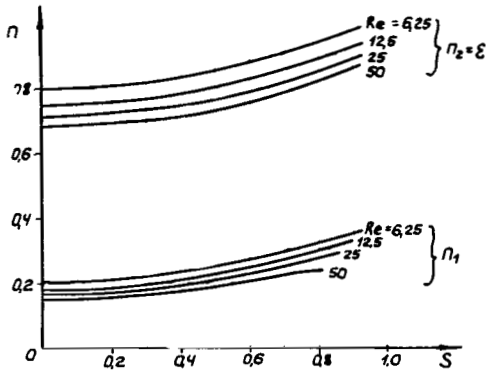

Figure 6.3. Boundaries of zones in physical plane at different numbers (flow around circular cylinder; M_∞ = 5.2; Pr = 0.72; $\varkappa$ = 1.4).

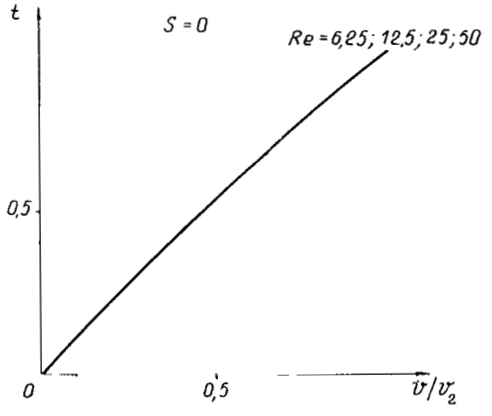

Figure 6.4. Distribution along axis of symmetry of tangential velocity component referred to value on line $n = n_2 \equiv \varepsilon(s)$ at different Re numbers (flow around a circular cylinder; M_∞ = 5.2; Pr = 0.72; $\varkappa$ = 1.4).

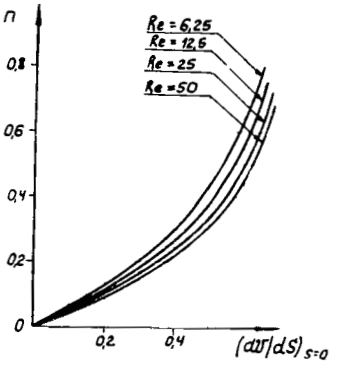

Figure 6.5. Profiles of gradient of tangential velocity component on axis of symmetry in physical plane at different Re numbers (flow around circular cylinder; M_∞ = 5.2; Pr = 0.72; $\varkappa$ = 1.4).

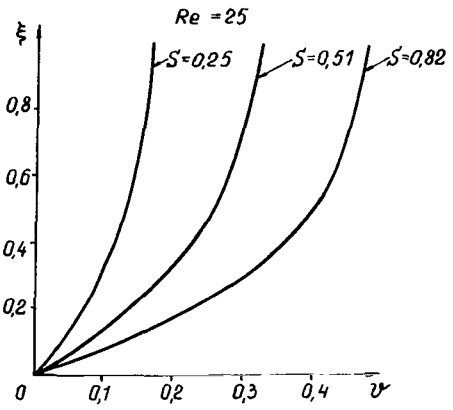

Figure 6.6. Profiles of tangential velocity component at different values of coordinate s (flow around circular cylinder; M_∞ = 5.2; Pr = 0.72; $\varkappa$ = 1.4).

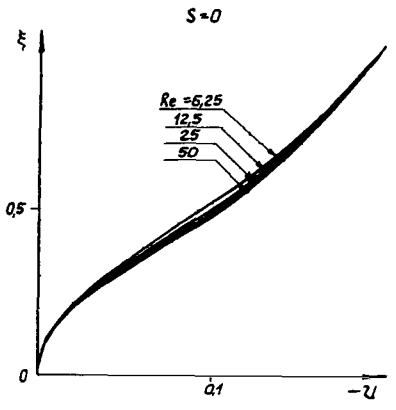

Figure 6.7. Profiles of normal vel component on axis of symmetry at different Re numbers (flow around lar cylinder; M_∞ = 5.2; Pr = 0.72; $\varkappa$ = 1.4).

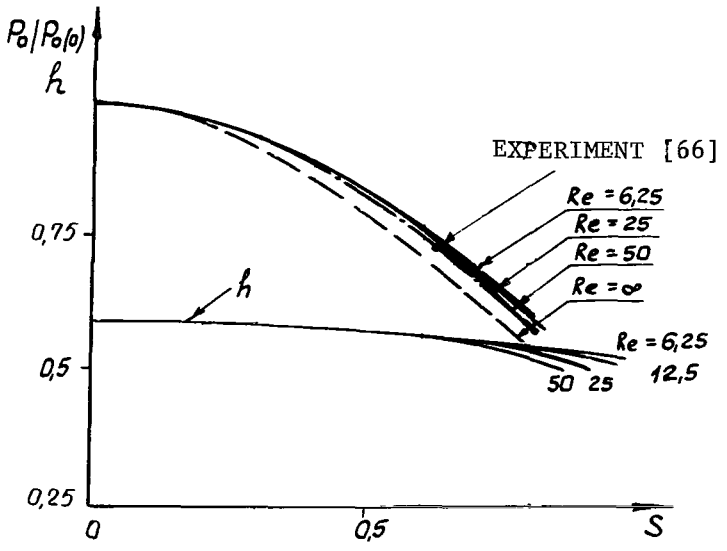

Figure 6.8. Distribution of pressure and enthalpy along surface of circular cylinder at different Re numbers (M_∞ = 5.2; Pr = 0.72; $\varkappa$ = 1.4).

$z_i^{(3)}$ the systems of algebraic equations were solved by the iterative method. After departure from the axis of symmetry integration was performed by the Runge-Kutta method with the use of the first two terms of the corresponding series. For the passage of the node the initial parameters were selected so that at their sufficiently small change the dependence Q(P) passed from one bundle of branches to another (bundles 1 and 2, Fig. 6.2). The principal criterion of the correctness of the selection of the holomorphic direction was the closeness of the values of the derivative da/ds before and after the singular point. The saddle points passed just as in the case of an ideal gas. The selection of the necessary values of the parameters when s = 0 was achieved as a result of multiple solution of the Cauchy problem. /252

Certain results of calculations in the second approximation (N = 2) of viscous gas flow around plane blunt bodies are given in [14] and in this chapter. In [14] bodies with a contour, the curvature of which varied according to the law $k = 1-bs^2$, were examined at numbers $M_\infty = 10$, Pr = 0.72, and Re = 50. Figures 6.3 - 6.10 and the tables presented here give the characteristics of flow around a circular cylinder obtained at $M_\infty = 5.2$; Pr = 0.72, and several values of the Re numbers (Re = 6.25; 12.5; 25; and 50). It was assumed that the surface of the body was insulated, and viscosity varied according to the law $\mu^* \sim h^{1/2}$; the adiabatic exponent is $\varkappa = 1.4$.

The position of the boundaries of zones n_1 and $n_2 = \varepsilon(s)$ (line Γ) in the physical plane n, s is shown in Fig. 6.3. Figure 6.4 shows, when s = 0, the velocity profiles of v/v_2 in the fictitious plane t, s which were obtained by means of interpolation polynomials, and Fig. 6.5 shows the same profiles in the physical plane constructed as the dependences $(dv/ds)_{s=0}$ on n. We see from a comparison of the curves that the function v(t), unlike v(n), is close to linear and in the examined range of Re numbers has an almost universal character.

Figure 6.6 shows the velocity profiles v(s) at different values of the coordinate s (Re = 25). From here we see that with an increase of distance from the stagnation point these profiles become more "filled." As an example of the change of the normal velocity components (with respect to the normal to the surface of the body), Fig. 6.7 shows the velocity profiles u on the axis of symmetry (just as the velocity profiles v, they were obtained by interpolation polynomials for corresponding complexes).

The distribution of pressure and enthalpy along the surface of the body is shown in Fig. 6.8. The same figure also shows the curve for the case of /253 an ideal gas plotted according to the data of [17] ($M_\infty = 5$, $\varkappa = 1.4$) and also the curve corresponding to the experimental data of O. Tewfik and W. Giedt obtained for an insulated cylinder at numbers $M_\infty = 5.73$ and $Re_\infty = 2050$ [66]. As we see from the curves, the distribution of the ratio of pressures $p_0(s)/p_0(0)$ changes little with a change of the Re number (the curves for

Re = 6.25, 12.5, and 25 relatively coincide and, comparatively, do not differ much from the corresponding distribution for an ideal gas (Re = ∞). However, the change of the friction coefficient along the surface of the body, shown i Fig. 6.9, depends largely on the Re number. For comparison with friction und conditions of a free molecular flow ($C_{f\ fr.m}$) the same figure shows the cur (dashed line) corresponding to diffuse reflection at an accommodation coeffici equal to 1. The dependences on Re numb of pressure $p_0(0)$ and the ratio $C_f/C_{f\ f}$ taken at the stagnation point are prese in Fig. 6.10. As the Re number decreas the value of $p_0(0)$, which can be identi with the usually measured quantity p_0' (stagnation pressure at the stagnation point), increases, although this increa becomes substantial only at sufficientl small Re numbers (Re < 10). When Re ≳ this quantity practically reaches the asymptote and differs from a correspond value of p_0' in an inviscid flow only at the third decimal point. The indicated difference can be treated to some exten as an estimate of the accuracy of the calculations of the method when N = 2. The ratio ($C_f/C_{f\ fr.m}$) increases with a decrease of the Re number and has a ten ency, when Re → 0, to approach its value in a free molecular flow, however, i is impossible to make definite conclusions here by virtue of the fact that th region of values of very small Re numbers is outside the limits of applicabil of both the method and of the Navier-Stokes equations. Furthermore, Fig. 6.1 shows the change of the coordinates s_* of the singular points as a function o the value of Re numbers (with a decrease of Re the singular points recede frc the stagnation point).

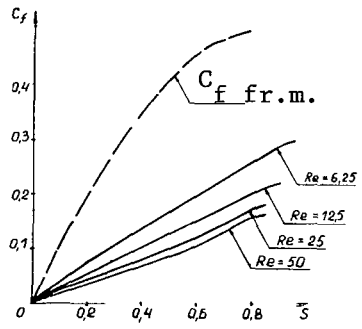

Figure 6.9. Distribution of coefficient of friction along surface of circular cylinder at different Re numbers (M_∞=5.2; Pr = 0.72; $\varkappa$ = 1.4); $C_{f\ fr.m}$ is value of friction coefficient in free molecular flow (diffuse reflection, accommodation coefficient equal to 1).

Tables 6.1 - 6.4 give the values of the flow parameters (u, v are the normal tangential velocity components, respectively; p is pressure; h is enthalpy) on the surface of a circular cylinder (t = 0, n = n_0 = 0), on the intermediate line (t = 1/2, n = n_1(s)), and on the external boundary of the integration range (line Γ, t = 1, n = n_2 = ε(s)) at various values of s. The Cartesian coordinates of the boundaries of zones $n_0(s) \equiv 0$, $n_1(s)$ and $n_2(s)$ i the physical plane are denoted, respectively, by (x_0, y_0), (x_1, y_1), (x_2, y_2) (the direction of the x axis coincides with the direction of the oncoming flow, the origin of the Cartesian coordinate system is placed at the center

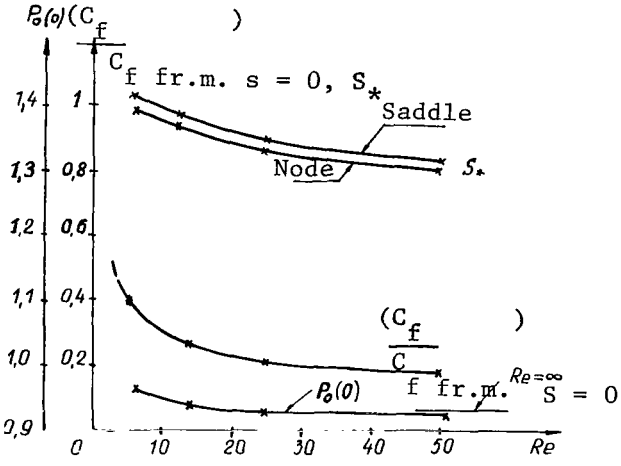

Figure 6.10. Dependence on Re number of pressure $p_0(0)$ at stagnation point, the ratio $(C_f/C_{f\ fr.m})_{s=0}$, and coordinates of position of singular points s_* (flow around a circular cylinder; $M_\infty = 5.2$; $Pr = 0.72$; $\varkappa = 1.4$).

of the cylinder); the angle of the oncoming flow is designated by σ. The tables also give the values of the coefficient of friction $C_f = \tau_w/\rho_\infty w_\infty^2$ (where $\tau_w = \frac{\mu_r^* w_\infty}{R_0}\mu_0\phi_0$ is friction on the surface of the body) and the values of the parameters a in transformation (6.8) which realizes transition to the fictitious plane s, t.

We must bear in mind that here the velocities are referred to w_∞, the pressure to $\rho_\infty w_\infty^2$, density to ρ_∞, enthalpy to w_∞^2, and all linear dimensions in the physical plane are referred to the radius of the circular cylinder R_0. All quantities on the body are designated by the subscript 0, on the line Γ. ($n = \varepsilon(s)$) by the subscript 2, and on the intermediate line ($n = \frac{1}{2}\varepsilon(s)$) by the subscript 1.

CALCULATION OF VISCOUS FLOWS. FLOW AROUND A CIRCULAR CYLINDER.

$M_\infty = 5.2$; Re = 6.25; 12.5; 25; 50; Pr = 0.72; $\varkappa = 1.4$

TABLE 6.1

Re = 50; $t = 0$ ($u_0 = 0$; $v_0 = 0$; $n_0 = 0$)

s	p_0	h_0	C_f	a	x_0	y_0
0.0000	0.925	0.589	0.0000	0.348	-1.000	0.000
0.1089	0.917	0.588	0.0191	0.351	-0.994	0.104
0.2337	0.889	0.585	0.0410	0.364	-0.972	0.231
0.3057	0.864	0.582	0.0533	0.376	-0.953	0.300
0.3921	0.826	0.578	0.0685	0.395	-0.924	0.342
0.4785	0.780	0.572	0.0844	0.421	-0.887	0.460
0.5647	0.726	0.565	0.102	0.452	-0.844	0.535
0.6129	0.693	0.559	0.112	0.471	-0.817	0.575
0.6993	0.625	0.547	0.133	0.503	-0.765	0.643
0.7281	0.600	0.542	0.140	0.511	-0.746	0.665
0.7713	0.560	0.533	0.151	0.517	-0.717	0.697
0.8049	0.527	0.525	0.160	0.518	-0.693	0.720

Re = 50; $t = 1/2$ ($n = n_1$)

s	v_1	u_1	p_1	h_1	n_1	x_1	y_1
0.0000	0.0000	-0.0228	0.920	0.591	0.151	-1.151	0.000
0.1089	0.0344	-0.0226	0.913	0.590	0.153	-1.146	0.125
0.2337	0.0753	-0.0220	0.886	0.586	0.159	-1.127	0.264
0.3057	0.100	-0.0212	0.862	0.585	0.164	-1.110	0.350
0.3921	0.131	-0.0196	0.826	0.581	0.173	-1.084	0.444
0.4785	0.164	-0.0171	0.783	0.576	0.184	-1.051	0.545
0.5647	0.200	-0.0137	0.733	0.569	0.199	-1.013	0.641
0.6129	0.221	-0.0115	0.703	0.565	0.207	-0.947	0.694
0.6993	0.261	-0.0072	0.642	0.555	0.223	-0.935	0.747
0.7281	0.275	-0.0059	0.619	0.551	0.227	-0.916	0.817
0.7713	0.296	-0.0044	0.584	0.544	0.234	-0.884	0.860
0.8049	0.314	-0.0037	0.555	0.539	0.237	-0.857	0.892

Re = 50; $t = 1$ ($n = n_2 = \varepsilon$)

s	v_2	u_2	p_2	h_2	ε	σ	x_2	y_2
0.0000	0.0000	-0.197	0.828	0.573	0.682	1.570	-1.682	0.000
0.1089	0.0747	-0.194	0.825	0.571	0.684	1.504	-1.674	0.143
0.2337	0.158	-0.182	0.812	0.563	0.692	1.429	-1.646	0.392
0.3057	0.205	-0.171	0.800	0.557	0.700	1.386	-1.621	0.511
0.3921	0.259	-0.155	0.783	0.547	0.712	1.336	-1.582	0.654
0.4785	0.309	-0.134	0.764	0.536	0.726	1.289	-1.532	0.794
0.5647	0.356	-0.109	0.742	0.523	0.747	1.243	-1.475	0.935
0.6129	0.379	-0.0944	0.730	0.516	0.759	1.220	-1.439	1.012
0.6993	0.416	-0.0635	0.709	0.504	0.784	1.183	-1.365	1.144
0.7281	0.426	-0.0523	0.703	0.501	0.794	1.172	-1.339	1.194
0.7713	0.438	-0.0347	0.695	0.496	0.810	1.159	-1.297	1.261
0.8049	0.445	-0.0204	0.690	0.494	0.823	1.152	-1.263	1.314

TABLE 6.2

/256

Re = 25; $t = 0$ ($u_0 = 0$; $v_0 = 0$; $n_0 = 0$)

s	p_0	h_0	C_f	a	x_0	y_0
0.0000	0.931	0.588	0.0000	0.365	-1.000	0.000
0.1062	0.924	0.588	0.0221	0.368	-0.994	0.106
0.1494	0.916	0.587	0.0311	0.372	-0.988	0.144
0.1926	0.907	0.586	0.0399	0.377	-0.981	0.191
0.2550	0.889	0.585	0.0526	0.386	-0.967	0.252
0.3318	0.861	0.582	0.0678	0.402	-0.945	0.325
0.3798	0.840	0.580	0.0772	0.414	-0.928	0.370
0.4278	0.817	0.578	0.0967	0.430	-0.909	0.414
0.5142	0.770	0.573	0.104	0.464	0.870	0.491
0.5622	0.741	0.569	0.114	0.488	-0.846	0.533
0.6198	0.703	0.564	0.128	0.522	-0.813	0.540
0.6678	0.669	0.558	0.140	0.553	-0.785	0.619
0.7158	0.632	0.552	0.152	0.587	-0.754	0.656
0.7638	0.593	0.544	0.165	0.622	-0.722	0.691
0.8214	0.542	0.532	0.179	0.660	-0.681	0.732
0.8550	0.511	0.525	0.182	0.676	-0.656	0.754

Re = 25; $t = 1/2$ ($n = n_1$)

s	v_1	u_1	p_1	h_1	n_1	x_1	y_1
0.0000	0.0000	-0.0240	0.922	0.590	0.164	-1.164	0.000
0.1062	0.0330	-0.0239	0.915	0.590	0.166	-1.159	0.123
0.1494	0.0466	-0.0237	0.908	0.589	0.167	-1.154	0.173
0.1926	0.0605	-0.0234	0.899	0.588	0.170	-1.148	0.223
0.2550	0.0809	-0.0228	0.882	0.586	0.174	-1.136	0.296
0.3318	0.107	-0.0216	0.856	0.584	0.181	-1.117	0.344
0.3798	0.124	-0.0205	0.837	0.582	0.187	-1.102	0.440
0.4278	0.141	-0.0191	0.815	0.579	0.193	-1.086	0.495
0.5142	0.174	-0.0157	0.772	0.573	0.208	-1.052	0.594
0.5622	0.193	-0.0132	0.746	0.570	0.217	-1.030	0.649
0.6198	0.218	-0.0095	0.711	0.564	0.230	-1.001	0.714
0.6678	0.239	-0.0060	0.681	0.560	0.242	-0.975	0.769
0.7158	0.261	-0.0021	0.649	0.554	0.254	-0.946	0.823
0.7638	0.284	+0.0019	0.614	0.549	0.266	-0.914	0.876
0.8214	0.313	+0.0068	0.570	0.539	0.281	-0.872	0.937
0.8550	0.330	+0.0094	0.543	0.534	0.288	-0.845	0.972

TABLE 6.2 Continued

/25

Re = 25; $t = 1$ ($n = n_2 = \varepsilon$)

s	v_2	u_2	p_2	h_2	ε	σ	x_2	y_2
0.0000	0.0000	-0.197	0.828	0.573	0.714	1.570	-1.714	0.000
0.1062	0.0717	-0.194	0.825	0.571	0.716	1.507	-1.706	0.141
0.1494	0.100	-0.191	0.821	0.569	0.718	1.481	-1.699	0.255
0.1926	0.129	-0.187	0.817	0.567	0.721	1.455	-1.689	0.329
0.2550	0.169	-0.179	0.809	0.562	0.727	1.419	-1.671	0.435
0.3318	0.218	-0.167	0.796	0.555	0.736	1.374	-1.641	0.565
0.3798	0.248	-0.157	0.787	0.550	0.743	1.347	-1.619	0.646
0.4278	0.277	-0.147	0.777	0.544	0.751	1.320	-1.593	0.726
0.5142	0.326	-0.125	0.755	0.532	0.768	1.272	-1.540	0.869
0.5622	0.353	-0.111	0.743	0.525	0.779	1.246	-1.505	0.944
0.6198	0.383	-0.0928	0.727	0.516	0.794	1.216	-1.460	1.042
0.6678	0.406	-0.0763	0.714	0.508	0.808	1.191	-1.419	1.119
0.7158	0.427	-0.0587	0.700	0.500	0.823	1.168	-1.375	1.196
0.7638	0.446	-0.0399	0.687	0.493	0.839	1.147	-1.324	1.272
0.8214	0.465	-0.0159	0.673	0.485	0.861	1.125	-1.267	1.362
0.8550	0.474	-0.0011	0.666	0.481	0.874	1.115	-1.230	1.414

TABLE 6.3

Re = 12.5; $t = 0$ ($u_0 = 0$; $v_0 = 0$; $n_0 = 0$)

s	p_0	h_0	C_f	a	x_0	y_0
0.0000	0.941	0.588	0.0000	0.388	-1.000	0.0000
0.0912	0.936	0.587	0.0244	0.390	-0.995	0.0910
0.1536	0.926	0.587	0.0409	0.395	-0.984	0.152
0.1968	0.916	0.586	0.0522	0.401	-0.980	0.195
0.2592	0.898	0.584	0.0681	0.410	-0.966	0.256
0.3456	0.865	0.582	0.0895	0.430	-0.940	0.334
0.3936	0.844	0.580	0.101	0.444	-0.923	0.343
0.4512	0.815	0.578	0.114	0.465	-0.899	0.436
0.4992	0.789	0.575	0.126	0.485	-0.877	0.474
0.5856	0.736	0.570	0.147	0.532	-0.833	0.552
0.6336	0.704	0.566	0.159	0.564	-0.805	0.592
0.6816	0.670	0.561	0.171	0.601	-0.776	0.630
0.7080	0.651	0.558	0.178	0.623	-0.759	0.650
0.7560	0.613	0.552	0.192	0.666	-0.727	0.646
0.8520	0.531	0.536	0.217	0.755	-0.658	0.752
0.9000	0.488	0.526	0.222	0.759	-0.621	0.743

TABLE 6.3 Continued

/258

Re = 12.5; $t = 1/2\ (n = n_1)$

s	v_1	u_1	p_1	h_1	n_1	x_1	y_1
0.0000	0.0000	-0.0256	0.924	0.589	0.180	-1.180	0.000
0.0912	0.0279	-0.0255	0.919	0.589	0.181	-1.176	0.107
0.1536	0.0472	-0.0252	0.910	0.588	0.184	-1.170	0.141
0.1968	0.0608	-0.0248	0.901	0.587	0.186	-1.163	0.232
0.2592	0.0809	-0.0241	0.884	0.585	0.191	-1.151	0.305
0.3456	0.109	-0.0225	0.854	0.582	0.200	-1.129	0.406
0.3936	0.126	-0.0213	0.834	0.580	0.206	-1.113	0.462
0.4512	0.147	-0.0193	0.808	0.576	0.215	-1.093	0.529
0.4992	0.164	-0.0172	0.785	0.573	0.223	-1.074	0.545
0.5856	0.196	-0.0121	0.738	0.567	0.241	-1.034	0.646
0.6336	0.217	-0.0086	0.710	0.562	0.252	-1.009	0.741
0.6816	0.237	-0.0046	0.681	0.557	0.265	-0.982	0.797
0.7080	0.249	-0.0021	0.664	0.555	0.272	-0.966	0.827
0.7560	0.270	+0.0026	0.632	0.549	0.286	-0.935	0.842
0.8520	0.316	+0.0130	0.563	0.535	0.314	-0.865	0.949
0.9000	0.340	+0.0180	0.526	0.527	0.326	-0.824	1.039

Re = 12.5; $t = 1\ (n = n_2 = \varepsilon)$

s	v_2	u_2	p_2	h_2	ε	σ	x_2	y_2
0.0000	0.0000	-0.198	0.828	0.574	0.750	1.570	-1.250	0.000
0.0912	0.0607	-0.195	0.825	0.573	0.751	1.516	-1.744	0.159
0.1536	0.101	-0.191	0.821	0.570	0.755	1.480	-1.734	0.264
0.1968	0.130	-0.187	0.817	0.568	0.758	1.455	-1.724	0.343
0.2592	0.170	-0.179	0.809	0.563	0.764	1.418	-1.705	0.452
0.3456	0.224	-0.165	0.794	0.555	0.774	1.369	-1.669	0.601
0.3936	0.253	-0.155	0.785	0.550	0.782	1.342	-1.646	0.643
0.4512	0.287	-0.142	0.772	0.542	0.792	1.310	-1.613	0.741
0.4992	0.314	-0.129	0.760	0.536	0.802	1.283	-1.542	0.862
0.5856	0.361	-0.104	0.737	0.523	0.822	1.236	-1.519	1.007
0.6336	0.386	-0.0894	0.723	0.515	0.835	1.210	-1.479	1.046
0.6816	0.410	-0.0730	0.709	0.507	0.849	1.184	-1.436	1.165
0.7080	0.422	-0.0635	0.701	0.503	0.858	1.171	-1.411	1.204
0.7560	0.443	-0.0455	0.686	0.494	0.874	1.147	-1.363	1.245
0.8520	0.479	-0.0064	0.657	0.479	0.909	1.103	-1.257	1.437
0.9000	0.492	+0.0147	0.645	0.472	0.930	1.085	-1.199	1.511

TABLE 6.4

/2

Re = 6.25; $t = 0$ ($u_0 = 0$; $v_0 = 0$; $n_0 = 0$)

s	p_0	h_0	C_f	a	x_0	y_0
0.0000	0.962	0.587	0.0000	0.422	-1.000	0.0000
0.0972	0.955	0.586	0.0357	0.425	-0.995	0.0970
0.1404	0.948	0.586	0.0513	0.429	-0.990	0.139
0.1836	0.939	0.585	0.0668	0.434	-0.983	0.142
0.2796	0.909	0.583	0.100	0.450	-0.961	0.275
0.3276	0.891	0.582	0.116	0.462	-0.946	0.321
0.3660	0.874	0.581	0.128	0.472	-0.933	0.357
0.4140	0.851	0.579	0.144	0.488	-0.915	0.402
0.4620	0.825	0.577	0.158	0.506	-0.895	0.445
0.5196	0.791	0.574	0.176	0.533	-0.868	0.496
0.5676	0.761	0.571	0.190	0.558	-0.843	0.537
0.6156	0.729	0.568	0.204	0.588	-0.816	0.577
0.6636	0.695	0.564	0.218	0.621	-0.787	0.615
0.7116	0.659	0.559	0.232	0.658	-0.757	0.653
0.7596	0.621	0.555	0.246	0.698	-0.725	0.644
0.8364	0.556	0.545	0.269	0.764	-0.670	0.742
0.9228	0.475	0.531	0.294	0.821	-0.603	0.797

Re = 6.25; $t = 1/2$ ($n = n_1$)

s	v_1	u_1	p_1	h_1	n_1	x_1	y_1
0.0000	0.0000	-0.0280	0.927	0.588	0.204	-1.204	0.000
0.0972	0.0292	-0.0278	0.921	0.587	0.205	-1.199	0.116
0.1404	0.0424	-0.0275	0.915	0.587	0.207	-1.195	0.168
0.1836	0.0557	-0.0272	0.907	0.586	0.209	-1.189	0.220
0.2796	0.0859	-0.0259	0.881	0.583	0.219	-1.172	0.336
0.3276	0.101	-0.0249	0.865	0.581	0.222	-1.157	0.393
0.3660	0.114	-0.0239	0.850	0.579	0.226	-1.145	0.439
0.4140	0.130	-0.0224	0.830	0.577	0.233	-1.129	0.496
0.4620	0.147	-0.0205	0.808	0.574	0.241	-1.111	0.553
0.5196	0.167	-0.0176	0.779	0.570	0.251	-1.046	0.621
0.5676	0.185	-0.0147	0.754	0.566	0.261	-1.063	0.674
0.6156	0.203	-0.0113	0.727	0.562	0.272	-1.038	0.734
0.6636	0.222	-0.0073	0.699	0.557	0.284	-1.011	0.790
0.7116	0.241	-0.0029	0.669	0.552	0.296	-0.981	0.846
0.7596	0.260	-0.0020	0.638	0.547	0.309	-0.949	0.901
0.8364	0.293	+0.0106	0.586	0.537	0.331	-0.892	0.988
0.9228	0.331	+0.0201	0.521	0.524	0.352	-0.816	1.178

TABLE 6.4 Continued

/260

Re = 6.25; $t = 1$ ($n = n_2 = \varepsilon$)

s	v_2	u_2	p_2	h_2	ε	σ	x_2	y_2
0.0000	0.0000	-0.197	0.827	0.575	0.800	1.570	-1.800	0.000
0.0972	0.0635	-0.196	0.825	0.574	0.802	1.514	-1.793	0.174
0.1404	0.0915	-0.193	0.822	0.572	0.804	1.489	-1.786	0.252
0.1836	0.119	-0.189	0.818	0.570	0.807	1.464	-1.776	0.329
0.2796	0.179	-0.177	0.805	0.563	0.816	1.406	-1.745	0.501
0.3276	0.209	-0.169	0.798	0.558	0.822	1.381	-1.725	0.586
0.3660	0.232	-0.161	0.791	0.554	0.828	1.360	-1.707	0.654
0.4140	0.260	-0.151	0.781	0.549	0.836	1.333	-1.681	0.734
0.4620	0.288	-0.140	0.770	0.543	0.845	1.306	-1.652	0.822
0.5196	0.320	-0.125	0.755	0.535	0.857	1.274	-1.612	0.922
0.5676	0.346	-0.112	0.742	0.528	0.869	1.247	-1,576	1.004
0.6156	0.371	-0.0974	0.729	0.520	0.881	1.221	-1.536	1.086
0.6636	0.395	-0.0818	0.714	0.512	0.895	1.195	-1.493	1.167
0.7116	0.418	-0.0653	0.698	0.504	0.910	1.169	-1.446	1.247
0.7596	0.440	-0.0478	0.682	0.496	0.926	1.143	-1.396	1.326
0.8364	0.471	-0.0181	0.657	0.482	0.954	1.104	-1.309	1.450
0.9228	0.498	+0.0180	0.629	0.469	0.990	1.066	-1.201	1.586

CHAPTER 7

THREE-DIMENSIONAL FLOWS

The problem of calculating flow of a supersonic gas stream around axisymmetric blunt bodies at an angle of attack is quite urgent and has been examined by a number of authors. /2

In the work of A. N. Minaylos [18] the method of integral relations was used to solve this problem, the functions having been approximated by polynomials both over the peripheral coordinate and across the boundary layer (scheme I, N = 1). The unquestionable virtue of this scheme is that it gives sufficiently complete information about the behavior of the initial parameters of the body. However, during the calculation certain computational difficulties arise which are associated with the solution of the multiparametric boundary-value problem and the construction of the numerical solution in the neighborhood of the singular points. A further advance with respect to approximations here is hampered in practice. G. F. Telenin and G. P. Tinyakov [67] used the method of straight lines to calculate three-dimensional flows.

We will examine below scheme II of the method of integral relations [25] which permits determining the flow field in the region of influence of blunting for the case of the flow of a perfect and equilibratory dissociating gas around axisymmetric bodies at an angle of attack.

The functions, just as in work [67], are represented approximately over the peripheral coordinate (trigonometric approximation) and along the shock layer (polynomial approximation), but in the supersonic region a characteristic limiting the region of the influence of mixed flow is used in place of the ray. To close the approximating system the condition of compatibility is used along the boundary characteristic, which permits in any approximation an exact satisfaction of the boundary conditions of the problem.

1. Statement of Problem. Let us examine supersonic flow around an axisymmetric blunt body at an angle of attack. As independent variables we used coordinates s, n, Θ, where s is the length of arc along the surface of the body; n is a normal to the body; Θ is an angle read off from the upper half-plane of symmetry of the flow (Figs. 7.1, 7.2).

Let us write out in these coordinates the dimensionless equations of gasdynamics in the divergent form

$$\frac{\partial \bar{z}}{\partial s}+\frac{\partial}{\partial n}A\bar{H}+\frac{\partial Nu}{\partial \Theta}=L\cos\delta+\frac{\bar{g}}{R};\quad \frac{\partial \bar{g}}{\partial s}+\frac{\partial A\bar{z}}{\partial n}+\frac{\partial Nv}{\partial \Theta}=L\sin\delta-\frac{\bar{z}}{R};$$

$$\frac{\partial \bar{t}w}{\partial s}+\frac{\partial Aw\bar{h}}{\partial n}+\frac{\partial L}{\partial \Theta}=-N(v\sin\delta+u\cos\delta);\quad \frac{\partial \bar{t}}{\partial s}+\frac{\partial A\bar{h}}{\partial n}+\frac{\partial N}{\partial \Theta}=0.$$

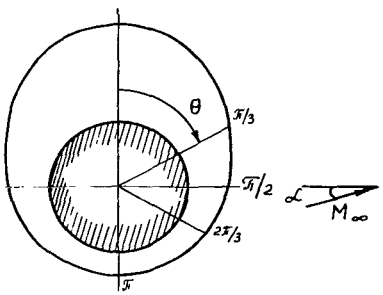

Figure 7.1. Separation of integration range in transverse plane.

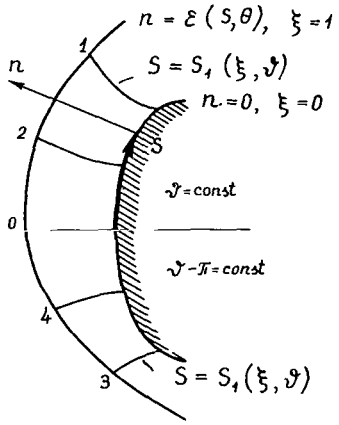

Figure 7.2. Separation of integration range in plane ϑ = const.

Before starting to approximate these equations with respect to coordinates s, Θ, we must compress the region in which the solution is present so that becomes rectangular. For this purpose we replace the variables. We will change from coordinates s, n, Θ , to coordinates η, ξ, ϑ, which are related in the following manner:

$$\eta = s/\hat{S}(\xi,\vartheta); \quad \xi = n/\varepsilon(s,\Theta); \quad \vartheta = \Theta,$$

where $s=\hat{S}(\xi,\vartheta)$ is the equation of the boundary characteristic of the surface and $n=\varepsilon(s,\Theta)$ is the equation of the shock wave.

In the new coordinates $\eta = 0$ is the axis of symmetry of the body, $\eta = 1$ is the characteristic, $\xi = 0$ is the body, $\xi = 1$ is the shock wave. The integration range will now look like $0 \le \zeta \le 1$, $0 \le \eta \le 1$, $0 \le \vartheta \le \pi$.

The equations of gasdynamics are transformed in the following manner:

$$\frac{\partial(\mathbf{K}_k r)}{\partial \eta} + \frac{\partial(\hat{s} r \mathbf{M}_k)}{\partial \xi} + \frac{\partial(\hat{s}\mathbf{N}_k)}{\partial \vartheta} = \hat{s}(\mathbf{Y}_k r + \mathbf{X}_k),$$

where k = 1 is the first equation of motion,

$$\mathbf{M}_1 = u\mathbf{M}_4 + A\mathbf{p}; \quad \mathbf{N}_1 = u\mathbf{N}_4; \quad \mathbf{X}_1 = 0;$$

$$\mathbf{K}_1 = u\mathbf{K}_4 - \eta A \hat{s}'_\xi \mathbf{p}; \quad \mathbf{Y}_1 = \left(L\frac{\cos\delta}{r} + \frac{g}{R}\right)\varepsilon;$$

k = 2 is the second equation of motion,

$$\mathbf{M}_2 = v\mathbf{M}_4 - \xi\varepsilon'_s \mathbf{p}; \quad \mathbf{N}_2 = v\mathbf{N}_4; \quad \mathbf{X}_2 = \varepsilon L \sin\delta;$$

$$\mathbf{K}_2 = v\mathbf{K}_4 + (\varepsilon + \xi\varepsilon'_\xi)\mathbf{p}; \quad \mathbf{Y}_2 = \frac{\varepsilon z}{R};$$

k = 3 is the third equation of motion,

$$M_3 = wM_4 - \xi A\frac{\varepsilon'_\Theta}{r}p;\quad N_3 = L\varepsilon;\quad X_3 = -N_4 v\sin\delta;$$
$$K_3 = wK_4 - \frac{\eta}{r}Ap(\varepsilon\hat{s}'_\vartheta - \hat{s}'_\xi\xi\,\varepsilon'_\Theta);\quad Y_3 = N_4 u\frac{\cos\delta}{r};$$

k = 4 is the equation of continuity,

$$M_4 = Ah - \xi\varepsilon'_s t - \xi\frac{\varepsilon'_\Theta}{r}N;\quad N_4 = N\varepsilon;\quad X_4 = 0;$$

$$K_4 = (\varepsilon + \xi\varepsilon'_\xi)t - \eta\hat{s}'_\xi Ah - \frac{\eta}{r}N(\varepsilon\hat{s}'_\vartheta - \hat{s}'_\xi\xi\varepsilon'_\Theta);\quad Y_4 = 0.$$

2. The question arises now of selecting the points for approximating the functions with respect to η and ϑ. At a fixed half-plane we select for the principal points of approximation with respect to η the axis of symmetry of the body and the characteristic (first approximation with respect to η). Further approximations are obtained by separating a given zone into N zones (N-th approximation with respect to η).

As the principal half-planes for approximation with respect to ϑ we must take the half-planes $\vartheta = 0,\ \pi$ (first approximation with respect to ϑ). Higher approximations can be obtained in two ways (P-th approximation with respe to ϑ):

$$1)\ \vartheta = \frac{i\pi}{2P-1}\qquad (i = 0, \ldots, 2P-1);$$
$$2)\ \vartheta = \frac{i\pi}{2(P-1)}\qquad (i = 0, \ldots, 2(P-1).$$

Figure 7.1 illustrates both forms of separation for N = 2, P = 2. /

We will present here the approximating system (N = 2, P = 2) for the first case. Using the condition of symmetry of flow relative to plane $\vartheta = 0;\ \pi$ and the condition of continuity on the axis of symmetry in any plane $\vartheta;\ \vartheta + \pi$, we can write out the formula of through approximation to functions in the plane $\vartheta;\ \vartheta + \pi$.

For the functions M_1, N_1, Y_1, X_2, M_3, N_3, Y_3, M_4, N_4 we have

$$f = f_0 + \left(\frac{8}{3}\varphi_2 - \frac{1}{3}\varphi_1\right)\eta + \left(\frac{16}{3}\varphi_4 - \frac{1}{3}\varphi_3 - 5f_0\right)\eta^2 + \left(\frac{4}{3}\varphi_1 - \frac{8}{3}\varphi_2\right)\eta^3 + \left(\frac{4}{3}\varphi_3 - \frac{16}{3}\varphi_4 + 4f_0\right)\eta^4,$$

where $\varphi_1 = \frac{f_1 - f_3}{2};\ \varphi_2 = \frac{f_2 - f_4}{2};\ \varphi_3 = \frac{f_1 + f_3}{2};\ \varphi_4 = \frac{f_2 + f_4}{2}.$

For functions M_2, N_2, Y_2, X_3, r, respectively,

$$f = f_0 + \left(\frac{8}{3}\varphi_4 - \frac{1}{3}\varphi_3\right)\eta + \left(\frac{16}{3}\varphi_2 - \frac{1}{3}\varphi_1 - 5f_0\right)\eta^2 + \\ + \left(\frac{4}{3}\varphi_3 - \frac{8}{3}\varphi_4\right)\eta^3 + \left(\frac{4}{3}\varphi_1 - \frac{16}{3}\varphi_2 + 4f_0\right)\eta^4.$$

For functions even with respect to ϑ :

$$\varphi_i = \frac{2}{3}(\varphi_i^0 + \varphi_i^1)\cos\vartheta + \frac{1}{3}(\varphi_i^0 - 2\varphi_i^1)\cos 3\vartheta, \quad i = 1,2;$$

$$\varphi_i = \frac{1}{3}(\varphi_i^0 + 2\varphi_i^1) + \frac{2}{3}(\varphi_i^0 - \varphi_i^1)\cos 2\vartheta, \quad i = 3,4.$$

For functions odd with respect to ϑ :

$$\varphi_i = \frac{2\varphi_i^1}{\sqrt{3}}\sin 2\vartheta, \quad i = 1,2; \quad \varphi_i = \frac{2\varphi_i^1}{\sqrt{3}}\sin\vartheta, \quad i = 3,4.$$

The superscript 0 pertains to the plane $\vartheta = 0, \pi$ and the superscript 1 pertains to the plane $\vartheta = \pi/3;\ 2\pi/3$. For functions M_2, N_2, Y_2, X_3, f_0 are approximated $\phi_{1,2}$ with respect to ϑ as $\phi_{3,4}$.

We will integrate the equations of gasdynamics from $\eta = 0$ to $\eta = i$:

$$K_{ki}r_i + \frac{\partial}{\partial\xi}\hat{s}\int_0^i M_k r\,d\eta + \frac{\partial\hat{s}\int_0^i N_k d\eta}{\partial\vartheta} = K_{ki}r_i + \hat{s}\frac{\partial}{\partial\xi}\int_0^i M_k r\,d\eta + \\ + \frac{\partial\hat{s}}{\partial\xi}\int_0^i M_k r\,d\eta + \frac{\partial\hat{s}}{\partial\vartheta}\int_0^i N_k d\eta + \hat{s}\frac{\partial}{\partial\vartheta}\int_0^i N_k d\eta = \hat{s}\int_0^i (Y_k r + X_k)\,d\eta. \qquad /265$$

Now approximating the functions with respect to η and ϑ we obtain a system of 8NP ordinary differential equations of the form

$$\sum_{l=1}^{4} a_{kil}^j \frac{d\tilde{M}_{kl}^j}{d\xi} = \sum_{l=0}^{4}\left[\tilde{Y}_{kl}^j b_{kil}^j + \tilde{X}_{kl}^j d_{kil} - \left(\frac{\hat{s}'_\xi}{\hat{s}}\right)_i^j a_{kil}^j \tilde{M}_{kl}^j - \right.$$

$$\left. - \left(\frac{\hat{s}'_\vartheta}{\hat{s}}\right)_i^j c_{kil}\tilde{N}_{kl}^j - \tilde{M}_{kl}^j \frac{da_{kil}^j}{d\xi} - c_{kil}\left(\frac{d\tilde{N}_k}{\partial\vartheta}\right)_l^j\right] - \left(\frac{1}{\hat{s}}K_k r\right)_i^j -$$

$$- a_{k0i}^j \frac{d}{d\xi}M_{k0}^j, \quad i = 1,2,3,4; \quad k = 1,2,3,4; \quad j = 0,1.$$

The index $\sim$ denotes that we must take not the functions themselves, but their half-sum of half-difference. For example,

$$\tilde{M}^j_{k1} = \frac{1}{2}(M^j_{k1} - M^j_{k3}), \quad \tilde{M}^j_{k2} = \frac{1}{2}(M^j_{k2} - M^j_{k4});$$
$$\tilde{M}^j_{k3} = \frac{1}{2}(M^j_{k1} + M^j_{k3}), \quad \tilde{M}^j_{k4} = \frac{1}{2}(M^j_{k2} + M^j_{k4}),$$

but $\tilde{M}^j_{k0} = \tilde{M}^j_{k0}$.

To close the system we must determine the quantities $\frac{d}{d\xi} M^j_{k0}$, which are expressed in terms of the derivatives $\frac{du_0}{d\xi}$, $\frac{dp_0}{d\xi}$, $\frac{dv_0}{d\xi}$, i.e., three more conditions are required. These additional conditions are the relations along the characteristics written in three half-planes. Here we will give the general form of these conditions of compatability and the equations of the boundary characteristic

$$v\frac{du}{d\xi} - \left(u - \xi\frac{\varepsilon'_\Theta}{r}w\right)\frac{dv}{d\xi} - \xi\frac{\varepsilon'_\Theta}{r}v\frac{dw}{\partial\xi} +$$
$$+ \frac{1}{\rho a^2}\frac{dp}{d\xi}\, a\sqrt{u^2+v^2-a^2+\left(\xi\frac{\varepsilon'_\Theta}{r}\right)^2(w^2+v^2-a^2) - 2uw\xi\frac{\varepsilon'_\Theta}{r}} =$$
$$= \frac{1}{r}\left(\varepsilon + \xi\varepsilon'_s\frac{d\hat{s}}{d\xi}\right)\left[w\frac{dv}{\partial\Theta} - v\frac{dw}{\partial\Theta} - (w^2+v^2)\sin\delta - vu\cos\delta\right] +$$
$$+ \frac{1}{r}A\frac{d\hat{s}}{d\xi}\left[u\frac{\partial w}{\partial\Theta} - w\frac{du}{\partial\Theta} + (u^2+w^2)\cos\delta + vu\sin\delta\right] + \frac{1}{R}\frac{d\hat{s}}{d\xi}\left(u^2 +\right.$$
$$\left. + v^2 - \xi\frac{\varepsilon'_\Theta}{r}uw\right) + \left[-\varepsilon vw + \left(gw + A\xi\frac{\varepsilon'_\Theta}{r}a^2\right)\frac{d\hat{s}}{d\xi}\right]\cdot\frac{1}{r\rho a^2}\frac{\partial p}{\partial\Theta};$$

$$\frac{1}{\varepsilon}\frac{d\hat{s}}{d\xi} = \frac{-vg - a^2\xi\varepsilon'_s + Aa\sqrt{(v^2-a^2)\left[1+\left(\xi\frac{\varepsilon'_\Theta}{r}\right)^2\right] + \left[u - w\xi\frac{\varepsilon'_\Theta}{r}\right]^2}}{a^2\left[A^2 + (\xi\varepsilon'_s)^2 + \left(A\xi\frac{\varepsilon'_\Theta}{r}\right)^2\right] - g^2},$$

where

$$g = \frac{M_4}{\rho}; \quad \frac{\partial f}{\partial\Theta} = \frac{\partial f}{\partial\vartheta} - \frac{\partial f}{\partial\eta}\frac{\eta\hat{s}'_\vartheta}{\hat{s}}.$$

The approximating system of ordinary differential equations has the form

$$\frac{du_0}{d\xi} = \frac{D_1}{D}; \quad \frac{dv_0^0}{d\xi} = \frac{D_2}{D}; \quad \frac{dT_0}{d\xi} = -\frac{1}{i_{T_0}}\left[i_p\frac{dp}{d\xi} + 2u\frac{du}{d\xi} + 2v\frac{dv}{d\xi}\right]_0^0;$$

$$\frac{dp_0}{d\xi} = \frac{D_3}{D}; \quad \frac{dp_i^j}{d\xi} = \frac{1}{\Delta_{0i}^j}\left[\sum_{l=1}^{4}\gamma_l Q_l + Q_6\right]_i^j;$$

$$\frac{du_i^j}{d\xi} = \frac{1}{M_{4i}^j}\left[Q_1 - uQ_4 - \frac{dA_p}{d\xi}\right]_i^j;$$

$$\frac{dv_i^j}{d\xi} = \frac{1}{M_{4i}^j}\left[Q_2 - vQ_4 + \frac{d\xi\varepsilon_s' p}{d\xi}\right]_i^j;$$

$$\frac{dw_i^j}{d\xi} = \frac{1}{M_{4i}^j}\left[Q_3 - wQ_4 + \frac{d\xi\frac{\varepsilon_\Theta'}{r}Ap}{d\xi}\right]_i^j;$$

$$\frac{dT_i^j}{d\xi} = -\frac{1}{i_{Ti}^j}\left[i_p\frac{dp}{d\xi} + 2u\frac{du}{d\xi} + 2v\frac{dv}{d\xi} + 2w\frac{dw}{d\xi}\right]_i^j, \quad i = 1,2,3,4; \; j = 0,1.$$

The known conditions on the shock wave and the non-flow condition on the body are the boundary conditions.

The problem is solved in the following manner: we assign the shape of the shock wave, and nine parameters (ε_0, ε_i^j, i = 1, 2, 3, 4, j = 0, 1) are selected so as to satisfy nine conditions of nonflow $u_i^j = 0$ on the body (i = 0, ..., 4, j = 0, 1). Iterations are performed by the Newton method. /267

Figure 7.3 and Table 7.1 present the results of calculating (scheme II, N = 2, p = 2) flow of an ideal gas ($\varkappa = 1.4$) around an ellipsoid of revolution ($\delta = 2$) at an angle of attack when $M_\infty = 10$, $\alpha = 5°$. The shape and position of the shock wave, coordinates of the boundary characteristic s, and the distribution of the normal and tangential velocity components (u, v), pressure (p), and temperature (T) along the boundaries of the zones across the shock layer are given for different meridional cross sections ($\vartheta = 0, \pi/3, 2\pi/3, \pi$).

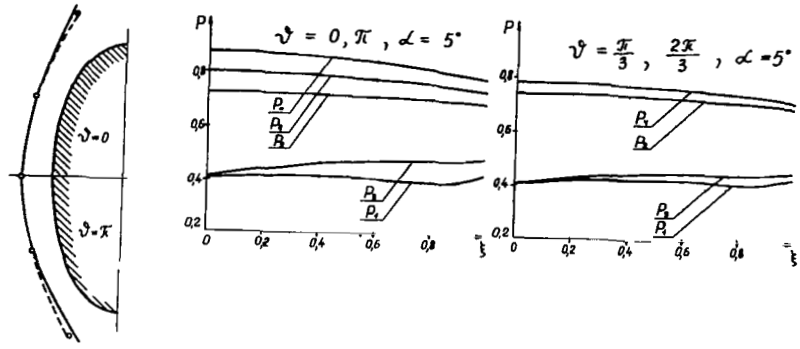

Figure 7.3. Shape of shock wave (---α = 0°; ooo α = 1°; —— α = 5°) and distribution of pressure for flow of perfect gas M_∞ = 10; $\varkappa$ = 1.4) around an ellipsoid of revolution (δ = 2) at angle of attack (α = 5°).

The subscript 0 pertains to quantities on the axis of symmetry of the body, the subscripts 1 and 3 on the boundary characteristic, and subscri 2 and 4 on the intermediate lines, respectively. The superscript 0 designates quantities in the meridional planes ϑ = 0, π, the superscript 1 in planes $\vartheta = \pi/3, 2\pi/3$. All data are given in a dimensionless form. The values of velocities are referred to w_{max}, pressure to $\rho_\infty w^2_{max}$, temperature to w^2_{max}/R, and linear dimensions to the vertical semiaxis of the ellipsoid

TABLE 7.1

CALCULATION OF THREE-DIMENSIONAL FLOWS. $M_\infty = 10$; $\varkappa = 1.4$; $\delta = 2$; $\alpha = 5°$. /268

$\vartheta = 0$

ξ	u_0	v_0	p_0	T_0	s_1^0	u_1^0	v_1^0	p_1^0	T_1^0	u_2^0	v_2^0	p_2^0	T_2^0
1.000	−0.170	0.0924	0.785	0.137	1.078	+0.157	0.651	0.432	0.0787	−0.149	0.347	0.695	0.122
0.875	−0.150	0.0829	0.806	0.138	1.033	+0.0991	0.584	0.402	0.0927	−0.134	0.331	0.703	0.124
0.750	−0.129	0.0721	0.826	0.139	0.998	+0.0591	0.531	0.403	0.101	−0.119	0.321	0.709	0.126
0.625	−0.108	0.0611	0.843	0.140	0.968	+0.0341	0.500	0.412	0.106	−0.103	0.312	0.714	0.127
0.500	−0.0874	0.0505	0.857	0.141	0.942	+0.0179	0.487	0.419	0.108	−0.0856	0.302	0.719	0.128
0.375	−0.0661	0.0408	0.867	0.141	0.916	+0.00639	0.484	0.423	0.109	−0.0660	0.289	0.724	0.130
0.250	−0.0446	0.0324	0.874	0.142	0.890	−0.00144	0.480	0.423	0.109	−0.0448	0.272	0.727	0.131
0.125	−0.0227	0.0258	0.878	0.142	0.867	−0.00429	0.466	0.419	0.111	−0.0225	0.253	0.728	0.133
0.000	0.0000	0.0216	0.879	0.142	0.848	0.0000	0.436	0.409	0.112	0.0000	0.236	0.727	0.134

$\vartheta = \pi$

ξ	s_3^0	u_3^0	v_3^0	p_3^0	T_3^0	u_4^0	v_4^0	p_4^0	T_4^0
1.000	1.078	+0.0665	0.613	0.490	0.0883	−0.176	0.244	0.739	0.129
0.875	1.035	+0.0239	0.565	0.479	0.0971	−0.148	0.221	0.756	0.132
0.750	1.000	−0.00385	0.527	0.477	0.103	−0.123	0.200	0.769	0.134
0.625	0.972	−0.0197	0.495	0.475	0.107	−0.0997	0.182	0.779	0.136
0.500	0.947	−0.0261	0.466	0.471	0.111	−0.0781	0.168	0.788	0.137
0.375	0.924	−0.0249	0.440	0.462	0.115	−0.0580	0.160	0.795	0.138
0.250	0.902	−0.0183	0.422	0.448	0.117	−0.0388	0.159	0.801	0.139
0.125	0.883	−0.00908	0.416	0.429	0.118	−0.0199	0.163	0.804	0.138
0.000	0.868	0.00000	0.435	0.409	0.115	0.0000	0.173	0.805	0.138

TABLE 7.1 Continued

$\vartheta = \pi/3$

ξ	s_1^1	u_1^1	v_1^1	p_1^1	T_1^1	w_1^1	u_2^1	v_2^1	p_2^1	T_2^1	w_2^1
1.000	1.078	+0.133	0.644	0.443	0.0805	-0.0475	-0.157	0.320	0.703	0.123	-0.0732
0.875	1.038	+0.0788	0.580	0.417	0.0935	-0.0473	-0.138	0.302	0.714	0.126	-0.0755
0.750	1.005	+0.0420	0.530	0.418	0.102	-0.0504	-0.120	0.289	0.722	0.127	-0.0752
0.625	0.978	+0.0196	0.497	0.424	0.106	-0.0569	-0.102	0.279	0.728	0.129	-0.0720
0.500	0.955	+0.00622	0.479	0.428	0.109	-0.0642	-0.0832	0.268	0.734	0.130	-0.0657
0.375	0.938	-0.00141	0.470	0.428	0.110	-0.0681	-0.0633	0.257	0.739	0.132	-0.0567
0.250	0.924	-0.00451	0.464	0.425	0.111	-0.0644	-0.0429	0.244	0.742	0.133	-0.0457
0.125	0.913	-0.00345	0.452	0.419	0.113	-0.0485	-0.0216	0.231	0.743	0.134	-0.0339
0.000	0.903	0.00000	0.421	0.407	0.117	-0.0160	0.0000	0.229	0.742	0.134	-0.0227

$\vartheta = 2\pi/3$

ξ	s_3^1	u_3^1	v_3^1	p_3^1	T_3^1	w_3^1	u_4^1	v_4^1	p_4^1	T_4^1	w_4^1
1.000	1.078	+0.0861	0.631	0.467	0.0844	-0.0494	-0.169	0.266	0.728	0.128	-0.0673
0.875	1.042	+0.0378	0.573	0.450	0.0952	-0.0461	-0.144	0.242	0.743	0.130	-0.0690
0.750	1.011	+0.00718	0.528	0.450	0.102	-0.0468	-0.121	0.223	0.754	0.132	-0.0690
0.625	0.985	-0.00995	0.492	0.452	0.107	-0.0510	-0.0998	0.207	0.763	0.134	-0.0668
0.500	0.963	-0.0173	0.464	0.451	0.111	-0.0572	-0.0793	0.196	0.771	0.135	-0.0621
0.375	0.946	-0.0175	0.443	0.446	0.114	-0.0618	-0.0596	0.188	0.777	0.136	-0.0549
0.250	0.935	-0.0127	0.430	0.436	0.115	-0.0638	-0.0402	0.185	0.781	0.137	-0.0458
0.125	0.927	-0.00535	0.427	0.422	0.116	-0.0645	-0.0207	0.185	0.784	0.137	-0.0356
0.000	0.919	0.00000	0.415	0.404	0.116	-0.0683	0.0000	0.192	0.784	0.136	-0.0255

CHAPTER 8

EXPERIMENTAL INVESTIGATION OF FLOW AROUND SOLIDS OF REVOLUTION IN A SUPERSONIC GAS FLOW

The calculation of gas flow in supersonic flow around axisymmetric bodies with a detached shock wave is a complex mathematical problem. Numerical methods with the use of electronic computers are presently employed to solve it. /270

To study the actual pattern of flow of a supersonic real gas around solids of revolution and also to evaluate the existing theoretical methods of calculation of flow around such bodies, we experimentally investigated flow around a sphere, cylinder, and two ellipsoids of revolution with a ratio of semiaxes equal to $b/a = 0.5$ and 1.5.

Experimental investigations set up to evaluate theoretical methods of calculating flow around bodies should have a quite high accuracy. Therefore, particular attention was devoted to the method of carrying out the experiments and to problems associated with ensuring a high accuracy of the measurements.

The investigations into supersonic gas flow around solids of revolution were carried out in the range $M_\infty = 2.00$–8.06. Curves of the distribution of pressure over the surface of the body and the shape and position of the nose shock wave were obtained.

In this work we will compare the obtained experimental data with the results of calculating flows in the region of influence of blunting by the method of integral relations [3 and 68] and of the supersonic zone by the method of characteristics [69 and 70].

Photographs of flow past a sphere and ellipsoids of revolution at different M_∞ numbers are also given.

Many of the results in this work were obtained in 1956.

1. Investigated Bodies and Measuring Equipment.

A sphere, cylinder, and three series of ellipsoids of revolution were manufactured for the experimental investigation of flow past axisymmetric bodies with a detached shock wave. /271

1. The sphere with a diameter of $D = 40$ mm is shown in Fig. 8.1. The figure shows that the sphere is fastened by means of a bracket on the lateral detachable caps of the working section of the tube. In the sphere are two pressure holes 0.4 mm in diameter arranged in one meridional section at an angular distance $\beta = 90°$ relative to one another.

2. The cylinder, with a diameter $D = 25$ mm, length $l = 150$ mm, and with pressure holes, is shown in Fig. 8.2. The two 0.4-mm-diameter holes are

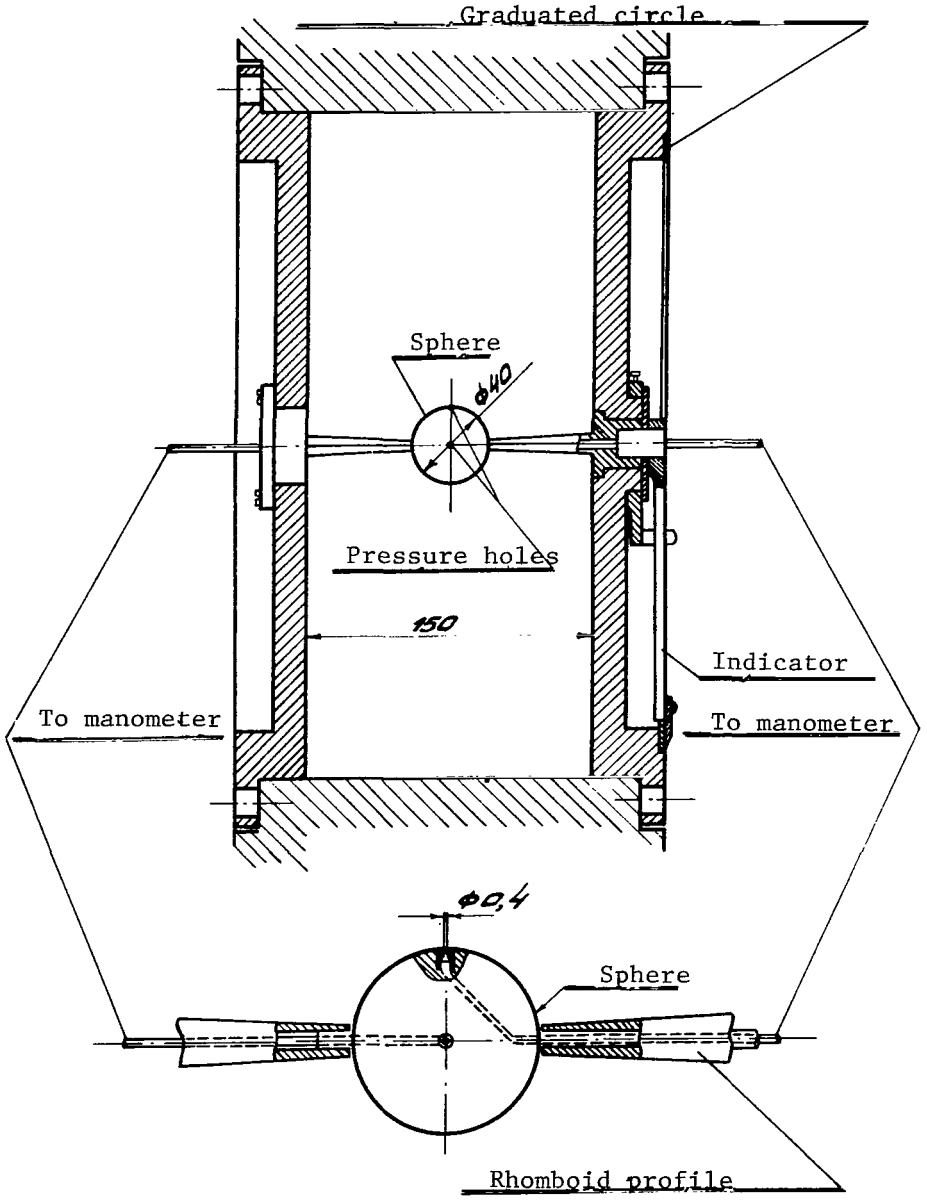

Figure 8.1. Sphere

arranged in the middle section of the cylinder at an angular distance $\beta = 90°$ relative to one another.

The second hole permits proper adjustment of the sphere or cylinder in the working section of the tunnel relative to the oncoming flow.

Along with solving a number of other methodological problems, we evaluated the effect of the diameter of the cylinder on the experimental results: two cylinders 10 and 15 mm in diameter and 150 mm long were additionally manufactured.

To carry out the experiments with the sphere and cylinder, a special device was designed and manufactured by means of which the test sphere or cylinder could be turned around the axis to any prescribed angle with an accuracy of $\pm$ 2'. This device consists of a removable cover on which is fastened a ring, a graudated circle calibrated in degrees. On the outside of this cover, on the cylindrical part of the holder of the sphere, or on the shank of the cylinder is rigidly fastened an indicator on the end of which is a vernier. The diagram of the attachment of the cylinder and of the device for measuring the angles are shown in Fig. 8.3.

3. The ellipsoids of revolution were made in three series.

The first series consisted of seven identical ellipsoids of revolution with a ratio of semiaxes $b/a = 0.5$. An ellipsoid of revolution of this series is shown in Fig. 8.4. The second series included three identical ellipsoids of revolution with the same ratio of semiaxes, but with a different arrangement of the holder (Fig. 8.5).

Eight identical ellipsoids of revolution with a ratio of semiaxes $b/a = 1.5$ made up the third series. An ellipsoid of revolution of this series is shown in Fig. 8.6.

The ellipsoid of revolution of a given series were manufactured from the /273
same pattern and differed from one another only by the arrangement of the pressure holes. This was done because it was impossible to place the necessary number of pressure holes on one ellipsoid.

On all ellipsoids of revolution of the same series (of the same shape) there were two identically arranged pressure holes, by means of which the pressure measurements were checked.

Some of the ellipsoids of revolution had two pressure holes which were /277
arranged at the top and bottom at an equal distance from the stagnation point. The pressure measured at these points enabled us to check the correctness of setting the model at a zero angle of attack.

Each ellipsoid of revolution had from eight to twelve holes.

All investigated bodies were manufactured with a tolerance of $\pm$ 0.03 mm.

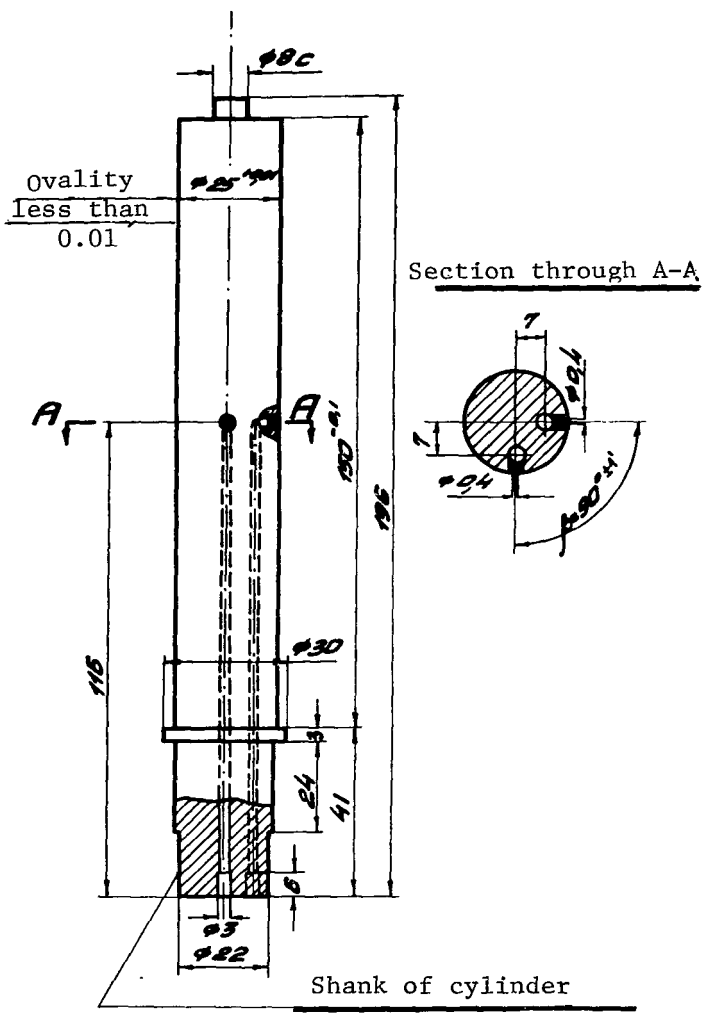

Figure 8.2. Cylinder

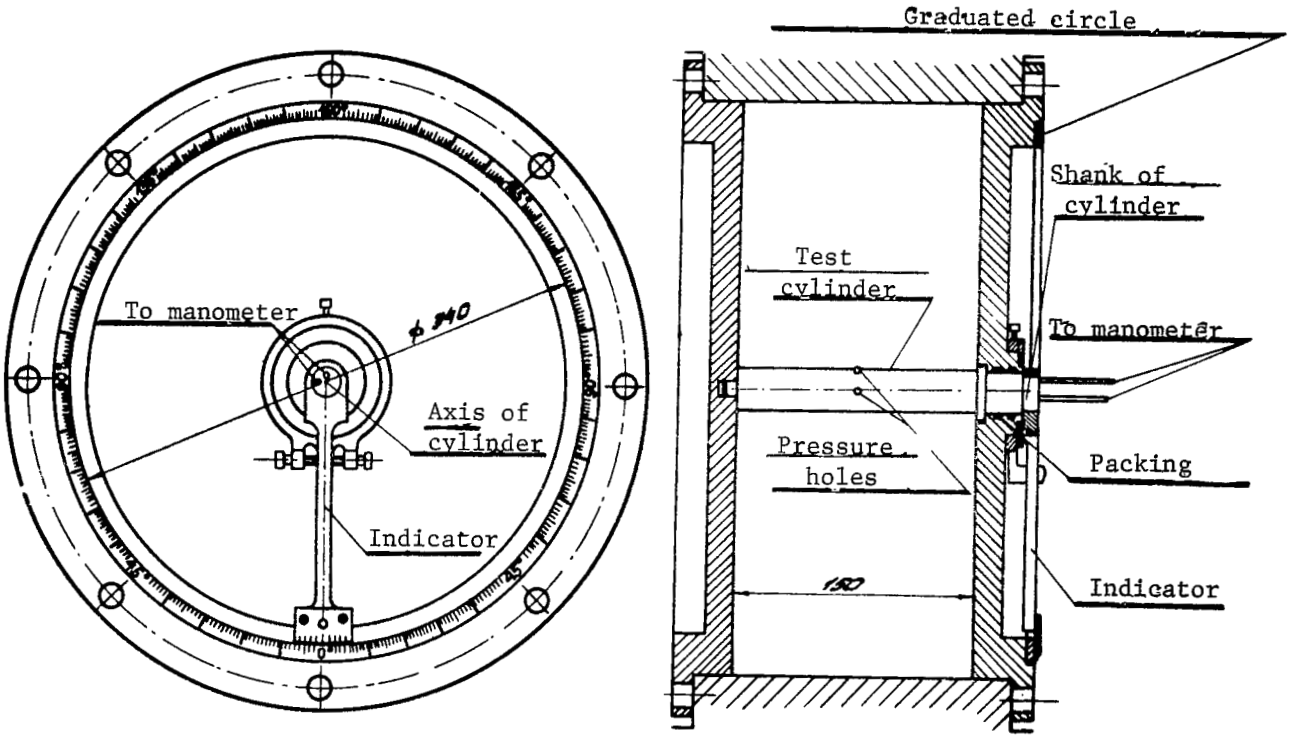

Figure 8.3. Diagram of device for measuring angles.

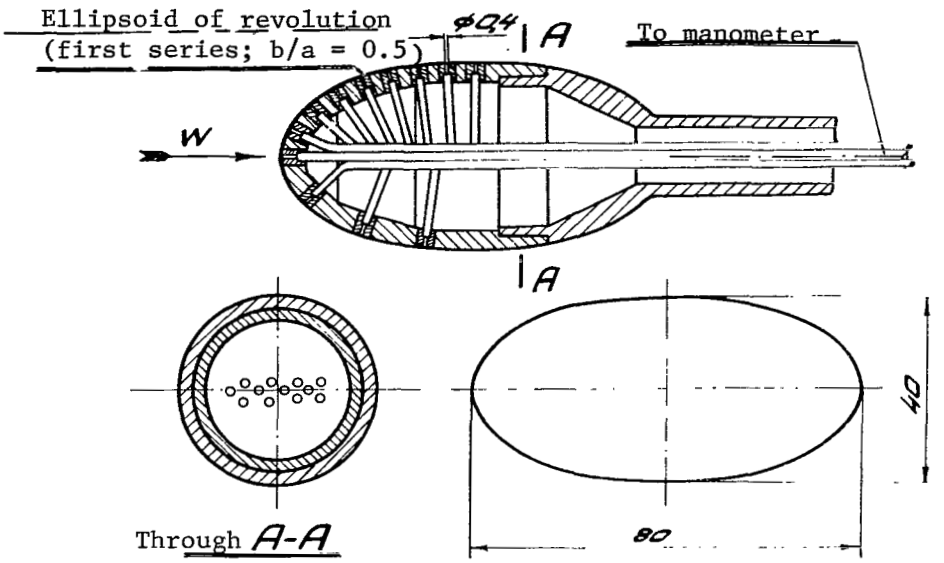

Figure 8.4. Ellipsoid of revolution, b/a = 0.5 (first series).

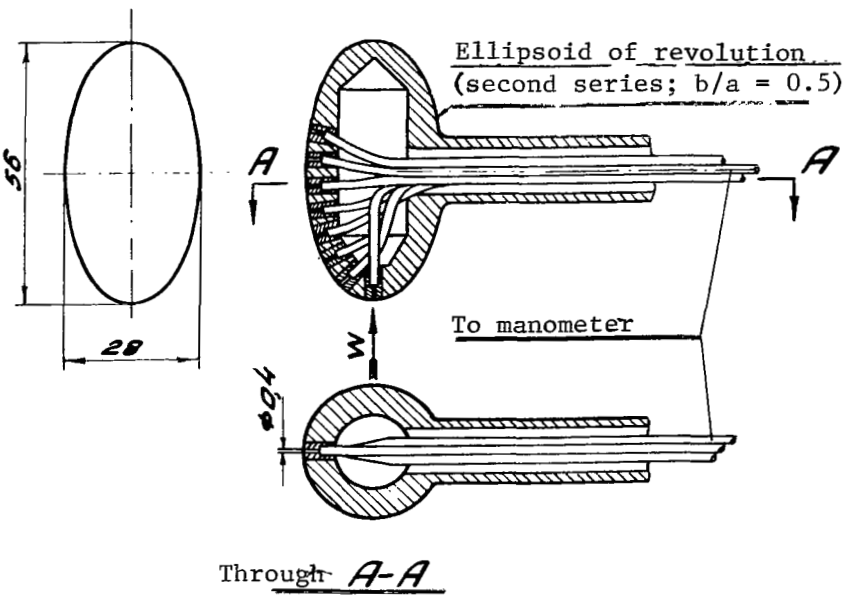

Figure 8.5. Ellipsoid of revolution, b/a = 0.5 (second series).

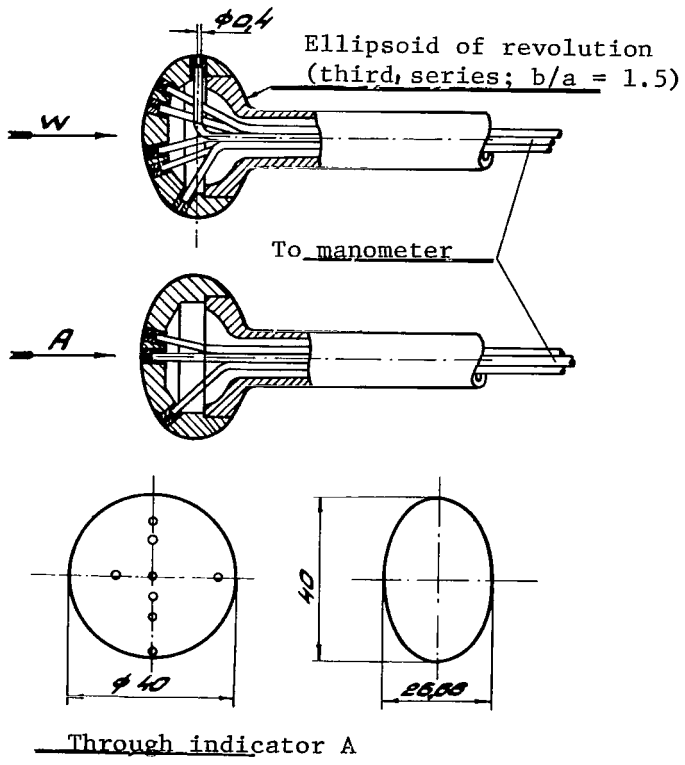

Figure 8.6. Ellipsoid of revolution, b/a = 1.5 (third series).

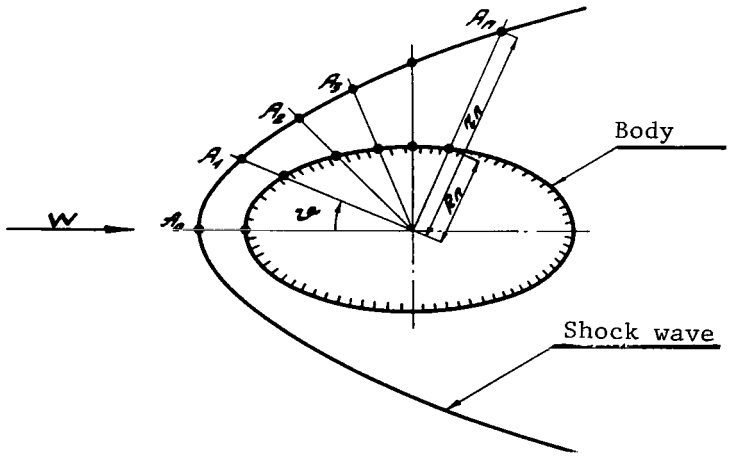

Figure 8.7. Diagram of determining angles $\hat{\chi}$.

The main geometric dimensions of the ellipsoids of revolution, coordinates of the outside contour, and the coordinates of the pressure holes are given in Tables 8.1 and 8.2.

The pressure in the forechamber of the wind tunnel was determined from the average value of the readings of two total-head tubes. At $M_\infty = 2$ the pressure was measured by a U-shaped mercury monometer. The presence of a vernier on a movable device with an optical sight ensured an accuracy of reading the measure pressure of $\pm$ 0.1 mm Hg at $M_\infty = 3$ the total-head tubes were connected with a Bourdon gauge which was calculated for a maximum mal pressure of 5 kg/cm^2. The installation of a special mechanism for turning the scale in the presence of th vernier provided an accuracy of reading the gauge pressure of $\pm$ 0.0016 kg/cm^2. The total-head tubes at $M_\infty = 4$ were connected with a standard tube-type manomet designed for a maximal pressure of 10 kg/cm^2. The scale division of this manometer was equal to 0.0333 kg/cm^2. The gauge pressure in the forechamber at $M_\infty = 6.05$ was measured by a standard manometer intended for a maximal pressure of 40 kg/cm^2, with a scale division equal to 0.1333 kg/cm^2. At $M_\infty = 8.06$ we used a standard manometer for 100 kg/cm^2 with a scale division equal to 0.333 k cm^2.

The temperature in the forechamber of the tunnel when $M_\infty = 2$, $M_\infty = 3$, and $M_\infty = 4$ was measured by a standard mercury thermometer with a scale division of 0.1°C. When $M_\infty = 6.05$ and 8.06 the temperature is measured by chromel-alumel thermocouples with a measurement range up to 800°C. The readings of the thermocouples were recorded by a EPP-9 potentiometer. In this case the temperature was measured with an accuracy of $\pm$ 5°C.

The pressure on the surface of the sphere, cylinder, and ellipsoids of revolution at numbers $M_\infty = 2$; 3, and 4 was measured by a U-shaped mercury manometer and a sliding scale. Since the pressure on the bodies of revolution with $M_\infty = 6.05$ and 8.06 varied within a wide range, a pressure less than 16 mm Hg was measured by a group recording manometer intended for a maximal pressure up to 16 mm Hg, and above 16 mm Hg the pressure was measured by the same type of instruments with upper limits up to 70 mm Hg and to 1 absolute atmosphere. The class of accuracy of the group recording manometers was $\pm$ 0.35 percent of the upper limit of measurement.

The pressure measured in the group recording manometer was sensed by a sylphon bellows mounted on a lever. The sylphon bellows transforms the pressu into a force acting on the lever, which is adjusted by the force of deformatio of a helical measuring spring. The magnitude of deformation of the measuring spring serves as a measure of the pressure. The instrument consists of a grou of such elements connected by a common drive and by a common recording mechani All measuring elements have the same principle of action. To measure the pressure of different ranges appropriate sylphon bellows and helical springs are installed and the size of the lever arms adjusted.

To obtain shadowgraphs we used the collimator part of the IAB-451 optical instrument with the flash light source and film holder from the AFA-BA aerial camera which was installed directly at the window of the working section of the wind tunnel.

The distance of the nose shock wave from the body was determined by means of a coordinatograph produced by the Swiss company Coradi, which was installed on a KP-8M copying instrument. Angles ϑ were measured with an accuracy of 0.5', and the linear dimensions in the direction of rays A_1, A_2, ..., A_n (Fig. 8.7) with an accuracy of $\pm$ 0.02 mm.

2. Conduction and Analysis of Results of Experiments

The investigations of the solids of revolution were carried out in a supersonic wind tunnel in the range M_∞ = 2.00 - 8.06. The installation could work indefinitely since the gas cylinders had a large volume in comparison with the air flow rate.

The values of total pressure, stagnation temperature in the forechamber of the tunnel, and the Re number calculated with respect to the linear dimension of the body in the direction of flow are given in Table 8.3 for various values of the numbers M_∞. The following quantities were measured simultaneously during the experiments: pressure on the solids of revolution, static pressure on the wall of the working section, total pressure, and stagnation temperature in the /279 forechamber of the tunnel.

The sphere was investigated at numbers M_∞ = 2, 3, 4, 6.05, and 8.06. The investigated sphere, at each value of M_∞, was installed in the working section so that the axis of one pressure hole coincided with the direction of the oncoming flow and the axis of the other hole formed an angle $\beta = 90°$ with it. After installing the sphere the pressure p was measured when $\Theta = 0$. Then the sphere was turned in the flow through angle $\Delta\theta$ relative to its own axis which was arranged normal to the direction of flow, and measurement of the pressure was repeated. In this manner pressure p was measured on the surface of the sphere for each value of $M\infty$ in the range θ = 0-180°.

In the same manner we measured the pressure on the two cylinders with a diameter of 15 and 25 mm. The 15-mm-diameter cylinder was tested at M_∞ = 2, 4, and 8.06, and the 25-mm-diameter cylinder was investigated at M_∞ = 3 and 6.05. Just as for the sphere, at each fixed value of the angle θ the pressure p was measured on the surface of the cylinder.

To elicit the effect of the diameter of the cylinder and the diameter of the pressure hole on the experimental results, additional tests were carried out at M_∞ = 3.00. The 25-mm-diameter cylinder was at first tested with two equal pressure holes (d = 0.4 mm), then one of the holes was enlarged and the experiment was repeated, in which case the diameter of the other hole was left constant. This hole served for control measurements of pressure. The tests for the distribution of pressure at M_∞ = 3 were carried out also with cylinders 10 and 15 mm in diameter.

The ellipsoids of revolution were tested at M_∞ = 3, 4, 6.05, and 8.06. A zero angle was established by means of a level with a subsequent check for the equality of the pressures which were measured at the pressure points symmetrically arranged on the bodies relative to the flow axis. As was already noted, a sufficient number of pressure holes could not be placed on one ellipsoid of revolution. To obtain a detailed picture of the distribution of pressure over the body, we tested identical ellipsoids of revolution with a ratio of semiaxes b/a = 0.5 and eight identical ellipsoids of revolution with a ratio of semiaxes b/a = 1.5 with a different arrangement of the pressure holes. The ellipsoids of the first and third series were tested under the same conditions in two positions, the change from the first position to the second being achieved by turning the ellipsoid through 180° around its own axis which coincided with the direction of the oncoming flow. The ellipsoids of revolution of the second series were tested by the same program as those of the first and third series, but their rotation was accomplished around an axis normal to the direction of flow. In this case we were careful that the test conditions of the ellipsoids were identical.

To determine the shape and position of the nose shock wave relative to th body at different values of M_∞, we photographed the pattern of flow around a sphere and two ellipsoids of revolution in the stream.

Pressure p measures on the surface of the solids of revolution at a value M_∞ = const and different values of the angle θ were referred to the pressure $p_{\theta = 0}$. For each value of M_∞ we obtained the dependence $p/p_{\theta = 0} = \bar{p}\ (\theta)$ wher θ is the value of the angle in radians (Fig. 8.8). Furthermore, the measured

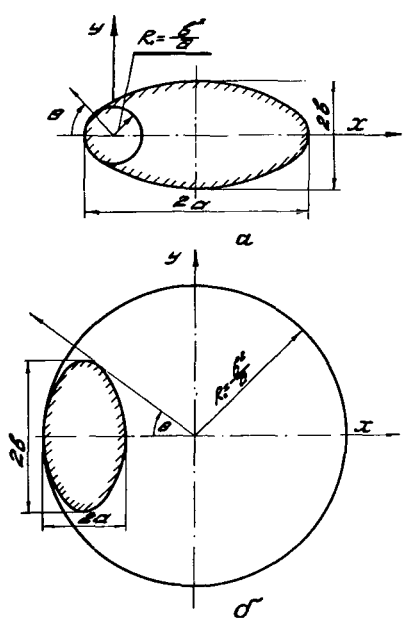

Figure 8.8. Diagram for determining angles θ:
a) b/a = 0.5; b) b/a = 1.5.

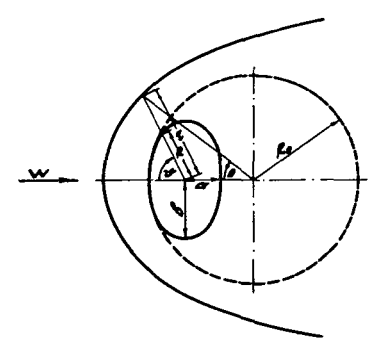

Figure 8.9. Diagram for converting angles θ to angles ϑ.

pressure p was referred to the total pressure p_0 in the forechamber of the tunnel. As a result we obtained the dependencies $p/p_0 = \tilde{p}(\vartheta)$.

The conversion from angles θ to ϑ for ellipsoids of revolution was accom- /281
plished by the formula

$$\vartheta = \operatorname{arcctn} \frac{ax}{b\sqrt{a^2 - x^2}},$$

where

$$x = \frac{(a^2 - b^2)a + b^2 \operatorname{ctn}\theta \sqrt{a^2 \operatorname{ctn}\theta + 2a^2 - b^2}}{a^2 + b^2 \operatorname{ctn}^2 \theta}.$$

For the sphere and cylinders the angles θ to ϑ coincide (Fig. 8.9), and the dimensionless distances from the body to the shock wave ε' and ε (ε' is the distance from the body to the shock wave along ray θ = const referred to $R_0 = b^2/a$) also coincide. For ellipsoids of revolution the formulas for converting from the coordinates of the shock wave ε' and θ to coordinates ε and ϑ have the following form:

$$\vartheta = \operatorname{arcctn} \frac{(A + \varepsilon')b^2 \cos\theta + a^2 - b^2}{(A + \varepsilon')b^2 \sin\theta};$$

$$\varepsilon = \frac{b}{a}\left(\sin^2\vartheta + \frac{b^2}{a^2}\cos^2\vartheta\right)^{1/2}\left[(A+\varepsilon')^2 - 2(A+\varepsilon') \times \left(1 - \frac{b^2}{a^2}\right)\cos\theta + \left(1 - \frac{a^2}{b^2}\right)^2\right]^{1/2} - 1,$$

where $A = \frac{c_1 + \sqrt{c_1^2 - cc_2}}{c}$ is the distance from the center of curvature (for point $\theta = 0$) to the ellipse, referred to the axis of curvature, when $\theta = 0$,

$$c = \frac{b^2}{a^2}\left(\sin^2\theta + \frac{b^2}{a^2}\cos^2\theta\right); \quad c_1 = \frac{b^2}{a^2}\left(\frac{b^2}{a^2} - 1\right)\cos\theta; \quad c_2 = \left(\frac{b^2}{a^2} - 1\right) - 1.$$

The distance from the body to the shock was defined as the distance between the points of intersection of the ray with the shock-wave contour and the body contour.

The relative distance ε_n from the body to the shock wave was defined as

the ratio $\frac{r_n - R_n}{R_n}$, where r_n is the distance between the center of symmetry of the model and the wave contour, and R_n is the distance between the center and contour of the body.

The number M_∞ in the working section of the tunnel was determined by the formula

$$\frac{p_0}{p_0'} = \left(\frac{2\varkappa}{\varkappa+1}M_\infty^2 - \frac{\varkappa-1}{\varkappa+1}\right)^{\frac{1}{\varkappa-1}} \left(\frac{1+\frac{\varkappa-1}{2}M_\infty^2}{\frac{\varkappa+1}{2}M_\infty^2}\right)^{\frac{\varkappa}{\varkappa-1}},$$

where p_0 is the total pressure measured in the forechamber of the tunnel; p_0' is the total pressure behind a direct shock wave, measured by a total-head tube in the working section of the tunnel; $\varkappa = \frac{c_p}{c_v}$ is the ratio of specific heat capacities, for air $\varkappa = 1.40$.

3. Experimental Results

As the result of these experiments at various values of M_∞ of the oncoming flow for a sphere, cylinder, and ellipsoids of revolution, we determined the dependences $\bar{p}(\theta)$, $\bar{p}(\vartheta)$, and $\varepsilon(\vartheta)$.

The dependence $\bar{p}(\theta)$ for a sphere at different values of M_∞ is presented in Figs. 8.10 - 8.14 and in Tables 8.4 and 8.5. In these figures the curves calculated by the method of integral relations [68] and by the method of characteristics [69]* are plotted by a solid line. We see from a comparison of the results of the experiment and theoretical calculation that the theory agrees nicely with the experiment.

We also measured the distribution of pressure p over the surface of a cylinder in its middle section at equal angular intervals. The results of the experiments are given in Tables 8.6 and 8.7 and are shown in Figs. 8.15 - 8.23 as the dependence $\bar{p}(\theta)$. The results of the experiments are compared in Fig. 8. with the results of theoretical calculations obtained in the first, second, and

---

* For the intermediate values of M_∞ of the oncoming flow (flow around a sphere when $M_\infty = 2$ and 8.06, cylinder when $M_\infty = 2$, 6.05, and 8.06, and ellipsoid of revolution with a ratio of semiaxes $b/a = 1.5$ when $M_\infty = 3$), the data on the calculations by the method of integral relations and the method of characteristics were presented by O. M. Belotserkovskiy.

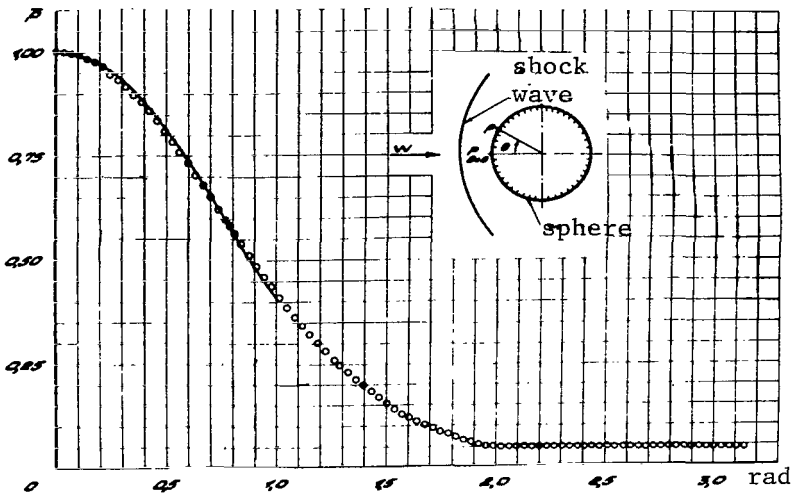

Figure 8.10. Distribution of pressure over surface of sphere when M_∞ = 2:
ooo experiment; ——— theory.

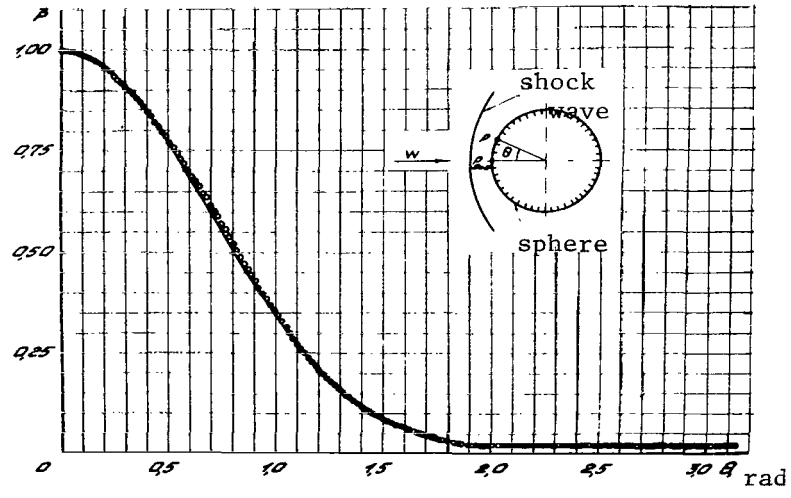

Figure 8.11. Distribution of pressure over surface of sphere when M_∞ = 3:
ooo experiment; ——— theory.

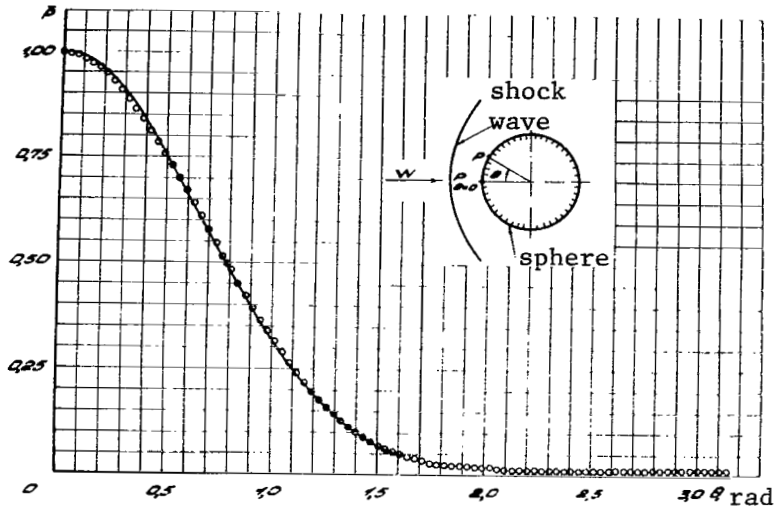

Figure 8.12. Distribution of pressure over surface of sphere when $M_\infty = 4$:
∘ ∘ ∘ experiment; —— theory.

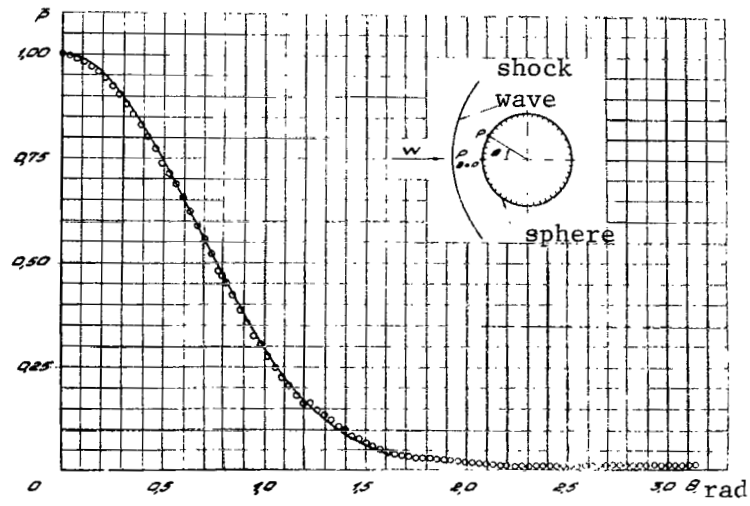

Figure 8.13. Distribution of pressure over surface of sphere when $M_\infty = 6.05$:
∘ ∘ ∘ experiment; —— theory.

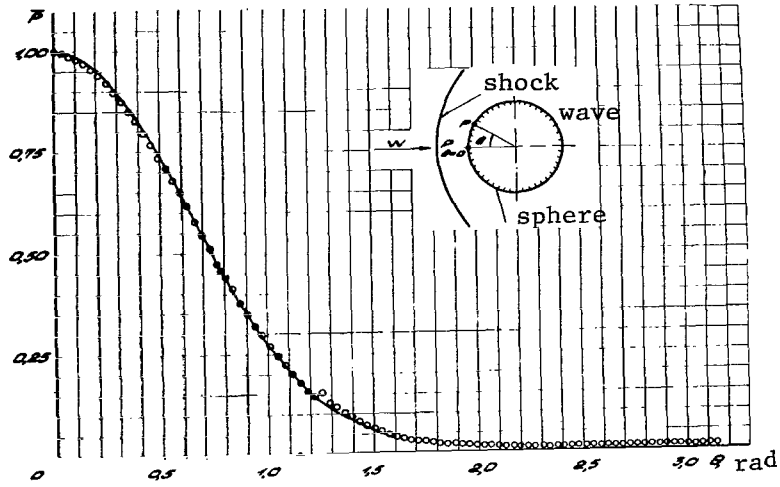

Figure 8.14. Distribution of pressure over surface of sphere when M_∞ = 8.06:
o o o experiment; ——— theory.

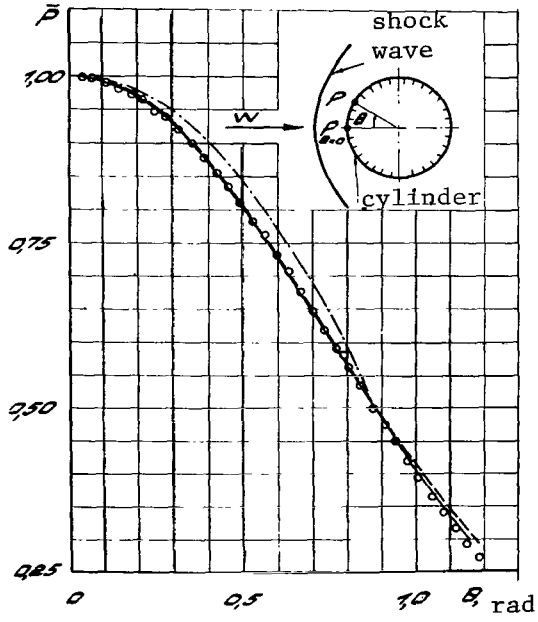

Figure 8.15. Distribution of pressure over surface of circular cylinder when M_∞ = 3:
o o o experiment; -.- approximation 1; --- approximation 2;
——— approximation 3.

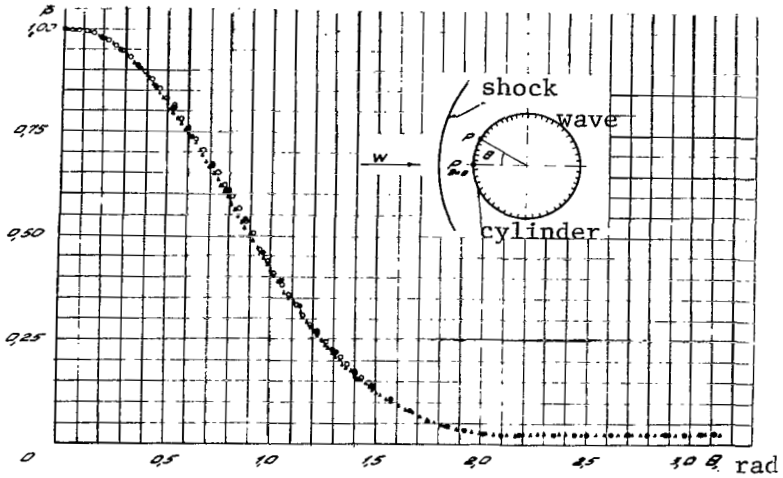

Figure 8.16. Distribution of pressure over surface of circular cylinder of different diameters when $M_\infty = 3$:
∘ ∘ ∘ D = 10 mm; • • • D = 15 mm;
ΔΔΔ D = 25 mm .

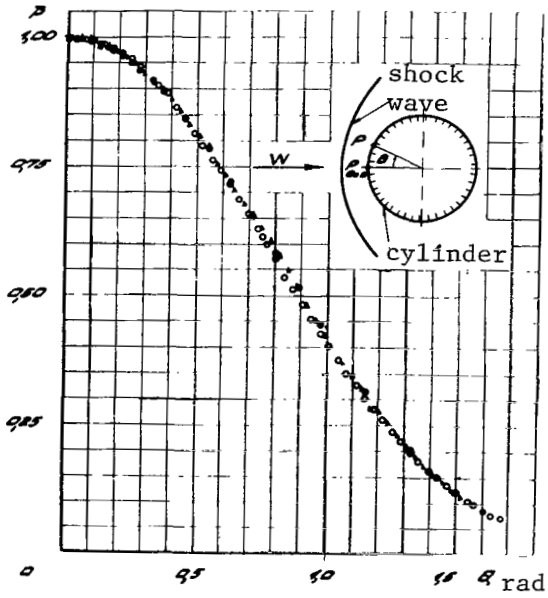

Figure 8.17. Distribution of pressure over surface of circular cylinder, D = 25 mm, when $M_\infty = 3$:
∘ ∘ ∘ experiment; $\bar{d} = 0.016$;
• • • $\bar{d} = 0.040$; ΔΔΔ $\bar{d} = 0.064$.

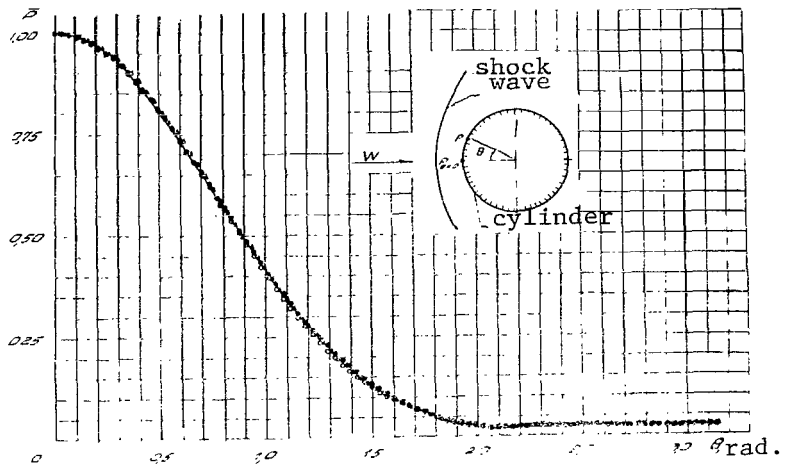

Figure 8.18. Distribution of pressure over surface of circular cylinder when $M_\infty = 3$:

ooo experiment 1956; ●●● 1959; ΔΔΔ 1965; ——— theory.

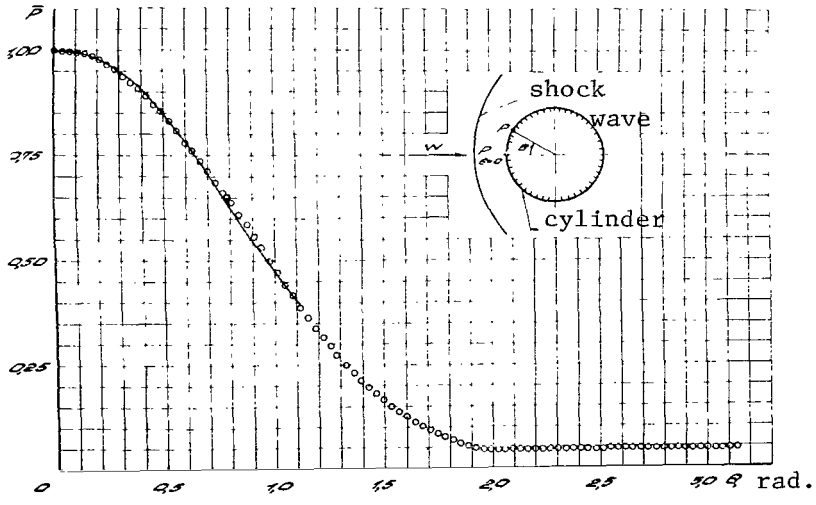

Figure 8.19. Distribution of pressure over surface of circular cylinder when $M_\infty = 2$:

ooo experiment; ——— theory.

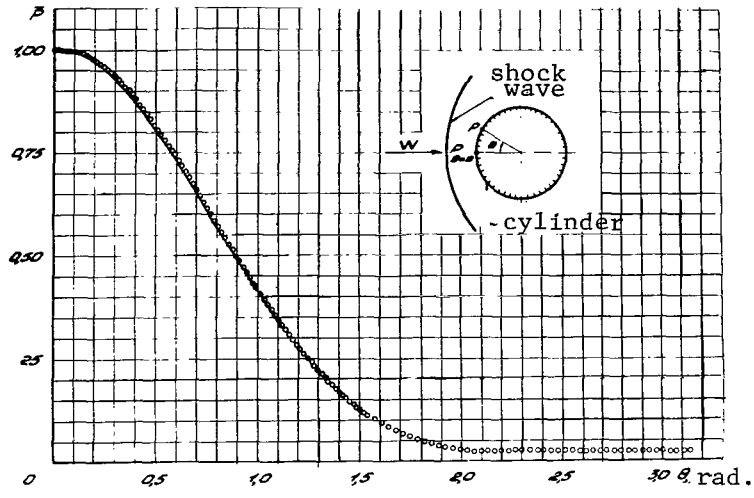

Figure 8.20. Distribution of pressure over surface of circular cylinder when $M_\infty = 3$:

ooo experiment; ——— theory.

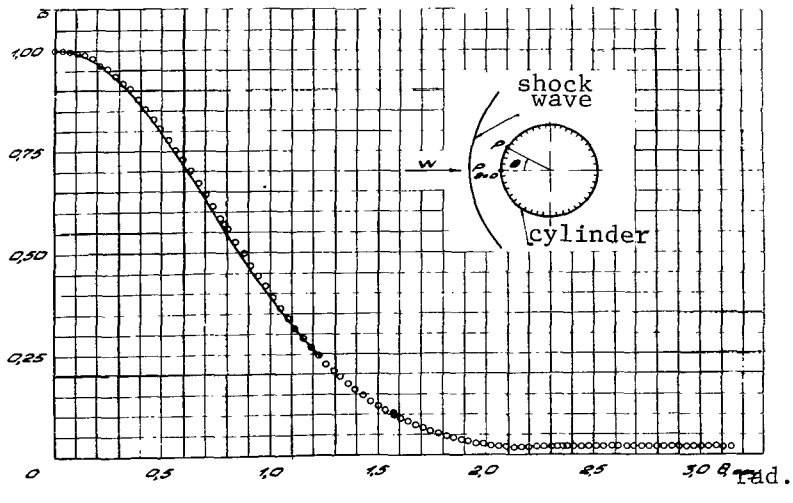

Figure 8.21. Distribution of pressure over surface of circular cylinder when $M_\infty = 4$:

ooo experiment; ——— theory.

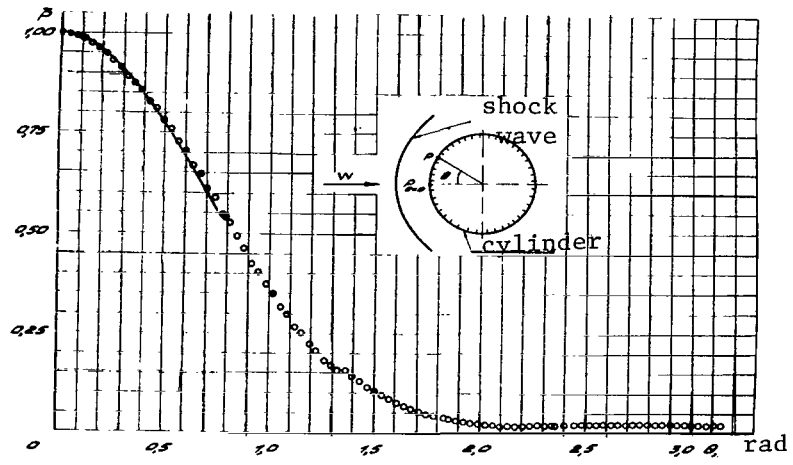

Figure 8.22. Distribution of pressure over surface of circular cylinder when M_∞ = 6.05: ooo experiment; ——— theory.

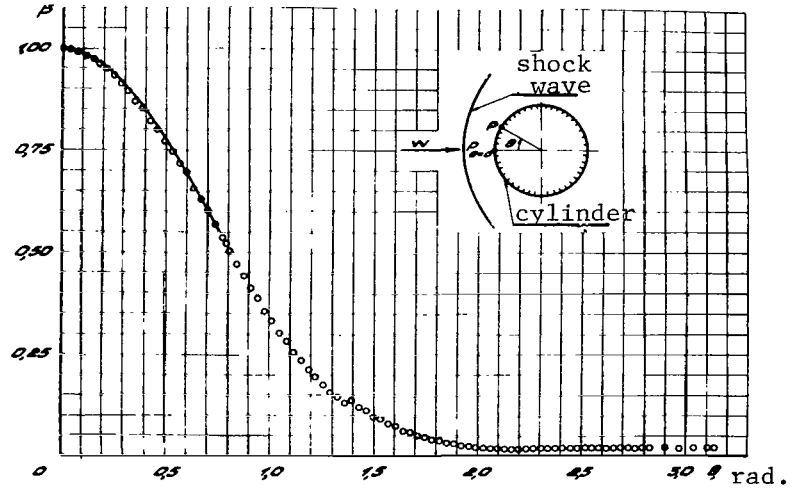

Figure 8.23. Distribution of pressure over surface of circular cylinder when M_∞ = 8.06: ooo experiment; ——— theory.

third approximations by scheme I of the method of integral relations. As we see from Fig. 8.15, in the entire range of angles θ the theoretical curve of the second and third approximations agree well with the results of the experiments. The results of experiments carried out with cylinders of different diameters when $M_\infty = 3$ are shown in Fig. 8.16. We see that the size of the diameter of the cylinder has almost no affect on the results of the experiment.

The dependence $\bar{p}(\theta)$ for cylinder D = 25 mm with different sizes of the pressure hole is shown in Fig. 8.17. A change of diameter of the pressure hole with limits from 0.4 to 1.6 mm has no substantial effect on the results of the experiments. Control experiments carried out with the same cylinder D = 25 mm when $M_\infty = 3$, as we see from Fig. 8.18, agree well with one another. /29

The curves calculated by the method of integral relations [3] and the method of characteristics [70] at corresponding values of M_∞ are plotted in Figs. 8.19 - 8.23 as solid lines. The results of the theoretical calculations and experimental investigations agree well with one another.

The experimental dependence $\bar{p}(\theta)$ for an ellipsoid of revolution with a ratio of semiaxes b/a = 0.5 at different values of M_∞ is shown in Figs. 8.24 - 8.27 and is given in Table 8.8. Figures 8.24 and 8.25 give the results of tests of this ellipsoid when $M_\infty = 3$ and 4. The same figures show the theoretical dependence $\bar{p}(\theta)$. A comparison of the calculation with the obtained results shows a good agreement between theory and experiment. Figures 8.26 and 8.27 give the experimental points obtained at values $M_\infty = 6.05$ and 8.06. We see that the theory agrees sufficiently well with the results of the experiments.

The results of the experiments carried out with an ellipsoid of revolution (ratio of semiaxes b/a = 1.5) when $M_\infty = 3$, 4, 6.05, and 8.06 are shown in Figs. 8.28 - 8.31 and are presented in Table 8.9. In Figs. 8.28 - 8.31 the dependence $\bar{p}(\theta)$ based on the data of the theoretical calculation is represented by a solid line. A comparison of the calculated curve with the experimental results shows a good agreement.

The results of measuring pressures at control points (Table 8.10) of ten ellipsoids of revolution with a ratio of semiaxes b/a = 0.5 in the entire range of M_∞ numbers agree well with each other. The same can be said about the results of testing eight ellipsoids of revolution with a ratio of semiaxes b/a = 1.5. This indicates that certain differences in geometric dimensions (within the tolerances) of manufactured models, the errors associated with installing the models in the working section of the tunnel, and the deviations in the operating conditions of the tunnel were comparatively small and did not have a substantial effect on the experimental results.

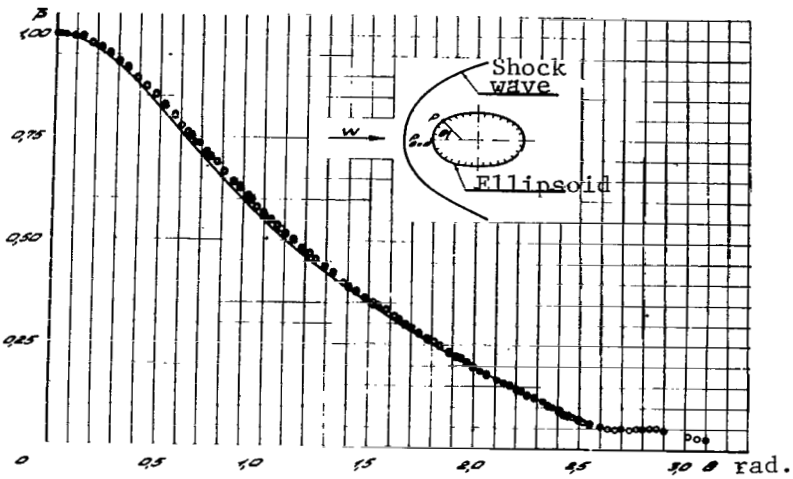

Figure 8.24. Distribution of pressure over surface of ellipsoid of revolution (b/a = 0.5) when M_∞ = 3: ooo experiment; ——— theory.

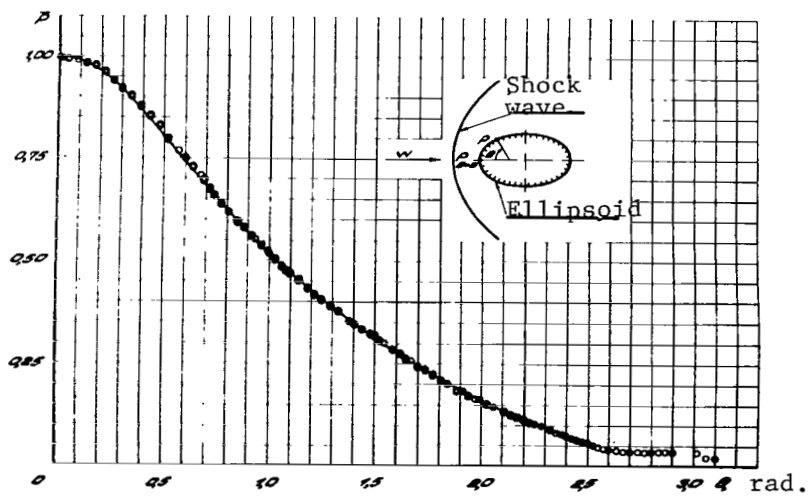

Figure 8.25. Distribution of pressure over surface of ellipsoid of revolution (b/a = 0.5) when M_∞ = 4: ooo experiment; ——— theory.

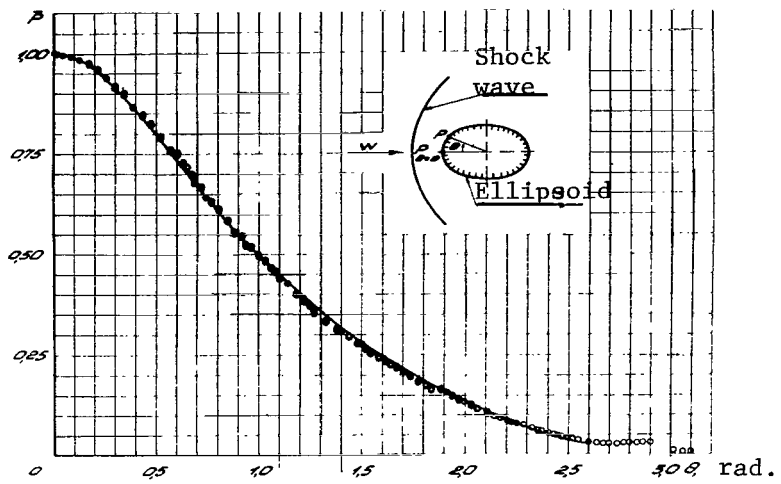

Figure 8.26. Distribution of pressure over surface of ellipsoid of revolution (b/a = 0.5) when M_∞ = 6.05: ooo experiment;——— theory.

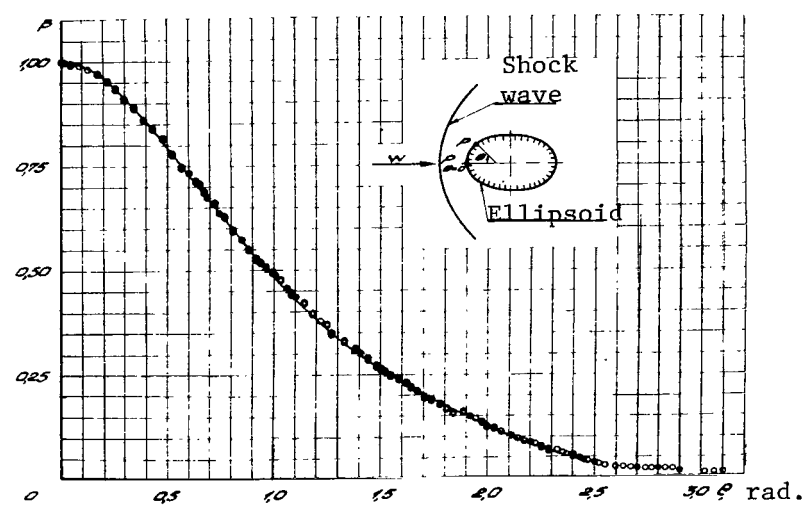

Figure 8.27. Distribution of pressure over surface of ellipsoid of revolution (b/a = 0.5) when M_∞ = 8.06: ooo experiment; ——— theory.

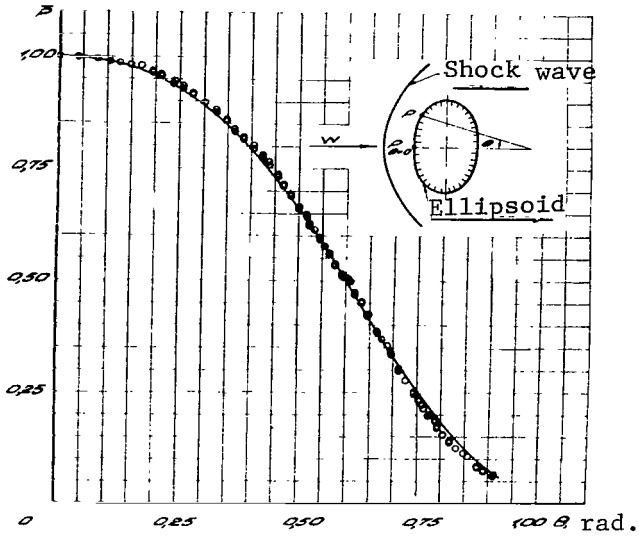

Figure 8.28. Distribution of pressure over surface of ellipsoid of revolution (b/a = 1.5) when M_∞ = 3: ooo experiment; ——— theory.

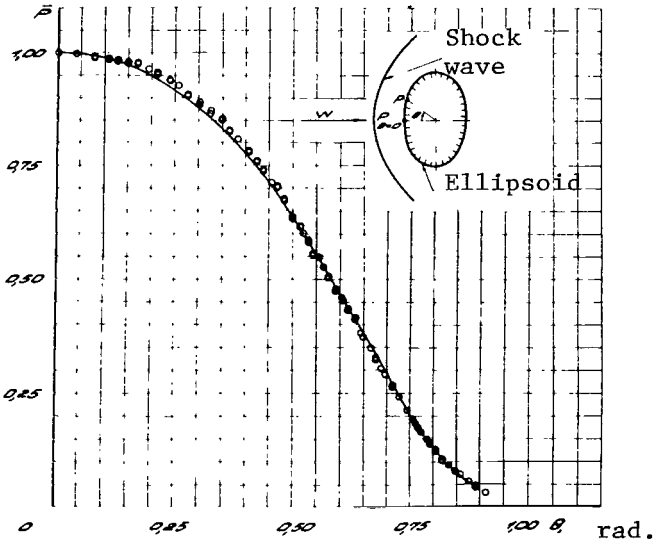

Figure 8.29. Distribution of pressure over surface of ellipsoid of revolution (b/a = 1.5) when M_∞ = 4: ooo experiment; ——— theory.

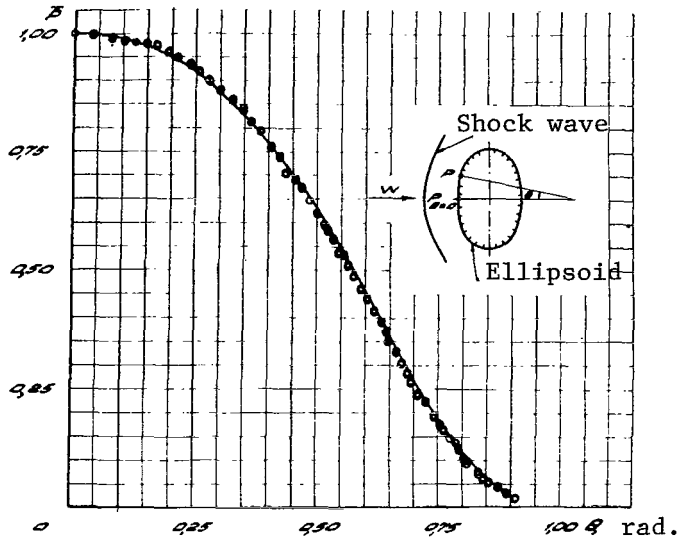

Figure 8.30. Distribution of pressure over surface of ellipsoid of revolution (b/a = 1.5) when M_∞ = 6.05: ooo experiment; —— theory.

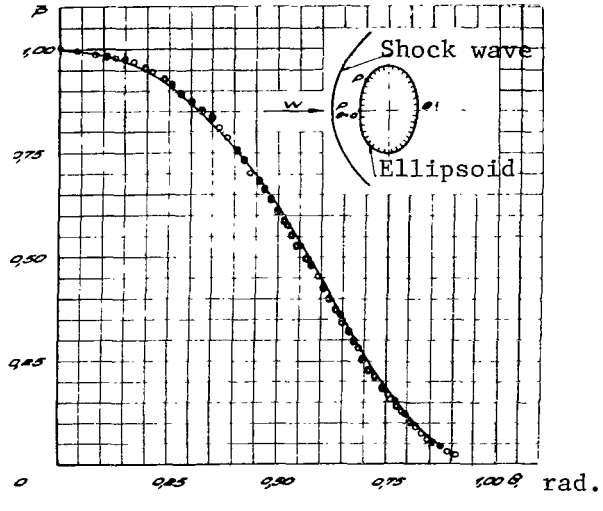

Figure 8.31. Distribution of pressure over surface of ellipsoid of revolution (b/a = 1.5) when M_∞ = 8.06: ooo experiment; —— theory.

We see from a comparison of the results of measuring pressure over the surface of a sphere, cylinder, and ellipsoids of revolution that the dispersion of the experimental points for ellipsoids at all values of M_∞ is somewhat greater than for the sphere and cylinder. This is apparently explained by the influence of insignificant defects in the manufacture (within the body) of the lines connecting the receiving (pressure) holes with the recording apparatus. /295

It is also necessary to note that as M_∞ increases, the dependence $\bar{p}(\theta)$ becomes rather weak with respect to the M_∞ numbers. At high values of M_∞ this relation changes so little that it can be considered virtually independent of M_∞.

The relation $\tilde{p}(\vartheta)$ is shown in Figs. 8.32 - 8.36 for a sphere. In these figures the calculated curves are plotted by a solid line. A comparison shows good agreement between the theory and experiment.

Figures 8.37 - 8.41 show the results of experiments on flow around a cylinder at various values of M_∞. A comparison of the experimental and calculated relations $\tilde{p}(\vartheta)$ at all M_∞ numbers also shows their good agreement.

Figures 8.42 - 8.45 depict the experimental points for an ellipsoid of revolution with a ratio of semiaxes $b/a = 0.5$ and the curves reflecting the theoretical calculations. As we see from the figures, the results of the theory agree nicely with the experimental data. The same (Figs. 8.46 - 8.49) can be said about the experiments carried out for an ellipsoid of revolution with a ratio of semiaxes $b/a = 1.5$.

We note that for all investigated solids of revolution (with a minor exception) the experimental data somewhat diverge from the theoretical in the initial section. The theoretical curves pass below or above the theoretical points. The maximal divergence between the theoretical and experimental values is about 4 percent.

We must also note that in experiments at values $M_\infty = 6.05$ and 8.06 the monotonic shape of the experimental relation $\bar{p}(\theta)$ is disrupted for all solids of revolution at a certain value of the angle θ. Thus, for example, the ratio of pressure $\bar{p}$ increases from 0.125 to 0.138 for the cylinder when $M_\infty = 8.06$ in the range $1.360 \leq \theta \leq 1.390$. This phenomenon is apparently explained by the occurrence at this place of a weak shock wave and separation of flow. It is characteristic that disruption of the monotonicity of the shape of the experimental curve for all bodies occurs approximately at the same value of $\bar{p}$.

The shape and position of the shock wave relative to the body were determined for the sphere and ellipsoids of revolution at various M_∞ values by the shadow method. The results of these experiments are shown in Figs. 8.50 - 8.55 and are presented in Tables 8.11 - 8.13. /305

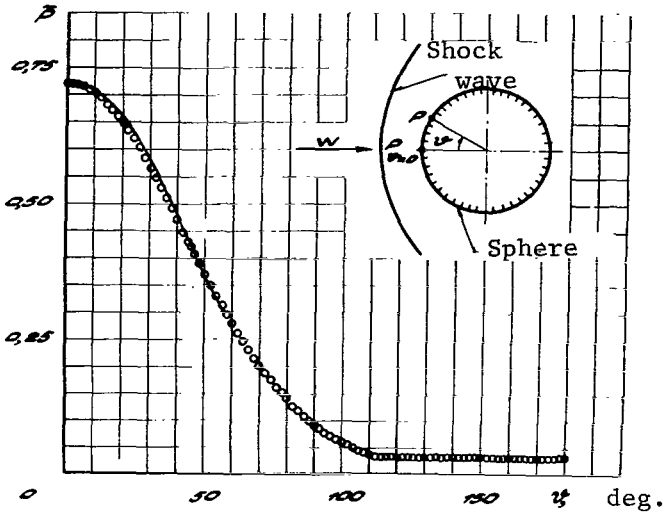

Figure 8.32. Dependence $\tilde{p}(\vartheta)$ for sphere when $M_\infty = 2$: ooo experiment; ——— theory.

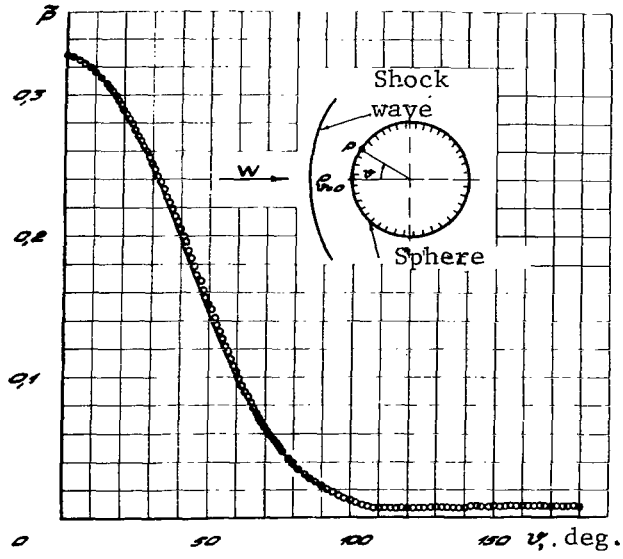

Figure 8.33. Dependence $\tilde{p}(\vartheta)$ for sphere when $M_\infty = 3$: ooo experiment; ——— theory.

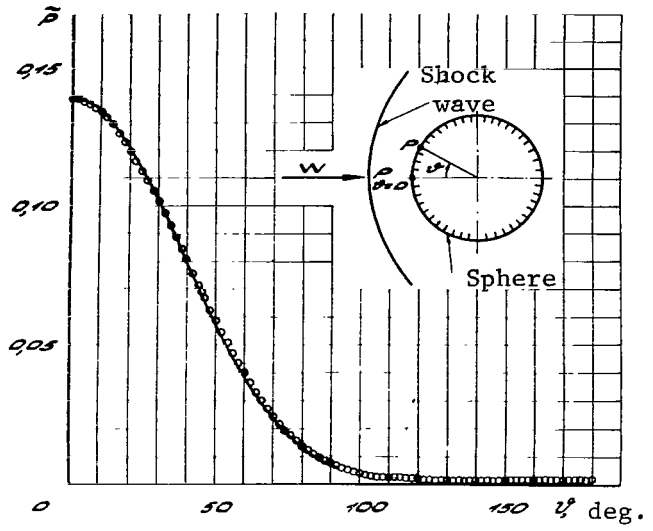

Figure 8.34. Dependence $\tilde{p}(\vartheta)$ for sphere when $M_\infty = 4$: ooo experiment; ——— theory.

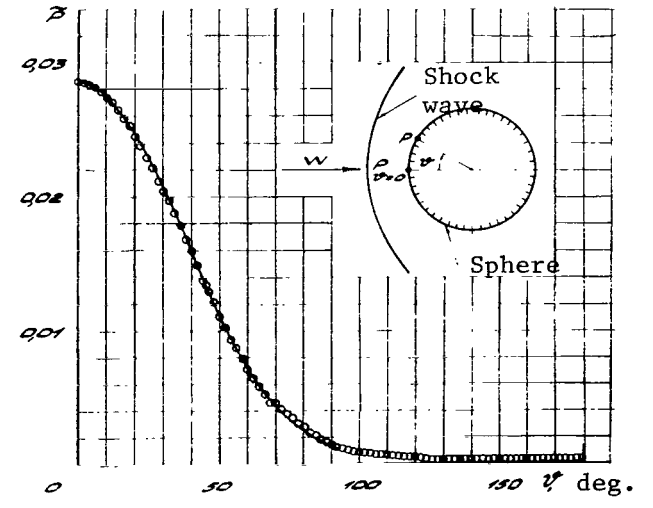

Figure 8.35. Dependence $\tilde{p}(\vartheta)$ for sphere when $M_\infty = 6.05$: ooo experiment; ——— theory.

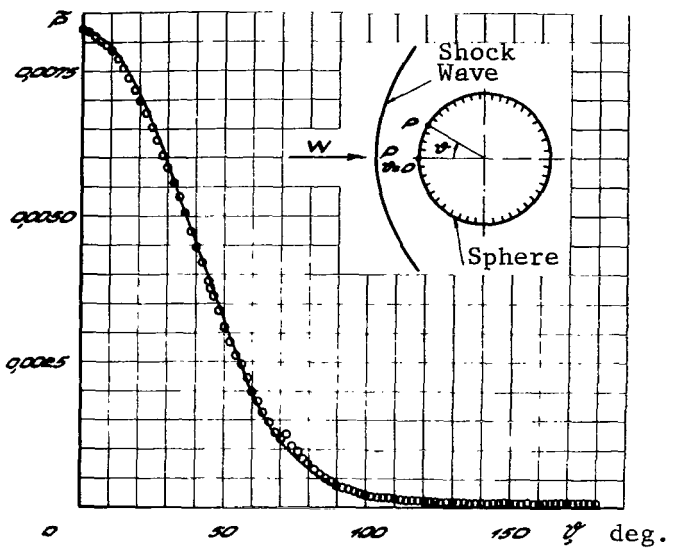

Figure 8.36. Dependence $\tilde{p}(\vartheta)$ for sphere when $M_\infty = 8.06$:
o o o experiment; —— theory

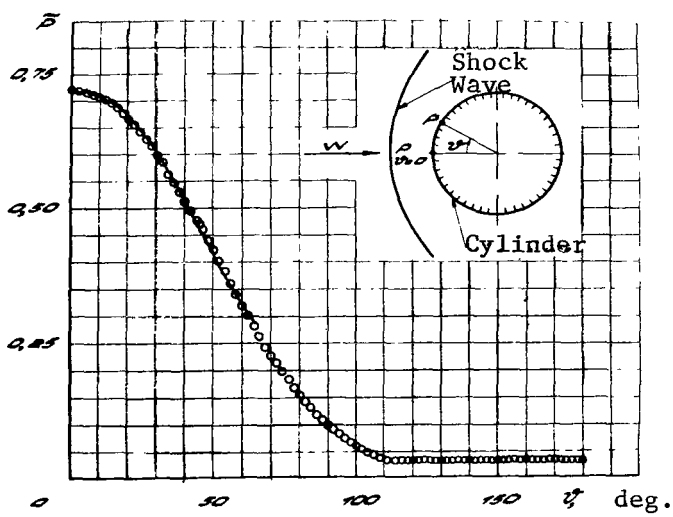

Figure 8.37. Dependence $\tilde{p}(\vartheta)$ for circular cylinder when $M_\infty = 2$:
o o o experiment; —— theory.

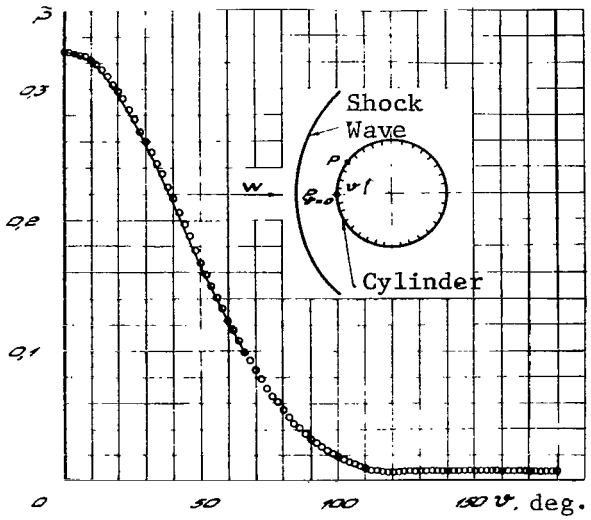

Figure 8.38. Dependence $\tilde{p}(\vartheta)$ for circular cylinder when $M_\infty = 3$:
o o o experiment; —— theory.

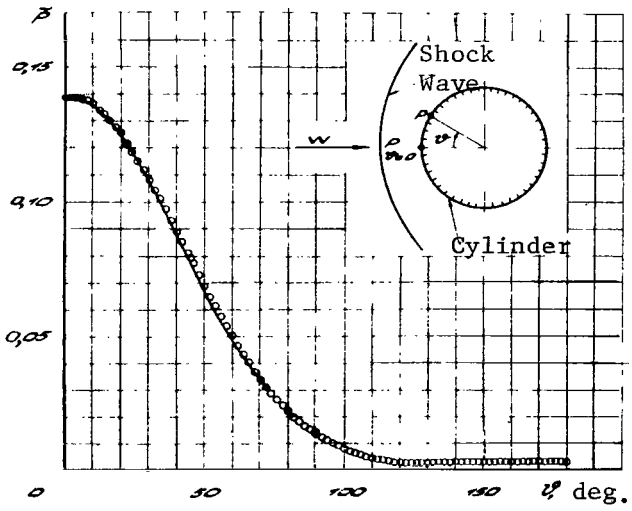

Figure 8.39. Dependence $\tilde{p}(\vartheta)$ for circular cylinder when $M_\infty = 4$:
o o o experiment; —— theory.

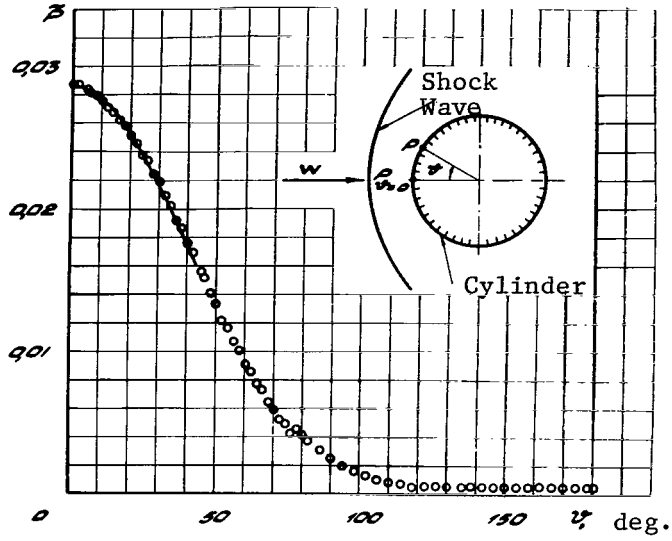

Figure 8.40. Dependence $\tilde{p}(\psi)$ for circular cylinder when $M_\infty = 6.05$: o o o experiment; —— theory.

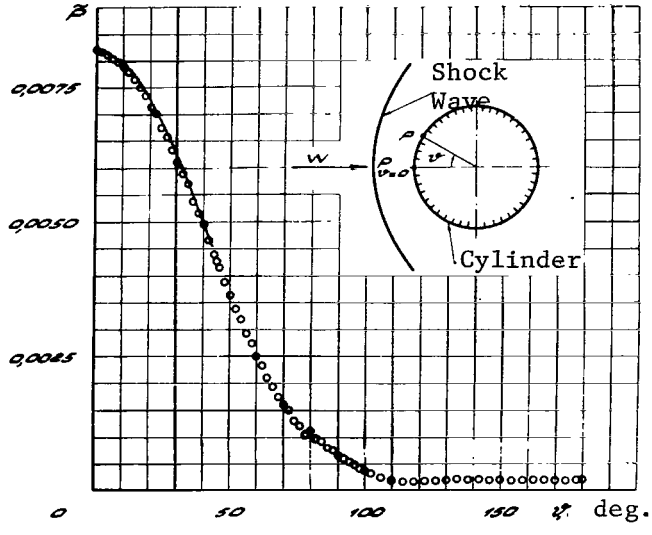

Figure 8.41. Dependence $\tilde{p}(\psi)$ for circular cylinder when $M_\infty = 8.06$: o o o experiment; —— theory.

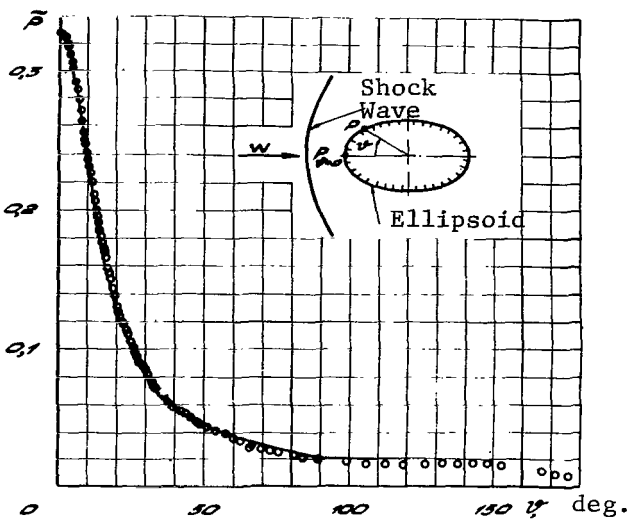

Figure 8.42. Dependence $\tilde{p}(\vartheta)$ for ellipsoid of revolution (b/a = 0.5) when M_∞ = 3: o o o experiment; —— theory.

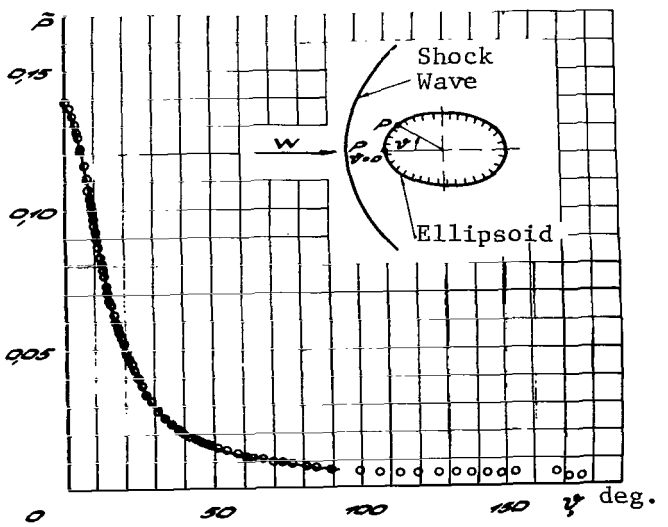

Figure 8.43. Dependence $\tilde{p}(\vartheta)$ for ellipsoid of revolution (b/a = 0.5) when M_∞ = 4: o o o experiment: —— theory.

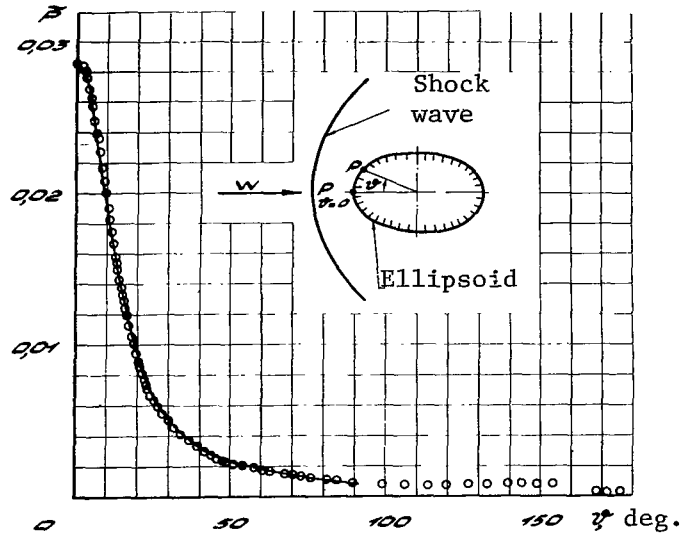

Figure 8.44. Dependence of $\tilde{p}(\vartheta)$ for ellipsoid of revolution (b/a = 0.5) when M_∞ = 6.05: ooo experiment; ——— theory.

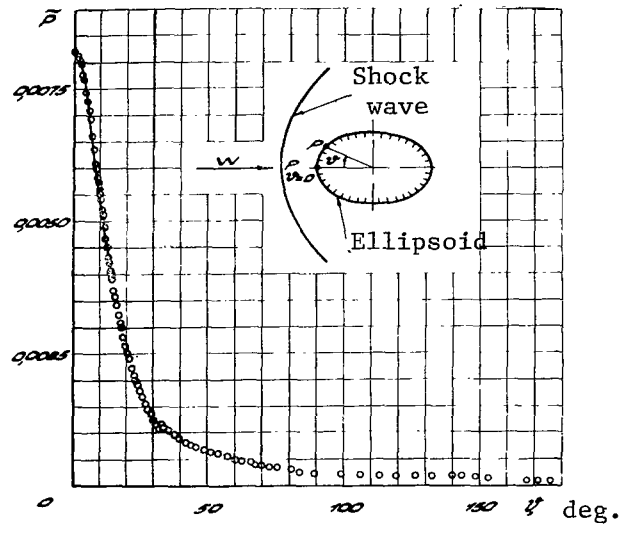

Figure 8.45. Dependence $\tilde{p}(\vartheta)$ for ellipsoid of revolution (b/a = 0.5) when M_∞ = 8.06: ooo experiment; ——— theory.

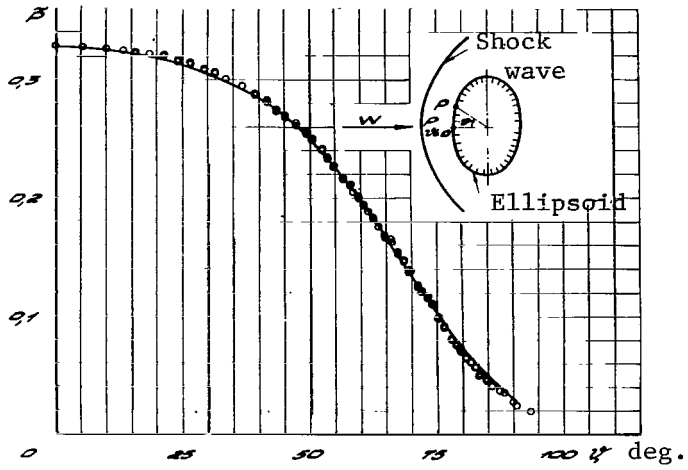

Figure 8.46. Dependence $\tilde{p}(\vartheta)$ for ellipsoid of revolution (b/a = 1.5) when M_∞ = 3: ooo experiment; —— theory.

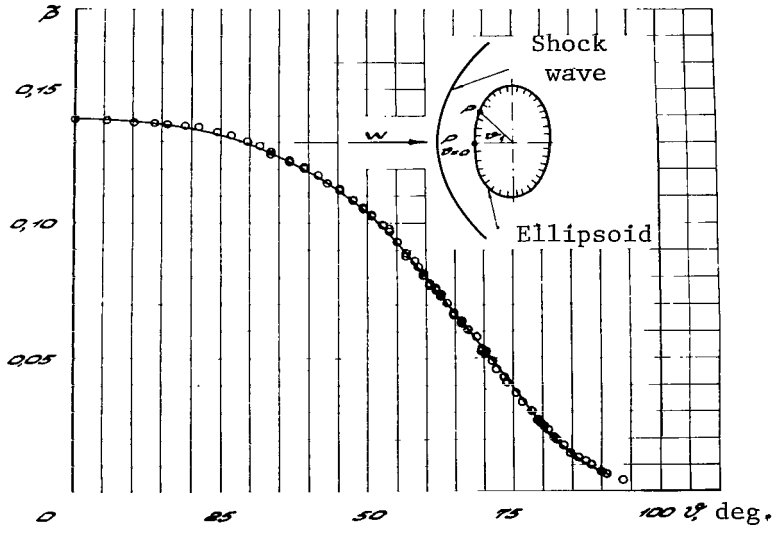

Figure 8.47. Dependence $\tilde{p}(\vartheta)$ for ellipsoid of revolution (b/a = 1.5) when M_∞ = 4: ooo experiment; —— theory.

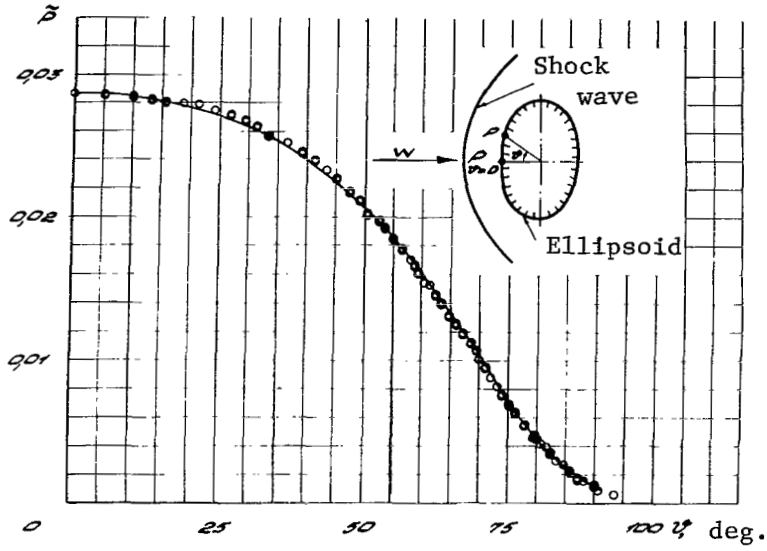

Figure 8.48. Dependence $\tilde{p}(\varphi)$ for ellipsoid of revolution (b/a = 1.5) when M_∞ = 6.05: ooo experiment; —— theory.

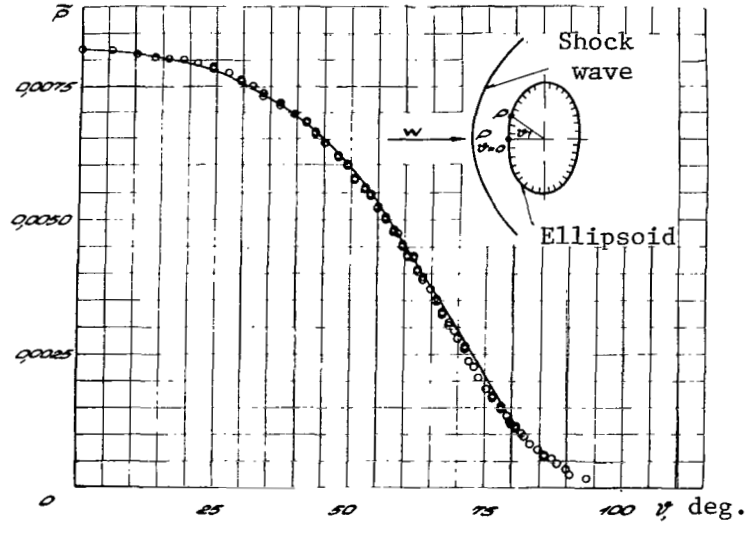

Figure 8.49. Dependence $\tilde{p}(\varphi)$ for ellipsoid of revolution (b/a = 1.5) when M_∞ = 8.06: ooo experiment; —— theory.

The dependence ε (ϑ) is shown in Fig. 8.50 and the dependence y/a=f(x/a) in Fig. 8.51 for the sphere in the range M_∞ = 2.00 - 8.06. In these figures the theoretical curves are plotted by a solid line. A comparison of the experimental data with the theoretical shows that the theory in the entire range of angles ϑ at different values of M_∞ agree well with the experiment.

Both for the ellipsoid of revolution with a ratio of semiaxes b/a = 0.5 (Figs. 8.52 - 8.53) and for the ellipsoid with a ratio of semiaxes b/a = 1.5 (Figs. 8.54 - 8.55) the obtained experimental results on determining the shape and position of the shock wave relative to the body agree well with the theoretical calculations.

The position of the nose shock wave was measured by shadow photography. The test bodies were depicted in natural size. The accuracy of the obtained results could be affected by the clarity of the image of the shock wave and test body, deviation from parallel of the light rays (normal to the flow in the working section of the tunnel), and possible distortion of the image owing to deflection of the rays, which is caused by a large density gradient behind the shock wave and near the test bodies. Special investigations were not carried out to determine the quantitative value of these errors in determining the shape and position of the shock wave relative to the body. Apparently they have a negligible influence on the experimental results.

Figure 8.56 shows the relation $\varepsilon_0 = f(M_\infty)$, i.e., the dependence of the dimensionless distance ε_0 of the shock wave on the body, for the sphere and ellipsoids of revolution when $\vartheta = 0$ and different values of M_∞. The points obtained from the experiment are plotted on these curves. As we see from the figure, the results of the experiment agree well with the calculation by the method of integral relations.

Figures 8.57 - 8.59 show photographs of bodies tested at different values of M_∞, which were obtained by means of the Töpler apparatus and interferometer.

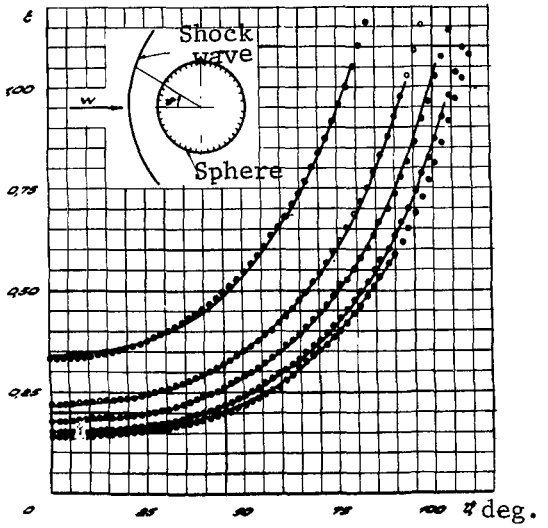

Figure 8.50. Sphere. Dependence of relative distance ε of shock wave on angle at different values of M_∞:

◎◎◎ – experiment $M_\infty = 2$; ○○○ – $M_\infty = 3$;
⊙⊙⊙ – $M_\infty = 4$; ◉◉◉ – $M_\infty = 6.05$;
●●● – $M_\infty = 8.06$; —— theory

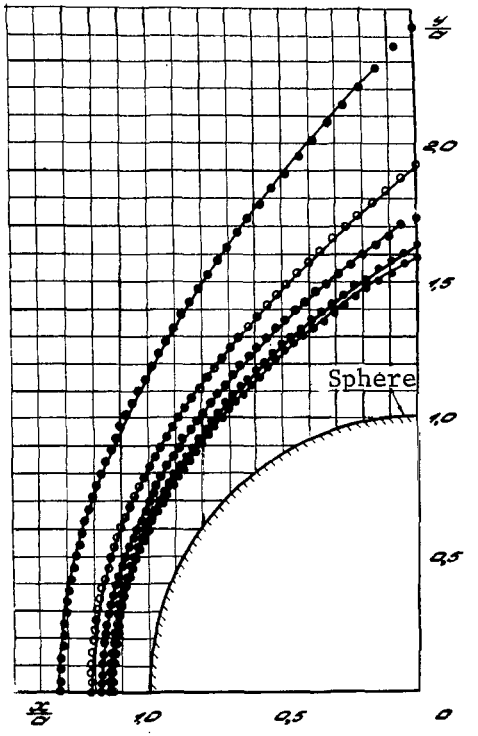

Figure 8.51. Sphere. Shape and position of shock wave relative to body at different values of M_∞:

◎◎◎ – experiment $M_\infty = 2$; ○○○ – $M_\infty = 3$; ⊙⊙⊙ – $M_\infty = 4$;
●●● – $M_\infty = 6.05$; ◑◑◑ – $M_\infty = 8.06$; —— theory.

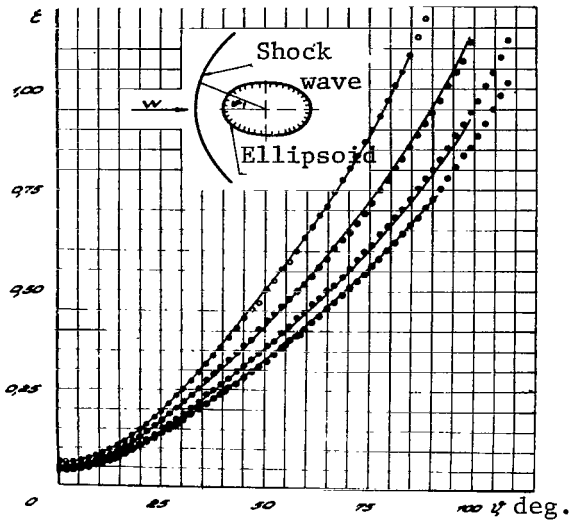

Figure 8.52. Ellipsoid of revolution (b/a = 0.5). Dependence of relative distance ε of shock wave on angle χ at different values of M_∞:

○○○-experiment $M_\infty = 3$; ⊙⊙⊙ - $M_\infty = 4$; ●●● - $M_\infty = 6.05$; ◑◑◑ - $M_\infty = 8.06$; —— theory

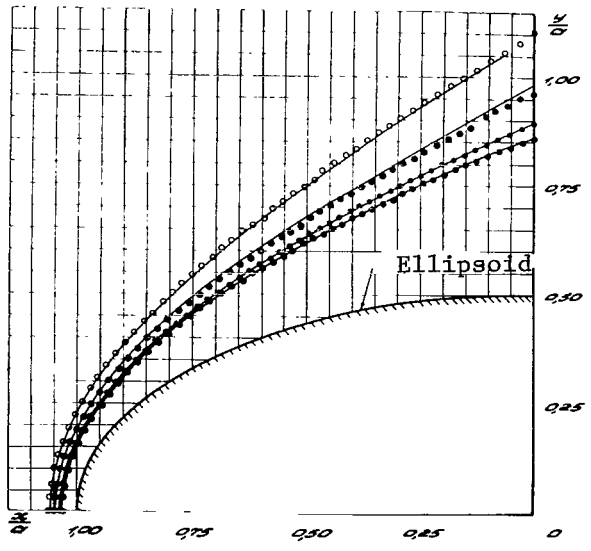

Figure 8.53. Ellipsoid of revolution (b/a = 0.5). Shape and position of shock wave relative to body at different values of M_∞:

○○○-experiment $M_\infty = 3$; ⊙⊙⊙ - $M_\infty = 4$; ●●● - $M_\infty = 6.05$; ◑◑◑ - $M_\infty = 8.06$; —— theory

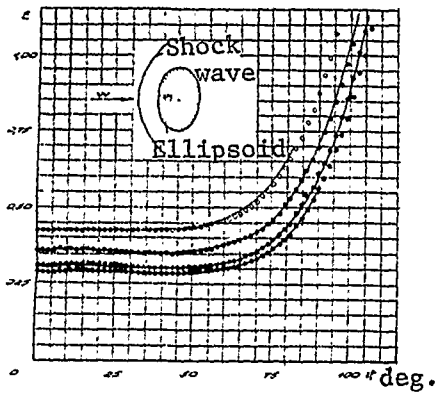

Figure 8.54. Ellipsoid of revolution (b/a = 1.5). Dependence of relative distance ε of shock wave on angle ϑ at different values of M_∞:

○ ○ ○–experiment; $M_\infty = 3$; ⊙ ⊙ ⊙– $M_\infty = 4$; ● ● ●– $M_\infty = 6.05$; ◑ ◑ ◑– $M_\infty = 8.06$; ——— theory.

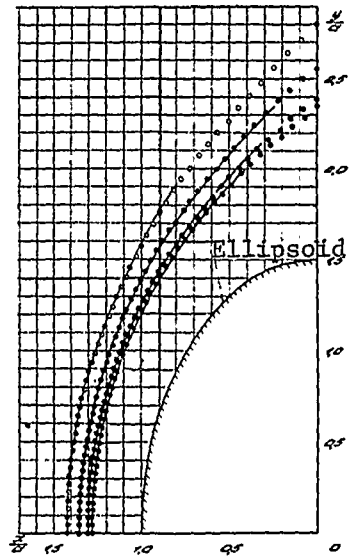

Figure 8.55. Ellipsoid of revolution (b/a = 1.5). Shape and position of shock wave relative to body at different values of M_∞:

○ ○ ○–experiment $M_\infty = 3$; ⊙ ⊙ ⊙ – $M_\infty = 4$; ◎ ◎ ◎– $M_\infty = 6.05$; ◑ ◑ ◑ – $M_\infty = 8.06$; ——— theory.

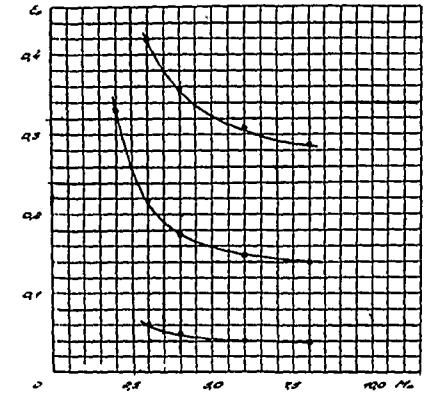

Figure 8.56. Sphere and ellipsoids of revolution (b/a = 0.5 and b/a = 1.5). Relative distance ε of shock wave from body when ϑ = 0 and at different values of M_∞:

● ● ●– experiment, sphere; ○○○ ellipsoid of revolution, b/a = 0,5; ⊙ ⊙ ⊙– ellipsoid of revolution, b/a = 1,5; ——— theory.

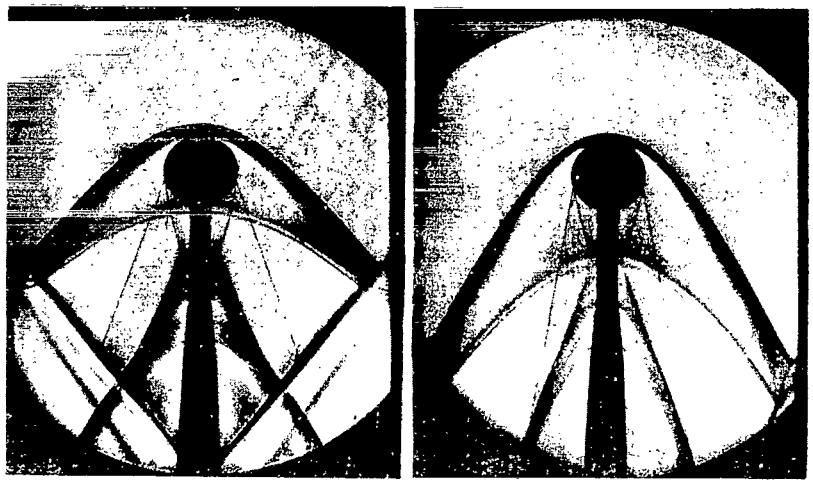

A B

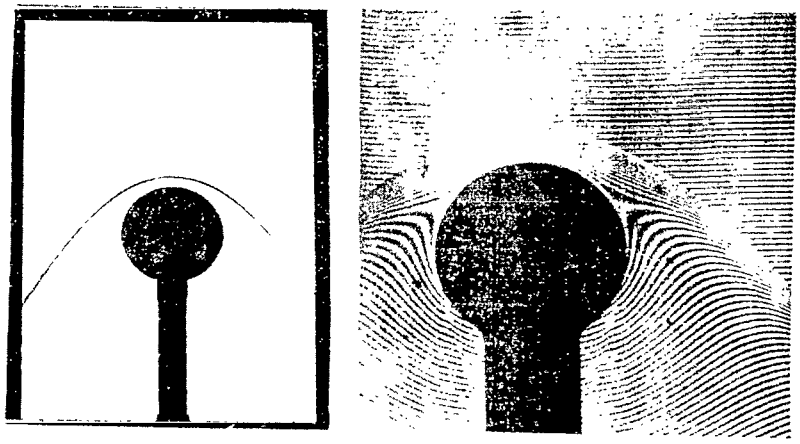

C D

Figure 8.57. Pattern of flow around sphere at different values of M_∞: a) $M_\infty = 2$ (Topler method); b) $M_\infty = 3$ (Topler method); c) $M_\infty = 3$ (shadow photography); d) $M_\infty = 3$ (interferogram).

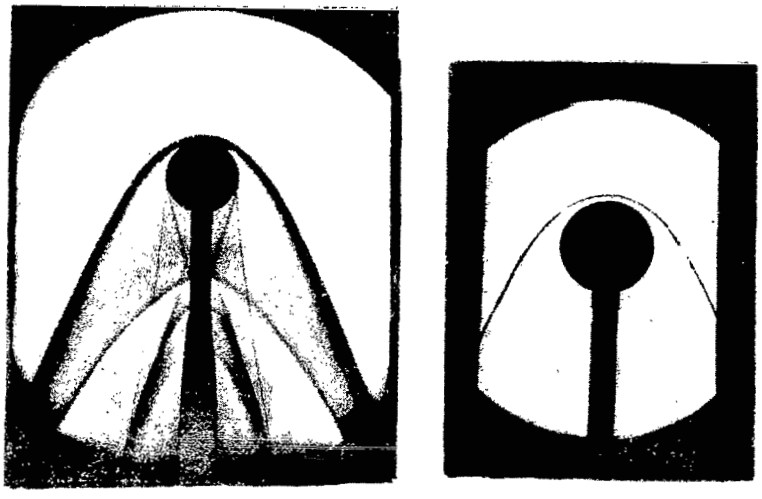

E F

Figure 8.57. Pattern of flow around sphere at different values of M_∞: e) $M_\infty = 4$ (Topler method); f) $M_\infty = 8.06$ (Topler method).

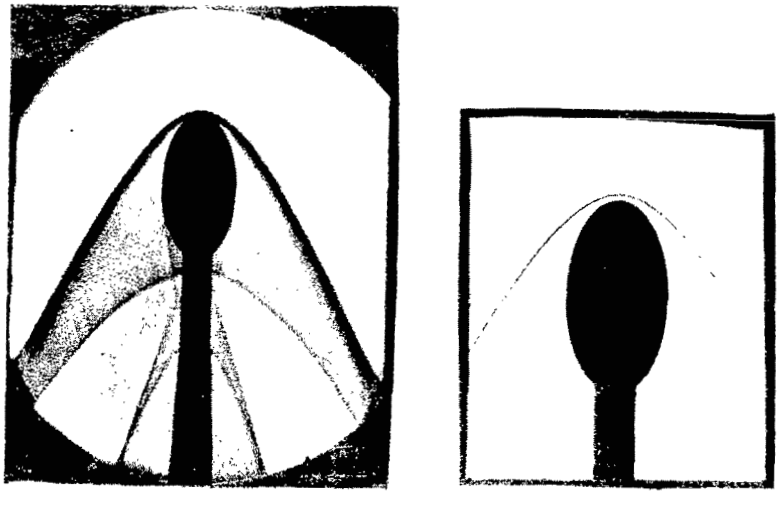

A B

Figure 8.58. Pattern of flow around ellipsoid of revolution (b/a = 0.5) at different values of M_∞: a) $M_\infty = 3$ (Topler method); b) $M_\infty = 3$ (shadow photography).

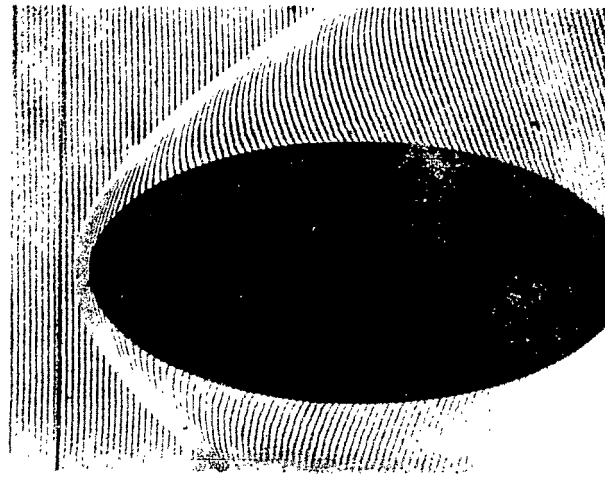

C

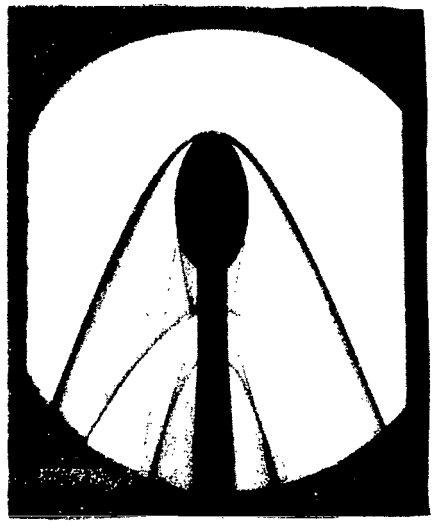

D

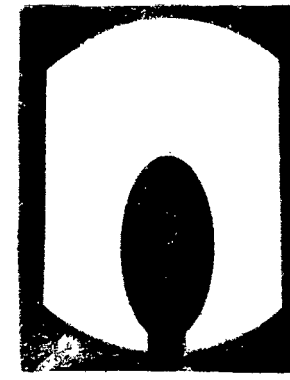

E

Figure 8.58. Pattern of flow around ellipsoid of revolution (b/a = 0.5) at different values M_∞: c) M_∞ = 3 (interferogram); d) M_∞ = 4 (Topler method); e) M_∞ = 8.06 (Topler method).

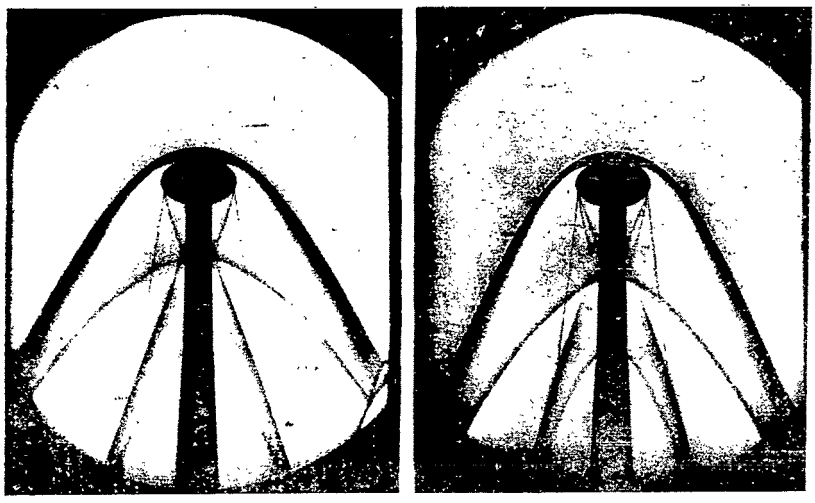

A B

C

Figure 8.59. Pattern of flow around ellipsoid of revolution (b/a = 1.5) at different values of M_∞: a) M_∞ = 3 (Topler method); b) M_∞ = 4 (Topler method; c) M_∞ = 8.06 (Topler method).

Conclusions

1. The results of experimental investigations into the distribution of pressure and determination of the shape of a shock wave and its position relative to the body during flow around a sphere when M_∞ = 2.00, 3.00, 4.00, 6.05, and 8.06, around a cylinder when M_∞ = 2.00, 3.00, 4.00, 6.05, and 8.06, and also around ellipsoids of revolution with a ratio of semiaxes b/a = 0.5 and 1.5 when M_∞ = 3.00, 4.00, 6.05, and 8.06 agree well in the entire range of angles with the results of the calculation of flows in the region of influence of blunting by the method of integral relations and of the supersonic zone by the method of characteristics. /313

2. On the basis of comparing the experimental data with those calculated we can conclude that the method of integral relations and the methods of characteristics are a reliable basis for calculating the flow of a supersonic gas stream around the leading part of smooth axisymmetric bodies.

3. A comparison of all experimental results shows that on flow around solids of revolution the dependence $\bar{p}(\theta)$ and the shape and position of the shock wave relative to the body at large values of M_∞ will depend little on M_∞.

TABLE 8.1

COORDINATES OF OUTSIDE CONTOUR OF ELLIPSOIDS OF REVOLUTION WITH DIFFERENT RATIOS OF SEMIAXES $\delta = b/a$.

x	y	x	y	x	y	x	y	x	y
$b/a = 0.5$; $a = 40$ mm ; $b = 20$ mm									
0.00	20.00	15.00	18.54	30.00	13.23	37.00	7.60	39.50	3.10
3.00	19.94	18.00	17.86	32.00	12.00	38.00	6.25	39.70	2.45
6.00	19.77	21.00	17.02	34.00	10.54	38.50	5.43	39.80	2.00
9.00	19.49	24.00	16.00	35.00	9.68	39.00	4.44	39.90	1.41
12.00	19.08	27.00	14.76	36.00	8.72	39.25	3.86	40.00	0.00
$b/a = 1.5$; $a = 13.33$ mm; $b = 20$ mm									
0.00	13.33	8.00	12.22	15.00	8.82	18.50	5.07	19.60	2.65
2.00	13.27	10.00	11.55	16.00	8.00	19.00	4.16	19.70	2.30
4.00	13.06	12.00	10.67	17.00	7.03	19.20	3.73	19.80	1.88
6.00	12.72	14.00	9.52	18.00	5.81	19.40	3.24	19.90	1.33
								20.00	0.00

TABLE 8.2

COORDINATES OF PRESSURE HOLES OF ELLIPSOID OF REVOLUTION WITH DIFFERENT RATIOS OF SEMIAXES $\delta = b/a$.

R	ϑ, deg	R	ϑ, deg	R	ϑ, deg	R	ϑ, deg	R	ϑ, deg
$b/a = 0.5$									
40.00	0.00	38.28	10.10	34.74	19.27	28.27	35.31	20.09	83.98
39.99	0.27	38.19	10.40	34.37	20.11	27.95	36.23	20.00	89.32
39.98	0.72	38.06	10.79	34.22	20.48	27.44	37.75	20.19	99.07
39.96	1.11	37.88	11.32	33.98	21.19	27.00	39.13	20.60	106.10
39.94	1.90	37.65	11.97	33.56	21.99	26.19	41.82	21.27	113.13
39.89	2.49	37.50	12.36	33.40	22.37	25.72	43.43	22.06	119.17
39.85	2.88	37.26	12.91	33.21	22.80	25.24	45.20	23.30	126.32
39.78	3.64	37.21	13.15	33.02	23.25	24.70	47.35	24.65	132.47
39.70	4.21	37.07	13.55	32.68	24.05	24.36	48.68	26.03	137.65
39.58	4.87	36.90	13.99	32.35	24.82	23.87	50.91	27.72	143.08
39.47	5.49	36.88	14.07	32.13	25.33	23.24	53.95	29.53	148.15
39.33	6.15	36.70	14.50	31.78	26.07	22.37	57.66	31.45	153.04
39.22	6.67	36.51	14.95	31.52	26.82	22.16	60.18	37.17	167.01
39.04	7.40	36.40	15.25	31.15	27.71	21.83	62.43	38.74	171.44
38.97	7.85	36.28	15.57	30.73	28.74	21.36	66.13	39.70	175.93
38.76	8.46	36.04	16.15	30.34	29.71	21.22	67.30		
38.65	8.87	35.77	16.80	29.99	30.65	20.96	69.85		
38.57	9.11	35.55	17.32	29.21	32.12	20.69	72.83		
38.50	9.43	35.35	17.83	29.02	33.20	20.48	75.70		
38.42	9.63	35.06	18.49	28.92	33.47	20.20	80.71		

TABLE 8.2 Continued

R	ϑ, deg	R	ϑ, deg	R	ϑ, deg	R	ϑ, deg
			$b/a = 1.5$				
13.33	0.00	15.52	43.35	17.90	63.49	19.56	78.93
13.36	5.36	15.71	45.19	18.06	64.82	19.60	79.53
13.44	10.09	15.95	47.51	18.20	65.95	19.62	79.79
13.50	13.36	16.15	49.20	18.22	66.12	19.69	80.75
13.62	15.83	16.31	50.57	18.35	67.18	19.75	81.81
13.73	18.67	16.54	52.61	18.51	68.48	19.78	82.35
13.85	21.36	16.66	53.53	18.62	69.43	19.84	83.39
13.99	24.16	16.86	54.95	18.64	69.70	19.89	84.65
14.14	26.69	17.03	56.56	18.82	71.24	19.93	85.87
14.33	29.44	17.22	58.09	18.91	72.08	19.97	87.17
14.48	31.58	17.29	58.66	19.03	73.13	19.99	88.12
14.63	33.54	17.40	59.55	19.10	73.85	20.00	89.99
14.89	36.65	17.53	60.55	19.24	75.21	20.00	90.62
15.09	39.24	17.66	61.63	19.35	76.41	19.96	93.50
15.34	41.58	17.78	62.53	19.48	77.96		

TABLE 8.3

VALUES OF PARAMETERS OF ONCOMING FLOW FOR THE INVESTIGATED BODIES

M_∞	p_0, atm abs	T_0, °K	Re	M_∞	p_0, atm abs	T_0, °K	Re
	Cylinder				Sphere		
2.00	1.94	293	$3.60 \cdot 10^5$	2.00	1.94	293	$9.60 \cdot 10^5$
3.00	4.04	293	$7.60 \cdot 10^5$	3.00	4.04	293	$1.22 \cdot 10^6$
4.00	7.43	293	$5.10 \cdot 10^5$	4.00	7.43	293	$1.36 \cdot 10^6$
6.05	20.78	513	$4.02 \cdot 10^5$	6.05	20.78	513	$6.43 \cdot 10^6$
8.06	88.06	813	$2.43 \cdot 10^5$	8.06	88.06	813	$6.49 \cdot 10^6$
	Absolute atmosphere						
	$b/a = 0.5$				$b/a = 1.5$		
3.00	4.04	293	$2.43 \cdot 10^6$	3.00	4.04	293	$8.11 \cdot 10^5$
4.00	7.43	293	$2.72 \cdot 10^6$	4.00	7.43	293	$9.07 \cdot 10^5$
6.05	20.78	513	$1.29 \cdot 10^6$	6.05	20.78	513	$4.29 \cdot 10^5$
8.06	88.06	813	$1.30 \cdot 10^6$	8.06	88.06	813	$4.33 \cdot 10^5$

TABLE 8.4

DISTRIBUTION OF PRESSURE $\bar{p}$ OVER SURFACE OF SPHERE AT DIFFERENT VALUES OF M_∞

θ, rad	M_∞				
	2	3	4	6.05	8.06
0.000	1.000	1.000	1.000	1.000	1.000
0.035	0.999	0.997	0.996	0.996	0.996
0.070	0.996	0.993	0.989	0.988	0.987
0.105	0.992	0.984	0.982	0.981	0.980
0.140	0.983	0.977	0.973	0.971	0.969
0.175	0.976	0.967	0.962	0.958	0.956
0.209	0.966	0.955	0.949	0.943	0.939
0.244	0.945	0.936	0.930	0.923	0.920
0.279	0.932	0.919	0.908	0.902	0.898
0.314	0.916	0.901	0.886	0.880	0.875
0.349	0.898	0.881	0.864	0.855	0.851
0.384	0.880	0.862	0.841	0.831	0.827
0.419	0.859	0.837	0.811	0.801	0.796
0.454	0.834	0.813	0.785	0.773	0.767
0.489	0.810	0.787	0.758	0.738	0.735
0.524	0.785	0.760	0.730	0.713	0.710
0.559	0.760	0.733	0.700	0.687	0.679
0.593	0.733	0.704	0.670	0.656	0.650
0.628	0.705	0.678	0.641	0.621	0.617
0.663	0.680	0.648	0.611	0.587	0.579
0.698	0.653	0.618	0.578	0.556	0.545
0.733	0.622	0.590	0.546	0.521	0.511
0.768	0.597	0.559	0.514	0.479	0.472
0.785	0.582	0.541	0.497	0.467	0.456
0.803	0.564	0.522	0.482	0.451	0.441
1.536	0.137	0.077	0.060	0.058	0.054
1.571	0.126	0.069	0.053	0.050	0.046
1.606	0.118	0.062	0.048	0.043	0.041
1.641	0.108	0.054	0.041	0.039	0.037
1.676	0.100	0.048	0.037	0.035	0.032
1.710	0.091	0.042	0.033	0.031	0.029
1.745	0.081	0.038	0.026	0.030	0.027
1.780	0.076	0.032	0.023	0.029	0.024
1.815	0.068	0.029	0.021	0.027	0.022
1.850	0.063	0.026	0.019	0.026	0.020
1.885	0.057	0.023	0.019	0.025	0.019
1.920	0.051	0.021	0.018	0.024	0.018
1.955	0.047	0.021	0.016	0.022	0.017
1.990	0.047	0.022	0.016	0.021	0.016
2.024	0.046	0.022	0.016	0.019	0.015
2.059	0.046	0.022	0.012	0.018	0.014
2.094	0.046	0.022	0.012	0.016	0.013
2.129	0.046	0.022	0.009	0.015	0.012
2.164	0.046	0.022	0.009	0.013	0.012
2.199	0.046	0.022	0.009	0.012	0.011
2.234	0.046	0.022	0.009	0.011	0.011
2.269	0.046	0.022	0.009	0.010	0.010
2.304	0.046	0.022	0.009	0.010	0.010
2.339	0.046	0.022	0.009	0.011	0.010
2.374	0.046	0.022	0.009	0.011	0.010

θ, rad	M_∞				
	2	3	4	6.05	8.06
0.838	0.539	0.489	0.450	0.423	0.412
0.873	0.512	0.459	0.421	0.385	0.376
0.908	0.484	0.430	0.391	0.355	0.347
0.942	0.459	0.400	0.362	0.324	0.318
0.977	0.435	0.368	0.338	0.305	0.297
1.012	0.409	0.344	0.312	0.276	0.269
1.047	0.386	0.315	0.287	0.247	0.243
1.082	0.362	0.285	0.262	0.224	0.221
1.117	0.341	0.261	0.237	0.204	0.199
1.152	0.320	0.238	0.216	0.181	0.177
1.187	0.299	0.216	0.194	0.161	0.157
1.222	0.280	0.197	0.174	0.162	0.142
1.257	0.256	0.179	0.157	0.144	0.153
1.292	0.244	0.161	0.141	0.132	0.127
1.326	0.227	0.146	0.126	0.121	0.117
1.361	0.210	0.129	0.111	0.105	0.102
1.396	0.196	0.116	0.099	0.097	0.093
1.431	0.180	0.104	0.088	0.081	0.080
1.466	0.165	0.095	0.078	0.076	0.071
1.501	0.150	0.084	0.068	0.064	0.062
2.409	0.046	0.022	0.009	0.011	0.010
2.443	0.046	0.022	0.009	0.011	0.010
2.478	0.046	0.022	0.009	0.011	0.011
2.513	0.046	0.022	0.009	0.012	0.011
2.548	0.046	0.022	0.009	0.011	0.011
2.583	0.046	0.022	0.009	0.011	0.011
2.618	0.046	0.022	0.010	0.011	0.011
2.653	0.046	0.022	0.010	0.011	0.010
2.688	0.046	0.022	0.010	0.011	0.010
2.722	0.046	0.022	0.010	0.011	0.010
2.757	0.047	0.022	0.010	0.011	0.010
2.793	0.047	0.022	0.011	0.011	0.010
2.827	0.047	0.022	0.011	0.011	0.010
2.862	0.047	0.022	0.011	0.011	0.010
2.897	0.047	0.022	0.011	0.011	0.010
2.932	0.046	0.022	0.011	0.011	0.010
2.967	0.046	0.022	0.011	0.011	0.010
3.002	0.046	0.022	0.011	0.011	0.010
3.037	0.046	0.022	0.011	0.011	0.010
3.072	0.046	0.022	0.011	0.011	0.010
3.107	0.046	0.022	0.011	0.011	0.010
3.142	0.046	0.022	0.011	0.011	0.010

TABLE 8.5

DISTRIBUTION OF PRESSURE OVER SURFACE OF SPHERE WHEN $M_\infty = 3$

θ, rad	$\bar{p}$	θ, rad	$\bar{p}$	θ, rad	$\bar{p}$	θ, rad	$\bar{p}$
0.017	0.998	0.715	0.605	1.413	0.110	2.110	0.022
0.052	0.994	0.750	0.573	1.448	0.099	2.146	0.022
0.087	0.990	0.785	0.541	1.484	0.088	2.180	0.022
0.122	0.980	0.820	0.507	1.518	0.080	2.216	0.022
0.157	0.969	0.855	0.473	1.553	0.071	2.250	0.022
0.191	0.958	0.890	0.445	1.590	0.066	2.290	0.022
0.227	0.945	0.925	0.415	1.620	0.058	2.320	0.022
0.262	0.928	0.961	0.386	1.660	0.051	2.350	0.022
0.296	0.912	0.995	0.357	1.690	0.045	2.390	0.022
0.332	0.891	1.030	0.329	1.730	0.040		
0.366	0.871	1.065	0.300	1.760	0.035		
0.401	0.848	1.100	0.272	1.800	0.030		
0.436	0.823	1.134	0.251	1.830	0.027		
0.471	0.797	1.169	0.227	1.868	0.024		
0.506	0.773	1.204	0.207	1.900	0.022		
0.541	0.748	1.239	0.188	1.937	0.021		
0.576	0.720	1.274	0.170	1.970	0.022		
0.611	0.688	1.309	0.153	2.010	0.022		
0.646	0.661	1.344	0.137	2.040	0.022		
0.680	0.638	1.378	0.123	2.076	0.022		

TABLE 8.6

/31

DISTRIBUTION OF PRESSURE $\bar{p}$ OVER SURFACE OF CIRCULAR CYLINDER AT DIFFERENT VALUES OF M_∞

θ, rad	M_∞				
	2	3	4	6.05	8.06
0.000	1.000	1.000	1.000	1.000	1.000
0.035	0.999	0.998	0.997	0.996	0.995
0.070	0.998	0.997	0.996	0.992	0.990
0.105	0.996	0.994	0.992	0.984	0.981
0.140	0.992	0.988	0.985	0.974	0.972
0.175	0.987	0.982	0.981	0.962	0.960
0.209	0.979	0.971	0.963	0.945	0.949
0.244	0.964	0.959	0.955	0.933	0.932
0.279	0.954	0.944	0.936	0.914	0.912
0.314	0.937	0.926	0.917	0.893	0.894
0.349	0.923	0.907	0.905	0.875	0.868
0.384	0.909	0.892	0.877	0.857	0.853
0.419	0.891	0.864	0.854	0.829	0.821
0.454	0.869	0.845	0.829	0.814	0.801
0.488	0.854	0.816	0.807	0.783	0.770
0.524	0.831	0.792	0.780	0.760	0.745
0.559	0.810	0.766	0.752	0.729	0.718
0.593	0.781	0.745	0.730	0.706	0.695
0.628	0.759	0.718	0.702	0.669	0.655
0.663	0.736	0.689	0.671	0.650	0.629
0.000	1.000	1.000	1.000	1.000	1.000
0.035	0.999	0.998	0.997	0.996	0.995
0.070	0.998	0.997	0.996	0.992	0.990
0.105	0.996	0.994	0.992	0.984	0.981
0.140	0.992	0.988	0.985	0.974	0.972
0.175	0.987	0.982	0.981	0.962	0.960
0.209	0.979	0.971	0.963	0.945	0.949
0.244	0.964	0.959	0.955	0.933	0.932
0.279	0.954	0.944	0.936	0.914	0.912
0.314	0.937	0.926	0.917	0.893	0.894
0.349	0.923	0.907	0.905	0.875	0.868
0.384	0.909	0.892	0.877	0.857	0.853
0.419	0.891	0.864	0.854	0.829	0.821
0.454	0.869	0.845	0.829	0.814	0.801
0.488	0.854	0.816	0.807	0.783	0.770
0.524	0.831	0.792	0.780	0.760	0.745
0.559	0.810	0.766	0.752	0.729	0.718
0.593	0.781	0.745	0.730	0.706	0.695
0.628	0.759	0.718	0.702	0.669	0.655
0.663	0.736	0.689	0.671	0.650	0.629

θ, rad	M_∞				
	2	3	4	6.05	8.06
0.698	0.712	0.659	0.643	0.613	0.603
0.733	0.684	0.629	0.614	0.590	0.568
0.767	0.661	0.600	0.584	0.549	0.535
0.785	0.651	0.584	0.571	0.543	0.520
0.803	0.637	0.571	0.558	0.528	0.504
0.838	0.610	0.541	0.527	0.492	0.471
0.873	0.586	0.515	0.498	0.464	0.442
0.908	0.558	0.485	0.467	0.425	0.412
0.942	0.530	0.457	0.443	0.405	0.386
0.977	0.498	0.431	0.417	0.372	0.355
1.012	0.470	0.405	0.389	0.349	0.333
1.047	0.439	0.378	0.363	0.315	0.303
1.082	0.416	0.353	0.338	0.297	0.281
1.117	0.387	0.330	0.313	0.266	0.255
1.152	0.363	0.306	0.289	0.252	0.235
1.186	0.336	0.283	0.265	0.223	0.212
1.222	0.315	0.262	0.245	0.206	0.195
1.257	0.294	0.240	0.223	0.181	0.175
1.292	0.272	0.220	0.207	0.170	0.158
1.326	0.249	0.201	0.192	0.155	0.147
0.698	0.712	0.659	0.643	0.613	0.603
0.733	0.684	0.629	0.614	0.590	0.568
0.767	0.661	0.600	0.584	0.549	0.535
0.785	0.651	0.584	0.571	0.543	0.520
0.803	0.637	0.571	0.558	0.528	0.504
0.838	0.610	0.541	0.527	0.492	0.471
0.873	0.586	0.515	0.498	0.464	0.442
0.908	0.558	0.485	0.467	0.425	0.412
0.942	0.530	0.457	0.443	0.405	0.386
0.977	0.498	0.431	0.417	0.372	0.355
1.012	0.470	0.405	0.389	0.349	0.333
1.047	0.439	0.378	0.363	0.315	0.303
1.082	0.416	0.353	0.338	0.297	0.281
1.117	0.387	0.330	0.313	0.266	0.255
1.152	0.363	0.306	0.289	0.252	0.235
1.186	0.336	0.283	0.265	0.223	0.212
1.222	0.315	0.262	0.245	0.206	0.195
1.257	0.294	0.240	0.223	0.181	0.175
1.292	0.272	0.220	0.207	0.170	0.158
1.326	0.249	0.201	0.192	0.155	0.147

TABLE 8.7

/321

DISTRIBUTION OF PRESSURE $\bar{p}$ OVER SURFACE OF CIRCULAR CYLINDER WHEN $M_\infty = 3$

θ,rad	$\bar{p}$	θ,rad	$\bar{p}$	θ, rad	$\bar{p}$
0.017	0.999	0.541	0.780	1.064	0.364
0.052	0.997	0.576	0.755	1.100	0.341
0.087	0.997	0.611	0.731	1.134	0.318
0.122	0.996	0.646	0.703	1.169	0.294
0.157	0.985	0.680	0.674	1.204	0.274
0.192	0.977	0.716	0.644	1.239	0.250
0.227	0.965	0.750	0.614	1.274	0.230
0.262	0.951	0.785	0.584	1.309	0.213
0.297	0.936	0.820	0.555	1.344	0.193
0.332	0.918	0.855	0.526	1.379	0.175
0.367	0.901	0.890	0.496	1.414	0.159
0.401	0.880	0.925	0.470	1.448	0.145
0.436	0.855	0.960	0.443	1.484	0.131
0.471	0.832	0.994	0.420	1.518	0.118
0.510	0.803	1.030	0.391		

TABLE 8.8

DISTRIBUTION OF PRESSURE OVER SURFACE OF ELLIPSOID OF REVOLUTION WITH RATIO OF SEMIAXES b/a = 0.5 AT DIFFERENT VALUES OF M_∞

θ, rad	M_∞							
	3		4		6.05		8.06	
	$\bar{p}^*_{su}$	$\bar{p}^{**}_{mod}$	$\bar{p}^*_{su}$	$\bar{p}^{**}_{mod}$	$\bar{p}^*_{su}$	$\bar{p}^{**}_{mod}$	$\bar{p}^*_{su}$	$\bar{p}^{**}_{mod}$
0.000	1.000	1.000	1.000	1.000	1.000	1.000	1.000	1.000
0.013	0.998	0.999	0.998	0.997	0.998	0.997	0.997	0.996
0.042	0.998	0.998	0.995	0.996	0.994	0.993	0.992	0.994
0.084	0.995	0.994	0.993	0.996	0.991	0.990	0.990	0.991
0.126	0.990	0.994	0.985	0.987	0.983	0.982	0.981	0.980
0.169	0.982	0.986	0.979	0.977	0.976	0.971	0.971	0.968
0.215	0.967	0.964	0.962	0.963	0.961	0.957	0.951	0.953
0.254	0.951	0.954	0.942	0.945	0.938	0.936	0.935	0.932
0.297	0.931	0.935	0.921	0.925	0.912	0.917	0.904	0.910
0.341	0.917	0.921	0.903	0.906	0.894	0.899	0.885	0.889
0.385	0.888	0.891	0.872	0.874	0.864	0.865	0.858	0.859
0.432	0.872	0.875	0.854	0.857	0.842	0.845	0.836	0.839
0.474	0.850	0.855	0.832	0.835	0.820	0.825	0.813	0.815
0.520	0.825	0.829	0.802	0.799	0.786	0.791	0.775	0.778
0.566	0.801	0.804	0.769	0.772	0.753	0.759	0.742	0.746

KEY:

* su - Surface

** mod - Model

TABLE 8.8 Continued

θ, rad	M_∞ = 3		4		6.05		8.06	
	$\bar{p}_{su}$*	$\bar{p}$ ** mod	$\bar{p}$ * su	$\bar{p}$ ** mod	$\bar{p}$ * su	$\bar{p}$ ** mod	$\bar{p}$ * su	$\bar{p}$ ** mod
0.600	0.776	0.777	0.751	0.755	0.745	0.749	0.732	0.734
0.631	0.759	0.763	0.734	0.731	0.721	0.727	0.710	0.714
0.647	0.751	0.754	0.723	0.726	0.709	0.715	0.703	0.708
0.671	0.732	0.736	0.711	0.712	0.694	0.697	0.686	0.684
0.683	0.731	0.734	0.695	0.701	0.679	0.675	0.673	0.674
0.719	0.711	0.715	0.676	0.680	0.662	0.666	0.657	0.660
0.740	0.700	0.704	0.661	0.664	0.638	0.640	0.635	0.636
0.768	0.689	0.692	0.641	0.646	0.625	0.630	0.624	0.626
0.805	0.667	0.665	0.623	0.623	0.607	0.612	0.591	0.595
0.850	0.641	0.644	0.595	0.599	0.581	0.583	0.572	0.570
0.880	0.626	0.632	0.581	0.584	0.549	0.553	0.549	0.545
0.918	0.606	0.609	0.559	0.564	0.540	0.543	0.527	0.525
0.934	0.595	0.600	0.551	0.555	0.517	0.522	0.515	0.517
0.962	0.578	0.581	0.537	0.541	0.511	0.516	0.501	0.505
0.995	0.564	0.568	0.522	0.527	0.495	0.498	0.491	0.493
1.000	0.560	0.565	0.519	0.522	0.490	0.493	0.488	0.490
1.030	0.549	0.552	0.504	0.508	0.478	0.481	0.475	0.473
1.059	0.535	0.538	0.484	0.487	0.461	0.463	0.450	0.455
1.080	0.525	0.528	0.476	0.479	0.451	0.455	0.437	0.442
1.100	0.515	0.517	0.469	0.473	0.439	0.434	0.432	0.433
1.140	0.501	0.504	0.451	0.455	0.425	0.422	0.417	0.420
1.180	0.478	0.481	0.433	0.434	0.399	0.395	0.394	0.392
1.215	0.468	0.471	0.417	0.420	0.377	0.382	0.376	0.374
1.246	0.456	0.453	0.405	0.407	0.368	0.370	0.368	0.365
1.287	0.436	0.439	0.390	0.393	0.348	0.352	0.342	0.345
1.327	0.421	0.425	0.375	0.378	0.327	0.332	0.324	0.326
1.379	0.397	0.401	0.352	0.356	0.310	0.312	0.305	0.310
1.402	0.385	0.391	0.345	0.347	0.305	0.305	0.299	0.301
1.437	0.375	0.379	0.335	0.336	0.291	0.294	0.283	0.286
1.480	0.361	0.365	0.321	0.325	0.275	0.277	0.265	0.269
1.500	0.355	0.357	0.316	0.321	0.269	0.273	0.259	0.263
1.521	0.350	0.346	0.305	0.307	0.261	0.263	0.252	0.254
1.544	0.344	0.345	0.301	0.301	0.253	0.250	0.245	0.247
1.582	0.333	0.336	0.285	0.283	0.243	0.241	0.236	0.240
1.618	0.317	0.321	0.274	0.276	0.231	0.234	0.225	0.227
1.641	0.307	0.312	0.265	0.261	0.221	0.224	0.215	0.218
1.670	0.295	0.301	0.258	0.257	0.214	0.216	0.204	0.207
1.702	0.289	0.293	0.241	0.244	0.203	0.205	0.192	0.195
1.737	0.273	0.279	0.235	0.238	0.193	0.195	0.186	0.188
1.775	0.267	0.263	0.223	0.225	0.182	0.184	0.175	0.177

KEY:

* su - Surface
** mod - Model

TABLE 8.8 Continued

θ, rad	M_∞							
	3		4		6.05		8.06	
	$\bar{p}_{su}$*	$\bar{p}_{mod}$**	$\bar{p}_{su}$*	$\bar{p}_{mod}$**	$\bar{p}_{su}$*	$\bar{p}_{mod}$**	$\bar{p}_{su}$*	$\bar{p}_{mod}$**
1.810	0.260	0.257	0.211	0.210	0.172	0.174	0.167	0.163
1.839	0.246	0.250	0.201	0.202	0.161	0.164	0.152	0.155
1.885	0.230	0.235	0.187	0.185	0.162	0.164	0.155	0.158
1.915	0.221	0.224	0.182	0.184	0.152	0.154	0.147	0.148
1.940	0.217	0.221	0.171	0.174	0.146	0.148	0.140	0.140
1.971	0.206	0.210	0.166	0.165	0.136	0.138	0.132	0.134
1.995	0.135	0.200	0.161	0.163	0.130	0.131	0.122	0.124
2.030	0.187	0.187	0.151	0.158	0.121	0.125	0.118	0.116
2.060	0.178	0.181	0.143	0.145	0.112	0.114	0.111	0.112
2.110	0.166	0.166	0.132	0.135	0.101	0.105	0.100	0.101
2.140	0.158	0.160	0.125	0.126	0.095	0.094	0.093	0.091
2.170	0.155	0.157	0.118	0.118	0.091	0.091	0.087	0.087
2.202	0.140	0.145	0.112	0.114	0.085	0.085	0.084	0.083
2.220	0.140	0.143	0.110	0.111	0.082	0.082	0.079	0.080
2.250	0.130	0.133	0.101	0.101	0.076	0.076	0.070	0.076
2.285	0.122	0.125	0.099	0.099	0.074	0.074	0.073	0.070
2.325	0.115	0.115	0.089	0.091	0.066	0.066	0.065	0.065
2.351	0.106	0.105	0.081	0.081	0.061	0.061	0.060	0.060
2.370	0.100	0.100	0.079	0.079	0.058	0.060	0.055	0.056
2.402	0.090	0.095	0.075	0.075	0.054	0.053	0.053	0.050
2.410	0.094	0.095	0.072	0.072	0.053	0.053	0.049	0.048
2.430	0.083	0.085	0.067	0.067	0.050	0.050	0.046	0.045
2.450	0.079	0.082	0.065	0.065	0.049	0.049	0.043	0.043
2.470	0.077	0.077	0.062	0.062	0.044	0.044	0.041	0.041
2.500	0.070	0.072	0.057	0.057	0.040	0.041	0.035	0.035
2.520	0.065	0.066	0.052	0.052	0.038	0.038	0.032	0.032
2.550	0.060	0.062	0.046	0.046	0.036	0.034	0.028	0.028
2.600	0.054	0.054	0.043	0.043	0.029	0.029	0.025	0.025
2.635	0.051	0.051	0.041	0.041	0.028	0.028	0.024	0.024
2.670	0.048	0.048	0.037	0.037	0.027	0.027	0.022	0.022
2.700	0.050	0.050	0.035	0.035	0.028	0.028	0.022	0.022
2.737	0.048	0.048	0.035	0.035	0.029	0.029	0.021	0.021
2.770	0.051	0.051	0.035	0.035	0.029	0.029	0.021	0.021
2.800	0.050	0.050	0.034	0.034	0.030	0.030	0.021	0.021
2.833	0.051	0.051	0.034	0.034	0.029	0.029	0.029	0.020
2.865	0.051	0.051	0.034	0.034	0.029	0.029	0.019	0.019
2.900	0.045	0.045	0.034	0.034	0.030	0.030	0.015	0.015
3.016	0.033	0.033	0.032	0.034	0.010	0.010	0.010	0.010
3.058	0.027	0.027	0.020	0.020	0.010	0.010	0.010	0.010
3.100	0.025	0.025	0.020	0.020	0.010	0.010	0.010	0.010

KEY:

* su - Surface
** mod - Model

TABLE 8.9

DISTRIBUTION OF PRESSURE OVER SURFACE OF ELLIPSOID OF REVOLUTION WITH RATIO OF SEMIAXES b/a = 1.5 AT DIFFERENT VALUES OF M_∞

θ, rad	M_∞							
	3		4		6.05		8.06	
	$\bar{p}^{*}_{su}$	$\bar{p}^{**}_{mod}$	$\bar{p}^{*}_{su}$	$\bar{p}^{**}_{mod}$	$\bar{p}^{*}_{su}$	$\bar{p}^{**}_{mod}$	$\bar{p}^{*}_{su}$	$\bar{p}^{**}_{mod}$
0.000	1.000	1.000	1.000	1.000	1.000	1.000	1.000	1.000
0.037	0.996	0.998	0.995	0.997	0.995	0.997	0.995	0.995
0.078	0.994	0.992	0.990	0.988	0.987	0.986	0.986	0.985
0.104	0.991	0.989	0.987	0.986	0.985	0.983	0.980	0.982
0.125	0.988	0.986	0.984	0.981	0.980	0.979	0.978	0.978
0.147	0.983	0.981	0.980	0.978	0.978	0.976	0.975	0.974
0.169	0.980	0.977	0.975	0.974	0.971	0.973	0.968	0.969
0.193	0.965	0.968	0.962	0.963	0.960	0.957	0.956	0.953
0.211	0.960	0.955	0.954	0.951	0.945	0.948	0.943	0.944
0.237	0.945	0.940	0.939	0.937	0.931	0.935	0.927	0.931
0.256	0.931	0.934	0.928	0.926	0.921	0.917	0.915	0.914
0.276	0.915	0.917	0.908	0.902	0.901	0.896	0.892	0.894
0.301	0.898	0.899	0.885	0.888	0.876	0.877	0.875	0.872
0.325	0.875	0.879	0.865	0.869	0.855	0.859	0.850	0.852
0.347	0.857	0.861	0.849	0.852	0.841	0.835	0.837	0.832
0.364	0.834	0.839	0.824	0.827	0.814	0.812	0.811	0.809
0.382	0.821	0.817	0.807	0.809	0.790	0.794	0.786	0.787
0.405	0.803	0.795	0.782	0.779	0.761	0.758	0.757	0.755
0.422	0.780	0.776	0.761	0.757	0.741	0.738	0.735	0.732
0.436	0.760	0.765	0.736	0.740	0.705	0.703	0.701	0.700
0.455	0.734	0.738	0.713	0.711	0.691	0.687	0.684	0.682
0.465	0.715	0.712	0.704	0.699	0.675	0.672	0.666	0.663
0.482	0.691	0.694	0.670	0.675	0.645	0.644	0.639	0.637
0.500	0.664	0.659	0.637	0.634	0.621	0.617	0.611	0.614
0.516	0.647	0.643	0.616	0.614	0.595	0.592	0.584	0.587

KEY:

* su - Surface
** mod - Model

TABLE 8.9 Continued

θ, rad	M_∞ = 3		4		6.05		8.06	
	$\bar{p}^*_{su}$	$\bar{p}^{**}_{mod}$	$\bar{p}^*_{su}$	$\bar{p}^{**}_{mod}$	$\bar{p}^*_{su}$	$\bar{p}^{**}_{mod}$	$\bar{p}^*_{su}$	$\bar{p}^{**}_{mod}$
0.522	0.627	0.625	0.601	0.600	0.584	0.581	0.579	0.575
0.532	0.614	0.612	0.584	0.581	0.566	0.563	0.550	0.554
0.543	0.595	0.591	0.557	0.554	0.538	0.536	0.529	0.527
0.555	0.577	0.577	0.549	0.547	0.534	0.530	0.524	0.528
0.565	0.561	0.558	0.528	0.526	0.510	0.506	0.494	0.497
0.576	0.537	0.535	0.506	0.503	0.488	0.485	0.477	0.479
0.591	0.514	0.510	0.477	0.473	0.461	0.458	0.452	0.453
0.604	0.506	0.503	0.459	0.455	0.441	0.437	0.425	0.427
0.606	0.502	0.500	0.453	0.451	0.435	0.438	0.424	0.425
0.618	0.472	0.467	0.434	0.431	0.416	0.413	0.397	0.399
0.633	0.452	0.449	0.412	0.414	0.391	0.388	0.373	0.375
0.644	0.421	0.425	0.379	0.382	0.372	0.370	0.361	0.363
0.647	0.421	0.424	0.376	0.372	0.351	0.349	0.340	0.341
0.665	0.387	0.382	0.349	0.347	0.331	0.327	0.319	0.322
0.675	0.367	0.370	0.326	0.321	0.305	0.303	0.297	0.293
0.687	0.355	0.353	0.304	0.301	0.284	0.282	0.277	0.279
0.695	0.334	0.339	0.293	0.290	0.266	0.263	0.251	0.254
0.711	0.303	0.299	0.262	0.265	0.241	0.238	0.227	0.225
0.726	0.279	0.278	0.238	0.239	0.220	0.222	0.208	0.211
0.743	0.251	0.247	0.213	0.211	0.193	0.190	0.182	0.185
0.754	0.231	0.234	0.193	0.191	0.174	0.171	0.166	0.167
0.761	0.222	0.224	0.186	0.184	0.165	0.161	0.154	0.155
0.764	0.213	0.214	0.175	0.174	0.155	0.158	0.151	0.153
0.775	0.201	0.197	0.164	0.162	0.145	0.143	0.138	0.141
0.787	0.189	0.185	0.148	0.146	0.138	0.135	0.126	0.124
0.793	0.176	0.173	0.139	0.140	0.124	0.120	0.119	0.121
0.805	0.156	0.152	0.124	0.121	0.105	0.101	0.101	0.102
0.819	0.143	0.139	0.104	0.101	0.095	0.091	0.089	0.087
0.832	0.125	0.126	0.093	0.091	0.075	0.071	0.075	0.073
0.846	0.113	0.112	0.078	0.077	0.067	0.068	0.060	0.062
0.856	0.105	0.105	0.071	0.069	0.056	0.055	0.055	0.053
0.876	0.084	0.082	0.055	0.054	0.045	0.043	0.043	0.042
0.890	0.075	0.073	0.045	0.041	0.032	0.033	0.030	0.032
0.911	0.065	0.062	0.031	0.030	0.022	0.022	0.021	0.020

KEY:

* su - Surface
** mod - Model

TABLE 8.10

PRESSURES MEASURED AT CONTROL PRESSURE (WITH IDENTICAL COORDINATES) POINTS FOR ELLIPSOIDS OF REVOLUTION WITH DIFFERENT RATIOS OF SEMIAXES

No. of model	θ, rad	M_∞ = 3		M_∞ = 4		M_∞ = 6.05		M_∞ = 8.06	
		$\bar{p}^*_{su}$	$\bar{p}^{**}_{mod}$	$\bar{p}^*_{su}$	$\bar{p}^{**}_{mod}$	$\bar{p}^*_{su}$	$\bar{p}^{**}_{mod}$	$\bar{p}^*_{su}$	$\bar{p}^{**}_{mod}$
				$b/a = 0.5$					
I	0.385	0.889	0.890	0.868	0.871	0.867	0.865	0.860	0.859
	2.170	0.152	0.156	0.117	0.119	0.090	0.091	0.086	0.087
II	0.385	0.886	0.888	0.875	0.878	0.866	0.864	0.859	0.861
	2.170	0.156	0.159	0.120	0.120	0.091	0.092	0.087	0.087
III	0.385	0.887	0.884	0.875	0.876	0.866	0.867	0.856	0.858
	2.170	0.155	0.157	0.119	0.116	0.092	0.093	0.088	0.087
IV	0.385	0.891	0.891	0.874	0.876	0.862	0.864	0.861	0.857
	2.170	0.152	0.153	0.118	0.119	0.090	0.091	0.086	0.086
V	0.385	0.890	0.892	0.875	0.877	0.862	0.864	0.858	0.858
	2.170	0.153	0.157	0.117	0.117	0.090	0.091	0.087	0.087
VI	0.385	0.885	0.887	0.877	0.877	0.863	0.863	0.858	0.861
	2.170	0.156	0.159	0.118	0.119	0.092	0.091	0.087	0.086
VII	0.385	0.889	0.889	0.869	0.878	0.864	0.862	0.858	0.861
	2.170	0.156	0.158	0.119	0.119	0.090	0.090	0.085	0.086
VIII	0.385	0.891	0.892	0.874	0.876	0.862	0.863	0.857	0.854
	2.170	0.151	0.153	0.118	0.119	0.092	0.091	0.087	0.088
IX	0.385	0.890	0.892	0.868	0.869	0.864	0.862	0.855	0.858
	2.170	0.155	0.157	0.117	0.118	0.090	0.091	0.087	0.087
X	0.385	0.889	0.890	0.869	0.870	0.865	0.864	0.854	0.858
	2.170	0.156	0.158	0.120	0.119	0.091	0.091	0.086	0.087
				$b/a = 1.5$					
I	0.301	0.897	0.897	0.885	0.887	0.879	0.880	0.873	0.877
	0.726	0.279	0.281	0.242	0.239	0.221	0.224	0.212	0.214
II	0.301	0.898	0.899	0.887	0.890	0.874	0.873	0.871	0.874
	0.726	0.281	0.277	0.236	0.239	0.217	0.217	0.210	0.212
III	0.301	0.897	0.898	0.885	0.887	0.880	0.879	0.869	0.876
	0.726	0.280	0.281	0.237	0.239	0.223	0.223	0.207	0.207
IV	0.301	0.897	0.897	0.884	0.887	0.873	0.877	0.871	0.874
	0.726	0.277	0.279	0.235	0.237	0.220	0.223	0.209	0.211
V	0.301	0.897	0.899	0.884	0.886	0.876	0.879	0.874	0.876
	0.726	0.279	0.281	0.241	0.243	0.219	0.222	0.207	0.210
VI	0.301	0.898	0.904	0.888	0.890	0.874	0.877	0.875	0.877
	0.726	0.277	0.278	0.236	0.238	0.221	0.223	0.206	0.208
VII	0.301	0.905	0.902	0.885	0.887	0.876	0.879	0.873	0.875
	0.726	0.280	0.282	0.240	0.242	0.221	0.224	0.211	0.213
VIII	0.301	0.898	0.903	0.886	0.887	0.878	0.879	0.871	0.874
	0.726	0.278	0.280	0.237	0.239	0.221	0.223	0.212	0.214

KEY:

* su - Surface
** mod - Model

TABLE 8.11

/327

RELATIVE DISTANCE ε OF SHOCK WAVE FROM SURFACE OF SPHERE AT DIFFERENT VALUES OF ϑ, AND M_∞

ϑ, deg	M_∞				
	2	3	4	6.05	8.06
0.0	0.330	0.218	0.174	0.147	0.137
1.8	0.330	0.218	0.174	0.147	0.137
3.6	0.331	0.219	0.175	0.147	0.137
5.4	0.332	0.220	0.176	0.147	0.137
7.2	0.333	0.222	0.179	0.147	0.137
9.0	0.335	0.223	0.181	0.148	0.138
10.8	0.337	0.224	0.184	0.149	0.138
12.6	0.339	0.226	0.185	0.152	0.140
14.4	0.343	0.228	0.186	0.152	0.142
16.2	0.347	0.230	0.186	0.154	0.144
18.0	0.352	0.232	0.188	0.157	0.146
19.8	0.357	0.234	0.189	0.159	0.148
21.6	0.363	0.236	0.191	0.162	0.149
23.4	0.368	0.241	0.194	0.162	0.151
25.2	0.375	0.246	0.197	0.166	0.154
27.0	0.385	0.250	0.200	0.168	0.157
28.8	0.393	0.255	0.204	0.169	0.158
30.6	0.403	0.260	0.209	0.172	0.161
32.4	0.411	0.266	0.214	0.177	0.165
34.2	0.421	0.271	0.220	0.183	0.169
36.0	0.432	0.278	0.226	0.189	0.173
37.8	0.442	0.286	0.234	0.196	0.176
39.6	0.455	0.292	0.240	0.200	0.180
41.4	0.468	0.300	0.245	0.204	0.186
43.2	0.481	0.309	0.252	0.211	0.192
45.0	0.496	0.319	0.262	0.217	0.198
46.8	0.511	0.328	0.272	0.225	0.203
48.6	0.528	0.340	0.279	0.235	0.213
50.4	0.546	0.351	0.289	0.242	0.219
52.2	0.565	0.362	0.299	0.251	0.227
54.0	0.585	0.376	0.309	0.261	0.236
55.8	0.607	0.391	0.323	0.273	0.246
57.6	0.635	0.403	0.336	0.282	0.254
59.4	0.654	0.420	0.348	0.295	0.263
61.2	0.680	0.438	0.365	0.306	0.280
63.0	0.710	0.455	0.377	0.319	0.291
64.8	0.738	0.477	0.392	0.331	0.312
66.6	0.767	0.495	0.410	0.347	0.324
68.4	0.803	0.520	0.428	0.362	0.339
70.2	0.837	0.541	0.445	0.377	0.353

TABLE 8.11 Continued

ϑ,deg	M_∞				
	2	3	4	6.05	8.06
72.0	0.872	0.566	0.463	0.392	0.366
73.8	0.914	0.594	0.485	0.413	0.384
75.6	0.956	0.621	0.512	0.431	0.400
77.4	0.999	0.652	0.526	0.452	0.420
79.2	1.049	0.685	0.551	0.475	0.441
81.0	1.103	0.718	0.577	0.497	0.461
82.8	1.159	0.751	0.603	0.520	0.485
84.6	1.222	0.790	0.633	0.549	0.509
86.4	1.286	0.832	0.665	0.574	0.533
88.2	1.357	0.876	0.699	0.600	0.566
90.0		0.925	0.734	0.633	0.586
91.8		0.975	0.776	0.666	0.617
93.6		1.030	0.815	0.700	0.650
95.4		1.089	0.863	0.740	0.687
97.2		1.152	0.917	0.784	0.725
99.0		1.217	0.961	0.823	0.767
100.8			1.025	0.872	0.813
102.6			1.075	0.924	0.860
104.4			1.141	0.977	0.915
106.2			1.213	1.035	0.970
108.0			1.289	1.097	1.020
109.8					1.080

TABLE 8.12

RELATIVE DISTANCE ε OF SHOCK WAVE FROM SURFACE OF ELLIPSOID OF REVOLUTION WITH RATIO OF SEMIAXES b/a = 0.5 AT DIFFERENT VALUES OF AND M_∞

ϑ,deg	M_∞			
	3	4	6.05	8.06
0.0	0.062	0.049	0.040	0.039
1.8	0.062	0.052	0.043	0.040
3.6	0.064	0.054	0.045	0.044
5.4	0.066	0.056	0.050	0.045
7.2	0.071	0.060	0.052	0.050
9.0	0.078	0.068	0.059	0.054
10.8	0.084	0.072	0.062	0.058
12.6	0.095	0.084	0.073	0.063
14.4	0.100	0.095	0.076	0.074
16.2	0.116	0.106	0.088	0.084
18.0	0.131	0.120	0.098	0.092
19.8	0.144	0.131	0.107	0.102
21.6	0.157	0.143	0.120	0.114
23.4	0.178	0.161	0.134	0.123
25.2	0.191	0.175	0.151	0.137
27.0	0.214	0.193	0.161	0.147
28.8	0.232	0.206	0.174	0.160
30.6	0.252	0.225	0.188	0.172
32.4	0.271	0.239	0.202	0.187
34.2	0.292	0.256	0.217	0.197
36.0	0.317	0.277	0.237	0.212
37.8	0.336	0.292	0.247	0.227
39.6	0.358	0.309	0.263	0.238
41.4	0.382	0.326	0.278	0.255
43.2	0.405	0.346	0.297	0.265
45.0	0.430	0.362	0.311	0.282
46.8	0.453	0.378	0.327	0.294
48.6	0.466	0.404	0.343	0.308
50.4	0.502	0.424	0.361	0.323
52.2	0.526	0.443	0.374	0.340

TABLE 8.12 Continued

ϑ, deg	M_∞			
	3	4	6.05	8.06
54.0	0.555	0.462	0.394	0.359
55.8	0.574	0.481	0.410	0.375
57.6	0.597	0.499	0.432	0.388
59.4	0.633	0.515	0.445	0.404
61.2	0.659	0.541	0.467	0.420
63.0	0.687	0.564	0.480	0.437
64.8	0.711	0.583	0.501	0.457
66.6	0.744	0.611	0.512	0.470
68.4	0.774	0.628	0.534	0.490
70.2	0.804	0.648	0.556	0.508
72.0	0.834	0.670	0.578	0.525
73.8	0.870	0.695	0.595	0.543
75.6	0.900	0.720	0.612	0.562
77.4	0.934	0.750	0.640	0.582
79.2	0.972	0.775	0.659	0.599

ϑ, deg	M_∞			
	3	4	6.05	8.06
81.0	1.012	0.802	0.683	0.619
82.8	1.043	0.825	0.703	0.640
84.6	1.084	0.856	0.728	0.662
86.4	1.127	0.885	0.752	0.680
88.2	1.172	0.914	0.777	0.704
90.0	1.219	0.941	0.799	0.725
91.8	1.241	0.972	0.826	0.752
93.6	1.296	1.010	0.854	0.778
95.4	1.339	1.041	0.886	0.807
97.2	1.400	1.072	0.912	0.834
99.0		1.116	0.942	0.855
100.8		1.151	0.971	0.885
102.6		1.194	1.007	0.914
104.4		1.240	1.041	0.950
106.2		1.287	1.077	0.983
108.0		1.342	1.119	1.015

TABLE 8.13

RELATIVE DISTANCE ε OF SHOCK WAVE FROM SURFACE OF ELLIPSOID OF REVOLUTION WITH RATIO OF SEMIAXES b/a = 1.5 AT DIFFERENT VALUES OF ϑ AND M_∞

ϑ, deg	M_∞			
	3	4	6.05	8.06
0.0	0.444	0.357	0.309	0.287
1.8	0.443	0.357	0.309	0.285
3.6	0.443	0.359	0.310	0.285
5.4	0.442	0.361	0.311	0.285
7.2	0.443	0.364	0.312	0.287
9.0	0.444	0.363	0.312	0.289
10.8	0.445	0.362	0.314	0.290
12.6	0.446	0.359	0.314	0.292
14.4	0.447	0.362	0.315	0.293
16.2	0.446	0.361	0.315	0.290
18.0	0.445	0.359	0.315	0.289
19.8	0.444	0.356	0.314	0.289
21.6	0.443	0.360	0.312	0.290
23.4	0.442	0.357	0.312	0.291
25.2	0.441	0.356	0.311	0.289
27.0	0.440	0.348	0.310	0.290
28.8	0.439	0.352	0.308	0.290
30.6	0.438	0.350	0.306	0.287
32.4	0.437	0.350	0.305	0.285
34.2	0.431	0.348	0.304	0.286
72.0	0.532	0.427	0.367	0.342
73.8	0.547	0.447	0.381	0.352
75.6	0.574	0.459	0.395	0.366
77.4	0.600	0.479	0.411	0.379
79.2	0.626	0.513	0.431	0.396
81.0	0.656	0.529	0.445	0.411
82.8	0.690	0.560	0.480	0.442
84.6	0.720	0.590	0.510	0.465
86.4	0.759	0.620	0.539	0.494
88.2	0.810	0.657	0.567	0.527

ϑ, deg	M_∞			
	3	4	6.05	8.06
36.0	0.436	0.349	0.303	0.284
37.8	0.436	0.349	0.302	0.283
39.6	0.435	0.346	0.301	0.283
41.4	0.435	0.349	0.302	0.284
43.2	0.434	0.345	0.302	0.285
45.0	0.434	0.350	0.301	0.286
46.8	0.435	0.352	0.302	0.286
48.6	0.436	0.352	0.305	0.287
50.4	0.437	0.354	0.304	0.290
52.2	0.438	0.354	0.303	0.290
54.0	0.440	0.361	0.307	0.292
55.8	0.443	0.362	0.310	0.294
57.6	0.446	0.370	0.311	0.296
59.4	0.451	0.374	0.315	0.301
61.2	0.461	0.382	0.319	0.302
63.0	0.470	0.385	0.323	0.305
64.8	0.476	0.393	0.328	0.311
66.6	0.489	0.401	0.339	0.316
68.4	0.502	0.410	0.346	0.325
70.2	0.517	0.419	0.355	0.330
90.0	0.863	0.697	0.612	0.561
91.8	0.917	0.747	0.646	0.595
93.6	0.983	0.792	0.687	0.637
95.4	1.057	0.844	0.738	0.690
97.2	1.133	0.903	0.798	0.740
99.0	1.232	0.973	0.857	0.792
100.8	1.326	1.040	0.925	0.862
102.6	1.435	1.117	1.012	0.945
104.4	1.564	1.215	1.083	1.001
106.2	1.693	1.299	1.177	1.090
108.0		1.415	1.282	1.169

REFERENCES

1. Dorodnitsiyn, A. A.: Method of Numerical Solution of Certain Nonlinear Problems of Aerodynamics (Ob odnom metode chislennogo resheniya nekotorykh nelineynykh zadach aerogidrodinamiki). Transactions of the Third All-Union Mathematical Congress, vol. 3. Moscow, Izd. AN SSSR, 447 - 453, 1958.
2. Belotserkovskiy, O. M. and P. I. Chushkin: Numerical Method of Integral Relations, Zh. vyvhisl. matem. i matem. fiz., vol. 2, No. 5, 731 - 759, 1962.
3. Belotserkovskiy, O. M.: Flow Around a Circular Cylinder with a Detached Shock Wave, Dokl. AN SSSR, vol. 113, No. 3, 509 - 512, 1957.
4. Chushkin, P. I.: Calculation of Certain Sonic Gas Flows. Prikl. matem i mekhan., vol. 21, No. 3, 353 - 360, 1957.
5. Van Dyke, M. D.: The Supersonic Blunt-Body Problem-Review and Extension. J. Aero-space Science, 1958, vol. 25, No. 8, 485 - 496. (Russian translation. Mekhanika., Sb. perev. i obz. in. period. lit., No. 5 (51), 3 - 22, 1958).
6. Vaglio-Laurin, R.: Transonic Rotational Flow Over a Convex Corner. J. Fluid Mech., vol. 9, Pt. 1, 81 - 103, 1960.
7. Belotserkovskiy, O. M.: Symmetric Flow of a Supersonic Ideal and Real Gas Around Blunt Bodies, Zh. vychisl. matem. i matem. viz., vol. 2, No. 6, 1062 - 1085, 1962.
8. Belotserkovskiy, O. M., A. Bulekbaev, and V. G. Grudnitskiy: Algorithms of Numerical Schemes of the Method of Integral Relations for Calculating Mixed Gas Flows, Zh. vychisl. matem. i matem. viz., vol. 6, No. 6, 1966 (In press).
9. Popov, F. D. : On One Scheme of the Method of Integral Relations in the Supersonic Blunt-Body Problem, Zh. tekhn. fiz., vol. 36, No. 2, 239 - 245, 1966.
10. Belotserkovskiy, O. M., M. M. Golomazov, and N. P. Shulishnina: Calculation of the Flow of an Equilibrium Dissociating Gas Around Blunt Bodies with a Detached Shock Wave, Zh. vychisl. matem. i. matem. fiz., vol. 4, No. 2, 306 - 316, 1964.
11. Ivanov, V. F.: Calculation of a Supersonic Flow Around Blunt Bodies with a Discontinuity of the Contour Generatrix (Raschet sverkhzvukovogo obtekaniy. zatuplennykh tel s izlomom obrazuyushchey kontura) (In press).
12. Lun'kin, Yu. P. and F. D. Popov: Effect of Nonequilibrium Dissociation on Supersonic Flow Around Blunt Bodies, Zh . vychisl. matem. i matem. fiz., vol. 4, No. 5, 896 - 904, 1964.
13. Lun'kin, Yu. P. and F. D. Popov: Effect of Vibrational-Dissociation Relaxation of Supersonic Flow Around Blunt Bodies, Zh. tekhn. fiz., vol. 36, No. 4, 661 - 671, 1966.
14. Tolstykh, A. I.: Numerical Calculations of Supersonic Viscous Gas Flow Around Blunt Bodies, Zh. vychisl. matem. i matem. fiz., vol. 6, No. 1, 113 - 120, 1966.
15. Bazzhin, A. P.: Calculation of Flow in Front of a Blunt Solid of Revolution Having a Corner Point, Inzhenernyy zh., vol. 1, No. 1, 154 - 159, 1961.

16. Shih, W. C. and J. R. Baron: Nonequilibrium Blunt-Body Flow Using the Method of Integral Relations. AIAA J., vol. 2, No. 6, 1062 - 1071, 1964.
17. Belotserkovskiy, O. M.: Calculation of Flow Around a Circular Cylinder with a Detached Shock Wave (Raschet obtekaniya krugovogo tsilindra s otoshedshey udarnoy volnoy). In the collection: Computational Mathematics. Izd. AN SSSR, No. 3, 149 - 185, 1958.
18. Minaylos, A. N.: Calculation of Flow Near a Blunt Solid of Revolution at an Angle of Attack in a Supersonic Gas Stream, Zh. vychisl. matem. i matem. fiz., vol. 4, No. 1, 171 - 177, 1964.
19. Golomazov, M. M.: Calculation of Supersonic Flow Around Blunt Bodies with a Discontinuity of Contour Curvature (Raschet sverkhzvukovogo obtekaniya zatuplennykh tel s razryvom krivizny kontura.). Report. Moscow, VTs AN SSSR, 1964.
20. Lun'kin, Yu. P., F. D. Popov, T. Ya. Timofeyeva, and Yu. M. Lipnitskiy: Passage of Singular Points in the Numerical Solution of Problems of Supersonic Flow Around Bodies, Trudy LPI, No. 248, 7 - 13, 1965.
21. Belotserkovskiy, O. M. and V. K. Duskin: Supersonic Nonequilibrium Gas Flow Around Blunt Bodies, Zh. vychisl. matem. i matem. fiz., vol. 4, No. 1, 61 - 77, 1964.
22. Dushin, V. K. and Yu. P. Lun'kin: Supersonic Nonequilibrium Dissociating Air Around Blunt Bodies, Zh. tekhn. fiz., vol. 35, No. 8, 1461 - 1470, 1965.
23. Fromin, V. N.: Hypersonic Gas Flow Around Blunt Bodies with Consideration of Radiation, Zh. vychisl. matem. i matem. fiz., vol. 6, No. 4, 1966.
24. Belotserkovskiy, O. M., Ye. S. Sedova, and F. V. Shugayev: Supersonic Flow Around Solids of Revolution with a Surface Discontinuity, Zh. vychisl. matem. i matem. fiz., vol. 6, No. 5, 1966 (In press).
25. Golomazov, M. M.: Calculation of Three-Dimensional Supersonic Flows in the Region of Influence of Blunting (Raschet trekhmernykh sverkhyvukovykh techeniy v oblasti vliyaniya zatupleniya). Report. Moscow, VTs AN SSSR, 1965.
26. Isayev, V. K. and V. V. Sonin: Modification of the Newton Method of Numerical Solution of Boundary-Value Problems, Zh. vychisl. matem. i matem. fiz., vol. 3, No. 6, 1114 - 1116, 1963.
27. Gilinskiy, S. M., G. F. Telenin, and G. P. Tinyakov: Method of Calculating Supersonic Flow Around Blunt Bodies with a Detached Shock Wave, Izv. AN SSSR, Mekhan. i mashinostr., No. 4, 9 - 28, 1964.
28. Li Li-kan: Certain Problems of Supersonic Gas Flow Around Bodies (Nekotoryye zadachi obtekaniya tel sverkhzvukovym potokom gaza.). Dissertation presented for scientific degree of candidate of physicomathematical sciences. VTs AN SSSR, 1966.
29. Godunov, S. K., A. V. Zabrodin, and G. P. Prokopov: Difference Scheme for Two-Dimensional Nonstationary Problems of Gas Dynamics and Calculation of Flow with a Detached Shock Wave, Zh. vychisl. matem. i matem. fiz., vol. 1, No. 6, 1020 - 1050, 1961.
30. Naumova, I. N.: Approximation of Thermodynamic Functions of Air, Zh. vychisl. matem. i matem. fiz., vol. 1, No. 2, 295 - 300, 1961.
31. Kraiko, A. N.: Analytical Representation of Thermodynamic Functions of Air, Inzhenernyy zh., vol. 4, No. 3, 548 - 550, 1964.

32. Molodtsov, V. K.: Calculation of Equilibrium Flows of Gas (In press). In collection: Numerical Methods of Solving Problems of Mathematical Physics (supplement to Zh. vychisl. matem. i matem. fiz.). Moscow, Izd. Nauka, 1966.
33. Maslennikov, V. G. and A. M. Studenkov: Position of Nose Shock Wave at M Numbers Close to One (O polozhenni golovnoy udarnoy volny pri chislakh M blizkikh k 1.). In the collection: Aerophysical Investigations of Supersonic Flows (Aerofizicheskiye issledovaniya sverkhzvukovykh techeniy Edited by Yu. A. Dunayev (In press).
34. Maslennikov, V. G.: Shape of a Detached Shock Wave Formed During Supersonic Motion of a Hemisphere and Cylindrical End in Different Gases (O forme otoshedshey udarnoy volny, obrazuyushcheysya pri sverkhzvukovom dvizhenii polusfery i tsilindricheskogo tortsa v razlichnykh gazakh.). In collection: Aerophysical Investigations of Supersonic Flows (Aerofizicheskiye issledovaniya sverkhzvukovykh techeniy). Edited by Yu. A. Dunayev (In press).
35. Lick, W.: Inviscid Flow of a Reacting Mixture of Gases Around a Blunt Body. J. Fluid Mech., vol. 7, No. 1, 128 - 144, 1960.
36. Hall, J. G., A. Q. Eschenroeder, and P. V. Marrone: Blunt-Nose Inviscid Air Flows with Coupled Nonequilibrium Processes. J. Aero-space Sci., vol. 29, No. 9, 1038 - 1051, 1962.
37. Predvoditelev, A. S., Ye. V. Stupochenko, A. S. Pleshanov, Ye. V. Samuylov, and I. B. Rozhdestvenskiy: Tables of Thermodynamic Functions of Air (Tablitsy termodinamicheskikh funktsiy vozdukha.). Three volumes, Moscow, Izd., AN SSSR, 1957, 1959, 1961.
38. Duff, R. E. and N. Davidson: Calculation of Reacting Profiles Behind Steady Shock Waves. II. Dissociation of Air. J. Chem. Phys.., vol. 31, No. 4, 1018 - 1027, 1959.
39. Losev, S. A. and N. A. Generalov: Investigation of the Phenomena of Excitation of Vibrations and Disintegration of Oxygen Molecules at High Temperatures, Dokl. AN SSSR, vol. 141, No. 5, 1072 - 1075, 1961.
40. Wray, K. L.: Shock-Tube Study of the Coupling of the O_2-Ar Rates of Dissociation. J. Chem. Phys., vol. 37, No. 6, 1254 - 1963, 1962.
41. Hammerling, P., J. D. Teare, and B. Kivel: Theory of Radiation From Luminous Shock Waves in Nitrogen. Phys. Fluids, vol. 2, No. 4, 422 - 426 1959.
42. Treanor, C. E. and P. V. Marrone: Effect of Dissociation on the Rate of Vibrational Relaxation. Phys. Fluids, vol. 5, No. 9, 1022 - 1026, 1962.
43. Lun'kin, Yu. P.: Change of Gas Parameters During Nonequilibrium Dissiciatic Behind a Shock Wave, Zh. takhn. fiz., vol. 30, No. 6, 622 - 626, 1960.
44. Osipov, A. I. and Ye. V. Stupochenko: Nonequilibrium Distribution of Energy with Respect to Vibrational Degrees of Freedom in Gases, Usp. fiz. nauk, vol. 79, No. 1, 81 - 113, 1963.
45. Nikitin, Ye. Ye.: Current Theories of Thermal Decomposition and Isomerizati of Molecules in the Gas Phase (Sovremennyye teorii termicheskogo raspada i izomerizatsii molekul v gazovoy forme.). Moscow, Izd. Nauka, 1964.
46. Losev, S. A.: Rate of Oxygen Decomposition at High Temperatures, Dokl. AN SSSR, vol. 141, No. 4, 894 - 896, 1961.

47. Millikan, R. C. and D. R. White: Systematics of Vibrational Relaxation. J. Chem. Phys., vol. 39, No. 12, 3209 - 3213, 1963.
48. Vaglio-Laurin, R.: On the PLK Method and the Supersonic Blunt-Body Problem. J. Aero-Space Sci., vol. 29, No. 2, 185 - 206, 248, 1962.
49. Gilinskiy, S. M. and G. F. Telenin: Supersonic Flow Around Bodies of Different Shape with a Detached Shock Wave. Izv. AN SSSR, Mekhan i mashinostr., No. 5, 148 - 156, 1964.
50. Fraasa, D.: An Experimental Investigation of Hypersonic Flow Over Blunt-Nosed Bodies at a Mach Number of 5.8. GALCIT Rep., No. 2, 75, 1957.
51. Fal'kovich, S. V. and I. A. Chernov: Sonic Gas Flow Around Solids of Revolution. Prikl. matem. i mekh., vol. 28, No. 2, 280 - 284, 1964.
52. Shmygelevskiy, Yu. D.: Calculation of Axisymmetric Supersonic Gas Flows in the Neighborhood of a Discontinuity of the Generator of a Solid Revolution. (Raschet osesimmetrichnykh sverkhzvukovykh potokov gaza v okrestnosti izloma obrazuyushchey tela vrashcheniya). Collection of Theoretical Works in Aerodynamics (Sbornik teoreticheskikh rabot po aerodinamike.). Moscow, Oborongiz, 1957.
53. Lees. L.: Current State of Aerodynamics of Hypersonic Flows. In the collection: Problems of the Motion of the Nose Cone of Longrange Rockets. Moscow, IIL, 1959.
54. Kuznetsov, Ye. S.: Radiant Heat Transfer in a Moving Liquid Medium, Izv, AN SSSR, Georgr. i geofiz., No. 1, 3 - 28, 1941.
55. Prokof'yev, V. A.: Stationary One-Dimensional Gas Motion with Consideration of Radiation (Statsionarnoye odnomernoye dvizheniye gaza s uchetom izlucheniya.). Dissertation. Inst. mekhan. AN SSSR, 1950.
56. Zel'dovich, Ya. B. and Yu. P. Rayzer: Physics of Shock Waves and High-Temperature Hydrodynamic Phenomena (Fizika udarnykh voln i vysoko-temperaturnykh gidrodinamicheskikh yavleniy.). Moscow, Fizmatgiz, 1963.
57. Mikhaylov, V. V.: Approximate Analytic Representation of Thermodynamic Functions of Air, Inzhenernyy sb., Izd. AN SSSR, vol. 31, 1961.
58. Mikhaylov, V. V.: Approximation of Enthalpy and Equation of State of Carbon Dioxide, Inzhenernyy zh., vol. 2, No. 2, 239, 1962.
59. Kibel, B.: Radiation from Hot Air and Its Effect on Stagnation-Point Heating. J. Aero-Space Sci., vol. 28, No. 2, 96 - 102, 1961.
60. Ho, H. T. and R. F. Probstein: The Compressible Viscous Layer in Rarefied Hypersonic Flow. Rarefied Gas Dynamics, Academic Press, 525 - 552, 1961.
61. Kao, H. C.: Hypersonic Viscous Flow Near the Stagnation Streamline of a Blunt Body. AIAA J., vol. 2, No. 11, 1892 - 1906, 1964.
62. Shidlovskiy, V. N.: Contribution to the Problem of Flow Around a Sphere by a Supersonic Stream of Rarefied Gas, Izv. AN SSSR, Mekhan. i mashinostr., No. 2, 17 - 24, 1962.
63. Levinskiy, Ye. and Kh. Iosikhara: Hypersonic Rarefied Gas Flow Around a Sphere (Obtekaniye sfery giperzvukovym potokom razrezhennogo gaza.). In collection: Investigations of Hypersonic Flows (Issledovaniya giperzvukovykh techeniy.). Moscow, Izd. Mir, 62 - 77, 1964.
64. Cheng, H. K.: The Blunt-Body Problem in Hypersonic Flow at Low Reynolds Number. JAS Paper, 63 - 92, 1963.
65. Van Dyke, M.: Theory of a Compressible Boundary Layer in the Second Approximation with Application to Hypersonic Flow Around Blunt Bodies. In collection: Investigations of Hypersonic Flows (Russian translation. Issledovaniya giperzvukovykh techeniy.). Moscow, Izd. Mir, 35 - 58,1964.

66. Tewfik, O. and W. Giedt: Heat Transfer Recovery Factor and Pressure Distributions Around a Circular Cylinder Normal to a Supersonic Rarefied Air Stream. J. Aero-Space Sci., vol. 27, No. 10, 721 - 729, 1960.
67. Telenin, G. F. and G. P. Tinyakov: Method of Calculating Three-Dimensional Flow Around Bodies with a Detached Shock Wave. Dokl. AN SSSR, vol. 154, No. 5, 1964.
68. Belotserkovskiy, O. M.: Calculation of Flow Around Axisymmetric Bodies wit a Detached Shock Wave (Raschet obtekaniya osesimmetrichnykh tel s otoshedshey udarnoy volnoy). Moscow, VTs AN SSSR, 1961.
69. Chushkin, P. I. and N. P. Shulishnina: Tables of Supersonic Flow Around Blunt Cones (Tablitsy sverkhzvukovogo techeniya okolo zatuplennykh konusov.). Moscow, VTs AN SSSR, 1961.
70. Chushkin, P. I.: Blunt Bodies of Simple Shape in a Hypersonic Gas Flow, Prikl. matem. i mekhan., vol. 24, No. 5, 1960.

Translation prepared for the National Aeronautics and Space Administration by INTERNATIONAL INFORMATION INCORPORATED, 2101 Walnut St., Philadelphia, Pa. 19103
Contract No. NASw-1499.

"The aeronautical and space activities of the United States shall be conducted so as to contribute . . . to the expansion of human knowledge of phenomena in the atmosphere and space. The Administration shall provide for the widest practicable and appropriate dissemination of information concerning its activities and the results thereof."

—NATIONAL AERONAUTICS AND SPACE ACT OF 1958

NASA SCIENTIFIC AND TECHNICAL PUBLICATIONS

TECHNICAL REPORTS: Scientific and technical information considered important, complete, and a lasting contribution to existing knowledge.

TECHNICAL NOTES: Information less broad in scope but nevertheless of importance as a contribution to existing knowledge.

TECHNICAL MEMORANDUMS: Information receiving limited distribution because of preliminary data, security classification, or other reasons.

CONTRACTOR REPORTS: Scientific and technical information generated under a NASA contract or grant and considered an important contribution to existing knowledge.

TECHNICAL TRANSLATIONS: Information published in a foreign language considered to merit NASA distribution in English.

SPECIAL PUBLICATIONS: Information derived from or of value to NASA activities. Publications include conference proceedings, monographs, data compilations, handbooks, sourcebooks, and special bibliographies.

TECHNOLOGY UTILIZATION PUBLICATIONS: Information on technology used by NASA that may be of particular interest in commercial and other non-aerospace applications. Publications include Tech Briefs, Technology Utilization Reports and Notes, and Technology Surveys.

Details on the availability of these publications may be obtained from:

SCIENTIFIC AND TECHNICAL INFORMATION DIVISION

NATIONAL AERONAUTICS AND SPACE ADMINISTRATION

Washington, D.C. 20546